THE STRESS-DEFORMATION BEHAVIOUR OF A COMPACTED CLAY

A thesis presented for the
degree of Ph.D. in Civil Engineering
to the University of Canterbury,
Christchurch, New Zealand.

by

M.J. PENDER

1971

TO JANNE

ERRATA

p.xix 3rd line from bottom should read: q : $(\sigma'_1 - \sigma'_3)$

xx 14th line should read: δij : kronecker delta ...

20 line 1, last word should be: macro-

20 line 2, insert the word "level" before "or"

30 equation at bottom of page should be (2.3a)

70 1st line 2nd paragraph: insert "this" after "complete"

78 the R.H.S. of Eq.(3.3) should read: $1/6\{(\sigma_{11}-\sigma_{22})^2 + (\sigma_{22}-\sigma_{33})^2 + (\sigma_{33}-\sigma_{11})^2\}$

81 the 1st line of Eq(3.7) should read:

$$\partial f/\partial \sigma_{ij} d\sigma_{ij} < 0,\ f = 0,\ df = 0$$

3rd line should read:

$$\partial f/\partial \sigma_{ij} d\sigma_{ij} > 0,\ f = 0,\ df > 0$$

103 In Fig.3.7 one of the lines between and parallel to DC and EF should be labelled KL

125 3rd and 9th lines should have (-3.0, 0.0) rather than vice versa.

130 1st line should have (-3.0, 0.0) rather than vice versa.

132 lines 8, 22 and 25 should read $\pm$1.79 psi rather than $\pm$ 1.29 psi

134 3rd line Section 4.6 should have (-3.0, 0.0)

148 4th line from bottom should be $\pm$1.79 psi rather than $\pm$ 1.29 psi

153 R.H.S. of Eq.(4.5) should read: $0.068\{3.24 - (\xi'-2.55)^2\}$ for $\xi' < 2.55$

191 8th line Roscoe is misspelt

194 8th line "Terzaghi" should read "Terzaghi[83]"

210 R.H.S. of Eq.(5.8) should read:

$$\frac{kdp}{p''(1+e)}\left\{1 + \frac{0.068\,\xi'(\xi'-2.55)}{(1-\zeta')(\zeta'-0.24)}\right.$$

227 R.H.S. of Eq.(3.32) should read:

$$Mpd\varepsilon + \frac{kdp}{(1+e)}$$

228 6th line replace "second" with "secant"

235 R.H.S. of third Equation from bottom should be:

$$\int \frac{dv}{F(v)-v} + c$$

243 6th line from bottom: "Now from the definition of η': "

244 6th line, insert "λ" after "constant"

266 14th line, insert "the" before "difference"

277 11th line, insert "linear elastic" before "behaviour"

286 2nd line, replace "test" with "text"

Last line of Eq.(6.15) should read: $(A_{3333} - A_{3322})/2$

291 1st line third paragraph: (3.23) not (3.24)

A B S T R A C T

The work presented in this thesis is an initial investigation into the stress-deformation behaviour of a compacted clay under axisymmetric stress conditions. This behaviour is explained in terms of the theory of plasticity.

In the early chapters the basic concepts underlying the treatment are discussed. One chapter considers soil behaviour in terms of an hypothesis that the nature of the interparticle force system is a controlling factor determining soil behaviour. Basic ideas of the theory of plasticity are then set out and the power of Drucker's stability postulate is highlighted. This is followed by an exposition of the main aspects of the theory developed by the Cambridge research team under Roscoe, and its unity with the standard concepts of the theory of plasticity is explained.

Described next is the behaviour of a series of triaxial tests on compacted samples saturated by the application of back pressure. This is followed by the development of a theory of plasticity which can account for the main features of the deformation of the material. The essential step in this development is the integration of an expression for the direction of the plastic strain increment vectors derived from the experimental results. This integration gives an expression for the successive yield curves during work hardening. Also

at this stage it is noted that the Terzaghi effective stress is not the simplest means of describing the soil behaviour. A modified effective stress is defined and is used in the remainder of the thesis. Further experimental work shows that the theory developed can only be applied when the material is loaded in the direction in which the compactive effort was applied.

ACKNOWLEDGEMENTS

Grateful acknowledgement is made to the following:

Professor H.J. Hopkins, Head of the Civil Engineering Department, who initially encouraged the writer to study for the degree of Ph.D.

Mr T.A.H. Dodd, supervisor of this study, for his interest and support.

Dr D.G. Elms for his interest and helpful criticism during the writing of this thesis.

Mr P.J. Alley for his encouragement.

The Technical Staff of the Civil Engineering Department, especially Mr V. Gavars whose craftsmanship was responsible for most of the apparatus used.

The Staff of the Mobil Computer Laboratory, for punching cards and the Staff of the Engineering Faculty Library for their assistance.

Mrs R. Brennan for her painstaking work in typing this thesis and Mrs A. Lynch who prepared the diagrams.

My parents and friends for encouragement.

The Ministry of Works and the University Grants Committee for financial assistance.

C O N T E N T S

Page

L I S T O F F I G U R E S

INDEX OF NOTATION

The following is an index of the more essential mathematical symbols used throughout this thesis. Only those symbols used throughout the whole thesis are included here. In several places symbols are introduced and used for a page or so to ease presentation, these are not included in this index.

a : proportion of sample cross sectional area occupied by interparticle contacts

$[\underline{a}]$: the matrix of the nine coefficients in the top left corner of the matrix $[\underline{A}]$

a_{ij} : the direction cosine between the i and j directions

$[a_{ki}]$: matrix of direction cosines for a coordinate transformation

A : pore pressure parameter

$[\underline{A}]$: matrix of the 36 non-zero coefficients of A_{ijkl}

A_{ci} : area of i^{th} interparticle contact

A_f : face area of a small element of soil

A_H : horizontal projected area of a typical soil particle

A_V : vertical projected area of a typical soil particle

A_{ijkl} : 4th order tensor of material coefficients

c_e : Hvorslev's true cohesion

C_c : slope of compression e, $\log_{10}$ p curve

C_c' : slope of swelling e, $\log_{10}$ p curve

dA : face area of an infinitesimal element of material

$d\epsilon_{ij}$: strain increment tensor

$d\epsilon^{e}_{ij}$: elastic strain increment tensor

$d\epsilon^{p}_{ij}$: plastic strain increment tensor

$d\sigma_{ij}$: stress increment tensor

$d\lambda$: a variable factor of proportionality between increments of stress and increments of plastic strain

dF : increment of work dissipated as friction

dU : increment of stored energy of volume change

dU_D : increment of stored energy of distortion

dW : increment of external work

dv^{e} : increment of elastic volumetric strain

dv^{p} : increment of plastic volumetric strain

e : void ratio

f : loading function

f_i : resultant force at the i^{th} interparticle contact

$f_1(\xi',\zeta')$: a function used in calculating the plastic volumetric strain

$\underset{\sim}{F}$: the resultant force acting on an infinitesimal area of material

F_H : seepage force in the horizontal direction acting on a typical soil particle

F_V : Seepage force in the vertical direction acting on a typical soil particle

g : plastic potential function

$g(\eta')$: gradient of the yield curve

G_s : specific gravity of soil particles

G_{us} : undrained unloading secant modulus

h : a function appearing in the expression for plastic strain increments

I_1 : first invariant of the stress tensor

J_2 : second invariant of the deviatoric stress tensor

J_3 : third invariant of the deviatoric stress tensor

ln : natural logarithm

p : isotropic component of the stress tensor $(=\frac{1}{3}(\sigma_{11}+\sigma_{22}+\sigma_{33})$

p_c : consolidation pressure

p_i : initial value of p

p_o : value of p at which yield curve cuts p axis

p_{max} : maximum value of p during the loading phase of an undrained test

p_{ul} : value of p after complete undrained unloading of a sample

p'' : isotropic component of actual effective stress tensor

p_{kc} : isotropic stress built into soil during kneading compaction

Pc_i : normal force at i^{th} interparticle contact

q : $\frac{1}{2}(\sigma'_1-\sigma'_3)$

q_r : value of q corrected for energy expended during volume change in a drained test

q_{max} : maximum value of q reached during a loading phase of an undrained test

$r(\eta')$: slope of consolidation curves at constant stress ratio in the (e, lnp) plane

s_{ij} : deviatoric stress tensor

S : slope of undrained stress path

Tc_i : tangential force at i^{th} interparticle contact

u : pore water pressure

v : specific volume = (1+e)

V : volume of sample

W : work

α : work hardening parameter

γ_w : density of water

δ_{ij} : kronicker delta, = 1 when i=j, = 0 when $i \neq j$

ϵ_{ij} : strain tensor

ϵ_{ij}^{e} : elastic strain tensor

ϵ_{ij}^{p} : plastic strain tensor

$\epsilon_{11}, \epsilon_{22}, \epsilon_{33}$: principal components of the strain tensor

ζ' : a dimensionless parameter used in describing the decrease in p on complete unloading under undrained conditions

η : the stress ratio: q/p

η' : the stress ratio: q/(p+3.0)

η'_r : the stress ratio: $q_r/(p+3.0)$

θ : inclination of the plastic strain increment vector

κ : slope of swelling line in the (e, lnp) plane

λ : slope of compression line in the (e, lnp) plane

M : value of η at critical state

ξ : the ratio: p/p_c

ξ' : the ratio: $(p+3.0)/(p_c+3.0)$

$\underset{\sim}{\sigma}$: stress vector on a small area of material

σ : a component of total stress

σ' : a component of effective stress

$\sigma'_1, \sigma'_2, \sigma'_3$: principal effective stresses

$\sigma_{11}, \sigma_{22}, \sigma_{33}$: principal components of the stress tensor

σ_{ij} : the stress tensor

ϕ' : angle of internal friction in terms of effective stress

ϕ_{cv} : angle of internal friction at constant volume

ϕ_μ : angle of interparticle friction

ϕ_e : Hvorslev's true angle of internal friction

LIST OF REFERENCES

1. ARGON, A.S., McCLINTOCK, F.A., Mechanical Behaviour of Materials, Addison-Wesley, 1966, pp. 54-55.

2. BACCHUS, D.R., "Cyclic Deformation of Clay", Unpublished Ph.D. thesis, University of Auckland, 1969.

3. BADILLO, E.J., "Failure Theory for Clays", Proceedings, 7th International Conference on Soil Mechanics and Foundation Engineering, Mexico City, 1969, Vol.I, pp. 203-213.

4. BARDEN, L., KHAYATT, A.J., Incremental Strain Ratios and the Strength of Sand in the Triaxial Test", Geotechnique, Vol.16, No.4, December 1966, pp.338-357.

5. BISHOP, A.W., BJERRUM, L., "The Relevance of the Triaxial Test to the Solution of Stability Problems", ASCE, Research Conference on Shear Strength of Cohesive Soils, Boulder, 1960, pp. 437-501.

6. BISHOP, A.W., HENKEL, D.J., The Measurement of Soil Properties in the Triaxial Test, 2nd edition, Edward Arnold, London, 1962, pp. 1-211.

7. BISHOP, A.W., Correspondence on: "Shear Characteristics of Saturated Silt Measured in Triaxial Compression", by A.D.PENMAN, Geotechnique, Vol. 4, March 1954, pp. 43-45.

8. BLAND, D.R., "The Associated Flow Rule of Plasticity", Journal of Mechanics and Physics of Solids, Vol.6, 1957, pp. 71-78.

9. BOWDEN, F.P., TABOR, D., The Friction and Lubrication of Solids, Chapter V, Oxford, 1950.

10. BROWN, E.H., "A Theory for the Mechanical Behaviour of Sand". Proceedings, 11th International Congress of Applied Mechanics, Munich, 1964, pp. 183-191.

11. BURLAND, J.B., Discussion, Proceedings, 7th International Conference on Soil Mechanics and Foundation Engineering, Mexico City, 1969, Vol.III, pp. 196.

12. CALLADINE, C.R., Correspondence on, "A Theoretical and Experimental Study of Strains in Triaxial Compression Tests on Normally Consolidated Clays", by K.H.ROSCOE and H.B. POOROOSHASB, Geotechnique, Vol. XIII, No.3., September 1963, p. 250.

13. CASAGRANDE, A., HIRSCHFELD, R.C., "Investigation of the Stress-Deformation and Strength Characteristics of Compacted Clays", 1st Progress Report, Harvard Soil Mechanics Series, No. 61, May 1960.

14. CHANG, T.Y., KO, H.Y., SCOTT, R.F., WESTMAN, R.A., "An Integrated Approach to the Stress Analysis of Granular Materials", Research Report, California Institute of Technology, 1967, pp. 1-51.

15. CHAPLIN, T.K., "Inner and Outer Plastic Yield Surfaces in Clays", Proceedings, 7th International Conference on Soil Mechanics and Foundation Engineering, Mexico City, 1969, Vol. I, pp. 73-80.

16. COON, M.D., EVANS, R.J., "Recoverable Deformation of Cohesionless Soils", Proceedings ASCE, Journal of Soil Mechanics and Foundations Division, Vol. 97, No.SM2, February, 1971, pp. 375-391.

17. DAVIS, E.H., POULOS, H.G., "The Use of Elastic Theory for Settlement Prediction Under Three-Dimensional Conditions", Geotechnique, Vol. 18, No.1, March 1968, pp. 67-91.

18. DRUCKER, D.C., "Coulomb Friction, Plasticity and Limit Loads," Transactions ASME, Journal of Applied Mechanics, Vol. 21, 1954, pp. 71-74.

19. DRUCKER, D.C., GIBSON, R.E., HENKEL, D.J., "Soil Mechanics and Work Hardening Tehories of Plasticity", Transactions ASCE, Vol. 122, 1957, pp. 338-346.

20. DRUCKER, D.C., "A Definition of Stable Inelastic Material", Transactions ASME, Journal of Applied Mechanics, Vol. 26, 1959, pp. 101-106.

21. DRUCKER, D.C., "On Stress-Strain Relations for Soils and Load Carrying Capacity", Proceedings, International Conference on Mechanics of Soil Vehicle Systems, Turin, 1961, p.15.

22. DRUCKER, D.C., "Concept of Path Independence and Material Stability for Soils", Proceedings, IUATM, Symposium on Rheology and Soil Mechanics, Grenoble, 1964, pp. 23-43.

23. DRUCKER, D.C., "On the Postulate of Stability of Material in the Mechanics of Continua", Journal de Mechanique, Vol.3, No.2, June 1964, pp. 235-249.

24. DUNCAN, J.M., CHANG, C.Y., "Nonlinear Analysis of Stress and Strain in Soils", Proceedings ASCE, Journal of Soil Mechanics and Foundations Division, Vol.96, No. SM5, September 1970, pp. 1629-1653.

25. GERRARD, C.M., "Some Aspects of the Stress-Strain Behaviour of Sand", Journal of the Australian Road Research Board, Vol.3, No.4, December 1967, pp. 67-90.

26. GIRIJAVALLABHAN, C.V., REESE, L.C., "Finite Element Method for Problems in Soil Mechanics", Proceedings ASCE, Journal of Soil Mechanics and Foundations Division, Vol.94, No. SM2, March 1968, pp. 473-496.

27. HENKEL, D.J., "The Shear Strength of Saturated Remoulded Clays", ASCE Research Conference on the Shear Strengths of Cohesive Soils, Boulder, 1960, p.544.

28. HENKEL, D.J., SOWA, V.A., Discussion, Symposium on Laboratory Shear Testing of Soils, ASTM, STP No. 361, 1963, p. 104.

29. HILL, R., The Mathematical Theory of Plasticity, Oxford, 1950, pp. 33-34.

30. HORNE, M.R., "The Behaviour of an Assembly of Rotund, Rigid, Cohesionless Particles, I and II". Proceedings Royal Scoiety, Series A, Vol.286, 1965, pp. 62-97.

31. HORNE, M.R., "The Behaviour of an Assembly of Rotund, Rigid, Cohesionless Particles, III". Proceedings Royal Society, Series A, Vol.310, 1969, pp.21-34.

32. HVORSLEV, M.J., "Physical Components of the Shear Strength of Saturated Clays", ASCE Research Conference on the Shear Strength of Cohesive Soils, Boulder, 1960.

33. JANBU, N., "Soil Compressibility as Determined by Oedometer and Triaxial Tests", Proceedings, European Conference on Soil Mechanics and Foundation Engineering, Wiesbaden, 1963, Vol. I, pp. 19-25.

34. KENNY, T.C., "Shear Strength of Soft Clay", Proceedings, Geotechnical Conference, Oslo, 1967, Vol. II, p.51.

35. KIRKPATRICK, W.M., BELSHAW, D.J., "On the Interpretation of the Triaxial Test", Geotechnique, Vol. XVIII, No.3, September 1968, pp.336-350.

36. KOITER, W.T., "Stress-Strain Relations, Uniqueness and Variational Theorems for Elastic-Plastic Materials with a Singular Yield Surface", Quarterly Journal of Applied Mathematics, Vol.11, 1953, pp. 350-354.

37. KONDNER, R.L., ZALESKO, J.S., "A Hyperbolic Stress-Strain Formulation for Sands," Proceedings, Second Pan American Conference on Soil Mechanics and Foundation Engineering, Sao Paulo, 1963, Vol. I., pp. 289-324.

38. LADANYI, B., Discussion on, "An Evaluation of Test Data Selecting a Yield Criterion for Soils", by K.H.ROSCOE, A.N.SCHOFIELD and A.THURAIRAJAH, Laboratory Shear Testing of Soils, ASTM STP 361, 1963, p.129.

39. LADD, C.C., "Stress-Strain Modulus of Clay in Undrained Shear", Proceedings ASCE, Journal of Soil Mechanics and Foundations Division, Vol. 90, No. SM5, September 1964, pp. 103-132.

40. LAMBE, T.W., WHITMAN, R.V., "The Role of Effective Stress in the Behaviour of Expansive Soils", Quarterly of the Colorado School of Mines, Vol.54, No.4., October 1959.

41. LAMBE, T.W., "A Mechanistic Picture of Shear Strength in Clay", ASCE Research Conference on the Shear Strength of Cohesive Soils, Boulder, 1960.

42. LAMBE, T.W., "Methods of Estimating Settlement", Proceedings ASCE, Journal of Soil Mechanics and Foundations Division, Vol.90, No. SM5, September 1964, pp. 43-67.

43. LAMBE, T.W., "The Stress-Path Method", Proceedings ASCE, Journal of Soil Mechanics and Foundations Division, Vol. 93, No. SM6, November 1967, pp. 309-331.

44. LEE, I.K., "Stress-Dilatancy Performance of Feldspar" Proceedings ASCE, Journal of Soil Mechanics and Foundations Division, Vol.92, NO. SM2, March 1966.

45. LOMIZE, G.M., KRYZHANOVSKY, A.L., "On the Shear Strength of Sand", Proceedings, Geotechnical Conference, Oslo, 1967, Vol.I, pp. 215-219.

46. LOWE, J., JOHNSTONE, T.C., "Use of Back Pressure to Increase the Degree of Saturation of Triaxial Test Specimens", ASCE Research Conference on Shear Strength of Cohesive Soils, Boulder, 1960.

47. LOVE, A.E.H., A Treatise on the Mathematical Theory of Elasticity, 2nd Edition, Cambridge, 1906, pp. 72-73.

48. MIKASA, M., "A Point of View on the Strength of Clay", Soil and Foundation, Vol. IV, 1964.

49. MITCHELL, J.K., "Components of Pore Water Pressure and their Engineering Significance", Proceedings, Ninth Conference on Clays and Clay Minerals, 1960, pp. 162-184

50. MITCHELL, J.K., CAMPANELLA, R.G., "Creep Studies on Saturated Clays", Laboratory Shear Testing of Soils, ASTM STP 361, 1963, pp. 90-103.

51. NAGHDI, P.M., "Stress-Strain Relations in Plasticity and Thermoplasticity", Proceedings, 2nd Symposium on Naval Structural Mechanics, Plasticity, Brown University, 1960, pp. 121-169.

52. OLSEN, R.E., CAMPBELL, L.M., "Bushing Friction in Triaxial Shear Testing", ASTM Materials, Research and Standards, Vol.7, No.2, February 1967, pp. 45-52.

53. PALMER, A.C., "On Stress Relations for Soils", Unpublished Ph.D. Thesis, Brown University, 1965, pp. 1-87.

54. PALMER, A.C., "A Limit Theorem for Materials with Non-Associated Flow Laws", Journal de Mechanique, Vol. 5, No.2, June 1966, pp.218-222.

55. PALMER, A.C., "Stress-Strain Relations for Clays: An Energy Theory," Geotechnique, Vol. XVII, December 1967, pp. 348-358

56. PENDER, M.J., "Deformation Properties of Undisturbed Sandy Silt from the Site of the Pukaki High Dam", Unpublished Ministry of Works Central Laboratories Report No. 375, 1971, pp. 1-35.

57. PENDER, M.J., "Some Properties of Weathered Greywacke", Proceedings, 1st Australia-New Zealand Geomechanics Conference, Melbourne, 1971.

58. PICKERING, D.J., "Anisotropic Elastic Parameters for Soils", Geotechnique, Vol. XX, No.3, September 1970, pp. 271-276.

59. POOROOSHASB, H.B., ROSCOE, K.H., "The Correlation of the Results of Shear Tests with varying degrees of Dilation", Proceedings, 5th International Conference on Soil Mechanics and Foundation Engineering, Paris, 1961, Vol.I, pp. 297-304.

60. POOROOSHASB, H.B., HOLUBEC, I., SHERBOURNE, A.N., "Yielding and Flow of Sand in Triaxial Compression", Canadian Geotechnical Journal, Vol.3., No.4, 1966, pp. 179-190.

61. POULOS, S.J., "Control of Leakage in the Triaxial Test", Harvard Soil Mechanics Series, No.71, March 1964, pp. 1-230.

62. PRAGER, W., Introduction to Mechanics of Continua, 1st Edition, Ginn and Company, Boston, 1961, Chapters, 1, 2, 3 and 4 , pp. 3-94.

63. ROSCOE, K.H., SCHOFIELD, A.N., WROTH, C.P., "On the Yielding of Soils," Geotechnique, Vol. VIII, March 1958, pp. 22-53.

64. ROSCOE, K.H., POOROOSHASB, H.B., "A Theoretical and Experimental Study of Strains in Triaxial Compression Tests on Normally Consolidated Clays", Geotechnique, Vol. XIII, No.1, March 1963, pp. 12-38.

65. ROSCOE, K.H., SCHOFIELD, A.N., THURAIRAJAH, A., "Yielding of Clays in States Wetter than Critical", Geotechnique, Vol. XIII, No.3, September 1963, pp. 211-240.

66. ROSCOE, K.H., THURAIRAJAH, A., "On the Uniqueness of Yield Surfaces for Wet Clays", Proceedings IUATM Symposium, Rheology and Soil Mechanics, Grenoble, 1964, pp. 364-391.

67. ROSCOE, K.H., BURLAND, J.B., "On the Generalised Stress-Strain Behaviour of Wet Clay", Proceedings, Conference Engineering Plasticity, Cambridge, March 1968, pp. 535-609.

68. ROSCOE, K.H., "The Influence of Strains in Soil Mechanics", Geotechnique, Vol. XX, No.2, June 1970, pp. 129-170.

69. ROWE, P.W., "The Stress-Dilatancy Relation for Static Equilibrium of an Assembly of Particles in Contact", Proceedings Royal Society, Series A, Vol. 269, 1962, pp. 500-527.

70. ROWE, P.W., BARDEN, L., "Importance of Free Ends in Triaxial Testing", Proceedings ASCE, Journal of the Soil Mechanics and Foundations Division, Vol.90, No. SM1, January 1964.

71. ROWE, P.W., "Progressive Failure and Strength of a Sand Mass", Proceedings, 7th International Conference on Soil Mechanics and Foundation Engineering, Mexico City, 1969, Vol. I, pp. 341-349.

72. SANDERS, J.L., "Plastic Stress-Strain Relations Based on Infinitely Many Plane Loading Surfaces", Proceedings, 2nd United States National Congress of Applied Mechanics, 1954, pp. 455-460.

73. SCHMID, W.E., "Rheological Shear and Consolidation Behaviour of Soils", Research Report Princeton University, 1960, pp. 1-52.

74. SCHMERTMANN, J.H., OSTERBERG, J.O., "An Experimental Study of the Development of Cohesion and Friction with Axial Strain in Saturated Cohesive Soils", ASCE Research Conference on the Shear Strength of Cohesive Soils, Boulder, 1960, p. 658.

75. SCHOFIELD, A.N., WROTH, C.P., Critical State Soil Mechanics, McGraw-Hill, London, 1968, pp. 165-206.

76. SCOTT, R.F., Principles of Soil Mechanics, 1st Edition, Addison Wesley, 1963, p.35, p.165, pp.336-356.

77. SCOTT, R.F., "Stress-Deformation and Strength Characteristics", Proceedings, 7th International Conference on Soil Mechanics and Foundation Engineering, Mexico City, 1969, "State of the Art Volume", pp. 1-47.

78. SEED, H.B., MITCHELL, J.K., CHAN, C.K., "The Strength of Compacted Cohesive Soils", ASCE Research Conference on Shear Strength of Cohesive Soils, Boulder, 1960, pp. 877-964.

79. SIMONS, N.E., SOM. N.W., "The Influence of Lateral Stresses on the Stress Deformation Characteristics of London Clay," Proceedings, 7th International Conference on Soil Mechanics and Foundation Engineering, Mexico City, 1969, Vol. I, pp. 369-377.

80. SKEMPTON, A.W., "Effective Stresses in Soils, Concrete and Rocks," Proceedings, Conference on Pore Pressure and Suction in Soils, London, 1960, pp. 4-16.

81. SKEMPTON, A.W., "Terzaghi's Discovery of Effective Stress", From Theory to Practice in Soil Mechanics, Wiley, 1960, p.42.

82. SOKOLNIKOFF, I.S., The Mathematical Theory of Elasticity, 2nd Edition, McGraw-Hill, 1956, p.64 problem No.1.

83. TERZAGHI, K., "Design and Performance of the Sasuma Dam", Proceedings Institution of Civil Engineers, Vol.9, 1958, p.369.

84. TROLLOPE, D.H., "The Fabric of Clays in Relation to Shear Strength", Proceedings, Third Australia-New Zealand Conference on Soil Mechanics and Foundation Engineering, Sydney, 1960, pp.197-202.

85. WEIDLER, J.B., PASLAY, P.R., "Constitutive Relations for Inelastic Granular Medium", Proceedings, ASCE Journal of the Engineering Mechanics Division, Vol.96, No. EM4, August 1970, pp. 395-406.

86. WHITMAN, R.V., RICHARDSON, A.M., HEALY, K.A., "Time Lags in Pore Pressure Measurements", Proceedings, 5th International Conference in Soil Mechanics and Foundation Engineering, Paris, 1961, Vol. I, pp. 407-411.

87. WILSON, S.D., "Small Soil Compaction Apparatus Duplicates Field Results Closely", Engineering News Record, Vol.145, No.18, November 1950.

88. YONG, R.N., McKYES, E., "Yield and Failure of a Clay Under Triaxial Stresses", Proceedings ASCE, Journal of Soil Mechanics and Foundations Division, Vol.97, No. SM1, January 1971, pp. 159-176.

CHAPTER 1

INTRODUCTION

1.1 BACKGROUND

There is a widespread opinion that a major area in need of development in soil mechanics is the understanding of the manner in which soil deforms under stress. Typical expressions of the inadequacy of present means of calculating the deformation of soils and the need for a more reliable approach have come from Coon and Evans[16], Gerrard[25], Janbu[33], Kondner and Zalesko[37], Lambe[42], Lomize and Kryzhanovsky[45], Palmer[55], Rowe[71], Simons and Som[79], and Weidler and Paslay[85] but perhaps the most lucid statements of the situation have been given by Roscoe[68] and Scott[77].

The problem can be illustrated with reference to the calculation of the settlement of a foundation. Much effort in soil mechanics has been spent on defining the stress conditions that lead to failure of soils, but only a comparatively small amount of effort has been concerned with describing the deformations at stress levels below failure. For example the classical means of calculating settlement has hardly changed since its introduction in the twenties by Terzaghi. During this time there have been considerable developments in structural analysis so that methods for taking full account of the deformations of indeterminate structures are now commonplace. This

situation presents the civil engineering profession with an inconsistency. On one hand the methods of calculating the behaviour of an indeterminate structure have reached a high degree of sophistication whereas the methods in use for calculating the response of the soil on which these structures are founded have reached a much lesser degree of sophistication. Yet the deformations imposed on the structure by the foundation settlement play a particularly important role in determining the stresses in the structure. This inconsistency can only be resolved by developing a thorough quantitative understanding of soil deformation. The complex way in which soils are known to behave suggests that this task is not a simple one.

Much work has been based on the assumption that soil is simply a linear elastic material with modulus values that are presumed to be independent of stress and strain. Practical experience both in the laboratory and in the field shows that the number of situations to which this idealisation can be applied is indeed very limited. However, a development of this elastic assumption considers how the modulus values, either tangent modulus or secant modulus, vary with stress and strain. Once ascertained for a particular material the variation in the modulus can be included in calculations using the equations of elasticity if an incremental loading procedure is used. Some success has been achieved with this method. Chang, Ko, Scott and Westman[14], Davis and Poulos[17], Janbu[33],

Ladd[39], and Pender[56,57] have shown how the deformation properties of various materials do depend on stress and strain conditions and how they can be expressed in terms of the applied stresses for monotonic loading. Using such procedures Chang, Ko, Scott and Westman[14], Duncan and Chang[24] and Girijavallabhan and Reese[26] have used the finite element method to calculate the non-linear stress strain behaviour of soils. This work has indicated that the method may lead to a useful compromise between the complexities of the material behaviour of real soils and the practical necessity to provide a means of calculation that can be used by non-specialists. However there are many aspects of this procedure that must be investigated further before the worth of the approach is definitely established. Of special importance is the effect of different stress paths on the modulus values.

A significant disadvantage of the above procedure is that it can be applied only to loading, because the modulus values are merely pseudo-elastic and cannot be applied to unloading. It is a common observation when soils are unloaded even from very low values of stress that most of the deformation is not recovered. This phenomenon suggests that a plastic deformation theory may be more generally valid. If this were verified some doubt would be cast on the validity of a pseudo-elastic approach because, as has been pointed out by Burland[11] there is a fundamental difference between the type

of behaviour predicted by an elastic theory and that predicted by a plastic theory. Recently there has been some interest in describing the behaviour of both clays and sands in terms of the theory of plasticity. Drucker, Gibson and Henkel[19] and Drucker[22] have outlined the general requirements which a theory must fulfil to describe the behaviour of soils. In addition to the work of the Cambridge research group, introduced below, the theory of plasticity has been used by Chaplin[15], Palmer[53], Poorooshasb, Holubec and Sherbourne[60], Weidler and Paslay[85] and Yong and McKyes[88]. Also Barden and Khayatt[4] have suggested that the stress dilatancy theory of Rowe[69] and Horne[30,31], implies the existence of a plastic potential. However the stress dilatancy theory was originally developed to describe the failure of sand, and deformation was involved only in consideration of energy, and so this theory is not primarily a treatment of soil deformation.

The references cited, suggest that approaches based on the theory of plasticity have some promise. Additionally there is the work of the research group at Cambridge University, until recently led by the late K.H.Roscoe. Their work over the last two decades has been by far the most thorough and persistent of all investigations of the manner in which soil deforms under stress. Their major achievement has been the development of a complete theory for predicting the deformation of normally consolidated clay, Roscoe and Burland[67]. The predictions of this theory have been tested by very careful

experimental investigations and it has been established that for laboratory prepared normally consolidated clay the theory is capable of predicting very accurately the deformational behaviour of this class of material. It is the opinion of the writer that of all the work discussed so far this treatment is the most satisfactory. The theory itself is founded on well established principles of mechanics and the experimental work has been of a particularly high standard. The other theories mentioned have in one way or another certain elements of simplification or restriction which makes them of value only in specific circumstances, whereas the Cambridge theory is a general one. To the present it has been applied only to laboratory prepared normally consolidated or lightly over-consolidated materials. As yet there are no published reports of attempts to apply the work to undisturbed samples from natural soil deposits. This is an important area for further development. The possible extension of the theory to naturally occurring soils is obviously worth consideration in view of the success achieved with laboratory prepared specimens, and one aspect of this task is undertaken in this thesis.

The use of compacted soil is common in many aspects of civil engineering practice. A considerable amount of work, summarised by Seed, Mitchell and Chan[78], has been done on the strength of compacted soils. Although there has been some

consideration of the stress-strain curves for various types of compacted soils there has never been, to the writer's knowledge, any attempt to study the deformation rather than the strength of compacted materials. An initial approach to this problem is presented in this thesis.

The research project reported here was undertaken to examine the stress-deformation behaviour of a compacted clay with the object of describing this behaviour in terms of the concepts of the theory of plasticity. The particular choice of a compacted material was made so that a material with anisotropic properties could be investigated. The Cambridge work assumes that the soil is isotropic but it is expected that many soils encountered in civil engineering would be anisotropic and so this additional complication should be considered. Because of the mode of formation one would expect a compacted soil to be anisotropic.

Because of limitations in time and previous work the scope of this investigation has had to be very restricted. The behaviour of one particular soil compacted in a particular manner at a given moisture content is described. Even with a given soil there are several possible means of compaction and a whole range of possible moisture contents. However it seemed more useful to investigate one situation in depth rather than a range of situations very briefly. In the succeeding chapters it is shown that a theory of plasticity can predict

the general features of the deformation of this material under axisymmetric loading. A limitation of this theory is also explained which restricts its application to loading in the direction in which the compactive effort was applied. Because this is an initial study there are many aspects that require further investigation and these are discussed. However the work in this thesis shows that the theory of plasticity does provide a promising means of describing the deformation of a particular compacted soil.

In the remainder of this chapter the contents of the thesis are summarised chapter by chapter.

1.2 CHAPTER 2

The material presented in Chapter 2, entitled "Soil as a Particulate Material", forms part of the conceptual basis on which the remainder of the thesis is built. In the first part of the chapter a basic hypothesis that the fundamental factor in soil mechanics is the nature of the interparticle force system is stated and its implications discussed. This is then followed by a discussion of the concept of stress and its application to soil mechanics. It is explained how the use of the concepts of continuum mechanics, such as stress and strain, in soil mechanics depends on the assumption that the size of smallest element considered is sufficient for a large

number of separate particles to be included, in other words these concepts tell nothing about the forces and displacements to which individual particles are subjected. It is explained how a common assumption made in soil mechanics is that the area of the inter-particle contacts is very small. The first important consequence developed from this is the justification of the usual assumption of the symmetry of the stress tensor. This part of Chapter 2 is completed with a discussion of the idea of effective stress. Rather than considering the equilibrium of part of a soil particle which is usually given when analysing the concept the equilibrium of a whole particle is discussed. It is shown that if the area taken up by inter-particle contacts is small then the pore water pressure makes a negligible contribution to the equilibrium of the particle. This leads to the conclusion that changes in the magnitude of the pore pressure can have no local effect on the magnitude of the interparticle forces and hence on the behaviour of the material. Thus the importance of pore water pressure must come into the picture elsewhere. Further consideration reveals that this is a boundary phenomenon depending on the relative stiffness of the soil structure and the fluid filling the voids.

The second half of Chapter 2 is devoted to reviewing briefly some of the more basic aspects of soil behaviour underlying their frictional and cohesive properties. The explanation of the phenomenon of cohesion offered in this section is

important to the rest of the thesis. It is suggested that the cohesive component of strength is caused by the shearing of bonds between particles or groups of particles. The stresses that these bonds provide in the way of shear resistance are not normally taken into account but as can be seen in Chapters 4 and 5 the inclusion of these stresses leads to a major simplification in the description of the behaviour of this material.

1.3 CHAPTER 3

Chapter 3 is entitled "Soil as a Plastic Material" and here the basic mechanics of the theory of plasticity are developed in the initial part of the chapter and in the second part the theory of plasticity developed by the Cambridge team is outlined. The material presented in this chapter as in Chapter 2 can be found in various places throughout the literature. However these review chapters are, in the opinion of the writer, more than repetitions of an eclectic nature because when required additional development of standard material is incorporated or a differing point of view is expressed.

In the first half of Chapter 3 Drucker's concept of a stable plastic material is explained and its three very powerful consequences are considered. These are that a stable plastic material has a yield surface to which the plastic strain increment vector is perpendicular, that this

yield surface is convex and that the only way the stress increment comes into the calculation of the plastic strain increment is in determining the magnitude of the strain increment.

In Chapter 3 it is also shown how the principal axes of the strain increment tensor and of stress tensor coincide when a sample deforms in the triaxial apparatus. One of the features of the triaxial apparatus that is undesirable is that failure of some materials may occur in thin zones, referred to in the rest of this thesis as slip planes, and so the deformation is not homogeneous. Now, although this means that the strains calculated from boundary displacements are not true strains it is shown how the ratio between the strain components is independent of the inhomogeneity of deformation so that the ratio between the components remains accurate despite the nonuniform deformation. This finding is used later in deriving a yield curve for the compacted clay from the results of a series of undrained triaxial tests.

The final half of Chapter 3 is taken up with explaining the general concepts underlying the "critical state" theory of plasticity developed by Roscoe et al for normally consolidated clay. After doing this it is pointed out how the theory derived does not use any of the concepts that have been explained in the early part of the chapter. To show that the two are compatible the expressions derived

from the Cambridge theory for the plastic strain increments are taken and used in conjunction with the equations from the theory of plasticity given in the first part of the chapter. From these the yield curve is derived as are several other features of the theory developed by Roscoe's team. This means that although the Cambridge approach did not make any direct appeal to the concepts of the conventional theory it is nevertheless consistent with this.

1.4 CHAPTER 4

This chapter is confined to describing the results of a series of triaxial tests, mostly undrained, in which the stress deformation behaviour of the material is measured. The chapter is concerned merely with describing the results of these tests; any interpretation and analysis is left to Chapter 5. All the samples tested were first compacted by kneading compaction, then mounted in a triaxial cell and saturated by the application of back pressure, and after this consolidated before testing.

Along with the usual stress-strain curves and stress paths the deformation of the material and shape of the stress paths on unloading are described. In addition the results of two drained tests are presented and the chapter is completed with a discussion of the consistency of the prepared samples and accuracy of the testing procedure.

The major finding in this chapter is that the description of the stress paths and stress-strain curves is greatly simplified if the isotropic component of effective stress acting on the material is modified by the addition of 3 psi. When this is done it is shown how a unique curve is found when the ratio of the maximum shearing stress in the sample to the modified isotropic component of stress is plotted against the distortion, and in addition it is shown how the stress paths for the undrained tests can be plotted as a unique two dimensional curve by the correct choice of parameters. In Chapter 4 the modification to the isotropic component of stress is treated as a purely empirical fact and a physical interpretation for the phenomenon is discussed in Chapter 5.

1.5 CHAPTER 5

This is probably the most significant chapter of the whole thesis and as with Chapters 2, 3 and 6 it is divided roughly into two parts. The first part is a qualitative discussion of the results presented in Chapter 4 and the second part is concerned with the development of a plastic stress-strain law for this particular compacted soil.

There are two major aspects of the initial qualitative part of the chapter. Firstly it is explained how a three-dimensional surface is defined by the stress paths for the undrained tests. It is shown how certain features of this

surface are similar to those of the State Boundary Surface developed by Roscoe for normally consolidated clays. Secondly the behaviour is discussed in terms of the hypothesis of Chapter 2, that the behaviour is determined by the interparticle force system. It is explained how three separate aspects of the behaviour indicate that if the isotropic component of stress is increased by 3 psi the parameters needed to describe the behaviour are greatly simplified. In addition it is shown in Chapter 6 how this component of stress is independent of the orientation of the sample. Because of this the stress must be isotropic and so the hypothesis is made that during the compaction process an isotropic component of stress equivalent to 3 psi is built into the sample. The singular feature of this phenomenon that is so important here is that for axial strains up to and beyond 10% this component remains constant. The connection with Chapter 2 is taken further at this stage and it is postulated that a modified effective stress law is more appropriate for describing the behaviour of this soil than the Terzaghi effective stress. This is called the "actual effective stress" here and is calculated simply by increasing the Terzaghi effective stress by 3 psi.

Before the expression for successive yield curves is derived in the second part of the chapter it is first explained that the means of calculating volumetric strain developed by the Cambridge group implies a contradiction when applied to

this compacted soil, because on unloading there is some decrease in the isotropic component of stress. A modified procedure for calculating the elastic and plastic components of volumetric strain is explained. This implies that the section of the boundary surface on which only elastic strains can occur is a curved, rather than a vertical, wall as is explained in Chapter 3 for normally consolidated clay. After this the stress paths for the drained tests are corrected for the energy involved in the volume change. The energy correction used is the standard one that has been used on a variety of materials; however it is seen that for the drained tests on the compacted material the corrected stress paths do not lie on the boundary surface defined by the undrained tests. This is important because, as is explained, the theory developed can only be applied to stress paths that lie on the boundary surface.

The function defining the successive yield curves during the work hardening is found by integrating the expression for the direction of the plastic strain increment vector that was determined from the results of the undrained tests. During the process of deriving this function it is shown that the friction parameter for the material, calculated from a modified version of Roscoe's energy equation, is not constant with stress and strain for this material. Using the yield curve derived and the process outlined at the end of Chapter 3, expressions for the plastic strain increments are determined. The expression

for the plastic distortion increment is applied to the stress paths for an undrained and a drained test and also to an isotropic consolidation test. It is seen from this that the theory predicts the general features of the manner in which the soil deforms. For the drained test there is a problem because the corrected stress paths do not lie on the boundary surface.

1.6 CHAPTER 6

As was explained above, one of the writer's reasons for choosing a compacted material for this investigation was because it would be expected to be anisotropic; in Chapter 6 this feature of the material behaviour is discussed. A series of undrained triaxial tests was performed on samples mounted in the triaxial apparatus so that the major principal stress was applied at right angles to the direction of compactive effort.

From the results of these tests it is shown that the deformation properties of the soil are definitely anisotropic and that the samples become more isotropic as the consolidation pressure is increased. However it is seen that for samples compacted and then consolidated under the same stresses the undrained stress paths swept out are the same regardless of the direction of the major principal stress relative to the direction of the compactive effort. From this it is seen that the same surface is defined by the results of undrained tests whether the material is oriented parallel or perpendicular

to the direction of compactive effort. This in turn implies that although the material is anisotropic with respect to deformation the values of the usual friction angle and cohesion for the material are isotropic.

For the remainder of Chapter 6 the particular type of anisotropy exhibited by the compacted soil is discussed. It is shown that when the material is loaded in the direction of the compactive effort there are only two independent components of deformation for an axially symmetric stress system such as the triaxial test, which itself has only two independent components of stress. However when the material is loaded at right angles to the direction in which the compactive effort was applied it is seen that there are now three independent components of deformation despite the fact that there are still only two independent components of stress. Because of this it is concluded that the theory developed in Chapter 5 can be applied correctly to this compacted material only when the direction of loading is parallel to that of the compactive effort. However the theory in its present state cannot be applied to loading perpendicular to the direction of the compactive effort because it cannot account for the third component of deformation.

1.7 CHAPTER 7 AND APPENDICES

In Chapter 7 the major conclusions reached in the

thesis are listed in order of importance. It has already been explained in the introduction how the project was a preliminary exploration of the deformation properties of a particular compacted clay. Because of this there are many aspects of the work that the writer feels need further more intensive investigation. These are listed, once again in order of importance, after the conclusions.

At the end of this thesis a number of appendices are included. In these the details of the equipment used and experimental procedure are set out, as are the listing of the computed experimental results. In the main body of the thesis only scant reference is made to these things because it was felt that these would be asides and would cloud the main lines of the discussion. In saying this it is not desired to play down the details of the experimental technique used as these form a very important part of what is presented in Chapters 2 to 7, particularly because so much trouble was taken with the details of this work. It goes without saying that nothing less than very careful experimental work is needed to elucidate the characteristics of the deformation of a material as complex as compacted soil.

CHAPTER TWO

SOIL AS A PARTICULATE MATERIAL

2.1 INTRODUCTION

The treatment of a compacted soil as a continuous material presented in this thesis should not be taken as a suggestion that the continuum approach is the only valid means of describing the stress-strain behaviour of a particulate material. One would expect that an alternative, and perhaps complementary, approach could be based on the fact that soil is an assemblage of individual particles. However even when soil is regarded as a continuum some of its properties are essentially dependent on its discrete composition. It is the purpose of this chapter to review and discuss these properties. Some of this discussion could be criticised on the grounds that it is rather speculative. This point is conceded: however, it does seem necessary to present these ideas because they reflect some aspects of the current understanding of soil behaviour in the literature. Although this understanding may be far from complete, as suggested by Kenny[34] in the following quotation: "---- there remain more questions than answers on the subject of strength properties at the particle level ----", there does seem to be some recognition of the importance of attempting to understand soil behaviour at this level. At least it does provide some hypothetical back-

ground from which to interpret and make predictions about the behaviour of soils.

The chapter is divided into three parts. Initially the hypothesis taken as fundamental by the writer is stated along with some of its implications. This includes some consideration of how the idea of stress can be applied to a particulate material. Secondly the concept of effective stress is discussed and finally the hypothesis is used to provide an explanation for the phenomena of cohesion and internal friction.

2.2 THE FUNDAMENTAL HYPOTHESIS

Throughout this thesis it is assumed that the fundamental variable responsible for all the diverse types of soil behaviour is the nature of the interparticle force system. This hypothesis is given the status of an axiom and its validity is not discussed any further. Although it might not be possible to measure these interparticle forces directly it is suggested that the recognition of their fundamental importance is vital in any explanation of soil behaviour.

Since it is probably not possible to demonstrate the validity of this hypothesis directly one should consider if there are any alternatives that are as appealing intuitively. When thinking about soil from the macroscopic or continuum viewpoint, as is done in the next chapter, such quantities as the stored and dissipated energy or the entropy of the material come to mind.

However at the interparticle level, as opposed to the microscopic or molecular level, it is not easy to suggest an alternative to the interparticle force system as the factor controlling the mechanical behaviour of soils.

When investigating many soil mechanics phenomena it is common to give a list of variables that can influence the observed behaviour of the material. Some of the more common of these are: void ratio, structure, stress history, composition, time and temperature. Separations like this could be interpreted as efforts to isolate various factors that contribute in a particular way to the interparticle force system. For example void ratio could be regarded as the factor primarily responsible for determining the average number of interparticle contacts per unit volume of a given soil. Structure the way in which these contacts are distributed with direction throughout the sample. While composition might reflect the manner in which the nature of the minerals composing the particles and the chemical composition of the fluid filling the pore space affect the interparticle forces. A caution that must be added here is that when selecting such a list of suitable variables care must be taken to ensure that they are all independent. When approaching such a task from the background of the hypothesis the choice of variables becomes somewhat more rational and the possibility of selecting variables that are not independent is reduced.

At this point it might be appropriate to consider the types of contact that may exist between particles and across which these all important interparticle forces are transmitted. There seem to be three possible types of contact. Those between non-cohesive sand and silt particles give rise to a good deal less argument in the literature than the two types of contact that may exist between clay particles.

Skempton[80], Scott[76] and Schmid[73] all agree that for non-cohesive particles the actual area of contact is extremely small and that the contact is of the type described by Bowden and Tabor[9] in Chapter V of their book. According to these researchers when two smooth metallic surfaces are in apparent contact the actual area of contact is only a very small proportion of the gross area. Even the smoothest metallic surfaces have a large number of irregularities on the microscale. When two surfaces approach the contact takes place between the irregularities or asperities and the contact stresses are so high that the material yields locally. Bowden and Tabor have demonstrated the validity of this idea for contact between metallic surfaces. Unfortunately the nature of contact between mineral surfaces has not been studied as extensively. However it does seem likely that the actual area of contact is extremely small and as stated above there is substantial agreement about contact between non-cohesive particles. Scott[76] and Schmid[73] have given lucid discussions of the implications of Bowden and

Tabor's theory of friction for soil mechanics. They have pointed out that because the material yields at the contacts the interparticle stress will be approximately constant. Secondly because the interparticle contacts occur at very small irregularities on the particle surfaces an increase in the stress applied to the soil is accommodated by the formation of new contacts rather than an increase in the area of existing contacts.

Two general classes of contact can exist between particles of a cohesive soil. The discussion in the literature of these contacts seems to have provoked more controversy than that about contact between non-cohesive particles. Because clay particles are very small and have a plate or rod-like form they have a large ratio of surface area to volume so that surface forces will play an important part at the interparticle contacts. When two planar clay sized particles approach in an aqueous environment so that their planar faces are parallel a repulsive force is exerted between the particles because of the interaction of their electrical double layers. This means that a compressive stress can be resisted while no real physical contact is made between the particles. The significance of this situation in relation to the fundamental hypothesis is not considered here as the type of clay mineral predominating in the soil tested in this project has a rod-like rather

than a planar form.

When clay particles approach in such a way that the contact is edge to edge or edge to face there has been some argument as to whether mineral to mineral contact is made or whether some adsorbed water remains between the particles acting as a contaminant. Regardless of the actual role played by the water at the interparticle contact it does not seem unreasonable to assume that the actual area of contact is small when edge to face contact is made. Even if the actual area of contact is small this type of contact differs considerably from that found in non-cohesive soils. All forces between contacts of sand and silt particles are caused by externally applied stresses and the weight of the material. For contact between clay particles other forces can arise. As mentioned above the interaction of the double layers results in an electrical force of repulsion. Also since the edges of the clay particles carry a positive electrical charge and their faces a net negative charge an attractive force will exist when edge to face contact is made. Another type of attractive force that can have a considerable effect at very small particle spacings is the Van der Waals-London force of attraction, the nature of this force is explained by Scott[76]. So that when the forces at the contact in a cohesive soil are considered not only those due to applied stresses must be considered, but also all the

forces of physico-chemical origin.

A deficiency in almost all of the discussion about the arrangement of various particles in soil is related to the idealised nature of the systems discussed. For example when discussing the structure of clays most authors consider materials composed only of clay particles whereas most natural deposits of soil have an extensive fraction of sand and silt particles. Thus what must be a very important type of contact in a real soil, that between a clay and a sand or silt particle, does not seem to have been considered. In view of what has been said above it does seem likely that this contact is also of the type involving a very small true area of contact.

In summary then it is assumed that in many types of soil the area occupied by the interparticle contacts is very small. A major exception to this assumption is to be found when a pure clay has a structure of plate-like particles arranged parallel to one another so that the externally applied stresses are resisted by the interaction of the double layers without any physical contact between the particles. The actual mechanism accounting for the behaviour of a soil in which this happens is not clear as explained by Mitchell[49] and Lambe[41]. The considerations in the remainder of this chapter are strictly applicable only to a soil where the contact area is small. This poses

no real problem for interpreting the behaviour of the particular soil examined in this thesis because this material has such a high proportion of silt.

Finally in this section some important implications of the fundamental hypothesis will be considered.

Firstly the postulation that interparticle forces are the controlling factor in soil behaviour suggests that the state of stress within the particle is of little importance. In coarse soils and broken rock particle fracturing may be significant, but in soil mechanics particle breakage is definitely of secondary importance at normal stress levels. Thus it is suggested that internal particle stresses play no important part in the mechanical behaviour of soil and consequently any discussion of the basic behaviour should make no reference to the stresses within the particles.

Secondly observations of the macroscopic behaviour of soils, and the suggestion that the interparticle contacts are of the type described by Bowden and Tabor suggests that the mechanism by which soil gains strength is interparticle friction. This means that a given contact will be able to sustain the load placed on it according to whether the ratio of the normal to the tangential component of the contact force is greater or less than the coefficient of friction between the two particles. If the ratio of the components is less than the coefficient of friction, then no interparticle move-

ment occurs, but if it is greater then some relative sliding will occur between the particles if the excess load cannot be distributed to other contacts.

Finally any relative motion that takes place between particles because of frictional failure of a contact or contacts will generally be irrecoverable when the sample is unloaded. This implies that the origin of the irreversible part of the deformation is slippage between particles or groups of particles.

2.3 THE DEFINITION OF STRESS FOR A PARTICULATE MATERIAL

In this section only a particulate material with empty voids is considered; the more general case of a material with fluid filled voids is discussed in section 2.4. The concept of stress used in continuum mechanics and developed in any of the standard texts, for example chapter 2 of Prager[62], is outlined in the following paragraphs and then the manner in which this concept must be modified to apply to a particulate material is explained.

The stress vector acting on a given elemental area within a continuum is defined as:

$$\underline{\sigma} = \lim_{dA \to 0} (\underset{\sim}{F}/dA) \qquad \ldots\ldots\ldots\ldots\ldots\ldots\ldots\ldots\ldots\ldots \quad (2.1)$$

where $\underline{\sigma}$ is the stress vector acting on a surface of area

dA and $\underset{\sim}{F}$ is the resultant force acting over this area.

A further aspect of this definition is concerned with the relation between the various stress vectors acting on surfaces with different orientations at a given point within the continuum. By considering the equilibrium of a small homogeneous tetrahedron of material and allowing its physical dimensions to tend to zero it can be shown that there is a linear relationship between the stress vectors acting on faces oriented in different directions at a point within the material. This leads to the concept of the stress tensor which is a quantity, denoted by σ_{ij} in this thesis, having nine components. The indices i and j can each have any value in the range 1 to 3 independently. When the indices have particular values, say L and M, the component σ_{LM} of the stress tensor is interpreted as the component of stress acting in the M direction on a plane whose unit normal vector is oriented in the L direction. If it is assumed that the only actions on the tetrahedron are surface and body forces then it can be shown by considering the rotational equilibrium of the element that the stress tensor is symmetric, that is $\sigma_{ij} = \sigma_{ji}$, which means that the number of independent stress components is reduced from 9 to 6.

In applying these ideas to a particulate material some modifications must be made. When considering a small element of the material care must be taken to choose an element

large enough to contain many individual soil particles and yet small enough to be representative of conditions at a point. This is to ensure that the material is uniformly distributed throughout the element so that the macroscopic homogeneity of the material is preserved in the small, but finite, element considered. Secondly, because the behaviour is supposed to be independent of the stresses within the particles the element must be chosen so that only whole particles exist along the boundaries, i.e. that no particles are cut. Since it is unlikely that all the contacts will occur in a plane the small element of soil considered will not have planar faces. However, this has no effect on the discussion below. This method of representing the conditions at a point within a soil by considering a small but finite element will only be successful if the space-rate of change of the quantities defined is such that the quantities have essentially uniform values over the sides of the element. If the scale of the element required is such that there are significant changes in the values then it is no longer possible to describe the behaviour of a particulate material from the viewpoint of continuum mechanics.

Now that an element of soil has been chosen the nature of stress in a particulate material can be considered. Along any face of the element there will be a number of interparticle contacts and at each of these contacts there will be a resultant

force exerted on the element of soil. This suggests that the stress vector on any face can be defined by:-

$$\underline{\sigma} = \left(\sum_{i=1}^{n} \underset{\sim}{f}_i\right)/A_f \qquad \text{.....} \quad (2.2)$$

where $\underset{\sim}{f}_i$ is the resultant force at the i^{th} interparticle contact, there being n contacts on the face which has a total area A_f (this is supposed to be small but finite as distinct from Eq.2.1 where the area, dA, was infinitesimal). On each face this stress vector can be resolved into three components, one normal to the face and two perpendicular components lying in the face, so the idea of a stress tensor arises as before. It is evident that the stress defined by Eq.(2.2) has a much smaller magnitude than the actual stresses at the interparticle contacts.

An important assumption made when defining stress is that there are no body or surface couples acting on the element of material considered. This has been justified by Love[47] on the grounds that as the size of the element tends to zero the magnitude of any couple will also tend to zero so when considering an infinitesimal element couples can be disregarded. However this may not be the case for the small element of soil considered. At each of these interparticle contacts on any face one should assume, for generality, that not only a direct force is transmitted but also a couple. However, the possibility that body couples can exist is discounted as there

is no obvious physical mechanism that could generate such actions. The presence of these contact couples cannot be explained away by the size of the element as this is no longer infinitesimal; their effect is considered by introducing a couple stress tensor defined in a similar way to the force stress tensor σ_{ij}. Argon and McClintock[1] define couple stress as the distributed couple per unit area. It is denoted here by M_{ij}. In the following paragraph it is shown that the existence of couple stresses requires the stress tensor to be asymmetrical.

Assuming that the stress tensor is asymmetrical and that the symmetric part is denoted by A_{ij} and the asymmetric part by B_{ij}, according to the well known identity of tensor analysis as set out in Prager[62] that an asymmetric tensor can be expressed as the sum of an asymmetric and a symmetric part, the equilibrium of forces on a small element requires that:

$$\partial A_{ij}/\partial x_i + \partial B_{ij}/\partial x_i + \rho f_j = 0 \quad \ldots\ldots\ldots\ldots\ldots\ldots\ldots\ldots \quad (2.3)$$

where ρf_j is the body force in the j^{th} direction. Considering the rotational equilibrium of the element the following equation is obtained:

$$\epsilon_{ijk} B_{jk} + \partial M_{ki}/\partial x_k = 0 \quad \ldots\ldots\ldots\ldots\ldots\ldots\ldots\ldots\ldots\ldots \quad (2.4)$$

where M_{ki} is the couple stress tensor and ϵ_{ijk} is the alternating tensor having a value of +1 when i, j and k have any of the values 1, 2 or 3 in a cyclic order and a value of -1 when i, j and k are taken in a non-cyclic way and a value of 0 when any two of i, j or k are equal. The symmetric part of the stress tensor is not included in Eq.(2.4) because the moment of its components is zero. Eq.(2.4) shows that the asymmetric part of the stress tensor is required to equilibrate the gradient of the couple stress tensor. The presence of these couple stresses and the resulting asymmetry of the stress tensor introduces a very considerable complexity into any theoretical treatment of the behaviour of a particulate material. Therefore it would be desirable to show either that the couple stresses cannot exist or that their magnitude is very small. The second of these alternatives can be achieved if it is known that the area of the interparticle contacts is very small. The magnitude of the stress defined in Eq.(2.2) arising from a force transmitted at a given interparticle contact is proportional to $(d/L)^2$, where d is a characteristic dimension of the contact and L is the characteristic length of the small element of soil considered. This assumes that the contact stress is constant. The basis for this has been explained earlier on page 22. Now when considering the magnitude of the couple stress arising from a couple applied at a given contact it seems reasonable to

discuss the maximum possible couple that a contact can withstand. In other words it is assumed that just as the direct forces cause yielding of the contact so too does the couple. It can be shown that the maximum couple a section can sustain under a fully plastic state of torsional stress is a function of d^3, where d is a characteristic dimension of the section. From the above definition of couple stress this means that the magnitude of the couple stress applied to the element by the couple applied at a contact is a function of $d(d/L)^2$. Since it was concluded in section 2.2 that the area of the contacts is very small the term $d(d/L)^2$ will be very much less than $(d/L)^2$ consequently the magnitude of the couple stresses will be very much less than that of the force stresses. Thus the effect of any torque transmitted at the interparticle contacts can be disregarded and the stress tensor can be considered as symmetric.

2.4 THE CONCEPT OF EFFECTIVE STRESS

The treatment of stress in a particulate material having empty voids given in the previous section is now generalised to include the case where the voids are filled with fluid. The so called principle of effective stress has traditionally been used in soil mechanics to handle this situation. According to this principle the stress controlling the compression and strength behaviour of a saturated soil is given by:

$$\sigma' = \sigma - u \qquad \ldots\ldots\ldots\ldots\ldots\ldots\ldots\ldots\ldots\ldots\ldots\ldots \quad (2.4)$$

where σ is the total stress and u the pore water pressure, while σ' is used to denote the effective stress. When soil behaviour is related to this stress rather than the total stress it is well known that several otherwise quite confusing phenomena can be explained in a rational manner. At this stage it is desirable to discuss the relation between this principle and the fundamental hypothesis stated in section 2 of this chapter.

Equation (2.4) implies that the observed behaviour of soil depends on the pressure in the fluid filling the voids between the particles. Recently there has been criticism of the effective stress principle by Schmid[73] and Mikasa[48] and although the writer does not agree with the conclusions reached by these authors it does seem that the soil mechanics literature reflects a preoccupation with pore pressure measurement, surprisingly little attention having been given to the physical significance of pore pressure response. The writer suggests that the hypothesis in section 2.2 is a statement of the principle of effective stress, in as much as it is postulated that the interparticle force system is the controlling factor in soil mechanics. For convenience the following distinction is made. The term "actual effective stress" is used to describe the stress arising from interparticle contact forces, that is the stress defined by Eq.(2.2), as distinct from the effective

stress of Eq.(2.4) called the Terzaghi effective stress. In the following paragraphs the influence of pore water pressure on the interparticle force system is examined. Initially this is done by considering the equilibrium of a single particle and assuming that the pore water pressure and the interparticle forces are independent and then the more complicated case where the two are interrrelated is discussed. The conclusion is reached that the phenomenon of pore pressure response under shear loading is an effect resulting from the making or breaking of interparticle contacts. Furthermore, although the actual effective stress cannot be measured its value can often be inferred from the Terzaghi effective stress, and any changes in the pore water pressure during shear loading imply an equal and opposite change in the actual effective stress.

In considering the equilibrium of a single particle the stress within the particle is not considered because, as pointed out towards the end of section 2.2, this should have no influence on the behaviour of the soil. It is also assumed that the soil is saturated and that the particles are non-cohesive, i.e. the effects of surface forces and osmosis are neglected at present. Fig.2.1 shows a cross-section of a particle in contact with several other particles. The resultant interparticle force at each contact is resolved into a normal and a tangential component, denoted for the i^{th} inter-

particle contact as Pc_i and Tc_i respectively. The area of the i^{th} contact is Ac_i and the angle that the normal force makes with the vertical is Θ_i. Along with the buoyant weight, $(G_s-1)\gamma_W V$ (where G_s is the specific gravity of the particle, γ_W the density of water and V the particle volume), the particle is subject to the local pore water pressure, u, and also a seepage force having vertical and horizontal components F_v and F_H respectively. Because the situation treated is a static one it is reasonable to omit inertial forces.

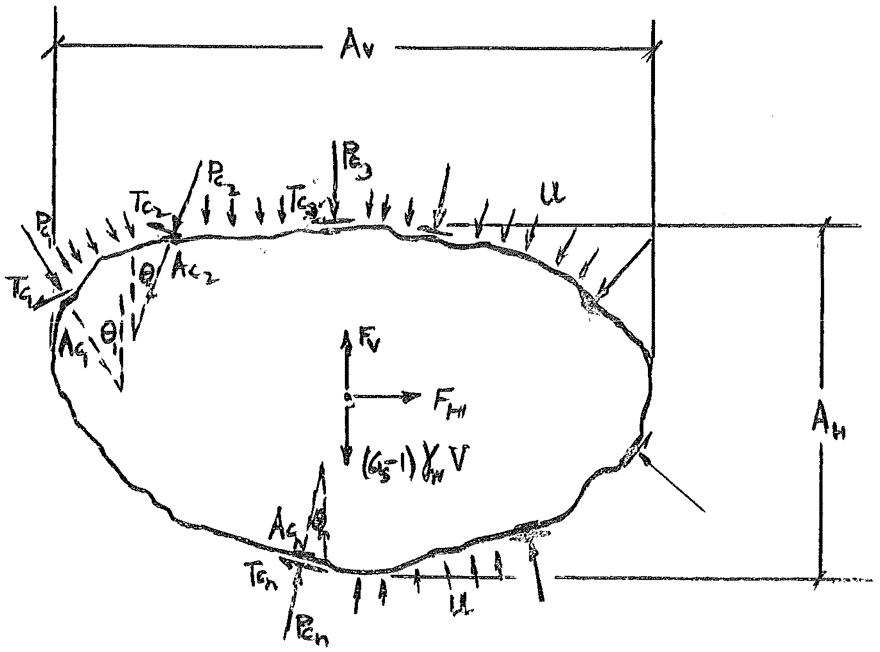

FIG.2.1 ACTIONS ON A TYPICAL SOIL PARTICLE

Considering first the vertical equilibrium of the particle:

$$\sum_{i=1}^{n} Pc_i \cos\Theta_i - \left(\sum_{i=1}^{n} Ac_i \cos\Theta_i\right)u + \sum_{i=1}^{n} Tc_i \sin\Theta_i - F_V + (G_s-1)\gamma_W V = 0 \quad \ldots\ldots\ldots\ldots\ldots (2.5)$$

The pore pressure terms in the above equation need some explanation. The presence of the buoyant weight implies that the pore water acts over the whole surface of the particle. Since this is not possible at the contacts the above expression for the downward forces has been written as if the water did act over the whole surface and compensating forces equal to the area of the contact times the pore water pressure acting outwards from the particle have been added. Thus this compensating force acts downwards for all those contacts where Pc_i acts upwards. The use of the buoyant weight and the average local pore water pressure, u, also has the advantage that the small variation in hydrostatic pressure around the particle is accounted for.

Two similar equations can be derived for equilibrium in two perpendicular horizontal directions. Since both have the same form only one is given here:

$$\sum_{i=1}^{n} Pc_i \sin\Theta_i - \left(\sum_{i=1}^{n} Ac_i \sin\Theta_i\right)u + \sum_{i=1}^{n} Tc_i \cos\Theta_i + F_H = 0 \quad \ldots\ldots (2.6)$$

Both Eqs.(2.5) and (2.6) indicate that pore water pressure

does contribute some force to the equilibrium of the particle. There is, of course, the possibility that the terms $\sum Ac_i \cos\Theta_i$ and $\sum Ac_i \sin\Theta_i$ may sum to zero, but in general these terms will have some magnitude so that the total projected area of the interparticle contacts in a given direction will not be zero. This means that the relationship between the areas Ac_i and the forces Pc_i and Tc_i must be evaluated so that the relative magnitude of the pore pressure term can be determined. The obvious approach to this problem would be to postulate a yield criterion for the material of the soil particles and use this to calculate Ac_i. Although attractive this idea is not pursued here simply because there is far too much uncertainty involved in applying any given yield criterion at the minute interparticle contacts. Because there is no simple experimental check on the validity of such an assumption more questions are raised than are answered. All that is used in the following discussion is the conclusion reached in section 2.2 of this chapter that the contact area is very small and that the contact stresses are large. Dividing Eq.(2.5) by the term $(\sum_{i=1}^{n} Ac_i \cos\Theta_i)$ gives:

$$\left(\sum_{i=1}^{n} Pc_i \cos\Theta_i\right)\Big/\left(\sum_{i=1}^{n} Ac_i \cos\Theta_i\right) + \left(\sum_{i=1}^{n} Tc_i \sin\Theta_i\right)\Big/\left(\sum_{i=1}^{n} Ac_i \cos\Theta_i\right)$$

$$- F_v\Big/\left(\sum_{i=1}^{n} Ac_i \cos\Theta_i\right) + (G-1)\gamma_w V\Big/\left(\sum_{i=1}^{n} Ac_i \cos\Theta_i\right) - u = 0 \qquad \text{..... (2.7)}$$

and similarly dividing Eq.(2.6) by $(\sum_{i=1}^{n} Ac_i \ Sin\Theta_i)$ gives:

$$(\sum_{i=1}^{n} Pc_i \ sin\Theta_i)/(\sum_{i=1}^{n} Ac_i \ sin\Theta_i) + (\sum_{i=1}^{n} Tc_i \ cos\Theta_i)/(\sum_{i=1}^{n} Ac_i \ sin\Theta_i)$$

$$+ F_H/(\sum_{i=1}^{n} Ac_i \ sin\Theta_i) - u = 0 \quad \ldots\ldots\ldots\ldots\ldots\ldots\ldots\ldots \quad (2.8)$$

The terms of the type $(\sum_{i=1}^{n} Pc_i \ sin\Theta_i)/(\sum_{i=1}^{n} Ac_i \ sin\Theta_i)$ in Eqs.(2.7) and (2.8) are in effect the average values of the direct stresses for all the interparticle contacts around the particle; these are the stresses that according to section 2.2 have a large magnitude. Also the remaining terms in which the divisor is of the type $(\sum_{i=1}^{n} Ac_i \ sin\Theta_i)$ will have a considerable magnitude because the total interparticle contact area of the whole particle is small. Thus all the terms in Eqs.(2.7) and (2.8) with the exception of the pore pressure term, u, will have a large magnitude; a magnitude that is considerably greater than the range of values for pore water pressure commonly encountered in practice. Hence the contribution of the pore water pressure to the equilibrium of the soil particle may be taken to be negligible.

So far the soil particle has been treated as non-cohesive. The more general case of a cohesive soil, in which there are electrical forces of attraction and repulsion and Van der Waals-London forces of attraction, can be included with

the above because the origin of the components of the inter-particle forces has not been specified. If the contact area still remains small then the conclusion reached above can be extended to cohesive soils. These physico-chemical inter-particle forces are sensitive to a number of factors such as temperature, concentration and type of ions in the pore water etc., and a change in any of these will lead to a change in the interparticle force system. For instance if both σ and u are maintained constant in drained loading of a cohesive soil and say the temperature changes then the soil behaviour will also change. This shows that the Terzaghi effective stress may not always be the stress controlling the strength and deformation properties of soil. Although at this stage the relationship between the fundamental hypothesis and the Terzaghi effective stress has not been settled it does seem that Eq.(2.4) has limitations when applied to cohesive soils. In other words, for a cohesionless soil the Terzaghi and actual effective stress are identical, but for a cohesive material this may not be so and Lambe and Whitman[40] have suggested this is why Eq.(2.4) does not account fully for the behaviour of swelling clays.

If the equilibrium of a small group of particles is considered, such as was discussed when defining stress in section 2.3, rather than the equilibrium of a single particle, the same conclusion is reached, that the pore water pressure

has only a negligible effect on the forces transmitted at the interparticle contacts. It was suggested earlier that the real significance of the interparticle forces is realised by considering them as the effective stress. However the above conclusion suggests that the pore water pressure has no local effect on the interparticle forces. What effect then does pore water pressure have on soil behaviour? This problem is discussed in the paragraphs below by considering not only the equilibrium of a single particle but also the equilibrium of the whole sample, including the effect of boundary conditions.

For the following discussion in which the boundary conditions are considered it is convenient to divide the stress system applied to the sample into two parts. Firstly the isotropic component of the stress tensor is defined as:

$$p = \frac{1}{3} \sigma_{ij} \delta_{ij} \qquad \ldots\ldots\ldots\ldots\ldots\ldots\ldots\ldots\ldots\ldots\ldots\ldots \quad (2.9)$$

where the indices i and j are summed over the range of values 1 to 3 independently, and where δ_{ij} is equal to 1 when i = j and 0 when i $\neq$ j. This can be expanded to:

$$p = \frac{1}{3} (\sigma_{11} + \sigma_{22} + \sigma_{33})$$

This equation shows that the isotropic component of the stress tensor, also known as the spherical component, is equal to the hydrostatic component of stress. The other component

of the stress system known as the deviatoric component is defined by:

$$s_{ij} = \sigma_{ij} - p\delta_{ij} \quad \ldots\ldots\ldots\ldots\ldots\ldots\ldots\ldots \quad (2.10)$$

The stress deviator thus represents all those components of stress associated with shearing stress.

In many laboratory test procedures and field situations the soil is effectively sealed around the boundaries so that pore water pressure and interparticle forces cannot be regarded as independent. When a section of a soil sample, including the boundaries, is considered all the interparticle forces along the section and the pore water pressure must equilibrate the forces applied at the sample boundary. It is now proposed to discuss the behaviour of the whole sample including the boundaries when subjected to the components of stress defined above. The first case, in which the sample is subjected to an isotropic component of stress under undrained loading, has been well discussed in the literature. The well known result is that the behaviour depends on the relative volumetric stiffness of the soil particle structure and on the fluid filling the voids. For the case of a fully saturated soil the volumetric stiffness of the water is so great in comparison with the volumetric stiffness of the soil particle structure that any increment of hydrostatic pressure in undrained loading will be transmitted entirely to the pore water and none of the stress

increment will be equilibrated by the interparticle forces. This explains the well known fact that the undrained behaviour of a saturated soil is not affected by changes in hydrostatic pressure because none of the stress change is transferred to the interparticle contacts. Thus at least one well known aspect of soil behaviour can be explained in terms of the fundamental hypothesis. Of course, if the sample is allowed to consolidate after the application of such a hydrostatic stress increment, the pore pressure will dissipate and the stress will gradually generate additional interparticle forces which lead to a volume change of the soil.

The behaviour when the deviatoric part of the stress tensor is applied to the soil sample under undrained loading is rather different. Before the soil can sustain any deviatoric stress component it must first be consolidated under an isotropic stress system. This isotropic stress is equilibrated by forces at the interparticle contacts, and because of the frictional nature of soil no shear stresses can be resisted until direct forces have been set up at the interparticle contacts by the isotropic stress. When the deviatoric component of the stress tensor is applied all the load must be taken by the soil particle structure and transferred from particle to particle at the interparticle contacts, because the fluid filling the voids has no shear stiffness. Now when this shear stress is applied to the sample

the existing interparticle contacts may be able to support their share of this new stress. In this case there will be no pore pressure response. More often the existing interparticle contacts cannot accommodate the new increment of stress without some rearrangement so that some of the existing contacts are broken and possibly some new ones are formed. Those contacts that are broken originally equilibrated some of the isotropic component of stress; for equilibrium to be maintained the sum of the normal contact forces and the force provided by the pore water pressure must balance the component of isotropic stress applied at the sample boundaries. If the total contribution of the interparticle direct forces to the isotropic component of the stress tensor is reduced in the process of breaking and reforming interparticle contacts, then there must be an increase in the pore water pressure. On the other hand if the sum of the direct forces at the interparticle contacts is increased after the shear stress is applied to the sample, then there will be a decrease in the pore water pressure. In the light of this explanation pore pressure response is just a consequence of the redistribution of load carrying capacity within the soil sample. The rate at which contacts are broken in comparison with the rate at which they are formed depends on how tightly the soil particles are packed together. For loosely packed soils the chances of a compensating contact being made after one has been broken are less than for a densely packed soil where there are

many more interparticle contacts per unit volume. Consequently loosely packed soils have a positive pore pressure response under undrained shear loading in contrast to densely packed soils which have a negative response. Under drained loading loosely packed soils decrease in volume and densely packed soils increase in volume. This suggests that there is a correlation between the tendency of a soil to have a positive pore pressure response on undrained loading and decrease in volume under drained loading.

The conclusion reached from this consideration of pore pressure response is that the phenomenon is the result of the interaction between the ways in which soil resists the isotropic and deviatoric components of the stress tensor. The important consequence of this is that the pore pressure response is not an independent effect, it is merely a result of the transfer of the mechanism by which the applied isotropic stress is equilibrated when interparticle bonds are broken and reformed. This explanation also shows that the reason for the success of the Terzaghi effective stress, given by Eq.(2.4) is that as an expression of equilibrium it portrays the interchange that takes place between pore water and interparticle forces. As pointed out earlier with regard to swelling clays, a deficiency of the Terzaghi effective stress is that it does not always account of physico-chemical interparticle forces.

It is interesting to consider if there are any situations

in nature where the conclusion reached earlier applies, namely that the pore water pressure has no local effect on the interparticle forces. In other words, are there any situations where the interparticle forces and the pore water pressure are truly independent. One example comes readily to mind; the behaviour of a sediment with a horizontal surface at the bottom of a lake or sea. Fluctuations in the water level have no affect on the behaviour of the sediment, provided it remains submerged, because the interparticle forces which are generated by the buoyant weight of the material are not affected by changes in water level. This was realised as long ago as 1871 by Sir Charles Lyell. The following quotation from Lyell's "Student's Elements of Geology" is part of a longer quotation given by Skempton[81]:

"When sand and mud sink to the bottom of a deep sea, the particles are not pressed down by the enormous weight of the encumbent ocean; for the water which becomes mingled with the sand and mud resists pressure with a force equal to that of the column of fluid above".

Since the interparticle forces are generated within the soil mass by the buoyant weight of the particles, no loads are transferred across impermeable boundaries and so there is no sharing of the hydrostatic components of stress between the contacts and the pore water as the sediment is loaded. An application of this idea that is of more relevance to soil mechanics applied

to foundation engineering is the behaviour of a deposit of soil with a fluctuating water table. At any point below the water table the effective stress is due to the weight of material above. This effective stress is made up of two parts: above the water table the total weight of soil contributes to the effective stress and below the water table only the buoyant weight contributes. When the water table rises the effective stress at a given level below falls and when the water table falls the effective stress increases. Application of Eq.(2.4) to this situation gives the change of effective stress due to a change in the water level. However the reason that the effective stress changes is not because the water pressure has changed but because the depth of soil contributing its buoyant weight has changed and it so happens that this is equal to the change computed using the pore water pressure.

Just before concluding this part of the chapter some aspects of Skempton's[80] paper on effective stress will be reviewed. At several places in the preceding discussion it has been emphasised that stresses within the soil particle are not considered. From this point of view the approach used by Skempton to derive the equilibrium equations for an inter-particle contact appears to be misleading. His diagram is given in Fig. 2.2 :

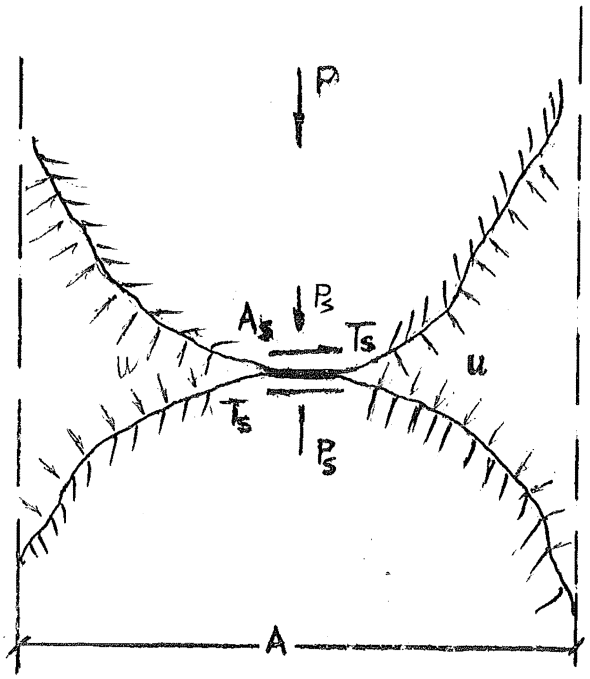

FIG.2.2 EQUILIBRIUM OF TWO PARTICLES IN CONTACT AFTER SKEMPTON (1960)

The shear and direct forces at the interparticle contact are given as T_s and P_s respectively and the contact area is A_s, the pore water pressure is denoted by u and the total normal force transmitted across the area A is P. In the original paper it is stated that two particles in contact are being considered. The difficulty is to explain the origin of P; in Fig.2.2 the impression is given that this might include the stresses within the soil particle. Skempton eventually concludes that the Terzaghi effective stress is adequate for the range of stresses normally encountered in engineering and since this conclusion is similar to the one

reached above it seems that there is nothing in Skempton's analysis that conflicts with the present discussion. It is suggested here that the problem about specifying the origin of the force P in Fig.2.2 can be resolved by changing the interpretation of Skempton's diagram. It was argued earlier that the real significance of pore water pressure does not become clear until the whole sample including boundaries is considered. Thus it is suggested that Fig.2.2 is merely a diagrammatic representation of a section through the whole sample. Along this section there will be a number of interparticle contacts each of which equilibrates some part of the stresses applied at the sample boundaries and represented here as the forces P and T. This means that the equation given by Skempton:

$$P = P_s + (A-A_s)u$$

can be regarded as the equation for equilibrium of vertical forces across the section of the sample. On dividing by the total area, A, this reduces to:

$$\sigma = \sigma' + (1-a)u \quad \ldots\ldots\ldots\ldots\ldots\ldots\ldots\ldots \quad (2.11)$$

where σ', the effective stress, has the same meaning as the stress defined by Eq.(2.2) and a is the proportion of the sample area occupied by the interparticle contacts. When a is small, as has been assumed in this thesis, Eq.(2.11) reduces to the Terzaghi effective stress given by Eq.(2.4).

To conclude this discussion of effective stress the relevance of effective stress analysis to foundation engineering is commented upon. As has been emphasised effective stress provides the most logical basis for interpreting soil behaviour, but, as pointed out by Mikasa[48] and Schmid[73] the accurate measurement of pore water pressure is not a simple matter and they are inclined to favour the total stress approach. When a sample is tested under conditions and imposed stresses identical with those in the field then there is no problem with the use of total stress analysis and it should yield results just as reliable as an effective stress study of the same situation. However it is never a simple matter to prepare or obtain samples with the same properties as the in-situ material and Bishop and Bjerrum[5] have pointed out that the great advantage of effective stress parameters is that they can be applied to a wider range of problems than total stress parameters. Also the determination of the cohesion and friction angle in terms of effective stress from undisturbed samples would seem to be less sensitive to stress changes caused by sampling and subsequent consolidation. Along with this there is the added advantage that measurement of pore water pressure provides some insight into the physical processes by which the sample is able to sustain the deviatoric component of the stress tensor.

2.5 FRICTION ANGLE AND COHESION RELATED TO INTERPARTICLE FORCES

In this part of the chapter the phenomena of internal friction and cohesion are discussed for a saturated soil and suggestions are made as to how these may be related to the interparticle forces. A good deal of confusion has resulted in soil mechanics because of the multiplicity of ways in which these parameters have been defined and no attempt is made here to discuss all these various definitions in detail. It is not intended here to give a detailed discussion of the very complex frictional and cohesive properties of soils. Instead an attempt is made to discuss the general features of the frictional and cohesive properties in terms of interparticle forces.

As mentioned in section 2.2 the hypothesis that the controlling factor in soil mechanics is the nature of the interparticle force system implies that interparticle friction is an important aspect of soil behaviour. Thus the coefficient of interparticle friction should be a basic physical parameter needed. It seems reasonable to assume that for a given soil this is constant and independent of the state of stress or deformation. This is not to say that the nature of every interparticle contact is such that the coefficient of friction at each is identical because most soils consist of mixtures of various minerals, contacts between various combinations of which have different coefficients. Even so, it should still be possible to nominate an average value for the material regardless

of the state of stress or strain. Such an assumption implies that the distribution of contacts between the various types of particles in a soil is not changed by the stress or strain.

Before considering internal friction, cohesion, and the interparticle forces in more detail it might be as well to list and comment briefly upon certain aspects of soil behaviour that have been well established by experiment. Any explanation of friction and cohesion must take the following five points into account:

(i) The multiplicity of definitions of friction angle and cohesion referred to above are all connected with failure conditions and are defined in terms of maximum principal stress differences or maximum principal effective stress ratios. However friction (and cohesion) are developed with strain and by plotting Mohr's circles for a number of samples at equal strains it is possible to get an idea of how the parameters develop. Schmertmann and Osterberg[74] have developed a method in which the sample is made to undergo changes in effective stress at essentially constant void ratio so that the way in which the friction and cohesion develop with strain can be studied. An example of this is shown in Fig.2.3. This diagram demonstrates how the friction angle and the cohesion of a remoulded specimen of Boston Blue clay are mobilised with strain.

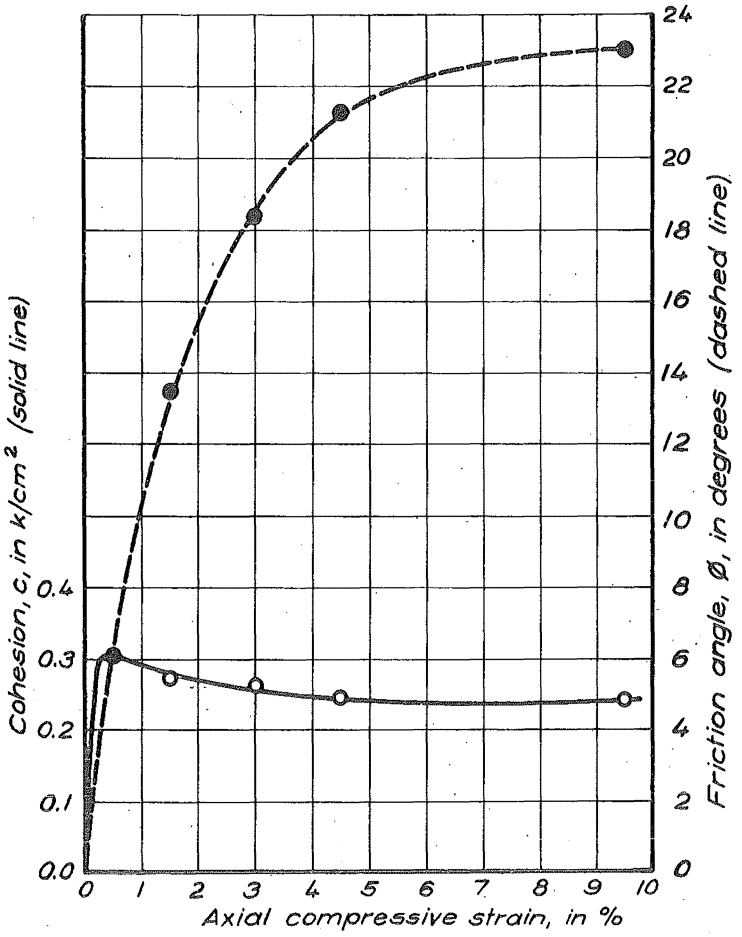

FIG. 2.3
DEVELOPMENT OF FRICTION AND COHESION WITH STRAIN

After Schmertmann

(ii) Cohesion is observed only for soils that contain some clay particles and then only when the soil is overconsolidated. It would be possible to quote many examples to illustrate how the cohesion is zero when samples consolidated from well above the liquid limit are tested while normally consolidated. Only that of Henkel[27] is given here, his results for tests on Weald clay are shown in Fig.2.4. This series of tests, both drained and undrained, for normally consolidated samples shows that for failure in axial compression and axial extension the cohesion is zero.

(iii) When samples of clay are overconsolidated in such a way that all have the same void ratio but different effective stresses, as illustrated in Fig.2.5, it is found that the friction angle is somewhat less than that for a series of normally consolidated samples. Also when determined for a range of void ratios it is found that this angle is independent of void ratio. On the other hand the cohesion turns out to be an exponential function of void ratio. Hvorslev[32] called these parameters the true angle of internal friction and the true cohesion.

(iv) When samples are tested under different conditions of drainage different friction angles are derived. This is because some of the work applied to the soil is used in changing the volume of the sample. To relate tests with

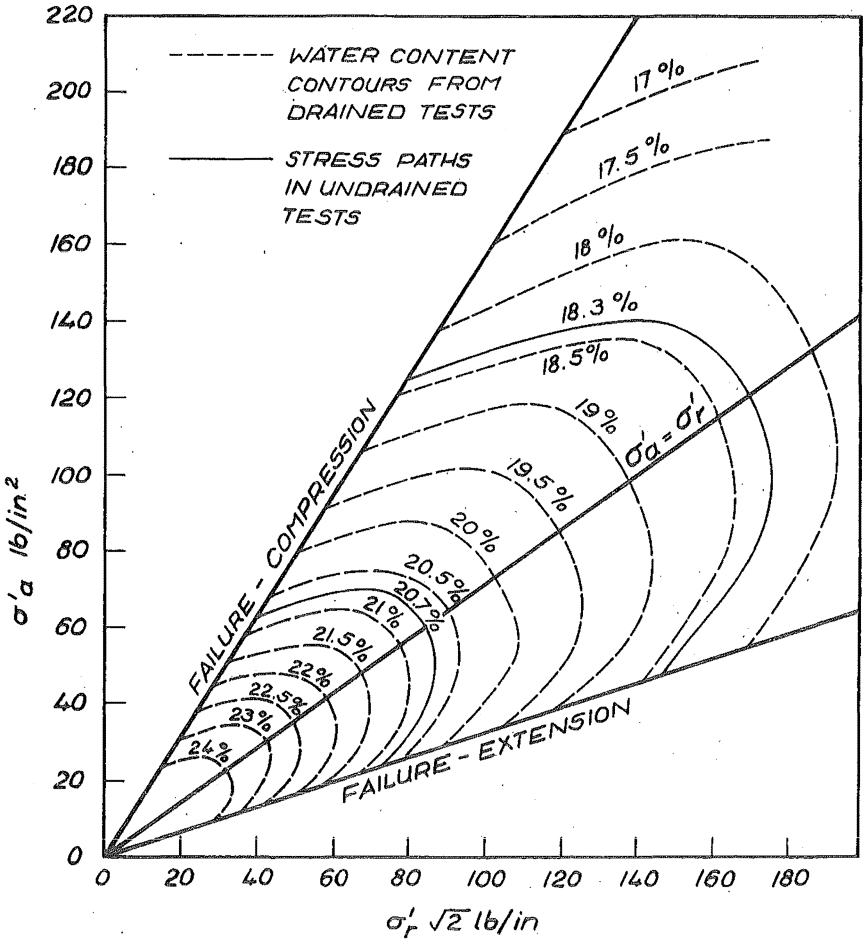

σ'_a = AXIAL EFFECTIVE STRESS
σ'_r = RADIAL EFFECTIVE STRESS

FIG. 2.4 FAILURE ENVELOPES FOR NORMALLY CONSOLIDATED WEALD CLAY

After Henkel

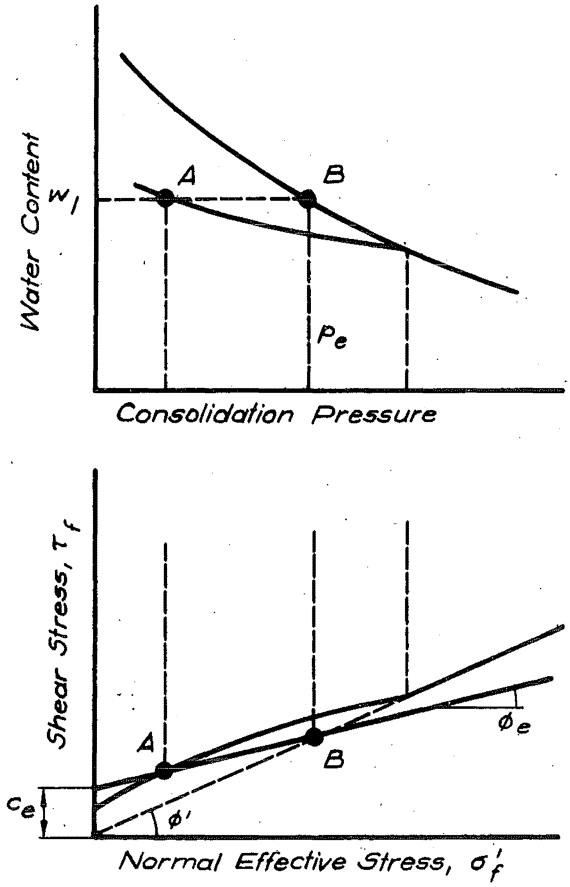

FIG. 2.5
DETERMINATION OF HVORSLEV'S TRUE ANGLE OF INTERNAL FRICTION AND TRUE COHESION

varying degrees of drainage many authors have suggested the use of boundary energy corrections to account for the work done in producing this volume change. When a suitable correction is applied the friction angle is supposed to be independent of the degree of drainage during the test. In the example given in Fig.2.4 the results of the drained and undrained tests give the same friction angle because at the failure point for a normally consolidated clay the rate of volume change in a drained test is zero and no boundary energy correction is necessary. But in the case of an overconsolidated clay or a dense sand or silt the volume is still changing at failure and the correction is required.

It has been demonstrated by Poorooshasb and Roscoe[59] that for tests on normally consolidated clays that no energy corrections are necessary at any stage of the stress path for these materials. However for over-consolidated cohesive soils this is not so. An example of how a correction can be used in this case is given in Chapter 5 section 8 where the results of some drained tests are discussed.

(v) The macroscopic friction angle measured for a given material is generally greater than the interparticle coefficient of friction. As an example the following table taken from Lee[44], gives values of the interparticle

friction angle ϕ_μ and the friction angle for deformation at constant volume ϕ_{cv} for a range of materials:

Material	ϕ_μ (degrees)	ϕ_{cv} (degrees)
Steel balls, $\frac{3}{32}$" dia.	7	14
Glass ballotini, 0.25 mm	17	24
Medium fine quartz sand	26	32
Feldspar 25-200 sieve	37	42

In the following pages these five aspects of soil behaviour are considered in terms of interparticle forces.

The first point to discuss is the reason why a material with a constant angle of friction on the microscale can have a variable angle on the macroscale as shown in Fig.2.3. As explained earlier the process of consolidating a soil under hydrostatic pressure results in a system of forces being set up at the interparticle contacts. These contacts can only be broken and relative movement take place between pairs of particles or groups of particles when the ratio of the normal component of the contact force to the tangential component is equal to the coefficient of interparticle friction. However after consolidation the contacts are not likely to be arranged in such a way that the maximum shearing resistance is available immediately some shearing stress is applied to the soil.

During the process of loading some contacts are broken and new ones are made so that there is a chance for some rearrangement to take place between various particles and groups of particles and the shear resistance of the soil increases. Eventually the stage is reached where the soil has mobilised the maximum possible resistance to shearing stress. At this point the sample continues to deform while the friction angle remains constant or in some soils the friction angle may then decrease. Thus the phenomenon of friction angle observed in soil mechanics depends on the organisation of particle contacts within the sample and reflects the extent to which a soil is able to rearrange the existing contacts when shearing stress is applied.

In the soil mechanics literature such reorganisation within the soil sample is known as structural change; where structure is regarded as the geometrical arrangement of the particles among themselves and is influenced by such things as particle shape and size. The concept has gained great popularity and is indeed most helpful when suggesting explanations for phenomena such as those discussed above. However it does seem to the writer that this is definitely an area of soil mechanics where much more research is needed to fully justify the present appeal to structural ideas. Also it is not easy to appreciate how these ideas can be applied to soils that contain a considerable proportion of sand and silt particles

because these particles do not have the characteristic plate-like shape associated with clay particles that is regarded as such an essential element in most considerations based on structural concepts. It is suggested here that for these cohesionless materials the function normally ascribed to the geometrical packing dependent on particle shape is associated with the way in which the interparticle contacts are distributed with direction throughout the sample. That is to say a change in structure for such a material would not be associated with any apparent change in the geometrical arrangement of the particles, rather, it would be linked with a change in the way that the contacts are distributed with direction throughout the soil.

A further aspect that has an important effect on the friction angle measured is related to the restrictions that are placed on the way in which the sample may deform. An obvious example is the difference between an axially symmetric test and a plane strain test. According to the stress dilatancy theory developed by Rowe[69] the measured friction angle for a given material lies somewhere between the interparticle friction angle ϕ_μ and the value when the sample deforms at constant volume ϕ_{cv}. In the case of axisymmetric deformation there are a large number of possible directions in which interparticle slip can occur while in the case of plane strain deformation the directions in which interparticle slip can occur are very much more restricted. This is reflected in the measured friction angles

after energy corrections: those for axially symmetric deformation tend to approach ϕ_{μ} while those for plane strain are greater and lie nearer to ϕ_{cv}. In other words there are more degrees of freedom in the axially symmetric case so that less work is required to deform the soil. Another aspect that is probably related to the freedom of interparticle movement is interlocking between particles because of surface irregularities. When there are more allowable directions for interparticle movement it is less likely that interlocking between particles because of irregular surfaces, sharp corners, etc. will contribute to the frictional resistance.

To complete this brief discussion of internal friction the effect of void ratio on the observed friction angle is considered, two cases have to be discussed. These are soils with and without cohesion.

Firstly cohesionless materials. It was suggested earlier in this chapter that void ratio may be regarded as a measure of the number of interparticle contacts per unit volume. When the void ratio is decreased the number of contacts is increased. On page 22 a current opinion was stated that the contact stress is approximately constant and any increase in the applied stress is resisted by the formation of new contacts rather than by an increase in stress at existing contacts. Now as the number of contacts per unit volume increases the number of contacts that may be able to contribute to the soil

strength increases and so the strength will increase as the void ratio decreases. However the discussion of this section implies that if the fundamental hypothesis is valid then the friction angle developed by cohesionless materials should be constant and independent of the number of inter-particle contacts per unit volume. Experiment shows that when the angle of internal friction of cohesionless materials is measured there is a characteristic decrease in the friction angle as the void ratio increases. However it is found that this decrease in the friction angle is related to the rate of volume change at failure and when corrections are applied for the work done by or against the cell pressure an angle that is approximately constant is found.

It is always found that completely dry or fully saturated sands and silts have no cohesion. This suggests that under zero stress all the interparticle contacts are broken thus explaining why the shear resistance is zero. A possible explanation for the breaking of the interparticle contacts appeals to the energy stored in the particles around the contact. Although the material is plastic in the immediate vicinity of each contact the elastic energy stored in the surrounding volume of particle may be sufficient to break the contact on unloading.

To explain the frictional properties of cohesive materials in terms of interparticle forces the explanation

of the behaviour at interparticle contacts given so far has to be extended. In section 2.2 it was pointed out that contact stresses arising from forces of a physico-chemical origin are important in cohesive soils. These forces lead to the formation of bonds between clay particles that are retained when the material is unloaded. The mechanism is set out in the following paragraphs.

The phenomenon of interparticle bonds can be explained by considering the nature of the clay particles that are the characteristic component of cohesive soils. It is well known that when two clay particles are forced close together that electrical forces of repulsion and attraction and physical forces of attraction come into play. The two most significant forces are the electrical repulsion between the electrical double layers that surround the clay particles in an aqueous environment and the Van der Waals-London attractive force that is effective when the particles are sufficiently close. When two isolated particles are made to approach from some considerable distance the electrical repulsion first manifests more than the attraction but when they are forced very close together the attraction will predominate. This has been discussed by several writers, including Scott[76], and is illustrated in Fig.2.6. When the force between the two particles is great enough to reduce the spacing to just below that at point A in Fig.2.6 there will be a spontaneous reduction in the spacing

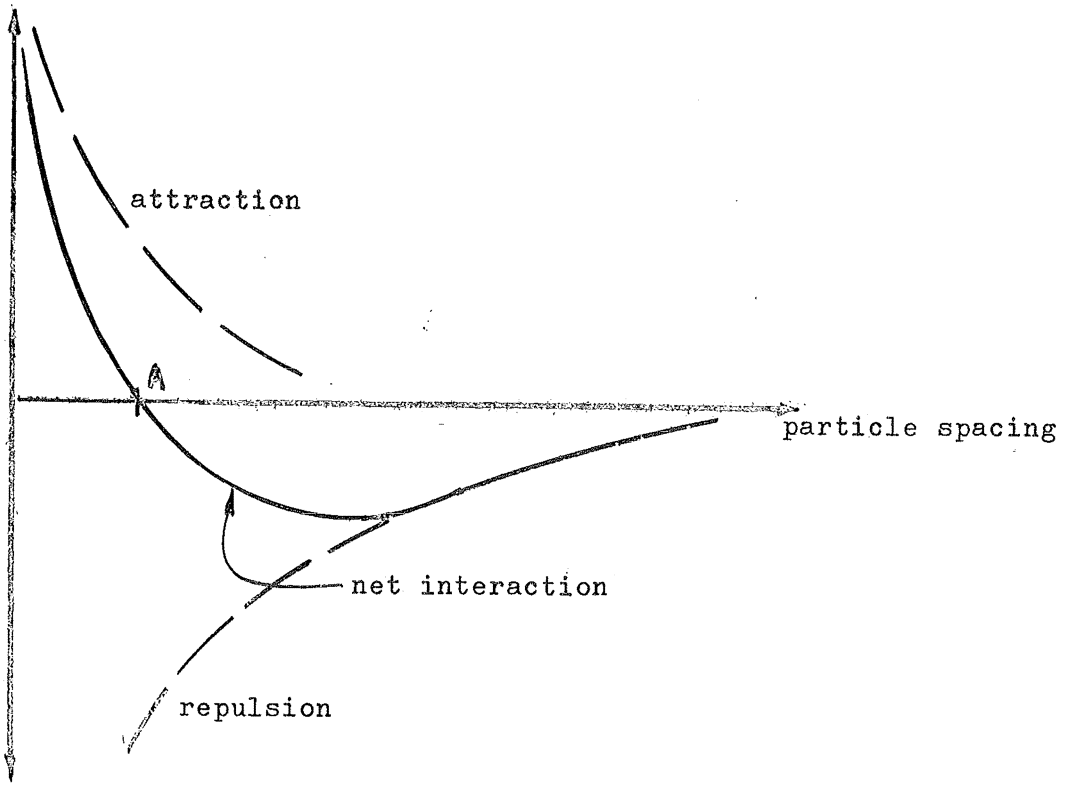

FIG.2.6 INTERACTION BETWEEN A PAIR OF CLAY PARTICLES

and the attraction will bond the particles when the force is removed. For a mass of clay particles subjected to a consolidation pressure which is later removed, i.e. becomes overconsolidated, various pairs of particles and groups of particles are bonded together and are capable of providing some resistance to shearing stress.

When a cohesive soil is unloaded after the formation of these bonds there is a decrease in the stress at the bond although it is not broken as happens with cohesionless materials. If the

stress is later increased the contact stress at the bonds will increase. It is suggested here that during unloading or reloading no new interparticle contacts are formed until the previous maximum value of the applied stress is reached. In other words this suggestion implies that in an overconsolidated cohesive soil the number of interparticle contacts is constant at stresses below the preconsolidation pressure and that changes in the applied stresses are accommodated by changes in the contact stress. Thus the interpretation suggested here of the behaviour at interparticle contacts in a cohesive soil is not the same as that of Scott[76] and Schmid[73]. It is the opinion of the writer that the constant contact stress situation is probably valid for cohesionless materials. It has already been suggested that on unloading contacts between cohesionless particles are broken but for a cohesive material the behaviour is complicated by the presence of the attractive forces. At the interparticle contacts there are forces originating from the attraction and also forces required to equilibrate the externally applied stresses. When these externally applied stresses are removed or reduced a decrease in the stress at the contacts would seem likely. Such a decrease in stress would be unlikely to lead to the breaking of interparticle contacts because the formation of the attractive bonds is not reversible by simply removing the applied stresses that lead to their formation. Hence it is suggested that the maximum stress occurs at a given contact during the formation of a bond. At that stage both the

force due to the attractive bond and due to the applied stress must be equilibrated. On removal of the external stress the contact stress decreases and on reapplication of the external stress the contact stress increases. While the applied stress is equal to or less than the previous maximum no new interparticle contacts would be formed. This idea is now used in discussing the two distinct friction angles associated with cohesive soils, that for the normally consolidated state and that for the overconsolidated state.

Hvorslev's true angle of friction is valid only for overconsolidated materials and is determined from a series of overconsolidated samples all at the same void ratio but under different stress conditions. Using the suggestion made earlier this requires that the number of interparticle contacts in each sample is the same. Possibly then Hvorslev's so called true angle of internal friction reflects the increase in shearing resistance when the average load at a constant number of interparticle contacts is increased. On the other hand the friction angle for normally consolidated clay, such as that illustrated in Fig.2.5, probably combines two effects, that due to the resistance provided by existing contacts and that due to the formation of new contacts. The combination of these two

effects would lead to the higher measured friction angle for normally consolidated materials.

Finally the phenomenon of cohesion is now discussed. As mentioned above cohesion is only observed for overconsolidated clays. It is manifested by a soil having some resistance to shearing stress even when the isotropic component of the stress tensor is zero. To be consistent with the fundamental hypothesis this requires that when clay soils are allowed to swell back to zero consolidation pressure there must be some normal force effective at the interparticle contacts built into the material. Such resistance could be provided by the bonds that exist in overconsolidated material.

Consequently there are two mechanisms that provide shearing resistance in an overconsolidated cohesive soil. Firstly the balancing of the isotropic component of the stress system at the particle contacts gives rise to a certain amount of resistance. The mobilisation of this resistance is responsible for the friction angle discussed above. To balance the applied stresses requires that at the component of the force transferred at the contacts is one of repulsion. On the other hand there are the contacts between clay particles and groups of clay particles discussed above which are formed during the consolidation process and across which there is a net force of attraction. The observed shear resistance is the summation of these two effects. The first is directly

related to the applied stress system and the result of inter-particle friction. The other component is more or less independent of the applied stress system because the attractive forces have been built into the sample by the previous consolidation history. Although these forces will provide some shear resistance they will not be greatly influenced by the isotropic component of the stress system as long as the previous maximum consolidation pressure is not exceeded. That is provided no new contacts are formed by the process considered above. This explanation of cohesion implies that physically there is no difference between friction and cohesion, and that both are explained in terms of inter-particle friction. The difference at the phenomenological level is one of ignorance: the cohesive component of strength is caused by attractive forces whose magnitude is unknown but which can be inferred in some cases if Hvorslev's true angle of internal friction is known.

This proposition also implies that if the interpretation of Hvorslev's true angle of friction given on page 64 is correct, that is if it does reflect the coefficient of friction at a constant number of interparticle contacts, then some restriction must be placed on the method of determination shown in Fig.2.5. Samples at various void ratios are prepared by subjecting the soil to cycles of loading and unloading. By this means it is possible to prepare samples at constant void ratio and yet with

different values of the isotropic component of the stress tensor. It would seem that the situation in which the number of inter-particle attractive bonds is constant can only be achieved when the maximum past consolidation pressure is the same for all the samples. Any increase in the consolidation pressure above the previous maximum will result in the formation of new attractive bonds between particles and hence lead to different values of the cohesive component of strength. Similarly this would explain why Hvorslev's true cohesion is a function of void ratio, increasing as the void ratio decreases. Lower void ratios require larger consolidation pressures so that there will be a greater number of particles aggregated by the forces of attraction. On shearing the cohesion will be greater because a larger number of these bonds are able to contribute to the shearing resistance.

On the basis of this approach to cohesion in terms of interparticle friction it is possible to suggest that the cohesive component of strength can be accounted for by adding an extra term to the isotropic component of the stress tensor. This idea has been suggested by Badillo[3], Schmid[73], Trollope[89] and others. The magnitude of the stress component could be determined by projecting the failure envelope and taking the intercept on the pressure axis. However there are two possible disadvantages associated with such an idea. In the first place the cohesion is not constant but is a function of

strain as shown in Fig.2.3. This change is no doubt associated with the gradual shearing and rupture of some of the attractive bonds. Secondly the addition of a small component of pressure could be objected to on the grounds that the actual types of stress responsible for cohesive resistance and frictional resistance are rather different in nature and cannot simply be added. As explained earlier the interparticle action necessary to equilibrate the applied stress system must be one of repulsion while that between clay particles pushed very close together is one of attraction. Even though these attractive forces do not contribute to equilibrating the externally applied hydrostatic pressure they are capable of providing shear resistance because friction can be mobilised under forces of repulsion and attraction.

One further aspect of the phenomenon of cohesion that needs clarification is related to the lack of cohesion in normally consolidated clays. The above discussion of the process by which the aggregation of clay particles takes place leads one to expect that these bonds are formed during the consolidation process and consequently must exist in normally consolidated soil. The following explanation is based on the suggestion made on page 65 that the difference between the friction angle of a normally consolidated clay and an overconsolidated clay is due to the contribution of the attractive bonds.

Consider a very wet slurry of clay at a moisture content

well above the liquid limit. For the clay to remain in such a state the applied stresses must be negligible and the strength is effectively zero. This means that at such low stress levels the number of interparticle contacts is insignificant and thus there will be effectively no interparticle attractive bonds. This means that when the applied stresses are virtually zero the clay can mobilise no strength either from friction or cohesion because there are effectively no interparticle contacts.

Now as the applied stresses are increased the void ratio of the slurry decreases and the strength increases. As the applied stresses are increased more and more interparticle contacts are required to equilibrate the applied stress. It is well known that for consolidation from a slurry a linear relation is found between the void ratio and the logarithm of the applied stress. The fact that Hvorslev's true cohesion is an exponential function of void ratio means that there is also a linear relation between the logarithm of c_e and the void ratio. This in turn implies that there must be a linear relation between the applied stress and c_e. Thus at any void ratio the component of strength due to the shearing of interparticle bonds for a normally consolidated clay is linearly related to the applied stress as is the component due to interparticle friction. This can be expressed as:

$$(\tau_{nc})_e = C + F$$

where $(\tau_{nc})_e$ is the strength of a normally consolidated clay at

void ratio e, C is the strength component derived from the shearing of interparticle attractive bonds and F is the component due to interparticle friction. Because of the linear relations mentioned above the expression for $(\tau_{nc})_e$ can be expressed as:

$$(\tau_{nc})_e = (\tan\beta_c + \tan\phi_e)\, p_{nc}$$

where p_{nc} is the applied stress required to produce normally consolidated clay at a void ratio e, ϕ_e is Hvorslev's true angle of internal friction and β_c is the angle defined by the linear relation between the applied stress and Hvorslev's true cohesion. Thus it is seen that the friction angle for a normally consolidated clay is the sum of the above angles and also that when p_{nc} is zero there can be no strength derived from cohesion or friction and thus the failure envelope for a normally consolidated clay passes through the origin as demonstrated in Fig.2.4.

A final comment required to complete section is related to the mechanism by which clay particles become aggregated. So far only one mechanism has been considered - the predominance of the Van der Waals-London force of attraction at small particle spacings. However, it is probable that there exist many other natural processes that lead to the bonding of particles. None of these is discussed here because it is thought that regardless of the actual mechanism of bonding the mechanics of cohesion will be similar.

These tentative ideas about effective stress, internal friction and cohesion are discussed further and applied to the

behaviour of the particular soil examined in this thesis in chapter 5.

CHAPTER THREE

SOIL AS A PLASTIC MATERIAL

3.1 INTRODUCTION

In this chapter the possibility of using one branch of continuum mechanics, the theory of plasticity, to predict the stress-strain behaviour of soils is discussed. Thus the viewpoint is different from that of Chapter 2 where the soil was regarded as an assemblage of individual particles. Now the soil is regarded as a continuum although the conclusions derived from Chapter 2 are still presumed to apply.

The object of any complete theory about the mechanical behaviour of a material is to describe completely the state of stress and strain at all points of the material. The solution of such problems, subject to certain specified boundary conditions, is the task of continuum mechanics and the general method is to set up such appropriate differential equations as are required to describe the problem in hand and solve the equations for the unknown quantities.

Certain features of this process are common to all continua. Firstly the same basic equilibrium equations must be satisfied for any material, regardless of its properties. Secondly some condition is required on the allowable deformations, e.g. the compatibility equations used in the theory of elasticity or the continuity equation used in fluid mechanics.

Thirdly a constitutive relation, describing the properties of the material under consideration, is needed. This usually has the form of a relation between stress and strain or increments of stress and strain.

Only the third of these common features is considered in this thesis, in that all the work is directed towards clarifying the type of relation needed to describe the stress-strain behaviour of a compacted soil. There is no discussion of methods needed to solve the boundary value problems mentioned above.

Evidently calculations based on the assumption that soil is a linearly elastic solid are used commonly to predict stresses and strains occurring in a loaded soil. This assumption may be justified in some (but by no means all) soil mechanics situations and one suspects that the widespread use of the theory of elasticity is more a matter of convenience rather than realistic representation of soil properties.

Experimental investigations show that many soils are susceptible to time dependent shear and (after the completion of primary consolidation) volumetric deformation, and this has suggested the use of viscoelastic models to predict soil behaviour. In this case the additional variable, time, introduces one further element of complexity and solutions become more difficult to obtain. Two further problems associated with the use of these models are firstly that the more complex models do not give a unique representation of the contribution

of the various components, and secondly, that the models are essentially one-dimensional, so that the representation of two and three dimensional behaviour is rather difficult.

Another different approach is to treat the soil as a plastic material, and to develop incremental stress-strain relations. This is the method used in the remainder of this thesis. In common with the hypothesis that soil is an elastic material, or that it can be represented by a simple rheological model, there are certain disadvantages in regarding a soil as a plastic material. Perhaps the most significant of these is that the theory of plasticity makes no allowance for time effects, so that time-dependent shear and volumetric deformation have to be neglected. Of course, there is no difficulty in accounting for the most significant time effect in soil mechanics - primary consolidation. This is because primary consolidation can be regarded simply as a time dependent increase in effective stress which leads to a corresponding change of volume. However, creep and secondary consolidation are apparently associated with constant effective stress and can not be allowed for. At this stage the introduction of a distinction pointed out to the writer by Elms* is worthwhile. The equations of continuum mechanics apply at a point within a material. Now in the theory of plasticity it is assumed that the material has no time dependent properties. This requires that when the state of stress is

---

* Private communication.

altered at a point there is an immediate response in the state of strain at that point. In dealing with a finite body of material the observed response is the summation of the response at a large number of distinct points within the body. Soil is a multiphase material so there is the additional complication of the coupling between the phases. When an arbitrary stress increment is applied to a body of soil there is usually some pore water pressure generated. As has been explained in Chapter 2 such pore pressures will equilibrate some of the applied stress increment. If drainage is allowed there will be a time dependent deformation of the material as the pore water pressure dissipates. The time required for this process depends on the permeability of the material and the size of the body of soil, but not on the equations governing behaviour at a point within the material. Thus time dependent consolidation of soils is not an inherent property of the material itself, it is merely a consequence of the limited permeability of the material and the physical dimensions of the body of soil. On the other hand creep and secondary consolidation are inherent time dependent properties and so these must be accounted for in the equations that describe the behaviour at a point within the material.

The inability of the plastic theory to account for creep deformation is not too great a disadvantage for the particular soil investigated in the compacted state in this work,

as the tendency of this material to creep is not very significant. It is the contention of the writer that the theory of plasticity gives the most satisfactory interpretation of the behaviour of the soil investigated here. Although the plastic approach gives, at best, only an approximation to the very complex behaviour exhibited by the material, it can predict stress-strain behaviour that is much more realistic than the elastic idealisation, and yet in a way that is a good deal simpler than a realistic rheological model.

3.2 APPLICATION OF THE THEORY OF PLASTICITY TO SOIL MECHANICS

The first serious attempt to examine the stress-strain behaviour of soils in the light of the theory of plasticity seems to have been made by Drucker, Gibson and Henkel[19], whose conclusions were reasonably encouraging. The approach has also been applied to normally consolidated clays by Roscoe, Schofield and Thurairajah[65] with some success, and further extended and refined by Roscoe and Burland[67]. Thus it is not unreasonable to expect that a similar approach might be valid for a compacted soil, which has properties similar to those of an overconsolidated clay. This possibility is examined in Chapter 5, while the remainder of this chapter is divided into two distinct parts. Firstly the concepts of the theory of plasticity are presented and the way in which they must be modified to account for soil behaviour is indicated and then

the work of the Cambridge research group is briefly reviewed and its relation to the theory of plasticity examined.

As explained in Chapter 2 it is convenient to refer to the state of stress in a continuous material by means of the stress tensor, σ_{ij}. The beauty of this shorthand notation by which all nine stress components can be represented with a single term is that it provides an elegant means of writing otherwise clumsy equations. The way in which the components of a tensor are affected by changing the axes of reference is important. It can be shown that certain quantities always remain the same regardless of the orientation of the axes; these quantities are called invariants and are extensively used in the theory of plasticity. The first invariant of the stress tensor is defined as:

$$I_1 = \sigma_{ii} = (\sigma_{11} + \sigma_{22} + \sigma_{33}) \quad \ldots\ldots\ldots\ldots\ldots\ldots\ldots\ldots \quad (3.1)$$

Where σ_{11} etc. are the principal values of the stress tensor. Equation (3.1) shows that the first invariant of the stress tensor is three times the hydrostatic pressure (or isotropic component defined in Eq.(2.9). Because it is convenient to distinguish between effects caused by the isotropic or hydrostatic component of the stress tensor and those caused by the remaining part the so-called deviatoric stress tensor, introduced in Eq.(2.10), is used. It can be defined by

$$s_{ij} = \sigma_{ij} - \frac{1}{3} I_1 \delta_{ij} \quad \ldots\ldots\ldots\ldots\ldots\ldots\ldots\ldots\ldots\ldots\ldots\ldots \quad (3.2)$$

where $\delta_{ij} = 1$ when $i = j$ and $\delta_{ij} = 0$ when $i \neq j$. The first invariant of the deviatoric stress tensor is zero but the second and third invariants are important in the theory of plasticity and are given by:

$$J_2 = \tfrac{1}{2}s_{ij}s_{ji} = \frac{1}{6}\left[(\sigma_{11}-\sigma_{22})^2 + (\sigma_{22}-\sigma_{33})^2 + (\sigma_{33}-\sigma_{11})^2\right] .$$

and ..... (3.3)

$$J_3 = \tfrac{1}{3}s_{ij}s_{jk}s_{ki} = \sigma_{11}\sigma_{22}\sigma_{33} + \tfrac{1}{3}J_2I_1 - \frac{1}{27}I_1^3$$

Any function of the invariants is, of course, itself invariant.

Similar definitions apply to the strain tensor, ϵ_{ij}. Also in the theory of plasticity the strain tensor is supposed to consist of two independent parts, an elastic and a plastic component, so that:

$$\epsilon_{ij} = \epsilon^e{}_{ij} + \epsilon^p{}_{ij} \quad \ldots\ldots\ldots\ldots\ldots\ldots\ldots\ldots\ldots\ldots\ldots\ldots \quad (3.4)$$

where $\epsilon^e{}_{ij}$ and $\epsilon^p{}_{ij}$ are the tensors of elastic and plastic strain respectively. The notation $\dot{\epsilon}_{ij}$ and $\dot{\sigma}_{ij}$ is commonly used in the theory of plasticity to denote the strain and stress increment tensors. However in this thesis the notation $d\epsilon_{ij}$ and $d\sigma_{ij}$ will be used as it is more convenient.

The most important concept used in the theory is that in the stress space* a yield surface exists which gives the boundary

---

* The stress space is defined by a three dimensional Cartesian coordinate system the axes of which give the directions of the principal stresses.

between those states of stress in which the deformation of the material is entirely elastic and those in which elastic and plastic deformation is involved. In the principal stress space, this surface encloses the origin. All stress points inside this surface give elastic, and only elastic, strains while those on the surface give elastic and plastic strains. The stress point can lie anywhere on or within the current yield surface but not outside it.

When the stress point is on the yield surface a further distinction is introduced. For a material that is perfectly plastic there can be no further increase in stress when the yield surface is reached. So while the stress point is on the yield surface, plastic deformation results. However for a work-hardening material there are three possibilities when the stress point is on the yield surface. Firstly a stress increment can be directed inside the yield surface and the stress point moves away from the surface. This is known as unloading and some elastic strain will be measured. Secondly, from a stress increment directed outwards from the surface plastic deformation occurs and the material work-hardens. This work-hardening changes the yield surface and, in general, a change in its position, shape and size can occur. However the new yield surface, known as a subsequent yield surface, must be such that the new stress point lies on it. Thirdly it is possible for the stress increment to be tangential to the yield surface.

In this case no work-hardening occurs so there can be no plastic deformation for a work-hardening material under this type of loading, called neutral loading. These three cases are shown in Fig.3.1.

It is usual to assume that for isothermal deformation the equation describing the initial and current yield surface is a function of current stress, current plastic strain and a parameter describing the amount of work-hardening. This function is referred to as the loading function and is given by Naghdi[51] as:

$$f(\sigma_{ij}, \epsilon^{p}_{ij}, \alpha) = 0 \quad \ldots\ldots\ldots\ldots\ldots\ldots\ldots\ldots\ldots\ldots\ldots\ldots \quad (3.5)$$

where α is a work-hardening parameter. During work-hardening the incremental change in f is:

$$df = \frac{\partial f}{\partial \sigma_{ij}} d\sigma_{ij} + \frac{\partial f}{\partial \epsilon^{p}_{ij}} d\epsilon^{p}_{ij} + \frac{\partial f}{\partial \alpha} d\alpha \quad \ldots\ldots\ldots\ldots\ldots\ldots \quad (3.6)$$

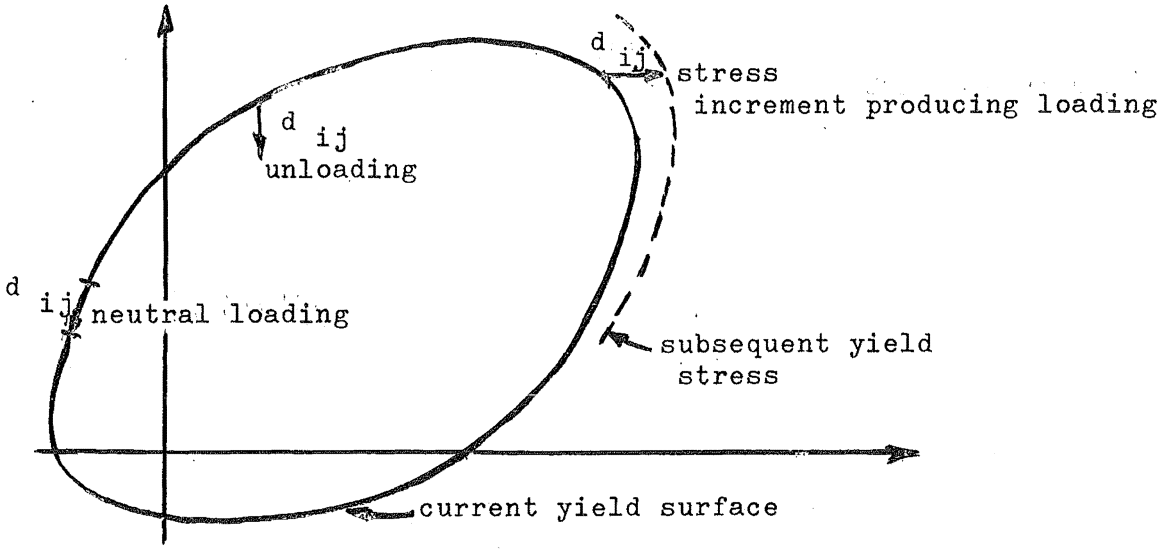

FIG.3.1 TWO DIMENSIONAL SECTION OF YIELD SURFACE SHOWING TYPES OF LOADING

When the stress point is on the yield surface, f = 0, the three types of loading can be described by the following criteria:

$$\text{UNLOADING} \qquad \frac{\partial f}{\partial \sigma_{ij}} d\sigma_{ij} < 0 \ , \quad f = 0, \ df = 0$$

$$\text{NEUTRAL LOADING} \qquad \frac{\partial f}{\partial \sigma_{ij}} d\sigma_{ij} = 0, \quad f = 0, \ df = 0 \qquad \ldots\ldots\ldots\ldots \quad (3.7)$$

$$\text{LOADING} \qquad \frac{\partial f}{\partial \sigma_{ij}} d\sigma_{ij} > 0, \quad f = 0, \ df > 0$$

It is usual to take a work-hardening parameter of the following form:

$$\alpha = \int \sigma_{ij} \, d\epsilon^{p}_{ij} \qquad \ldots\ldots\ldots\ldots\ldots\ldots\ldots\ldots \quad (3.8)$$

The work-hardening discussed up to this point is of a very general nature; however there seems to be some justification, as explained below, for assuming that the work-hardening of soil is of a much simpler kind. It is assumed that the work-hardening of soil is isotropic, i.e. for an increment of plastic deformation the whole yield surface expands uniformly. The series of triaxial compression and extension tests performed by Henkel[27] on normally consolidated and overconsolidated clay seems to justify this, particularly if one agrees with the explanation, given by Ladanyi[38], of the discrepancies between compression and extension tests. This assumption of isotropy represents the first of two major departures from the conventional theory of plasticity as it was developed to account for the properties of metals. It is well known that many metals work-harden anisotropically and exhibit the Bauschinger effect which complicates the theoretical treatment of the deforma-

tion of metals.

Another commonly used term in the theory is plastic potential. This is similar to the velocity potential used to describe irrotational flow in fluid mechanics. It is a scalar function, the derivitives of which give the direction of the components of the plastic strain increment tensor. It is usually denoted by $g(\sigma_{ij}, \epsilon^p{}_{ij}, \alpha)$. Since the gradient of a scalar function is a vector whose direction is that of the outward normal to the function, one can conclude that the existence of a plastic potential requires that the plastic strain increment vector be normal to the plastic potential function.

Using the loading criterion, Eq.(3.7), it is now possible to postulate a general constitutive relation for a work hardening plastic material after Hill[29]:

$$d\epsilon^p{}_{ij} = h \frac{\partial g}{\partial \sigma_{ij}} \frac{\partial f}{\partial \sigma_{kl}} d\sigma_{kl} \quad \ldots\ldots\ldots\ldots\ldots\ldots\ldots\ldots\ldots\ldots (3.9)$$

where g is the plastic potential function,

f is the function describing the current yield surface

and $h(\sigma_{ij}, \epsilon^p{}_{ij}, \alpha)$ is a scalar function.

In the terminology of the theory of plasticity a relation like this between increments of plastic strain, the loading function, and the plastic potential function is known as a flow law. Apart from assuming that the functions f and g exist and that they are not functions of increments of stress and plastic strain, Eq.(3.9)

is based on the assumption that the principal axes of the strain increment tensor coincide with the principal axes of the stress tensor. The generality of Eq.(3.9) obviously rules out any description of plastic behaviour simple enough to have practical appeal, so that it is necessary to look for realistic simplifications. Two lines of attack are possible. One could proceed on a rational basis and from known properties of the plastic deformation impose restrictive conditions; alternatively, quite arbitrary simplifications can be made and their validity checked by experiment. The usual approach falls somewhere between these two.

As an example, it is known that the isotropic component of the stress tensor has no effect on the yielding and plastic deformation of metals and that there is no plastic volumetric strain. From this experimentally observed fact the so called condition of incompressibility is applied, i.e. $d\epsilon^p_{ii} = 0$. However it is equally well known that the behaviour of soils is very dependent on the isotropic component of stress so that the incompressibility condition cannot be used in soil mechanics. This is the second major difference between a theory of plasticity valid for soils and one suitable to describe the behaviour of a metal. When dealing with the plastic deformation of metals it is not uncommon to simplify Eq.(3.5) by assuming that the work hardening can be accounted for in the loading function by a simple scalar parameter and the stresses included as functions

of the invariants of the stress tensor. Because of the condition of incompressibility it is appropriate to use the invariants of the deviatoric stress tensor, the first invariant of which is zero. Thus Eq.(3.5) is simplified to:

$$f(J_2,J_3) = C \quad \ldots\ldots\ldots\ldots\ldots\ldots\ldots\ldots\ldots\ldots\ldots\ldots \quad (3.5a)$$

where C is a function of the work hardening parameter α defined in Eq.(3.8). Now in a soil in which the plastic volume change is not, in general, zero a slightly different form is needed in which the first invariant of the stress tensor appears:

$$f(I_1,J_2,J_3) = C \quad \ldots\ldots\ldots\ldots\ldots\ldots\ldots\ldots\ldots\ldots\ldots\ldots \quad (3.5b)$$

where I_1 is the first invariant of the stress tensor defined in Eq.(3.1) and J_2 and J_3 are the second and third invariants of the deviatoric stress tensor defined in Eq.(3.3).

A further assumption or restriction on Eq.(3.9) is related to the direction of the plastic strain increment vector. Regardless of one's position it is most convenient to assume that the plastic strain increment vector is normal to the current yield surface. However one's reason for wanting to make this assumption will be very dependent on viewpoint. For example a mathematician will want to solve boundary value problems associated with the plastic behaviour of a given material and normality of the strain increment vector leads to very useful conclusions about the uniqueness of the solutions. The emphasis in this thesis is on

the physical behaviour of soils, so that it would be very satisfying if the assumption of normality could be justified on physical grounds. To this end the approach of Drucker[20,23] is most attractive.

Drucker starts by making a simple postulate about the material behaviour, a postulate whose validity is easily checked when inspecting the results of actual tests. The postulate is based on consideration of a body under an existing state of stress σ_{ij}, to which some external agency applies a small increment of stress $d\sigma_{ij}$. Drucker postulates that a stable material is such that:

> "The work done by the external agency on the change in displacements it produces must be positive or zero."
>
> i.e.

$$d\sigma_{ij}\, d\epsilon_{ij} \geq 0 \qquad \ldots\ldots\ldots\ldots\ldots\ldots\ldots\ldots\ldots\ldots\ldots\ldots \quad (3.10)$$

where the strain increment is produced by $d\sigma_{ij}$. The interpretation of this postulate in the case of a one dimensional test is given in Fig.3.2.

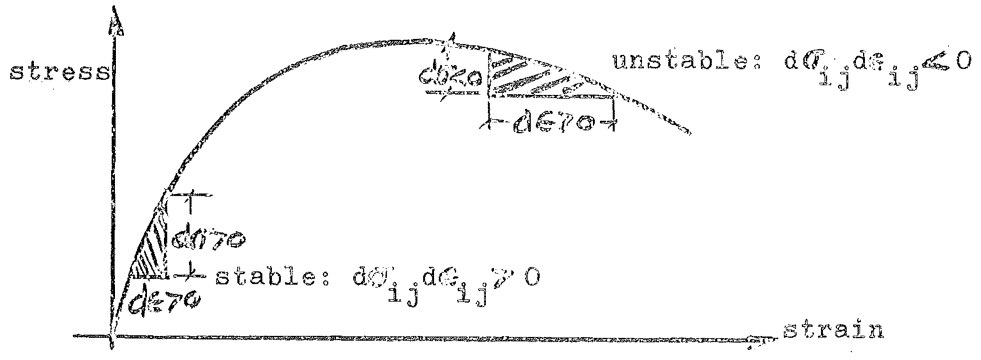

FIG.3.2 ILLUSTRATION OF DRUCKER'S STABILITY POSTULATE FOR A SIMPLE ONE DIMENSIONAL TEST

In a simple test like this the material is stable while the stress-strain curve is rising but when the curve is falling the material violates the stability postulate because an increase in strain leads to a decrease in stress so that $d\sigma_{ij}\, d\epsilon_{ij} < 0$. In the stress space instability is manifested by a shrinking of the yield surface. During the application of an outward directed stress increment the yield surface contracts at the stress point rather than expands as required for work-hardening.

On the basis of the satisfaction of this postulate Drucker was able to derive the following two most significant conclusions:

(i) In the stress-space the yield surface must be convex.

(ii) The plastic strain increment vector must be in the direction of the outward normal to the yield curve at the stress point.

It was pointed out in the introduction to this chapter that the laws of mechanics must hold for all continua. So that in addition to the equilibrium equations mentioned the laws of thermodynamics must be satisfied. Drucker emphasises that his postulate is not a statement of any law of thermodynamics, rather it is applied to the material in addition to the laws of mechanics and thermodynamics. In other words the postulate can be regarded as a definition of a stable plastic material. The work done by the external agency is only part of the total work, W, done by the application of $d\sigma_{ij}$, which is:

$$W = \sigma_{ij}\, d\epsilon_{ij} + d\sigma_{ij}\, d\epsilon_{ij} \qquad \ldots\ldots\ldots\ldots\ldots\ldots\ldots\ldots\ldots\ldots \quad (3.11)$$

It is this total work that must be zero or positive by the second law of thermodynamics. It is clearly positive even when $d\sigma_{ij}\, d\epsilon_{ij} < 0$. Drucker also emphasises that fulfilment of the postulate means that the only type of flow law possible is one with the plastic strain increment vector normal to the yield surface. Application of any other type of flow law is invalid.

When the stability postulate can be applied to a material a considerable simplification of Eq.(3.9) is possible. The normality of the plastic strain increment to the yield surface implies that the loading function and the plastic potential function are identical - this was shown to be the case by Bland[8]. Eq.(3.9) can now be written:

$$d\epsilon^{p}_{ij} = h\frac{\partial f}{\partial \sigma_{ij}}\frac{\partial f}{\partial \sigma_{kl}}\, d\sigma_{kl} \qquad \ldots\ldots\ldots\ldots\ldots\ldots\ldots\ldots\ldots\ldots \quad (3.12)$$

In this form the stress-strain relation is known as an associated flow law.

Drucker was able to extend the implications of his postulate even further. In ref.20 he showed that the function h in Eq.(3.12) could depend on σ_{ij}, ϵ^{p}_{ij} and the history of loading but must be independent of $d\sigma_{ij}$. This brings out an important property of the constitutive relation, Equation (3.12), that has been emphasised by Burland[11]. Equation (3.12) may be rewritten as:

$$d\epsilon^{p}_{ij} = h\frac{\partial f}{\partial \sigma_{ij}}\, df \qquad \ldots\ldots\ldots\ldots\ldots\ldots\ldots\ldots\ldots\ldots \quad (3.12a)$$

where df is the incremental change in the loading function during

work-hardening. The terms h and df are scalar quantities but the components of the plastic strain increment tensor and the components of $\partial f/\partial \sigma_{ij}$ are vectors. And so it is evident that the direction of the components of the plastic strain increment given by Eq.(3.12) depends only on the gradient, $\partial f/\partial \sigma_{ij}$. Thus at any point on the yield surface the direction of the components of the plastic strain increment tensor is a function of the yield surface at that point and is quite independent of the direction of the stress increment. This is the major difference between a constitutive relation for a plastic material and one for an elastic material. There is always a relation between the direction of the applied stress increment and the corresponding strain increment for an elastic material. The only significance that the stress increment has in Eq.(3.12) is in determining the magnitude of df and hence the magnitude of the plastic strain increment. Thus although Eq.(3.12) can be written as a linear relation between increments of stress and increments of strain it is a very different type of linear relation from that for an elastic material. This linear version of Eq.(3.12) has the following form:

$$d\epsilon^{p}_{ij} = A_{ijkl}\, d\sigma_{kl} \qquad \ldots\ldots\ldots\ldots\ldots\ldots\ldots\ldots\ldots\ldots\ldots\ldots\ldots\ldots \quad (3.13)$$

where A_{ijkl} is a fourth order tensor, depending on the properties of the material. It is not a physical constant and must be evaluated at each stage of the loading. However for much work the following form of the associated flow law is used:

$$d\epsilon^{p}_{ij} = d\lambda \frac{\partial f}{\partial \sigma_{ij}} \qquad (3.14)$$

where $d\lambda$ is a positive scalar multiplier that varies during loading.

An assumption underlying Eqs.(3.12), (3.13) and(3.14) that is required when proving that Drucker's stability relation leads to the normality of the plastic strain increment vectors is that the principal axes of the stress tensor and of the plastic strain increment tensor coincide. Apparently this was first introduced to the theory by St.Venant. Examination of the behaviour of metals undergoing plastic deformation justifies this assumption, but for soils it would seem necessary to reconsider the matter. This can be done with the aid of Eq.(3.13) and some knowledge of the conditions to which the sample under test is subject.

The first step is to derive a relationship between the various components of the tensor A_{ijkl} so that the principal axes of the stress-increment tensor coincide with the principal axes of the plastic strain-increment tensor. The approach used here is similar to that suggested by Sokolnikoff[82] in connection with a similar problem in the theory of elasticity. Assume that the principal axes of the stress-increment tensor are known. Then the principal axes of the stress-increment and plastic strain-increment tensors will coincide if it can be shown that all the components of the plastic strain-increment tensor, $d\epsilon^{p}_{ij}$, for which $i \neq j$, are zero in the three orthogonal planes defined by the principal directions of the stress increment tensor.

Because of the symmetry of the stress and plastic strain-increment tensors the following relation holds:

$$A_{ijkl} = A_{ijlk} \text{ and } A_{ijkl} = A_{jikl} \quad \ldots\ldots\ldots\ldots (3.15)$$

This reduces the number of independent components of A_{ijkl} from 81 to 36. In the principal planes of the stress-increment space those components of $d\sigma_{ij}$ for which $i \neq j$ are zero, so using this and Eq.(3.15) the expanded form of Eq.(3.13) is:

$$d\epsilon^p_{11} = A_{1111}d\sigma_{11} + A_{1122}d\sigma_{22} + A_{1133}d\sigma_{33}$$

$$d\epsilon^p_{22} = A_{2211}d\sigma_{11} + A_{2222}d\sigma_{22} + A_{2233}d\sigma_{33}$$

$$d\epsilon^p_{33} = A_{3311}d\sigma_{11} + A_{3322}d\sigma_{22} + A_{3333}d\sigma_{33}$$

$$d\epsilon^p_{13} = A_{1311}d\sigma_{11} + A_{1322}d\sigma_{22} + A_{1333}d\sigma_{33}$$

$$d\epsilon^p_{32} = A_{3211}d\sigma_{11} + A_{3222}d\sigma_{22} + A_{3233}d\sigma_{33}$$

$$d\epsilon^p_{21} = A_{2111}d\sigma_{11} + A_{2122}d\sigma_{22} + A_{2133}d\sigma_{33}$$

Actually this expansion presumes that the principal directions of A_{ijkl} coincide with those of $d\sigma_{ij}$. This is not severe as normally one would have sufficient knowledge about a material to nominate the principal directions of its properties. The last three equations in the above expansion must all be equal to zero if the principal directions of $d\sigma_{ij}$ and $d\epsilon^p_{ij}$ are the same. Since the stress components are not zero this occurs when the

value of the following determinant is zero; i.e.:-

$$\begin{vmatrix} A_{1311} & A_{1322} & A_{1333} \\ A_{3211} & A_{3222} & A_{3233} \\ A_{2111} & A_{2122} & A_{2133} \end{vmatrix} = 0 \quad \ldots\ldots\ldots\ldots\ldots\ldots\ldots\ldots \quad (3.16)$$

This is true for isotropic materials and for materials with most of the common types of anisotropy. Its application to the particular soil considered in this thesis will be discussed in Chapter 6.

Now Eq.(3.16) gives a requirement for the coincidence of the principal axes of the stress-increment and plastic strain-increment tensors. However St. Venant's hypothesis was concerned not with the stress increment tensor, $d\sigma_{ij}$, but with the stress tensor, σ_{ij}. So that the relationship between the principal directions of the stress-increment tensor and those of the stress tensor is now required. This can be obtained by examining the nature of the test to which the sample is subjected. In the case of the triaxial test, the only test used in this project, the principal directions are fixed and do not vary during the test. Thus in triaxially tested specimens the principal directions of the stress-increment tensor coincide with the principal directions of the stress tensor.

Therefore one can conclude that for a sample tested in the triaxial apparatus, provided the sample is mounted so that the

principal directions of the soil properties are oriented in the principal directions of the applied stress system and if Eq.(3.16) is satisfied, then the principal axes of the stress tensor will coincide with the principal axes of the plastic strain-increment tensor.

A further question that must be considered is: Is it reasonable to expect Drucker's postulate to be fulfilled for a frictional material such as soil? Drucker[18], Brown[10] and Palmer[54] have all shown by means of simple models that a frictional material can violate the postulate. Furthermore it has been suggested by Drucker[21] that frictional and plastic deformation are fundamentally different. During frictional deformation sliding takes place between the two bodies, there being no displacement normal to the plane of sliding. But for plastic deformation, normality of the strain increment vector requires some displacement normal to the direction of sliding. These two cases are shown in Fig.3.3.

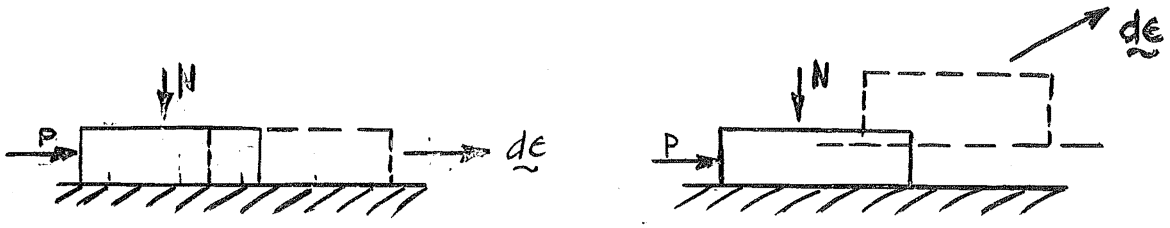

(a) Frictional (b) Plastic

FIG.3.3 PLASTIC AND FRICTIONAL DEFORMATION

The models proposed by these authors show that for a frictional material the stability postulate may not be fulfilled. However none of these models leads one to conclude immediately that because a soil is basically a frictional material the postulate does not apply. Soil is a very much more complex material than any of these simple models suggest and because of this additional complexity one can imagine ways in which the material can deform in a frictional manner and yet not violate the stability postulate. For example soil, although frictional, certainly does not deform in the manner of Fig.3.3a. This is because soils generally dilate during deformation.

Thus the suggestion, based on simple models, that frictional materials may not fulfil the stability postulate serves as a reasonable caution but any specific case can only be decided by examining the results of actual tests.

One further assumption that is implicit in all the discussion up to here is the homogeneity of the state of stress and strain throughout the sample. This is a necessary requirement for all the work reported in this thesis because the stresses and strains throughout the sample are calculated from the stresses applied to and the displacements observed at the boundaries of the sample. When a sample approaches failure by deforming uniformly throughout homogeneity can be assumed, but when failure is related to the formation of a slip plane or planes, inhomogeneity of deformation has developed and the strains calculated from boundary

displacements are no longer those that actually occur along the slip plane. However an interesting relation is found if the ratio of the components of deformation is considered for a sample deforming with a slip plane in a triaxial test.

For the sample deforming with a single inclined slip plane as shown in Fig.3.4 and assuming that all the volume change occurs in the slip plane then the full increment of volumetric strain is:-

$$dv_T = \frac{\Delta V \cos\theta}{\pi R^2 t}$$

where ΔV is the change in volume and the other factors are defined in Fig.3.4. The apparent volumetric strain is:

$$dv_A = \frac{\Delta V}{\pi R^2 H}$$

So that:

$$\frac{dv_T}{dv_A} = \frac{H}{t}\cos\theta$$

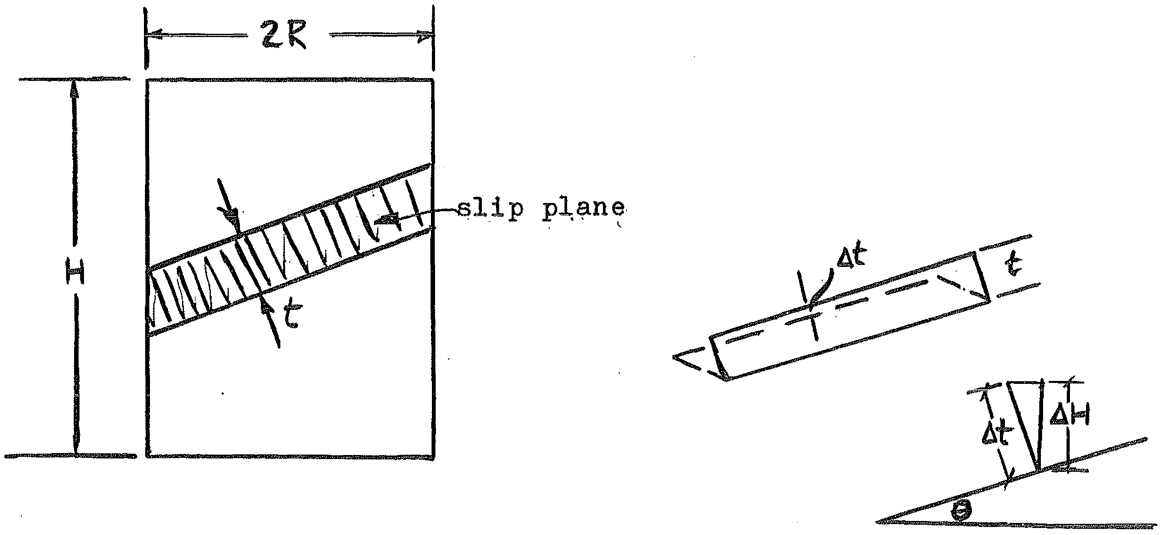

FIG. 3.4 SAMPLE WITH A SLIP PLANE

Using the definition of shear strain given in Eq.(3.24) the true shear deformation is:

$$d\epsilon_T = \frac{\Delta t}{t} - \frac{1}{3}\frac{\Delta V \cos\Theta}{\pi R^2 t}$$

$$= \frac{1}{t}\left\{\Delta t - \frac{1}{3}\frac{\Delta V \cos\Theta}{\pi R^2}\right\}$$

The apparent shear deformation is:

$$d\epsilon_A = \frac{\Delta H}{H} - \frac{1}{3}\frac{\Delta V}{\pi R^2 H}$$

$$= \frac{1}{H \cos\Theta}\left\{\Delta t - \frac{1}{3}\frac{\Delta V \cos\Theta}{\pi R^2}\right\}$$

So that

$$\frac{d\epsilon_T}{d\epsilon_A} = \frac{H}{t}\cos\Theta$$

Therefore:

$$\frac{d\epsilon_T}{dv_T} = \frac{d\epsilon_A}{dv_A} \quad \text{..... (3.17)}$$

Thus the ratio of the increments of true strain is equal to the ratio of the increments of apparent strain when a slip plane forms in a sample deforming in a triaxial test so that any relation depending on the ratio of strain components should not be influenced by inhomogeneous deformation. Because of the incremental form of the relation given in Eq.(3.17) it remains true even though the thickness and inclination of the slip plane may change as the material deforms. The relation also remains valid when a certain proportion of the total change in height occurs along the slip plane

and the remainder in the rest of the sample.

Finally in this section a possible generalisation of Eq.(3.14) is discussed. The equation describing the loading function, Eq.(3.5), is sufficiently general to include the possibility of the yield surface, although remaining convex, having corners and edges and so not being a surface of uniformly changing curvature. Such portions of the yield surface are called singular in distinction to other parts called regular. Koiter[36] suggested that in this case the yield surface could be specified by several distinct loading functions. At a state of stress within the closed space formed by all these surfaces only elastic deformation can occur and so all the loading functions must have negative values. For a state of stress in the yield surface at least one yield function vanishes and none of the remainder can be positive. Koiter's generalisation of Eq.(3.14) is written:-

$$d\epsilon^{p}_{ij} = \sum_{i=j}^{n} d\lambda(n)\frac{\partial f^{(n)}}{\partial \sigma_{ij}} \qquad \ldots\ldots\ldots\ldots\ldots\ldots\ldots\ldots\ldots\ldots (3.18)$$

where $f^{(n)}$ are the separate loading functions, and where the summation is taken over only those loading functions that vanish at the loading point, i.e. $f^{(n)}(\sigma_{ij}) = 0$. From Eq.(3.18) the plastic strain increment vector consists of several independent components, but each component is normal to its respective yield surface. This implies that at a corner or edge in the yield surface the plastic strain increment vector must lie somewhere between the normals to the adjacent parts of the yield surface.

This is illustrated in Fig.3.5:

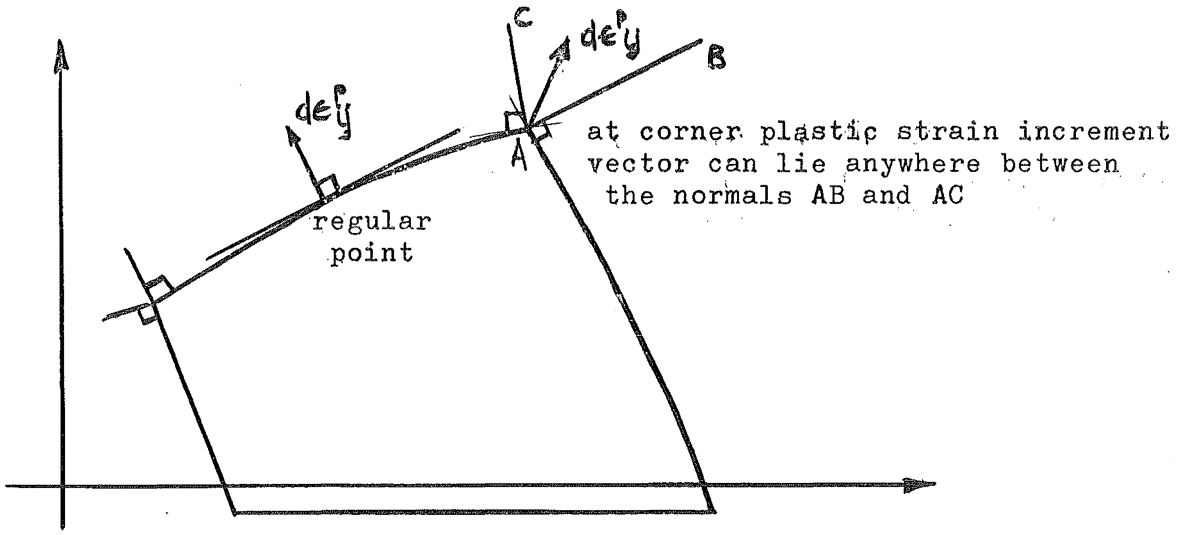

FIG.3.5 TWO DIMENSIONAL SECTION OF A YIELD SURFACE WITH CORNERS

The functioning of a yield surface with corners has been discussed in geometrical terms by Sanders[72].

Drucker's stability postulate requires that at a corner the plastic strain increment vector must lie somewhere between the normals to the adjacent parts of the yield surface. Therefore Koiter's generalisation, Eq.(3.18), is quite compatible with the concept of material stability.

Thus Drucker's simple postulate, the applicability of which can easily be checked by experiment, leads to three important conclusions; that the plastic strain increment is perpendicular to the yield surface, that the yield surface is convex, and that although the magnitude of the plastic strain increment is related to the magnitude of the stress increment its direction is entriely independent from the direction of the stress increment.

These conclusions greatly simplify the form of the plastic stress strain relations needed to describe a material. In the remaining section of this chapter the work of Roscoe et al is outlined. It is shown how further considerable simplifications have been made to Eqs.(3.5) and (3.12) verified experimentally for normally consolidated clays.

3.3 THE APPROACH OF THE CAMBRIDGE GROUP

So far the discussion in this chapter has been concerned with outlining the concepts of the theory of plasticity for a material with an associated flow law. The general way in which these concepts have to be modified to account for soil behaviour has been indicated. In the rest of the chapter the theory for describing the deformation of normally consolidated clays developed by the research group at Cambridge University, under the leadership of the late K.H.Roscoe, is outlined.

Although several researchers have considered the possibility of using the concepts of the theory of plasticity to predict the stress-strain behaviour of soils, at the time of writing, only the group at Cambridge can be said to have made a persistent attack from both the theoretical and experimental viewpoints. Their approach, with some modifications, is the basis used to describe the behaviour of a compacted soil in this thesis. No attempt has been made here to give a complete coverage of all the various aspects of the Cambridge theories. Only those that are relevant

to the work in this thesis are explained.

It is assumed that soil can be regarded as an isotropic work-hardening continuum which remains isotropic during plastic deformation.

The stress system imposed by the triaxial apparatus can be described by just two independent components. In preference to the usual major and minor principal effective stresses, σ'_1 and σ'_3, the following are used:

$$p = \tfrac{1}{3}(\sigma'_1 + 2\sigma'_3) = \tfrac{1}{3} I_1 \quad \ldots\ldots\ldots\ldots\ldots\ldots\ldots\ldots \quad (3.19)$$

$$q = (\sigma'_1 - \sigma'_3) = \sqrt{3 J_2} \quad \ldots\ldots\ldots\ldots\ldots\ldots\ldots\ldots \quad (3.20)$$

where I_1 is the first invariant of the stress tensor and J_2 is the second invariant of the deviatoric stress tensor, these are defined in Eqs.(3.1) and (3.3). Use of such a simple stress system having only two independent components means that the third invariant of the deviatoric stress tensor is not independent being a function of J_2 and I_1. Because of the radial symmetry of the imposed stress system the triaxial apparatus can be used only to investigate soil behaviour in a planar section of the stress space. In recognition of this fact the term yield curve will be used in place of yield surface in the remainder of this chapter. As the material is supposed to remain isotropic under the action of the stresses p and q only two components are required to describe the state of deformation. Firstly the strain increment, for example, in the axial direction, is defined as:

$$d\epsilon_1 = -\frac{d\ell_1}{\ell_1} \quad \ldots\ldots\ldots\ldots\ldots\ldots\ldots\ldots\ldots\ldots\ldots\ldots\ldots\ldots \quad (3.21)$$

where ℓ_1 is the length of the sample. The total strain at any point is given by summing all the increments to that point, so that:

$$\epsilon_1 = -\sum \frac{d\ell_1}{\ell_1} = \ln\left\{\frac{\ell_{1(o)}}{\ell_1}\right\} \quad \ldots\ldots\ldots\ldots\ldots\ldots\ldots\ldots \quad (3.22)$$

where $\ell_{1(o)}$ is the original length of the sample. The volumetric strain increment is defined as:

$$dv = (d\epsilon_1 + 2d\epsilon_3) = -de/(1+e) \quad \ldots\ldots\ldots\ldots\ldots\ldots \quad (3.23)$$

where dv is the volumetric strain increment, $d\epsilon_3$ the lateral strain increment and e the current void ratio. A measure of the shear strain, or distortion increment is:

$$d\epsilon = (d\epsilon_1 - \tfrac{1}{3}\, dv) \quad \ldots\ldots\ldots\ldots\ldots\ldots\ldots\ldots\ldots\ldots\ldots\ldots \quad (3.24)$$

The two components of deformation used here are $d\epsilon$ and dv. These definitions of strain are such that compressive strains are positive.

The first important aspect of the Cambridge approach is the unified presentation of soil behaviour in the (p,q,e) space. Three orthogonal axes can be used for p, q and the void ratio, e, and the behaviour of the soil represented in a three dimensional diagram rather than the three separate (p,e), (q,e) and (p,q) planar diagrams often used. When the results of tests conducted on normallyconsolidated clays are plotted in this three dimensional

space it is seen that they form a surface. The first basic hypothesis of the Cambridge group is that for a given normally consolidated soil this surface is unique, i.e. when a sample under test is subjected to an arbitrary stress path the change in void ratio must be such that the point describing the state of the sample always lies on the surface. Roscoe and Poorooshasb[64] call this the "State Boundary Surface" and it is shown as the surface ABCDEFGH in Fig.3.6. The question of uniqueness has been investigated by Roscoe and Thurairajah[66] who suggest that despite certain experimental difficulties the idealisation is a reasonable approximation to soil behaviour. This surface represents the limit of all states that the soil may take. The virgin consolidation line, ABCD, represents the limit of all possible states for the soil in the (p,e) plane so that points on or inside the line are valid but those outside it have no physical meaning. Similarly for the whole of the surface ABCDEFGH all points on or within are possible but no point outside it.

The virgin consolidation line, ABCD, forms one boundary of the surface shown in Fig.3.6. Another boundary is the so called "Critical State Line", EFGH. It is a second basic hypothesis of the Cambridge approach that all samples under test tend towards a final state defined by the following conditions:

$$\frac{\partial q}{\partial \epsilon} = \frac{\partial p}{\partial \epsilon} = \frac{\partial \eta}{\partial \epsilon} = \frac{\partial v}{\partial \epsilon} = 0 \; ; \quad d\epsilon \gg 0 \; ; \quad \eta = M \quad \ldots\ldots\ldots\ldots \quad (3.25)$$

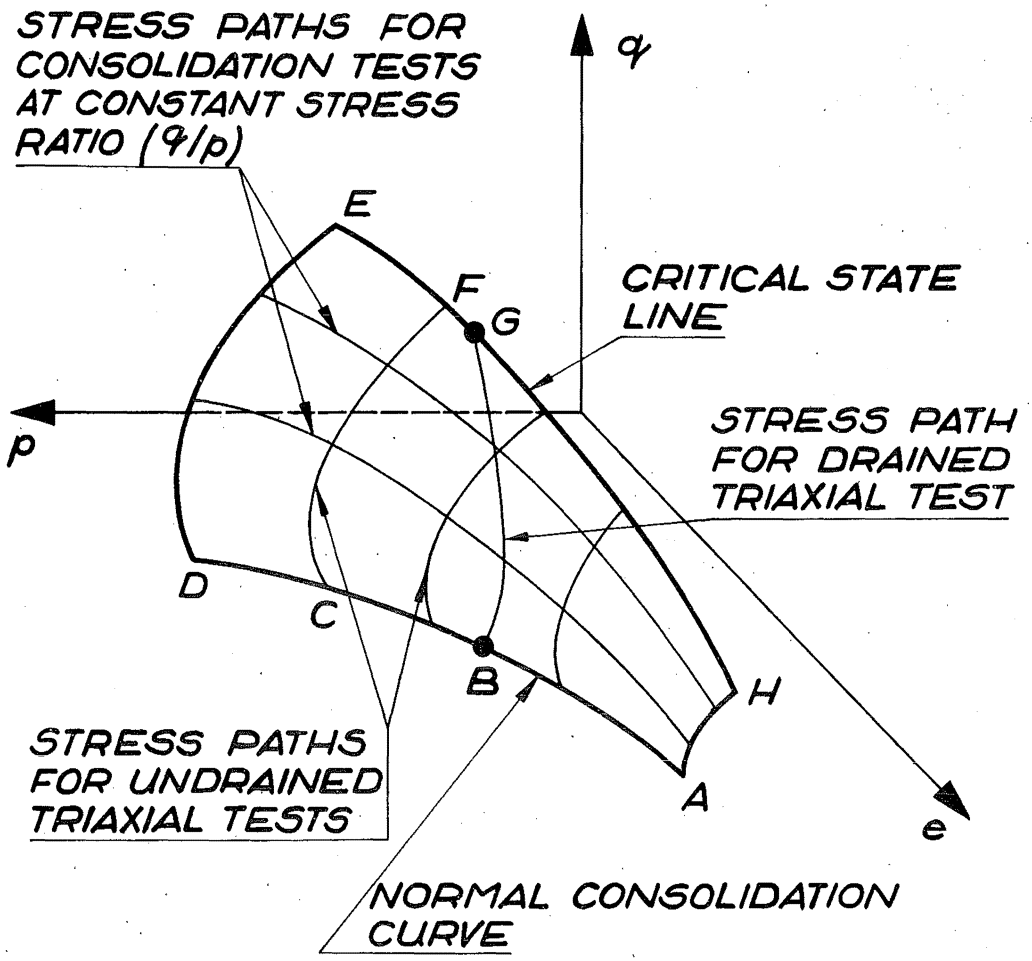

FIG. 3.6 AN ISOMETRIC VIEW OF THE STATE BOUNDRY SURFACE (WET SIDE)

where η is the stress ratio q/p, M is a soil constant and V is the sample volume.

When the conditions of Eq.(3.25) are satisfied the sample is said to have reached the "Critical State". In such a state there is no further change in q, p or e but the sample may continue to distort. The critical state line is the locus of all the critical states reached by samples from various initial conditions and state paths. The projection of the critical state line on the (p,q) plane is a straight line with the equation : q = Mp. The projection of the critical state line on the (e, lnp) plane is a straight line parallel to the virgin consolidation line, this is illustrated in Fig.3.7. Samples whose state point is on or below that part of the state boundary surface between the critical state line and the virgin consolidation line are called "wet" and other samples are called "dry".

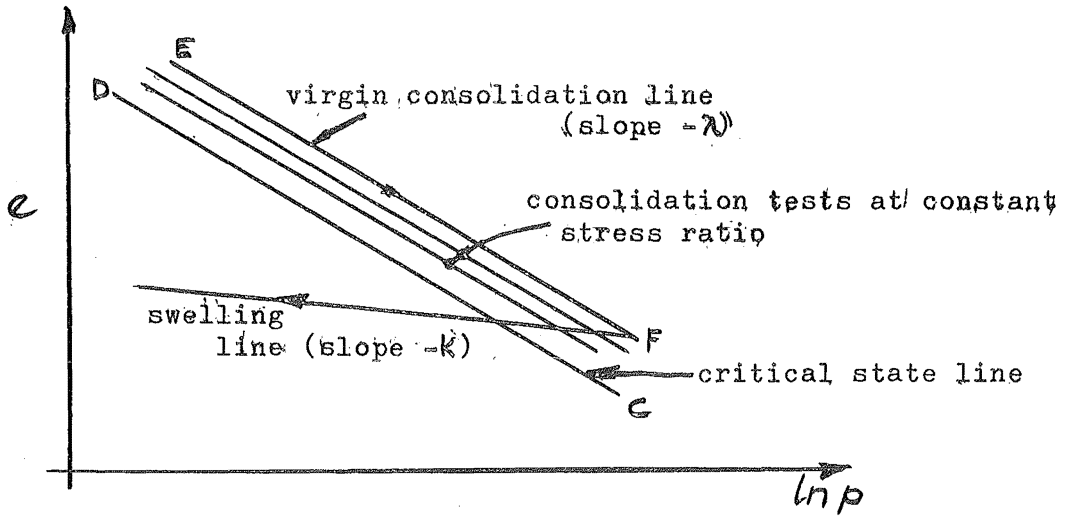

FIG.3.7 BEHAVIOUR OF NORMALLY CONSOLIDATED CLAY IN THE (e, np) PLANE

The state path for a consolidation test conducted at constant stress ratio lies on the state boundary surface and when projected into the (e, lnp) plane this line is parallel to and lies between the virgin consolidation curve and the critical state line, for example line KL in Fig.3.7. Using this experimentally observed fact Roscoe et al[65] were able to calculate the volumetric strain increment due to a stress increment dp, dq for a sample whose state point lies on the state boundary surface. This is given as (Eq.(3.14) in Ref.65).

$$dv = \frac{\lambda}{p(1+e)(S+\eta)} \{ dq + Sdp \} \quad \ldots\ldots\ldots\ldots\ldots\ldots \quad (3.26)$$

where λ is the slope of the virgin consolidation line in the (e, lnp) plane and S is the slope of the stress path followed during an undrained test, i.e.

$$S = -(dq/dp)_e \quad \ldots\ldots\ldots\ldots\ldots\ldots\ldots\ldots\ldots\ldots \quad (3.27)$$

It must be noted that Eq.(3.26) contains both an elastic and a plastic component of volume change.

The component of shear deformation, $d\epsilon$, corresponding to the component of volume change given by Eq.(3.26) can be determined by considering work done during the deformation of the sample. The external work done by the applied stresses during an increment of deformation is:

$$dW = pdv + qd\epsilon \quad \ldots\ldots\ldots\ldots\ldots\ldots\ldots\ldots\ldots\ldots \quad (3.28)$$

This work can either be stored as elastic energy or dissipated

within the sample. Both these processes are assumed to occur within the soil. The third hypothesis of Roscoe et al is that there is no recoverable component of shear deformation. The elastic volume change is given by considering the slope of the rebound line in the (e,lnp) plane, illustrated in Fig.3.7. Thus:

$$dv^e = \frac{\kappa dp}{p(1+e)} \quad \ldots\ldots\ldots\ldots\ldots\ldots\ldots\ldots\ldots\ldots\ldots\ldots \quad (3.29)$$

where κ is the slope of the swelling line in the (e, lnp) plane. Then the elastic energy stored during the application of dp is:-

$$dU = \frac{\kappa dp}{(1+e)} \quad \ldots\ldots\ldots\ldots\ldots\ldots\ldots\ldots\ldots\ldots\ldots\ldots \quad (3.30)$$

The fourth, and final, basic hypothesis of the Cambridge approach is that all the work not stored as elastic energy is dissipated as interparticle friction. This dissipated work is defined as:

$$dF = Mpd\epsilon \quad \ldots\ldots\ldots\ldots\ldots\ldots\ldots\ldots\ldots\ldots\ldots\ldots \quad (3.31)$$

Thus the soil constant M, defining the stress ratio at the critical state, can be interpreted as a macroscopic coefficient of friction. Using Eqs.(3.28), (3.30) and (3.31) and equating the work done externally to the work done inside the sample the following equation is obtained:

$$qd\epsilon + pdv = \frac{\kappa dp}{(1+e)} + Mpd\epsilon \quad \ldots\ldots\ldots\ldots\ldots\ldots\ldots \quad (3.32)$$

This equation (Eq.(2.9) in Reference 65) will be referred to as Roscoe's energy equation.

From Eqs.(3.26) and (3.32) the increment of distortion

when dp, dq is applied to the sample is:-

$$d\epsilon = \frac{\kappa}{p(1+e)} \left\{ \frac{(\lambda/\kappa)dq + [S(\lambda/\kappa - 1) - \eta]dp}{(S+\eta)(M-\eta)} \right\} \quad \ldots\ldots\ldots\ldots \quad (3.33)$$

This is given as Eq.(4.1) in Reference 65. Because it is assumed that there is no recoverable distortion Eq.(3.33) gives a plastic strain increment.

In as much as Eqs.(3.26) and (3.33) give increments of elastic and plastic deformation they can be regarded as plastic stress-strain relations. However they have been derived without using any of the concepts of the theory of plasticity. This is possible because two novel ideas were introduced by the Cambridge group. Firstly the existence of a unique state boundary surface makes the calculation of dv, Eq.(3.26), immediate. Secondly the postulation of a mechanism accounting for the manner in which work is dissipated within the sample is a new concept and makes calculation of $d\epsilon$ possible. To the writer's knowledge no equivalent ideas are to be found in the conventional theory of plasticity. Therefore it is interesting and important to ask whether Eqs.(3.26) and (3.33) can be expressed in the form of Eq.(3.12), i.e. whether expressions for the functions f and h can be found.

Using the Cambridge parameters the expansion of Eq.(3.12) is:

$$d\epsilon^p = h\frac{\partial f}{\partial q}\,df = h\frac{\partial f}{\partial q}\left[\frac{\partial f}{\partial q}\,dq + \frac{\partial f}{\partial p}\,dp\right]$$

$$dv^p = h\frac{\partial f}{\partial p}\,df = h\frac{\partial f}{\partial p}\left[\frac{\partial f}{\partial q}\,dq + \frac{\partial f}{\partial p}\,dp\right]$$

For convenience put $\frac{\partial f}{\partial q} = A$ and $\frac{\partial f}{\partial p} = B$, substitution gives:

$$d\epsilon^p = hA^2 dq + hABdp \quad \ldots\ldots\ldots\ldots\ldots\ldots\ldots\ldots \quad (3.34)$$

$$dv^p = hBAdq + hB^2 dp \quad \ldots\ldots\ldots\ldots\ldots\ldots\ldots\ldots \quad (3.35)$$

Since it is assumed that there is no recoverable shear deformation Eq.(3.33) can be written:

$$d\epsilon^p = \frac{\kappa}{p(1+e)}\left\{\frac{(\lambda/k)dq + [S(M/k - 1) - \eta]\,dp}{(S+\eta)(M-\eta)}\right\} \quad \ldots\ldots\ldots\ldots \quad (3.33a)$$

Using Eqs.(3.26) and (3.29) the plastic component of volume change is:

$$dv^p = \frac{\lambda}{p(1+e)}\left\{\frac{dq + Sdp}{(S+\eta)}\right\} - \frac{k\,dp}{p(1+e)} \quad \ldots\ldots\ldots\ldots\ldots\ldots \quad (3.36)$$

Equating the coefficients of dq and dp between Eqs.(3.34) and (3.33a) gives:

$$hA^2 = \frac{\lambda}{p(1+e)(S+\eta)(M-\eta)} \quad \ldots\ldots\ldots\ldots\ldots\ldots\ldots\ldots \quad (3.37)$$

$$hAB = \frac{\kappa[S(M/k - 1) - \eta]}{p(1+e)(S+\eta)(M-\eta)} \quad \ldots\ldots\ldots\ldots\ldots\ldots\ldots\ldots \quad (3.38)$$

Similarly equating coefficients of dq and dp between Eqs.(3.35) and (3.36) gives:

$$hAB = \frac{\lambda}{p(1+e)(S+\eta)} \quad \ldots\ldots\ldots\ldots\ldots\ldots\ldots\ldots \quad (3.39)$$

$$hB^2 = \frac{S\lambda - k(S+\eta)}{p(1+e)(S+\eta)} \quad \ldots\ldots\ldots\ldots\ldots\ldots\ldots\ldots \quad (3.40)$$

Equating coefficients in this manner is possible because it is

known from section 3.2 that h is independent of increments of stress and that f is also independent of stress increments because of Eq.(3.5) defining the form of f. For consistency Eq.(3.38) and (3.39) must be identical, thus:

$$K\left[S(\lambda k-1) - \eta\right] / (M-\eta) = \lambda$$

Which simplifies to:

$$S = \frac{M}{(1-K/\lambda)} - \eta \qquad \ldots\ldots\ldots\ldots\ldots\ldots\ldots\ldots\ldots\ldots \quad (3.41)$$

Eq.(3.41) is identical to Eq.(4.2) in reference 65 although the procedure used by Roscoe et al in deriving it was slightly different to that used here. Equation (3.41) can be used to simplify the expressions for the plastic strain increments given by Eqs.(3.33a) and (3.36). These reduce to:

$$d\epsilon^p = \frac{(\lambda-K)}{Mp(M-\eta)(1+e)}\left\{ dq - (M-\eta)dp \right\} \qquad \ldots\ldots\ldots\ldots\ldots\ldots \quad (3.33b)$$

and

$$dv^p = \frac{(\lambda-K)}{Mp(1+e)}\left\{ dq - (M-\eta)dp \right\} \qquad \ldots\ldots\ldots\ldots\ldots\ldots\ldots\ldots \quad (3.36a)$$

As these equations are still fairly complex comparison with Eqs.(3.12) and (3.12a) is worthwhile. It was pointed out in discussing Eq.(3.12) on page 88 that the only way the stress increments come into the equation is in the increment of the loading function, i.e. in the term df. Thus it is possible to say that in Eqs.(3.33b) and (3.36a) the term $dq - (M-\eta)\,dp$ is at least part of the increment in the loading function during the

application of the stress increment (dq,dp). The remainder of these equations, the terms $(\lambda-\kappa)/Mp(M-\eta)(1+e)$ and $(\lambda-\kappa)/Mp(1+e)$ must be related to the $h\partial f/\partial\sigma_{ij}$ part of Eq.(3.12).

Substitution of Eq.(3.41) leads to the following simplifications of Eqs.(3.37) to (3.40):

$$hA^2 = \frac{(\lambda-\kappa)}{pM(1+e)(M-\eta)} \quad \ldots\ldots\ldots\ldots\ldots\ldots\ldots\ldots \quad (3.42)$$

$$hAB = \frac{(\lambda-\kappa)}{pM(1+e)} \quad \ldots\ldots\ldots\ldots\ldots\ldots\ldots\ldots \quad (3.43)$$

and

$$hB^2 = \frac{(\lambda-\kappa)(M-\eta)}{pM(1+e)} \quad \ldots\ldots\ldots\ldots\ldots\ldots\ldots\ldots \quad (3.44)$$

Using either Eqs.(3.42) and (3.43) or (3.43) and (3.44) h can be eliminated and the following obtained:

$$\frac{A}{B} = \frac{1}{(M-\eta)}$$

$$\text{i.e.} \quad \frac{\partial f}{\partial q} \cdot \frac{\partial p}{\partial f} = \frac{1}{(M-\eta)}$$

At this stage it is necessary to solve the above equation for f, i.e. the equation of the current yield surface is required. Considering a neutral change of stress and using the condition given in Eq.(3.7):

$$\frac{\partial f}{\partial q}\,dq + \frac{\partial f}{\partial p}\,dp = 0$$

This simple relation holds because for a neutral change in stress no additional work-hardening occurs and no additional plastic strain takes place and so the last two terms in Eq.(3.6) are zero,

so that:

$$\frac{dq}{dp} = -\frac{\partial f}{\partial p} \cdot \frac{\partial q}{\partial f}$$

Thus f is a function along which:

$$\frac{dq}{dp} = -(M-\eta) \quad \ldots\ldots\ldots\ldots\ldots\ldots\ldots\ldots\ldots\ldots\ldots\ldots \quad (3.45)$$

Using $\frac{1}{p}$ as an integrating factor and the initial condition that when $q=0$, $\eta=0$ and $p=p_o$

$$q = Mp\ln\left(\frac{p_o}{p}\right)$$

So that the function f is given as:

$$f = q - Mp\ln\left(\frac{p_o}{p}\right) \quad \ldots\ldots\ldots\ldots\ldots\ldots\ldots\ldots\ldots\ldots\ldots\ldots \quad (3.46)$$

Differentiation of Eq.(3.46) and substitution into Eqs.(3.42), (3.43) and (3.44) leads to:

$$A = 1, \quad B = (M-\eta) \quad \text{and}$$

$$h = \frac{(\lambda-\kappa)}{Mp(1+e)(M-\eta)} \quad \ldots\ldots\ldots\ldots\ldots\ldots\ldots\ldots\ldots\ldots\ldots\ldots \quad (3.47)$$

Evidently Eqs.(3.46) and (3.47) give the two functions, f and h, that can be used in conjunction with Eq.(3.12) to give increments of deformation equivalent to those calculated from Eqs.(3.26) and (3.33). However before one can make a definite conclusion that the approach of the Cambridge group is compatible with the conventional theory of plasticity the physical meaning of Eq.(3.46) must be examined. Eq.(3.12) requires that

f must represent both the yield curve and the plastic potential function for a work-hardening material.

As explained in section 3.2 the stress point can move around the yield surface for a work-hardening material without incurring any additional plastic deformation. In the (p,e) plane the swelling or rebound line, ABR in Fig.3.8, is considered to be a curve along which only elastic deformation occurs. This suggests that the curve in the state boundary surface vertically above the swelling line, curve AXF in Fig.3.8, is a path that can be traversed while only elastic deformation occurs. However such a curve cannot strictly be regarded as a yield curve in the sense discussed in section 3.2. The idea that a curve or surface exists giving the boundary between regions where only elastic deformation occurs and those where elastic and plastic deformation occurs has been discussed in section 3.2 only with reference to the stress space. One could perhaps suggest that the concept of a yield surface be broadened to include such a boundary between elastic and elastic-plastic states in the (p,q,e) space. However the disadvantage of doing this is much greater than any advantage. The very useful consequences of Drucker's stability postulate, which have been derived for a yield surface in the stress space, would not apply to a curve in the (p,q,e) space. Calladine[12] has made a suggestion that overcomes this problem. He proposed that the projection of the elastic section of the state boundary surface onto the (p,q)

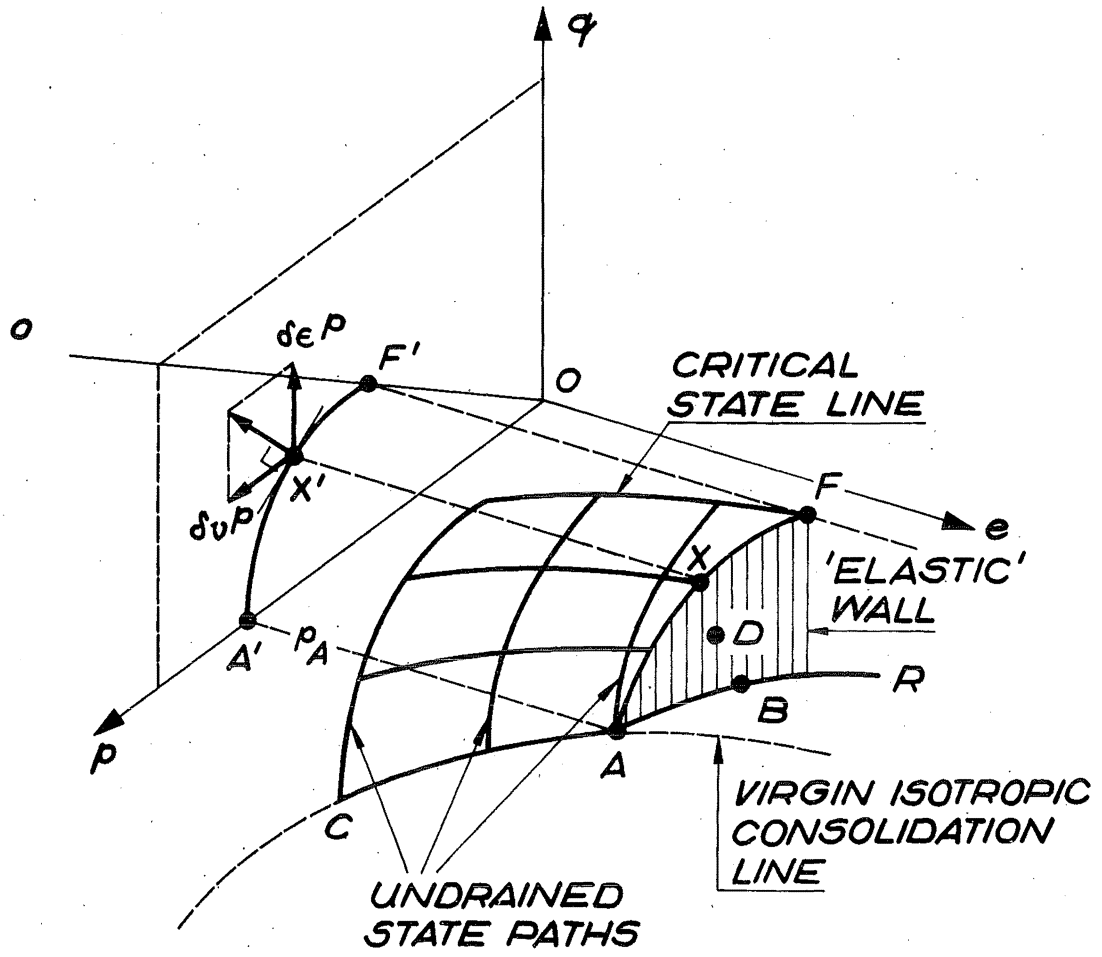

FIG. 3.8 YIELD CURVE AND STATE BOUNDARY SURFACE

plane be used as the yield curve. This projection is shown as A'X'F' in Fig.3.8. Such a yield curve would be described, using the normality condition, by:

$$\left(\frac{dq}{dp}\right)_{A'F'} = -\frac{dv^p}{d\epsilon} \quad \ldots\ldots\ldots\ldots\ldots\ldots\ldots\ldots\ldots\ldots \quad (3.48)$$

Using Eqs.(3.33) and (3.36) this becomes:

$$\left(\frac{dq}{dp}\right)_{A'F'} = -(M-\eta) \quad \ldots\ldots\ldots\ldots\ldots\ldots\ldots\ldots\ldots\ldots \quad (3.49)$$

Since this equation is the same as Eq.(3.45) the yield curve obtained by this procedure is identical with the function f given in Eq.(3.46). Comparison of this expression for the yield curve with Eq.(3.5b) is worthwhile. In Eqs.(3.19) and (3.20) the relation of the stress parameters p and q to the invariants of the stress tensor and deviatoric stress tensor is shown. Using this the equation defining the loading function, Eq.(3.46), can be written as:

$$f(I_1, J_2, M, p_o) = 0 \quad \ldots\ldots\ldots\ldots\ldots\ldots\ldots\ldots\ldots\ldots \quad (3.46a)$$

This illustrates that the loading function implied by the work of the Cambridge group on normally consolidated clays is a function of the first invariant of the stress tensor, the second invariant of the deviatoric stress tensor, a single material parameter that is independent of stress and strain and the value of p at which the current yield curve intersects the p axis of the (q,p) plane. The third invariant of the deviatoric stress

tensor, J_3, does not appear in Eq.(3.46a) because for the simple stress conditions imposed by the triaxial apparatus J_3 reduces to a function of J_2 and I_1. During the work-hardening the current yield curve expands although each successive yield curve is geometrically similar to the previous one. A useful measure of the amount of expansion of the yield curve and consequently an indication of the amount of work hardening is the change in the value of p_o from one yield curve to another.

In summary, two equations (3.26) and (3.33) were obtained by Roscoe, Schofield and Thurairajah[65] giving the components of deformation when the state point of the sample moves along the boundary surface. These equations were arrived at without using any of the concepts of the theory of plasticity. When these two equations were combined with the plastic stress-strain relation, Eq.(3.12), a solution for f was obtained. It was then shown that this function satisfies the physical conditions needed for a yield curve. Therefore the equations derived by the Cambridge group are quite compatible with the conventional theory of plasticity, even though they are based on some new ideas.

During a loading path that gives some plastic deformation the state point moves around the state boundary surface effectively crossing a number of elastic limit curves. In the (p,q) plane this means that the position of the yield curve is changing

continuously. However this change in position is accomplished without a change in shape. Since the shape of the yield curve is independent of the state of work-hardening, the strain increment associated with a particular stress increment is independent of the stress path followed in reaching the present state of stress.

So far only the deformation associated with state points on the boundary surface has been considered. For a point below the surface, such as B or D in Fig.3.8, the sample is supposed to behave elastically until the state point reaches the boundary surface.

In subjecting the predictions of their theory to experimental test the Cambridge group have concentrated on the behaviour of normally consolidated and lightly overconsolidated clays. This has been done because these samples tend to behave more uniformly than dry samples which may become unstable. As only the behaviour of wet samples is well supported by experimental evidence, only the wet side of the state boundary surface has been shown in Figs.3.6 and 3.8. A range of test results presented by Schofield and Wroth[75] shows that the theory gives a good representation of soil behaviour under undrained conditions. Furthermore in reference 65 Roscoe et al have indicated that, despite some experimental problems the strains occurring during a drained test can be predicted from the results of undrained tests. Roscoe and Burland[67] have introduced some refinements which lead

to even better correspondence between predicted and observed behaviour. Also the correlation between predictions and observations has improved as experimental methods have been refined.

The comparative simplicity of this theoretical approach has some interesting implications for design procedures used in foundation engineering. If the results of the Cambridge theory could be generalised to encompass more complex stress conditions, then it might be possible to simplify some of the applications of Lambe's "Stress Path Method"[43]. In essence this method estimates the performance of a foundation by conducting laboratory tests on samples subjected to the same stress paths as similar elements of soil within the actual foundation. The disadvantage of this approach is that rather complex testing conditions may sometimes be required. With the aid of a generalised theory one could use simple test conditions and the theory to predict the strains in the more complicated case.

Perhaps the most surprising aspect of this theory is its relative simplicity. It would be reasonable to expect the plastic behaviour of soil to be more complex than that of metal because soil not only distorts when subjected to stress but also undergoes considerable change in volume. A tentative explanation of this simplicity can be based on the hypothesis that soil is basically a frictional material and that plastic deformation is due to relative motion between adjacent particles or groups of

particles. The particles move past one another when the ratio of the tangential component of the contact force to the normal component exceeds the coefficient of friction for the material. This coefficient will be more or less constant for a soil of given composition. Furthermore it will not change with the state of deformation and orientation of the particles. Such a situation is indeed very simple when contrasted with the deformation process in metals. Even a metal that is macroscopically isotropic is composed of crystals whose properties are very dependent on direction. Plastic deformation is accompanied by reorientation and gliding of the crystals so the bulk properties of a specimen in a given direction are dependent on the state of deformation. Thus at the macroscopic level the deformation of metal is simpler than that of soil but the converse could well be the case at the microscopic level. This simplicity should also apply to a dry soil which is just as much a frictional material as a wet soil. The main difference between wet and dry soils is the direction of the dilation during shear. A wet soil tends to reduce the number of interparticle contacts during shear so that the volume decreases. On the other hand a dry soil tends to increase the number of interparticle contacts and so the volume increases during shear. However, for a dry soil the coefficient of friction between particles will still be independent of deformation. Thus the simple path independence that is predicted, and has been observed, for a wet soil should also be expected for

a dry soil. If this proposition is correct then the ideas of the Cambridge theory could be extended to include dry soils. Chapter 5 is devoted to exploring this possibility.

CHAPTER FOUR

BEHAVIOUR OF SAMPLES LOADED PARALLEL TO THE DIRECTION OF THE COMPACTIVE EFFORT

4.1 INTRODUCTION

In this chapter the results of a series of tests conducted on samples of a clay, prepared wet of optimum moisture content by kneading compaction, and loaded parallel to the direction in which the compactive effort was applied, are presented. All the tests were made in the triaxial apparatus on samples that had been saturated by the application of back pressure and consolidated under hydrostatic pressures ranging from 0.90 to 63.60 psi. The tests were a mixture of strain controlled and stress controlled types and a very great deal of effort was directed towards minimising the influence of those sources of error inherent in the triaxial method of testing.

The emphasis in the chapter is placed on the description of the observed soil behaviour. Interpretation and discussion are left to the next chapter. The equipment used and the testing procedures followed are described in detail in appendices B, C and D while the properties of the soil tested are given in appendix A and so only essential reference is made to these things here.

4.2 STRESS-STRAIN BEHAVIOUR

In Fig.4.1 the curves of q plotted against the axial strain, ϵ_1, are presented for most of the undrained tests. The definition of q and ϵ has already been given in Eqs. (3.20) and (3.24) but for convenience they are repeated here:-

$$q = (\sigma'_1 - \sigma'_3) \quad \ldots\ldots\ldots\ldots\ldots\ldots\ldots\ldots\ldots\ldots \quad (3.20)$$

$$\epsilon = \epsilon_1 - \tfrac{1}{3}(\epsilon_1 + 2\epsilon_3) \quad \ldots\ldots\ldots\ldots\ldots\ldots\ldots\ldots \quad (3.24)$$

where ϵ_1 is the axial strain and ϵ_3 the radial strain. For an undrained test the volumetric strain $(\epsilon_1 + 2\epsilon_3)$ is zero so that the distortion, ϵ, is equal to the axial strain.

At the top right hand end of each curve in Fig.4.1 the code number for each test is given along with the consolidation pressure in brackets. The stress controlled tests are referred to as "STC" and the strain controlled tests by the letters "CSR", in each case the test number is preceded by this designation of the type of test. The tests have been numbered in the order in which they were performed. A complete listing of the reduced experimental results for the undrained tests can be found in appendix F.

All these stress strain curves have a similar form, the main features being two points of inflexion and almost completely rigid behaviour for small values of q. The curves have been plotted only for axial strains up to 10 per cent. To this

level of strain the assumption that the deformed shape of the sample is uniform seems reasonable. At strains greater than about 10 per cent the sample begins to barrel and slip planes become visible. Because much of the discussion in this thesis is applicable only to samples that are deforming uniformly, 10 per cent is taken as the upper limit of strain to be considered. However a few tests were continued to see if the samples reached a critical state. Even when slip planes had become quite noticeable the values of q and p continued to increase and were still increasing at strains in excess of about 25 per cent although the shape of the sample had become quite non-uniform. In fact none of the samples ever reached a critical state in which the values of q and p reached stationary values and ϵ continued to increase, although it can be said that the samples were tending towards such a state because the rate at which q was increasing with strain was decreasing towards the end of the tests. To check that this behaviour was truly a feature of the soil tested a few special tests were performed. Firstly two tests (CSR 003 and CSR 004) were made on conventional 3" x $1\frac{1}{2}$"D samples rather than the $1\frac{1}{2}$" x $1\frac{1}{2}$"D samples with free ends used throughout the rest of the testing programme. These showed very similar behaviour to the short samples and no maximum value of q was found for strains up to 30 per cent. Some of the slip planes occurring at high strains crossed the filter paper side drains. This might have given rise to an artificial increase in strength and

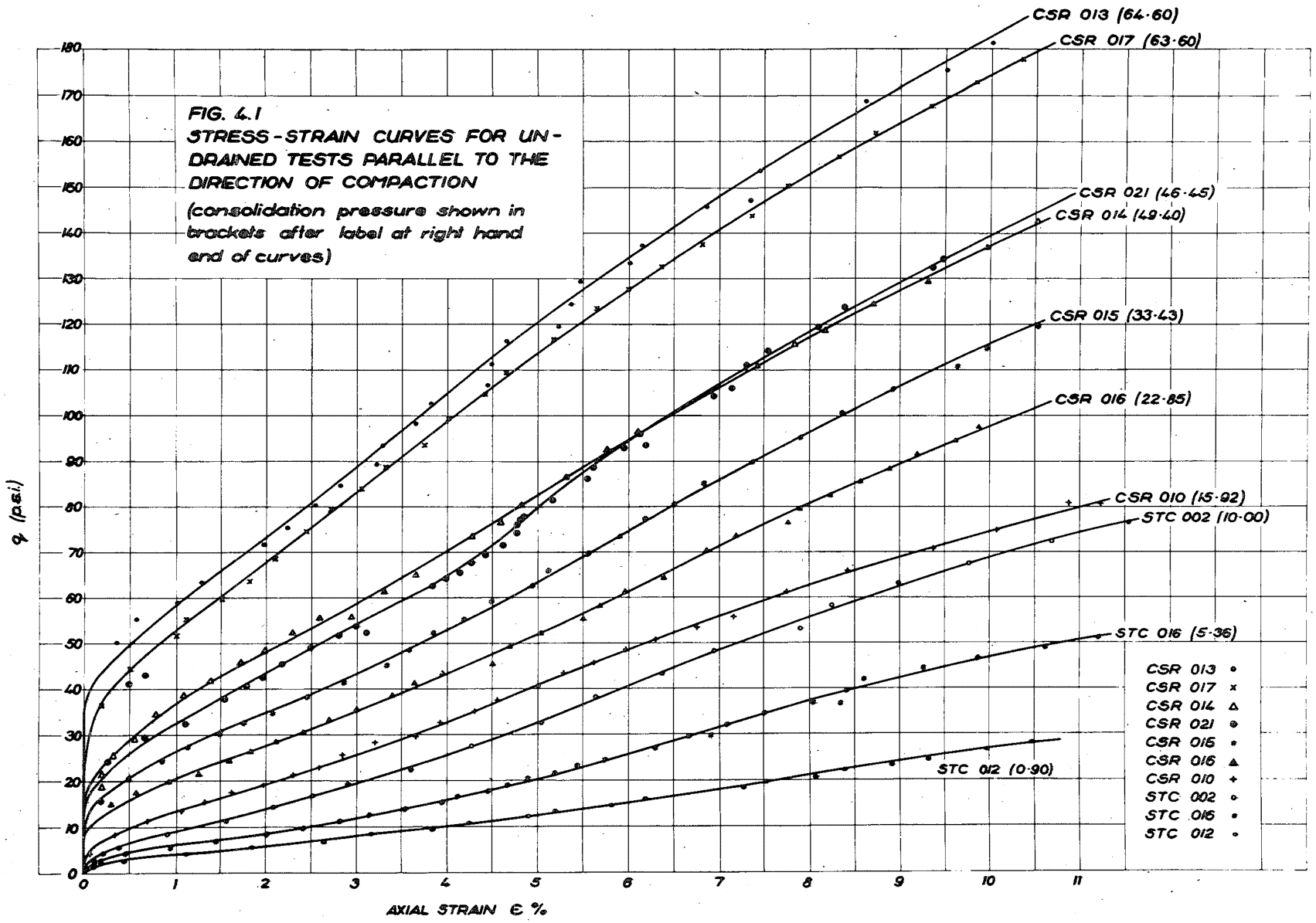
FIG. 4.1
STRESS-STRAIN CURVES FOR UN-DRAINED TESTS PARALLEL TO THE DIRECTION OF COMPACTION
(consolidation pressure shown in brackets after label at right hand end of curves)
CSR 013 (64·60)
CSR 017 (63·60)
CSR 021 (46·45)
CSR 014 (49·40)
CSR 015 (33·43)
CSR 016 (22·85)
CSR 010 (15·92)
STC 002 (10·00)
STC 016 (5·36)
STC 012 (0·90)
CSR 013
CSR 017
CSR 014
CSR 021
CSR 015
CSR 016
CSR 010
STC 002
STC 015
STC 012
q (p.s.i.)
AXIAL STRAIN ε %
0
10
20
30
40
50
60
70
80
90
100
110
120
130
140
150
160
170
180
1
2
3
4
5
6
7
8
9
10
11

so a test on a $1\frac{1}{2}$" x $1\frac{1}{2}$"D sample with no side drains (CSR 005) was made as a check. No significant difference was observed for strains up to 26 per cent.

4.3 STRESS PATHS

The stress paths for all the undrained tests are plotted in Fig.4.2. All the paths have a similar form, firstly a decrease in p as q is increased and then both p and q increase together. The end portions of all these stress paths are tangential to a straight line that passes through the point $q = 0$, $p = -3.0$, the slope of this line varies a little from test to test; however, as discussed in section 4.6 a reasonable idealisation is that all the stress paths are tangential to one line. The first of the two points of inflexion mentioned in section 4.2 is associated with the minimum values of p along the stress path. The fact that p continues to increase as q increases at the end of the test means that the $p \nu \epsilon$ curve continues to rise as does the $q \nu \epsilon$ curve. The shape of the stress paths eventually requires that the pore water pressure in the samples becomes negative. Fortunately this presented no experimental problem because the high back pressure ensured that although the pore water pressure was negative with respect to the cell pressure the absolute value was still very much greater than zero.

One test (CSR 021) was continued after the strain had reached 10% to investigate the effect of the formation of slip

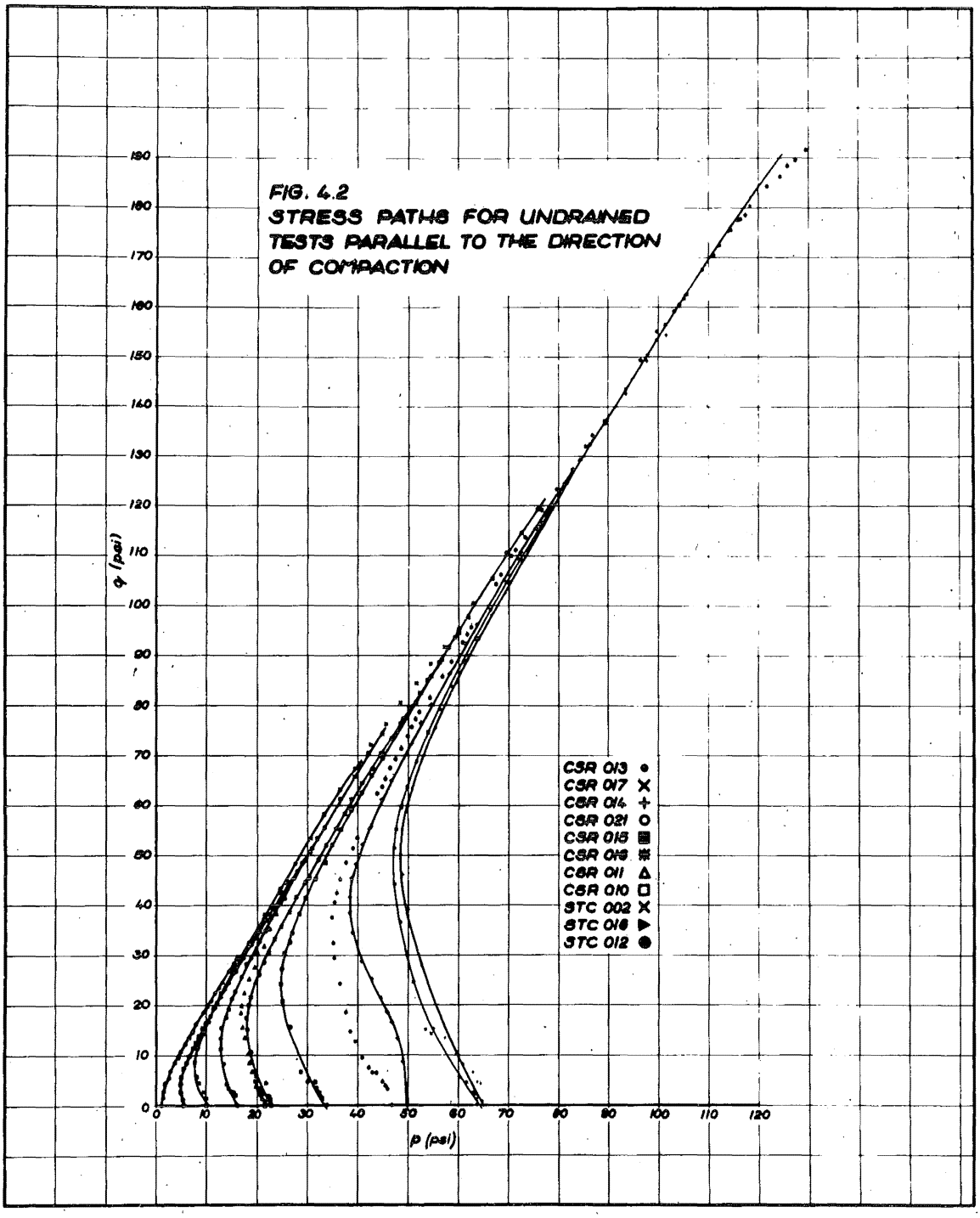
FIG. 4.2
STRESS PATHS FOR UNDRAINED TESTS PARALLEL TO THE DIRECTION OF COMPACTION
q (psi)
p (psi)
0
10
20
30
40
50
60
70
80
90
100
110
120
130
140
150
160
170
180
190
CSR 013
CSR 017
CSR 014
CSR 021
CSR 015
CSR 019
CSR 011
CSR 010
STC 002
STC 016
STC 012

planes on the shape of the stress path. The stress path for the test is shown in Fig.4.3. When the axial strain reached 7% the path approached the line that passes through (0.,-3.0) and at a strain of 10% slip planes first became visible on the surface of the sample. The appearance of the slip planes made no difference to the form of the stress path and the points still lay along the same line until the axial deformation reached 17½% at which point the stress path began to move away from the tangent through (0.,-3.0). However at a strain of 17% the sample had become fairly non-uniform in shape and the divergence of the stress path was no doubt caused by errors in the calculated stress resulting from the assumption that the sample is a uniform right circular cylinder. The result of this test does illustrate that shape of the stress paths for all the tests terminated at a strain of 10% is not affected by the presence of slip planes.

4.4 CURVES OF STRESS RATIO VERSUS STRAIN

The curves of the stress ratio $\eta = q/p$, have been plotted against strain for some of the undrained tests in Fig.4.4. The samples with the lowest consolidation pressures, i.e. those nearest the "as compacted" condition, have a peak value of η, after which the curve settles down to a constant value of η. On the other hand the samples with the higher consolidation pressures do not have a peak value in the curve. At least this general tendency is clear from Fig.4.4 even if some of the samples seem

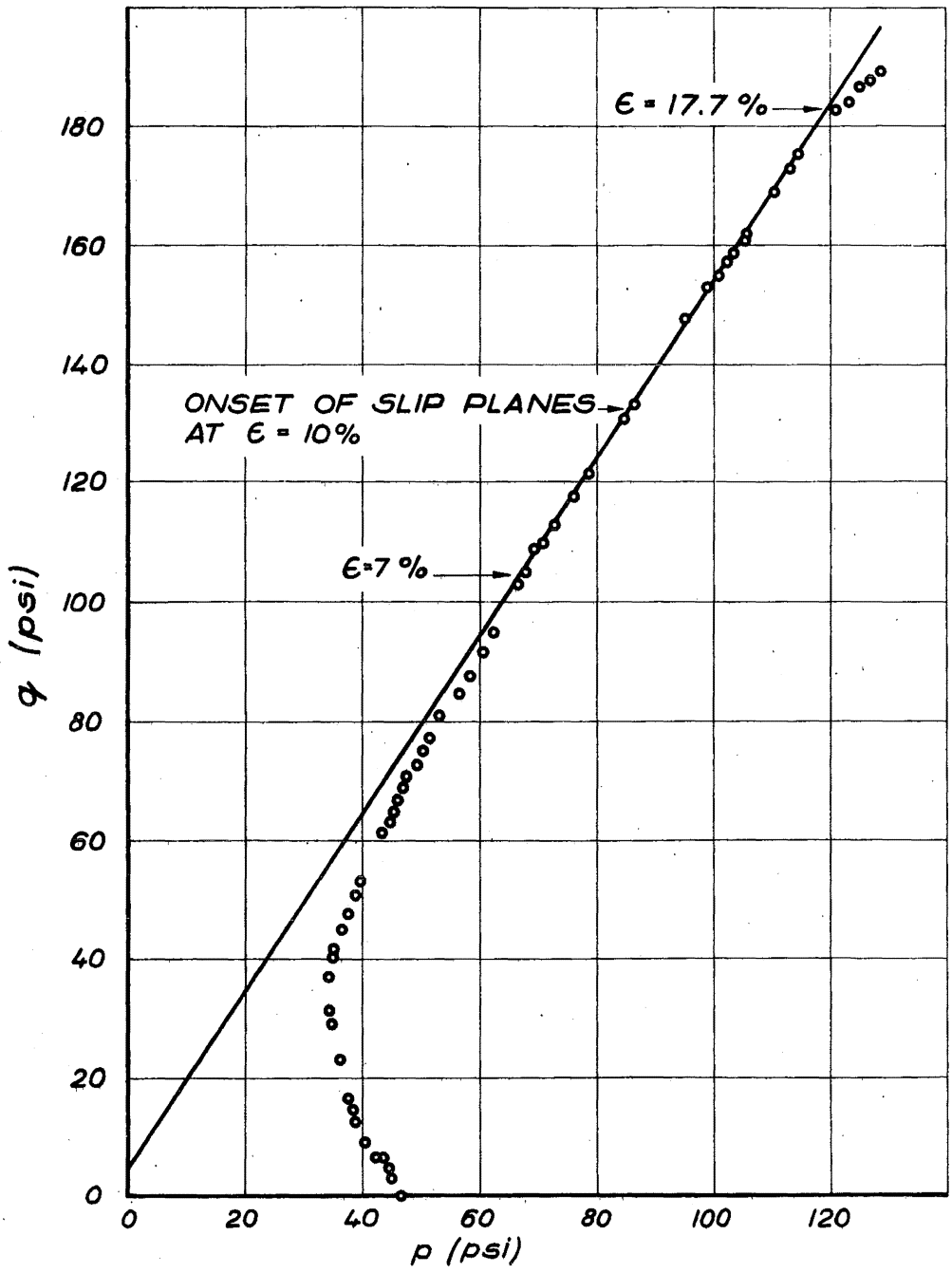

FIG. 4.3 STRESS PATH FOR TEST CSR 021

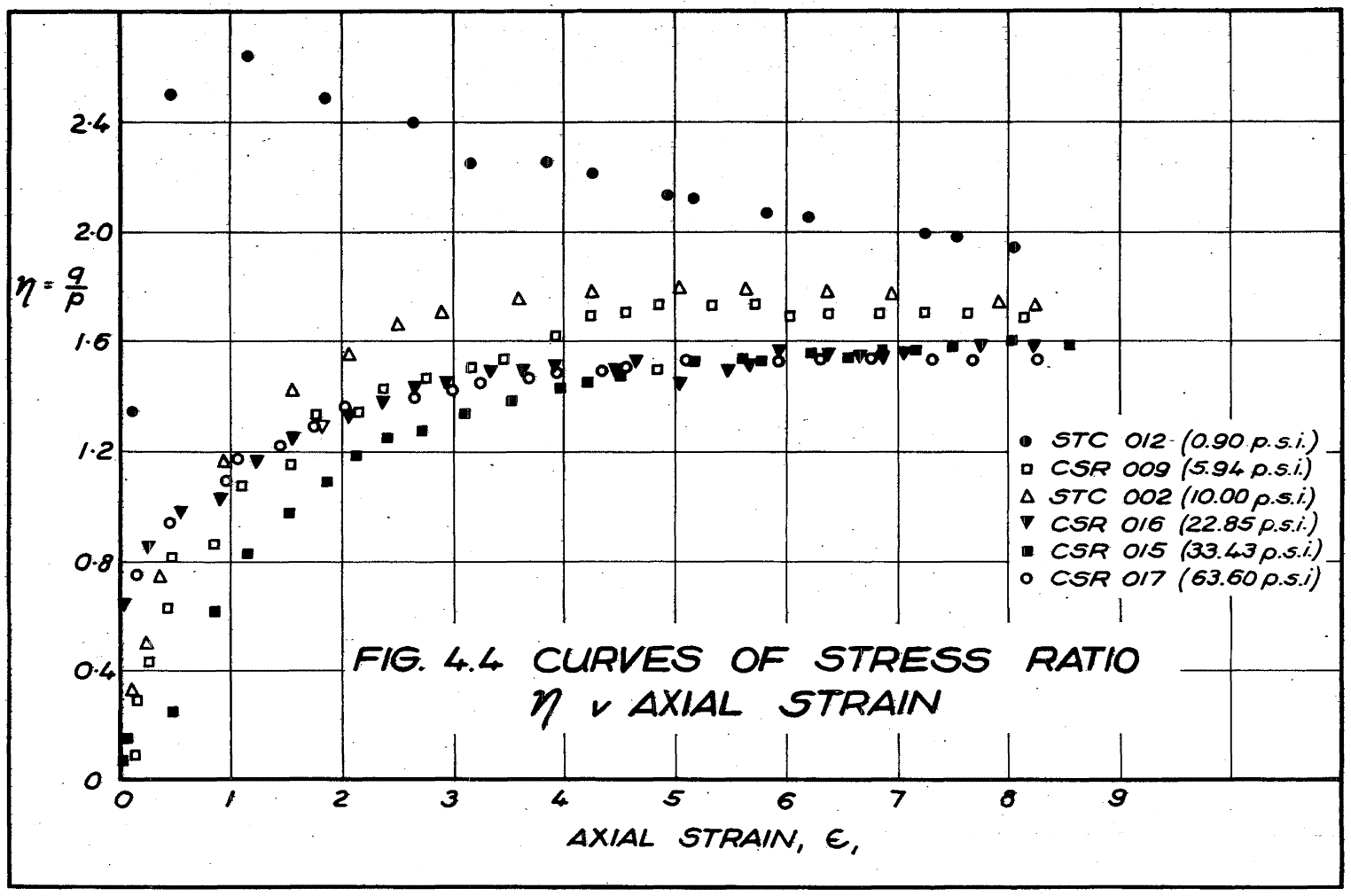

FIG. 4.4 CURVES OF STRESS RATIO
η v AXIAL STRAIN

to be exceptions. STC 012 with a consolidation pressure of 0.90 psi passed through a very pronounced peak, and STC 002 with a pressure of 10.00 psi passed through a somewhat smaller peak. On this basis one would expect that the samples with consolidation pressures of around 5 psi (CSR 009 and STC 016) would have a peak value somewhere between the other two. The fact that this does not occur has not been investigated any further but it could well be related to the scatter in the "as compacted" samples discussed in section 4.13.

It is also worth noting that the peak value in the $\eta v \epsilon$ curve occurs at low strains and this always occurs well before slip planes become visible along the side of the sample.

Fig.4.4 is important because it shows that the $\eta v \epsilon$ curve tends to depend on the particular test. It is shown in the next section that a slightly different ratio is more useful for this soil as it leads to a single curve for all the undrained tests.

4.5 CONTOURS OF EQUAL TOTAL AXIAL STRAIN

Contours of equal total axial strain (i.e. elastic plus plastic) were plotted onto the undrained stress paths to see if there was any relationship between the shape of the various undrained stress paths and the deformation of the sample at any point. The result is plotted in Fig.4.5 and shows that the contours are straight lines all of which seem to pass through

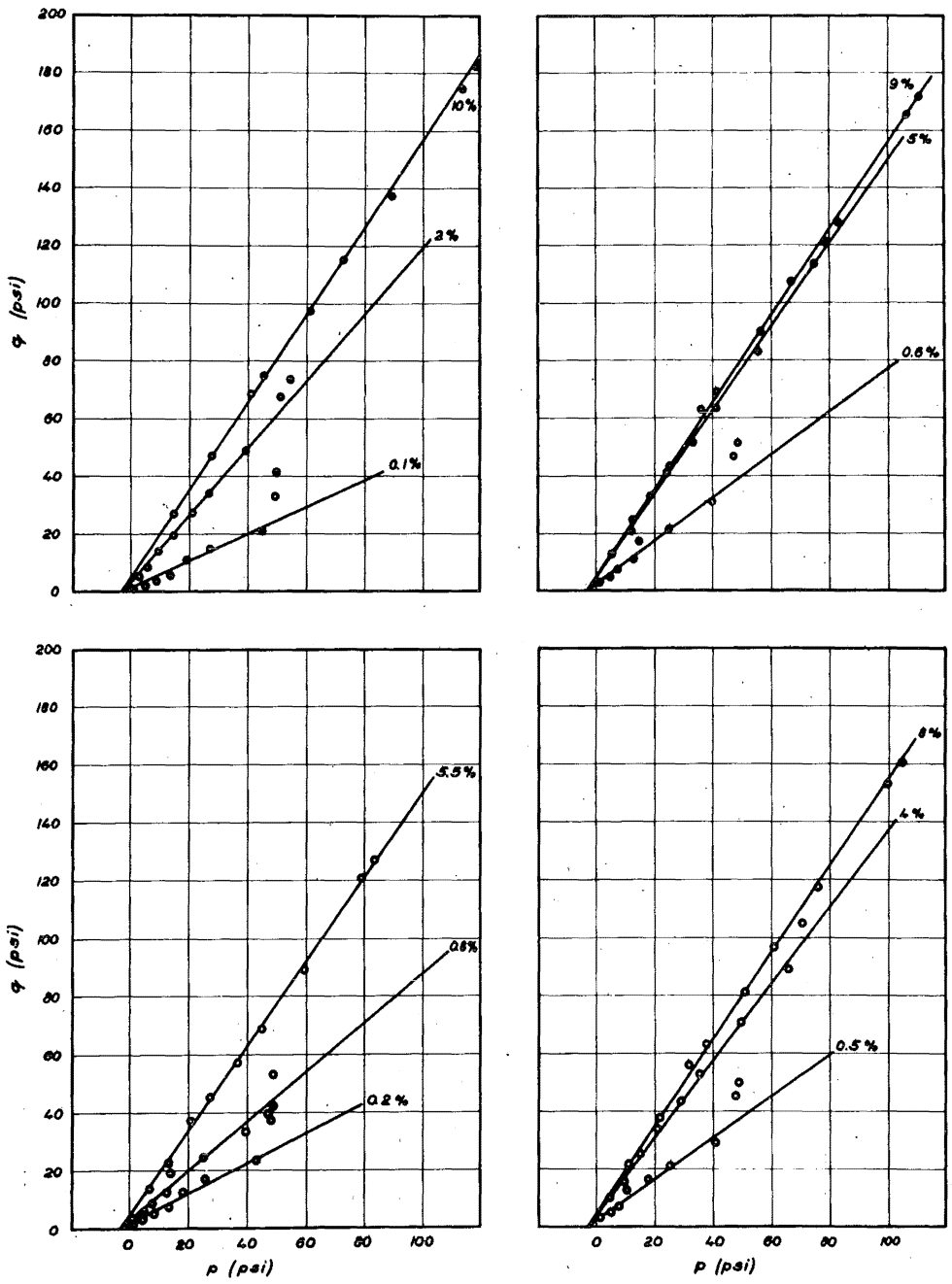

FIG. 4.5 CONTOURS OF EQUAL TOTAL STRAIN

the point (0.,-3.0). Fig.4.5 has been presented as four separate figures because if all the contours are plotted on one diagram the result tends to be confused, and for the same reason the actual stress paths have not been drawn in Fig.4.5.

In the next chapter it will be seen that the observation that all these contours of equal strain seem to pass through a common point on the p-axis is a most important part of the argument presented in this thesis. And also in the rest of this chapter it is important because it leads to a simplification of the description of the behaviour of this particular compacted soil. In fact this phenomenon is perhaps the most significant property observed for the material, consequently the determination of the intercept of these linear contours of equal strain is discussed in detail.

A more accurate assessment of the intercept of each contour on the p-axis of the stress path diagram is obtained using the least squares curve fitting method to calculate a "best straight line". This was done and the results are presented in Table 4.1. In calculating these contours only the first seven points on the contours at lower strains were used rather than the nine values plotted on Fig.4.4. This is clearly justifiable because the upper two values on these contours are not consistent with the remainder. These points, and the tests from which they were derived, are discussed in section 4.13. No results are quoted in Table 4.1

TABLE 4.1

PARAMETERS OF LINEAR CONTOURS OF EQUAL STRAIN FOR UNDRAINED TESTS FROM LEAST SQUARES CURVE FITTING

Strain (%)	Slope	Intercept on p axis (psi)
0.2	0.537	-2.184
0.3	0.584	-2.176
0.5	0.689	-3.049
0.8	0.905	-3.578
1.0	0.919	-2.623
1.5	1.077	-2.334
2.0	1.158	-2.656
3.0	1.291	-2.663
5.0	1.449	-2.874
7.0	1.496	-3.308
10.0	1.474	-4.769

for a 0.1% contour because of the difficulty in determining the position of this accurately. The probable error in measuring the sample deformation is about half the deformation needed for a strain of 0.1%.

From Table 4.1 it can be seen that the value of the intercept is approximately the same for each contour. The average value is -2.98 psi and all the values tabulated lie in the range -2.98 ± 1.29 psi. This range of values is rather wide because of the low value for the 0.2% contour and the rather higher value for the 10% contour, the remainder of the values fall into a much narrower range. Unfortunately, because these values of the intercept on the p-axis are not measured data but have been deduced by the least squares procedure it is not valid to apply a simple calculation to determine confidence limits. However an indication that the values are distributed much more closely about the mean value than the above range suggests is given by noting that the range of values -2.98 ± 0.68 encompasses one standard deviation either side of the mean value. For a normal distribution 68% of the values lie in the range one standard deviation each side of the mean value.

In fact the way in which the value of this intercept is used in this thesis means that the range of ± 1.29 psi about the mean value is not so significant because the value of the intercept is added to the value of the p component of stress and so it is the range of values of $(p + 2.98) \pm 1.29$ psi that

is more relevant than the range for the intercept alone. In view of the range of the values given in Table 4.1 a value of 3.0 psi is used in the remainder of this thesis and it seems reasonable to assume that the value is constant and there is no significant tendency for it to change with stress or strain.

The fact that all these contours pass through (0.,-3.0) suggests that a new stress ratio might be more appropriate for describing the behaviour of this material. This is defined by:

$$\eta' = q/(p+3.0) \quad \ldots\ldots\ldots\ldots\ldots\ldots\ldots\ldots\ldots\ldots \quad (4.1)$$

This is in effect the same as moving the q axis in the stress space to the left by 3 psi. The contour for each axial strain value is associated with a definite value of η' and in Fig.4.6 these values of η' have been plotted against the corresponding total axial strain on a logarithmic scale. The curve can be divided into three distinct regions. There is one linear portion up to a strain of approximately 0.45%, after a transition this is followed by another linear region up to a strain of 5.5% after which there is only a small increase in η' for quite large increases in strain. The significance of the abrupt change in slope of this semilogarithmic plot at a strain of 0.45% is not clear at this stage. It may reflect some change in material behaviour but as there does not seem to be any other indication of this the possibility is not investigated here. On the other hand it may be simply a property of the type of

mathematical function needed to describe the $\eta'v\epsilon$ relation for this material. An example of such a phenomenon is the plot of settlement versus log(time) of the common one dimensional consolidation test. The primary consolidation phase consists of two linear portions separated by a fairly sharp transition, this transition is not associated with any change in the material behaviour. The points plotted in Fig.4.6 are the slopes of the strain contours plotted in Fig.4.5. In Fig.4.7 these same values are plotted on a natural scale for η'. The values plotted in Fig.4.6 are marked with the round points. Also at each point a bar has been added to show the range of values for η' at each strain for all the tests, this indicates that there is some scatter particularly at the lower strains. However the most significant aspect of this curve is that η' does not have any tendency to pass through a peak value and then decrease as does η.

4.6 RELATION BETWEEN THE ULTIMATE VALUE OF η' AND VOID RATIO

When describing the stress paths followed by the various tests it was mentioned that the tangent passing through the point (0.,-3.0) could be drawn to the end part of the stress path. Now that the modified stress ratio η' has been introduced it is worth examining its value for the end part of the stress path of each test. These values have been plotted against the void ratio in Fig.4.8. Despite some scatter, particularly in tests CSR 010 and STC 002, it is evident that there is a strong tendency for

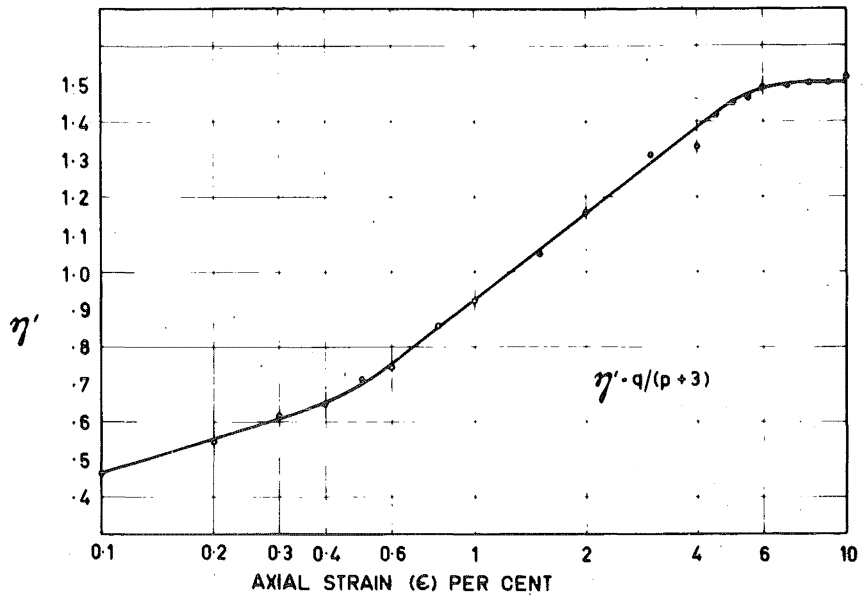

FIG. 4.6 SLOPE OF CONTOURS OF EQUAL TOTAL STRAIN FROM STRESS PATHS (LOGARITHMIC SCALE)

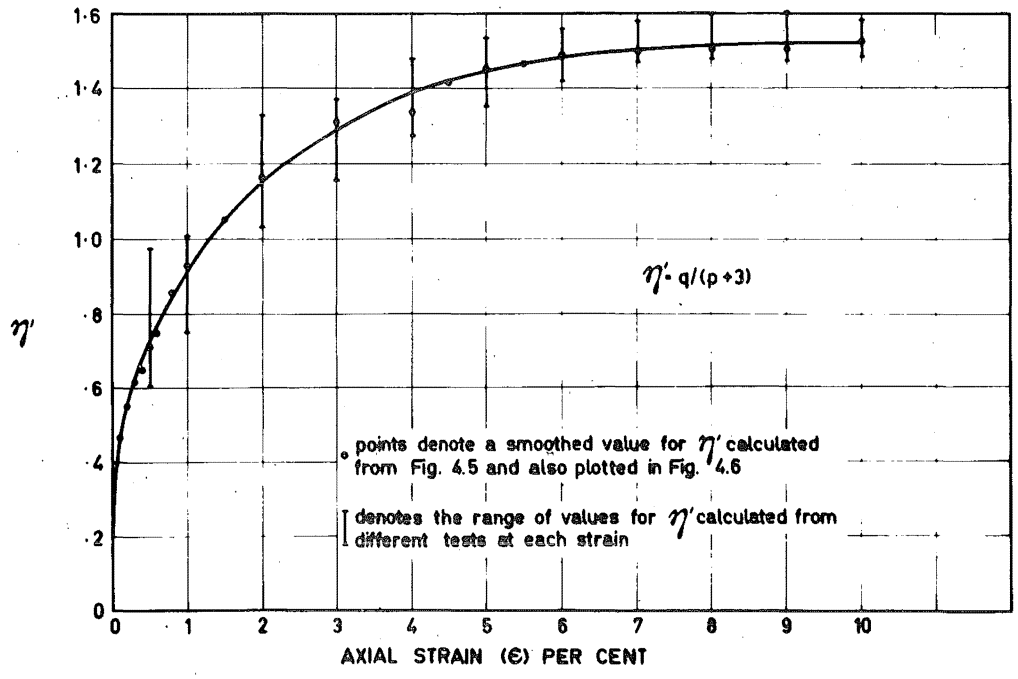

FIG. 4.7 SLOPE OF CONTOURS OF EQUAL TOTAL STRAIN FROM STRESS PATHS (NATURAL SCALE)

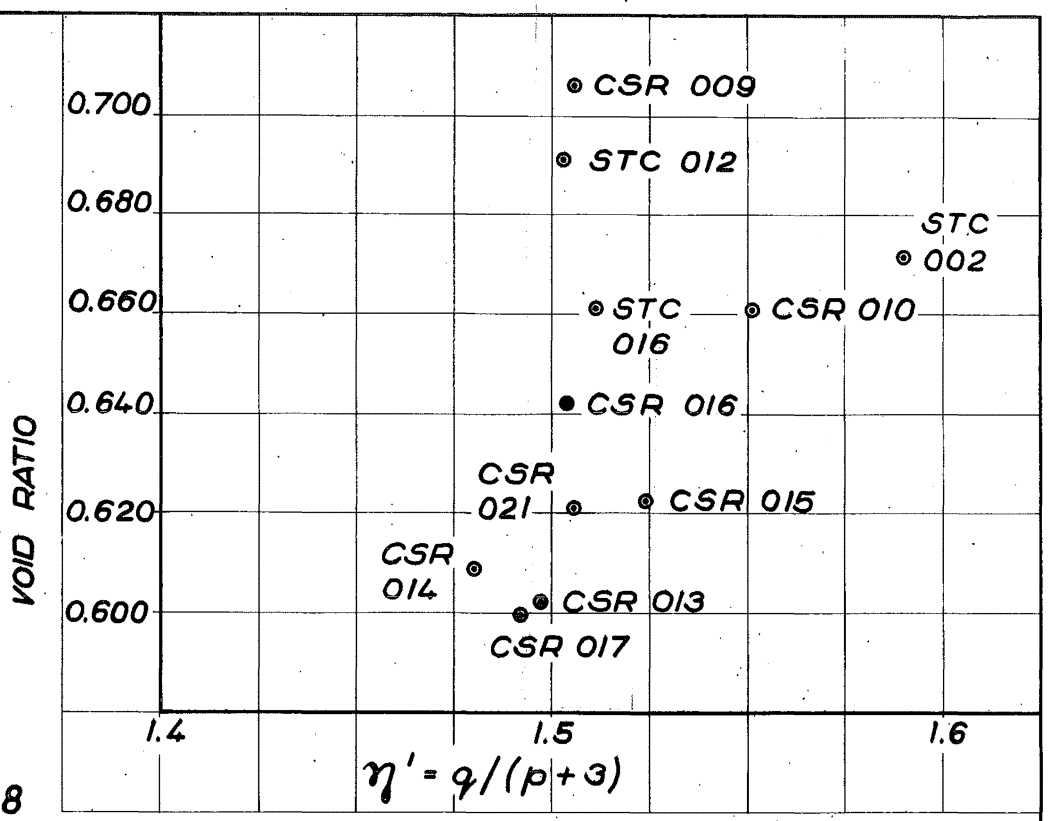

FIG. 4.8
VALUES OF η' ALONG FINAL PART OF STRESS PATHS

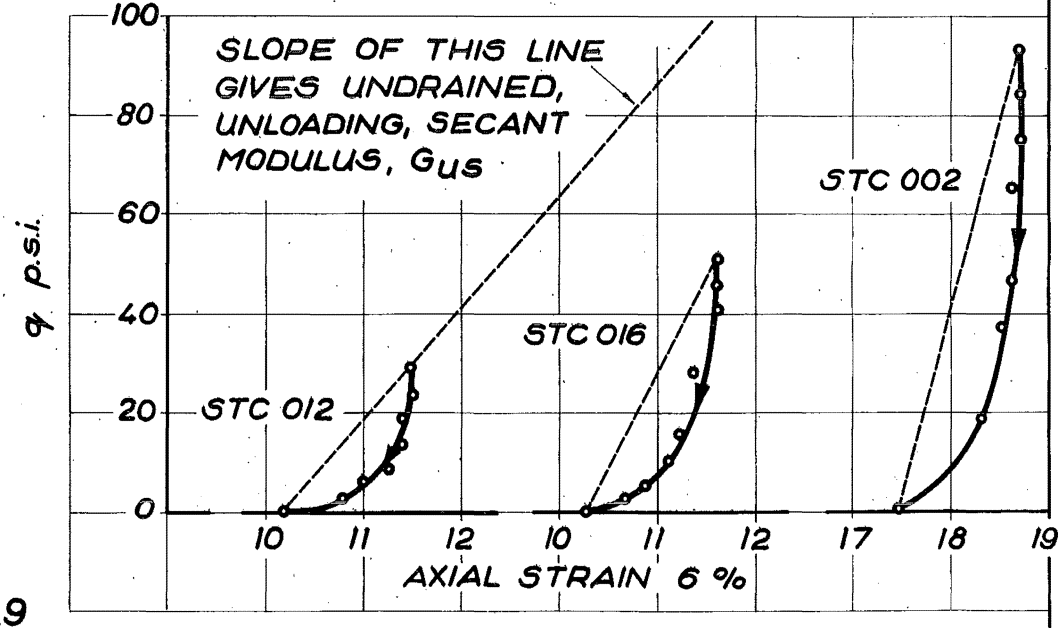

FIG. 4.9
SOME TYPICAL UNLOADING STRESS-STRAIN CURVES

the final value of η' to be independent of void ratio. The point for test STC 002 seems to lie so far away from the other values that it is probable that this sample was not representative and so its value of η' was discarded. The mean value and range for the other points is 1.51 ± 0.04.

4.7 UNLOADING BEHAVIOUR

The behaviour of the material when unloaded in an undrained test was examined in several ways. At the completion of most of the tests, i.e. when the axial strain had reached about 10%, the sample was unloaded in stages, and the recovery recorded. In each case a characteristic non-linear curve was obtained. Some typical results are shown in Fig.4.9.

In the remainder of this thesis only complete unloading, i.e. from a given value of q down to zero, is considered and the non-linear unloading stress-strain curves are characterised by the slope of the dotted straight lines between the ends of the curves in Fig.4.9. In other words the unloading behaviour is described by the secant modulus and this is denoted by G_{us}.

When this unloading modulus is determined for each of the tests discussed so far it is seen that the value of G_{us} increases as the consolidation pressure increases. This result is plotted in Fig.4.10, which suggests that there is a linear relation between the undrained unloading modulus and the consolidation pressure. Once again discarding the value from test

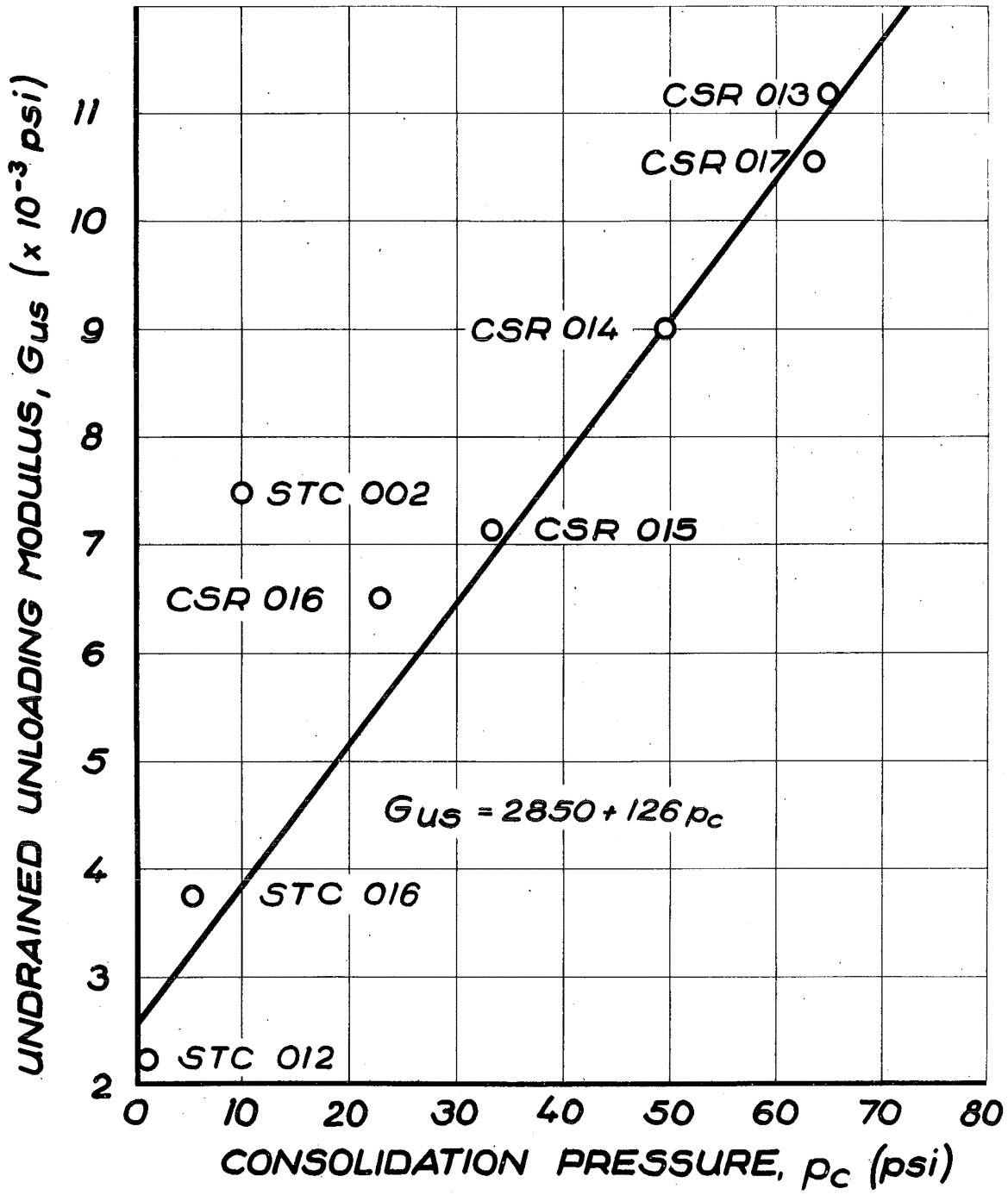

FIG. 4.10
VARIATION OF UNDRAINED, UNLOADING MODULUS WITH CONSOLIDATION PRESSURE

STC 002 which is apparently anomalous a least squares procedure was used to calculate a "best straight line" through the points. The equation of this line is:

$$G_{us} = (2850 + 126p_c) \text{ psi} \quad \ldots\ldots\ldots\ldots\ldots\ldots\ldots (4.2)$$

where p_c is the consolidation pressure to which the sample was subjected after compaction and back pressure saturation.

Next the variation of the unloading modulus when a sample was unloaded from various stress levels and strains was investigated. This was done in the test STC 004 (that is the fourth stress controlled test) in which a sample consolidated at 10 psi was loaded to various stress levels and unloaded before being reloaded to a higher stress level. The stress strain curve for this test, given in Fig. 4.11, shows that as before a non-linear recovery curve results on unloading and that the general shape of these unloading curves is similar for each cycle and apparently independent of strain. In Fig.4.13 the values of G_{us} for the various cycles have been plotted against strain. Unfortunately the scatter is fairly considerable, there being a factor of two between the smallest and largest values, although there does not seem to be any consistent tendency for the value of G_{us} to increase or decrease as the strain increases. The unloading curves in Fig.4.11 look as if they might have the form : $q = \epsilon_r^n$, where ϵ_r is the recoverable axial strain on complete unloading. The value of n can be determined by comparing the area under the

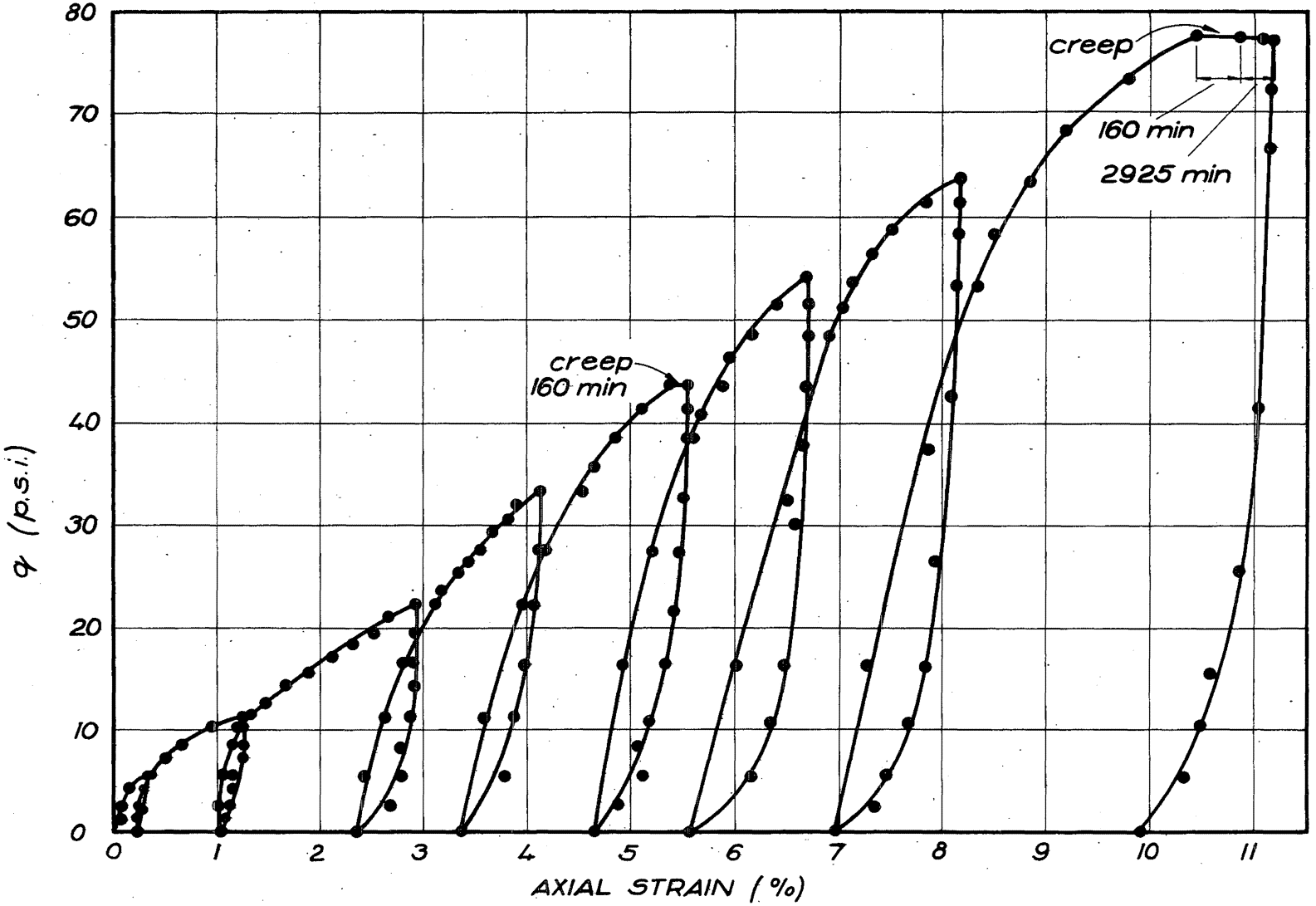

FIG. 4.11 STRESS STRAIN CURVE FOR TEST STC 004

unloading curve with that of the triangle beneath the straight line joining the point of maximum to zero stress. It is a property of a curve with the form $y = x^n$ that the ratio of the area under the curve to that of the triangle is $1/(n-1)$. The results are plotted out in Fig.4.14 and the average value of 0.5 suggests that the value of n is 3, i.e. the unloading curve is a cubic.

Having determined that the unloading modulus is proportional to the consolidation pressure and that it seems to be independent of q and ϵ, it now remains to investigate the behaviour of G_{us} when the sample is repeatedly loaded to the same value of q. The object of this is to determine whether the value of G_{us} determined by the initial unloading from a given stress includes some contribution from creep deformation. In test STC 001 a sample that had been consolidated to 10 psi was loaded and unloaded 8 times with a load of 40 lb (i.e. to a value of q_{max} about 22 psi) then 10 times with a load of 80 lb (q_{max} in the range 43-42 psi) and 4 times to 160 lb (q_{max} in the range 80 to 75 psi). The stress-strain curve for this test is plotted in Fig.4.15 while in Fig.4.17 the values of G_{us} for each cycle have been plotted. This demonstrates that G_{us} is constant for all unloading cycles from a given stress, although it does suggest that G_{us} increases slightly when q increases, contrary to Fig.4.13 where despite much scatter no tendency was evident.

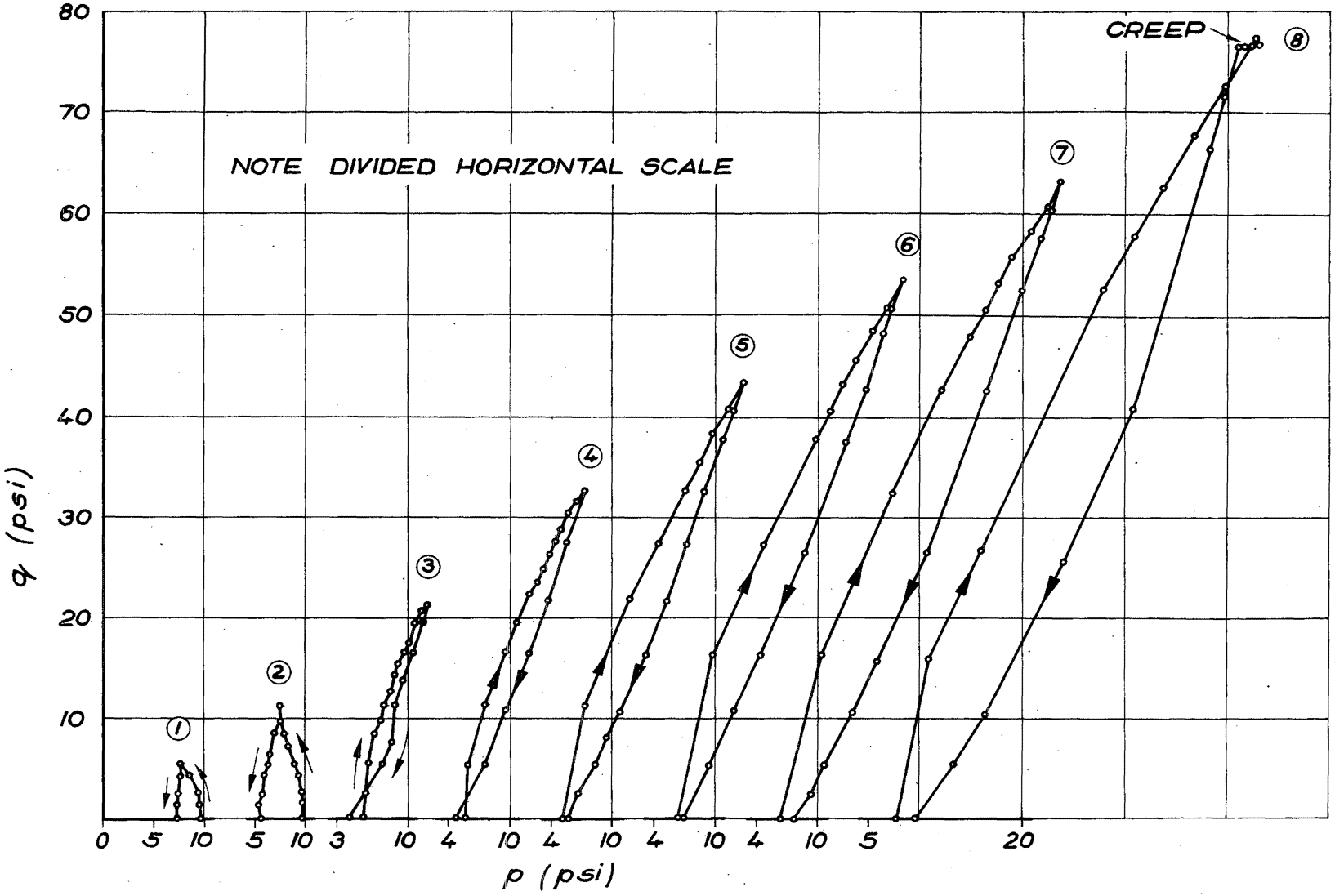

FIG. 4.12 STRESS PATH FOR TEST STC 004

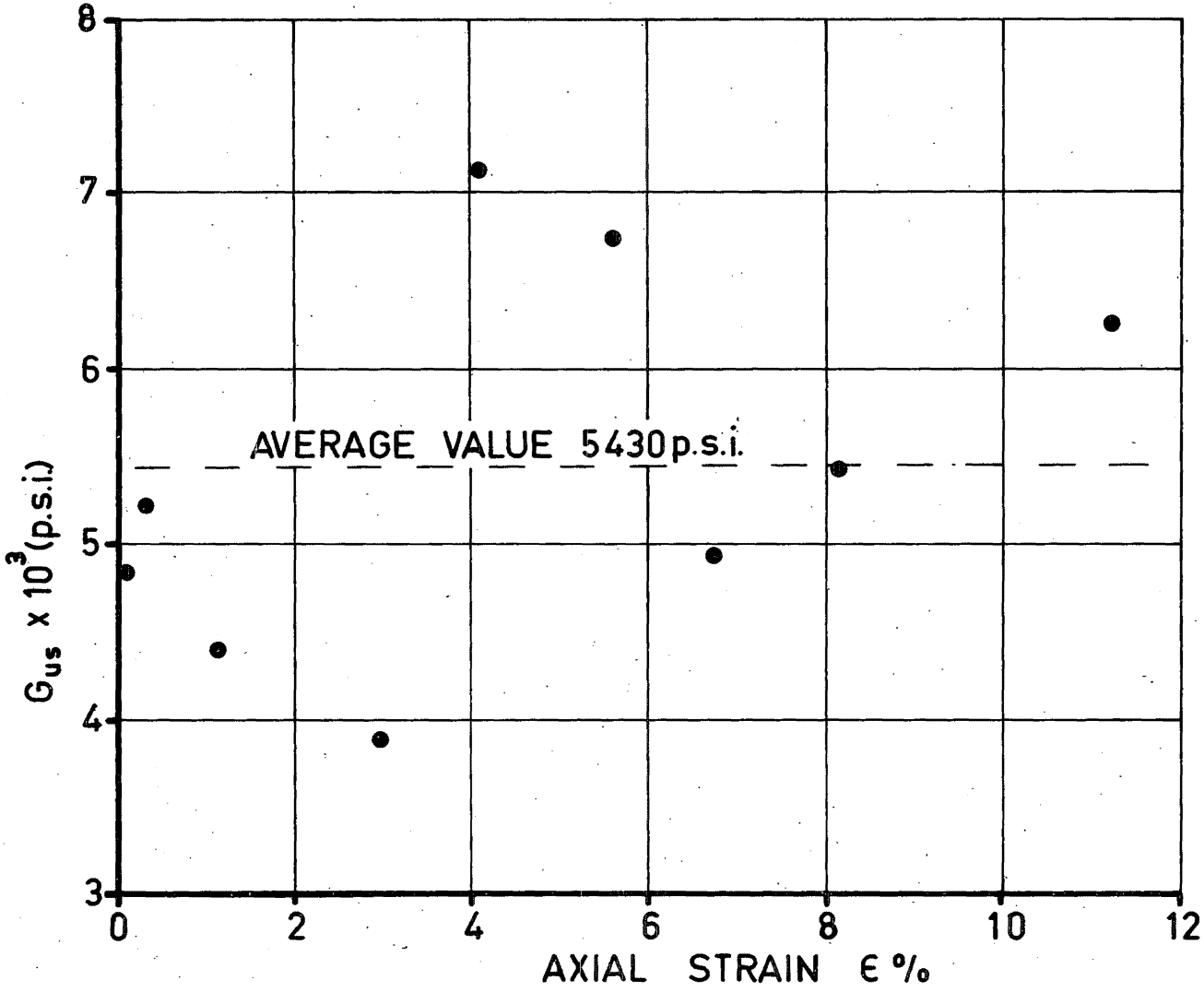

FIG. 4.13 VARIATION OF G_{us} WITH STRAIN FOR TEST STC 004

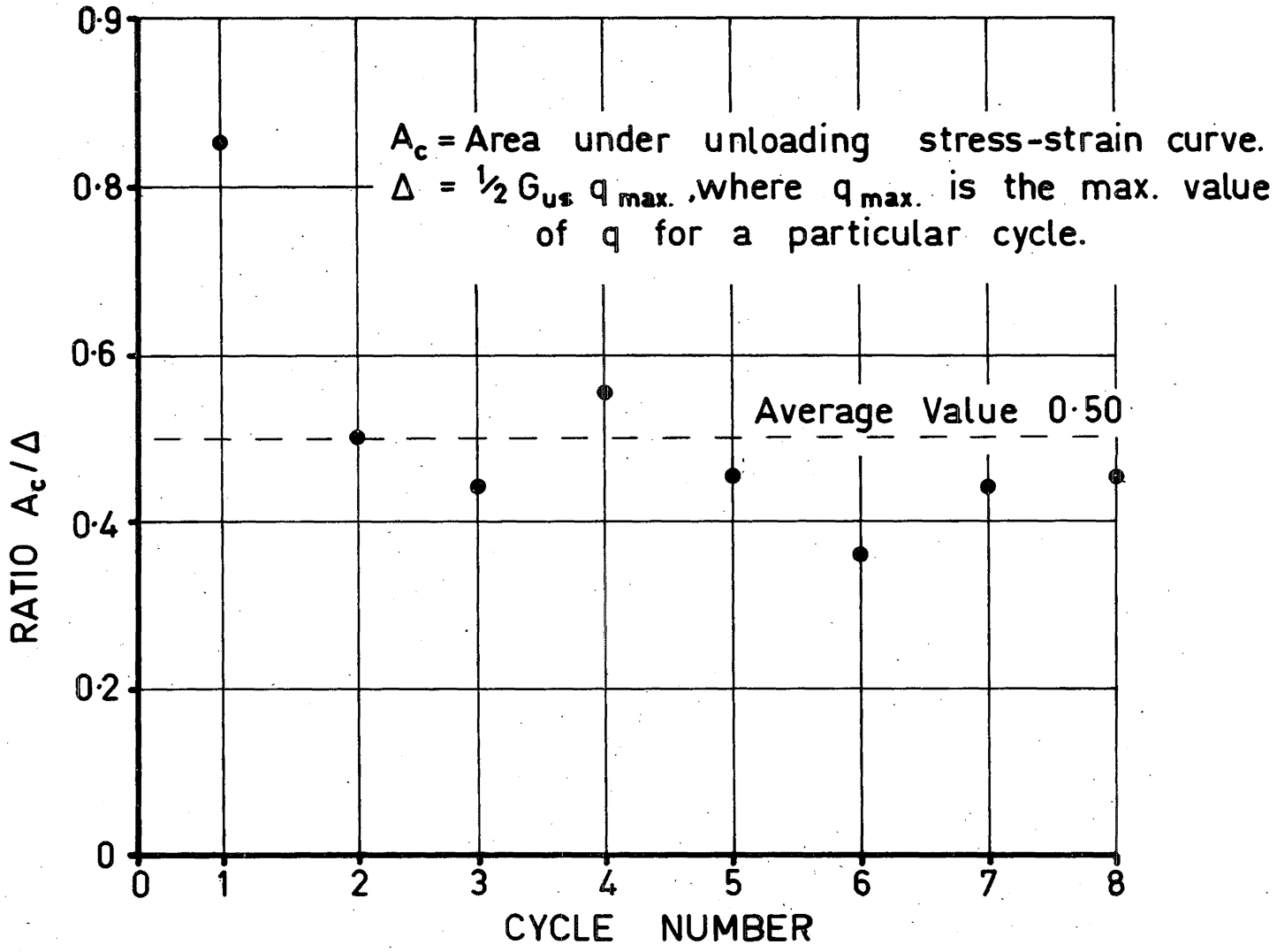

FIG. 4.14 SHAPE OF UNLOADING STRESS-STRAIN CURVES FOR STC 004

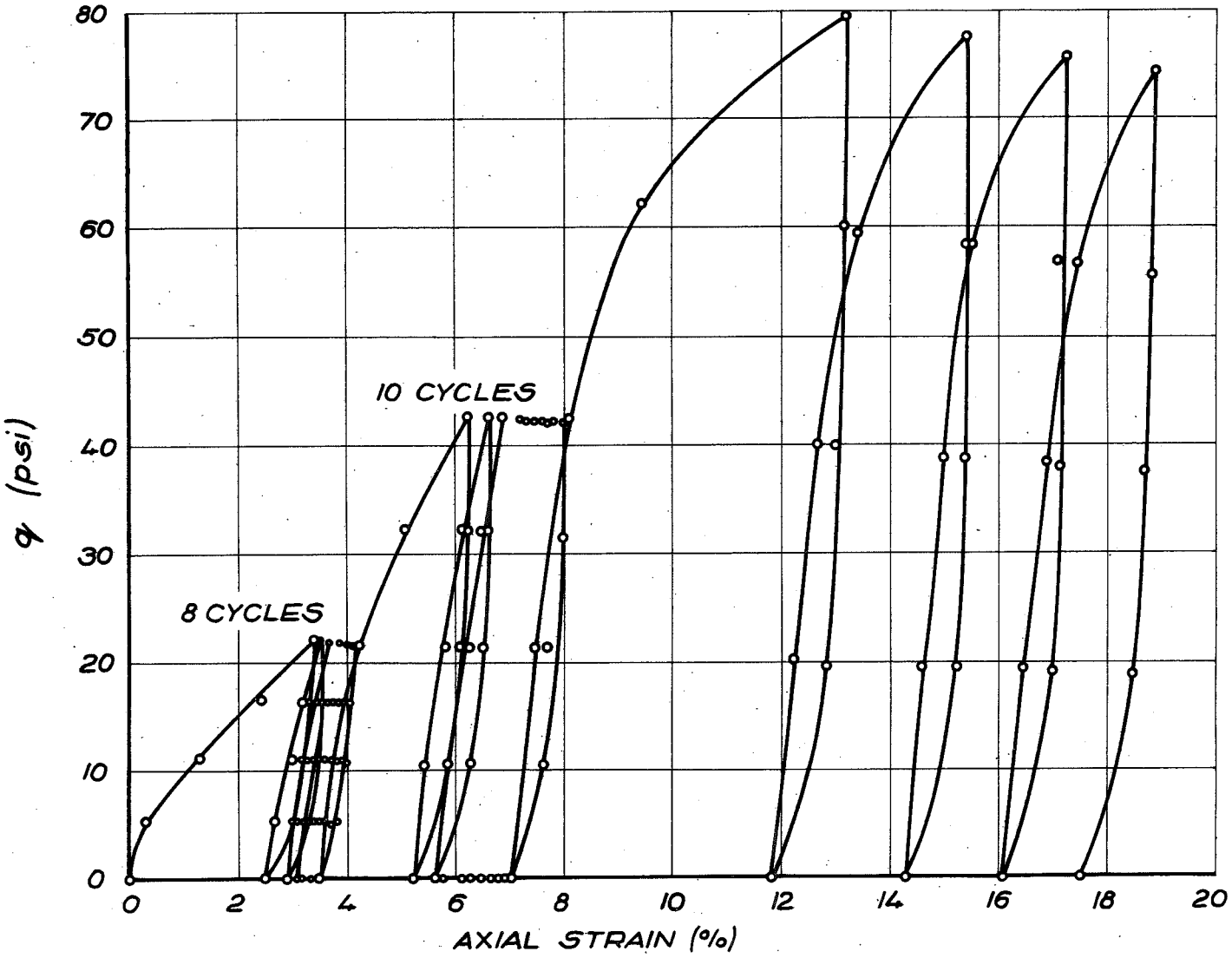

FIG. 4.15 STRESS STRAIN CURVE FOR TEST STC 001

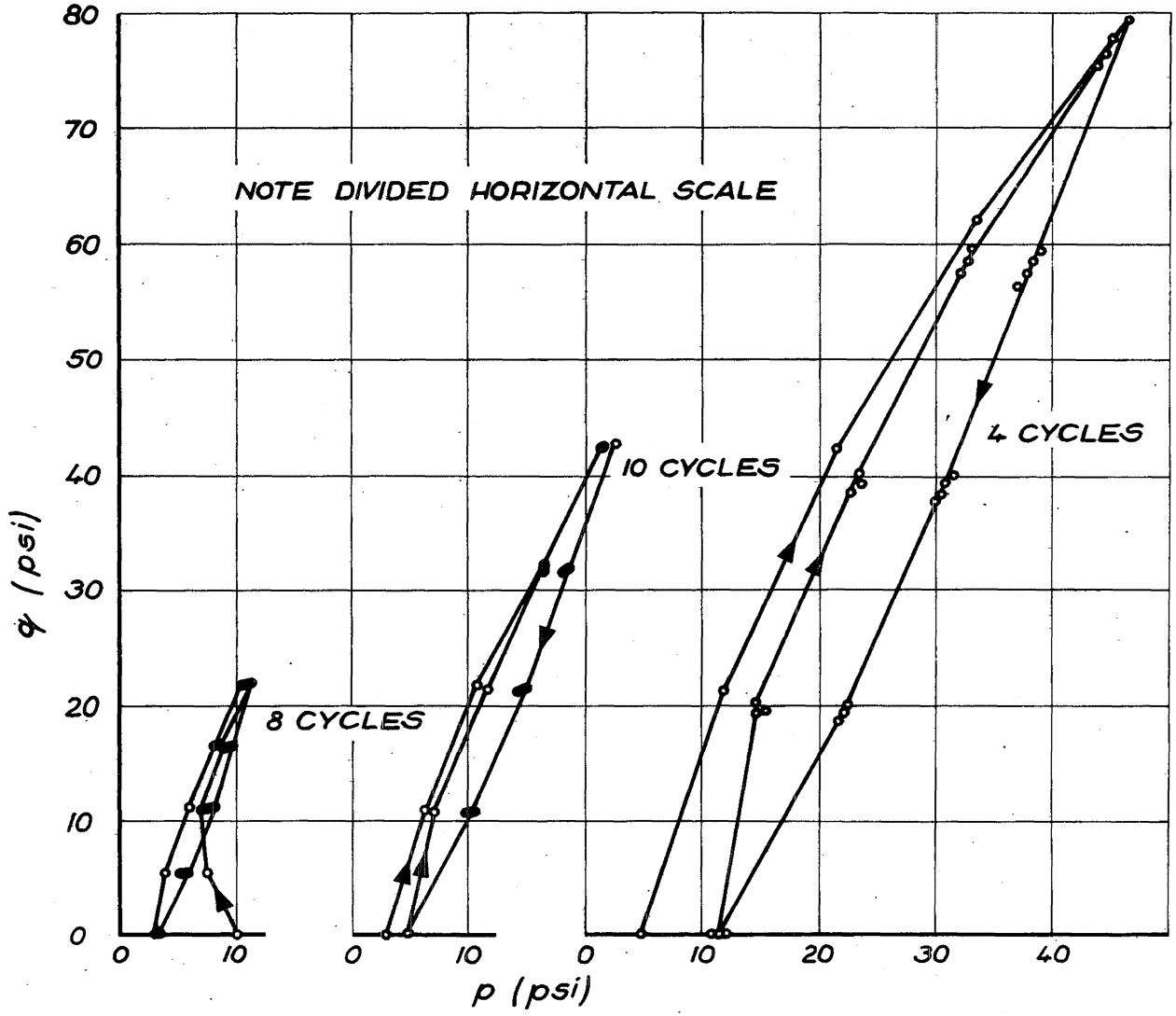

FIG. 4.16 STRESS PATH FOR TEST STC 001

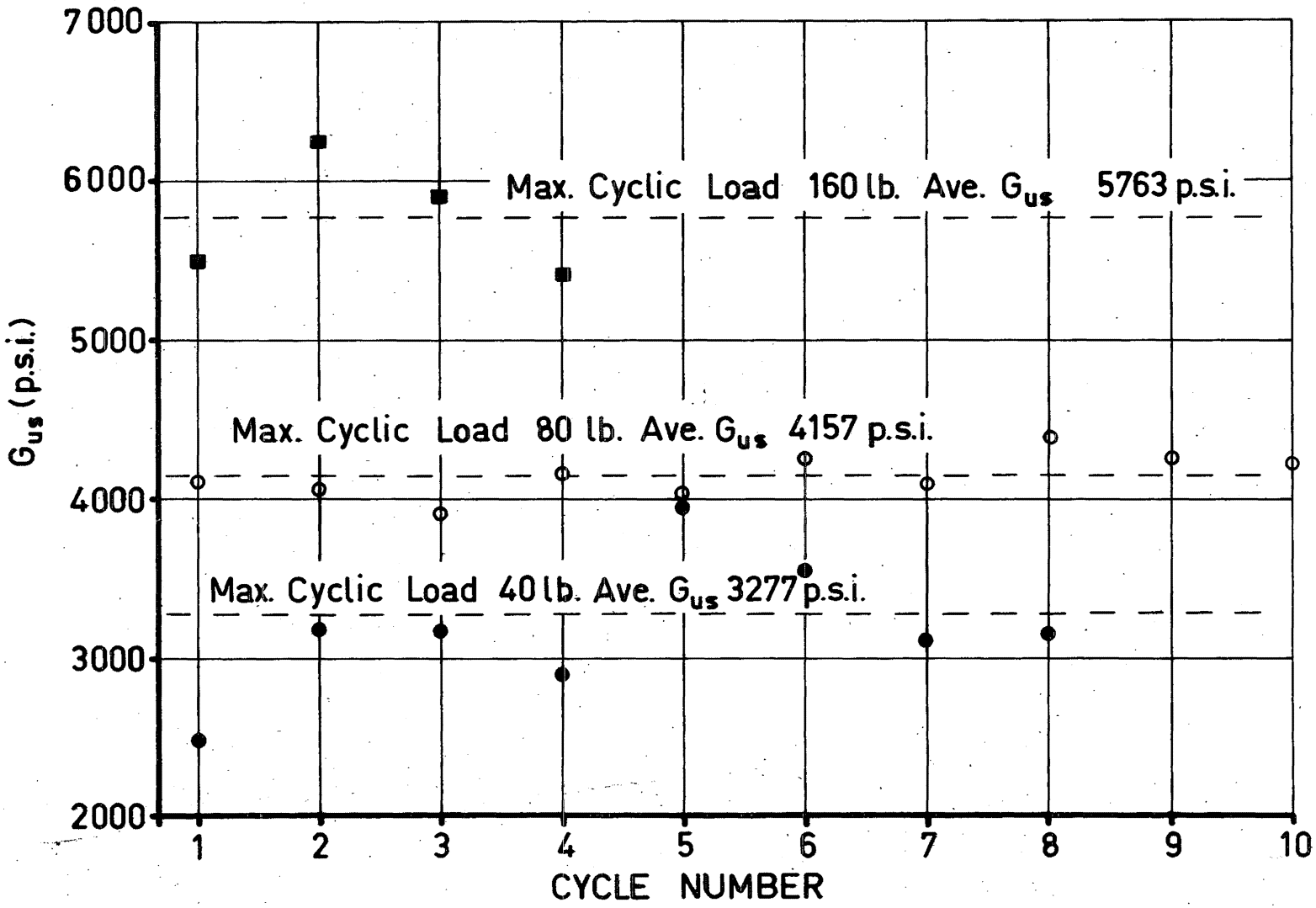

FIG. 4.17 VARIATION OF G_{us} FOR UNLOADING CYCLES OF STC001

The stress paths for these cyclic loading tests are given in Fig.4.12 and 4.16; they have been plotted on a divided horizontal scale to avoid the confusion that would result if the horizontal scale was continuous. In Fig.4.12 the stress paths for the load-unload cycles are almost closed except for those at the very beginning of the test where p decreases as the sample is loaded. The paths for STC 001 also have similar shape and likewise have been plotted on a divided horizontal scale. It is interesting to note that for each of the cycles to the same maximum load the stress paths are almost identical.

4.8 UNDRAINED STRESS PATHS IN TERMS OF DIMENSIONLESS PARAMETERS

It is possible to plot the stress paths in a three dimensional space with void ratio as one axis and q and p as the other two axes. If this is done the stress paths will define a surface in the (p, q, e) space. However, such a procedure is clumsy and it is not easy to interpret soil behaviour in terms of this three dimensional diagram. Roscoe and Thurairajah[66] have shown how it is possible to represent this three dimensional surface for normally consolidated clay as a unique two dimensional curve by plotting certain dimensionless parameters. The parameters they used were η (=q/p) and ξ defined by:

$$\xi = p/p_c$$

where p_c is the pressure at which the sample was consolidated before it was sheared. In the undrained tests discussed here

similar parameters are used: η' already defined in Eq.4.1

and

$$\xi' = (p+3.0)/(p_c+3.0) \quad \ldots\ldots\ldots\ldots\ldots\ldots\ldots\ldots \quad (4.3)$$

These curves have been plotted for most of the tests in Fig.4.18. This shows that all the points are grouped into a fairly narrow band so that one curve can be used to represent all the stress paths.

The curves plotted in Fig.4.18 provide another means of confirming the value of 3.0 psi used in defining η' and ξ'. Values of η' and ξ' were calculated for all the points with p increased by 2.0 psi rather than 3.0 psi and another set of values was calculated with p raised by 4.0 psi. Curves similar to those in Fig.4.18 were plotted and in each case there was a good deal more scatter so that the calculated points fall into a much wider band, particularly at low values of η'. Thus it seems that the η' v ξ' curve plotted in Fig.4.18 is reasonably sensitive to the stress component added to the value of p when calculating η' and ξ'. When a value of 3.0 psi is used as has been done in Eqs.(4.2) and (4.3) the best overall plot is obtained with least scatter. This provides further confirmation of the choice of 3.0 psi in section 4.5 where it was suggested that the average of the range of values -2.94 ± 1.29 psi is valid for the intercept of the contours of equal strain on the p-axis.

Hence it is suggested that the description of the stress-strain curves and the stress paths for this material can be

simplified by modifying the value of the stress component p by the addition of 3.0 psi. This results in the single η' v ϵ curve for all the stress-strain curves and the single η' v ξ' curve for all the stress paths. The value of 3.0 psi has been determined independently in three ways. Firstly the final section of each stress path was tangential to a straight line passing through the point q = 0 and p = -3.0 psi. Secondly the contours of equal total strain were seen to be approximately linear. The intercept of each of these contours on the p-axis was calculated by the least squares procedure and although there was some scatter the average value was -3.0 psi. Finally the η' v ξ' plot was found to be sensitive to the value by which p was increased when calculating η' and ξ' and that the best overall curve was obtained when a value of 3.0 psi was used.

In Fig.4.18 only those tests with consolidation pressures greater than 10 psi are plotted. Now in Fig.4.19 the solid line gives the smoothed curve from Fig.4.18 and the plotted points are for tests STC 012 and STC 016 which were consolidated at 0.90 psi and 5.36 psi respectively. These two tests deviate from the points in Fig.4.18 quite considerably: thus the idealised relation between η' and ξ' is used only for samples consolidated at pressures greater than 10 psi. The divergence for tests STC 012 and STC 016 is considered in Chapter 5.

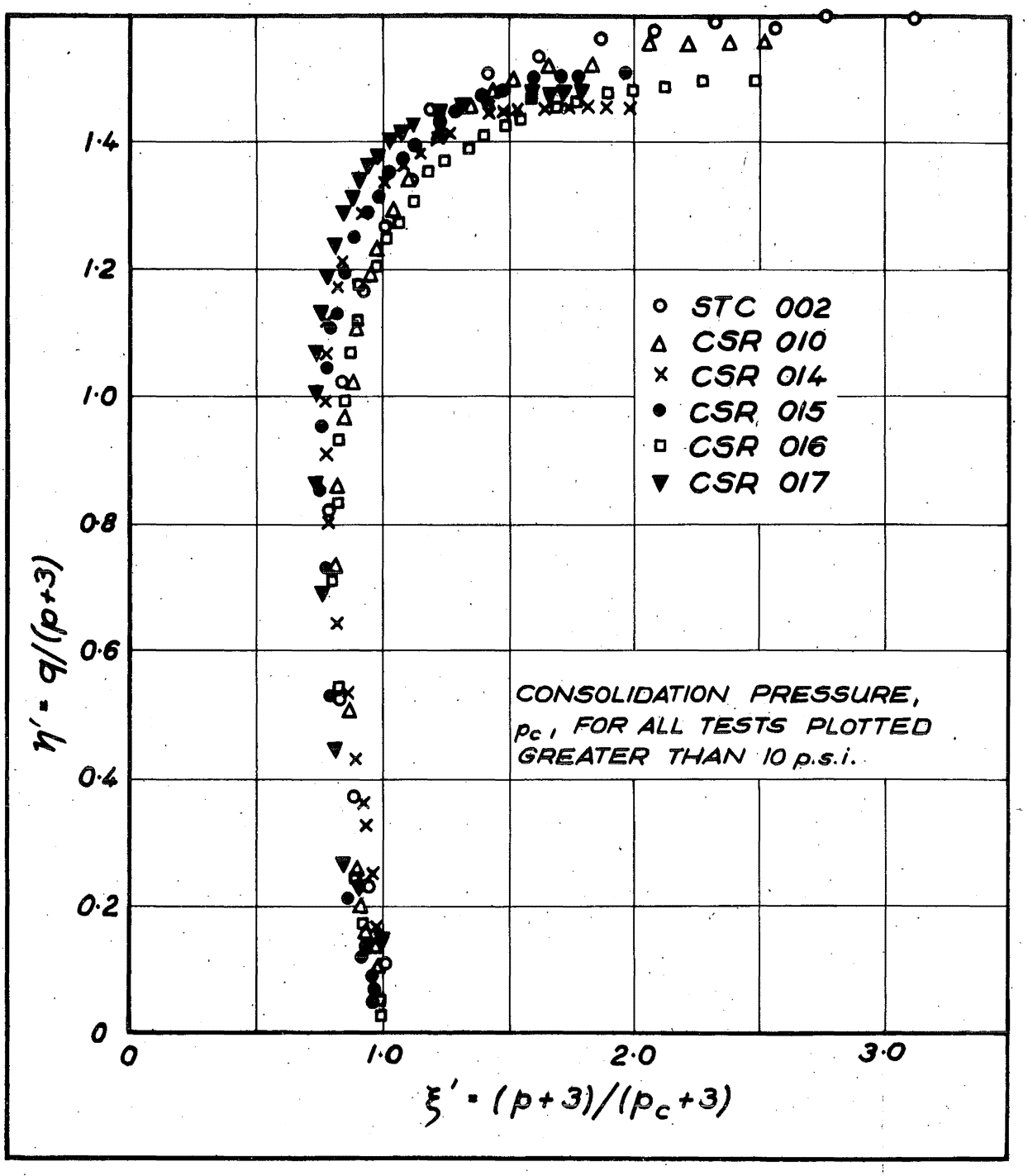

FIG. 4.18 UNDRAINED STRESS PATHS IN TERMS OF DIMENSIONLESS PARAMETERS η' AND ξ'

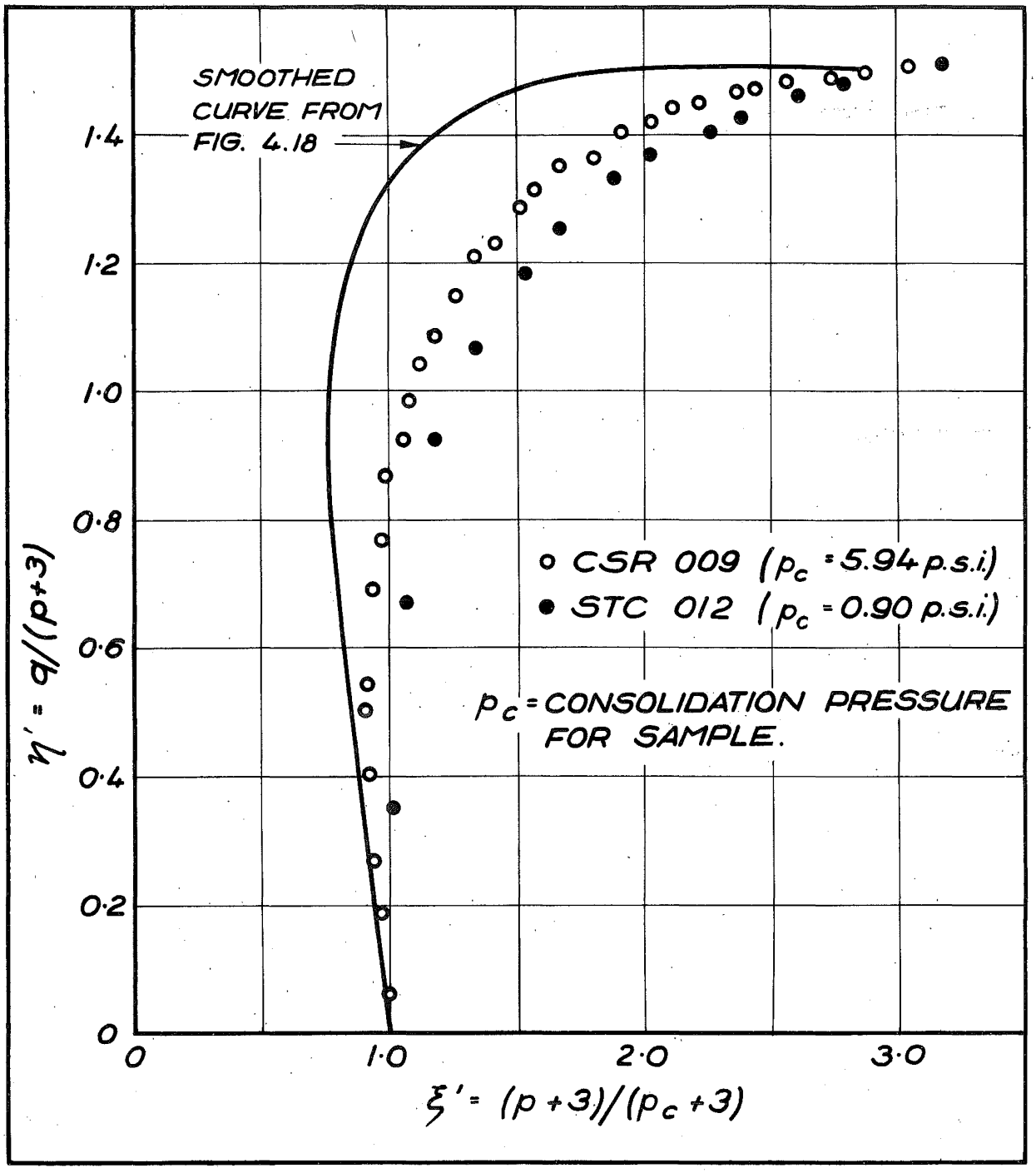

FIG. 4.19 UNDRAINED STRESS PATHS FOR TESTS WITH CONSOLIDATION PRESSURES LESS THAN 10 p.s.i.

4.9 UNDRAINED UNLOADING STRESS PATHS

In Section 4.7 the magnitude of the axial strain recovered when the samples were unloaded, under undrained conditions, was discussed. In this section the shape of the stress path during this undrained unloading process is described. Fig.4.12 shows how the shape of these unloading parts of the undrained stress paths varies with increase in the value of q reached before unloading. These successive unloading cycles show that in all cases there is a decrease in p on unloading, and that the decrease tends to be greater with increase in the value of η' to which the sample was loaded. The shape of the loading portion of the stress paths was discussed in the previous section using the dimensionless parameters η' and ξ'. One more dimensionless parameter is now introduced to describe the form of this unloading portion. The essentials of this are illustrated in the following diagram, Fig.4.20.

The intention of this section is to relate the change in p on unloading, $(p_{max} - p_{ul})$ to ξ' and p_{max}. The new dimensionless parameters ζ' is now defined:

$$\zeta' = \frac{(p_{max} - p_{ul})}{(p_{max}+3.0)} \quad \ldots\ldots\ldots\ldots\ldots\ldots\ldots\ldots\ldots\ldots \quad (4.4)$$

For all the tests on which unloading data were recorded the values of ζ' for each unloading cycle have been plotted against the value

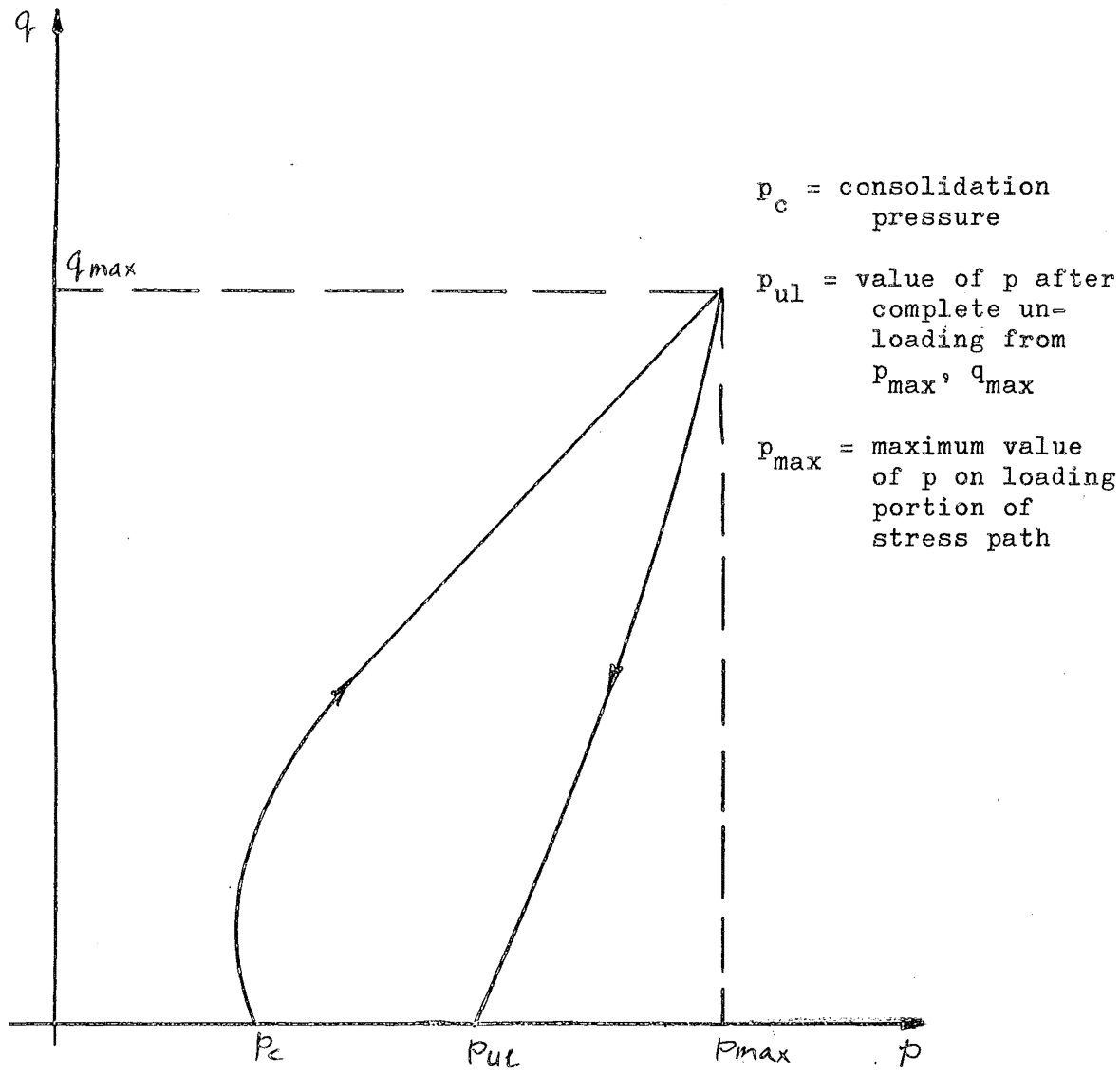

FIG.4.20 LOADING AND UNLOADING UNDRAINED STRESS PATHS

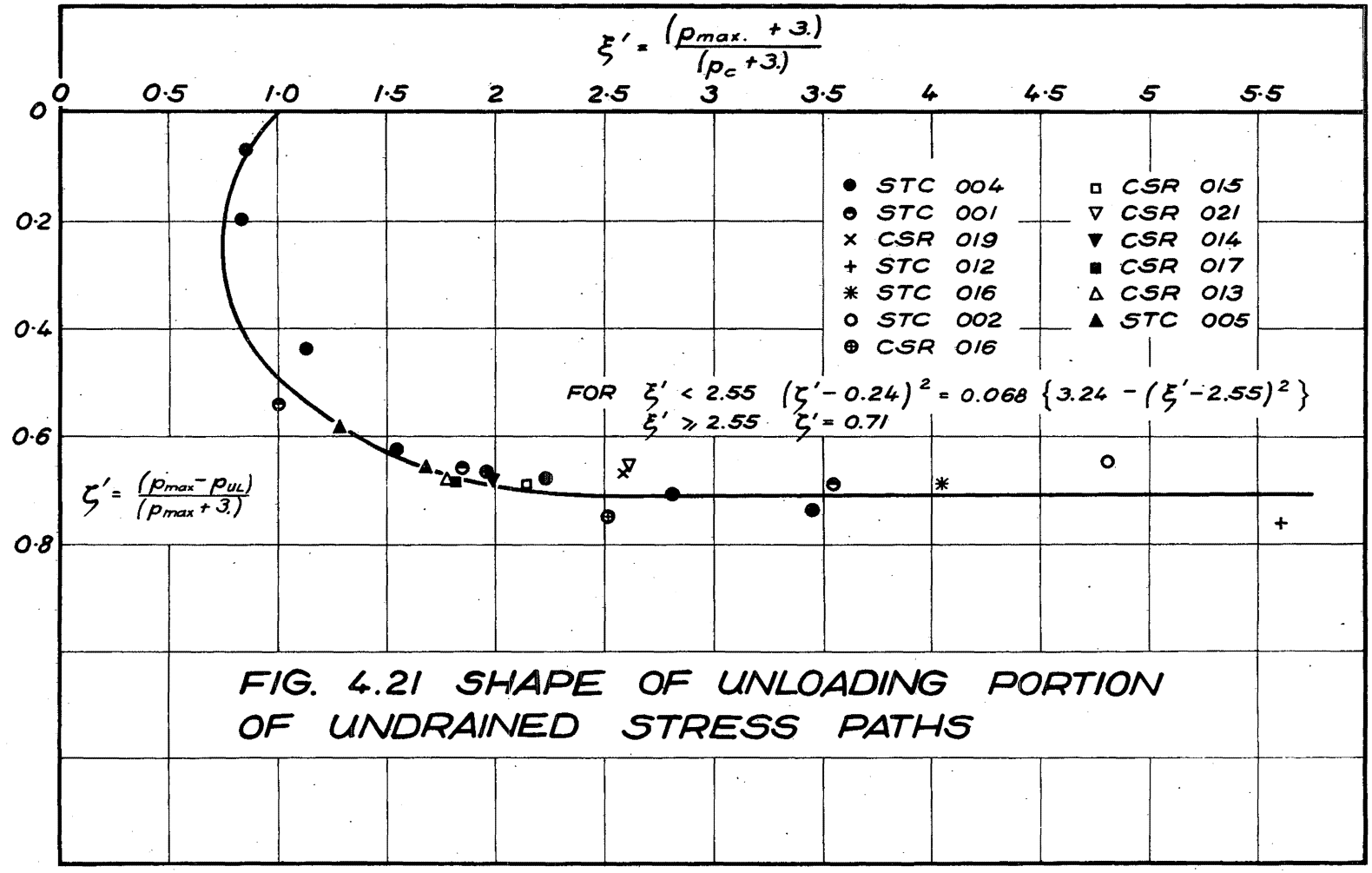

FIG. 4.21 SHAPE OF UNLOADING PORTION OF UNDRAINED STRESS PATHS

of ξ' for the stresses at the beginning of the unloading phase in Fig.4.21. This graph shows a uniform trend. The major features of the curve are defined by the eight points furnished by test STC 004. The remainder of the points provided by the unloading portions of the remainder of the tests confirm that this curve is characteristic of the material and not of test STC 004.

The curve can be divided into two portions. The initial curved portion for ξ' values less than 2.55 which is approximately elliptical and the final portion for ξ' values greater than 2.55 when ζ' is constant at 0.71. This is expressed as:

$$(\zeta' - 0.24)^2 = 0.066 \left\{ 3.35 - (\xi' - 2.55) \right\}^2 \text{ for } \xi' < 2.55$$

$$\zeta' = 0.71 \text{ for } \xi' \geqslant 2.55 \qquad \ldots\ldots\ldots\ldots (4.5)$$

In the next chapter this parameter ζ' will be used in calculating the plastic volumetric strain along an undrained stress path.

4.10 SAMPLES ALLOWED TO SWELL AFTER INITIAL CONSOLIDATION

All the test results considered so far have been from undrained tests on samples which have been consolidated to a given pressure and then loaded. Two special tests were made in which the samples were allowed to swell under a lower pressure after the initial consolidation and then loaded. The first of these, CSR 019, was consolidated at 63.45 psi and then rebounded to 32.59 psi and the second, CSR 020, was allowed to swell under 12.69 psi after initial consolidation at 47.60 psi. The final

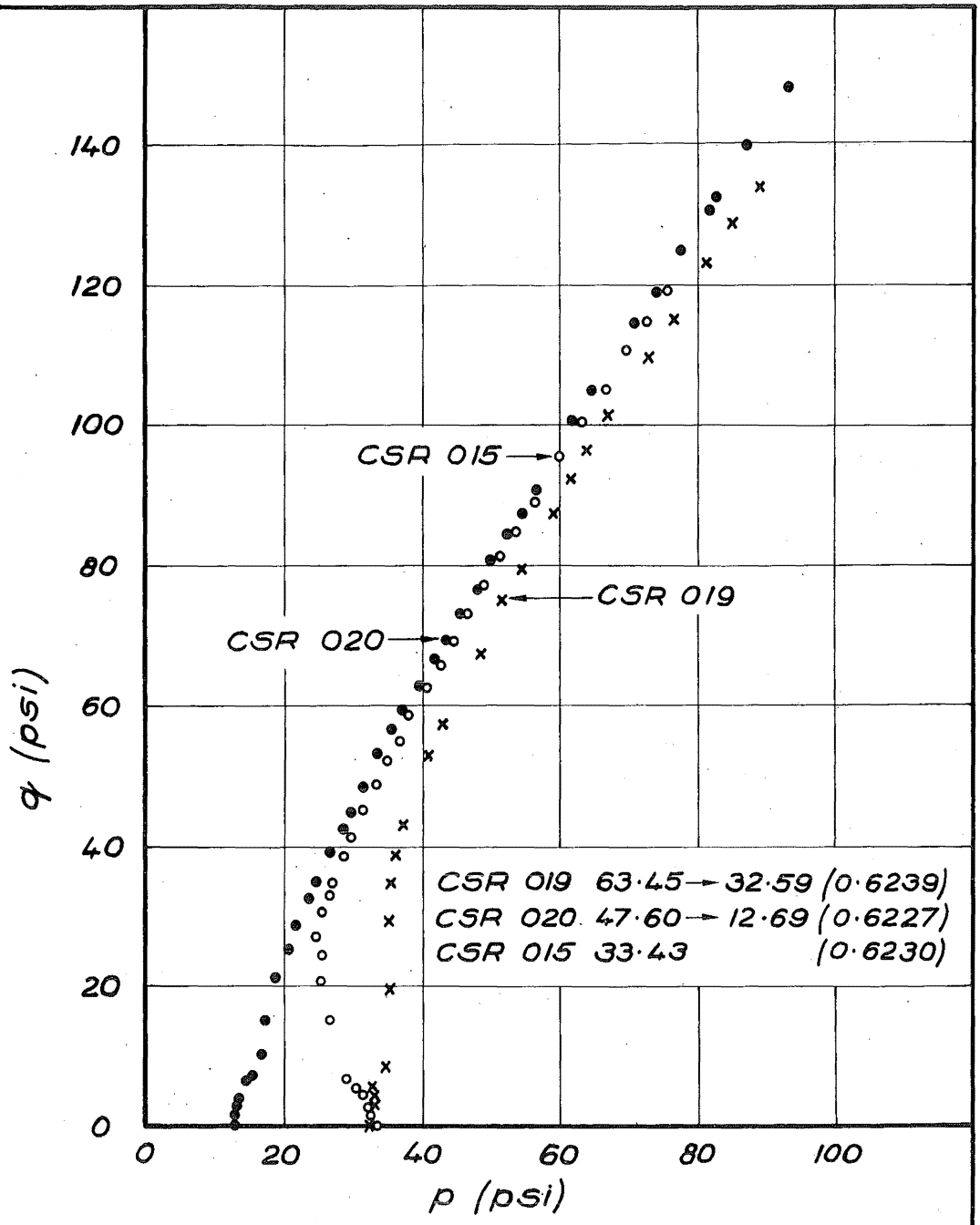

FIG. 4.22 STRESS PATHS FOR TESTS CSR 020, CSR 019 & CSR 015

void ratios of these samples were very close: 0.624 for CSR 019 and 0.623 for CSR 020. Tests such as these would normally be classed as overconsolidated, but this term has been avoided here because even when not allowed to swell to a lower pressure the samples behave as if overconsolidated.

The stress paths for the tests have been plotted in Fig.4.22 and for comparison the stress path for CSR 015 has been included. The void ratio of test CSR 015 was 0.623, so that the void ratios of all three tests shown in this diagram are very nearly the same. The shape of the stress paths for the two tests allowed to swell to lower consolidation pressures before loading are slightly different to that of CSR 015. However the tendency noted in Section 4.3 for the ultimate portions of the stress paths to lie along a unique line is repeated with these tests. But in this case the contours of equal total axial strain from section 4.5 do not apply. This is illustrated in Fig.4.23, where the η'v ϵ curve for test CSR 019 is compared with the curve from Fig.4.7. It is apparent from this diagram that in the early stages of the test sample CSR 020 is a great deal stiffer than CSR 015 for a given value of η' but that at the later stages the two curves converge.

The value of the unloading modulus for each of the tests is: CSR 015, 7135 psi, CSR 019, 7285 psi and CSR 020 6850 psi. The similarity of these values suggests that G_{us} might be a function of void ratio rather than consolidation pressure as

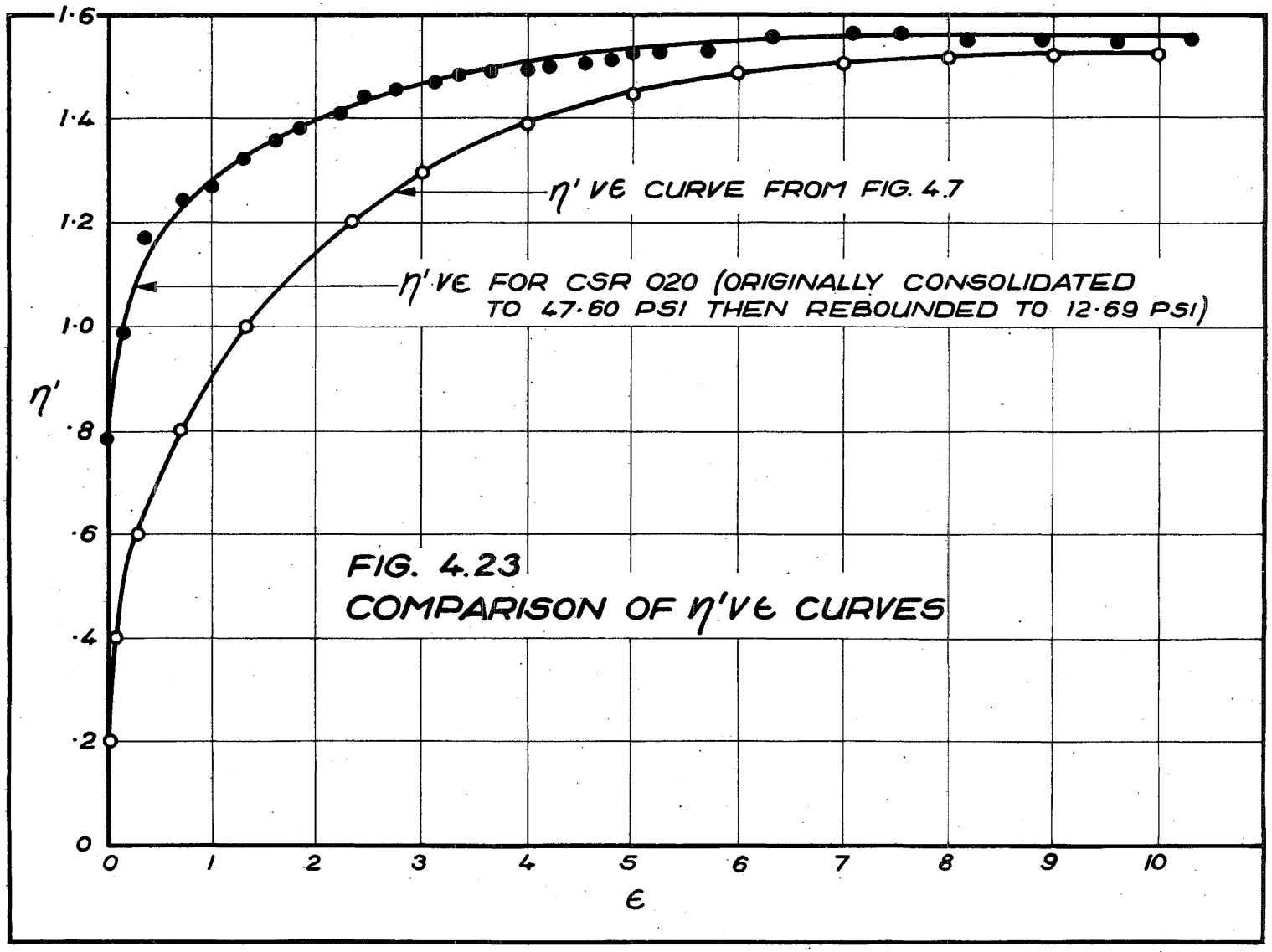

FIG. 4.23
COMPARISON OF η' VE CURVES

suggested in section 4.7. Of course this comment does not imply that there is anything incorrect about the relation between G_{us} and p_c given in Eq.(4.2) because there is a well defined relation between the void ratio and the consolidation pressure given in Appendix A and Fig.4.27. However if it was confirmed by a more extensive series of tests that G_{us} was a unique function of void ratio the very useful result that it was not dependent on consolidation history would follow.

4.11 CREEP BEHAVIOUR

On several occasions samples were left under constant load for some time to examine the creep behaviour of the soil. In all cases undrained creep effects were found to be of little significance. For example the stress-strain curve for test STC 004 given in Fig.4.10 shows that there is definitely some creep deformation when constant load is maintained. However the rate at which this deformation proceeds decreases rapidly. On the final load cycle the amount of creep deformation in the first 160 minutes of sustained load was 0.4% while a further 2925 minutes was then required for the creep strain to increase by another 0.3%. Another example is test STC 012 in which the sample was left under load for nearly six days (8320 mins.) during which time the axial strain increased from 10.80% to 11.47%. However for the final $3\frac{1}{2}$ days the strain remained virtually constant.

It is possible that this lack of continuous creep deformation under constant undrained load might be associated with the increase in p that accompanies an increase in strain. Thus any tendency for the sample to creep under constant load will be stabilised because of the corresponding tendency for p to increase, consequently it might be more appropriate to investigate the creep of this material under drained rather than undrained conditions.

4.12 DRAINED SHEAR TESTS

In addition to the undrained test so far described two drained tests were performed on the soil. Although the majority of the work reported in this thesis is on undrained tests it was felt to be worthwhile to do a few drained tests to get some idea of how the soil behaves when subjected to different stress paths and also to check how the concept of stability is fulfilled under this type of stress path. Two tests were performed. DSC 001 was initially consolidated after back pressure saturation under a pressure of 20.55 psi to a void ratio of 0.626 and DSC 002 was consolidated at 35.79 psi to a void ratio of 0.612.

The stress strain curves for these two tests are plotted in Fig.4.24 and are of a quite different form to those for the undrained tests plotted in Fig.4.1. Two features distinguish these stress-strain curves from the undrained tests. The curves do not have the changes in curvature and points of inflection of the undrained tests, and also they reach a maximum

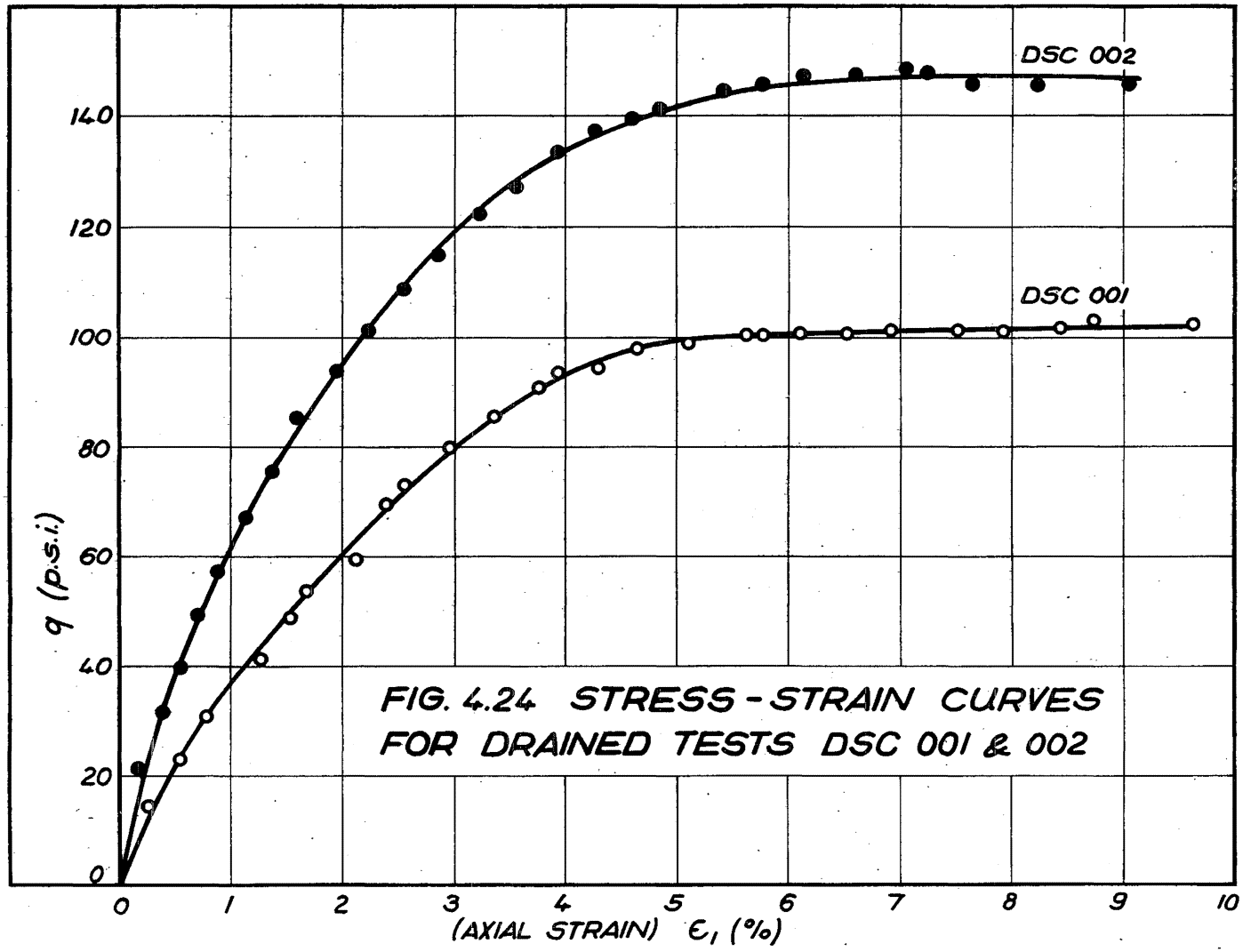

FIG. 4.24 STRESS - STRAIN CURVES FOR DRAINED TESTS DSC 001 & 002

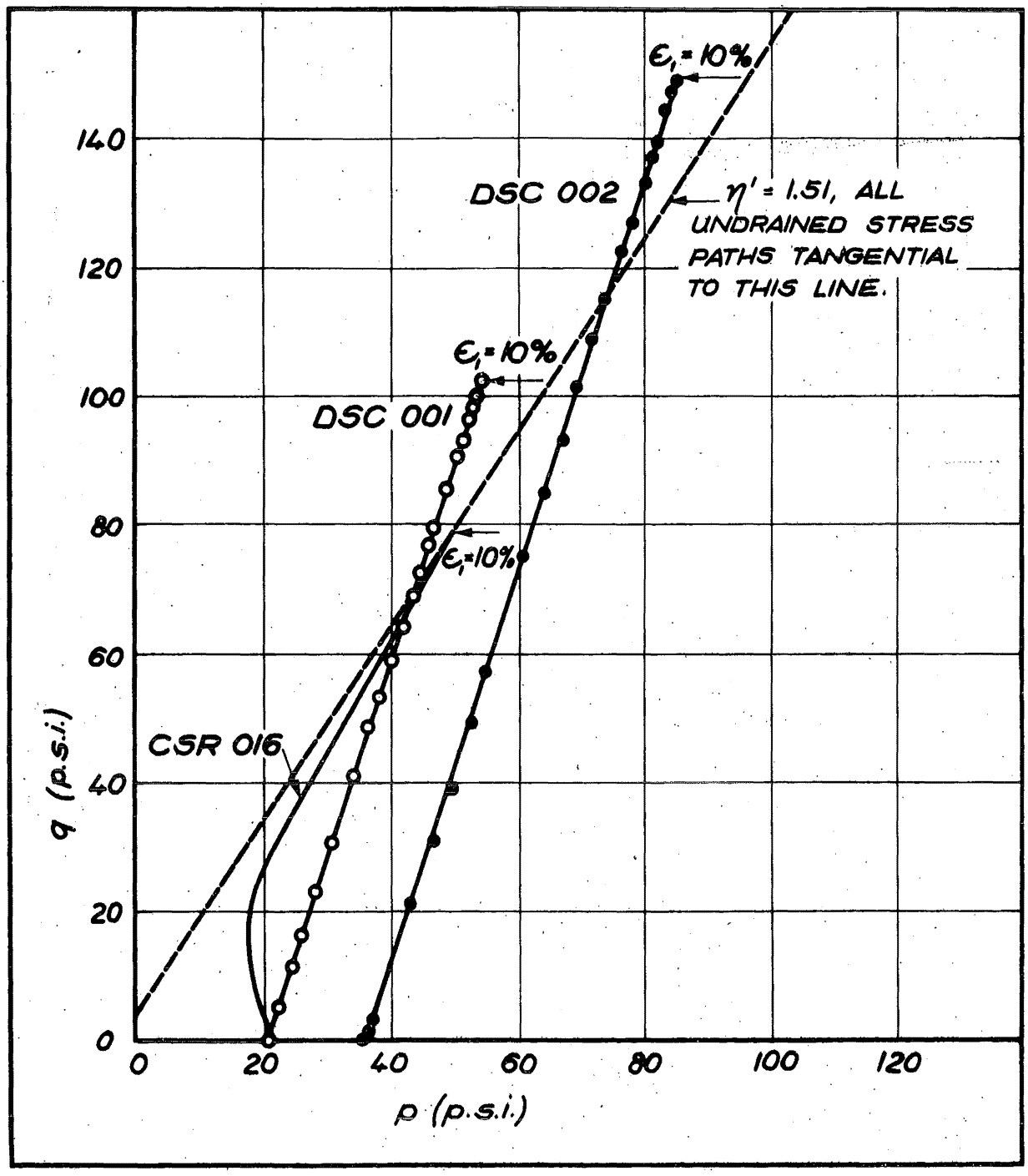

FIG. 4.25 STRESS PATHS FOR DRAINED TESTS DSC 001, DSC 002 & UNDRAINED TEST CSR 016.

value of q that remains constant as the strain increases. It is significant that this maximum stress is held while the strain increases by several per cent and that there is no marked tendency for it to decrease. The points do show a slight tendency to fluctuate but it can be seen that there is no general tendency for q to decrease as the strain increases. This is important for deciding if the deformation is stable.

The stress paths for the two tests have been plotted in Fig.4.25. Because σ'_3 remains constant in a drained test the stress path has a slope of 3 in a (q,p) diagram. To aid comparison with the undrained tests a typical undrained stress path, that for test CSR 016, has also been plotted and also the line with $\eta' = 1.51$ which is tangential to the undrained stress paths. This diagram clearly shows that the end points of the drained stress paths lie above the contour of 10% axial strain for the undrained tests and indicates that the stresses required for the drained tests to reach an axial strain of 10% are somewhat larger than those required for the undrained tests. This aspect is discussed further in Chapter 5.

The final diagram presented for these two drained tests is a plot of the ratio $\Delta e/(1+e)$ versus axial strain ϵ_1, in Fig.4.26. This ratio is a measure of the volumetric strain undergone by the samples during shearing. The upper half of the graph, where the sign of $\Delta e/(1+e)$ is negative, shows where there is a net increase in sample volume. It is seen how sample DSC 002 with a higher consolidation pressure shows a lesser tendency to increase in

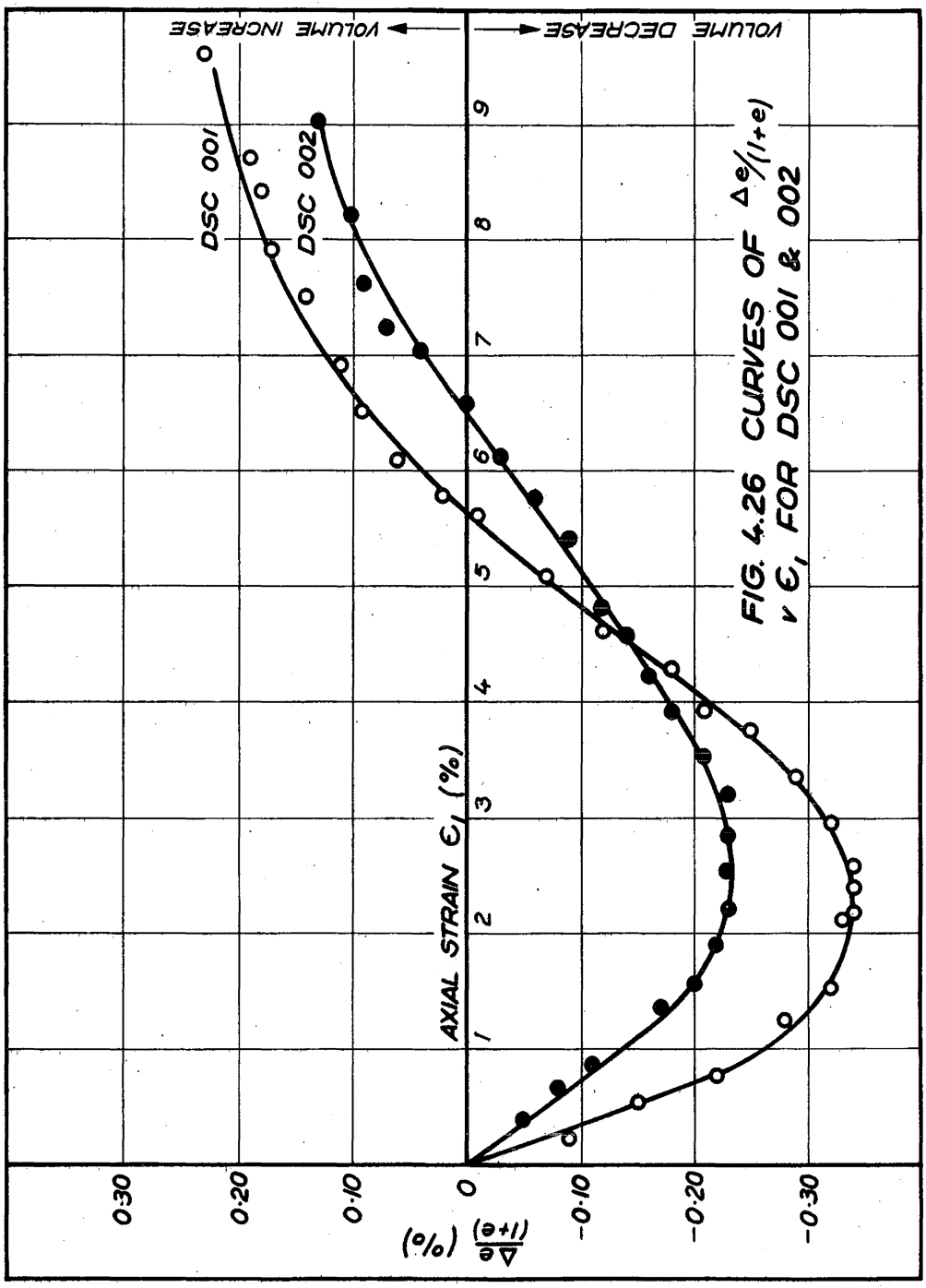

FIG. 4.26 CURVES OF $\Delta e/(1+e)$ v ϵ_1 FOR DSC 001 & 002

volume at large strains.

4.13 UNIFORMITY OF SAMPLES TESTED AND EXPERIMENTAL ERRORS

The results presented so far in this chapter fall into a fairly consistent pattern. However there is some scatter and it is the purpose of this section to examine whether this scatter could be a result of any variability in the method of sample preparation or a consequence of errors in measurement. This topic is considered under three headings. Initially the uniformity of the "as compacted" samples is considered. This is followed by a brief consideration of the accuracy of the various measurements taken and finally consideration is given to errors involved because of the assumptions on which the measurements are reduced to stresses and strains.

(i) Uniformity of Samples

It is well known that as a method of sample preparation compaction tends to produce more variable results than do other methods such as consolidation from a slurry. In Fig.4.27 the void ratio of the samples from the undrained tests is plotted against the consolidation pressure on a logarithmic scale. The void ratios were calculated, on the assumption that the sample was saturated, from the two smallest of the three final moisture contents. The figure shows that for the higher consolidation pressures the points fall along a reasonably well defined straight line. But for consolidation pressures up to 10 psi there is a

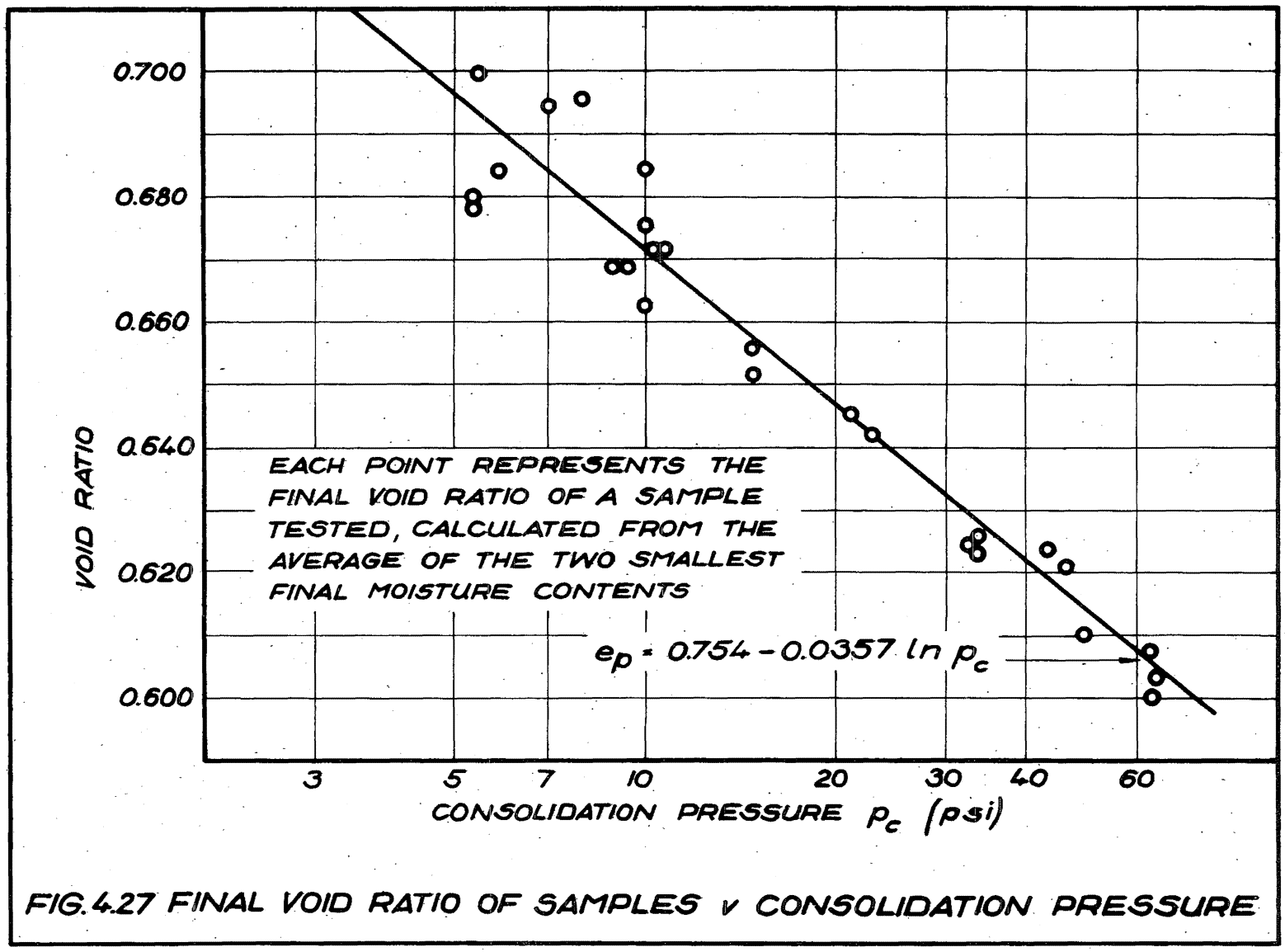

FIG. 4.27 FINAL VOID RATIO OF SAMPLES v CONSOLIDATION PRESSURE

considerable amount of scatter. This is probably caused by the inherent variability of the compaction process.

To investigate this variability the properties of twelve samples were determined immediately after compaction; the results are plotted in Fig.4.28. It can be seen that the wet weight, moisture content and dry density of the samples as compacted do fluctuate but the range of these variations is quite small. This is not the case for the unconfined compressive strength which appears to undergo fairly large fluctuations apparently unrelated to the variations in moisture content and dry density. Since the strength properties of the samples so far discussed are very much more consistent than the results of these unconfined compression tests, it is suggested that the wide variations are the result of fluctuations in the negative pore pressure in the samples on compaction. This was not measured but it would not be related directly to small changes in density and moisture content, and since all the samples discussed here were saturated these negative pore pressures would not be present.

The minimum value of the dry density of 92.5 lb/ft^3 for these "as compacted" samples is equivalent to a void ratio of 0.713 and the maximum value of 93.6 lb/ft^3 corresponds to a void ratio of 0.690. The difference of 0.023 between these two agrees fairly well with the scatter in void ratio at the lower consolidation pressures in Fig.4.26. Thus it seems that there is some scatter in the average void ratio of the samples on

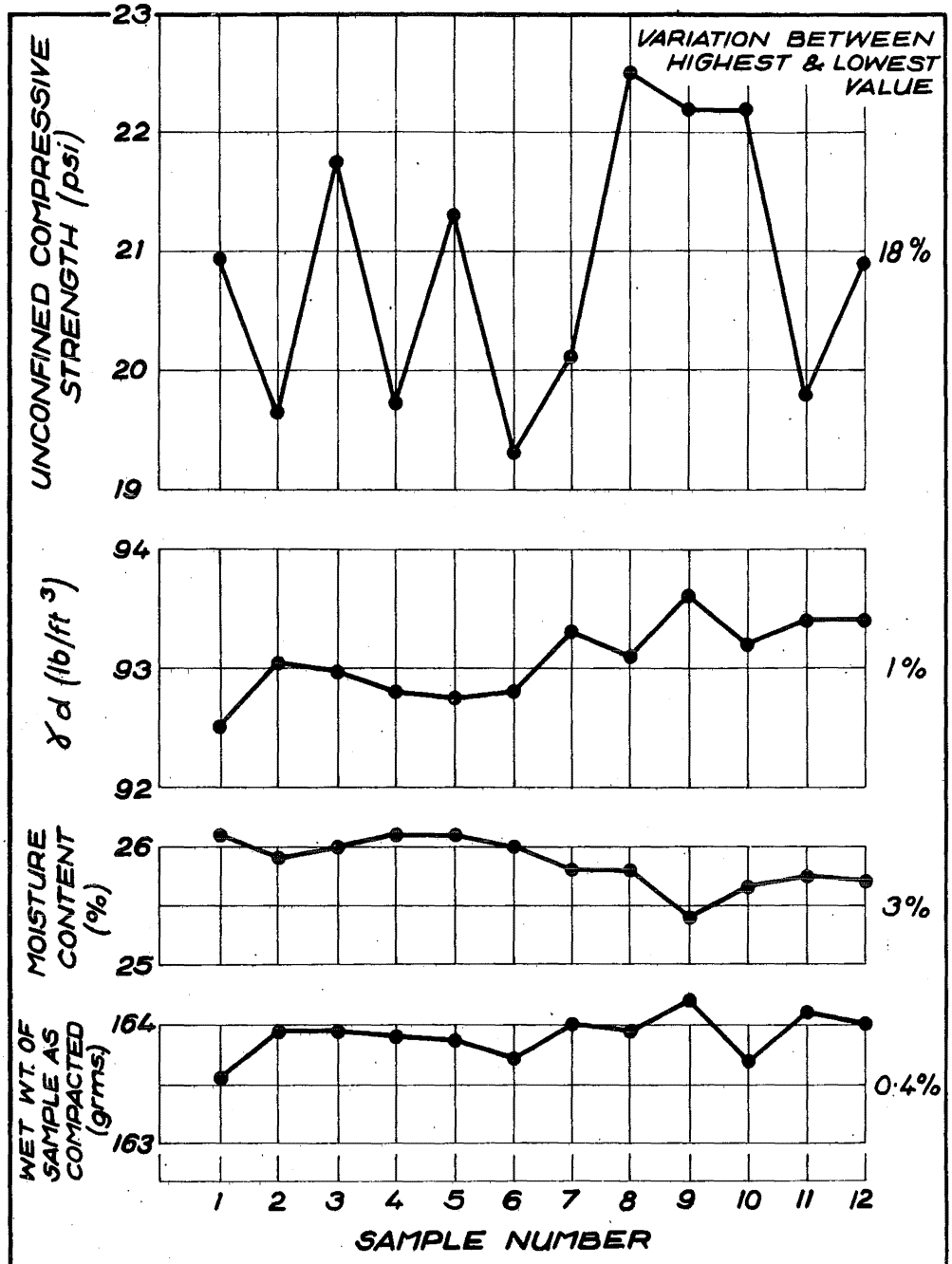

FIG. 4.28 VARIATION IN PROPERTIES OF SAMPLES IMMEDIATELY AFTER COMPACTION

compaction which is reduced as the consolidation pressure is increased.

As explained in Appendix C, at the completion of each test the samples were cut into three and the moisture content of each portion determined. In general the results were fairly consistent, the range between the three values being within 1%. However some of the tests (CSR 014 and CSR 015 for instance) showed a very high moisture content in the top third of the sample. Close examination of these moisture content samples revealed a crack across the top of the sample which might have been associated with this anomalous value. The cause of the crack is not clear. Since it only occurred in a few samples it might have been caused by not drilling the guide hole at the top of the sample deep enough. Because of this occasional high moisture content the average of the two smallest final moisture contents was used to calculate the void ratio.

And finally to check that moisture contents taken from the top, middle and bottom of the sample are sufficient to determine the average void ratio a few selected samples were cut into sixteen pieces and the moisture content of each piece was determined. These results are presented graphically in Fig.4.29. The first three sets of results presented at the top of this figure are from "as compacted" samples. These establish that although the moisture contents do fluctuate there is a noticeable tendency for the moisture content to decrease towards the

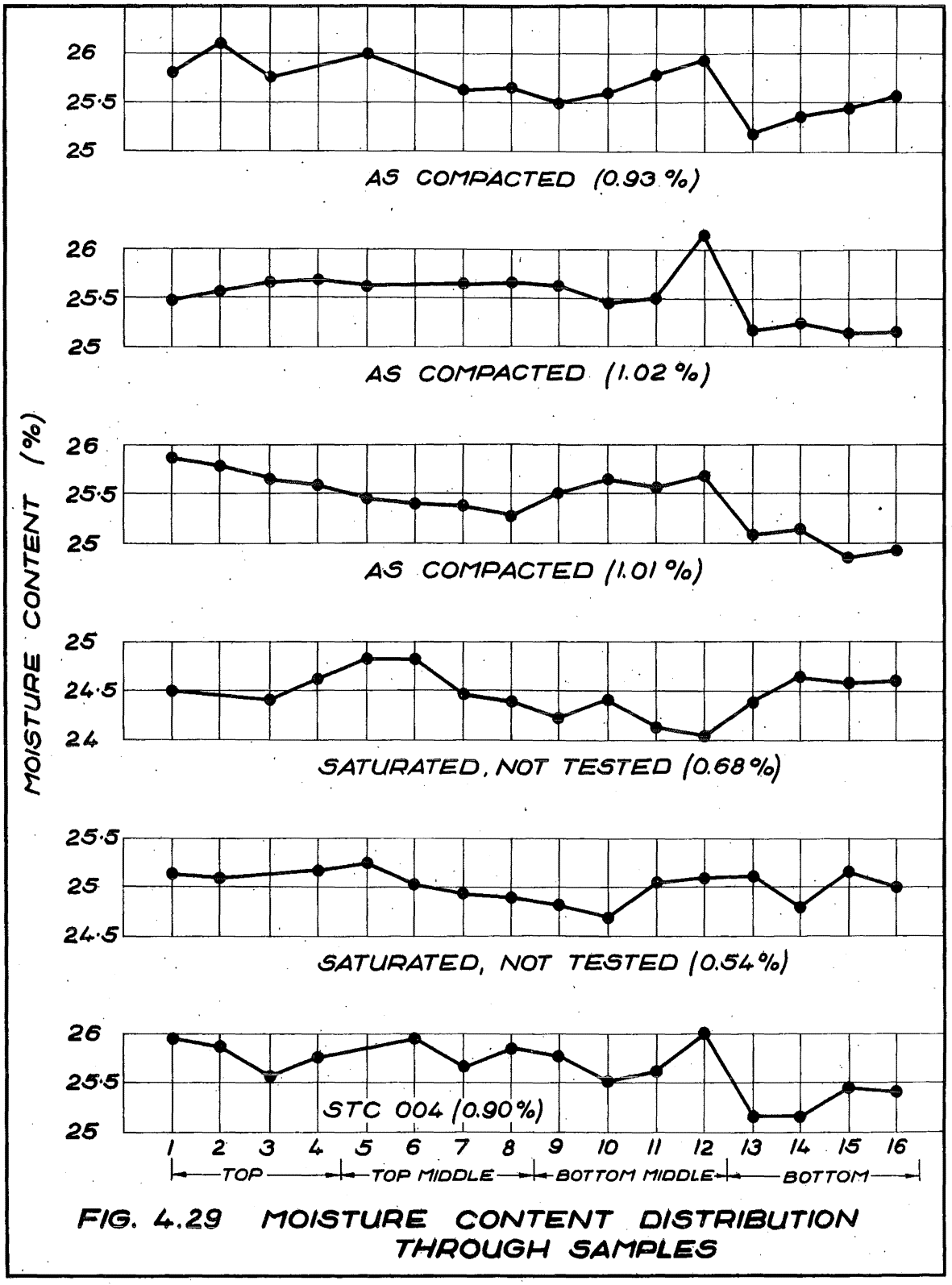

FIG. 4.29 MOISTURE CONTENT DISTRIBUTION THROUGH SAMPLES

bottom of the sample. However the fluctuations about this tendency are fairly considerable, the difference between the smallest and the largest values is about 1%. Next two samples were treated similarly after having been saturated and consolidated at 10 psi. As before there is some scatter although for these two samples the difference between the smallest and largest is somewhat smaller than for the "as compacted" samples but, perhaps more importantly, there is now no overall tendency for the moisture content to decrease towards the bottom. The sixth set of results comes from the sample for test STC 004 after testing. Once again there is scatter from point to point and the difference between the smallest and largest values is of the same order as that in the other five sets of moisture contents. These five sets of results show that back pressure saturation tends to make the moisture content distribution throughout the samples more uniform and they suggest that it is unlikely that the overall moisture content of the samples can be determined to better than 0.5% and that in many cases 1% is a more likely value. This means that the void ratio quoted for the samples may be in error up to $\pm$ 0.0015.

In summary it has been shown in this section that there is some variability in the void ratios of the as compacted samples. It seems that differences in void ratio of 0.020 are possible between samples on compaction but when the samples are consolidated these differences from sample to sample are reduced

as the consolidation pressure is increased. Within a particular sample immediately after compaction, or consolidated at pressures below 10 psi, it seems that the void ratio may vary throughout the sample by 0.002 or 0.003.

(ii) Accuracy of measurements

In all three measurements were taken during the undrained tests. These were axial deformation, axial load and pore water pressure. The details of these measurements are explained in the Appendices and all that is needed here is to repeat that considerable care was taken with these measurements. The accuracy of the measurement of axial deformation was $\pm$ 0.0005". That of the axial load was $\pm$ 0.5 lb and $\pm$ 0.15 psi for the pore water pressure

(iii) Accuracy of Reduced Experimental Results

The probable error associated with each of the measurements taken has just been given but it is not these errors that must be considered when discussing the accuracy of the results presented in this chapter. What must be considered are the values calculated from the three measurements. The calculation of stresses and strains is based on certain assumptions about the deformation of the samples. These are that there is no change in volume and that the sample remains cylindrical. The condition of no volume change during the course of an undrained test is important but, because of measures explained in Appendix D this presents no problem with the tests discussed here. Although

visual observation of the deformed samples showed that the cylindrical shape was maintained no measurements were taken to investigate this more thoroughly. This omission is usual in triaxial testing. However the calculation of the stresses is based on this assumption and thus it is unfortunately not possible to specify likely ranges of errors for the stress components because the uncertainty in the cross section of the sample is not known.

Nevertheless in view of the generally consistent pattern of behaviour reported in this chapter it does seem that random errors are not significant. Occasionally it has been noted that a few points on some of the graphs are not consistent with the interpretation suggested by the others. Examples are the points for test STC 002 in Figs.4.8 and 4.10 or the anomalous upper two points on some of the contours of equal strain in Fig.4.5. These effects are obviously related to the variability in the compaction process, already discussed, rather than to errors in measurement or errors associated with the assumptions in calculating stresses and strains from the measurements taken. Thus, although it is not possible to give quantitative probable errors for the reduced experimental results it is felt that the care taken with the experimental procedure is such that these errors are not important in comparison with the random variations caused by the compaction process.

It is possible to get some idea of the combined effect

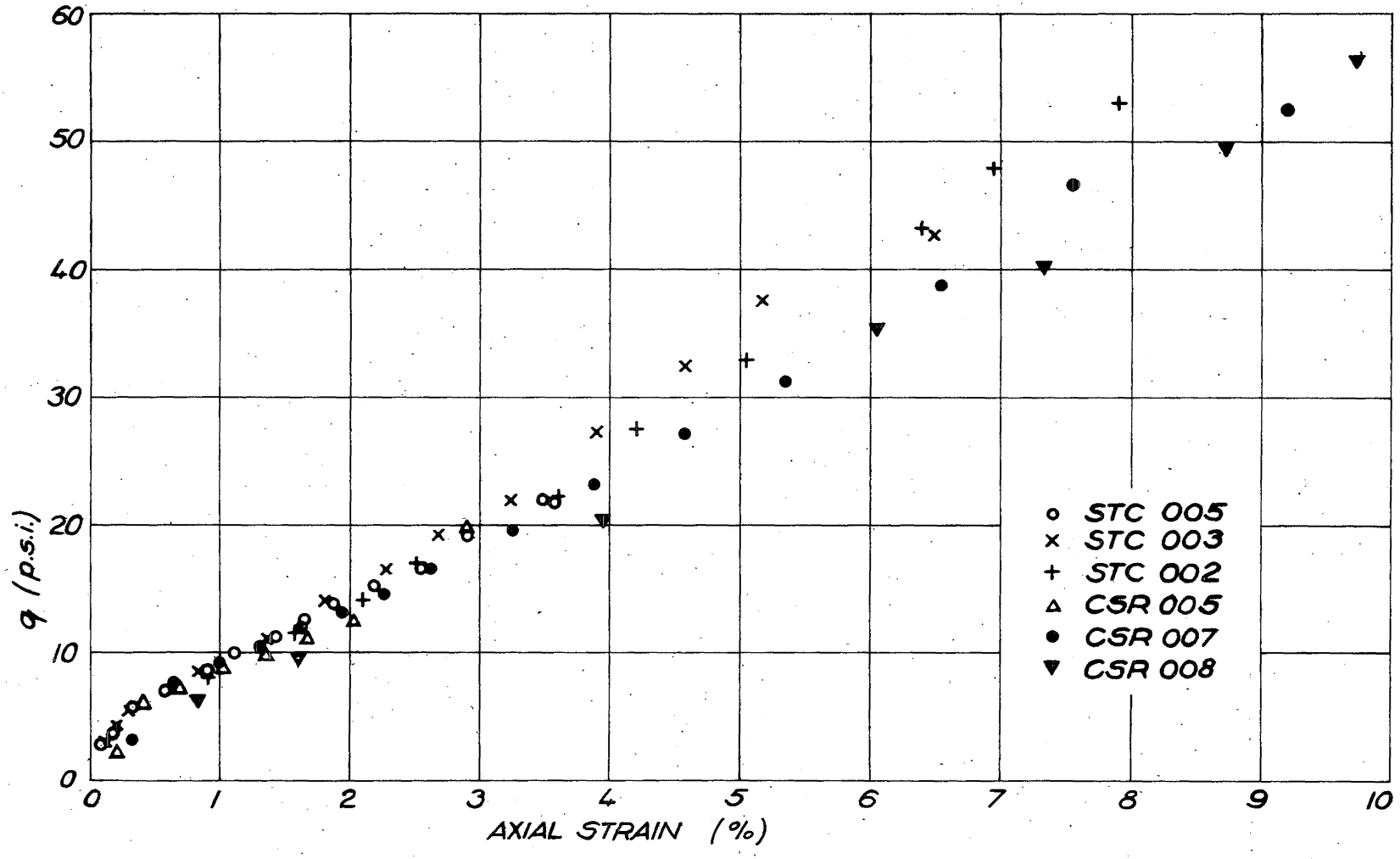

FIG. 4.30 COMPARISON OF STRESS-STRAIN CURVES (SAMPLES CONSOLIDATED AT 10 p.s.i.)

of all these sources of error by comparing the behaviour of samples consolidated at the same pressure. This is done in Fig.4.30 where the stress strain curves for several samples consolidated at 10 psi are compared. It is seen that they are all remarkably close thus supporting the claim made above that variations from sample to sample, errors in measurement and reduction of results have no significant affect on the pattern of behaviour reported in this chapter. Although it must be noted that Fig.4.30 is not capable of highlighting systematic errors.

CHAPTER FIVE

FORMULATION OF A PLASTIC STRESS-STRAIN RELATION

5.1 INTRODUCTION

In this chapter an attempt is made to use those concepts of the theory of plasticity, outlined in Chapter 3, to explain the behaviour described in Chapter 4. The approach used is along the lines of the theories developed by the soil mechanics research group at Cambridge University although some modifications are introduced to account for the properties characteristic of the soil treated in this thesis. In Chapter 4 the emphasis was placed on describing the observed behaviour with as little interpretation and analysis as possible while the object of the present chapter is the investigation of the possibility of using an incremental plastic stress-strain relation to predict the deformation of the soil.

Initially some of the basic aspects of the critical state model are reviewed and discussed in greater detail than in Chapter 3. This is followed by a discussion of the general features of the behaviour presented in Chapter 4 and it is shown how certain aspects of these are not incompatible with some of the critical state concepts. From here the way in which the ideas of Chapter 3 can be used to interpret the behaviour of the compacted silty clay is explored. It is explained how the approach adopted depends on two aspects of the material behaviour

which are known to be valid. The first of these aspects of the soil behaviour is that the deformation, for both drained and undrained tests, is stable in the Druckerian sense and consequently a yield surface must exist to which the plastic strain increment vector is perpendicular. Secondly it has been emphasised elsewhere that the deformation of the samples in the triaxial apparatus may not be homogeneous. This means that the strains calculated from the boundary displacements may not be true strains; however it has been shown in Chapter 3 that even though this may be so the ratio between the components of strain remains independent of this inhomogeneity. Thus more emphasis is placed on the prediction of this ratio than the prediction of the actual stress-strain curves.

The overall conclusion reached in this chapter, the most significant conclusion of the whole thesis, is that it is by no means unreasonable to attempt to describe the deformation behaviour of the particular compacted soil discussed here in terms of the theory of plasticity. Equations for calculating the strain increments of the soil are developed using the concepts for an ideal work hardening elastic-plastic material. The equation for the successive yield curves is derived and the form of the function h (cf. Eqs.3.12, 3.34 and 3.35) is inferred from this. Using these relations the general features of the deformation behaviour are derived. The correspondence between these predictions and the observations of Chapter 4 is certainly

not exact but they are sufficiently close to indicate that the method is indeed promising.

5.2 SOME ASPECTS OF THE CRITICAL STATE MODEL

The following paragraphs contain an elaboration of some features of the critical state theory that will be used explicitly when attempting to develop a stress-strain relation. Most of this work has already been outlined in Chapter 3, but some of the points need amplification.

The concept of the state boundary surface, S.B.S., in the (p,q,e) space was discussed in Chapter 3 and was illustrated mainly with respect to cohesive soil that is wet of critical. This boundary surface has been illustrated in Figs.3.6 and 3.8 but for convenience another diagram, Fig.5.1, which shows the part of the surface on the dry side of the critical state line more clearly is included here.

Just as the virgin consolidation curve, EPP'F in Fig.5.1, in the (p,e) plane represents the boundary of all possible states for the soil so too the whole surface ABCDEFGH represents the boundary of all possible combinations of p, q and e to which the material may be subjected. The soil may exist in any state on or below the surface of the space bounded by the S.B.S. and the (p,q), (p,e) and (q,e) planes but in no state outside the surface.

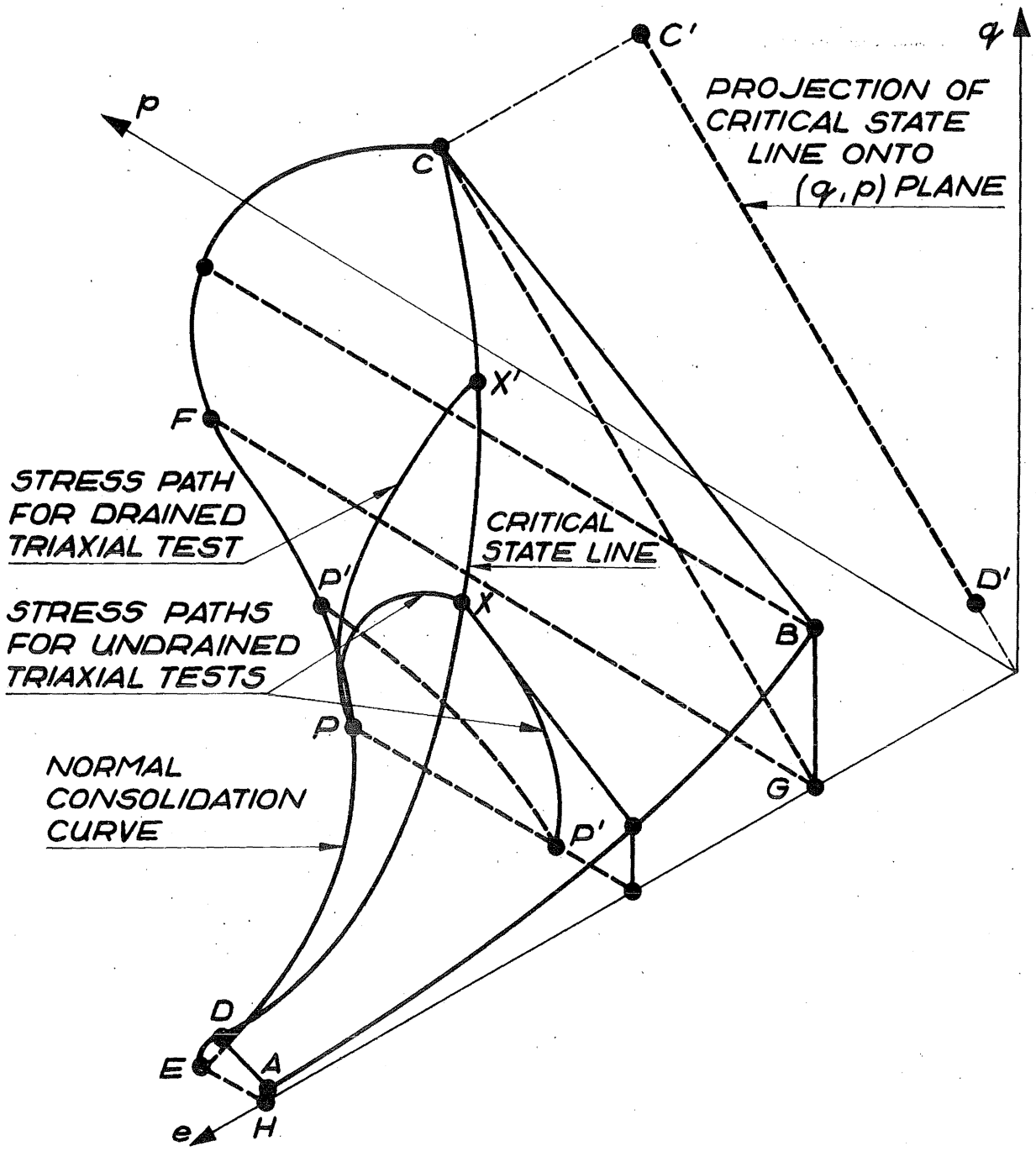

FIG. 5.1 AN ISOMETRIC VIEW OF THE STATE BOUNDRY SURFACE

The line CX'XD is known as the critical state line. The behaviour of soil in any state along this line is described by equation 3.25 which states that although unlimited shear distortion can occur at a critical state, after the critical state is reached, there will be no further volumetric strain or change in the state of stress or of stress ratio, η, (which is then equal to the friction parameter M). i.e.:-

$$(q/p)_{\text{critical state}} = M$$

The state boundary surface is divided into two parts by the critical state line. The part of the surface between the critical state line and the q,e plane, ABCD in Fig.5.1, is known as the dry side and the other part, CDEF, is called the wet side of the state boundary surface.

A constant void ratio section of the state boundary surface, hereafter abbreviated as S.B.S., can be seen in Fig.5.2.

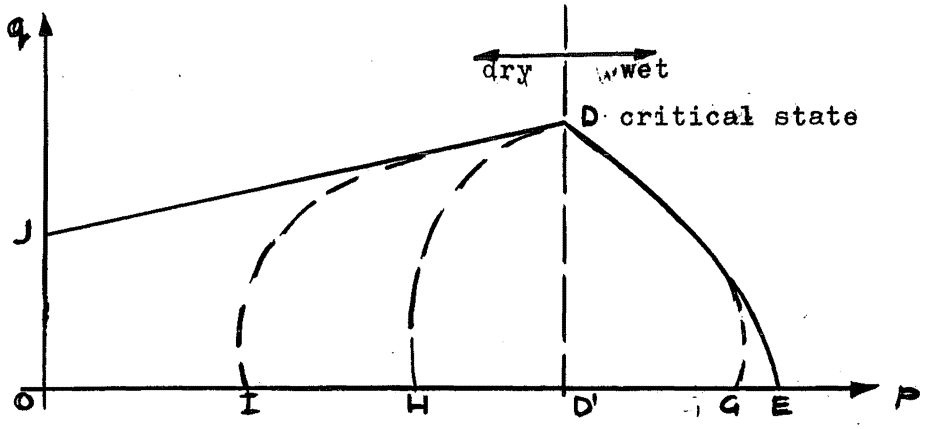

FIG.5.2 CONSTANT VOID RATIO SECTION OF THE S.B.S.

The diagram shows that a constant void ratio section of the dry side of the S.B.S. is linear so that the dry side is a ruled surface the slope of which is the same for all constant void ratio sections. It has been suggested by Roscoe, Schofield and Wroth[63] that the slope of this is equivalent to Hvorslev's "true angle of internal friction", ϕ'_e, discussed in Section 2.5 and that the distance JO is related to Hvorslev's "true cohesion" for the particular void ratio in question. All constant void ratio sections of the boundary surface are geometrically similar; as the void ratio decreases the size of the section increases.

A sample at point E in Fig.5.2 is normally consolidated and the curve ED is the stress path followed by the sample, initially at state E, during undrained axial compression in a triaxial test. The end point for such a test occurs when the sample has reached the critical state for that particular void ratio, shown as point D. The line DD' is the division between states wet and dry of critical. Samples with the same void ratio as that at point E but having swelled under smaller pressures after initial consolidation such as those with state points at G, H and I are all overconsolidated and during an undrained triaxial test have stress paths GD, HD and ID respectively. This illustrates the importance of the critical state concept. Regardless of the initial state of the sample it is a basic postulate of the critical state model that the end point of any test lies somewhere along the critical state line. So when the samples

with initial states, E, G, H and I are tested in undrained triaxial compression all the tests end at point D. For samples with an initial state that is not on the S.B.S. there is a tendency for the stress path to approach the surface before the critical state is reached. During a drained test the same overall behaviour is observed, although because the void ratio changes the state point moves along as well as around the boundary surface.

Now that a constant void ratio section of the state boundary surface has been considered a section in which only elastic deformation is supposed to occur is discussed. In the (p,e) plane the rebound line is regarded as a line along which only elastic changes in volume take place. This is shown in Fig.3.8 (p.112) as the line ABR. It was explained in Chapter 3 how the section of the surface vertically above this line represents an "Elastic Wall" and when the stress point moves about in this section only elastic changes in void ratio will occur. It was further explained in Chapter 3 how the line in the S.B.S. vertically above ABR (in this case AXF) can be regarded as a yield curve. An undrained section of the S.B.S. can be said to cut many of these elastic walls; thus during an undrained test the stress path crosses a succession of these yield curves and hence the proposition that the soil work hardens when sheared.

Having completed this more detailed description of the S.B.S. it might be worthwhile to consider the significance of the words "state boundary surface". The reason for the words

"boundary surface" is obvious enough but what is the meaning of the word"state"? Roscoe and Poorooshasb[64] have defined the state of an element at any given instant: "as the sum of all the (macroscopic) quantities that can be associated with the element at that instant." This means that any of the characteristics of the material can be expressed in terms of the state variables at that time. It is a basic assumption of the Cambridge work (and in the work of many other soil mechanicians) that the state of a soil can be completely specified by the current state of stress and the void ratio; temperature and time effects are not considered. Thus the variables used in setting up the S.B.S. are important because they are regarded as the state variables for the material. This idea is of considerable significance in the development of the plastic stress strain relations given in Equations 3.33b and 3.36a. It leads to the assumption that at any given point on the S.B.S. an increment of stress will result in an increment of strain the direction of which is a function of the current stress and void ratio but is independent of the stress increment, that is the direction of the strain increment vector depends only on the current state of the material. This can be expressed as:

$$d\upsilon^p/d\epsilon^p = f(p,q,e) \quad \ldots\ldots\ldots\ldots\ldots\ldots\ldots\ldots \quad (5.1)$$

In assuming that the stress parameters p and q may be used to describe the state of stress the additional assumption is made

that the material is isotropic. Actually this is a fairly considerable restriction, the importance of which is discussed in Chapter 6, but for the meantime isotropy is assumed.

At this stage the writer would like to offer an alternative explanation of the term "state" and connect it with the fundamental hypothesis put forth in Chapter 2 where it was suggested that the stress deformation properties of a soil are determined by the nature of the interparticle force system. From this view point the term "state" could be defined as : the sum of all those macroscopic quantities that are necessary to specify the nature of the interparticle force system. The stress components p and q, and the void ratio, e, are obviously most important factors in determining the interparticle force system but what of other factors? Temperature and time effects come to mind immediately but as has already been emphasised these are not considered in this thesis. Another possibility is the concept often appealed to in soil mechanics and discussed in Chapter 2, namely soil structure. This is also not considered in the Cambridge work because of the assumption of isotropy.

Finally it should be emphasised that most of the data available about the S.B.S. are associated with states wetter than critical. Because of the non uniformities that control the mode of deformation for drier than critical samples these states have not been investigated, or the information available has been

regarded as questionable.

A second essential aspect of the Cambridge approach is the suggestion that the amount of work for a given strain increment dissipated internally as friction within the sample is independent of strain for stress paths on the S.B.S. That is to say the coefficient of interparticle friction is constant. How does this differ from the behaviour outlined in section 5 of Chapter 2 where it was explained that frictional resistance was developed as a function of strain? The friction angles discussed in that part of Chapter 2 were corrected only for the energy required to change the volume of the sample, which results in an angle that is a function of strain. However in addition to the boundary energy correction Roscoe's energy equation (Eq.3.32) includes the elastic energy stored within the sample as a consequence of deformation. This additional consideration which is applied only to stress paths on the S.B.S. leads to a constant friction parameter defined by:

$$q_{\text{critical state}} = Mp \qquad \ldots\ldots\ldots\ldots\ldots\ldots\ldots\ldots \quad (5.2)$$

It is a simple matter to show that this critical state friction parameter which is independent of the void ratio and the state of stress is related to the conventional friction angle, ϕ', defined in terms of the stresses σ'_1 and σ'_3 by:

$$\text{Sin } \phi'_{\text{crit}} = \frac{3M}{6+M} \qquad \ldots\ldots\ldots\ldots\ldots\ldots\ldots\ldots \quad (5.3)$$

An important step in formulating the energy equation was to

propose a suitable term for the work dissipated as friction. The one used by Roscoe is given in Eq.3.31 which is repeated here:

$$dU = Mpd\epsilon \quad \ldots\ldots\ldots\ldots\ldots\ldots\ldots\ldots\ldots\ldots \quad (3.31)$$

However this is by no means the only possible relation and in fact Roscoe and Burland[67] have suggested another possibility, and a modification of Eq.3.31 is used later in this chapter.

Finally in this section the method of calculation of the components of plastic strain is reviewed. An important basic assumption is that for states wet of critical there is no recoverable shear distortion, therefore:

$$d\epsilon^p = d\epsilon = d\epsilon_1 - \tfrac{1}{3}dv$$

Now in an undrained triaxial test dv = 0 so that $d\epsilon = d\epsilon_1$. Although it is assumed that there is no recoverable shear distortion an important aspect of the Cambridge treatment of soil deformation is the inclusion of some recoverable volumetric deformation. This has already been explained briefly in Chapter 3 but at this stage the interpretation of this recoverable volumetric strain in the (v,lnp) diagram is discussed. Fig.5.3 below is similar to Fig.3.7 but in this case the specific volume (v = 1+e) rather than the void ratio is plotted against lnp.

Consider a soil sample initially at state A and subjected to a small decrease in p under undrained conditions so that the state point moves to B. Using Eq.(3.29) the increment of elastic

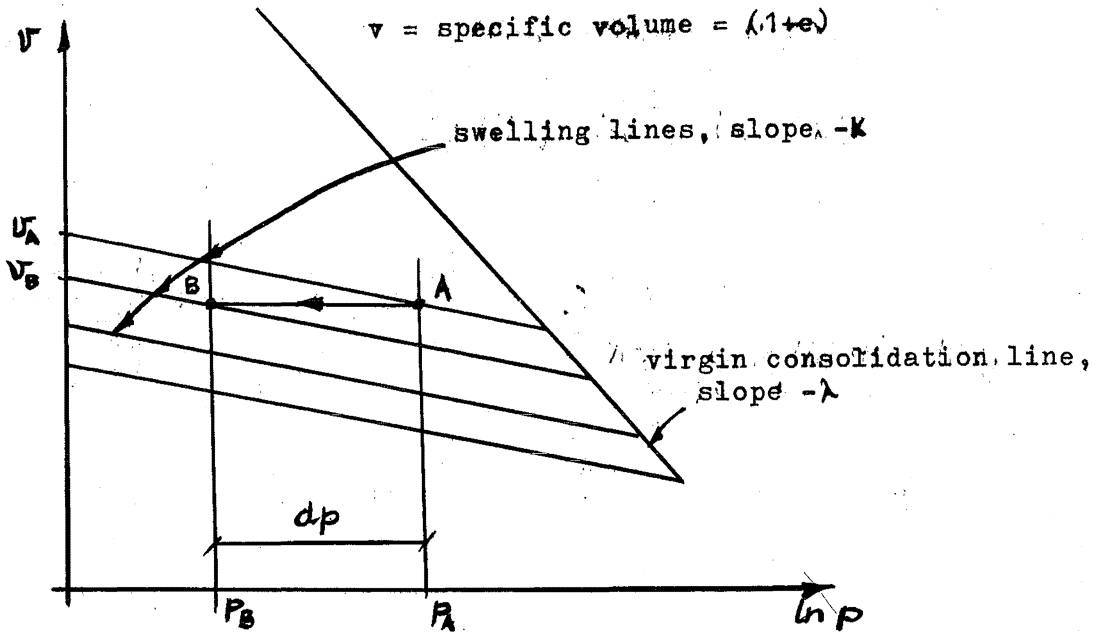

FIG.5.3 ELASTIC AND PLASTIC VOLUME CHANGE IN THE (v,lnp) PLANE

volumetric strain associated with this stress decrement is:

$$dv = -kdp/pv$$

However because it was specified that this stress increment takes place under undrained conditions there can be no overall volume change, so this elastic strain increment must be balanced by an equal and opposite plastic strain increment. Schofield and Wroth[75] have suggested another way of interpreting this plastic volume change on p.139 of their book. Through the points A and B swelling lines of slope -k can be drawn which have characteristic intercepts on the v axis. The difference between these two values ($v_A - v_B$) is equal for the plastic volume change kdp/pv. Thus

plastic volume change can be related to the change in the "k-line" associated with the various state points. In fact each of these "k-lines" represents a specific elastic wall in Fig.3.8, so that a change of "k-line" requires movement from one yield curve to another with the corresponding plastic strain. The same reasoning applies to an arbitrary stress path on the S.B.S. causing some plastic deformation - the plastic volumetric strain can be calculated from the difference between the intercepts of the initial and final k-lines on the v-axis.

For state paths on the wet side of the state boundary surface unloading from a given value of q produces no change in p, that is the unloading stress paths fall vertically from the S.B.S. towards the (q,e) plane in Fig.5.1. Thus any change in p associated with loading on the S.B.S. is in fact a permanent change so the total plastic volume strain for a given loading path is completely defined by the change in k-line during loading.

5.3 RELATION BETWEEN BEHAVIOUR OF COMPACTED SOIL AND CRITICAL STATE MODEL

In this section various aspects of the behaviour presented in Chapter 4 are discussed and the relation, if any, with the critical state model is explained. The stress-strain curves plotted in Figs.4.11 and 4.15 show that the soil work hardens when the stress is increased. The shape of the stress strain curves during the unload-reload cycles in these tests is quite different from those

parts of the curves where the current shearing stress is greater than any previous value. This occurs even at quite low values of q. As a first approximation it can be said that Fig.4.11 demonstrates that during the first-loading parts of the curves large irrecoverable deformations occur; during unloading only a relatively small proportion of the strain is recovered and during reloading the strains are small until the previous maximum value of q is approached. Fig.4.15 demonstrates that for repeated cyclic loading to stresses less than the previous maximum the increase in strain per cycle is small compared with the strain reached before unloading. On the basis of these two diagrams it is assumed that as a first approximation the stress-strain behaviour can be idealised as work hardening elastic-plastic. This represents a difference from the critical state behaviour which assumes, for samples wet of critical at least, that there is no recoverable shear deformation.

Closer examination of Figs.4.11 and 4.15 does show that this is an idealisation. Fig.4.15 suggests that repeated loading to the same stress level may introduce further hardening. The diagram indicates that after many cycles of loading and unloading to a constant value of q that the maximum past value of q must be exceeded considerably before there will be any further substantial increase in shear strain. Fig.4.5 also illustrates that with each successive reloading the strain increases slightly but after several cycles the effect is quite considerable even if the additional strain per cycle decreases as the number of cycles increases.

Fig.4.11 illustrates that for each reloading cycle the strain corresponding to the previous maximum value of q is exceeded at a smaller value of q. Nevertheless these are second order effects compared with the behaviour of the material when the value of q is increased monotonically and so the assumption of work hardening plastic behaviour is a reasonable starting point for analysing the behaviour presented in Chapter 4.

Perhaps the greatest difference between the behaviour observed in Chapter 4 and the critical state model is that the samples subjected to undrained tests did not seem to reach a critical state, at least not for strains up to 10%. It was explained in section 2 of Chapter 4 that even for quite large strains a critical state was not reached in any of the tests; however, it was also shown in Fig.4.3 that for strains greater than about 17% the non-uniformity of the sample deformation is such that it is not really possible to tell whether or not a critical state would be reached at large strains. However certain aspects of the behaviour of the soil suggest that a critical state is approached. In the first place the rate of change of the stresses q and p with respect to axial strain was decreasing rapidly as the strain increased, which implies that had the test continued long enough the stress point might have reached a stationary value and the shear strain become indeterminate.

The shape of the stress paths for the undrained tests has a form quite different from that for an undrained test on material wet of critical. They are suggestive of a material that tends to

expand on shearing. In the terminology of the critical state theory such a soil is dry of critical and so the value of p must increase as q increases if a critical state is to be reached.

The final positions of the stress paths for the undrained tests are tangential to a straight line passing through the point p = -3.0 on the p axis. The fact that the final part of each stress path is linear is in keeping with the idea that the constant void ratio sections of the dry side of the S.B.S. are linear (Fig.5.1). What is unexpected is the result that the stress paths for all the undrained tests are tangential to one line passing through the point(0,-3.0). The usual observation from the behaviour of over-consolidated cohesive soils is that the undrained stress paths are tangential to a series of parallel straight lines the intercepts of which in the q-axis are dependent on void ratio. Before considering this in too much detail a decision must be reached whether this aspect of the material behaviour can be regarded as truly characteristic of this compacted soil or whether it is a consequence of the method of testing. It was noted earlier that the samples tested did develop some non-uniformities as the axial strains increased and although it was emphasised that slip planes did not become visible until the axial strain approached about 10% there is still the possibility that this non-uniform deformation, although not visible, might have been important at low strains and be the major factor responsible for the planar surface in the (p,q,e) space. Bacchus[2] has suggested that rather than being a fundamental shear parameter of any importance the slope of the final position of an

undrained stress path for overconsolidated materials is a consequence of the development of non-uniformity. Before disputing this idea for the particular material treated here it is pointed out that the stress path had become linear long before any non-uniformity was visible. Examination of Fig.4.7 shows that η' had settled down to a constant value by the time the axial strain had reached about 6% whereas the slip planes were not visible until the strain reached about 10%. However, this fact is not really sufficient for one to claim that non-uniformity is unimportant because if slip planes become visible at axial strains of 10% they must be initiated at much lower strains. Such non-uniformity could arise from two aspects of soil behaviour. Firstly the non-uniform deformation could lead to non-uniform distribution of pore water pressure so that the calculated values of the stress p would be erroneous. Secondly there is a possibility that, even for an undrained test, the void ratio along a shear plane might be different from that of the rest of the sample.

If the first of these problems cannot be disregarded generally it definitely can be in this case. The use of free ends means that the deformed shape of the sample was very uniform so that the calculated areas of the sample must have been fairly accurate for axial strains up to 10%. Also the rate of loading was such that complete equalisation of pore water pressure had taken place so that the measured pore pressure would be equal to

that on the shear plane. Thus there is no reason to suppose that the measured values of the hydrostatic component of the effective stress are not accurate.

The second of these problems is a little more difficult. There has been some experimental evidence that suggests for undrained tests that the possibility of the void ratio along the slip plane increasing at the expense of the rest of the sample may not be significant. Rosecoe and Thurairajah[66] conducted a series of experiments to investigate the effect of stress path on the form of the S.B.S. In undrained and drained triaxial tests they noted some important differences. These were cleared up by using the more sophisticated simple shear apparatus which does not develop the non-uniformities of the triaxial apparatus. The tests in the simple shear apparatus showed that the S.B.S. determined was independent on the type of test and furthermore this S.B.S. was virtually the same as that determined from the undrained triaxial tests. Thus Roscoe and Thurairajah suggested that the S.B.S. determined from undrained triaxial tests is subject to less error than that determined from drained tests. It was with this suggestion in mind that most of the data presented in this thesis were determined in undrained triaxial tests and following Roscoe and Thurairajah it is suggested that the possibility of non-uniform void ratio on the slip plane is not likely to be important for the range of axial strains considered. This is also confirmed by the comments at the end of Chapter 4

about sample uniformity.

Thus it is assumed that the fact that the linear end portions of all the undrained stress paths are tangential to a line passing through the point p = -3.0 on the p-axis is not subject to serious experimental errors and is truly representative of the soil behaviour.

This behaviour is extremely interesting because it shows that the friction angle for the material is independent of void ratio at least for a range of void ratios between 0.72 and 0.62. This has been illustrated in Fig.4.8 where the void ratio was plotted against the slope of the final portion of the stress paths. As commented in Chapter 4 there is some scatter in this diagram but it is reasonable to make the idealisation that η' for the final part of the stress paths is independent of void ratio. Because the final part of each stress path is linear it is possible to determine the friction angle for each test. This is illustrated below in Fig.5.4.

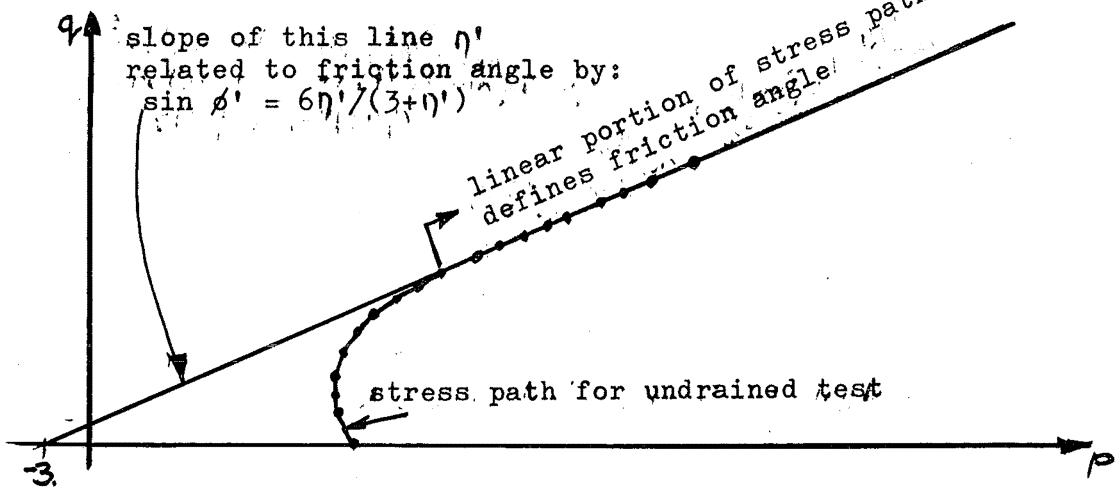

FIG.5.4 FRICTION ANGLE DETERMINED FROM FINAL PART OF STRESS PATH

Thus the constant slope of the final part of the stress path means that the friction angle is independent of void ratio. Referring to section 5 of Chapter 2 and Fig.2.5 it can be seen that this is the type of behaviour that would be expected of Hvorslev's true angle of internal friction. It is also possible to determine the cohesion for each test from the tangent to the final portion of the stress path. Cohesion is normally determined from a plot of $\frac{1}{2}(\sigma'_1 + \sigma'_3)$ against $\frac{1}{2}(\sigma'_1 - \sigma'_3)$. The cohesion is determined from the intercept of this plot on the $\frac{1}{2}(\sigma'_1 - \sigma'_3)$ axis, i.e. the intercept on the line where $\frac{1}{2}(\sigma'_1 + \sigma'_3)$ is zero. Now when $\frac{1}{2}(\sigma'_1 + \sigma'_3)$ is zero p is also zero and $\frac{1}{2}(\sigma'_1 - \sigma'_3)$ is $\frac{1}{2}q$. Thus the intercept of the tangent to the stress paths on the q axis can be related to the cohesion of the material. Now the fact that the stress paths are all tangential to the one line means that the cohesion of the material is also independent of void ratio. This is quite different from the behaviour exhibited by Hvorslev's true cohesion. It was explained in section 5.2 that Roscoe, Schofield and Wroth[63] suggested that the slope of the dry side of the S.B.S. is related to Hvorslev's true angle of friction and the intercept on the q axis is related to Hvorslev's true cohesion. For the particular compacted material discussed in this thesis the stress paths for undrained tests are tangential to a planar surface of constant friction angle and constant cohesion. It is explained below how this situation might arise using the concepts

of section 5 of Chapter 2.

Now if the slope of the end parts of these undrained stress paths are equated with Hvorslev's true angle of internal friction by using Eq.5.3 the resulting angle is 37^{o}. This is rather a large value for Hvorslev's true angle of friction but part of the cause of this may be due to the presence of halloysite as the predominant clay mineral in the particular soil tested. Terzaghi has commented that halloysite gives rise to large friction angles.

Before discussing the anomalous behaviour of the cohesion intercept it is worthwhile considering the processes by which the samples are formed. The importance of the line $\eta' = 1.51$ and the intercept $p = -3.0$ on the p-axis suggests that a consequence of the mode of formation of the samples is that an effective hydrostatic component of stress of 3 psi is built into the material. Because the stress paths were determined after the samples had been saturated by the application of back pressure this cannot be attributed to negative pore pressures following compaction. The samples were prepared by kneading compaction in which local areas of the sample are subjected to increases in vertical pressure under the foot of the kneading compactor and considerable shearing stresses at the edges. Although the final sample is built up by a large number of separate applications of the compactor the overall effect will not be unlike consolidation under both hydrostatic and shearing

stresses. The application of the shearing stresses at the edge of the compaction foot means that the void ratio of the final sample is somewhat smaller than if it was prepared by hydrostatic compression alone. This statement is based on the observation of Roscoe Schofield and Thurairajah[65] that consolidation under constant stress ratio, greater than unity, produces a smaller void ratio for a given value of p than does consolidation under hydrostatic stresses alone. When the sample is removed from the compaction mould the total stress applied to the sample is zero so that it can be said to be overconsolidated both with respect to hydrostatic pressure and shearing stress. It has already been shown in Chapter 4 how the inclusion of this 3 psi greatly simplifies the description of the soil behaviour. In Fig.4.3 it was demonstrated very clearly that there is no unique relationship between the η vϵ curves for the undrained tests. However when η' rather than η is used the resulting η'vϵ curve can be said to be unique for all the undrained tests, also the dimensionless plot in Fig.4.18 describing the stress paths depends on the inclusion of the extra 3 psi as does the description of the unloading part of the stress paths in Fig.4.21.

The overconsolidation of the material with respect to hydrostatic pressure can be seen from Fig.A.1 in Appendix A which is an (e,lnp) plot for increasing hydrostatic pressure. There is an initial curved portion followed by a linear part on the semi-logarithmic scale. Using Casagrande's construction this

suggests a preconsolidation pressure of 9-10 psi. There appears to be a similar preconsolidation effect with regard to the shearing stress q. Fig.4.1 in which the qvε curves for all the undrained tests are plotted shows that the soil behaves almost rigidly when the shearing stress is first applied. As the consolidation pressure is increased there is an increase in the value of q reached before any significant shear deformation is observed. Fig.4.7 shows that the value of η' at which any noticeable shear deformation first occurs is more or less constant. In other words it seems that the compaction process not only builds into the sample an apparent preconsolidation pressure as defined by Casagrande's construction but also a "preshearing effective stress ratio" below which the soil is almost rigid under the application of shearing stress.

It is postulated here that the constant cohesion exhibited by the material is a consequence of the compaction process. As explained above, the method of sample preparation was the same in all cases: a compaction process, analogous to consolidation at constant stress ratio, followed by unloading and then consolidation at various hydrostatic stresses. In Chapter 2 the hypothesis was put forward that a loading-unloading process such as this results in a series of attractive bonds being set up in a cohesive soil; when these bonds are sheared they contribute to the shearing strength of the soil and have the same effect on the material as if the hydrostratic or isotropic

component of stress was 3 psi higher than the externally applied value. Because this is actually built into the sample during the compaction process and not during the subsequent consolidation it is constant for all the samples and independent of void ratio. This is in contrast to the line AB in Fig.5.1. In the next chapter is discussed a series of tests performed on samples stressed at right angles to the direction of compactive effort. Once again the stress paths from these tests are tangential to the line $\eta' = 1.51$ which passes through the point $p = -3.0$ psi on the p-axis. This suggests that the compaction process builds in an isotropic component of stress, in other words it is hydrostatic. In Chapter 2 a distinction was made between the so called "Terzaghi effective stress" and the "actual effective stress". It is suggested that this soil is an example of such behaviour. The process of compacting the soil is thought to produce a series of attractive bonds between the soil particles. These bonds influence the soil behaviour in such a way that it is inferred that they are equivalent to an isotropic pressure of 3 psi existing in the soil. When this pressure is added to the value of p applied to the material during the undrained tests the observed behaviour seems to fit into a definite pattern. The hydrostatic component of effective stress can now be modified in the following way:

$$p'' = p + p_{kc} \quad \ldots\ldots\ldots\ldots\ldots\ldots\ldots\ldots \quad 5.4$$

where p is the Terzaghi effective hydrostatic component of stress

and p" is called the actual effective hydrostatic component of stress; p_{kc} is the stress built into the material as a consequence of compaction. For this particular soil prepared by kneading compaction wet of optimum moisture continent to a dry density of 93 lb/ft^3 p_{kc} is given by:

$$p_{kc} = 3.0 \text{ psi}$$

Unfortunately it is not possible to measure this actual effective stress independently so its existence must remain hypothetical. Nevertheless the concept does greatly simplify the description of the behaviour of this soil, resulting in the unique $\eta' v\epsilon$, $\eta' v\xi'$ curves discussed in Chapter 4. The simplicity of the idea, the fact that the 3 psi difference between the actual and Terzaghi effective stress is approximately independent of void ratio and strain and appears to be isotropic, adds to its appeal. The use of the concept is also a consequence of the fundamental hypothesis of Chapter 2 that the stress deformation behaviour of soils depends on the nature of the interparticle force system.

If the stress paths for the undrained tests are plotted in a three dimensional (p,q,e) space they sweep out a uniformly curved surface that develops into a plane inclined at a constant angle to the (p,e) plane and whose strike on the (q,e) plane is parallel to the void ratio axis. This surface is sketched for the material treated in this thesis in Fig.5.5 and

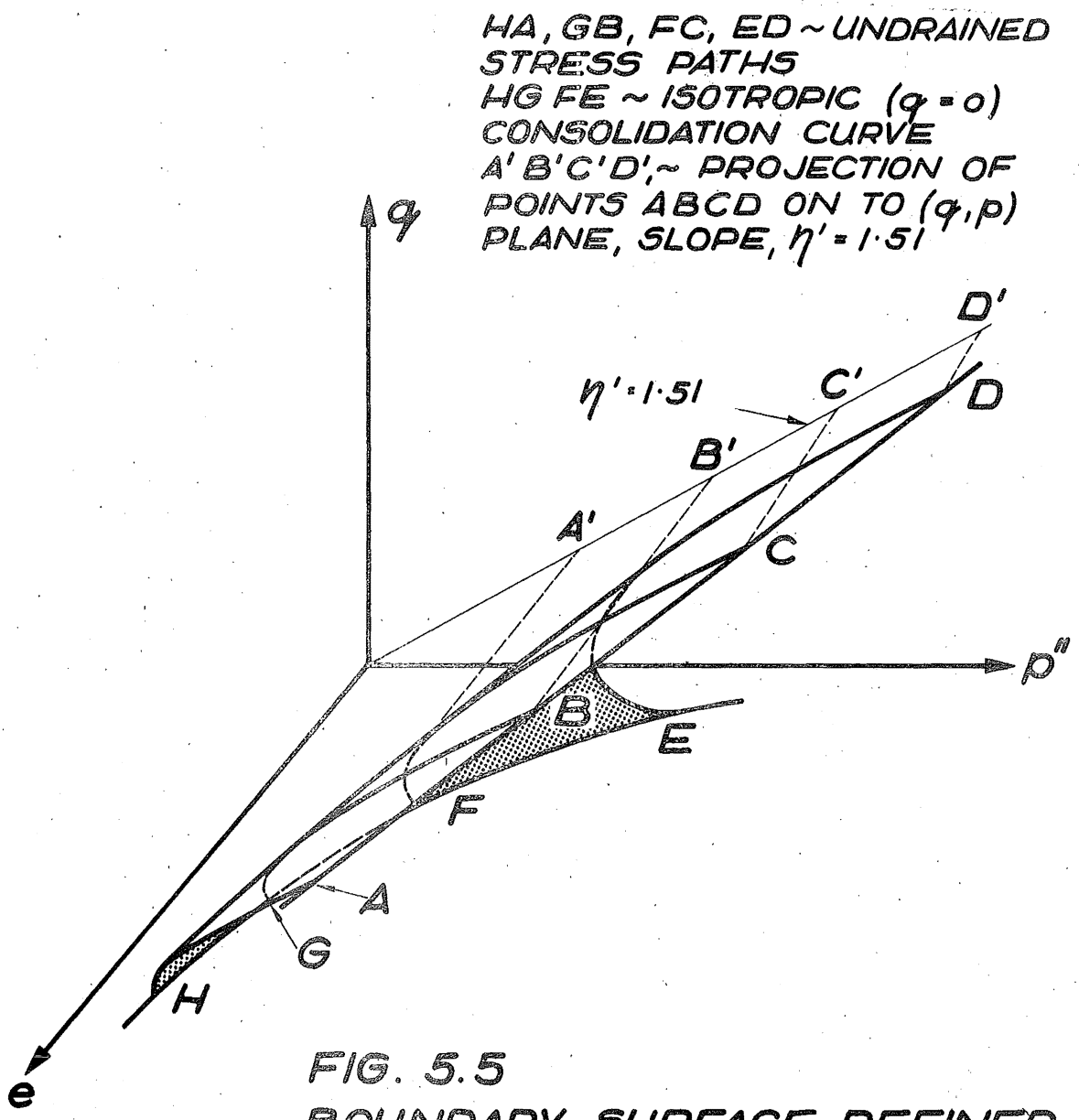

FIG. 5.5
BOUNDARY SURFACE DEFINED BY UNDRAINED STRESS PATHS

is represented as the two dimensional plot of η' v ξ' in Fig.4.18. Can this surface be regarded as a state boundary surface for the material? Evidently only in a very limited sense. As stated above the S.B.S. is the boundary of all possible states that a soil may take, it may exist in any combination of p,q and e that lies on or below the S.B.S. If this were so for the compacted soil tested here, only states on or inside this three dimensional surface in the p, q, e space would have been observed. However in the cyclic loading and unloading tests discussed in Chapter 4 this is violated. Figs.4.12 and 4.16 illustrate how at low values of q the stress point moves outside the surface during unloading. This is illustrated in Fig.5.6 for a constant void ratio section of this three dimensional surface.

Consider, for example, a sample initially consolidated to the state defined by point I and then subjected to undrained loading to the point K and subsequently unloaded. The final state point after such a load-unload cycle is at point I' outside the section of the surface defined by the undrained loading stress paths. This illustrates that the three dimensional surface defined by the stress paths is not a boundary that defines a limiting surface beyond which the state point cannot exist. However the surface is of use in that for initial loading all the state paths lie along it and after unloading and reloading, such as the cycle IKI', the state point does approach

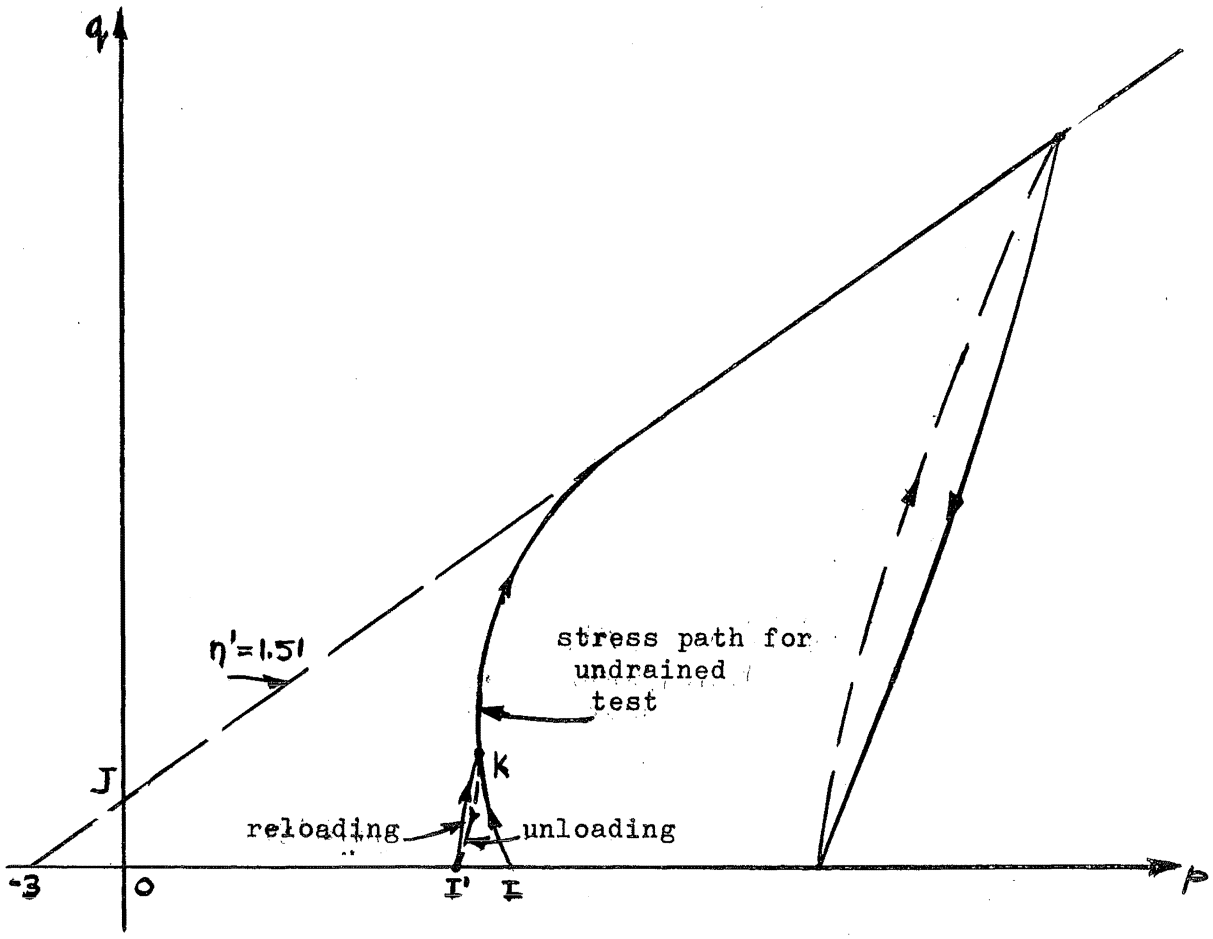

FIG.5.6 UNLOADING BEHAVIOUR OF UNDRAINED STRESS PATHS

the surface again.

Roscoe and Poorooshasb[64] have shown how the use of dimensionless parameters makes it possible to represent the whole of the boundary surface with a two dimensional curve. A similar thing was done in Chapter 4 where in Fig.4.18 the stress paths were plotted in terms of the parameters η' and ξ'. These parameters are equivalent to the ones used by Roscoe and Poorooshasb, the difference being that the actual rather than the Terzaghi effective stress is used here. This two dimensional plot of the stress paths provides an independent evaluation of the magnitude of the difference between the actual and Terzaghi effective stress. The significance of this 3 psi was initially suggested because the stress paths were all tangential to the line with $\eta' = 1.51$ and which passes through the point (0, -3.0). Next the contours of equal axial strain emphasised the importance of the point (0, -3.0) and demonstrated that the parameter η' rather than η was important in describing the stress-strain behaviour on initial loading. Finally the definition of the parameters ξ' and ζ' provided yet another way of confirming the 3 psi difference postulated between the Terzaghi and actual effective stress. The parameters ξ' and η' were calculated for each test for a range of values for p_{kc}. These values were plotted and showed that the η' v ξ' plot in Fig.4.18, with p_{kc} equal to 3 psi, provided the best representation of the stress paths. The plots with p_{kc} equal to 2 psi and 4 spi showed a

good deal more scatter. Using the least squares method of fitting a best straight line to the contours of equal strain the average value of the intercept was calculated to be -2.94 ± 1.29 psi. It was stated in Chapter 4 that the range of values associated with this mean value was fairly severe. The fact that the scatter in Fig.4.18 is increased noticeably when p_{kc} is changed from 3 psi to 2 psi or 4 psi confirms that the range -2.94 ± 1.29 psi for p_{kc} is severe and the choice of -3.0 psi is reasonable. The phenomenon represented in Fig.4.18 is important for two reasons. Firstly it shows, in a third independent way, the importance of the small component of hydrostatic stress built into the material by the compaction process. Secondly it demonstrates that the pattern of behaviour is relatively sensitive to the magnitude of p_{kc} because deviations from 3 psi of the order of 1 psi are sufficient to cloud the picture. It was mentioned above that it is not possible to measure the actual effective stress directly in the way that the Terzaghi effective stress can be measured; however, the persistent recurrence of the 3 psi that is required to derive a consistent picture of the soil behaviour suggests that the concept is not unreasonable.

When discussing the idea of actual effective stress in Chapter 2 it was mentioned that similar ideas have been put forward by others, that soil behaviour is frictional and cohesion is the result of stresses built into the sample because of the mode of formation

and composition. However, to the writer's knowledge, the soil discussed in this thesis is the first example of a material where the use of the concept results in such a major simplification. The fact that the component of stress, p_{kc}, seems to be constant for a range of void ratios, applied stresses and strains means that the soil behaviour can be described in a relatively simple manner.

Fig.4.18 shows that the stress paths for a majority of the tests can be represented by one η' v ξ' curve. Exceptions to this are samples with consolidation pressures less than 10 psi. The curves for the STC 012 and CSR 009 in Fig.4.19 lie well away from those in Fig.4.18. This phenomenon is probably connected with the shape of the (e,lnp) curve for the material given as Fig.A.1 in Appendix A. The initial part of the curve is much flatter than the final part and samples with consolidation pressures less than 10 psi lie along this portion of the curve. This suggests that the stress paths for samples at the lower consolidation pressures fall along an elastic part of the surface rather than on the boundary surface defined by the higher consolidation pressures, in other words the stress paths lie in an elastic wall rather than on the actual boundary surface and consequently the η' v ξ' curves are different from that in Fig.4.18.

The consolidation curve in Appendix A makes it possible to determine values of λ and k (cf. Fig.3.7). However in view of the concept of the actual effective stress introduced earlier it would seem more logical to determine λ and k in terms

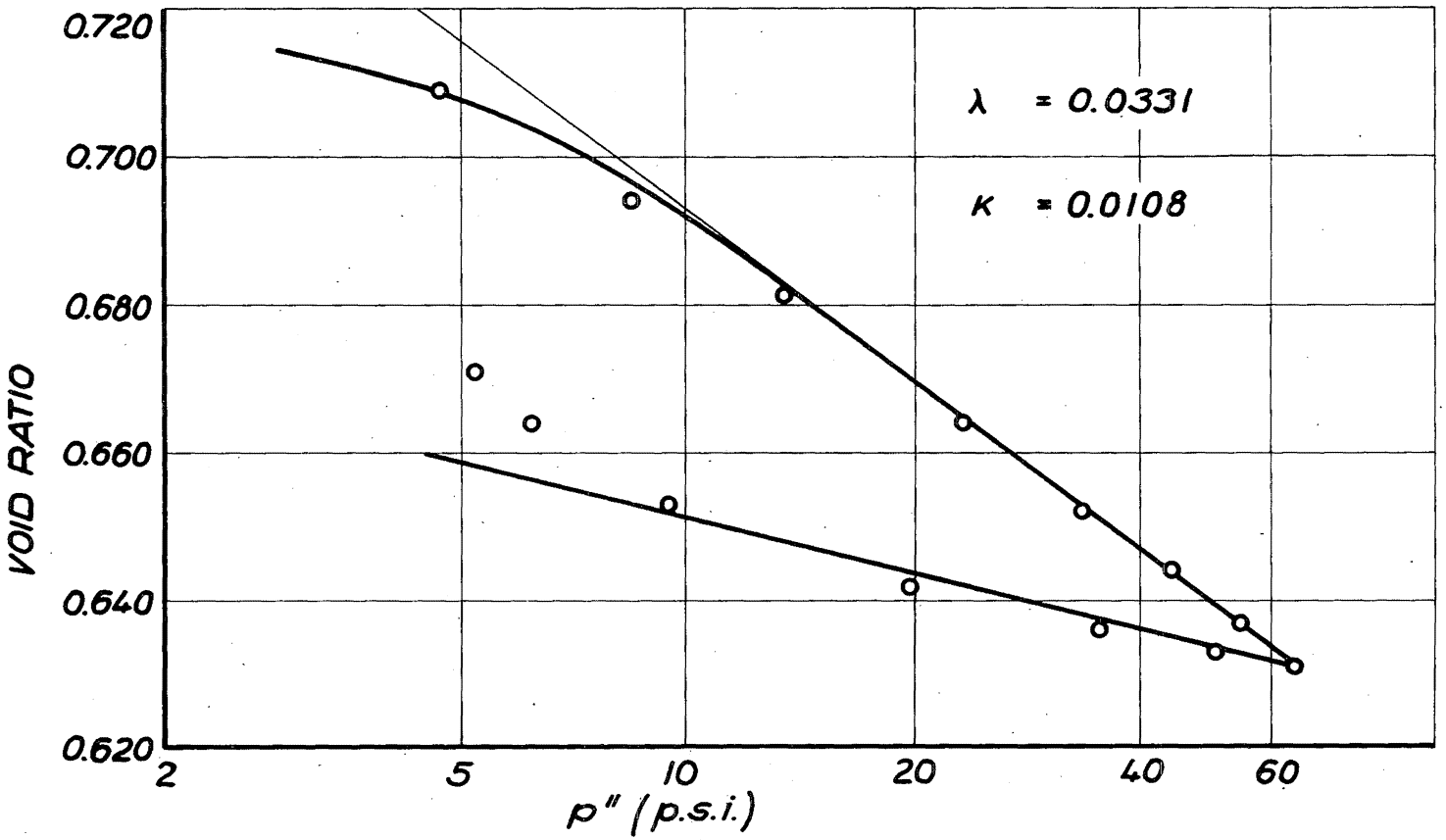

FIG. 5.7. ISOTROPIC ($q = 0$) CONSOLIDATION BEHAVIOUR IN TERMS OF ACTUAL EFFECTIVE STRESS

of actual effective stress. In Fig.5.7 the consolidation curve of Fig.A.1 has been replotted in terms of the actual effective stress. This results in a slight increase in the parameters and k: however, the difference is not significant, k increases from 0.010 to 0.011 and λ is increased from 0.031 to 0.033. These values of λ and k are very definitely a function of the mode of sample preparation so that it is no surprise that the and k values are quite different from those for a slurry also given in Appendix A.

One of the basic ideas of the Cambridge work is that the only recoverable component of deformation is volumetric strain which is represented by a straight line on the (e,lnp) curve with a slope k. There is supposed to be no recoverable shear deformation. An important graphical representation of this was the elastic wall in the S.B.S. in which the only component of strain was recoverable volumetric strain. Now it has been demonstrated in Chapter 4 how the material treated here has some recoverable shear deformation so the question arises as to whether this has to be represented on the boundary surface. The recoverable volumetric strain is represented on the S.B.S. because volumetric strain is in effect a change in void ratio and so a volumetric strain causes a change in a state variable. On the other hand shear strain is not a state variable and so it is not represented on the S.B.S.

In summary this section has been concerned with explaining

in qualitative terms the general features of the behaviour reported in Chapter 4. It has been postulated that as a consequence of the compaction process a hydrostatic component of stress is built into the material and this has been evaluated independently in three ways. All three of these approaches indicate that for the particular material discussed in this thesis the magnitude of this stress is approximately constant at 3.0 psi. Using a suggestion made in Chapter 2 it is suggested that this stress can be added to the measured effective stress to give the so called actual effective stress which describes the soil behaviour more satisfactorily than the Terzaghi effective stress. A consequence of using the actual effective stress is that it is possible to plot the three dimensional surface formed by the various undrained stress paths in the (p, q, e) space as a unique two dimensional plot of the dimensionless ratios η' and ξ'. In this way the results of these tests are similar to the critical state concepts, although the three-dimensional surface is only a S.B.S. for loading; unloading and reloading paths may lie outside it. Nevertheless the fact that the loading stress paths for the undrained tests do form a unique surface means that a general equation for the volumetric plastic strain increment can be developed for any stress increment lying in the surface. This is done in section 6 of this chapter.

5.4 CALCULATION OF INCREMENTS OF PLASTIC STRAIN

In this section the procedure used in calculating the components of plastic strain for the undrained tests is outlined. The calculation of the volumetric strain is discussed first and this is followed by procedure for calculating the distortion increment.

The relation between the plastic volumetric strain and the shift in the k line has been outlined in section 2 of this chapter. However this explanation was developed for a material that exhibited no change in the stress component p on unloading the stress component q, i.e. for normally consolidated or lightly overconsolidated clay. When it is applied to a material that has a decrease in p when the stress component q is reduced a contradiction results. It has been explained how the material treated in this thesis can be regarded as elastic-plastic work-hardening so that only elastic strains are supposed to occur during an unloading-reloading cycle. However for an undrained test the change in p on unloading implies that there must be some plastic volume change because of the shift in k-line associated with the decrease in the stress p. Stress paths for unloading and reloading cycles can be seen in Figs.4.12 and 4.16 and they show that there is a very definite decrease in p as q is reduced and Fig.4.21 shows that these unloading parts of the stress paths have a characteristic shape. To account for this change in p on unloading it is necessary to modify the concept

of the elastic wall. It is still possible to have elastic volume changes during unloading even when there is some change in p, provided that all the unloading stress path lies in an elastic wall. This is the modification introduced in this chapter, viz. that the unloading parts of the stress paths lie in an elastic wall and consequently this wall is no longer vertical in the (q, p, e) diagram. It is still assumed that the intercept of this modified elastic wall on the (p, e) plane is a straight line of slope -k in (e, lnp) diagram. The second of these requirements means that the particular k line associated with the elastic wall at a given loaded state is specified by the value of p" in the unloaded state and the change in k line during some loading process is related to the change in the value of p" at unloading. This idea is illustrated in the following diagram Fig.5.8 which is similar to Fig.4.20.

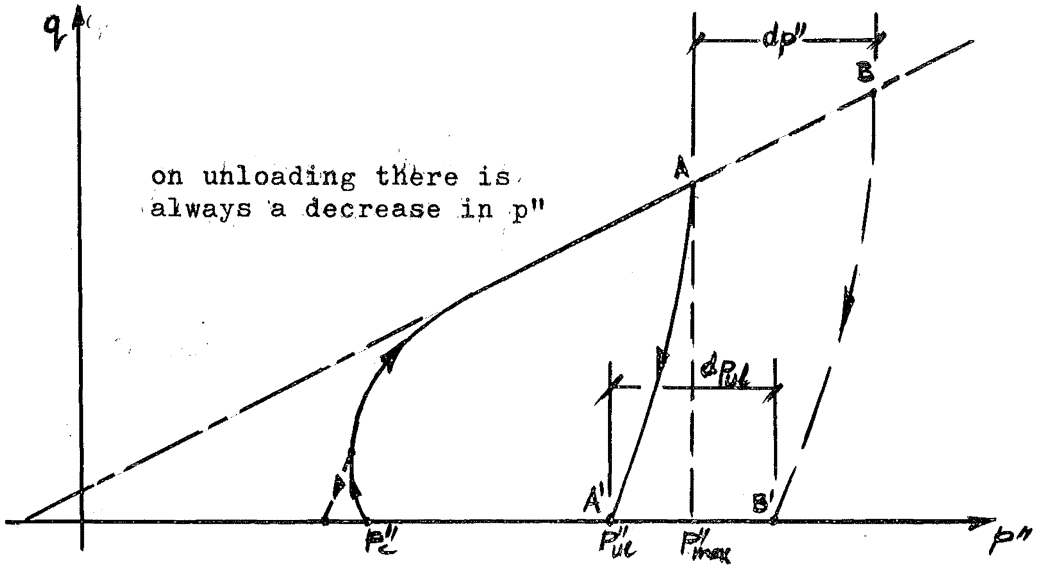

FIG.5.8 UNLOADING PART OF STRESS PATHS

Taking the suggestion made above, the plastic volume change during an undrained test is related not to dp but rather to dp_{ul}. Consider the case set out in the diagram above: a material stressed to point A on complete unloading would come to A'. Now if the stress was increased from A to B before unloading the material will end at B'. At this stage it is necessary to express dp_{ul} in terms of dp so that the increment of plastic volume change can be calculated. It has already been shown in Fig.4.21 that there is a unique relation between p_{max} and p_{ul}. This was achieved by using the following parameter:

$$\zeta' = \frac{p_{max} - p_{ul}}{p_{max} + 3} = \frac{p''_{max} - p''_{ul}}{p''_{max}} \quad \ldots\ldots\ldots\ldots (4.4)$$

and Fig.4.21 shows that for all the undrained tests the relation between ζ' and ξ' is unique, which means that at any stage of loading p_{ul} can be calculated. Thus the definition of plastic strain becomes:

$$dv^p = -\frac{k\, dp_{ul}}{(1+e)p''_{ul}} \quad \ldots\ldots\ldots\ldots\ldots\ldots\ldots\ldots (5.5)$$

where $p''_{ul} = p_{ul} + 3.0$. This equation represents two modifications of Eq.(3.29). Firstly dp_{ul} rather than dp is used in the top line and secondly p''_{ul}, the actual effective stress, is used rather than the Terzaghi effective stress. At this stage it is necessary to calculate dp_{ul}, this follows from the definition of ζ' given in Eq.(4.4). It gives:

$$dp_{ul} = (1-\zeta')dp - p''\, d\zeta' \quad \ldots\ldots\ldots\ldots\ldots\ldots \quad (5.6)$$

Substituting this into Eq.(5.5) and also substituting for p''_{ul} gives:

$$dv^p = -\frac{k}{(1+e)}\left\{\frac{dp}{p''} - \frac{d\zeta'}{(1-\zeta')}\right\} \quad \ldots\ldots\ldots\ldots\ldots\ldots \quad (5.7)$$

This equation gives an expression for the plastic volume change during an undrained test; it is possible to express $d\zeta'$ as a function of dp so that during an undrained test dv^p is still a function of dp. Using Eqs.(4.4) and (4.5) this gives:

$$dv^p = -\frac{k}{(1+e)} f_1(\xi',\zeta')\frac{dp}{p''} = -\frac{k}{p''(1+e)}\left\{1 + \frac{0.068\zeta'(\xi' - 2.55)}{(1-\zeta')(\quad - 0.24)}\right\} \quad \ldots \quad (5.8)$$

Now Fig.4.21 shows that at any position along the stress path ζ' is always positive and less than unity and so the plastic strain increment defined by Eq.(5.7) is smaller in magnitude than that calculated from Eq.(3.29) when dp is positive, and larger when dp is negative. (Actually Eq.(3.29) gives an expression for an elastic strain increment, but since an undrained test is under consideration the elastic and plastic volumetric strain increments are equal and opposite).

Equation (5.7) represents a considerable modification of the concept of the elastic wall outlined in Chapter 3 and amplified in section 2 of this chapter. Because of the curved unloading stress path which must be contained in the elastic wall the wall itself must be curved rather than vertical. As an aid

to visualising this the following diagram, Fig.5.9 shows a sketch of the modified elastic wall. Examination of the unloading stress paths, Figs.4.12 and 4.16, shows that these are almost linear but that the slope decreases as ξ' increases and so sections of the elastic wall parallel to the (q,p) plane are very nearly straight lines but the slope of these lines increases as ξ' increases.

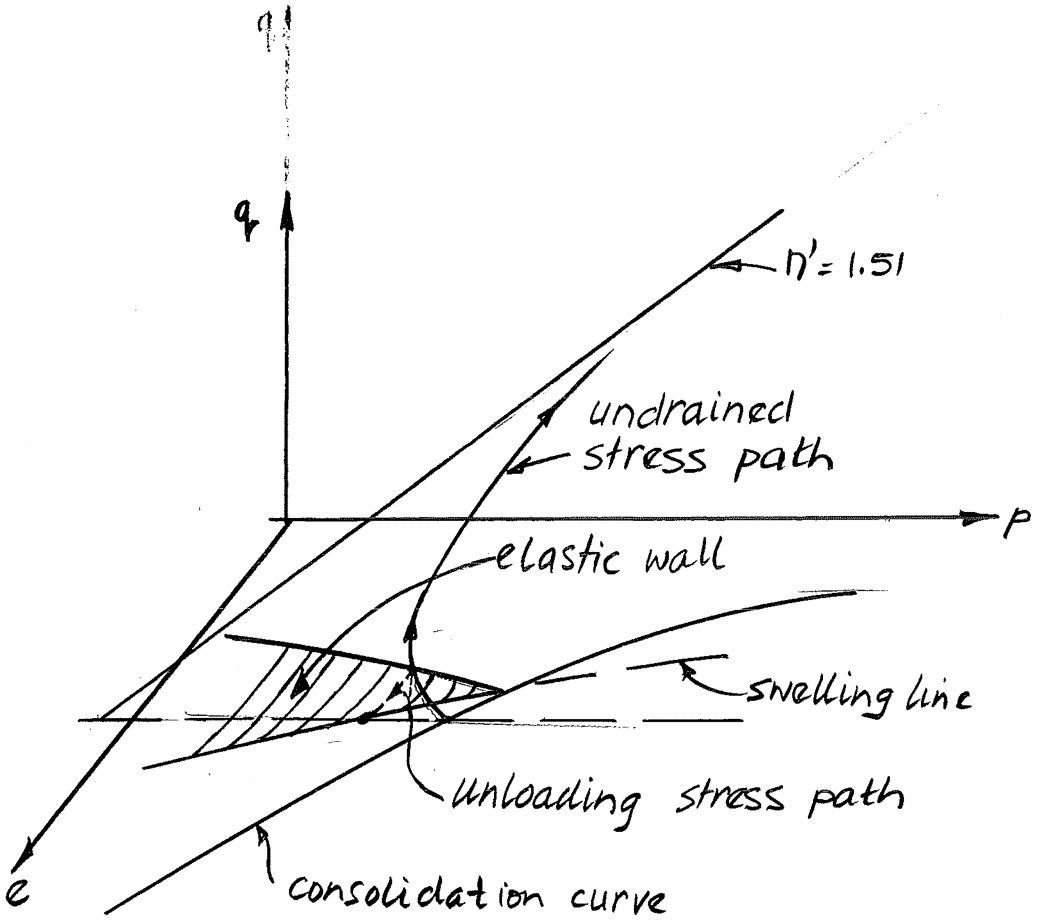

FIG.5.9 SKETCH OF MODIFIED ELASTIC WALL

Before moving on to the calculation of the increment of distortion the choice of a suitable value of k needs to be discussed. Fig.A.1 in Appendix A gives a means of determining k from the slope of the rebound curve. However it would seem more logical to do this in terms of the actual effective stress, and so k is determined from Fig.5.7 in which the void ratio is plotted against ln (p"). It can be seen that the initial part of the swelling curve is linear on the semi-logarithmic plot but that at the lowest values of p" the swelling line curves upward. Since the range of p" values for most of the tests considered is greater than 10 psi the slope of the linear part is used, thus the value of k used when calculating dv^p from Eq.(5.7) is:

$$k = 0.011$$

Now the procedure used for calculating the increment of plastic distortion is outlined. The basic equation used is Eq.(3.4) i.e.:-

$$d\epsilon^p = d\epsilon - d\epsilon^e$$

From equation (3.24)

$$d\epsilon = d\epsilon_1 - \tfrac{1}{3}\, dv$$

which continues the assumption of isotropy made in Chapter 3, and so:

$$d\epsilon^e = d\epsilon_1{}^e - \tfrac{1}{3}\, dv^e$$

where $d\epsilon_1$ is the axial strain increment. For the undrained tests at present under discussion dv^e is calculated from Eq.(5.7) using a plus rather than a minus sign. Thus all that remains to determine $d\epsilon^p$ is to calculate $d\epsilon_1{}^e$. This can be done with the undrained unloading secant modulus, G_{us}, introduced in section 4.7. It was discussed in Chapter 4 how this modulus remains approximately constant throughout an undrained test so that during the stress increment dq:

$$d\epsilon_1{}^e = dq/G_{us} \quad \ldots\ldots\ldots\ldots\ldots\ldots\ldots\ldots \quad (5.9)$$

Therefore:-

$$d\epsilon^p = d\epsilon - dq/G_{us} - \tfrac{1}{3}\, dv^p \quad \ldots\ldots\ldots\ldots\ldots\ldots \quad (5.10)$$

With the aid of equations (5.7) and (5.10) it is now possible to calculate the increments of plastic strain during the undrained tests; it has already been pointed out that in the triaxial test there are only two independent components of deformation, so that when $d\epsilon^p$ and dv^p are known the state of plastic deformation is completely specified.

5.5 CONTOURS OF EQUAL PLASTIC DISTORTION

In Fig.4.6 and 4.7 the contours of equal total axial strain have been plotted against the stress ratio η'. It has already been stated that in an undrained test the axial strain is equal to the distortion, so that Figs.4.6 and 4.7 are in fact plots of the contours of equal total (elastic + plastic)

distortion against the stress ratio η'. In this section the corresponding plot of the contours of equal plastic distortion are derived, i.e. η' v ϵ^p. The values of the plastic strains and strain increments have been calculated using a computer programme and the listing of this programme and the calculated results for the undrained tests can be found in Appendix H. In Fig.5.10 contours of equal plastic distortion have been plotted for ϵ^p = 0.1%, 1%, 2½% and 6%. This diagram is very similar to Fig.4.5 and shows that these contours are linear in the (q,p) plane as were the contours of equal total distortion. In Fig.5.11 the values of ϵ^p have been plotted against the value of η' for each of these contours and also the η' v ϵ curve from Fig.4.7 is included for comparison. The diagram shows that there is very little difference between the two curves. For a given value of ϵ the value of η' required for the same value of ϵ^p is seen to be slightly greater along the initial part of the curve for small values of ϵ and ϵ^p, and for larger values the two curves converge. At the small values of ϵ the difference between the curves is very much less than the scatter for the individual values of η', marked as a vertical line in Fig.4.7, so it is reasonable to assume that the η' v ϵ^p and the η' v ϵ curves for the undrained tests are practically the same.

5.6 STABILITY OF DEFORMATION

An essential requirement for applying the concepts of the

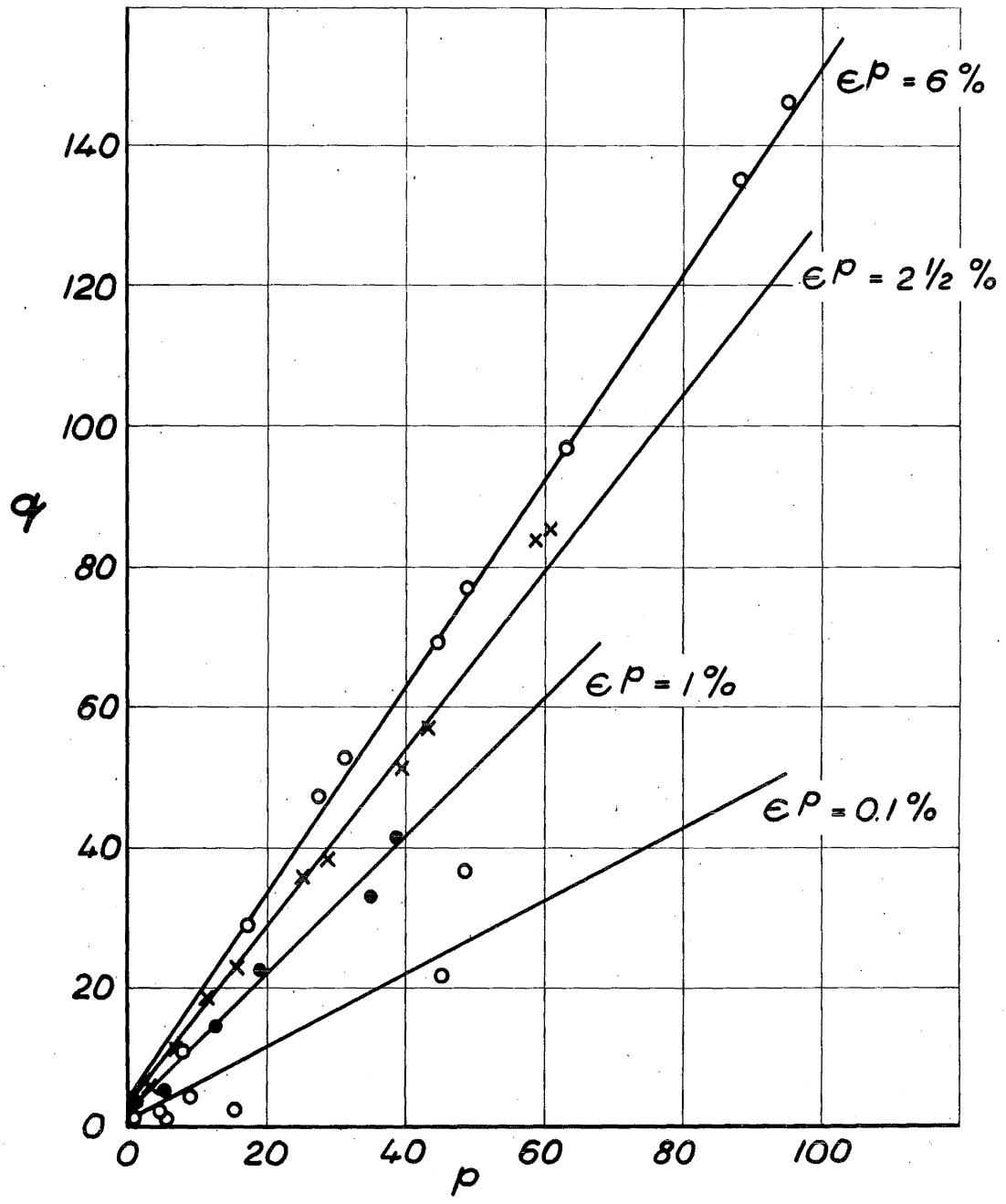

FIG. 5.10 CONTOURS OF EQUAL PLASTIC DISTORTION

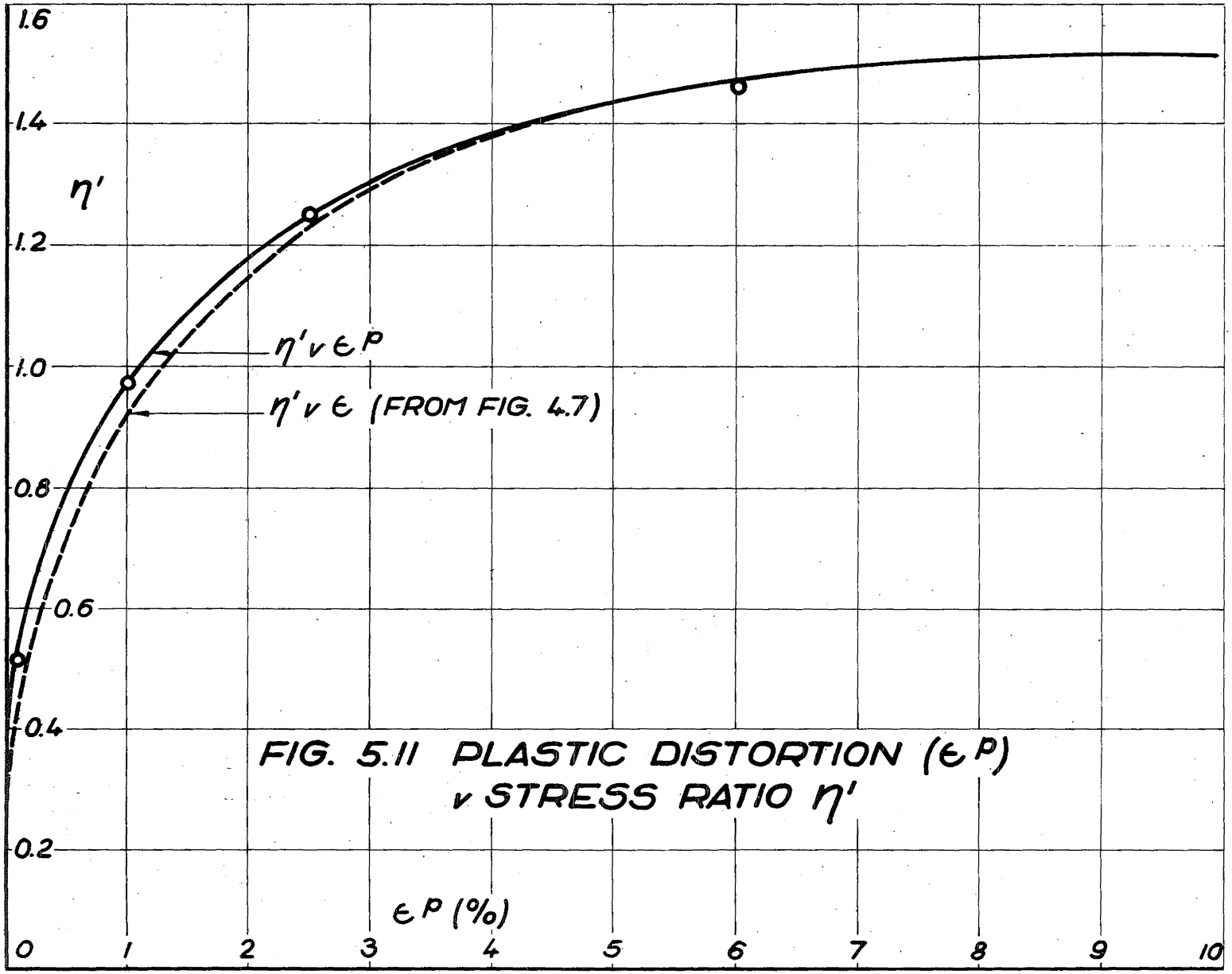

FIG. 5.11 PLASTIC DISTORTION (ϵ^P) v STRESS RATIO η'

theory of plasticity is that the material deformation must be stable in the sense defined by Drucker. This requires that at all stages of the deformation the following inequality must hold:-

$$d\sigma_{ij}\, d\epsilon^{p}_{ij} \geqslant 0 \qquad \ldots\ldots\ldots\ldots\ldots\ldots\ldots\ldots\ldots\ldots\ldots\ldots\ldots\ldots \quad (3.10)$$

For a material which is assumed to be isotropic, and which is tested under conditions of axial symmetry in the triaxial apparatus, there are only two independent components of stress and strain. In this case the above inequality can be expanded to:

$$dq\,d\epsilon^{p} + dp\, dv^{p} \geqslant 0 \qquad \ldots\ldots\ldots\ldots\ldots\ldots\ldots\ldots\ldots\ldots\ldots\ldots\ldots\ldots \quad (5.11)$$

This inequality was evaluated at each stage of the loading for the undrained tests. The results are given along with the plastic strain increments in Appendix H. The values are tabulated in the column headed DS and it is seen that the inequality is satisfaied at all stages of the loading. This observation carries with it the implication that a yield surface must exist which is also a plastic potential for the material.

For the two drained tests the plastic strain increments were evaluated and tabulated along with a listing of the results for these tests in Appendix G. The inequality given in Eq.(5.11) has been evaluated and, as before, tabulated in the column headed DS. These tabulated values show that for strains up to about 7% the inequality is satisfied and between strains of 7 and 10% the value of DS fluctuates between small negative and small positive

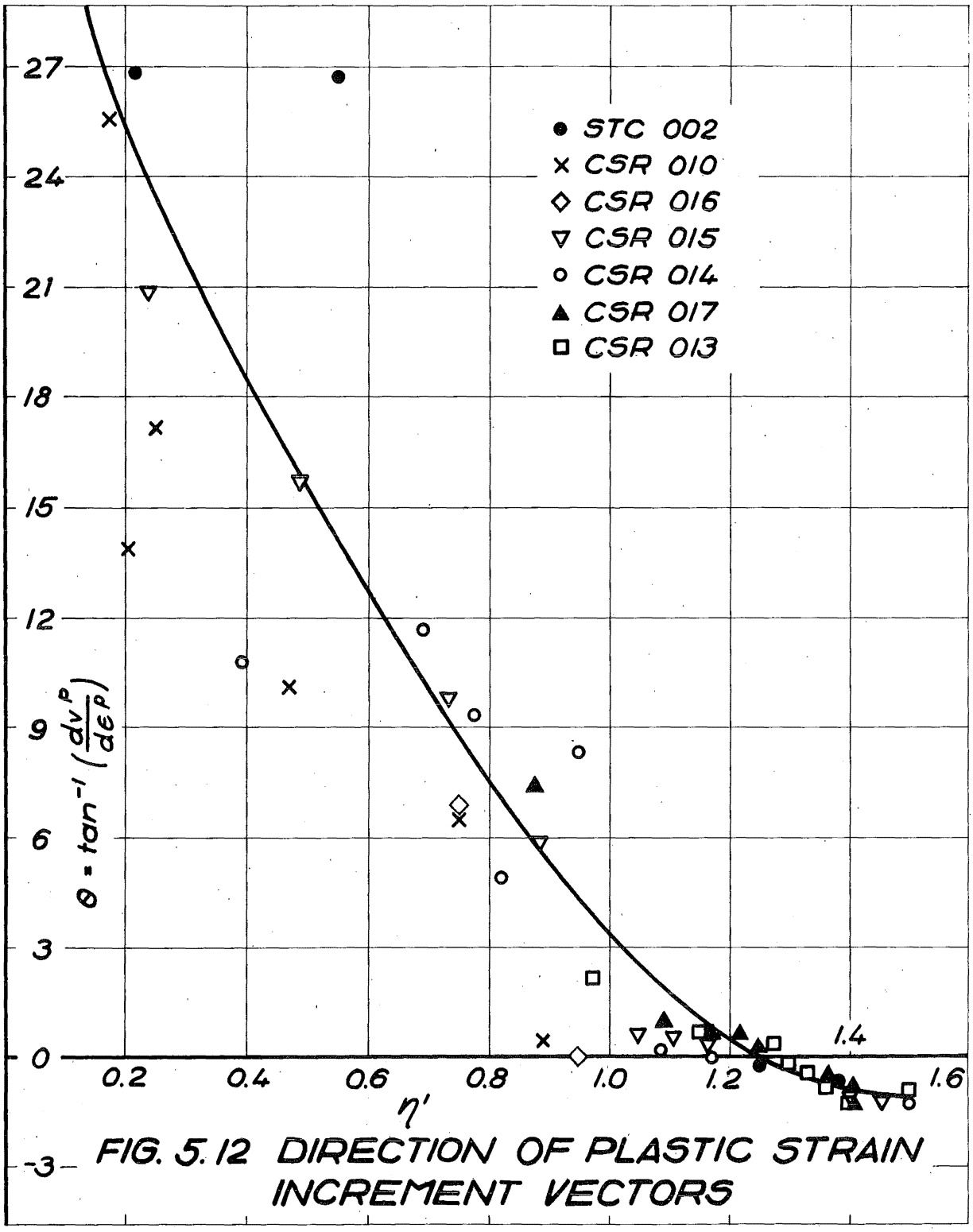

FIG. 5.12 DIRECTION OF PLASTIC STRAIN INCREMENT VECTORS

values. This suggests that in the range of strains between 7 and 10% the inequality is just satisfied.

For the initial stages of the loading $d\epsilon^p$ and dv^p are positive for both the drained and undrained tests. However at the latter stages dv^p becomes negative and so the inequality, Eq.(5.11), is still satisfied because the term $dqd\epsilon^p$ is greater in magnitude than the term $dpdv^p$. It is perhaps fortunate that k is small for this material because this keeps the magnitude of the actual volumetric strain increments small and so when dv^p is negative $dqd\epsilon^p$ is the dominant term. However if the value of k was larger this might not be so, and the negative values of dv^p could cause the inequality not to be satisfied.

5.7 DIRECTION OF THE PLASTIC STRAIN INCREMENT VECTORS

Using Eqs.(5.7) and (5.10) it is possible to calculate the inclination of a vector whose two components are dv^p and $d\epsilon^p$. Because the material is assumed to be isotropic the principal axes of the stress increment tensor and the strain increment tensor coincide, so that the direction of this vector can be plotted in the (q,p) plane with the stress paths. The angle is defined by the following equation:

$$\theta = \tan^{-1}(dv^p/d\epsilon^p) \quad \ldots\ldots\ldots\ldots\ldots\ldots\ldots\ldots \quad (5.12)$$

The calculated values are included with the listing of computer results in Appendix H. In Fig.5.12 the values of θ have been

plotted against η' for the undrained tests. It is clear that there is a uniform trend in this diagram despite a large amount of scatter. The fact that the points are scattered is not surprising because the values have been calculated directly from the stress paths and the stress-strain curves. None of these curves is absolutely smooth, although a good smoothed curve can be drawn through the points. However when incremental values are taken, any small fluctuations from point to point become important and result in large fluctuations in θ. This is overcome by drawing a smoothed curve through the points in Fig.5.12. Initially, when the samples just yield, the values of θ are large but as η' increases θ decreases and is zero when η' is about 1.26. For larger values of η' it can be seen that θ becomes negative but the angles remain small.

The curve shows that when η' is equal to 1.51 θ has a value of -1.3°. This means that along the final part of the stress paths which have a constant value of η' the inclination of the plastic strain increment vector is constant. This angle is so small that it is worth considering whether it is small because of some experimental error, and should in fact be zero along the final part of the stress paths. The answer to this is definitely no. Equation (5.7) and the curve of ζ' v ξ' (Fig.4.21) provide the explanation. The plot of ζ' v ξ' in Fig.4.21 shows that eventually ζ' reaches a constant value so the term $d\zeta'/(1-\zeta')$ will become zero, this happens when $\xi' = 2.55$. Now $\eta' = 1.51$

when $\xi' = 2.00$ so that $d\zeta'/(1-\zeta')$ is zero a short way along that part of the stress path where η' is constant. Also for all values of $\eta' > 1.0$ dp is positive, thus somewhere between $\xi' = 0.75$ ($\eta' = 1.0$) and $\xi' = 2.55$ the term $\{dp/p'' - d\zeta'/(1 - \zeta')\}$ changes from negative to positive values so that the plastic volumetric strain increment changes from positive to negative values. The only way that dv^p can be zero when η' is constant (and hence Θ be zero) is for dp/p" to be equal to $d\zeta'/(1 - \zeta')$, thus as p" increases $d\zeta'$ must also increase. This is quite contrary to Fig.4.21 which shows very definitely that along the final part of the stress paths ζ' is constant at 0.71. Thus there is no question about the validity of the small negative values of Θ along the final parts of the stress paths - they are a consequence of the η' v ξ' and ζ' v ξ' behaviour explained in Chapter 4.

Another question that needs to be considered is the effect on this behaviour of the use of Equation (5.7) rather than (3.29) for calculating the volumetric strain increment. The concepts underlying Eq.(5.7) have been introduced to account for the characteristic shape of the unloading stress paths but it has not been possible to put this idea to independent test because of the limitations of the testing equipment available, and so the existence of a curved elastic wall does remain hypothetical. However the use of equation (5.7) alters the shape of Fig.5.12 slightly but not the general features. It can be seen that if the ζ' term is neglected, Θ is zero when dp is zero, and also

that the initial values of θ will be smaller and the final values a little larger, but the overall shape of Fig.5.12 will still be the same - θ starts at positive values and eventually becomes negative.

The same is true of $d\epsilon^p$. In Chapter 4 it has been shown that there is clearly some recoverable shear deformation but some aspects of the behaviour of G_{us} are uncertain, for example Fig.4.13. However Figs.5.10 and 5.11 have shown that the effect of this recoverable shear deformation is small because there is very little difference between the ϵ v η' and ϵ^p v η' curves. Thus the actual value of G_{us} does not have a great influence on Fig.5.12 and so it can be concluded that a curve of the shape of Fig.5.12 is truly characteristic of this material although the actual details of the curve do depend on the definitions of $d\epsilon^p$ and dv^p used.

Figure 5.12 represents a very important simplification of Eq.(5.1). The fact that all the undrained tests give the same η' v θ curve means that the direction of the plastic strain increment vector is not dependent on the void ratio of the material as suggested by Eq.(5.1). Figure 5.12 shows that θ is a function only of the ratio of the stresses q and p", in other words the successive yield curves for the work hardening material are geometrically similar. The values plotted in Fig.5.12 are points determined from a whole range of yield curves but because of this geometrical similitude they are also the values that would be obtained when yielding takes place at various points around a

particular yield curve. Thus the smoothed curve in Fig.5.12, a function of η', can be integrated to give an expression for the yield curve for this material. This is done in section 10 of this chapter.

5.8 DRAINED TESTS

The details of the two drained tests performed have already been discussed in Chapter 4. At this point it is necessary to consider these tests further and examine the relationship between the measured behaviour and the boundary surface derived for the undrained tests. It has long been a classic problem of soil mechanics to relate the behaviour of drained tests to that of undrained tests. During a drained test the volume change means that a certain amount of the applied load is used in doing work against or with the cell pressure and to account for this the so called boundary energy correction has been applied. The correction used here is that proposed by Bishop[7]. In this an additional term is added to the applied shear stress to account for the volume change. The equation has the following form:

$$q_r = q + \sigma'_3 \frac{dv}{d\epsilon_1} \qquad \text{.....} \quad (5.13)$$

where q_r is the corrected stress. This correction has been applied to the stress paths for the drained tests. The stress ratio, $q_r/(p+3)$ has been plotted in Fig.5.13 against the value

of ξ'. The value of ξ' is defined in the same way as in Eq.(4.3), however when calculating ξ' for drained tests the value of p_c, the value of p on the isotropic consolidation line, must be determined for the current void ratio. In Fig.5.13 that part of the η' v ξ', Fig.4.18, for values of $\xi' > 1$ has been included for comparison.

The object of applying this correction to the measured stress paths of the undrained tests is to see if the corrected paths lie in the boundary surface defined by the undrained tests. Now along a drained stress path p (and therefore ξ') increases right from the start of the test and so it is evident that if the corrected path is to lie in the boundary surface then at the beginning of the test when η' is near zero η'_r must be about 1.3. It is clear from Fig.5.13 that this does not occur, although the corrected value for the early stages of the test is greater than the actual value of η' the difference is still not large enough. The diagram shows that η'_r increases fairly rapidly with ξ' and actually crosses the η' v ξ' curve from Fig.4.18 and so η'_r is greater than η' towards the end of the test.

It is not clear why the corrected values of η' do not lie on the η' v ξ' curve. This form of correction was used with reasonable results by Roscoe, Schofield and Wroth[63] in correcting the results of drained tests on silt. Poorooshasb and Roscoe[59] have made certain suggestions about the use of Bishop's boundary energy correction and although they have suggested a modified

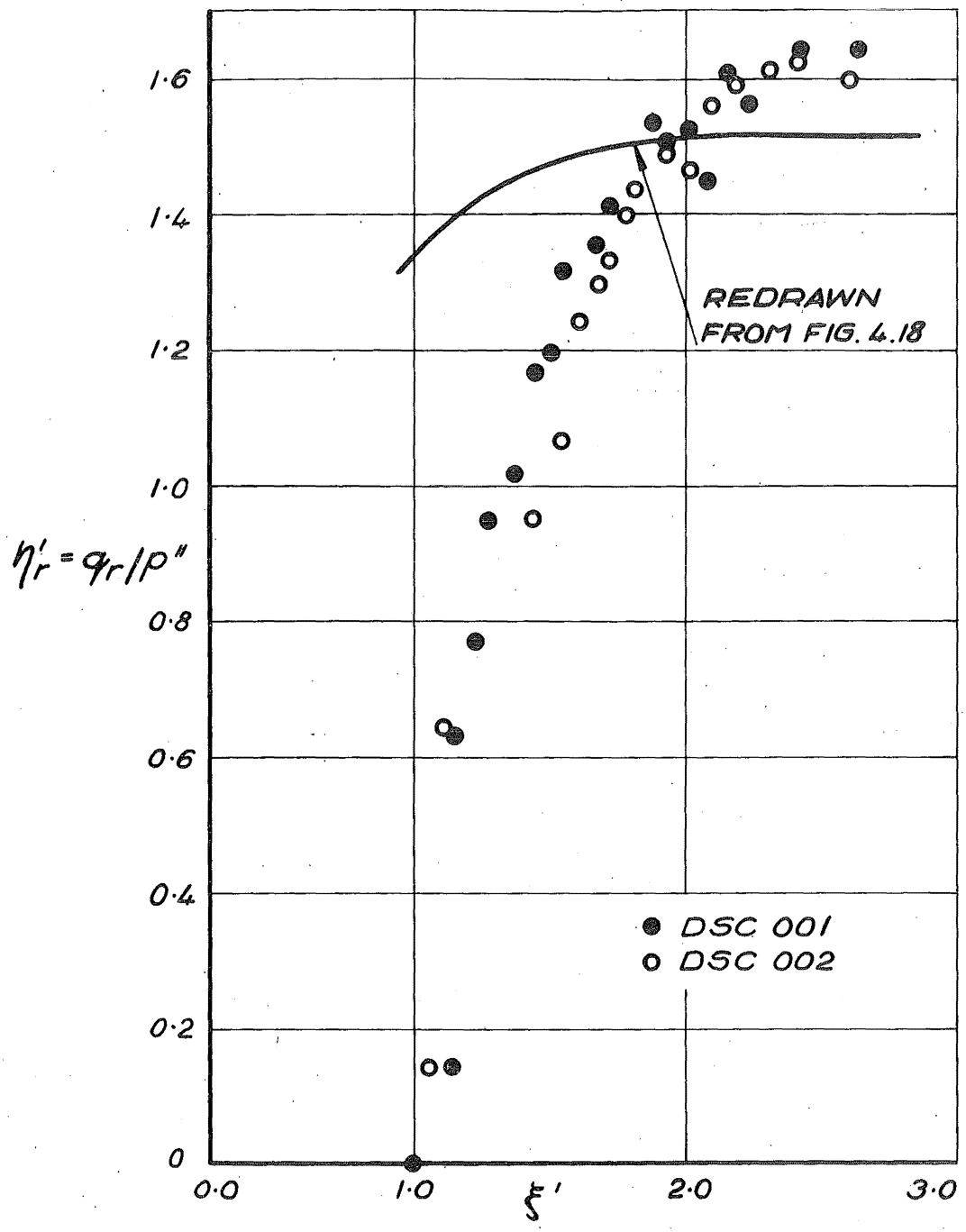

FIG. 5.13 DRAINED STRESS PATHS IN TERMS OF THE PARAMETERS η'_r & ξ'

form they have confined their discussion to normally consolidated clays. Thus it seems that it is necessary to find a suitable energy correction for this compacted material under drained conditions, a task that is not attempted in this thesis.

5.9 DEVELOPMENT OF A REVISED ENERGY EQUATION

Roscoe's energy equation, discussed in Chapter 3, has the form:

$$qd\epsilon + pdv = Mpd\epsilon + \frac{dkp}{(1+e)} \quad \ldots\ldots\ldots\ldots\ldots\ldots\ldots\ldots \quad (3.32)$$

The terms on the left hand side of this equation represent components of energy due to the externally applied stresses and their corresponding deformations. Those on the right hand side are the energy components stored or dissipated within the soil. The term $Mpd\epsilon$ is the work dissipated as friction, as explained in Chapter 3, M is a soil constant that is independent of void ratio, stress or strain. The second component on the right hand side is the recoverable energy of volume change, i.e. the energy associated with the rebound curve on the (e,lnp) plot.

As it stands Eq.(3.32) is not suitable for describing the behaviour of the soil discussed in this thesis for two reasons. Firstly the material has some recoverable shear deformation; Eq.(3.32) was formulated on the assumption that this is zero. Secondly there is the component of stress that seems to be built into the soil as a result of the compaction process which requires

that the actual rather than the Terzaghi effective stress be used.

The phenomenon of recoverable shear distortion was discussed from the experimental viewpoint in Chapter 4. In summary the discussion in section 4.7 leads to the following four conclusions:

(i) That the undrained unloading second modulus, G_{us} is directly proportional to the consolidation pressure, Fig.4.10.

(ii) That the non-linear unloading stress-strain curve has the form $q = \epsilon_r^n$, where ϵ_r is the recoverable distortion on complete unloading and n has the value 0.5, Fig.4.14.

(iii) That the magnitude of G_{us} is not changed by repeated loading to the same maximum stress, Fig.4.17.

(iv) That for an undrained test the magnitude of G_{us} seems to be independent of q.

Of these four conclusions the first three are quite well established in Chapter 4, but there is some uncertainty about the fourth. Fig.4.13 shows that although there is a fair amount of scatter there is no systematic change in G_{us} with q. Because of this it is assumed here that G_{us} is independent of q.

Fig.5.14 is a sketch of a typical stress-strain curve for an undrained test; some unloading curves are included to illustrate how the recoverable energy of distortion is calculated.

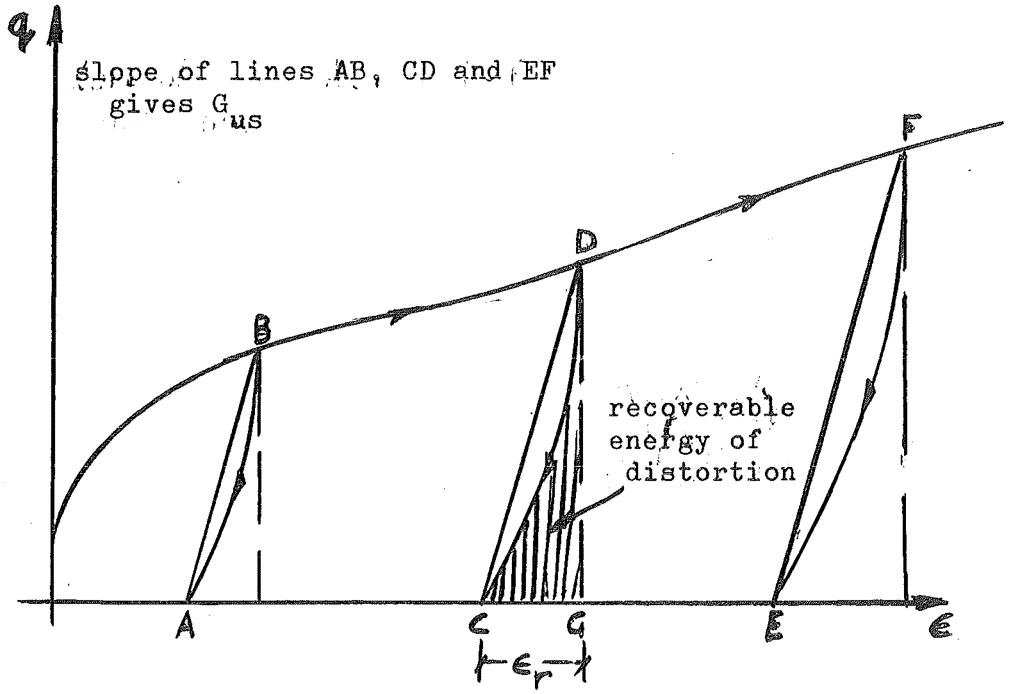

FIG.5.14 TYPICAL STRESS-STRAIN CURVE FOR AN UNDRAINED TEST WITH UNLOADING

The slope of the lines AB, CD and EF define the magnitude of G_{us}. The distortional energy stored at point D is given by the shaded area GDC. From Fig.4.14 the curve DC is assumed to be a third order curve. The area under the unloading curve gives the stored distortional energy U_D:

$$U_D = \tfrac{1}{2} \times \tfrac{1}{2} \times q \times \epsilon_r$$

where ϵ_r is the recoverable shear distortion. G_{us} is defined by:

$$\epsilon_r = q/G_{us}$$

So that:

$$U_D = q^2/4G_{us} \quad \ldots\ldots\ldots\ldots\ldots\ldots\ldots\ldots\ldots\ldots\ldots\ldots\ldots\ldots \quad (5.14)$$

Now when there is a small increase dq from q_1 to q_2 the incremental increase in stored energy is:

$$dU_D = \frac{dq}{4G_{us}} (q_2 + q_1)$$

which can be approximated to:

$$dU_D \approx qdq/2G_{us} \quad \ldots\ldots\ldots\ldots\ldots\ldots\ldots\ldots\ldots\ldots \quad (5.15)$$

This incremental increase in stored energy must be added to the right hand side of the energy equation as it is a component of stored energy. A question that should be considered is concerned with the mechanism underlying this recoverable deformation. Is it elastic or inelastic? Obviously the non-linear unloading curve demonstrates that, if elastic, the deformation is not of the linear variety. It is suggested here that the recoverable shear deformation can be regarded as elastic in the same sense that the recoverable energy stored on consolidation is regarded as elastic. If the rebound curve is plotted on a natural scale the resulting curve of e v p for unloading is curved and has much the same shape as the q v ϵ_r curve on unloading, i.e. the curvature increases as the stress decreases. Neither of these curves represents elastic behaviour in the usual linear sense but in as much as they represent deformation that is recoverable on unloading they imply the existence of stored energy. Thus if a correction is to be incorporated into the energy equation to account for the stored energy due to the nonlinear (e,p) curve on unloading it is

then consistent to include another correction to account for the nonlinear (ϵ_r,q) curve. In this thesis some effort is made to refer to these as corrections for stored or recoverable energy; reference to elastic energy is avoided because of the connotation that the word elastic has for linear behaviour.

The second modification to the energy equation incorporates the actual effective stress rather than the Terzaghi effective stress. That is, the component of p equal to 3.0 psi that seems to be built into the material as a result of the compaction process is included in the equation. This requires that three of the terms be modified. On the left hand side of equation 3.32 the term pdv becomes p"dv. On the right hand side the term for the work dissipated as friction has to be modified to $Mp"d\epsilon^p$ and the term for the stored energy of volume change must be changed. Comparing equations (3.29) and (3.30) it is seen that the increment of volumetric energy stored during the application of a stress increment dp is p times the corresponding recoverable volumetric strain increment. Thus the recoverable energy of volume change stored in the material during a stress increment dp is given by changing the sign of the right hand side of Eq.(5.7) and multiplying throughout by p". Thus the energy equation is now written:

$$p"dv + qd\epsilon = Mp"d\epsilon^p + \frac{k}{(1+e)}\left\{dp - p"d\zeta'/(1-\zeta')\right\} + \frac{qdq}{2G_{us}} \quad \ldots\ldots \quad (5.16)$$

At each stage of the loading all the terms in this equation, with

the exception of M are either measured directly or can be calculated from the measured values, thus M can be evaluated at each stage of the stress path. However this is not necessary. Equation (5.16) has an appearance rather different from Eq.(3.32) and this is so because of the corrections for recoverable volumetric and distortional energy, but in essence the two equations are identical. Eq.(5.16) uses the same terms to account for the dissipation of work as friction within the material as does Eq.(3.32). The apparent difference between the two equations is a consequence of the more complex terms needed to account for the stored energy in the compacted soil discussed here, however when written in terms of plastic strain increments the equations are similar. The only difference is that here actual effective stress is used and so Eq.(5.16) can be written as:-

$$p''dv^p + qd\epsilon^p = Mp''d\epsilon^p \quad \ldots\ldots\ldots\ldots\ldots\ldots\ldots\ldots \quad (5.17)$$

This can be rearranged to give:

$$M = \eta' + \tan\Theta \quad \ldots\ldots\ldots\ldots\ldots\ldots\ldots\ldots\ldots\ldots \quad (5.18)$$

Figure 5.12 gives $\tan\Theta$ as a function of η' and so M can be calculated as a function of η'. This has been done and the values are plotted in Fig.5.15. It is immediately obvious from this diagram that for the compacted clay considered in this thesis M is not constant. The idea that the friction parameter

M is constant is a key concept in the critical model however the reason for the variability is not considered further here, it may be that a different term for the work dissipated as friction is needed or it may be a characteristic of the material, but it does not pose any problem for the development of a yield curve. Fig.5.15 shows that at small values of η' M is approximately constant at 0.66 and that as η' increases M increases until the two are approximately equal for values of η' greater than 1.1.

5.10 DEVELOPMENT OF A YIELD CURVE

It is possible to fit a parabola through most of the points in Fig.5.15. This is shown as a solid line whereas the dots represent points calculated using Eq.5.18 and Fig.5.12. For values of η' greater than 0.8 the fit is very good but for smaller values of η' there is some divergence between the fitted curve and the measured points. It will be seen later that this difference does have an effect on the predicted stress-strain curves but the significance of this is not great. The curve fitting means that M can be expressed as the following function of η':-

$$M = 0.332\eta'^2 + 0.729 \quad \ldots\ldots\ldots\ldots\ldots\ldots\ldots\ldots \quad (5.19)$$

Substituting this into equations (5.18), using Eq.(5.12) and rearranging gives:

$$(dv^p/d\epsilon^p) = 0.332\eta'^2 - \eta' + 0.729 \quad \ldots\ldots\ldots\ldots\ldots \quad (5.20)$$

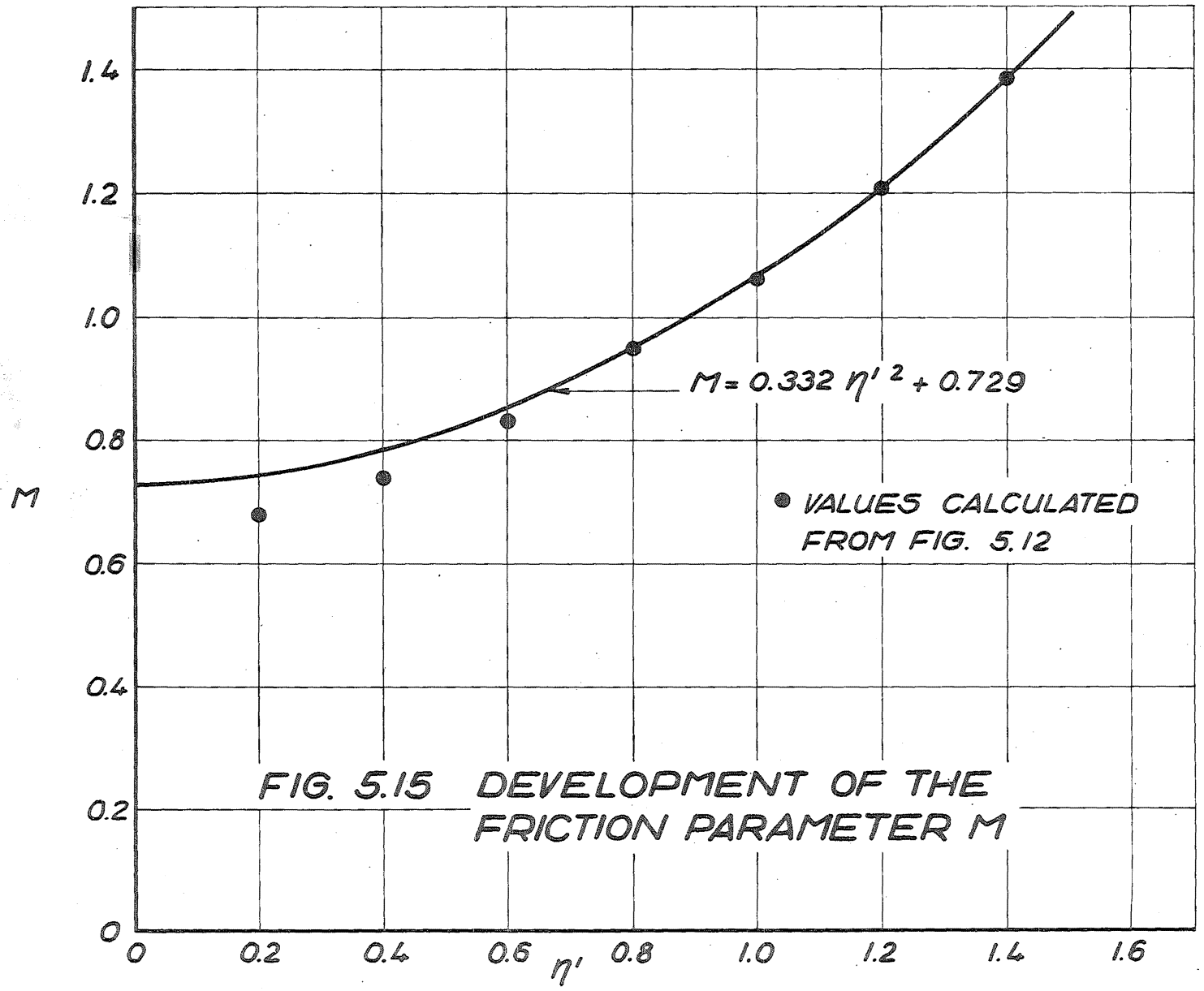

FIG. 5.15 DEVELOPMENT OF THE FRICTION PARAMETER M

This equation shows, for undrained loading at least, that the direction of the strain increment vector depends on η' and is independent of increments in stress and is thus a simplification of Eq.(5.1) but a little more complex than the relation that follows from Eqs.(3.48) and (3.49), i.e.:-

$$dv^p/d\epsilon^p = M - \eta'$$

However, as explained at the end of section 5.7, equation (5.20) can be integrated and a yield curve derived. As explained in Chapter 3 a yield curve for a work hardening material is such that along it:

$$dq/dp = - dv^p/d\epsilon^p \quad \ldots\ldots\ldots\ldots\ldots\ldots\ldots \quad (3.48a)$$

and so

$$dq/dp = -0.332\eta'^2 + \eta' - 0.729 \quad \ldots\ldots\ldots \quad (5.21)$$

On integration Eq.(5.21) gives the required yield curve, whose equation is of the form:-

$$\frac{dy}{dx} = F\left(\frac{y}{x}\right) = F(v)$$

and has the solution:-

$$\ln(x) = \frac{dv}{F(v) - v} + c$$

where $v = \left(\frac{y}{x}\right)$. Thus Eq.(5.20) integrates to:-

$$\ln(p'') = -3.01 \int \frac{d\eta'}{\eta'^2 + (1.481)^2}$$

which is:

$$\ln(p'') = -2.032 \tan^{-1}\{\eta'/1.481\} + c$$

Now when $\eta' = 0$, $p'' = p''_o$ (p''_o is the value of p" at which the yield curve cuts the p" axis) and thus the yield curve has the equation:

$$f = q - 1.481\ p'' \tan\left\{0.493 \ln(p''_o/p'')\right\} = 0 \quad \ldots\ldots\ldots\ldots\ldots\ldots \quad (5.22)$$

This function is a yield curve for the compacted clay considered in this thesis, prepared by kneading compaction wet of O.M.C. to a dry density of 93 lb/ft^3 and saturated by the application of back pressure, in the same way as Eq.(3.46) represents a yield curve for a normally consolidated clay. The partial derivatives of Eq.(5.22) with respect of q and p" are:

$$\frac{\partial f}{\partial q} = 1 \text{ and } \frac{\partial f}{\partial p} = g(\eta') = 0.332\eta'^2 - \eta' + 0.729 \quad \ldots \quad (5.23)$$

From Eqs.(5.23) it can be shown that when $\eta' = 1.23$, $dv^p/d\epsilon^p = 0$ and that $dv^p/d\epsilon^p > 0$ when $\eta' < 1.23$, and $dv^p/d\epsilon^p < 0$ when $\eta' > 1.23$. When $\eta' = 0$ $dv^p/d\epsilon^p = 0.729$ and when $\eta' = 1.51$ $dv^p/d\epsilon^p = -0.024$. Some of these yield curves have been sketched in Fig.5.16 and the general features of the curves are noted on the diagram. For any of the undrained stress paths in Fig.4.2 or the drained stress paths in Fig.4.25 each increment of stress results in a new yield curve being engaged and so the material work hardens and the range of states for which there can be only elastic deformation is increased.

Using the normality concept the values of θ for various values of η' can be calculated from Eqs.(5.23). This has been

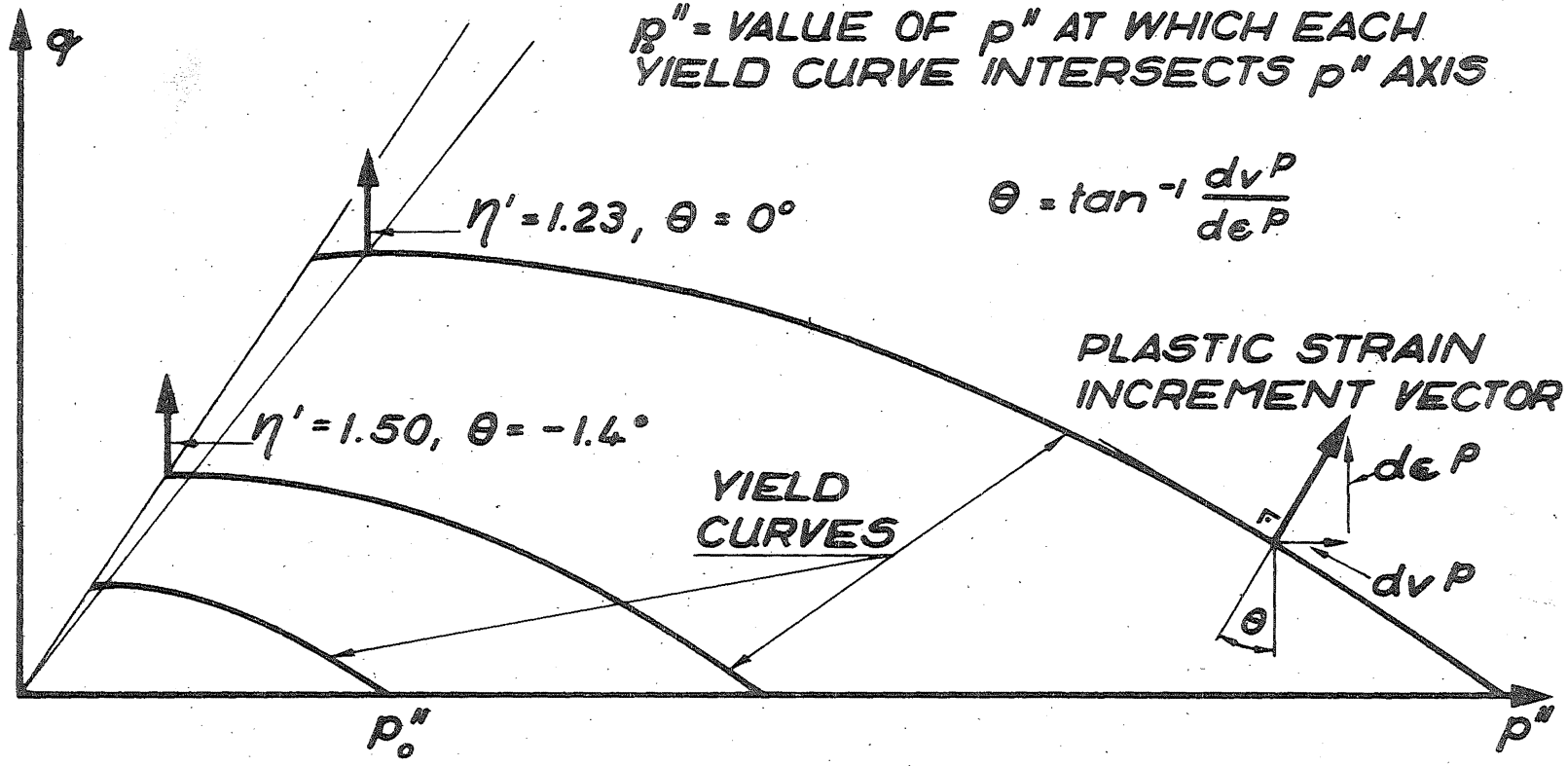

FIG. 5.16 SHAPE OF YIELD CURVES

$f = q - 1.481\, p'' \tan [0.493 \ln (p_o''/p'')]$

done and the results drawn as a solid line in Fig.5.17. Along with this calculated curve points for the smoothed curve from Fig.5.12 have been plotted. The diagram shows that the correspondence between the values of ϕ calculated for the yield curve and the values from Fig.5.12 agree very well for $\eta' \geq 0.8$. An alternative to the curve fitting used in Fig.5.15 would have been an exact fit of the curve at small values of η' with some discrepancy at larger values. However from the point of view of actually predicting stress-strain curves it would seem to be more important to fit the curve at larger values of η' as has been done here and tolerate some discrepancy at lower values because the greater part of the strains occur when η' is larger.

Finally in this section the geometrical interpretation of the yield curves is considered. In Chapter 3 it was shown how the yield curves can be interpreted as the projection on to the (q,p) plane of the line in which the elastic wall cuts the S.B.S. A similar suggestion is made here. This must be so because for a work hardening material the yield curve represents the limiting curve around which the stress point can move and yet give rise to no additional plastic deformation. Clearly there must be some path in the boundary surface for which this can occur and so it must be possible to project the yield curve on to the boundary surface and vice versa. For values of η' greater than 1.51 the function defined by Eq.(5.22) passes

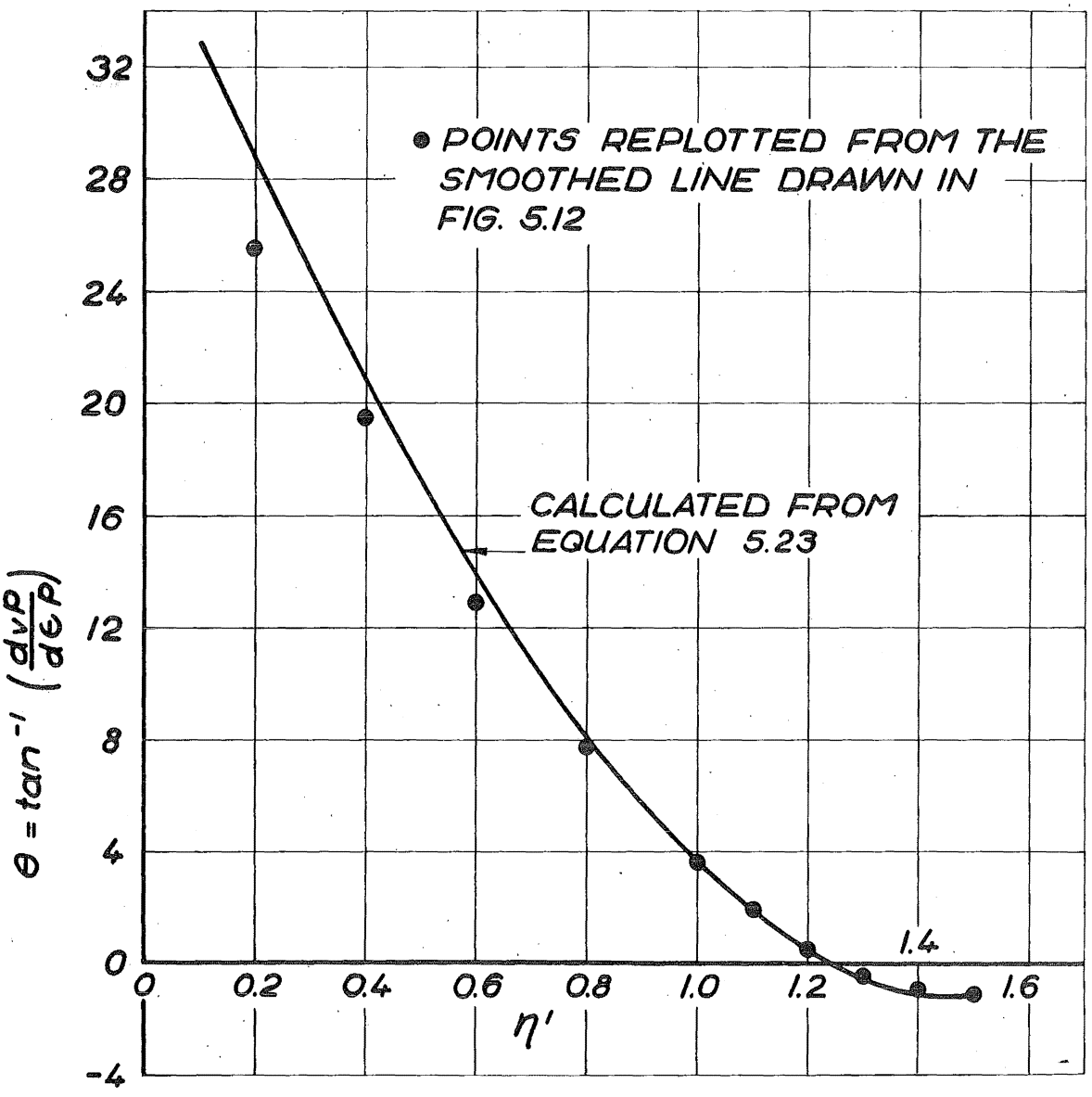

FIG. 5.17
RELATION BETWEEN θ DETERMINED FROM EQUATION 5.23 & EXPERIMENTAL VALUES

outside the yield curve and in fact tends to $+\infty$ when p'' is zero, but this is of no importance for the behaviour discussed in this chapter because here η' cannot have a value greater than 1.51.

In this section a function giving a yield curve for the material has been derived. It is a good deal more complex than that derived by the Cambridge group for wet clay because the compacted material does not seem to have a constant friction parameter M; however it can still be interpreted geometrically in the same way as the function derived for wet clay. As has already been pointed out the experimental results, Fig.5.12, on which this yield function is based, are independent of nonuniform sample deformation and so the same comment must apply to the function derived from these results. In the remaining parts of this chapter the relation between stress and strain for various stress paths is discussed, but since these are stress-strain curves there may be some difference between the observed and predicted values because of nonuniform deformation.

5.11 EVALUATION OF THE FUNCTION h

Equation (3.12) for a plastic material obeying Drucker's postulate has the form:

$$d\epsilon^{p}_{ij} = h \frac{\partial f}{\partial \sigma_{ij}} \frac{\partial f}{\partial \sigma_{kl}} d\sigma_{kl} \quad \ldots\ldots\ldots\ldots\ldots\ldots\ldots\ldots \quad (3.12)$$

The function for the yield curve, f, has already been determined

but the function h has yet to be found. The direction of the plastic strain increment vector is defined by the gradient of f, $\partial f/\partial \sigma_{ij}$, whilst the scalar function h and the increment in f, $\partial f/\partial \sigma_{kl}\ d\sigma_{kl}$, determine the magnitude of the plastic strain increment vector. The procedure used here for determining h is similar to that used in Chapter 3 where h was determined for a wet clay using the equation for the yield curve and equations (3.34) and (3.35). In Chapter 3 it was explained how Roscoe et al[65] calculated the volume change for an arbitrary stress increment in the boundary surface. The S.B.S. in the (p, q, e) space is unique, so the shape of the surface must define the change in void ratio associated with an arbitrary stress increment that lies in the surface. Using this and the observation that when the results of consolidation tests at constant stress ratio, η, were plotted on an (e,lnp) diagram a set of parallel straight lines of slope $-\lambda$ was obtained, one line for each test, they obtained Eq.(3.26) for the volumetric strain increment associated with a stress increment in the S.B.S. An almost identical procedure is followed here to determine the volumetric strain increment associated with an arbitrary loading stress increment lying in the boundary surface sketched in Fig.5.5. However in this case no information is available about the slope of consolidation curves at constant stress ratio η' in the (e,lnp) plane. This is overcome by assuming that the slope of these lines is a function of η'. The situation is illustrated in the following diagram:-

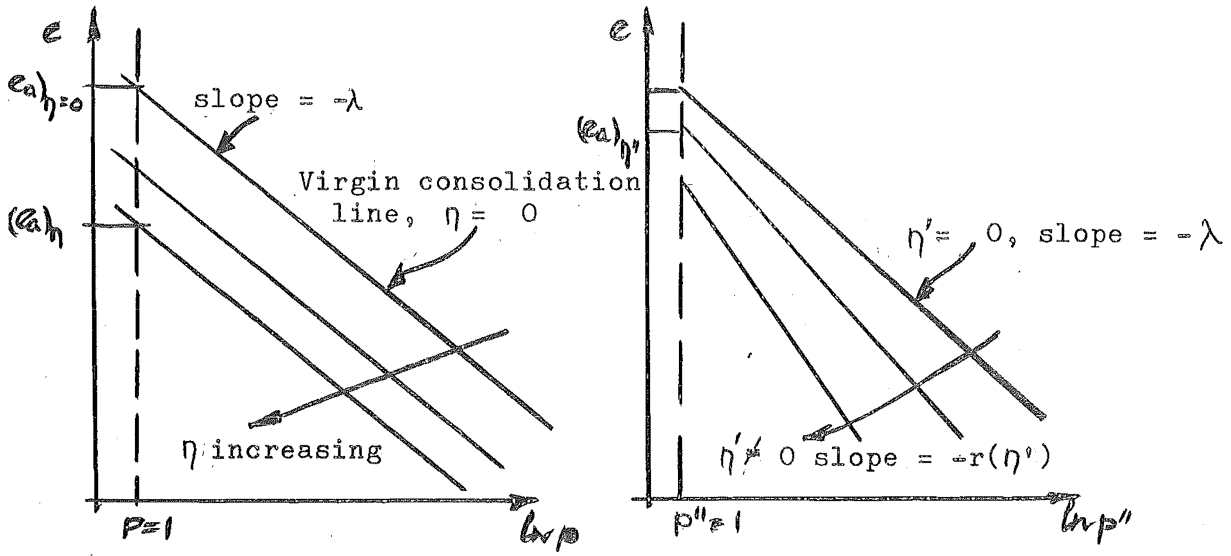

(a) wet clay (b) compacted clay

FIG.5.18 COMPARISON OF CONSOLIDATION TESTS AT CONSTANT STRESS RATIOS FOR WET CLAY AND SUGGESTED BEHAVIOUR FOR THE COMPACTED CLAY

This diagram illustrates the suggestion made here that the slope of the e,ln p" lines for consolidation tests at constant stress ratio η' may not be constant for the compacted clay, as has been observed for wet clay, but rather a function of η', denoted by $r(\eta')$. Each line for the compacted clay can be characterised by its void ratio when p" = 1 and its slope, i.e.

$$(e_a)_{\eta'} = e + r(\eta') \ln p'' \quad \ldots\ldots\ldots\ldots\ldots\ldots\ldots\ldots \quad (5.24)$$

where $(e_a)_{\eta'}$ is the void ratio for a line with a particular value of η' when p" = 1 psi. Now during the application of a stress increment the value of $(e_a)_{\eta'}$ will change by:

$$d(e_a)_{\eta'} = de + r(\eta') \frac{dp''}{p''} + r'(\eta') \ln(p'')d\eta' \quad \ldots\ldots\ldots\ldots \quad (5.25)$$

This change in $(e_a)_{\eta'}$ can also be related to the shape of the undrained stress paths. During one undrained stress increment:

$$\left\{\frac{d(e_a)_{\eta'}}{dp''}\right\}_e = s'(\eta') \left(\frac{d\eta'}{dp''}\right)_e$$

where $s'(\eta') = d(e_a)_{\eta'}/d\eta'$ and $(d\eta'/dp'')_e$ is the rate of change of η' with respect of p'' along an undrained stress path. Equation (5.24) can also be differentiated with respect to p'' for an undrained stress increment, and the result substituted into the above equation, which gives:

$$s'(\eta') \left(\frac{d\eta'}{dp''}\right)_e = r'(\eta')/p'' + r'(\eta') \ln(p'') \left(\frac{d\eta'}{dp''}\right)_e$$

and using the definition of $s'(\eta')$ this reduces to:

$$d(e_a)_{\eta'} = r(\eta') \left(\frac{dp''}{d\eta'}\right)_e \cdot \left(\frac{d\eta'}{p}\right) + r'(\eta') \ln(p'')d\eta'$$

Comparing this equation with (5.25) leads to:

$$de = \frac{r(\eta')}{p''} \left\{\frac{d\eta'}{(d\eta'/dp'')_e} - dp''\right\} \quad \ldots\ldots\ldots\ldots\ldots\ldots\ldots\ldots \quad (5.26)$$

Now from the definition of ':

$$\left(\frac{d\eta'}{dp''}\right)_e = \frac{1}{p''} \left\{\left(\frac{dq}{dp''}\right)_e - \eta'\right\}$$

The slope of the stress path for an undrained test, $(dq/dp'')_e$ has already been denoted by -S in Chapter 3 and the same will be done again here. Using this, Eq.(5.26) can be expressed as:-

$$de = -\frac{r(\eta')}{p''} \left\{\frac{dq + S\, dp''}{(S+\eta')}\right\} \quad \ldots\ldots\ldots\ldots\ldots\ldots\ldots\ldots \quad (5.27)$$

Using the relation:-

$$dv = -\frac{de}{(1+e)} \quad \ldots\ldots\ldots\ldots\ldots\ldots\ldots\ldots\ldots\ldots \quad (3.23)$$

it is possible to express Eq.(5.27) as:-

$$dv = \frac{r(\eta')}{p''(1+e)}\left\{\frac{dq + S\,dp''}{S+\eta'}\right\} \quad \ldots\ldots\ldots\ldots\ldots\ldots \quad (5.28)$$

This equation is very similar to Eq.(3.26) the only difference being that the constant λ has been replaced with the function $r(\eta')$. The equation fills the same purpose as Eq.(3.26), it provides an expression for the volumetric strain increment associated with a small increment of stress in the boundary surface. Because this expression is independent of any aspect of the theory of plasticity it can be used to evaluate the form of the function h. The expression given in Eq.(5.8) for the plastic volume change in an undrained test can be coupled with Eq.(5.27) to give the plastic volumetric strain increment associated with a stress increment in the boundary surface. Eq.(5.8) gives the plastic strain increment for an undrained test and this is equal and opposite to the elastic volumetric strain increment, so that:

$$dv^p = \frac{r(\eta')}{p''(1+e)}\left\{\frac{dq + S dp''}{S+\eta'}\right\} - \frac{k}{p''(1+e)}\, f_1(\xi', \zeta')dp \quad \ldots\ldots\ldots \quad (5.29)$$

Equation (3.12) can be expanded to give

$$dv^p = h\frac{\partial f}{\partial p''}\left\{\frac{\partial f}{\partial q}\,dq + \frac{\partial f}{\partial p''}\,dp''\right\}$$

From Eq.(5.23):

$$\frac{\partial f}{\partial q} = 1 \text{ and } \frac{\partial f}{\partial p} = g(\eta')$$

and thus:

$$dv^p = hg(\eta')\left\{ dq + g(\eta')\, dp''\right\} \quad \ldots\ldots\ldots\ldots\ldots\ldots\ldots\ldots \quad (5.30)$$

Equating coefficients of dq between Eqs.(5.29) and (5.30):

$$\frac{r(\eta')}{p''(1+e)(S+\eta')} \equiv hg(\eta')$$

and equating coefficients of dp gives:

$$\frac{1}{p(1+e)}\left\{ \frac{S\ r(\eta')}{(S+\eta')} - kf_1(\xi',\zeta')\right\} \equiv hg^2(\eta')$$

From these two identities it is possible to determine the functions $r(\eta')$ and h. Solving for h gives:-

$$h = \frac{kf_1(\xi',\zeta')}{p''(1+e)\ g(\eta')(S-g(\eta'))} \quad \ldots\ldots\ldots\ldots\ldots\ldots\ldots\ldots \quad (5.31)$$

This function h combined with the yield function f, Eq.(5.21), makes it possible to calculate the behaviour of the compacted soil under various stress paths as long as these stress paths lie in the boundary surface stretched in Fig.5.5. In the next section these calculations are done and the results compared with the observations of Chapter 4.

5.12 PREDICTION OF STRESS STRAIN BEHAVIOUR

Equation (5.30) gives the expansion of Eq.(3.12) for the

increment of plastic volume strain. The corresponding expansion for the distortion is:

$$d\epsilon^p = h\left\{ dq + g(\eta')dp'' \right\} \quad \ldots\ldots\ldots\ldots\ldots\ldots\ldots\ldots \quad (5.32)$$

On substitution of h from Eq.(5.31) this becomes:

$$d\epsilon^p = \frac{kf_1(\xi',\zeta')\left\{ \frac{dq}{dp''} + g(\eta') \right\}}{g(\eta')(1+e)(S-g(\eta'))} \frac{dp''}{p''} \quad \ldots\ldots\ldots\ldots\ldots\ldots \quad (5.33)$$

With this equation the distortion can be calculated for any stress path lying in the boundary surface. In this section the distortion which occurs during an undrained test, a drained test and during an isotropic consolidation test is calculated. The prediction of the soil behaviour during a drained test and during a consolidation test is the real test of the usefulness of the stress-strain theory developed in this chapter. It has been developed entirely from the results of undrained tests and obviously must be capable of predicting undrained behaviour but to be of general use it must be capable of predicting behaviour during an arbitrary loading stress path with any degree of drainage. The three cases are set out below.

(a) An Undrained Stress Path

There should not be any need to check on the predictions of the theory along an undrained stress path because the equations have been derived from the results of undrained tests. However, comparing the observed and predicted response will provide a means of assessing the importance of the difference

between the curve and the plotted points in Fig.5.17. For an undrained test $dq/dp'' = -S$ and $dp''/p'' = d\xi'/\xi'$ and so equation (5.33) reduces to:

$$(d\epsilon^p)_{\text{undrained stress path}} = - \frac{k f_1(\xi', \zeta') \left\{ \frac{d\xi'}{\xi'} \right\}}{(1+e) g(\eta')} \quad \ldots\ldots\ldots\ldots \quad (5.34)$$

Despite the minus sign $d\epsilon^p$ is always positive. Over the initial part of the curve, for $0 > \eta' > 1$, $d\xi' < 0$ and thereafter is always positive. The term $f_1(\xi', \zeta')$ is positive for $0 < \eta' < 1$ and for $\eta' > 1.23$ and negative when $1.0 < \eta' < 1.23$, while the function $g(\eta')$ is positive for all values of $\eta' < 1.23$ and then negative for values of η' between 1.23 and 1.51. Thus each of the main terms in Eq.(5.34) is negative over a certain range of values for η' while the other two remain positive and so the minus sign is cancelled.

Equation (5.34) suggests that the η' $v\epsilon^p$ curve for an undrained stress path must be influenced by the void ratio of the material since the term (1+e) occurs in the bottom line. However the range of void ratios for the undrained tests reported in Chapter 4 is fairly limited, between 0.70 and about 0.60, and so the term (1+e) does not vary much for any of the undrained tests discussed. In the following calculation a value of 1.65 is used for the term (1+e) regardless of the initial void ratio of the sample. This is certainly justified when Fig.4.7 is examined; at each value of ϵ there is a fair amount of scatter so any refinement of the (1+e) term is not justified.

TABLE 5.1 CALCULATION OF η' v ϵ^p CURVE FOR AN UNDRAINED STRESS PATH

η'	ξ'	$d\xi'$	$(d\xi'/\xi')$	$f_1(\xi',\xi')$	$g(\eta')$	$d\epsilon^p(\%)$	$\epsilon^p(\%)$
0.000	1.000	-0.035	-0.035	1.439	0.729	0.045	0.000
0.100	0.965	-0.030	-0.032	1.498	0.632	0.050	0.045
0.200	0.935	-0.030	-0.032	1.512	0.542	0.058	0.095
0.300	0.905	-0.030	-0.033	1.560	0.459	0.073	0.153
0.400	0.875	-0.030	-0.034	1.624	0.382	0.095	0.226
0.500	0.845	-0.030	-0.036	1.716	0.312	0.130	0.321
0.600	0.815	-0.030	-0.037	1.870	0.249	0.182	0.451
0.700	0.785	-0.025	-0.032	2.199	0.192	0.240	0.633
0.800	0.760	-0.006	-0.008	3.098	0.141	0.115	0.873
0.900	0.754	-0.002	-0.003	4.756	0.098	0.095	0.988
0.950	0.752	-0.002	-0.003	6.344	0.079	0.158	1.083
1.000	0.750				0.061		1.241
1.050	0.752	+0.002	+0.003	-4.663	0.045	0.204	1.445
1.100	0.754	0.002	0.003	-3.075	0.031	0.195	1.640
1.200	0.840	0.086	0.102	-0.086	0.007	0.821	2.461
1.250	0.885	0.045	0.051	0.034	-0.002	0.568	3.029
1.300	0.960	0.075	0.078	0.124	-0.010	0.634	3.663
1.350	1.040	0.080	0.077	0.165	-0.016	0.520	4.183
1.400	1.200	0.160	0.133	0.211	-0.020	0.919	5.102
1.450	1.400	0.200	0.143	0.240	-0.023	0.977	6.099
1.500	1.800	0.400	0.333	0.355	-0.024	3.226	9.325

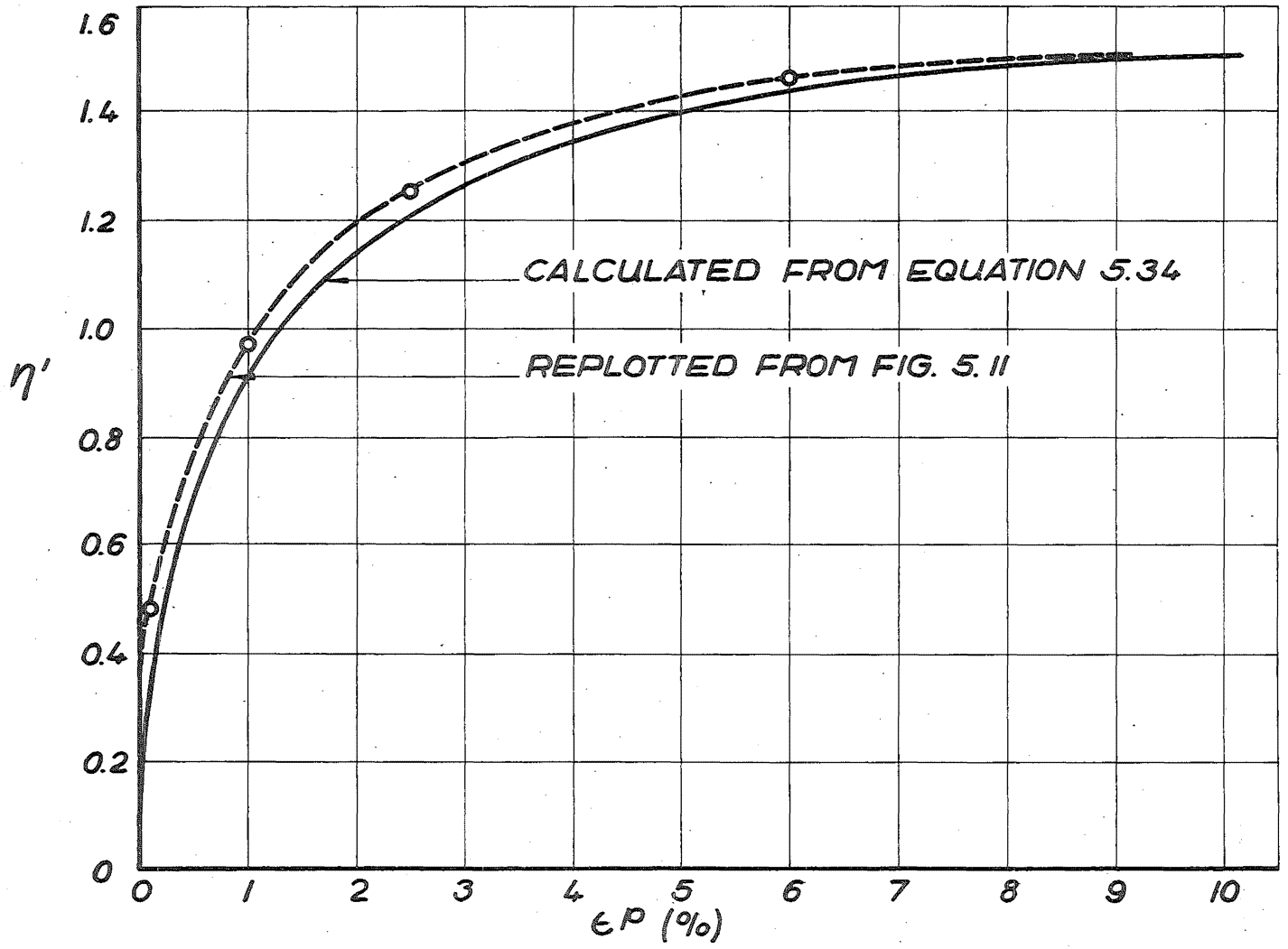

FIG. 5.19 COMPARISON BETWEEN PREDICTED AND MEASURED η' v ϵ^p CURVES FOR UNDRAINED TESTS

Table 5.1 sets out the evaluation of the terms in Eq.(5.34). The resulting curve of η' v ϵ^p for an undrained test is plotted in Fig.5.19. It is seen that the summation of the strain increments calculated according to Eq.(5.34) overpredicts slightly the measured distortion at any point. This would be a consequence of the fact that the angle θ is overpredicted at small values of η'. An unfortunate consequence of an incremental procedure for calculating a stress-strain curve is that any small initial error is propagated onwards throughout the curve. Fig.5.11 shows that there is no plastic distortion until η' reaches about 0.40 whereas the theory developed in this chapter predicts that the material will yield right from the application of shearing stress; however, the distortion during this initial part of the test is only 0.23%. Apart from this small initial error it is seen that the predicted curve follows the experimental curve fairly well. Thus it seems that even though the mathematical curve fitted to the experimental points in Fig.5.17 does not fit particularly well at low values of η' the experimental and predicted η' v ϵ^p curves are very close. This is because there is very little distortion at small η' values along an undrained stress path. It will be seen when discussing an isotropic consolidation test below that this is not so along other stress paths.

(b) A Drained Stress Path

Along a drained stress path dq/dp" is always equal to 3 and thus Eq.(5.33) reduces to:

$$d\epsilon^{p}_{\text{drained stress path}} = \frac{k f_{6}(\xi', \zeta') \{ 3+g(\eta') \}}{g(\eta')(1+e)(S-g(\eta'))} \left(\frac{dp''}{p''} \right) \quad \ldots\ldots\ldots \quad (5.35)$$

The various terms of this equation are evaluated in Table 5.2 and the η' v ϵ^{p} curve plotted in Fig.5.20. Also plotted in the diagram is the curve of η'_{r} v ϵ^{p} determined from the two drained tests. For a drained test η' must increase from the value of 1 and not decrease initially as with an undrained test because of the boundary energy and elastic energy corrections to the stress path as explained in section 5.8. In the diagram it is seen that there is some discrepancy between the observed and predicted results. Calculations based on Eq.(5.35) assume that the corrected drained stress path lies in the boundary surface. But it has already been shown in section 5.8 how the corrected values of η', η'_{r}, do not lie in the boundary surface defined by the undrained tests. Such behaviour has already been noted by Roscoe and Thurairajah[66] in other drained triaxial tests and they attribute it to non-uniform deformation in the drained triaxial test. In other words the discrepancy in Fig.5.20 between the observed and predicted η' v ϵ^{p} curves for the drained test may not be a consequence of any fault in the stress strain theory proposed here, but rather a consequence of the failure to make the corrected drained test results fit the boundary surface. Nevertheless it is still possible to conclude that the theory does predict the general features of deformation that occurs during a drained test.

TABLE 5.2 CALCULATION OF η' v ϵ^p CURVE FOR A DRAINED STRESS PATH

η'	ξ'	$(d\xi'/\xi')$	$f(\xi', \xi')$	$g(\eta')$	$3+g(\eta')$	$S-g(\eta')$	$d\epsilon^p$	ϵ^p
1.330	1.000	0.040	0.198	-0.015	2.985	-2.021	0.511	0.000
1.350	1.040	0.038	0.211	-0.016	2.984	-1.934	0.506	0.511
1.380	1.120	0.071	0.227	-0.019	2.981	-1.875	0.883	1.017
1.400	1.200	0.067	0.239	-0.020	2.980	-1.816	0.861	1.900
1.420	1.250	0.040	0.245	-0.021	2.979	-1.791	0.508	2.761
1.430	1.300	0.039	0.250	-0.022	2.978	-1.765	0.490	3.269
1.440	1.350	0.037	0.256	-0.022	2.978	-1.740	0.483	3.759
1.450	1.400	0.036	0.263	-0.023	2.977	-1.715	0.468	4.242
1.460	1.450	0.035	0.271	-0.023	2.977	-1.715	0.469	4.710
1.470	1.500	0.033	0.280	-0.023	2.977	-1.715	0.457	5.179
1.475	1.550	0.032	0.291	-0.024	2.976	-1.714	0.441	5.636
1.480	1.600	0.031	0.303	-0.024	2.976	-1.714	0.445	6.077
1.483	1.650	0.030	0.317	-0.024	2.976	-1.714	0.451	6.522
1.490	1.700	0.029	0.329	-0.024	2.976	-1.714	0.452	6.973
1.496	1.750	0.029	0.352	-0.024	2.976	-1.714	0.484	7.425
1.500	1.800	0.028	0.372	-0.024	2.976	-1.714	0.494	7.909

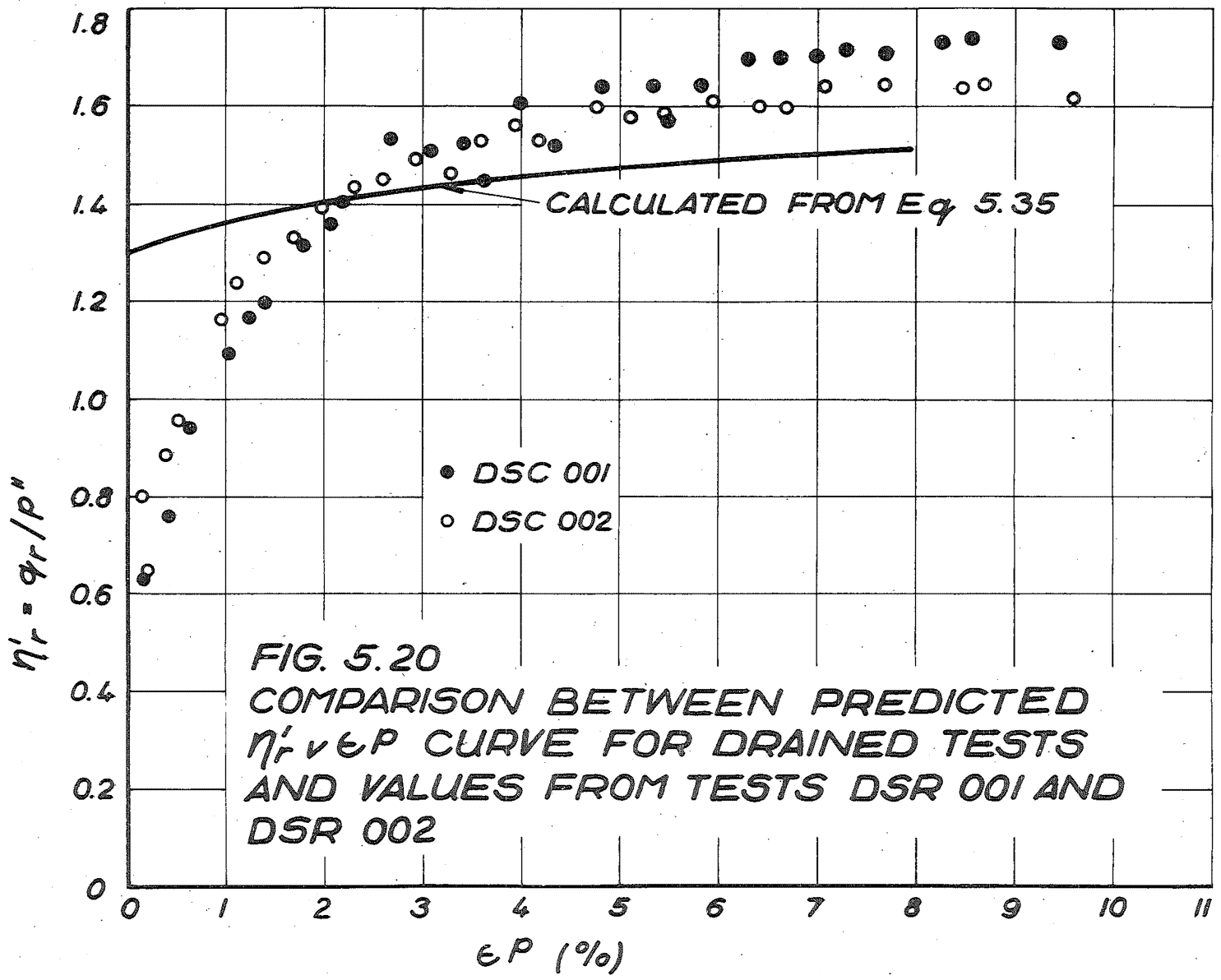

FIG. 5.20
COMPARISON BETWEEN PREDICTED η'_r v ϵ_P CURVE FOR DRAINED TESTS AND VALUES FROM TESTS DSR 001 AND DSR 002

(c) An Isotropic Consolidation Test ($\eta' = 0$)

During an isotropic consolidation test $q = 0$ and $\frac{dq}{dp} = 0$ and so Eq.(5.33) reduces to:

$$d\epsilon^p_{\text{consolidation test } (\eta'=0)} = \frac{k f_1(\xi', \xi')}{(1+e)(S-g(\eta'))} \left(\frac{dp''}{p''}\right) \quad \ldots\ldots\ldots \quad (5.36)$$

when $\eta' = 0$ the terms $f_1(\xi', \xi')$ and $(S-g(\eta'))$ are constant, and by inserting the appropriate values the equation reduces to:-

$$d\epsilon^p_{\text{consolidation test } (\eta'=0)} = 0.378 \left(\frac{dp''}{p''}\right) \quad \ldots\ldots\ldots\ldots\ldots\ldots \quad (5.37)$$

which can be integrated to give:

$$\epsilon^p_{\text{consolidation test } (\eta'=0)} = 0.378 \ln (p''/p''_i) \quad \ldots\ldots\ldots \quad (5.38)$$

where ϵ^p is the plastic distortion that occurs when the stress is increased from p''_i to p''. A consolidation test such as this was performed on the compacted soil and the distortion was measured. The results have been plotted in Fig.5.21 as has the relation given in Eq.(5.38). The graph shows that the theory overpredicts the strains by a factor of about a third. However this is not surprising because the theory overpredicts the angle of the plastic strain increment vector when $\eta' = 0$. What is more important is the observation that the theory does predict the correct form of the relationship for the plastic distortion during an isotropic consolidation test. In both cases there is a linear relation when ϵ^p is plotted against the logarithm of the stress p''.

The points plotted in Fig.5.21 suggest that the assumption of isotropy may be suspect. For an isotropic material it would be expected that only volumetric strain would result during the application of hydrostatic stress increment. The presence of the distortion plotted in Fig.5.21 obviously contradicts this and the situation is discussed in more detail in Chapter 6. The prediction made by Eq.(5.38) of distortion during hydrostatic compression is a consequence of the shape of the yield curve. Because of the normality of the plastic strain increment vector any yield curve that does not cross the p" axis at right angles will predict distortion during an increment of hydrostatic stress.

By calculating the stress-strain behaviour predicted by the theory for an undrained test, a drained test and an isotropic consolidation test it has been shown that the theory is capable of predicting the general features of material behaviour. Admittedly for a drained test there is the problem that the corrected loading path does not lie in the boundary surface but here the overall behaviour is still predicted. Also in the isotropic consolidation test the predicted strain is about twice the measured value; however the logarithmic form of the relationship is correctly predicted. It was explained in the introduction to this thesis that the work presented here is in the nature of a preliminary investigation into the worth of using the theory of plasticity to describe the deformation

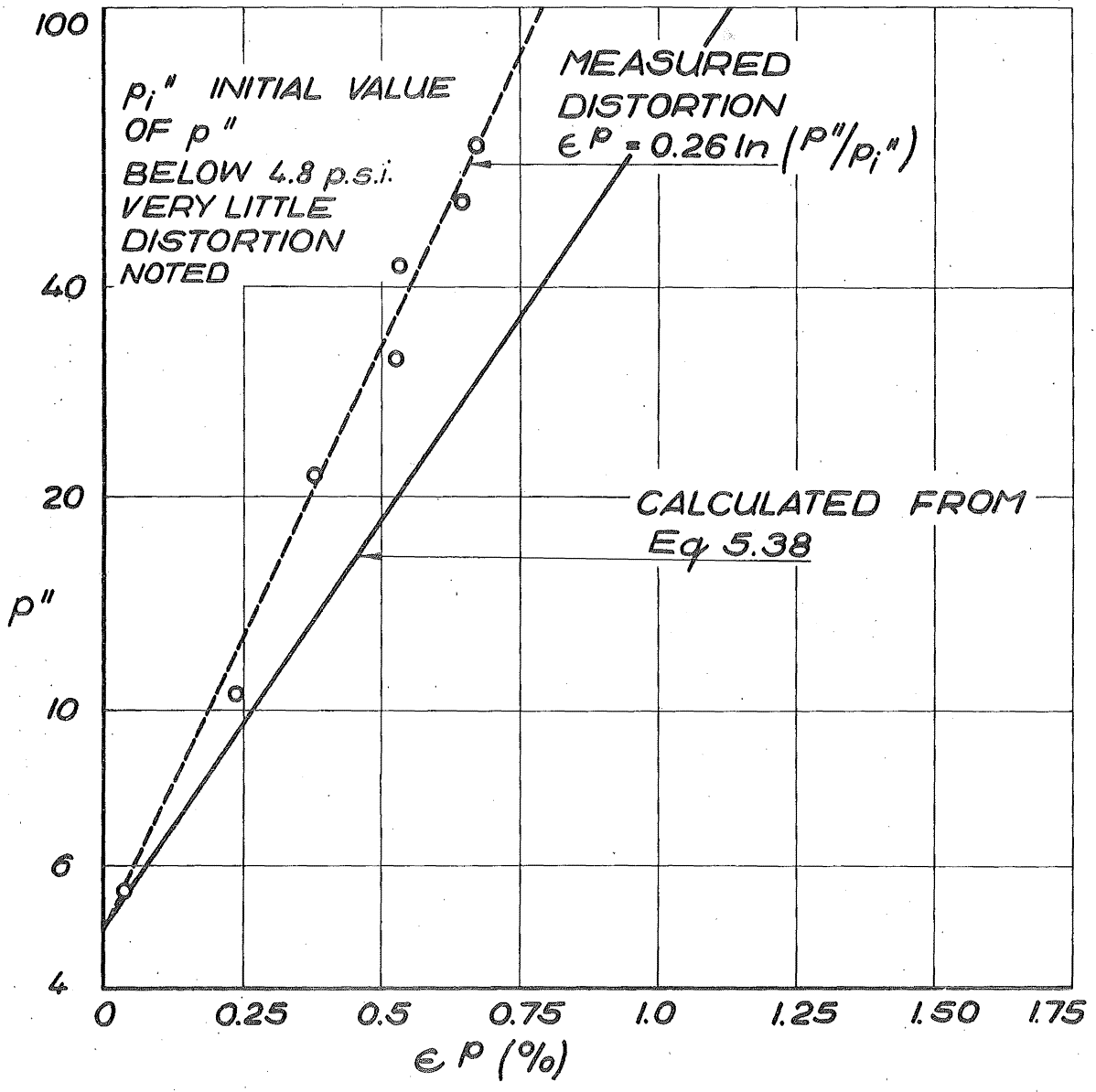

FIG. 5.21 MEASURED AND PREDICTED DISTORTION DURING AN ISOTROPIC CONSOLIDATION TEST

behaviour of a compacted material. It is concluded here that the approach is indeed very promising but before any more definite conclusion can be reached a number of more specific tests would have to be carried out to check on the validity of the yield curve and function h proposed. These would include a series of consolidation tests under constant stress ratios η'. This would provide an independent way of deriving data for Fig.5.12. In addition, once a given yield curve has been reached by a certain amount of work hardening, its general shape could be investigated by moving the stress point to some other part of the curve. Thirdly the independence of the direction of the plastic strain increment vector from the direction of the stress increment vector is an essential aspect of plastic behaviour as explained in Chapter 3. This could be checked by applying a series of stress increments in various directions at a given point on the yield curve.

5.13 CONCLUSIONS

The substance of this chapter represents the major achievement of this thesis. The work here has been divided into two parts. In the first the behaviour of the compacted soil was discussed in qualitative terms and in the second a plastic stress-strain relation has been developed.

In the first part it is explained how the major similarity between the behaviour discussed here and the critical state model

is the surface in the (p,q,e) space defined by the undrained tests. Both here and in the critical state model constant void ratio sections of this surface are geometrically similar. Although the surface for the compacted soil is a boundary surface for initial loading, it is not a state boundary surface in the way that the surface in the (p,q,e) space defined by the state paths for wet clays is. Possibly the most important part of this qualitative discussion is the suggestion that the Terzaghi effective stress does not provide the most suitable means of describing the soil behaviour. The hypothesis is made that the compaction process sets up a stress system in the material that has the same effect as increasing the isotropic component of stress by 3.0 psi. This component is added to the Terzaghi effective stress and the result, called the actual effective stress, has been postulated as the stress that controls the strength and deformation of the material.

In the second part of the chapter an expression was derived from which it is possible to calculate the successive yield loci as the material work hardens. From this, equations predicting the distortion during various types of test are derived. It was seen that although these predictions do not correspond exactly with the observations of Chapter 4 they do predict the general features of the behaviour.

CHAPTER SIX

BEHAVIOUR OF SAMPLES LOADED PERPENDICULAR TO THE DIRECTION OF COMPACTIVE EFFORT

6.1 INTRODUCTION

Towards the end of Chapter 5 it was suggested that anisotropy might have some affect on the stress-strain behaviour of a compacted soil. The current understanding of the behaviour of soils compacted wet of optimum moisture content by kneading compaction makes considerable appeal to the idea that the arrangement of particles is not isotropic. Unfortunately studies of the isotropy or anisotropy of the mechanical properties of compacted soils are rare and the work presented in this chapter is the result of a simple investigation of the properties of the soil when loaded at right angles to the direction of compactive effort rather than parallel to it as in Chapter 4.

It is not possible to present a complete analysis here because insufficient testing was performed and also because of the limitations of the triaxial method of testing. However some general conclusions are possible. The results suggest that the elastic properties of the material are nearly isotropic and that the plastic properties are anisotropic; the exact degree of anisotropy depends on the consolidation pressure. Furthermore, for samples loaded in perpendicular directions after consolidation at the same pressure the stress strain curve, q v ϵ, for the

sample tested with the direction of the major principal stress parallel to the direction of compaction lies above that of the sample tested perpendicular to it but despite this anisotropy the stress paths for the two tests are almost identical.

6.2 CONSOLIDATION BEHAVIOUR

The isotropic consolidation test already discussed briefly in Chapter 5 and presented in appendix A is discussed in a different context here. This test was performed on a sample prepared and mounted in the triaxial cell in the same way as those samples tested with the direction of the major principal stress parallel to the direction of compaction. Being an isotropic consolidation test only increments of cell pressure were applied so that q and η' were zero at all stages of the test. In addition to measurement of the volume change for each stress increment, the axial deformation was also measured, so that it was possible to determine the ratio between the increment of axial deformation and the volumetric strain increment. For isotropic behaviour this ratio equals 0.333. In Fig.6.1 the direction and magnitude of the elastic and plastic strain increment vectors have been plotted. These plastic strain increment vectors have been calculated by determining the total strain increment vectors for increasing pressure and then the vectors when the consolidation pressure is decreased. The latter have been plotted as the elastic strain increment vectors in the upper part of Fig.6.1

and the vectorial difference between the total and elastic strain increment vectors as the plastic strain increment vectors in the lower part of Fig.6.1. It seems that the plastic strain increments for low consolidation pressures exhibit considerable anisotropy but as the consolidation pressure is increased the direction of the vectors tends towards the isotropic line, suggesting that the material tends to become isotropic as the consolidation pressure increases. On the other hand it seems that the elastic behaviour tends to be very much more isotropic particularly at the low consolidation pressures.

The observation that the material tends to become more isotropic as the consolidation pressure increases is slightly in conflict with Fig.5.12 which was taken as evidence that the inclination of the plastic strain increment vector, $\tan^{-1}(dv^p/d\epsilon^p)$, is simply a function of η'. This would mean that the inclination of the vector would be constant for constant values of η'. The fact that the value of $d\epsilon_1^p/dv^p$ for each increment of p in Fig.6.1 decreases as the consolidation pressure increases suggests that when η' is zero $dv^p/d\epsilon^p$ depends on p. This possibility is not investigated any further here but the significance of this effect could be investigated by a series of tests at constant stress ratio η' as suggested at the end of Chapter 5 for confirming the form of the yield curves derived.

One aspect of this consolidation test is a departure from normal practice and should be mentioned in passing. It is

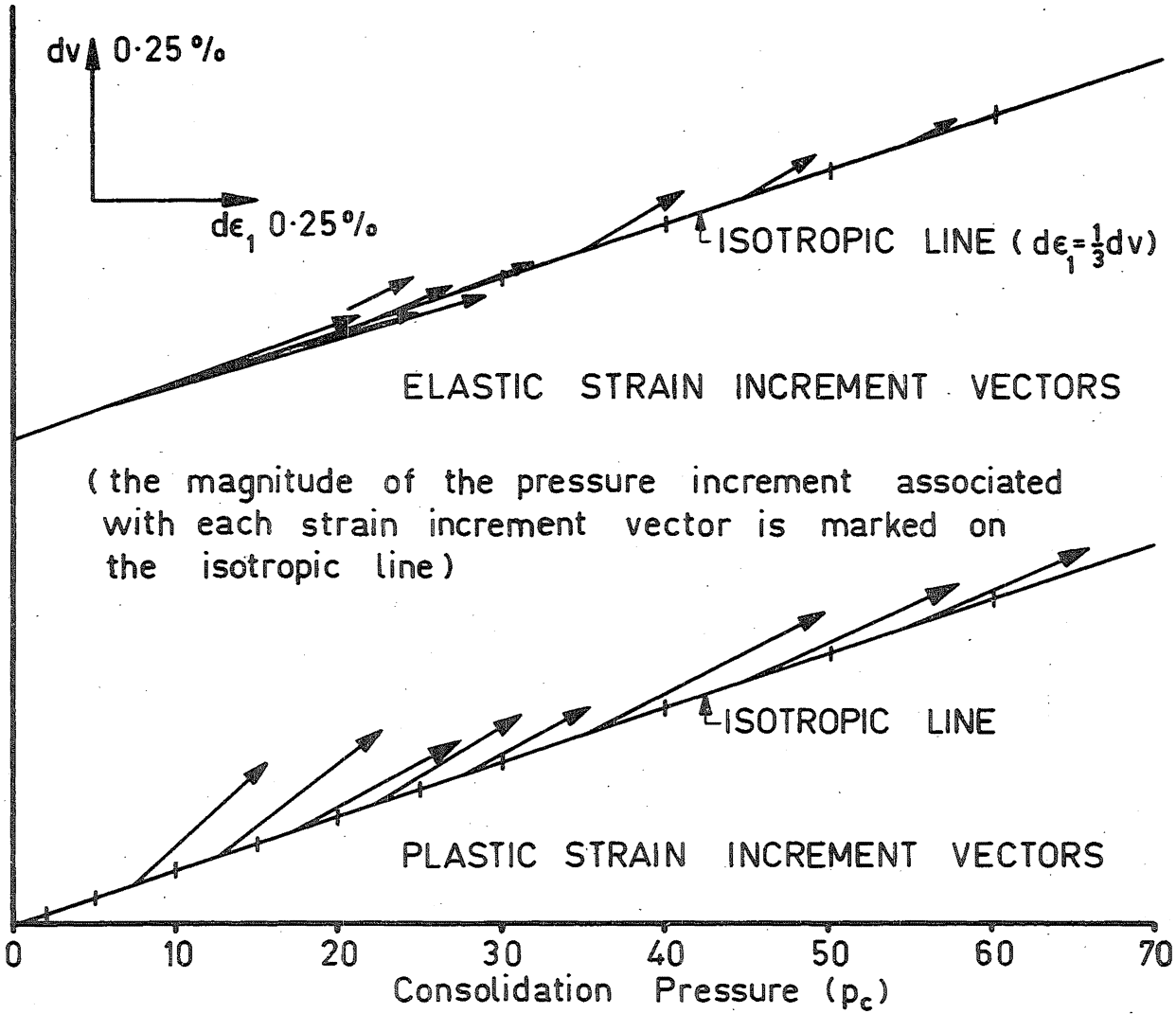

FIG. 6.1 DIRECTION OF ELASTIC & PLASTIC STRAIN INCREMENT VECTORS DURING CONSOLIDATION

common to use a load increment ratio of 1. This is done for two reasons. Firstly with load increment ratios of this order secondary consolidation effects are reduced and secondly the amount of secondary consolidation per load increment is consistent. However the use of a variable load increment ratio as in this test produces no problems because this material is not very susceptible to creep deformation as has already been explained in Chapter 4.

6.3 STRESS-STRAIN BEHAVIOUR

The samples of soil loaded perpendicular to the direction of compactive effort were prepared in a different manner from those loaded parallel to the direction of the compactive effort. Those loaded perpendicular were cut from samples compacted into a $2\frac{1}{4}$" x $2\frac{1}{4}$" x $2\frac{1}{4}$" mould whereas those loaded parallel were prepared from samples compacted into a $1\frac{1}{2}$" D cylindrical mould. The fact that both methods of sample preparation produced material with the same density was taken as evidence that there was no significant difference between the properties of the samples produced by the two methods of compaction.

In Figs.6.2 to 6.7 stress-strain curves for the samples loaded perpendicular to the direction of compactive effort are presented. Also included for comparison are the stress-strain curves for samples consolidated at similar pressures and loaded parallel to the direction of compactive effort. From these curves it can be seen that the samples are somewhat stiffer

when loaded parallel than when loaded perpendicular to the direction of compactive effort. Also plotted on these curves are the stress paths for each of the perpendicular and parallel tests. There is very little difference between the stress paths despite the considerable difference between the stress strain curves, so that for a sample consolidated to a given pressure it can be said that the stress path is independent of the direction of loading. This means that the surface discussed in section 4.7 defined in the (p,q,e) space by the undrained stress paths and plotted in a two dimensional diagram by use of the parameters η' and ξ' in Fig.4.18 is independent of the direction in which the samples are loaded. Because the stress-strain curves are not independent of the direction of loading the contours of equal axial strain will not be unique. The contours for the samples loaded parallel to the direction of compaction will lie further up the surface than those for the samples loaded perpendicular.

To achieve a truly valid comparison between the samples loaded perpendicular and parallel to the direction of compactive effort it is necessary to compare samples with the same void ratio in addition to using similar consolidation pressures as has been done here. In fact in almost all of Figs.6.2 to 6.7 the stiffer of the two samples is the one with the smaller void ratio. This suggests that the reason for the difference between the stress-strain curves is not connected with anisotropy at all

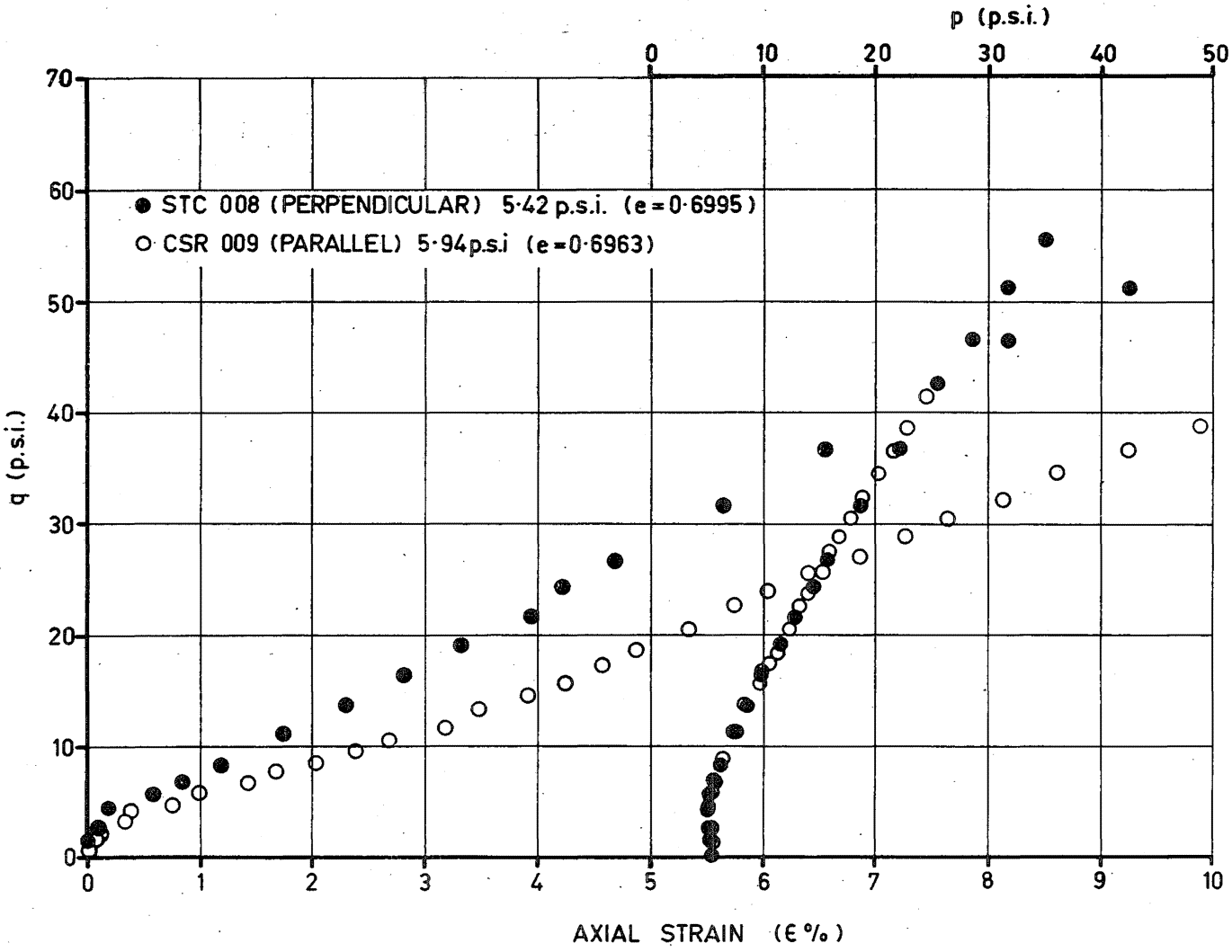

FIG. 6.2 STRESS STRAIN CURVES & STRESS PATHS FOR TESTS STC 008 & CSR 009

but is simply a consequence of one sample being slightly more dense than the other. Examination of the differences in void ratio shows that for the various pairs of samples compared the differences range between 0.001 and 0.011, generally being about 0.002 to 0.003. The effect of such small differences is examined in Figs.6.8 and 6.9 in which the stress-strain curves for pairs of samples with small differences in void ratio are compared. The curves for two samples loaded parallel to the direction of compaction with a void ratio difference of 0.007 are plotted in Fig.6.8 and in Fig.6.9 two samples loaded perpendicular to the direction of compactive effort with a difference in void ratio of 0.002 are shown. The small differences between the curves in these figures seem to be related more to difference in consolidation pressure than the difference in void ratio between the samples compared. This suggests that when comparing the results of loading tests the effect of small differences in void ratio is not great - certainly not of the order of the differences between the two directions of loading in Figs.6.2 to 6.7 - but that differences in consolidation pressure ought to be given some consideration when making comparisons.

Each of the pairs of samples compared in Fig.6.2 - 6.7 are now discussed separately.

The two samples STC 008 and CSR 009 in Fig.6.2 are exceptions to the conclusion that samples loaded parallel to the

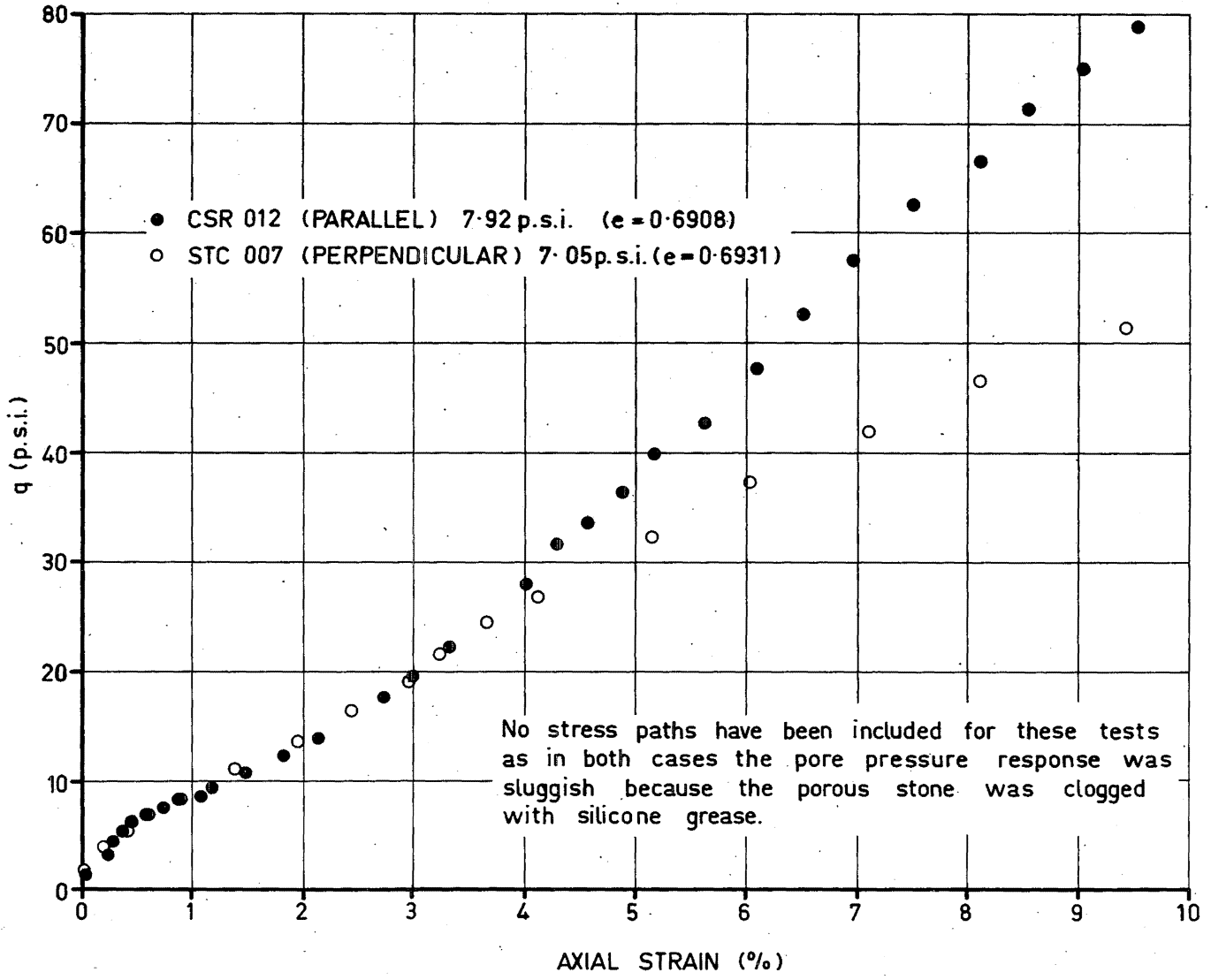

FIG. 6.3 STRESS STRAIN CURVES FOR TESTS CSR 012 & STC 007

direction of compaction are stiffer than those loaded perpendicular. The reason for this is not clear and cannot be explained by differences in void ratio or consolidation pressure. This apparent anomaly might be associated with the observation made in section 4.7 that the stress paths for samples with consolidation pressures below 10 psi do not fit the η', ξ' curve defined by the other stress paths. It has been suggested in Chapter 5 that this is probably because at low consolidation pressures the state point of the sample lies on an elastic swelling line and not on the true S.B.S. Nevertheless Fig.6.2 shows that the two stress paths are identical.

The difference between the curves for CSR 012 and STC 007 in Fig.6.3 is partly due to the higher consolidation pressure for CSR 012. Assuming that this accounts for a difference of the same order as that in Fig.6.9 this would still leave a fair range between the two curves to be accounted for by anisotropy. In both of these tests the porous tip for measuring pore pressures became clogged with silicone grease thus giving inaccurate readings, so that the stress paths for these tests cannot be plotted. However, this has no affect on the q v ϵ curves so the above comparison can be made.

Once again in Fig.6.4 some allowance has to be made for the slightly different consolidation pressures but in this case it would separate the curves even further. The two stress paths in this figure are slightly separated; however of all

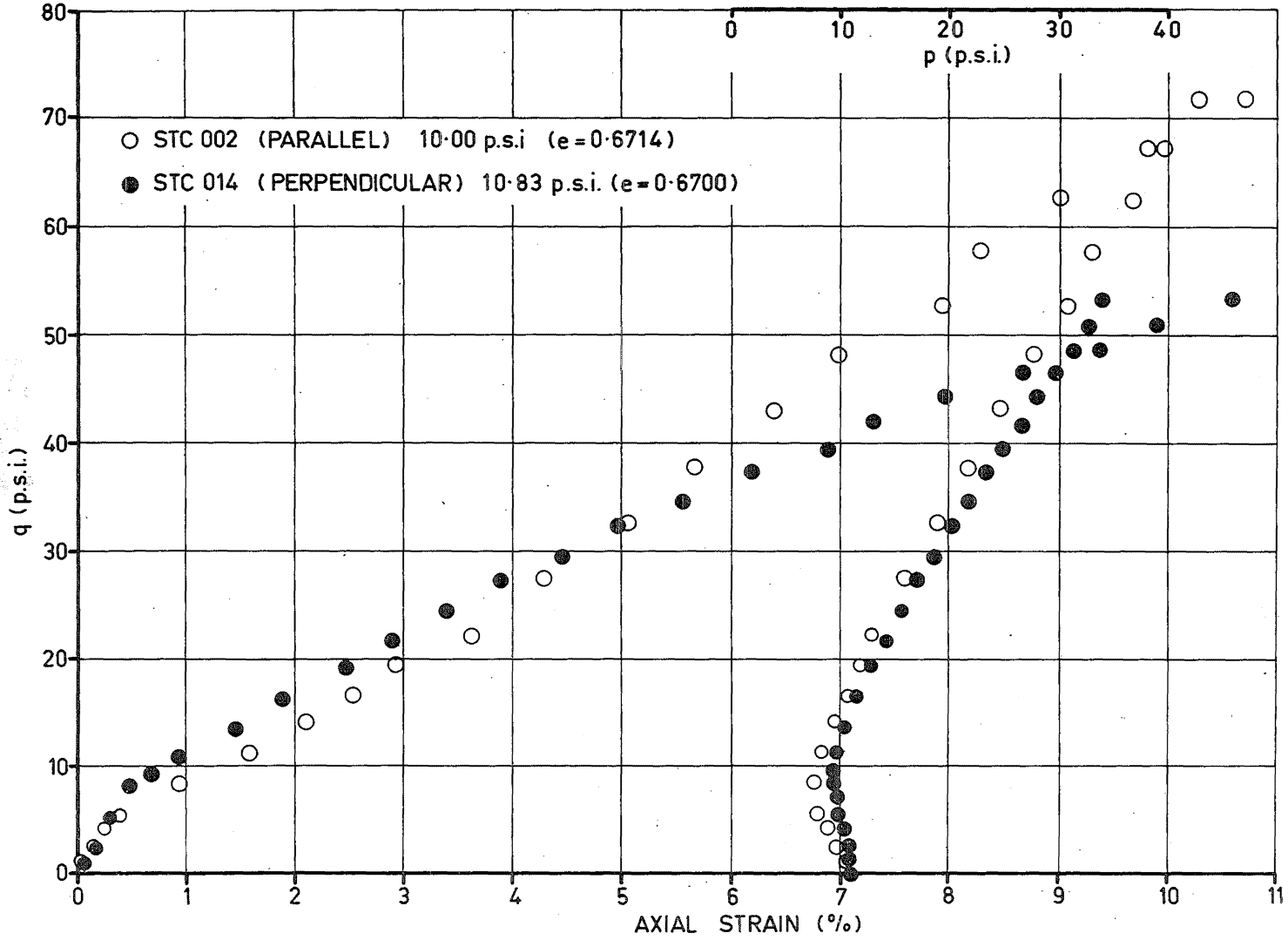

FIG. 6.4 STRESS STRAIN CURVES & STRESS PATHS FOR TESTS STC 002 & STC 014

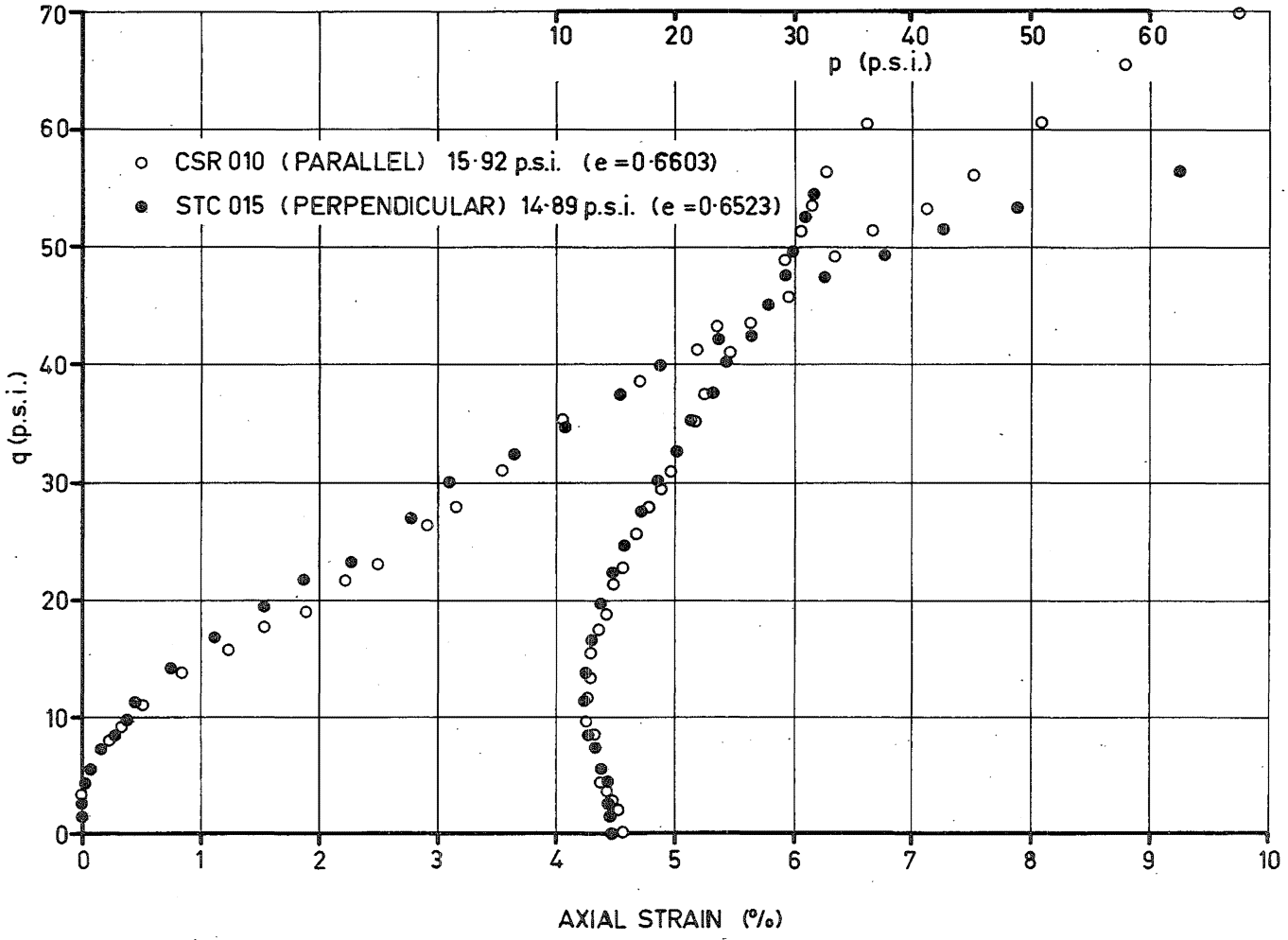

FIG. 6.5 STRESS STRAIN CURVES & STRESS PATHS FOR TESTS CSR 010 & STC 015

the pairs of stress paths compared from perpendicular and parallel loading the separation of these two is greatest.

When the 1.03 psi difference between the consolidation pressures for tests CSR 010 and STC 015 in Fig.6.5 is allowed for the separation of the stress-strain curves will be increased slightly, but even then the amount of anisotropy shown by these tests is somewhat less than the previous tests at lower consolidation pressures.

Allowing for the difference of 3 psi between the two tests in Fig.6.6 will make the curves approach thus reducing the apparent degree of anisotropy.

Finally in Fig.6.7 the difference in consolidation pressure will make the curves approach reducing even further the small amount of anisotropy. Furthermore in these tests the difference between void ratios is rather large (0.0112) and perhaps this is large enough to have some effect.

Thus from these tests it is concluded that there is definitely some anisotropy in this compacted soil. This conclusion is strengthened if small qualitative corrections are included to account for the difference in consolidation pressure between samples, which is shown to be of importance in Figs.6.8 and 6.9. It is also concluded from Figs.6.2 to 6.7 that as the consolidation pressure increases the curves for loading perpendicular and parallel to tend to approach indicating a trend for the samples to become isotropic, thus confirming the behaviour

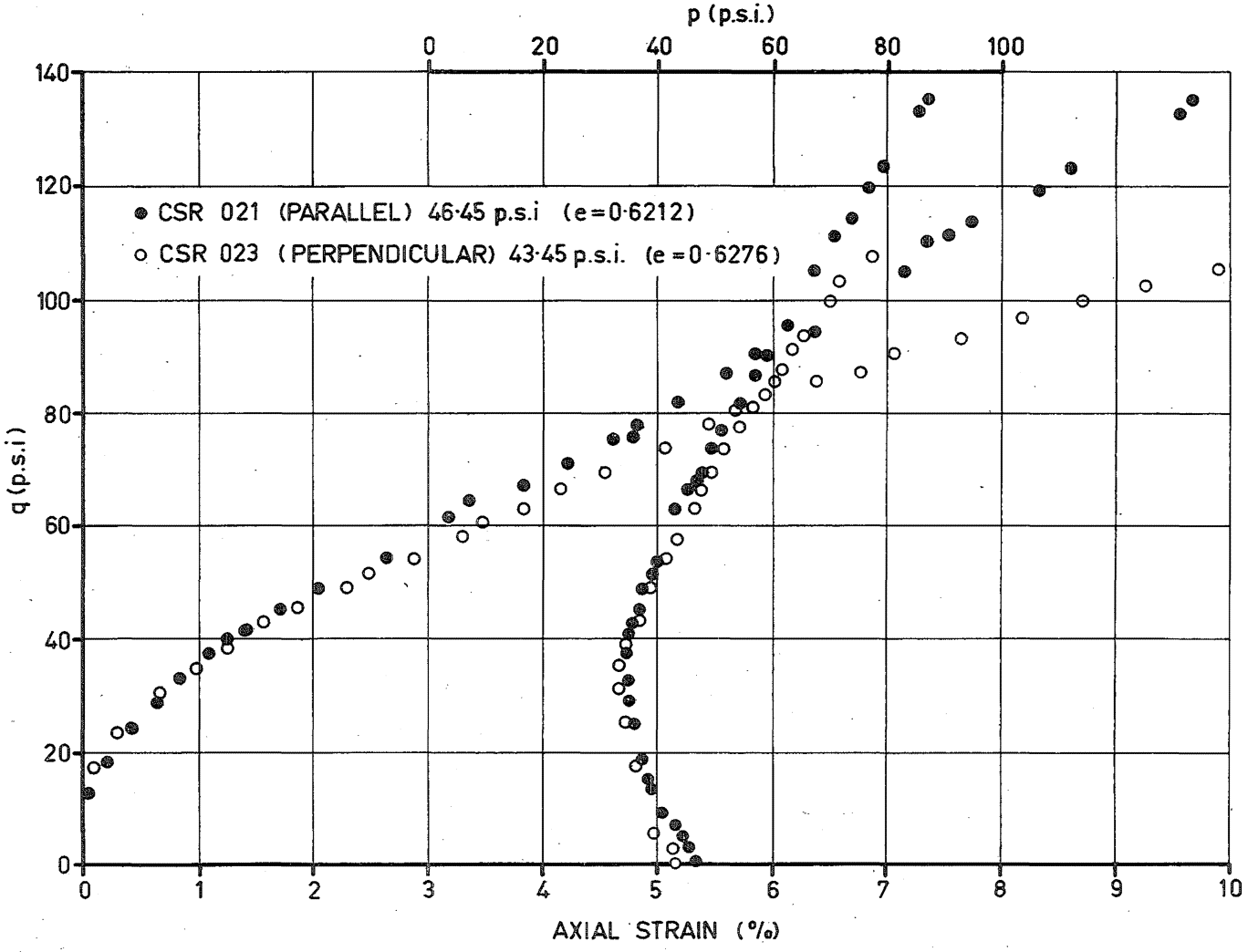

FIG.6.6 STRESS STRAIN CURVES & STRESS PATHS FOR TESTS CSR 021 & CSR 023

observed in Fig.6.1.

It is significant that the stress paths for the tests perpendicular and parallel to the direction of compactive effort are the same despite the anisotropy of deformation. This provides additional support for the hypothesis made in Chapter 5 that the compaction process results in a component of hydrostatic stress of 3.0 psi being built into the material. Since hydrostatic stress is, by definition, isotropic, the value of 3 psi must be independent of sample orientation if it is truly hydrostatic stress. The fact that the stress paths for parallel and perpendicular loading are identical means that they are tangential to the one line passing through the point (0.,-3.0) and so the value of 3.0 psi is independent of sample orientation thus suggesting that it is indeed a hydrostatic component of stress. This also means that the shear parameters, in terms of effective stress, determined as outlined in Fig.5.4 are also independent of sample orientation.

6.4 BEHAVIOUR OF UNLOADING MODULUS

As with the tests in Chapter 4 the undrained unloading modulus, G_{us}, was determined by unloading at the end of the test. The values have been plotted in Fig.6.10 in the same manner as Fig.4.10. Also included for comparison are the results from Fig.4.10 where the values were determined from loading parallel to the compaction. As with the samples loaded parallel there is

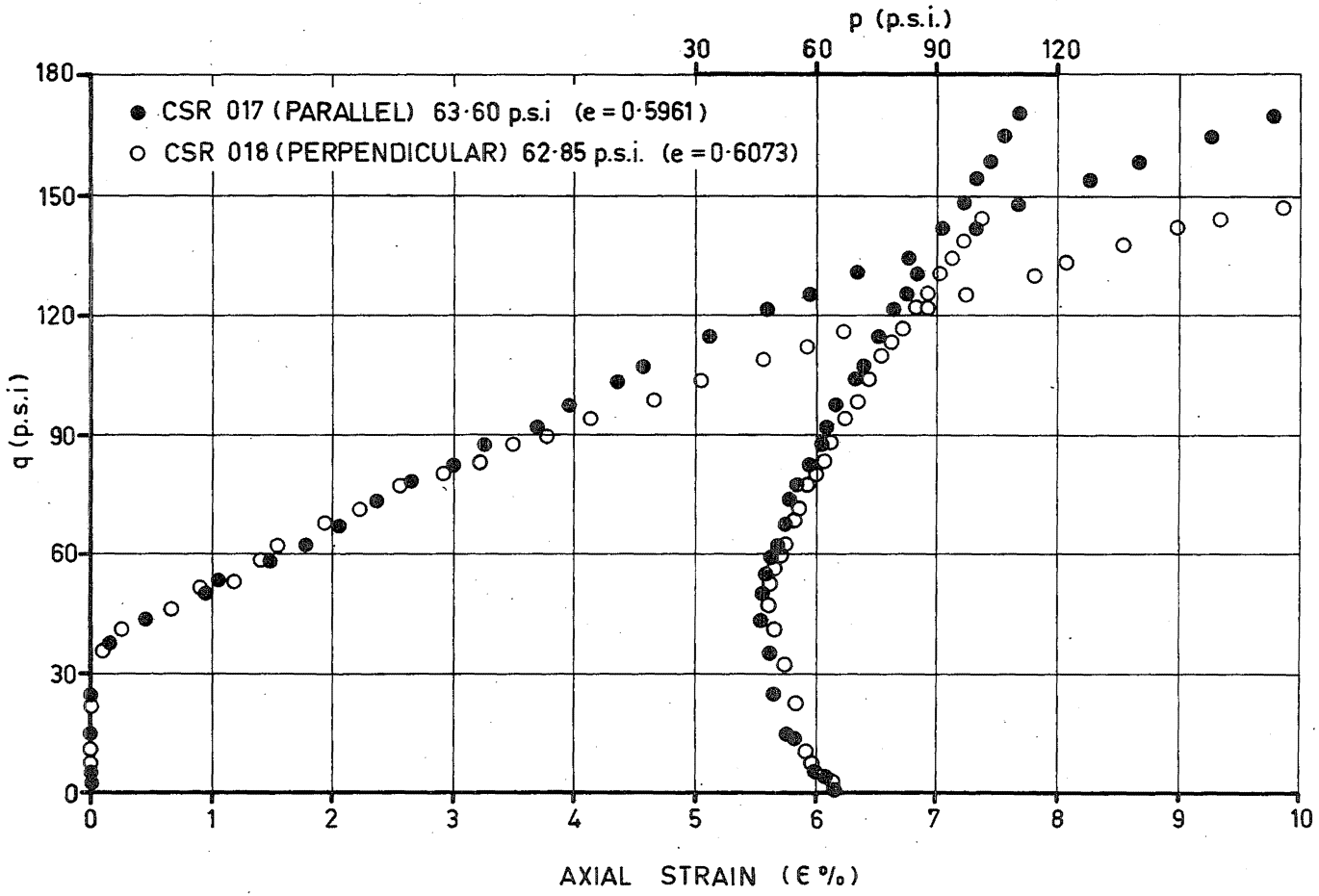

FIG. 6.7 STRESS STRAIN CURVES & STRESS PATHS FOR TESTS CSR 017 & CSR 018

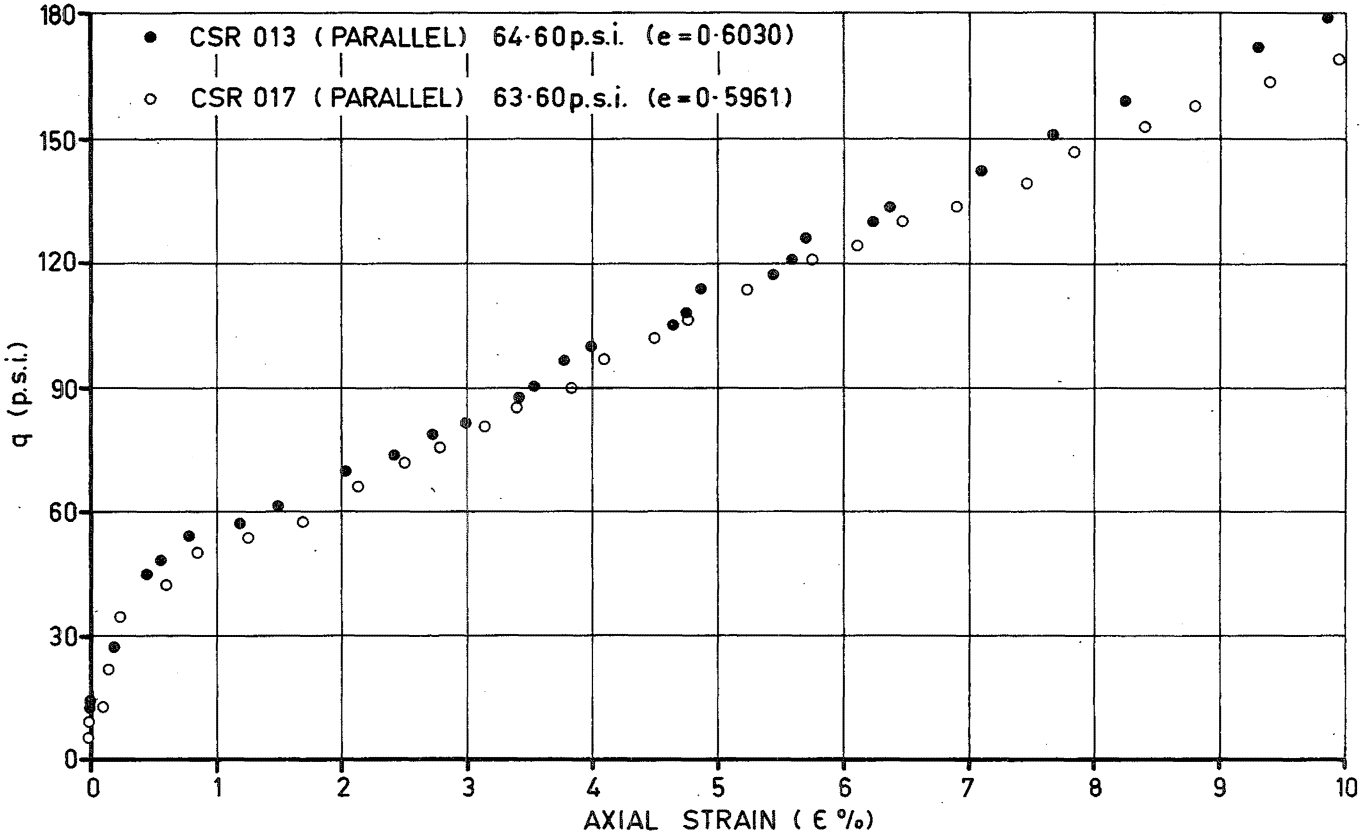

FIG. 6.8 STRESS STRAIN CURVES FOR TESTS CSR 013 & CSR 017

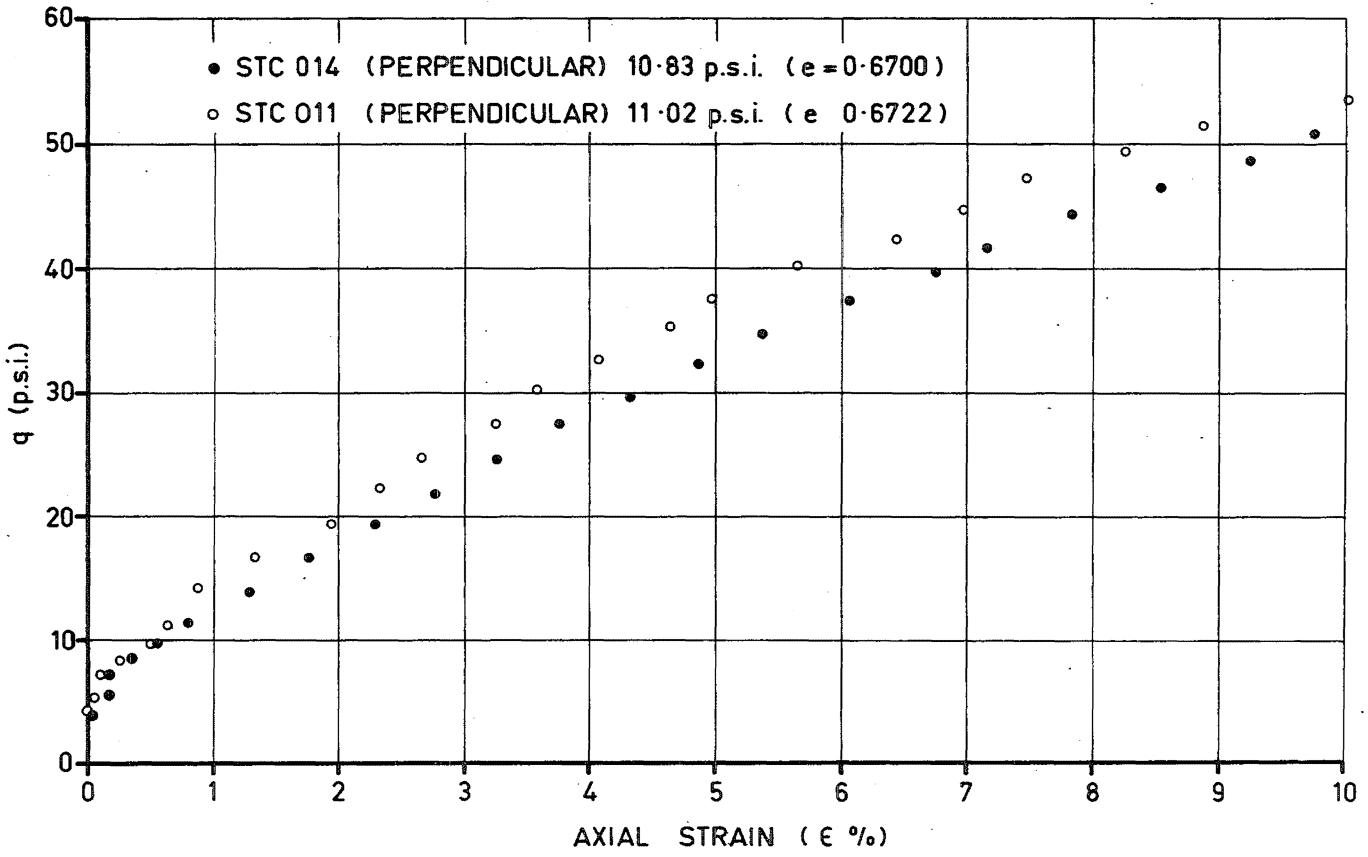

FIG. 6.9 STRESS STRAIN CURVES FOR TESTS STC 014 & STC 011

a fair amount of scatter particularly at the lower consolidation pressures when the void ratio tends to be variable. The graph does show that there is no significant difference between the values of G_{us} when the material is loaded parallel or perpendicular to the direction of compactive effort. This is in line with Fig.6.1 which suggests that the elastic properties of the soil are approximately isotropic.

Now there is one aspect of the material behaviour that is in conflict with this conclusion that the elastic, or unloading, behaviour is approximately isotropic. It is well known that for isotropic behaviour the pore pressure parameter A must be equal to $\frac{1}{3}$. In terms of the parameters p and q it is a simple matter to show that A can be expressed as:

$$A = \frac{1}{3} - \frac{dp}{dq} \qquad \ldots\ldots\ldots\ldots\ldots\ldots\ldots\ldots\ldots\ldots\ldots\ldots\ldots\ldots\ldots\ldots (6.1)$$

This demonstrates that for behaviour to be isotropic on unloading p must remain constant. As discussed in Chapters 4 and 5 there is a decrease in p as the material is unloaded under undrained conditions so that $A \neq \frac{1}{3}$. However it has been pointed out by Pickering[58] that this is a fairly severe test and that even for mild anisotropy A is likely to be significantly different from $\frac{1}{3}$. Thus it is concluded that the change of p during the unloading part of the stress paths does not conflict with the suggestion that on unloading the behaviour of the material was approximately isotropic.

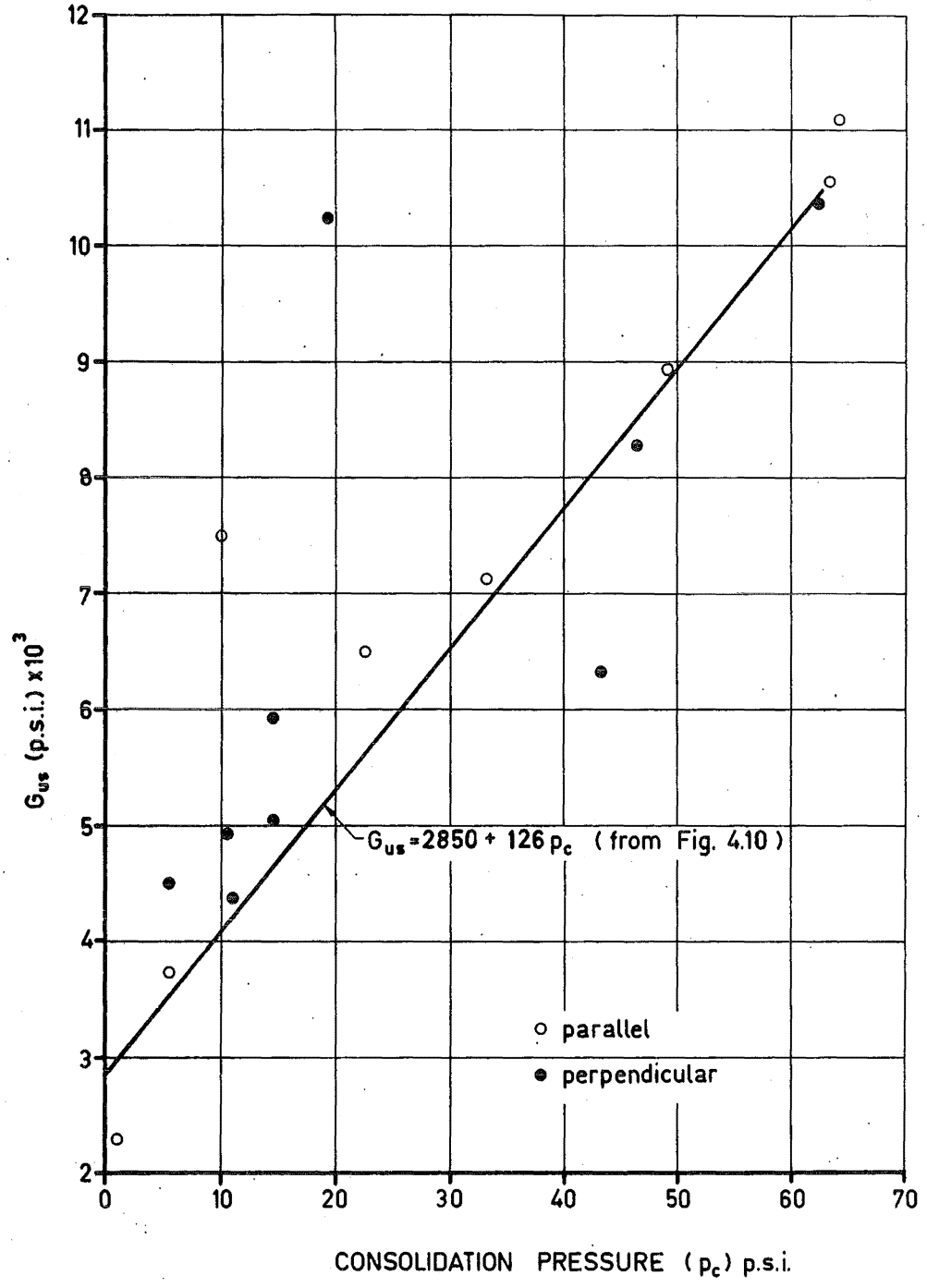

FIG. 6.10 UNLOADING MODULUS FOR SAMPLES LOADED PARALLEL & PERPENDICULAR TO THE DIRECTION OF COMPACTIVE EFFORT

6.5 DESCRIPTION OF THE ANISOTROPY

In this section the particular type of anisotropy exhibited by the soil is specified and the number of parameters necessary to describe it are determined. At this stage it is assumed that the deformation of samples when tested at right angles to the direction of compaction is stable in the Druckerian sense; it has already been shown in Chapter 5 that for samples tested parallel the deformation is stable. This assumption means that the linear relation between increments of plastic strain and increments of stress given in Eq.(3.13) can be used, i.e.

$$d\epsilon^{p}_{ij} = A_{ijkl}\, d\sigma_{kl} \qquad \ldots\ldots\ldots\ldots\ldots\ldots\ldots\ldots \quad (3.13)$$

A_{ijkl} is a fourth order tensor the components of which are not material constants but which are likely to depend on the state of stress and strain and also the amount of work hardening, but not on increments of these. There are 81 independent components of this tensor. Fortunately this number can be reduced in several ways.

Because of the symmetry of the stress tensor:

$$A_{ijkl} = A_{ijlk} \qquad \ldots\ldots\ldots\ldots\ldots\ldots\ldots\ldots \quad (6.2)$$

So that the 81 independent values are reduced to 54. Furthermore because of the symmetry of the strain tensor:

$$A_{ijkl} = A_{jikl} \qquad \ldots\ldots\ldots\ldots\ldots\ldots\ldots\ldots \quad (6.3)$$

which reduces the number of values to 36.

Using these simplifications Eq.(3.13) can be expanded to:

$$d\epsilon^p_{11} = A_{1111}d\sigma_{11}+A_{1122}d\sigma_{22}+A_{1133}d\sigma_{33}+A_{1112}d\sigma_{12}+A_{1113}d\sigma_{13}+A_{1132}d\sigma_{32}$$

$$d\epsilon^p_{22} = A_{2211}d\sigma_{11}+A_{2222}d\sigma_{22}+A_{2233}d\sigma_{33}+A_{2212}d\sigma_{12}+A_{2213}d\sigma_{13}+A_{2232}d\sigma_{32}$$

$$d\epsilon^p_{33} = A_{3311}d\sigma_{11}+A_{3322}d\sigma_{22}+A_{3333}d\sigma_{33}+A_{3312}d\sigma_{12}+A_{3313}d\sigma_{13}+A_{3332}d\sigma_{32}$$

$$d\epsilon^p_{12} = A_{1211}d\sigma_{11}+A_{1222}d\sigma_{22}+A_{1233}d\sigma_{33}+A_{1212}d\sigma_{12}+A_{1213}d\sigma_{13}+A_{1232}d\sigma_{32}$$

$$d\epsilon^p_{13} = A_{1311}d\sigma_{11}+A_{1322}d\sigma_{22}+A_{1333}d\sigma_{33}+A_{1312}d\sigma_{12}+A_{1313}d\sigma_{13}+A_{1332}d\sigma_{32}$$

$$d\epsilon^p_{32} = A_{3211}d\sigma_{11}+A_{3222}d\sigma_{22}+A_{3233}d\sigma_{33}+A_{3212}d\sigma_{12}+A_{3213}d\sigma_{13}+A_{3232}d\sigma_{32}$$

..... (6.4)

When dealing with elastic materials it is possible to show by considering the strain energy of the deformed body that:

$$A_{ijkl} = A_{klij} \quad \text{..... (6.5)}$$

which reduces the number of independent values in Eq.(6.4) to 21. Since energy considerations have proved useful for an elastic material there is the possibility that the concepts of irreversible thermodynamics might prove equally useful for plastic materials. This has been attempted by various authors and Naghdi[51] shows how the use of Onsager's reciprocal relations lead to the conclusion that $A_{ijkl} = A_{klij}$ for an irreversible material. However because of the assumptions involved this is little removed from theoretical speculation and it certainly has not been verified for soil. A second approach that is often used in the theory of

plasticity to obtain relationships between various components of A_{ijkl} by using the condition that the material is incompressible. However this cannot be used here because soil can undergo plastic changes in volume. The only remaining approach that can be used to further reduce the number of values of A_{ijkl} is to consider the type of symmetry that must be built into the material as a consequence of the process of compaction.

Compacting soil into a cylindrical mould produces a material whose properties in any horizontal direction are the same and which are different from those in the vertical direction. In other words the components of the tensor A_{ijkl} are not affected by rotating the coordinate system through any angle about a vertical axis. This is illustrated in Fig.6.11.

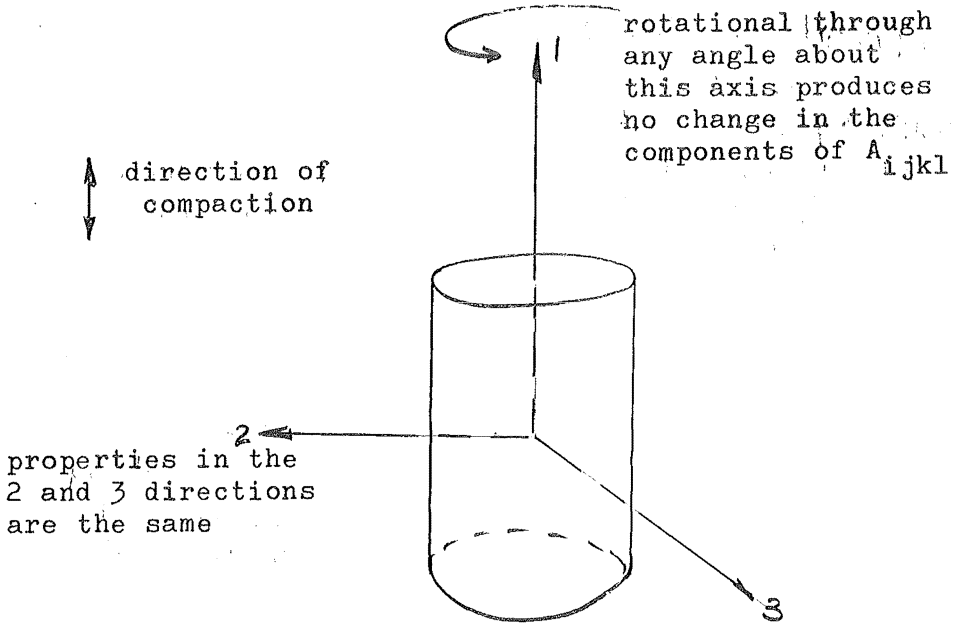

FIG.6.11 SYMMETRY OF THE COMPACTED SAMPLE

By a process of performing certain convenient transformations on the set of axes shown in Fig.6.11 it can be shown that certain of the components of A_{ijkl} are zero. As an example an anticlockwise rotation through 180^{o} about the 1 axis leads to the conclusion that 16 of the components are zero and that the remaining non-zero components are:

$$[\underline{A}] = \begin{bmatrix} A_{1111} & A_{1122} & A_{1133} & \cdot & \cdot & A_{1132} \\ A_{2211} & A_{2222} & A_{2233} & \cdot & \cdot & A_{2232} \\ A_{3311} & A_{3322} & A_{3333} & \cdot & \cdot & A_{3332} \\ \cdot & \cdot & \cdot & A_{1212} & A_{1213} & \cdot \\ \cdot & \cdot & \cdot & A_{1312} & A_{1313} & \cdot \\ A_{3211} & A_{3232} & A_{3233} & \cdot & \cdot & A_{3232} \end{bmatrix} \quad \ldots\ldots\ldots\ldots (6.6)$$

where $[\underline{A}]$ is a convenient symbol for the matrix of the 36 non-zero terms of the tensor A_{ijkl}. The procedure followed to obtain this result is set out in the following paragraph.

The first step is to find out how the stress and strain components are affected by this transformation. This operation is a standard one and is explained in any text on continuum mechanics, such as Prager[62]. Using the transformation formula for a second order tensor:

$$d\sigma'_{ij} = a_{ik}a_{jl}d\sigma_{kl}$$

and $\ldots\ldots\ldots\ldots\ldots\ldots\ldots\ldots\ldots\ldots\ldots\ldots (6.7)$

$$d\epsilon^{p'}_{ij} = a_{ik}a_{jl}d\epsilon^{p}_{kl}$$

where a_{ki} is the cosine of the angle between the axis in the k direction in the transformed system and the axis in the i direction of the old system. The matrix of a_{ki} values for the 180^{o} anticlockwise rotation about the 1 axis is:-

$$[a_{ki}] = \begin{bmatrix} 1 & 0 & 0 \\ 0 & -1 & 0 \\ 0 & 0 & -1 \end{bmatrix} \qquad \ldots\ldots\ldots\ldots\ldots\ldots\ldots\ldots \quad (6.8)$$

From Eqs.(6.7) and (6.8) the following is obtained:

$$d\sigma'_{11} = d\sigma_{11} \;,\; d\sigma'_{22} = d\sigma_{22} \;,\; d\sigma'_{33} = d\sigma_{33}$$

$$d\sigma'_{12} = -d\sigma_{12} \;,\; d\sigma'_{13} = -d\sigma_{13} \;,\; d\sigma'_{32} = d\sigma_{32}$$

and $\ldots\ldots\ldots\ldots\ldots\ldots\ldots\ldots \quad (6.9)$

$$d\epsilon'_{11} = d\epsilon_{11} \;,\; d\epsilon'_{22} = d\epsilon_{22} \;,\; d\epsilon'_{33} = d\epsilon_{33}$$

$$d\epsilon'_{12} = -d\epsilon_{12} \;,\; d\epsilon'_{13} = -d\epsilon_{13} \;,\; d\epsilon'_{32} = d\epsilon_{32}$$

It is not necessary to transform the components A_{ijkl} using the equivalent transformation rule for a fourth order tensor because these components are not affected by the rotation about the 1 axis as a consequence of the symmetry. The equation for $d\epsilon^{p'}_{11}$ in the transformed system is:

$$d\epsilon^{p'}_{11} = A_{1111}d\sigma'_{11}+A_{1122}d\sigma'_{22}+A_{1133}d\sigma'_{33}+A_{1112}d\sigma'_{12}+A_{1113}d\sigma'_{13} +A_{1132}d\sigma'_{32}$$

As explained above $d\epsilon^{p'}_{11} = d\epsilon^{p}_{11}$ and using the relations between

the transformed and old stress components in Eq.(6.9) this becomes:

$$d\epsilon^p_{11} = A_{1111}d\sigma_{11}+A_{1122}d\sigma_{22}+A_{1133}d\sigma_{33}-A_{1112}d\sigma_{12}-A_{1113}d\sigma_{13}+A_{1132}d\sigma_{32}$$

but from the top line of Eq.(6.4)

$$d\epsilon^p_{11} = A_{1111}d\sigma_{11}+A_{1122}d\sigma_{22}+A_{1133}d\sigma_{33}+A_{1112}d\sigma_{12}+A_{1113}d\sigma_{13}$$
$$+A_{1132}d\sigma_{32}$$

Comparing these two equations it is evident that A_{1112} and A_{1113} must be zero for the equality. Similarly by considering each of the stress components in the original and transformed systems it can be shown that several other components of A_{ijkl} are zero as set out in Eq.(6.6).

If now the system of axes is rotated through 180^o about the 2 axis of the original coordinate system further simplification results. Following the same procedure as above it is seen that $A_{1132} = 0$, $A_{2232} = 0$, $A_{3332} = 0$, $A_{1213} = 0$, $A_{1312} = 0$, $A_{3211} = 0$, $A_{3222} = 0$ and $A_{3233} = 0$. Thus Eq.(6.5) now becomes:

$$[\underline{A}] = \begin{bmatrix} A_{1111} & A_{1122} & A_{1133} & \cdot & \cdot & \cdot \\ A_{2211} & A_{2222} & A_{2233} & \cdot & \cdot & \cdot \\ A_{3311} & A_{3322} & A_{3333} & \cdot & \cdot & \cdot \\ \cdot & \cdot & \cdot & A_{1212} & \cdot & \cdot \\ \cdot & \cdot & \cdot & \cdot & A_{1313} & \cdot \\ \cdot & \cdot & \cdot & \cdot & \cdot & A_{3332} \end{bmatrix} \quad \ldots\ldots\ldots\ldots\ldots (6.10)$$

Many other transformations of this system of axes are possible, but with the exception of a rotation through an arbitrary angle about the 1 axis no new information is obtained. Because there is supposed to be symmetry about any horizontal plane in Fig.6.11 as a consequence of the compaction process, any terms of A_{ijkl} that are symmetrical in their 2 and 3 indices will be equal, thus:

$A_{2222} = A_{3333}$, $A_{2233} = A_{3322}$, $A_{1122} = A_{1133}$, $A_{2211} = A_{3311}$ and $A_{1212} = A_{1313}$. Now there are seven independent values:

$$[\underline{A}] = \begin{bmatrix} A_{1111} & A_{1133} & A_{1133} & \cdot & \cdot & \cdot \\ A_{3311} & A_{3333} & A_{3322} & \cdot & \cdot & \cdot \\ A_{3311} & A_{3322} & A_{3333} & \cdot & \cdot & \cdot \\ \cdot & \cdot & \cdot & A_{1313} & \cdot & \cdot \\ \cdot & \cdot & \cdot & \cdot & A_{1313} & \cdot \\ \cdot & \cdot & \cdot & \cdot & \cdot & A_{3232} \end{bmatrix} \quad \ldots\ldots\ldots\ldots (6.11)$$

This can be further reduced by considering a rotation through an arbitrary angle about the 1 axis. The transformation matrix for this is:

$$[a_{ki}] = \begin{bmatrix} 1 & 0 & 0 \\ 0 & m & -n \\ 0 & n & m \end{bmatrix} \quad \ldots\ldots\ldots\ldots\ldots\ldots\ldots\ldots\ldots\ldots (6.12)$$

where n is sinZ and m is cosZ, Z being the angle of rotation. The components of A_{ijkl} transform according to the formula:

$$A_{ijkl} = a_{im}\, a_{jn}\, a_{ko}\, a_{lp}\, A_{mnop} \quad \ldots\ldots\ldots\ldots\ldots\ldots \quad (6.13)$$

as explained in any standard test such as Prager[62]. Considering the way in which A_{3322} transforms leads to:

$$m^2n^2(A_{2222} + A_{3333}) - 4m^2n^2\, A_{2323} = A_{3322}(1-m^4)-n^4\, A_{2233}$$

which, by using the identity $m^2+n^2 = 1$ and remembering that $A_{3322} = A_{2233}$ and $A_{2323} = A_{3232}$ can be reduced to:

$$A_{3333} - A_{3322} = 2\, A_{3232} \quad \ldots\ldots\ldots\ldots\ldots\ldots\ldots\ldots \quad (6.14)$$

Transformed values of any of the other coefficients can be calculated but no new information is obtained.

Thus the final simplified matrix of coefficients contains only six independent values:

$$[\underline{A}] = \begin{bmatrix} A_{1111} & A_{1133} & A_{1133} & \cdot & \cdot & \cdot \\ A_{3311} & A_{3333} & A_{3322} & \cdot & \cdot & \cdot \\ A_{3311} & A_{3322} & A_{3333} & \cdot & \cdot & \cdot \\ \cdot & \cdot & \cdot & A_{1313} & \cdot & \cdot \\ \cdot & \cdot & \cdot & \cdot & A_{1313} & \cdot \\ \cdot & \cdot & \cdot & \cdot & \cdot & A_{3333}-A_{3322})/2 \end{bmatrix} \quad \ldots\ldots\ldots \quad (6.15)$$

These six independent coefficients are required to specify the type of anisotropy that the plastic deformation of this compacted soil would be expected to exhibit. The fact that six separate coefficients are required means that it is not

possible to determine all of them separately from the results of tests, such as the triaxial test, where there are only two independent components of the applied stress system.

Application of Eq.(3.16) shows that for a material with this type of anisotropy the principal axes of the stress increment and plastic strain increment tensors will coincide.

6.6 EQUATIONS FOR STRAIN INCREMENTS ON PARALLEL AND PERPENDICULAR LOADING

Equation (6.15) can now be applied to the triaxial test stress system to determine equations for the plastic strain increments. When Eq.(6.15) is applied to the triaxial test it becomes obvious that because of the simplicity of the stress system applied not all of the six components can be determined. As only two independent stress components are applied only two independent strain components can be measured:

$$\begin{aligned} d\epsilon^p_{11} &= A_{1111}d\sigma_{11} + 2A_{1133}d\sigma_{33} \\ d\epsilon^p_{33} &= A_{3311}d\sigma_{11} + (A_{3322} + A_{3333})d\sigma_{33} \end{aligned} \quad \text{..... (6.16)}$$

This gives the equations applicable to the loading test in Chapter 4, i.e. for loading parallel to the direction of compactive effort.

The next step is to find equations similar to Eqs.(6.16) that give the components of plastic strain when the sample is loaded perpendicular to the direction of compactive effort. The problem can be regarded as a rotation through 90^o about

the 2 axis as illustrated in Fig.6.12 below:

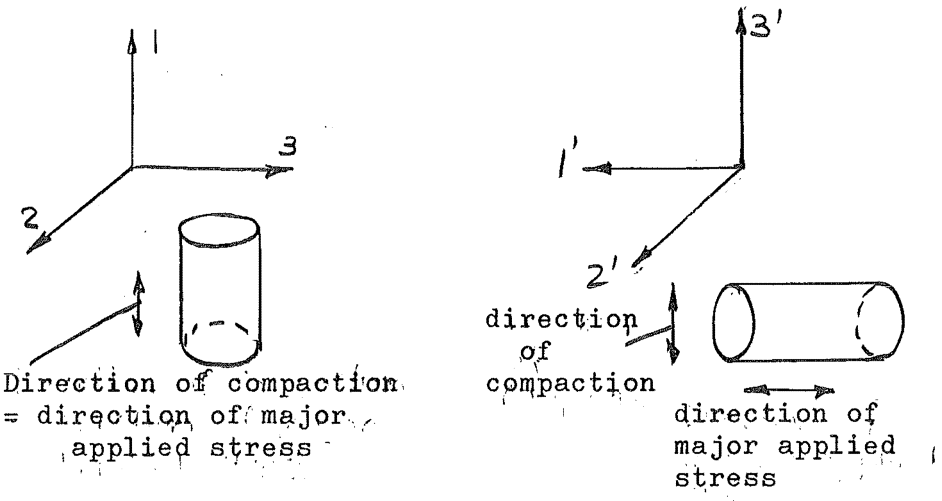

(a) Parallel (b) Perpendicular

FIG.6.12 SAMPLES MOUNTED PERPENDICULAR AND PARALLEL TO THE DIRECTION OF COMPACTIVE EFFORT

The transformation matrix for this rotation is:

$$[a_{ki}] = \begin{bmatrix} 0 & 0 & -1 \\ 0 & 1 & 0 \\ 1 & 0 & 0 \end{bmatrix} \quad \ldots\ldots\ldots\ldots\ldots\ldots\ldots\ldots \quad (6.17)$$

Using these values and Eq.(6.12) the manner in which the components of A_{ijkl} transform can be calculated. For example

$$A'_{1111} = a_{11}a_{11}a_{11}a_{11}A_{1111} + a_{11}a_{11}a_{12}a_{12}A_{1122} + a_{11}a_{11}a_{13}a_{13}A_{1133}$$
$$a_{12}a_{12}a_{11}a_{11}A_{2211} + a_{12}a_{12}a_{12}a_{12}A_{2222} + a_{12}a_{12}a_{13}a_{13}A_{2233}$$
$$a_{13}a_{13}a_{11}a_{11}A_{3311} + a_{13}a_{13}a_{12}a_{12}A_{3322} + a_{13}a_{13}a_{13}a_{13}A_{3333}$$
$$+a_{11}a_{12}a_{11}a_{12}A_{1212} + a_{11}a_{13}a_{11}a_{13}A_{1313} + a_{13}a_{13}a_{13}a_{12}A_{3332}$$

No other components of A_{ijkl} need be considered on the right of the preceding equation because they are zero. Substituting the values from the transformation matrix, Eq.(6.17), reduces this to:

$$A'_{1111} = A_{3333}$$

Similarly the other components can be transformed so that Eq.(6.10) now becomes:

$$[\underline{a}] = \begin{bmatrix} A_{3333} & A_{3322} & A_{3311} \\ A_{2233} & A_{2222} & A_{2211} \\ A_{1133} & A_{1122} & A_{1111} \end{bmatrix} \quad \ldots\ldots\ldots\ldots\ldots\ldots\ldots\ldots\ldots\ldots \quad (6.18)$$

where $[\underline{a}]$ is a convenient symbol for the submatrix of the nine terms in the top left hand corner of $[\underline{A}]$. Using the observation made on p.285 that all terms symmetrical in the 2 and 3 indices are equal this reduces to:

$$[\underline{a}] = \begin{bmatrix} A_{3333} & A_{3322} & A_{3311} \\ A_{3322} & A_{3333} & A_{3311} \\ A_{1133} & A_{1133} & A_{1111} \end{bmatrix} \quad \ldots\ldots\ldots\ldots\ldots\ldots\ldots\ldots\ldots\ldots \quad (6.19)$$

It is now possible to write the equations for the strain increments for loading perpendicular to the direction of compactive effort:

$$\begin{aligned} d\epsilon^p_{11} &= A_{3333}\, d\sigma_{11} + (A_{3322} + A_{3311})\, d\sigma_{33} \\ d\epsilon^p_{22} &= A_{3322}\, d\sigma_{11} + (A_{3333} + A_{3311})\, d\sigma_{33} \\ d\epsilon^p_{33} &= A_{1133}\, d\sigma_{11} + (A_{1133} + A_{1111})\, d\sigma_{33} \end{aligned} \quad \ldots\ldots\ldots\ldots \quad (6.20)$$

These three equations make the problem of mounting samples in the triaxial apparatus with the direction of the compactive effort perpendicular to the major principal stress immediately apparent. The applied stress system is symmetrical with only two independent components but the resulting strain system is not so simple and has three rather than two independent components of strain. Unfortunately no attempt was made to measure separately the two strain components in the direction of the minor principal stress in the tests perpendicular to the compactive effort, although it was noted that some of the samples had an elliptical rather than circular cross section at the end of the tests. However it is still possible to draw some conclusions about the material behaviour from the tests.

The observation explained earlier in this chapter, that the stress paths for samples loaded perpendicular and parallel to the direction of compactive effort in an undrained test are identical, has not been used yet. This fact provides yet another way of simplifying the matrix of coefficients given in equations (6.15) and (6.19) for an undrained test. It was explained on p.279 that the components of the tensor A_{ijkl} are not material constants but are likely to be functions of stress and strain. The fact that the undrained stress paths are identical leads one to suppose that when comparing the increments of deformation under equal stress increments the appropriate values of A_{ijkl} may be the same for the tests when the sample is

loaded perpendicular or parallel to the direction of compactive effort. In other words it is suggested that for these undrained tests the components of A_{ijkl} are functions of stress only. This is not unreasonable because in the undrained tests the total volume of the sample is constant. It has already been shown that the soil has elastic properties which are isotropic, and so for identical stress paths in an undrained test the plastic volumetric strain must be the same regardless of whether the samples are loaded parallel or perpendicular to the direction of compactive effort.

Having stated that these plastic volumetric strains must be equal for undrained tests it now remains to investigate what new information this implies.

The definition of volumetric strain given in equation (3.24) is not dependent on isotropic deformation so it holds for anisotropic behaviour. Thus in both types of test, loading perpendicular and parallel to the direction of compactive effort, the volumetric plastic strain increment is the sum of the principal plastic strain increments.

For loading parallel to the direction of compactive effort:

$$dv^p = (A_{1111} + 2A_{3311})\, d\sigma_{11} + 2(A_{1133} + A_{3322} + A_{3333})\, d\sigma_{33}$$

and for loading perpendicular to the direction of compactive effort

$$dv^p = (A_{3333} + A_{3322} + A_{1111})d\sigma_{11} + (A_{1111} + A_{3333} + A_{3322} + A_{1133} + 2A_{3311})d\sigma_{33}$$

equating the coefficients of $d\sigma_{11}$ or $d\sigma_{33}$ in each of these equations leads to the following result for an undrained test:

$$A_{3333} + A_{3322} = A_{1111} + 2A_{3311} - A_{1133} \quad \ldots\ldots\ldots\ldots\ldots \quad (6.21)$$

Using Eq.(6.21) equations (6.16) and (6.20) can be further simplified. In loading parallel to the direction of compactive effort Eq.(6.16) becomes:-

$$d\epsilon^p_{11} = A_{1111}\, d\sigma_{11} + 2A_{1133}\, d\sigma_{33} \quad \ldots\ldots\ldots\ldots\ldots\ldots \quad (6.22)$$

$$d\epsilon^p_{33} = A_{3311}\, d\sigma_{11} + (A_{1111} + 2A_{3311} - A_{1133})d\sigma_{33}$$

and for loading perpendicular to the direction of compactive effort Eq.(6.20) becomes:

$$d\epsilon^p_{11} = A_{3333}\, d\sigma_{11} + (A_{1111} - A_{3333} + 3A_{3311} - A_{1133})\, d\sigma_{33}$$

$$d\epsilon^p_{22} = (A_{1111} - A_{3333} + 2A_{3311} - A_{1133})d\sigma_{11} + (A_{3333} + A_{3311})\, d\sigma_{33} \quad \ldots\ldots \quad (6.23)$$

$$d\epsilon^p_{33} = A_{1133} d\sigma_{11} + (A_{1133} + A_{1111})\, d\sigma_{33}$$

Equation (6.22) shows that there are only two independent components of the plastic strain tensor when the compacted soil is loaded parallel to the direction of compactive effort. These two components can be expressed as an isotropic or spherical component of the tensor giving the volumetric strain, and a deviatoric strain tensor with only one component, giving the distortion. On the other hand Equation (6.23) results in a deviatoric strain

tensor with three distinct components and so there are three components of distortion when the compacted soil is loaded perpendicular to the direction of the compactive effort.

6.7 SIGNIFICANCE OF ANISOTROPY FOR THE PLASTIC STRESS-STRAIN RELATION DEVELOPED IN CHAPTER 5

In this section of the chapter the significance of the anisotropy set out above for the plastic stress-strain law developed in Chapter 5 is discussed.

The components of deformation given in Eq.(6.22) can be converted to the components $d\epsilon^p$ and dv^p for loading parallel to the direction of compaction as follows:-

$$dv^p = d\epsilon^p_{11} + 2d\epsilon^p_{33} = (A_{1111} + 2A_{3311})d\sigma_{11} + 2(A_{1111} + 2A_{3311})d\sigma_{33}$$

which reduces to:

$$dv^p = 3(A_{1111} + 2A_{3311})dp \quad \ldots\ldots\ldots\ldots\ldots\ldots\ldots\ldots \quad (6.24)$$

This equation shows that the plastic volumetric strain increment for loading parallel to the direction of compactive effort is independent of the stress increment dq, in other words it has the same form as equation (5.8). For the plastic distortion increment:

$$d\epsilon^p = \tfrac{2}{3}(d\epsilon^p_{11} - d\epsilon^p_{33}) = \tfrac{2}{3}(A_{1111} - A_{3311})d\sigma_{11} + (3A_{1133} - A_{1111} - 2A_{3311})d\sigma_{33}$$

which can be expressed as:-

$$d\epsilon^p = \tfrac{2}{3}(A_{1111} - A_{1133})dq + 2(A_{1133} - A_{3311})dp \quad \ldots\ldots\ldots\ldots (6.25)$$

Now this equation for the distortion increment has the same form as equation (5.32) given for the distortion increment in Chapter 5.

Equations (6.24) and (6.25) have been derived here for a material whose properties are not isotropic, yet it has been pointed out that the form of both of these equations is the same as those derived in Chapter 5 where it is assumed that the material is isotropic. This requires some explanation.

For a material to be truly isotropic three conditions must be fulfilled. The first of these is that under an arbitrary increment of stress there are only two independent components to the strain tensor. These are an isotropic component giving the volumetric strain and a deviatoric component giving only one component of distortion. Secondly the material must deform in the same way regardless of orientation with respect to the applied stress system. Finally two material constants completely describe the behaviour. Equations (6.24) and (6.25) show that there are only two components of deformation when the compacted material is loaded parallel to the direction of compactive effort, and so the first of the above requirements is fulfilled. However the preceding sections show that the other two requirements are not fulfilled, i.e. more than two material properties are needed

to describe the behaviour and the deformation is not independent of the orientation of the sample with respect to the applied stress system. Nevertheless this means that the material behaves simply enough when loaded parallel to the direction of compactive effort for an approach based on the assumption of isotropy to describe the deformation. In other words under these conditions the material is "pseudo-isotropic". However this does reveal the major restriction that must be applied to the plastic stress-strain theory developed in Chapter 5. The theory is based on the assumption that the material is isotropic and consequently can only describe the behaviour when the material is loaded parallel to the direction of compaction in an axisymmetric stress system. The possible modification to include the anisotropy of the compacted material is not attempted in this thesis. To measure this anisotropic behaviour completely some type of apparatus other than the triaxial equipment would be required.

Nevertheless the finding that a material with the particular type of anisotropy set out in Eq.(6.15) can be treated as pseudo-isotropic under an axisymmetric stress system when the major principal stress is applied in the same direction as was the compactive effort may have important ramifications. Many naturally occurring deposits of soil are laid down under conditions not unlike those during compaction. The resulting deposit of soil has properties like those illustrated in Fig.6.11 - the material is anisotropic with properties in a vertical plane

different from those in the horizontal plane and the properties in any direction in the horizontal plane are the same. Now if samples are obtained from such a deposit of soil and tested with the major principal stress applied in the vertical direction it would be possible to use a theory based on the assumption of isotropy, such as that developed by the Cambridge group, to describe the behaviour under axisymmetric stress conditions. Thus the apparently restrictive assumption of material isotropy may not preclude the application of theories such as that developed in Chapter 5 and that by the Cambridge group to many practical situations.

CHAPTER SEVEN

CONCLUSIONS AND SUGGESTIONS FOR FURTHER RESEARCH

In Chapter 1 it was explained that there is a widespread opinion that a major area in need of development in soil mechanics is the understanding of the manner in which soil deforms under stress. The work reported in this thesis is the result of an initial investigation into the behaviour of a particular soil prepared in a particular way subjected to the stress system applied by the triaxial apparatus.

The aim of the work reported in the previous chapters was twofold. Firstly it was desired to investigate the behaviour of a material in a state that might be encountered in engineering practice. Secondly it was desired to investigate a material with anisotropic stress deformation properties in order to assess the restrictions placed on the use of theoretical treatments based on the assumption of isotropy.

As this work was an initial investigation several aspects require further study and these are also explained in this chapter.

The eight conclusions reached are set out below in order of importance:-

1) In the second half of Chapter 5 a function describing the form of successive yield curves for the work hardening of

the compacted clay was derived from the results of a series of undrained triaxial tests in which the material was loaded in the direction of the compactive effort. It was demonstrated that although the plastic stress-strain relation developed using this function does not predict the behaviour of the material exactly, it does predict the general features of the behaviour. Thus the major conclusion of this thesis is that the use of a theory for an isotropic elastic-plastic work-hardening material to describe the behaviour of this particular compacted soil has some promise.

As explained below results from other types of tests would be needed before a more definite conclusion about the validity of the theory can be reached. But in Chapter 6 an important limitation to the theory was found. The results of a series of undrained triaxial tests in which the material was loaded at right angles to the direction of compactive effort show that the plastic deformation of this compacted soil is anisotropic. However the anisotropy was such that when the material is loaded parallel to the direction in which the compactive effort was applied the material behaves in a "pseudo-isotropic" manner and thus the deformation can be described by a theory based on the assumption of isotropy.

2) In the first part of Chapter 5 the concept of "actual effective stress" was introduced. It was postulated that this is more appropriate than the Terzaghi effective stress

for describing the behaviour of this particular soil compacted to a given dry density. The behaviour described in Chapter 4 and further discussed in Chapters 5 and 6 indicates that the description of the material behaviour is simplified by adding 3.0 psi to the hydrostatic component of effective stress. This 3.0 psi seems to be unaffected by the amount of consolidation after compaction and back pressure saturation, or by the amount of axial deformation, in other words it seems to be a characteristic of this material that remains constant over a range of states. Because of this it was suggested in Chapter 5 that one consequence of the compaction process is that a component of hydrostatic stress equal to 3.0 psi is built into the material. This idea is in line with the hypothesis made in Chapter 2 that the controlling factor determining the behaviour of any soil is the nature of the interparticle force system.

The magnitude of this stress component was determined independently by three separate aspects of the behaviour of the samples during undrained tests. The two drained tests performed did not give such a clear indication, but it has been explained in Chapter 5 that this may be a consequence of the limitations of the drained triaxial test.

3) In Chapter 3 some of the defects of the triaxial method of testing were discussed. It was shown by means of a simple analysis that the ratio of the increment of distortion to the

volumetric strain increment corresponding to given stress increment has the same value regardless of whether the sample deforms homogeneously or deforms in a narrow slip plane. This conclusion was used in Chapter 5 when deriving the function for the successive yield curves.

4) The work in Chapter 4 revealed that when the stress paths for the undrained tests are expressed in terms of the actual effective stress, the undrained stress paths are geometrically similar for samples consolidated at pressures greater than 10 psi. This means that these stress paths sweep out a three dimensional surface of which constant void ratio sections are geometrically similar.

5) In Chapter 6 it was shown that the elastic, or recoverable, properties of the material are approximately isotropic, whereas the plastic deformation is anisotropic. Despite this anisotropic deformation, it was shown that the stress paths are not dependent on the direction of the loading with respect to the direction in which the compactive effort was applied.

6) It was observed that when the samples were unloaded under undrained conditions there was a decrease in the effective hydrostatic component of stress. The definition of a new dimensionless parameter revealed that there was a well defined relation between the decrease in stress on complete

unloading and the change in the effective hydrostatic component of stress during the loading phase of the test.

7) Contours of equal axial deformation were plotted for the undrained tests in the stress path diagram in Chapter 4. It was seen that these are linear and that all the contours pass through a common point on the effective hydrostatic pressure axis. It was also shown that the shape of these contours is a unique function of axial strain for all the undrained tests.

8) On complete unloading under undrained conditions there was a certain amount of axial strain recovered. In Chapter 4 it was shown that the magnitude of this was defined by an undrained unloading secant modulus. The magnitude of this modulus was a linear function of the pressure at which the samples were consolidated before undrained loading. It was also found that the value of this modulus was not affected by repeated loading to a constant stress and was approximately constant throughout the undrained tests.

Finally five suggestions for further research are presented:

(i) It has been pointed out at the end of Chapter 5 that the direction of the plastic strain increment vector has been determined only for undrained tests. It would be valuable to

measure this for other stress paths such as the constant stress ratio paths discussed in Chapter 5. In addition, tests to check that the direction of the plastic strain increment vector at a given position on the yield curve is independent of direction of the stress increment at that point would provide an additional valuable test of the validity of the function for the successive yield curves developed in Chapter 5. Both these types of test could be performed in the conventional triaxial apparatus provided that facilities for controlling the stress path were available.

Another important development of Chapter 5 was the proposal of a modified elastic wall. The existence of this was inferred from the observed behaviour but was not measured directly and so it would be interesting to investigate experimentally the form of this wall.

(ii) The most important limitation of the incremental stress-strain theory developed in Chapter 5 was related to the anisotropy of this compacted material. A more thorough investigation of the anisotropic properties would provide further evidence on which the general validity of the theory could be decided. The major difficulty in Chapter 6 was that simple equipment, such as the triaxial apparatus, is not really suitable for measuring the deformation of an anisotropic material. A more versatile type of apparatus capable of applying a general stress system rather than a very specialised one would be required for

such an investigation.

(iii) It would be worthwhile to conduct a more extensive investigation of the concept of actual effective stress introduced in Chapter 5. This concept has emerged as a fairly clear characteristic of the undrained tests, but not of the drained tests, and yet if it is to be a valid concept it must apply to any stress path whether drained or undrained. This reduces to investigating the type of energy correction needed to correlate the results of drained tests with those of undrained tests. As suggested in Chapter 5 and mentioned again above, part of the problem might be related to the triaxial apparatus and so some other type of apparatus might be of more use in such an investigation.

(iv) As material prepared at only one point on a compaction curve has been investigated here it might be interesting to measure the deformation of the same material under stress when compacted to other initial states. Variables such as position on the compaction curve, compactive effort and type of compaction could be considered. Perhaps the most interesting aspect of such an investigation would be the effect, if any, of the initial state of the compacted soil on the value of the stress component built into the material as a result of the compaction process.

(v) The range of void ratios covered in this study has not been great. Another important extension of the work presented in this thesis would be an investigation over a greater range of void ratios, by consolidating samples under greater pressures before loading to failure.

APPENDIX A

PROPERTIES OF THE SOIL TESTED

A.1. INTRODUCTION

The soil used for testing was obtained from Webb Refineries Ltd., Henderson, who designate it as Mark 4 china clay. It was supplied in paper bags each containing 100 lb. of dry powdered soil. Determination of the liquid limit by taking samples from several bags showed that there was little difference in the soil from bag to bag, so the material was used from the bags as supplied, with no mixing or special treatment.

A.2. GENERAL PROPERTIES

The soil was found to have the following general properties:

Liquid Limit	=	49%
Plastic Limit	=	36%
Plasticity Index	=	13%
Clay Fraction ($<2\mu$)	=	18%
Activity (P.I./Clay Fraction)	=	0.72
Specific Gravity	=	2.54

Fig. A.1. gives the particle size distribution curve determined according to ASTM standard procedure D422-63. The particle size curve shows that most of the material falls into the silt category, only 18% being finer than 2 microns. If this

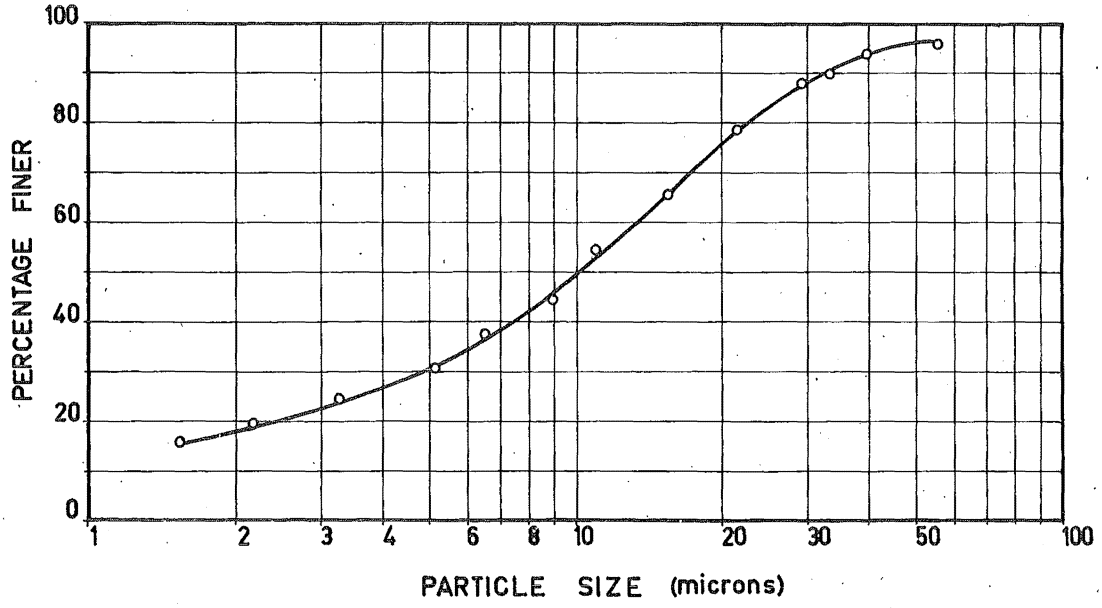

FIG. A1 PARTICLE SIZE DISTRIBUTION

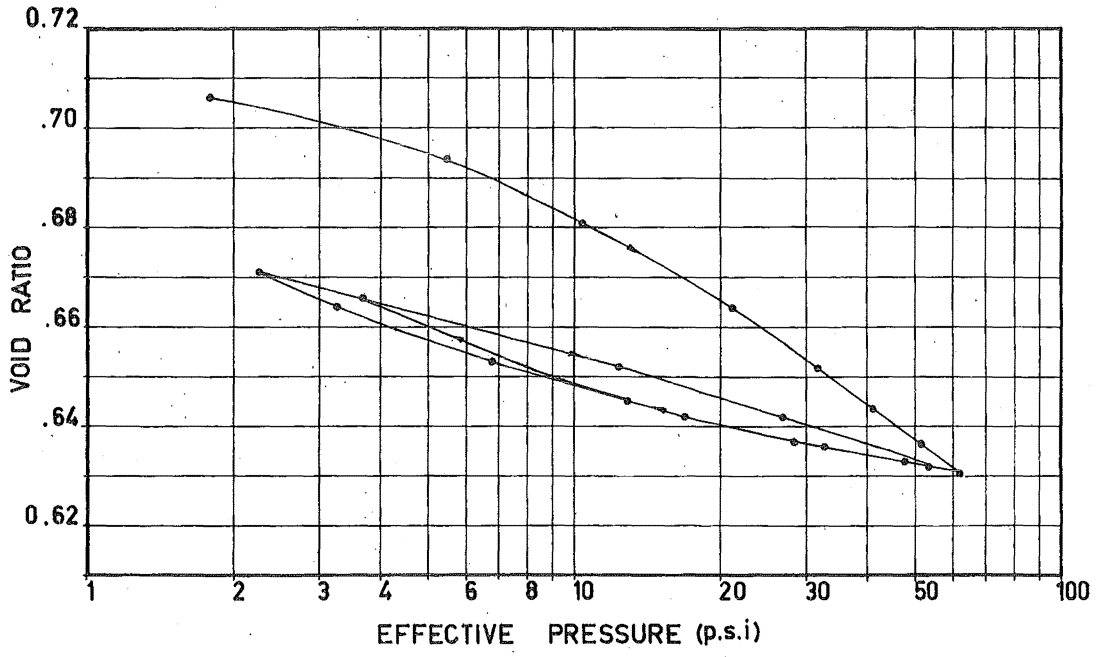

FIG. A4 ISOTROPIC CONSOLIDATION CURVES

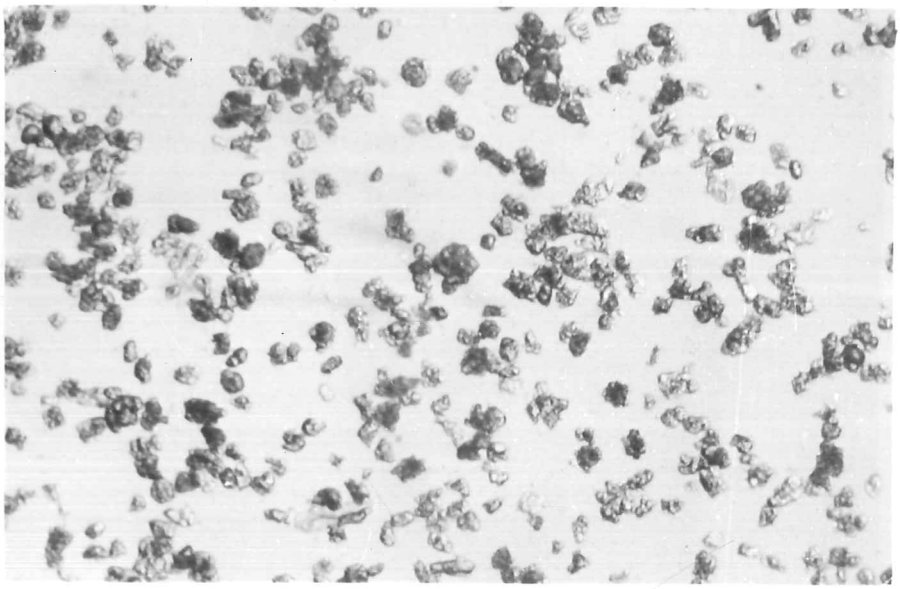

FIG. A2 PHOTOMICROGRAPH (×400) OF SILT PARTICLES EQUIVALENT SPHERICAL PARTICLE SIZE 15 to 20μ

×4000

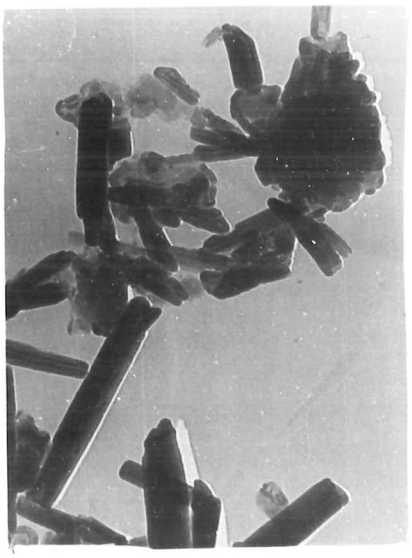

×20000

FIG. A3 ELECTRON MICROGRAPH OF CLAY PARTICLES EQIVALENT SPHERICAL PARTICLE SIZE LESS THAN 1μ

material was classified as the basis of particle size it would be a clayey silt. However with a liquid limit of 49% the material exhibits properties more characteristic of a clay than a silt so it has been termed a clay in this thesis.

A.3. TYPE AND SHAPE OF PARTICLES PRESENT

The photomicrograph, Fig. A.2. of silt particles from the soil, between 15 and 20 microns in size, shows that they have an irregular subangular shape.

Electronmicrographs of the clay fraction of the soil are shown in Fig. A.3. These were taken by Dr A.H.Bryant, formerly of the Civil Engineering Dept. A small volume was taken from the top of a suspension which had been prepared, as if to determine particle size distribution, after it had been standing for 24 hours. This was diluted many times, and a drop was dried on a glass plate. A carbon replica was made of the deposit, and the magnified image of this replica is shown in the photographs.

Two things are of interestfrom these electronmicrographs. Firstly the elongated, rod like, shape of the particles suggests that the clay mineral is Halloysite. Secondly there seems to be a tendency for the clay particles to form aggregates despite the presence of the dispersing agent. In discussing the properties of a soil containing Halloysite Terzaghi[82] considers that this tendency to form aggregates is responsible

for the comparatively low plasticity index and high angle of internal friction for soils containing this clay mineral.

A.4. CONSOLIDATION CHARACTERISTICS

The consolidation curve for a compacted sample of the soil is given in Fig.A.4. This was obtained by compacting a sample at the standard moisture content and compactive effort used for all samples tested. The sample was then mounted in a triaxial cell, and after saturation by the application of back pressure it was consolidated under hydrostatic pressure. From the void ratio-log pressure curve the following values were obtained:

C_c = 0.0135

C'_c (average for rebound) = 0.0049

C'_c (for linear portion at beginning at rebound) = 0.0032

The average value for the coefficient of consolidation was $3.10 \times 10^{-2} cm^2/sec$.

For purposes of comparison a consolidation test was conducted in an oedometer on a slurry whose initial moisture content was about twice the liquid limit. For this the following values were obtained:

$C_c = 0.179$

$C'_c = 0.035$

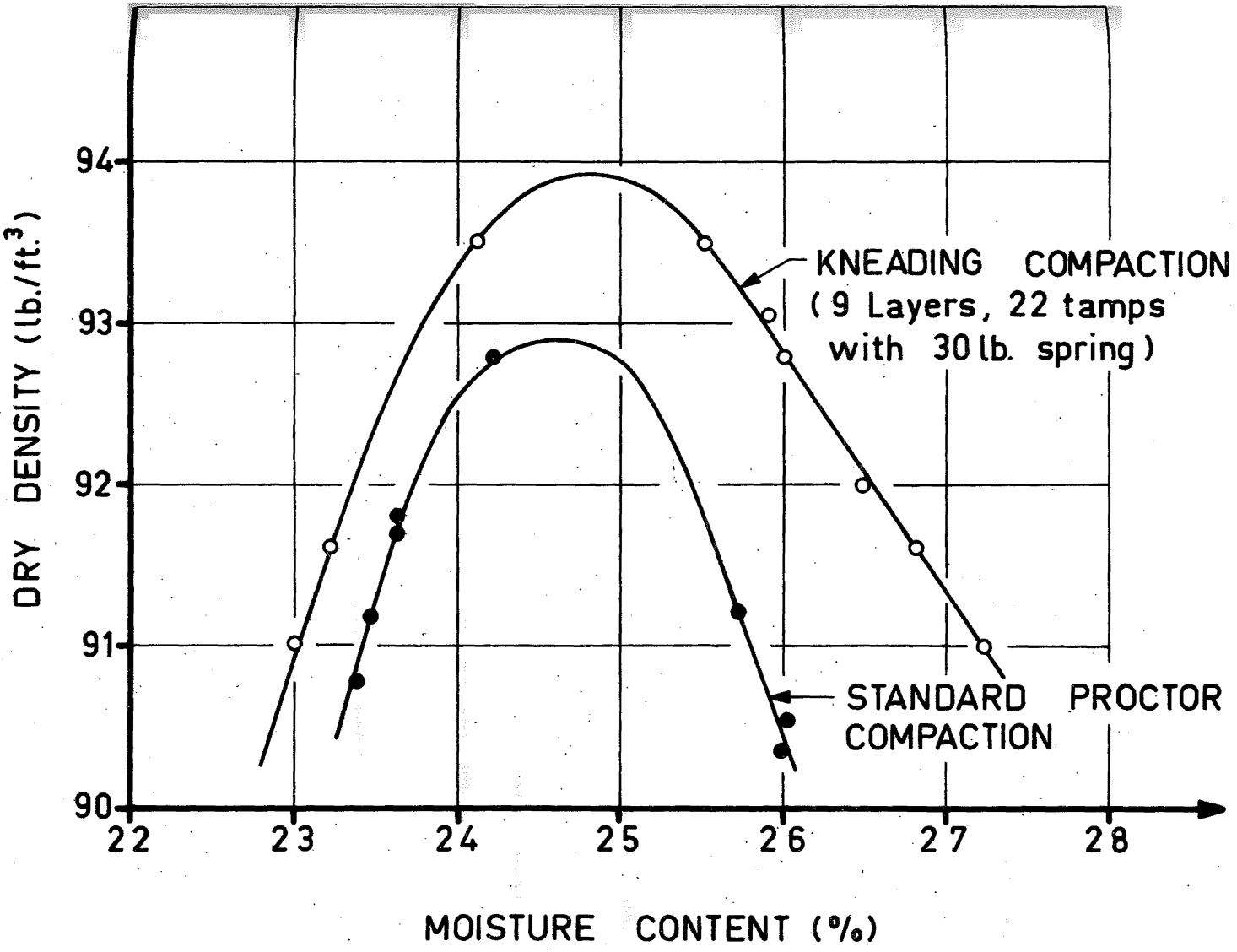

FIG. A 5 COMPACTION CURVES

A.5. COMPACTION CHARACTERISTICS

Compaction curves for the material are shown in Fig.A.5. All samples were prepared by kneading compaction in a 3" x $1\frac{1}{2}$"D split mould. Nine layers of moist soil were used, and each received 22 tamps of 30 lb with a hand compactor after the style of the Harvard miniature compactor. For purposes of comparison a standard Proctor compaction curve is included. This shows that the compaction used was somewhat greater than the standard Proctor effort, and as is usual with kneading compaction the slope of the curve on the wet side of O.M.C. was not as steep as that with dynamic compaction. All the points on these curves were obtained using moist soil which had been allowed to cure for 24 hours after mixing.

The target values for each triaxial test sample were: m/c 26% and dry density 93 lb/ft^3. If the values actually achieved for each test sample are plotted on the compaction curve, most of them lie above the curve. It is thought that the reason for this might be that the curing period in these cases was usually much greater than one day, as a new batch of moist soil was not prepared every time a sample was to be compacted.

APPENDIX B

DESCRIPTION OF APPARATUS

B.1. INTRODUCTION

As a preliminary to the detailed description of the experimental procedure given in appendices C and D this appendix describes the type of equipment used, to aid the presentation of the material in appendices C and D.

The apparatus followed the main features of the standard triaxial set-up described by Bishop and Henkel[6]. However over the years many useful developments have been noted in the literature and, where appropriate, the writer has incorporated these. Thus it is suggested that the equipment and experimental procedures used for this research project were of a high standard.

Essentially the equipment consisted of four triaxial cells with associated pressure generating equipment. Three of the cells, used for stress controlled tests, were mounted on a common loading frame and the fourth cell, used for strain controlled and consolidation tests, was set up in a Wykeham Farrance model T57 variable speed compression testing machine. Four hydraulic accumulators generated the cell and back pressures, the plumbing being so arranged that the systems could be coupled together. Fig.B.1 gives a diagrammatic presentation of the relationship between the various components.

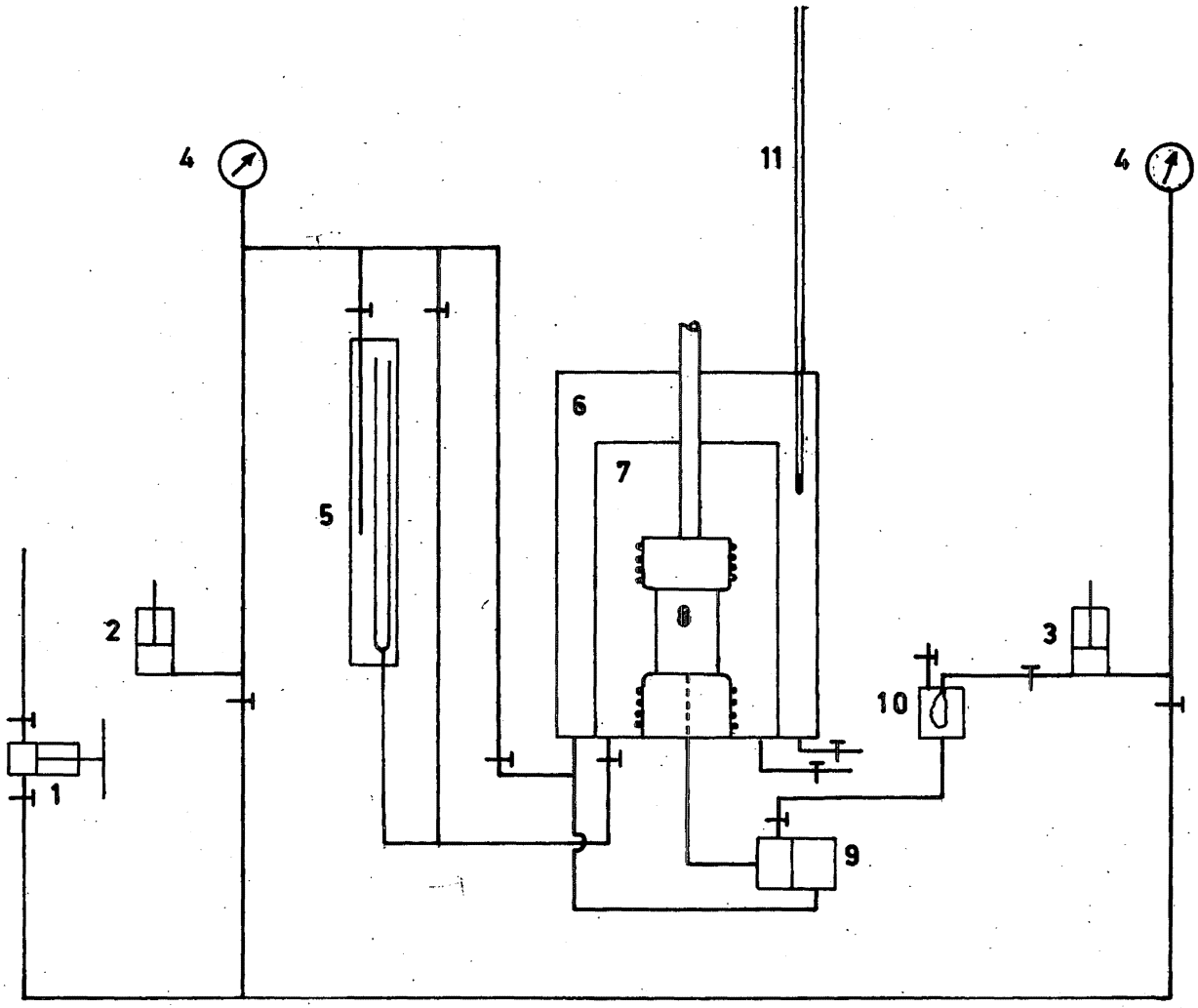

1 Screw pump

2 Cell pressure hydraulic accumulator

3 Back pressure hydraulic accumulator

4 Pressure gauge

5 Volume change gauge

6 Outer cell

7 Inner cell

8 Soil sample

9 Pore pressure transducer

10 Balloon interface between distilled, deaired water and mains water

11 Thermometer

Key: —| = valve

FIG. B1 DIAGRAMMATIC LAYOUT OF APPARATUS

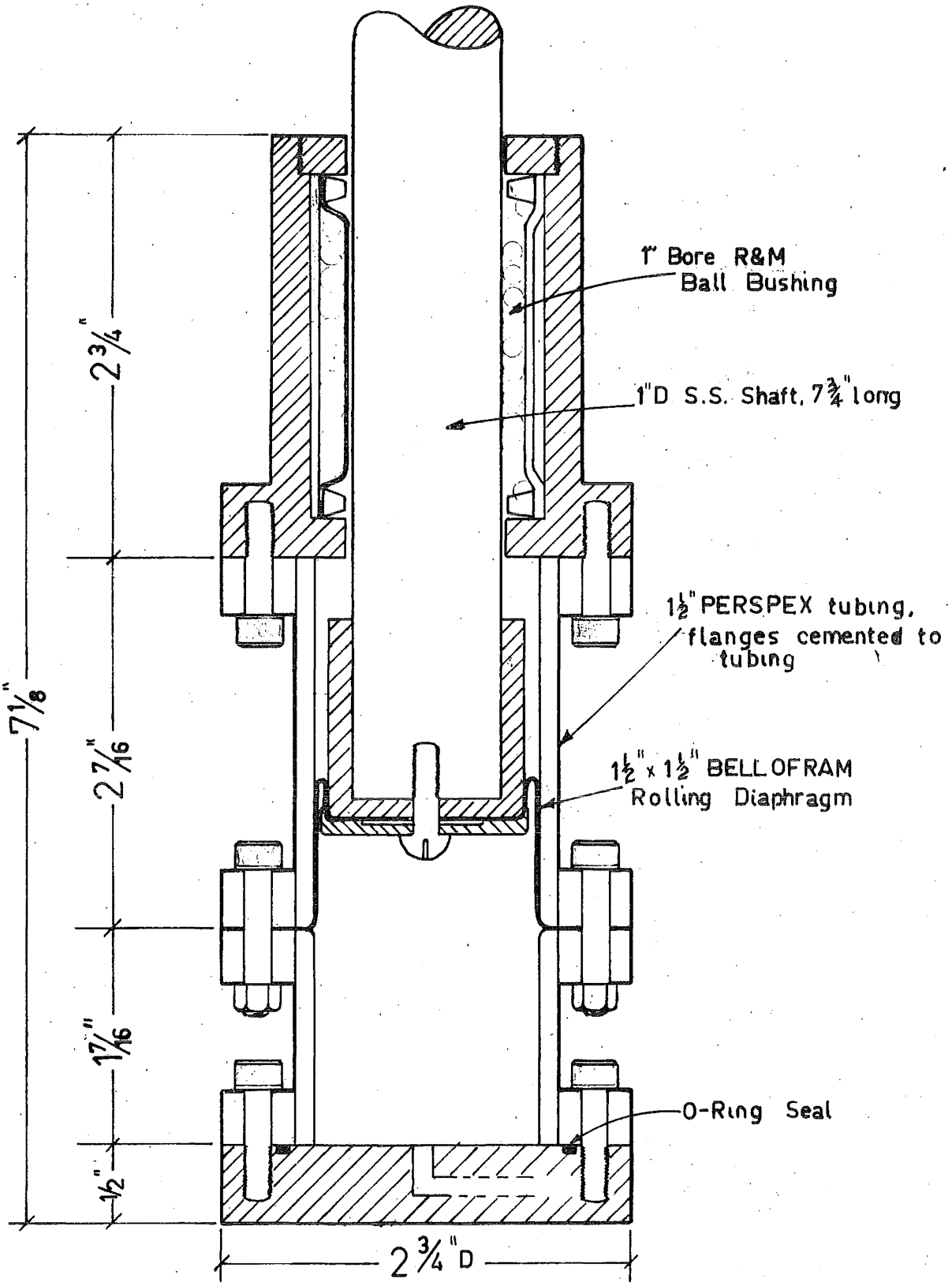

FIG. B2 HYDRAULIC ACCUMULATOR

To minimise the effects of temperature variations on the soil and apparatus everything was set up in a constant temperature room controlled to 20°C ±0.5°C.

B.2. HYDRAULIC ACCUMULATORS

Confining pressures for triaxial testing can be generated in several ways. The simplest way is to use air pressure, but this is undesirable for all but short term tests because of the problems that can arise when air diffuses through the rubber membrane into the sample. Perhaps the most elegant pressure generating device is the self compensating mercury control described by Bishop and Henkel[6]. Unfortunately the high cost of sufficient mercury meant that this system could not be used here. The remaining types of pressure generators include a whole range of devices, collectively described as hydraulic accumulators, in which a weighted piston generates pressure by acting on a confined volume of fluid.

The main requirements of a satisfactory hydraulic accumulator are negligible friction on the piston and sufficient capacity to accommodate the volume changes occurring during consolidation and those caused by any small leaks. These requirements were met in a relatively simple manner using a combination of a 1½"D Bellofram rolling diaphragm and a 1" Ransome and Marles ball bushing to provide an effective seal with negligible frictional loss. The accumulator has a

FIG. B3 GENERAL VIEW OF HYDRAULIC ACCUMULATORS

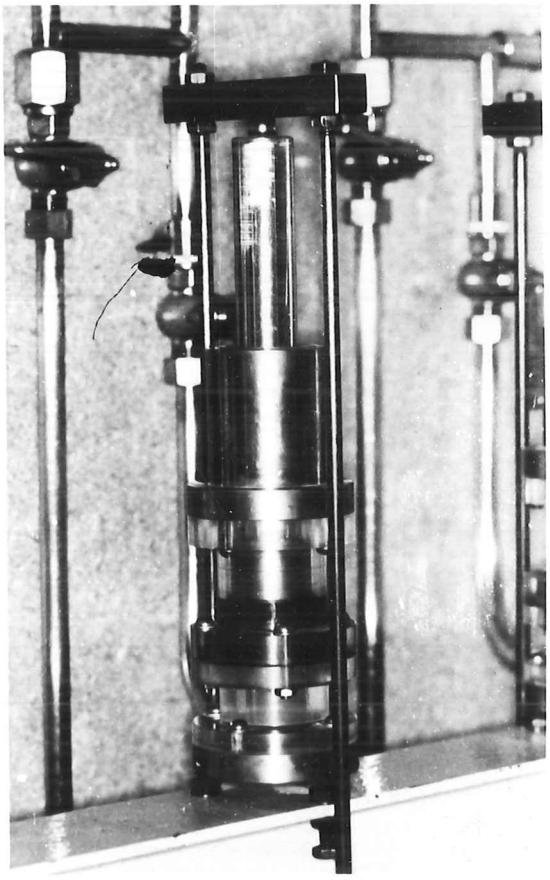

FIG. B4 CLOSE-UP OF A HYDRAULIC ACCUMULATOR

volumetric capacity of 50 ml and a pressure range of 10 psi to 200 psi. A cross-section of an accumulator can be seen in Fig.B.2 and Figs.B.3 and B.4 are photographs of the bank of accumulators and a close-up of a single accumulator respectively.

As a means of providing a constant pressure, the combination of a rolling diaphragm and a ball bushing seems to be very reliable. Only one qualification needs to be mentioned. At the extreme ends of the travel of the rolling diaphragm there seems to be a slight change in the effective area of the diaphragm which gives rise to an apparent frictional force. The significance of this force was investigated by traversing one hydraulic accumulator over its entire volumetric displacement at a nominal pressure of 140 psi and measuring the true pressure with one of the pore pressure transducers back pressured to a constant 140 psi. This test showed that over the central half of the travel the pressure generated by the accumulator was constant to within 0.1 psi but at the ends of the range the pressure changed by as much as 1 psi.

B.3. TRIAXIAL CELLS

(a) Cell for constant strain rate tests:

This was a standard Wykeham Farrance cell modified by the addition of a Geonor rotating bushing to reduce ram friction. The top and bottom platens were replaced with special $1\frac{3}{4}$"D stainless steel platens for the free ends.

Fig.B.5 shows this cell mounted in the Wykeham Farrance machine with a sample ready for testing.

At first the axial load carried by the samples in this type of test was measured with a proving ring. But on a test at supposedly constant strain rate the actual strain rate of the sample was subject to wide fluctuations, and so the proving ring was replaced with a stiffer device. A Phillips PR6101P/02 HK load beam, having a capacity of 200 kg. was used. The flexibility of this load beam was 0.00001"/lb while that of a proving ring of similar capacity was 0.0015"/lb. The read-out from the load beam was measured with a Budd model P350 static strain indicator. Fig.B.6 shows the load beam clearly.

(b) Cells for stress controlled tests:

The three cells for the stress controlled tests were specially designed and constructed for the work reported in this thesis. A cross-section of a complete cell can be seen in Fig.B.7, and photographs of the cells can be seen in Figs.B.8 and B.9. Various aspects of their construction are described under the following headings.

(i) Loading ram and bushing:

Consisting of a stainless steel ram running in two $\frac{1}{2}$" bore R & M ball bushings, and sealed with a rolling diaphragm, this was of similar design to the piston of the hydraulic accumulators. According to Olson and Campbell[52] this is the most satisfactory type of bushing for triaxial cells. The

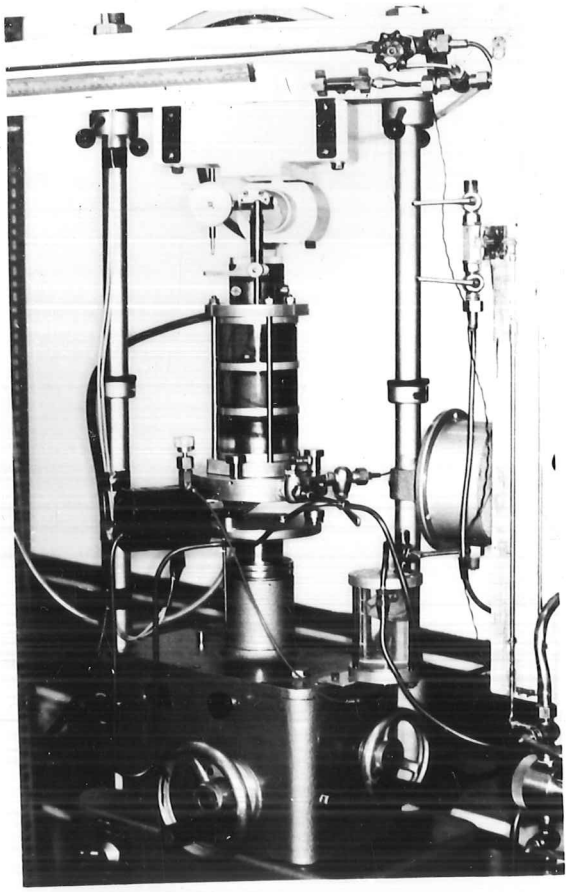

FIG. B5 CELL MOUNTED IN WYKEHAM FARRANCE MACHINE FOR A CONSTANT STRAIN RATE TEST

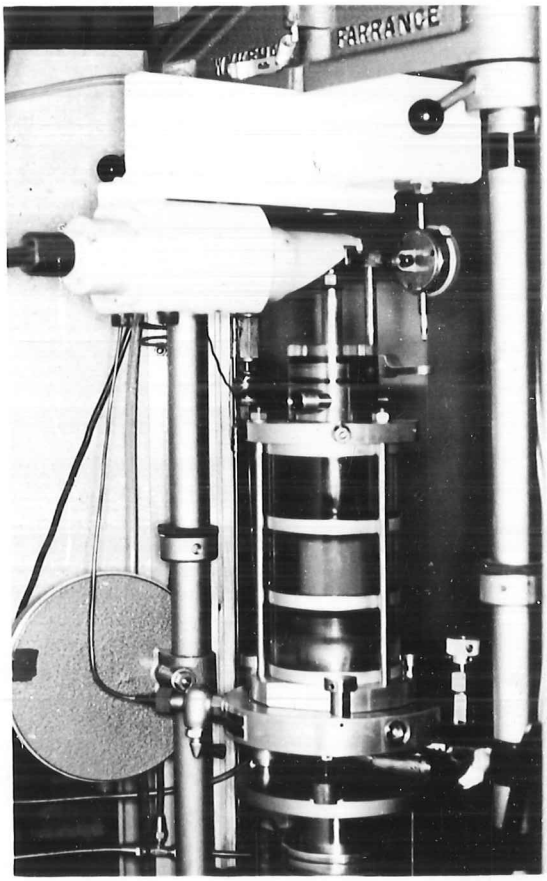

FIG. B6 REAR VIEW OF THE CELL SHOWING THE LOAD BEAM

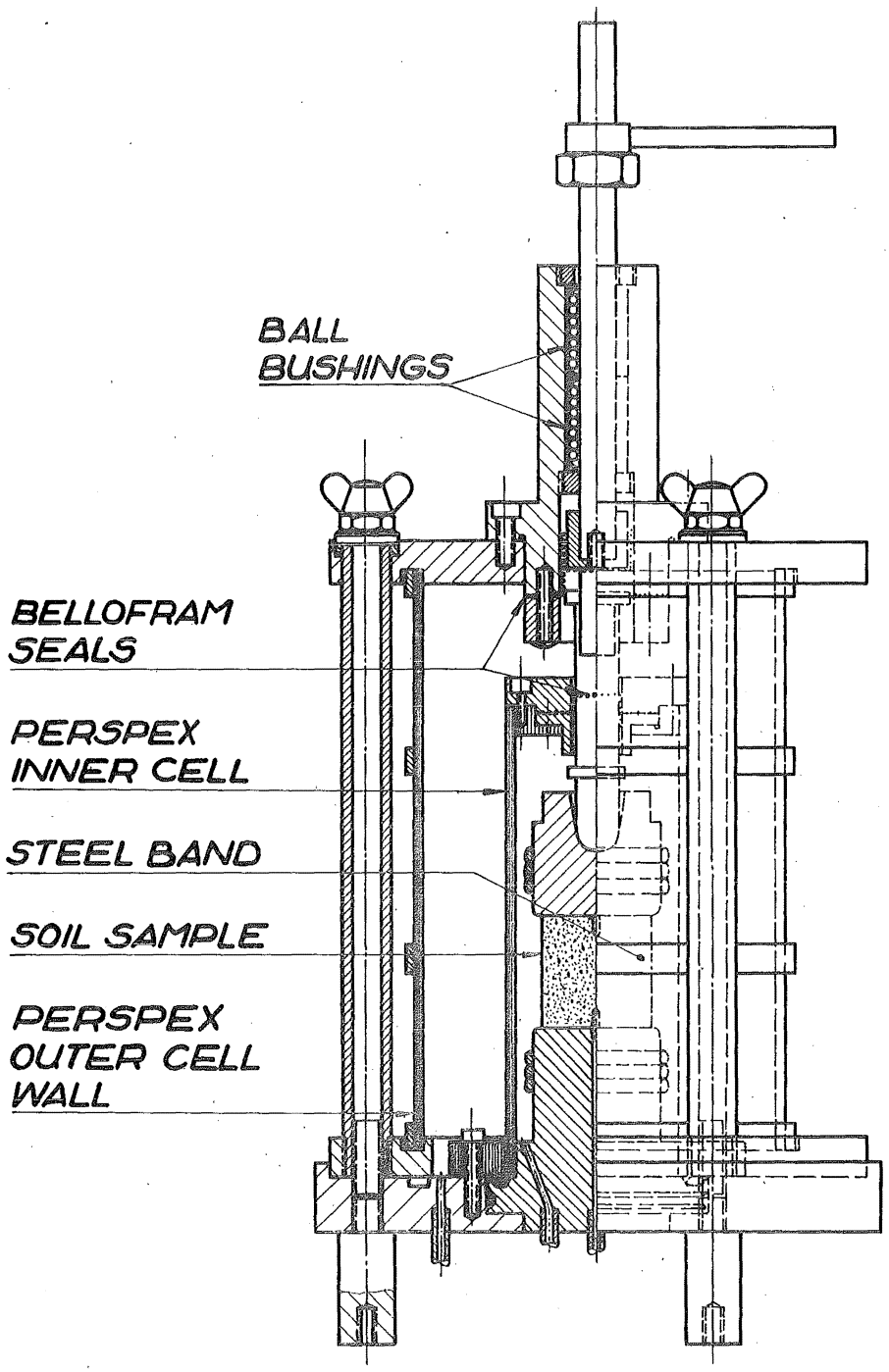

FIG. B7 CROSS-SECTION OF TRIAXIAL CELL USED FOR STRESS CONTROLLED TESTS

frictional loss is small and there is no vibration transmitted to the sample through the loading ram, as happens when a rotating bushing is used to reduce friction. The change in effective area of the rolling diaphragm at the extreme ends of travel was manifested by a variation in the load necessary to compensate for the cell pressure. However over the middle half of the travel, that used in the tests reported here, the load required to compensate for the cell pressure was constant to within $\frac{1}{5}$lb.

(ii) Bottom Pedestal:

The $1\frac{3}{4}$"D bottom pedestal was made from stainless steel and was finished with a very high polish to reduce the possibility of leakage into the sample under the O-rings used to seal the ends of the rubber membrane. A $\frac{3"}{16}$ D porous probe for pore pressure measurement was cemented with araldite in the centre of the pedestal. Similarly the tube leading from the underside of the pedestal to the pore pressure transducer was cemented in with araldite. The base of the cell was machined from a bronze casting and the stainless steel pedestal was bolted to it. A photograph of the cell base and bottom pedestal can be seen in Fig.B.11.

(iii) Outer Cell

The outer cell was made from $\frac{3"}{16}$ thick perspex tubing strengthened at the ends and third points with steel rings. Even with the steel rings some difficulty was experienced with

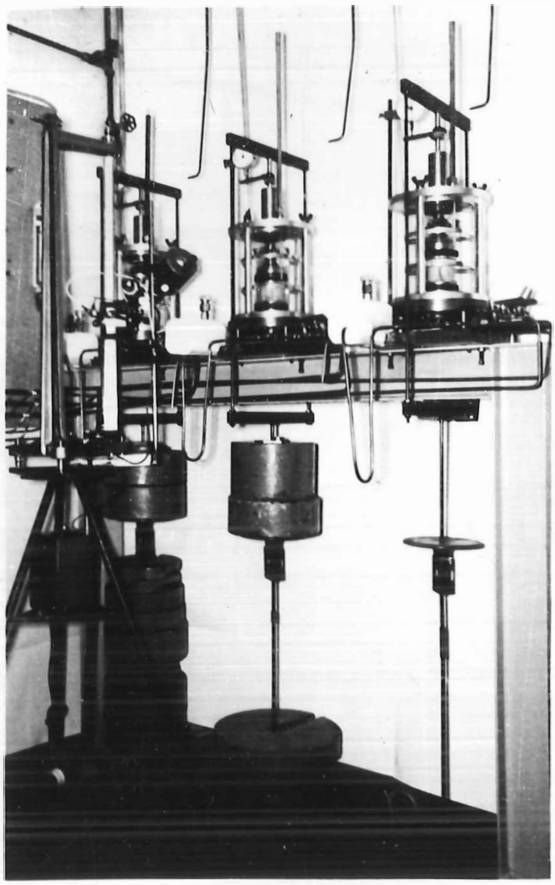

FIG. B8 GENERAL VIEW OF THE CELLS FOR THE STRESS CONTROLLED TESTS AND THE CATHET-OMETER

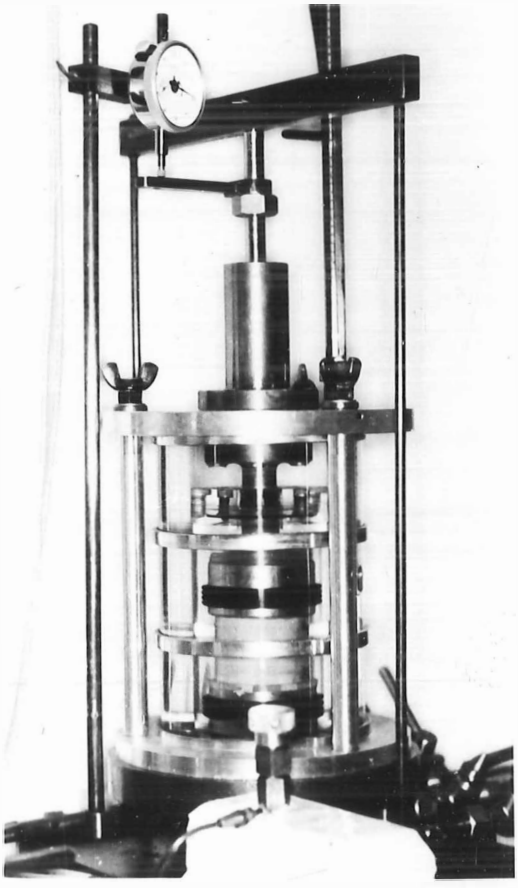

FIG. B9 CLOSE-UP OF A FULLY ASSEMBLED CELL WITH A SAMPLE UNDER TEST

the perspex, which had a tendency to fracture when under pressure. The trouble was eventually traced to the presence of tiny scratches on the surface of the perspex, which seemed to act as stress raisers. After a number of failures in this way, the outside of each new perspex cell was polished with Brasso before applying any pressure, and no further fractures occurred.

The alignment of each cell was checked during manufacture by mounting the cell base in a lathe so that it ran true. Then the outer cell was adjusted so that the centre line of the loading piston at the level of the top of the cell was within $\pm$0.005" for concentricity and wobble. This adjustment was maintained during subsequent re-assemblies of the cells because each cell was so constructed that the force in the holding down bolts did not affect the alignment of the various components.

(iv) Inner Cell

The writer's original intention in using an inner cell entirely separate from the outer cell was to allow measurement of the changes in volume that occur during undrained tests on unsaturated soils. This was to be done by taking an independent cell pressure lead to the inner cell via a kerosine-water burrette (seen in the background of Fig.B.3). As things developed this facility was not used to the extent originally envisaged. However two other features did make the inner cell useful. Firstly, the time required for the cell fluid (castor oil) to drain away after the completion of a test was considerable

and so the reduction in the volume of castor oil by the use of the inner cell is an advantage. Secondly, the cathetometer sightings for determining the deformation of the sample seem to be less reliable when taken through a considerable thickness of oil. Thus a further advantage of the inner cell was that it kept the sight distance through oil down to $\frac{3}{4}$". The arrangement of the inner cell can be seen in Fig.B.9.

The three cells were all mounted on a common loading frame. The base of each cell was bolted down to a heavy steel plate that had been attached to the frame and levelled.

B.4. PORE PRESSURE TRANSDUCER

The back pressure used was high and it was not possible to make a transducer that could measure the absolute pore pressure with sufficient sensitivity and yet have the required long term stability.

The standard null indicator method, Bishop and Henkel[6], was not used because of the need for constant adjustment. However the transducer developed was of sufficient stiffness to ensure negligible volume change.

Thus a type of differential pressure transducer was used which measured the difference between the cell pressure and the pore water pressure. Changes in the minor principal effective stress could then be measured in one step so that the inherently less accurate process of measuring separately

the cell pressure and pore water pressure and then subtracting them was avoided.

The transducers were specially built for this project. Essentially each consisted of a stainless steel diaphragm, back pressured by the cell pressure, on which four Budd C9-121-A strain gauges were mounted. Fig.B.10 shows a cross-section of a transducer.

At first some difficulty was encountered in cementing the strain gauges to the diaphragm in such a way that good long term stability resulted. A successful technique was eventually developed using Araldite AY103, and this is detailed in Appendix E along with the details of the design of the transducer. Castor oil had to be used to back pressure the diaphragm for two reasons. Firstly conventional waterproofing compounds are intended to protect the gauge from dampness and atmospheric moisture and certainly not from long term total immersion in water at high pressures. Secondly waterproofing compounds tend to be rather soft and plastic so that when the ambient pressure changes the waterproofing creeps and causes the gauge reading to change. Avoiding these two problems meant that the strain gauges could not be waterproofed so that a non-conductive fluid, castor oil, had to be used for back pressuring the diaphragm. Over the year and a half that the transducers were in use they were satisfactory in every way, and the back pressuring system was found to be reliable.

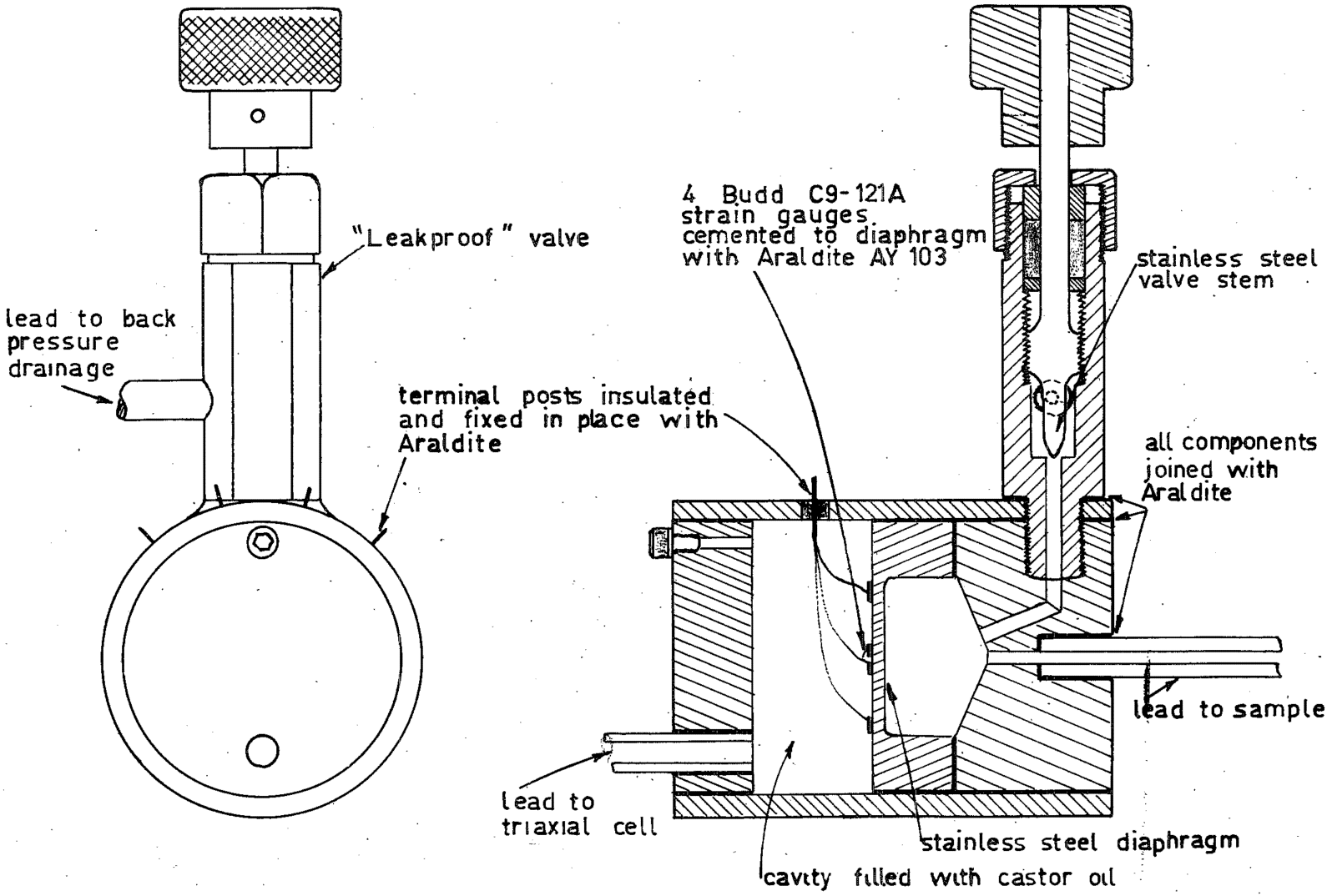

FIG. B 10 PORE PRESSURE TRANSDUCER SCALE: Full Size

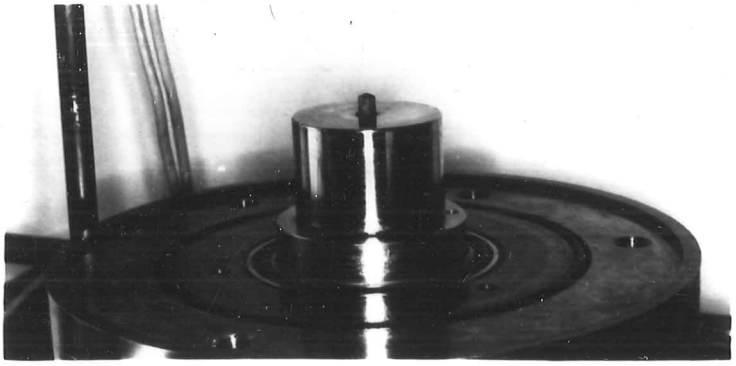

FIG. B11 CELL BASE AND BOTTOM PLATEN

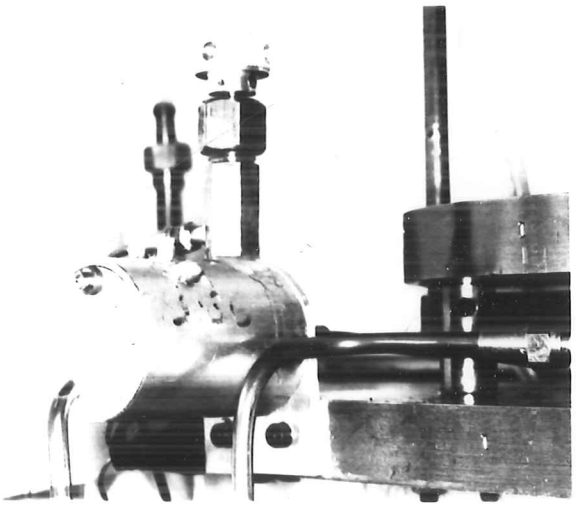

FIG. B12 PORE PRESSURE TRANSDUCER MOUNTED AT THE CELL BASE

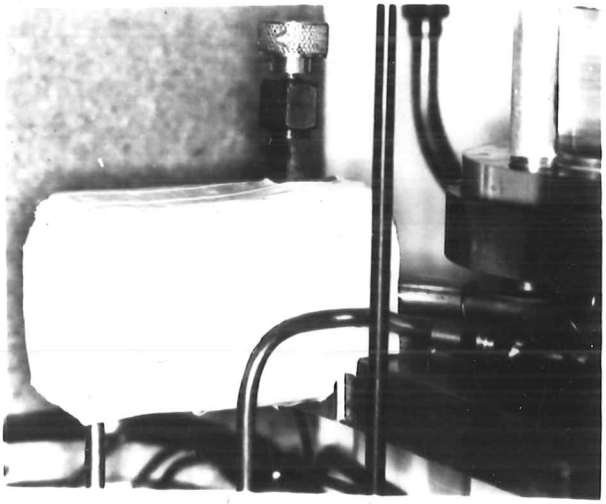

FIG. B13 COMPLETED PORE PRESSURE TRANSDUCER WITH THERMAL INSULATION FITTED

The valve described in Fig.B.10 as "leakproof" had to be capable of providing a very effective seal when closed after consolidation of the sample. Any leakage past this valve during an undrained test would produce a very significant error of unknown magnitude. None of the valves commercially available are suitable for this very stringent task, and so a satisfactory valve was developed in which a stainless steel stem can be screwed down tightly onto a brass seating.

When the pressure transducers had been constructed and fitted to the triaxial cells as shown in Fig.B.12 one further source of bother manifested itself. When a sample stood under undrained conditions under no load the pore pressure reading was observed to have an erratic variation about a mean value. The source of this variation was traced to the air conditioning plant in the constant temperature room in which the apparatus was mounted. The air temperature in the room tended to fluctuate about the mean value of $20^{o}C$ with a period of 20 to 30 minutes. These changes in air temperature were causing the changes in pore pressure readings. When the transducers were insulated with polystyrene foam as shown in Fig.B.13, and the flow of air about the room was controlled, the fluctuations in pressure disappeared.

The readout from the transducers was made with a Budd P350 static strain indicator capable of measuring a strain of 10^{-6}, so that pressure changes of 0.1 psi could be measured. When

the initial problems had been ironed out the transducers performed very well during the whole of the eighteen months in which they were used.

B.5. THE CATHETOMETER

The final item of equipment that needs mentioning is the cathetometer used to measure the axial deformation of each sample. This was loaned by the Physics Department of the University and had a range of $\frac{1}{2}$ a metre and could resolve distances down to 0.001 cm. with a 10X microscope. The cylindrical triaxial cell produced a considerable spherical aberration, so only a very restricted field of view could be used.

To achieve this restricted field of view the aperture of the objective lens had to be stepped down to 0.05 in. and a microscope illuminator was set up to provide a sufficiently bright image of the stationery pins which were used as targets.

APPENDIX C

DETAILS OF EXPERIMENTAL PROCEDURE

C.1. INTRODUCTION

In this appendix the basic procedure used throughout the experimental investigation is outlined. The appendix is divided into three parts dealing with the preparation of samples, the measurements of the stress-deformation behaviour and the final examination of the tested specimen. All items under these headings are described briefly giving an overall impression of the routine procedure. Several matters requiring further discussion are dealt with in Appendix D.

C.2. PREPARATION OF SAMPLES

(a) Preparation of moist soil

As all the samples for testing were not prepared at one time, several mixes of moist soil were required. The initial attempts to prepare a batch of moist soil at the desired moisture content of 26% in one mixing were not successful. To improve on this a method was used in which two mixes were prepared and subsequently blended. Two batches of soil were mixed, one about 2% dry, and the other about 2% wet of the desired moisture content. This was done by weighing out a given amount of dry soil and calculating the amount of water required (making some allowance for hydroscopic moisture). The dry soil was then placed in the

bowl of a Hobart dough mixer and the distilled water added slowly with the mixer operating at a slow speed. After all the water had been added the mixer was switched to the highest speed to ensure that any lumps were broken down. The overall mixing time was about 10 minutes. The mixed soil was then placed in a polythene bag, and after several moisture content samples had been taken it was stored in a fog room along with the bag of the second mix.

After 24 hours in the fog room the two mixes were blended in suitable proportions, using the Hobart mixer, to give the desired moisture content of 26%. The proportions mixed were calculated from the following formula:

$$R = \frac{(M_2 - M_D)}{(M_D - M_1)} \left\{ \frac{1 + M_1}{1 + M_2} \right\}$$

where M_D is the desired moisture content

M_1 is the moisture content of the mix dry of M_D

M_2 is the moisture content of the mix wet of M_D

and R is the ratio of the weight of mix M_1 to the weight of mix M_2 required.

The required quantities were mixed for several minutes and again stored in a plastic bag in the fog room until needed. Using this procedure no difficulty was encountered in preparing mixes to within +0.1, -0.2% of the desired value.

(b) Compaction of samples for testing

All the samples for testing parallel to the direction of

compactive effort were compacted into a 3" x 1½"D mould. The samples were compacted in 9 layers, each with 20 grams of moist soil. The compactive effort consisted of 22 tamps per layer, each of 30 lb, applied with a hand compactor similar to the Harvard miniature compactor[86]. After compaction the sample was trimmed flush with the ends of the mould and the sample plus mould was weighed on a Mettler balance that had been tared to read zero for the empty mould.

Next the sample was removed from the mould by extruding it with a piece of 1½"D bar. Casagrande and Hirschfeld[13] report that this does not alter the density of samples compacted wet of O.M.C. As an additional precaution the inner surface of the mould was coated with P.T.F.E. lubricant from an aerosol spray to reduce any tendency of the soil to adhere to the metal surface.

Upon removal from the mould, pieces were taken from each end of the sample for determination of the as-compacted moisture content. The test sample, about 1½" high, was trimmed from the remaining portion, and some care was taken to ensure that the ends of the trimmed sample were square and parallel. The final height and diameter of the sample were measured with a dial gauge comparator.

The samples for testing perpendicular to the direction of compactive effort were compacted into a 2¼" cubical mould rather than the 3" x 1½"D mould. As before 9 layers were

used, but with 43 grms. of moist soil per layer and 47 rather than 22 tamps of the compactor were applied so that the number of tamps/unit volume remained the same as in the samples tested parallel to the direction of compaction. Since this compaction procedure produced the same density as the other it is reasonable to assume that the compacted soil in both cases has similar properties. The final sample was trimmed from this $2\frac{1}{4}$" cube of soil by carefully cutting the soil away as a $1\frac{1}{2}$"D sampling tube was pushed gently into the cube. The inside of the mould and sampling tube were coated with P.T.F.E. spray.

(c) Mounting of the prepared samples

Fig.C.1 shows the way in which the samples were mounted for testing. Except for a few preliminary tests the height to diameter ratio of all the samples was 1, and free or "friction-less ends" were always used. The pore water pressure was measured from a probe at the base of the sample. This probe was also in contact with the side drains consisting of six strips of filter paper (Whatman No.1) $\frac{3}{8}$" wide over the full height of the sample. The actual mounting procedure was as follows:

(i) The locating holes at the centre of each end were drilled using a special guide.

(ii) The filter paper side drain was moistened and placed over a dummy bottom platen. The perspex disc with the bottom frictionless end was placed over this.

(iii) The sample was placed on the dummy bottom platen and the drainage strips placed in position along the sides of the sample. To ensure that the filter paper was not clogged with any excess silicone grease a small rubber strip was inserted between each drainage strip and the sample at the bottom end.

(iv) The rubber membrane was placed over the sample in the usual manner.

(v) The top of the membrane was peeled back and the whole assembly inverted and placed on the top platen. This had previously been prepared by assembling the frictionless end and smearing the sides with I.C.I. M490 silicone grease.

(vi) The sample was removed from the dummy bottom platen and placed onto the pedestal of the triaxial cell. The rubber membrane was folded down over the sides of the pedestal which had previously been coated with silicone grease.

(vii) Four O-rings were placed over each platen to seal the rubber membrane.

(viii) A stationery pin, used as a target for measuring the axial deformation, was pushed through the membrane into the sample about $\frac{1}{4}$" from each end. The places where the two pins pierced the membrane were sealed with Budd GW-1 strain gauge waterproofing compound.

This completed the mounting of the sample and when the waterproofing was dry (about 1 hour) the cell was assembled.

(d) Back pressure saturation and consolidation

After the assembly of the triaxial cell, the sample was saturated by the application of back pressure. Usually this was done over a period of 24 hours. The cell pressure and back pressure were equalised, and were increased simultaneously in 10 psi increments at the rate of one increment every 30 minutes to 1 hour. When the pressure had reached about 120 psi the whole system was left to stand for some hours to ensure that all the air was dissolved before the consolidation phase was begun.

The consolidation pressure was applied by adjusting the cell pressure by the required amount relative to the back pressure. In all cases the actual consolidation pressure was measured with the pore pressure transducer. To ensure good bedding of the specimen on the end platens, the samples for stress controlled tests were consolidated, while under an axial load of 1 lb. The consolidation period used was generally 24 hours after which the valve leading to the back pressure system was closed.

(e) Test for saturation

Between the closure of the drainage valve and the commencement of loading some of the samples were tested for saturation. This simply involved altering the cell pressure and noting any change of the pore pressure in the sample.

For those samples tested, it was found that the value of the pore pressure parameter B was always greater than 0.97,

and was usually >0.99 after a response time of 1 minute. In calculating B from observations of the change in pore water pressure, a small correction had to be applied to allow for the effect on the strain gauges of the change in oil pressure in the pressure transducer.

C.3. MEASUREMENT OF THE STRESS-DEFORMATION PROPERTIES

Three measurements had to be recorded at each stage of a test. These were: axial load, axial deformation, and pore water pressure (or volume change in the case of a drained test).

(a) Measurement of axial load

In the case of the strain controlled tests this simply required taking a reading of the strain bridge connected to the load beam. No allowance had to be made for ram friction because of the rotating bushing, and no correction was made for the strength of the filter paper side drain or for the load taken by the rubber membrane.

For the stress controlled tests the axial load was determined by counting up the weights on the hanger. The load required to counterbalance the cell pressure was subtracted from the total on the hanger, this had been determined previously for a range of cell pressures by finding the weight that would just cause the piston to fall through the middle $\frac{1}{2}$" of its travel. As with the strain controlled tests no correction was

made for the strength of the filter paper side drains or the rubber membrane.

(b) Measurement of axial deformation

Two measurements were taken to determine the change in length of the sample. Firstly the conventional procedure was used in which readings are taken from a dial gauge mounted between the top of the cell and the top of the piston. Although very straightforward, this method has the disadvantage that all the various bedding errors are included. To eliminate these bedding errors a second method was measured. This was done by measuring the distance between the heads of the two pins with a cathetometer.

(c) Measurement of pore water pressure and volume change

As explained in appendix B the pore water pressure was measured using a specially built differential pressure transducer.

Before taking a pore pressure reading it was necessary to ensure that the pressure was equalised throughout the sample. For the stress controlled tests this was determined quite simply by waiting till the pore pressure reading had reached a steady value. The time for equalisation was generally less than 10 minutes from the application of the stress increment. Partly as an added precaution to ensure equalisation, and partly for convenience, a time interval of 15 minutes was used between the application of successive stress increments.

For the constant strain rate tests a suitable strain rate could be determined from the results of the stress controlled tests. Such a strain rate, calculated to ensure equalisation at all stages of the test, results in a test of excessively long duration. This is because, at the initial stages of loading, the rate at which the pore pressure increases with strain is rather large. This difficulty was overcome by starting the test at a strain rate slow enough to ensure equalisation for the early part of the test. At some later stage when the pore pressure response was not so rapid the strain rate was changed and the test was completed at a greater rate of strain.

The rate of loading to ensure complete drainage for the drained tests was determined while the drained tests were being performed. As drainage was from the top end of the sample only, the pore water pressure at the bottom end could be measured. The rate of strain was adjusted so that the pore pressure reading was always within 0.2 psi of zero.

C.4. FINAL EXAMINATION OF SAMPLE

Once the measurement of the stress deformation behaviour of the sample, both for loading and unloading, had been completed, a visual assessment was made of the uniformity of deformation, presence of slip planes etc. After this the cell was emptied and the sample stripped down for determination of the final moisture content. The time lapse between the

completion of unloading and the weighing of the sample for the final moisture content determination was generally about one hour.

The stripped sample was removed intact from the cell and the final height and diameter were measured using the dial gauge comparator. The sample was then cut into three pieces, each of which was trimmed and weighed for a determination of the final moisture content of the sample.

① O-Ring

② Filter paper side drain

③ Target for measuring deformation

④ Sample

⑤ Rubber membrane

⑥ Porous probe

⑦ Rubber disk of free end

⑧ Silicone grease

⑨ Sealing compound around target

⑩ Rubber barrier between side drain and grease

⑪ Perspex disk of bottom free end

⑫ Bottom platen

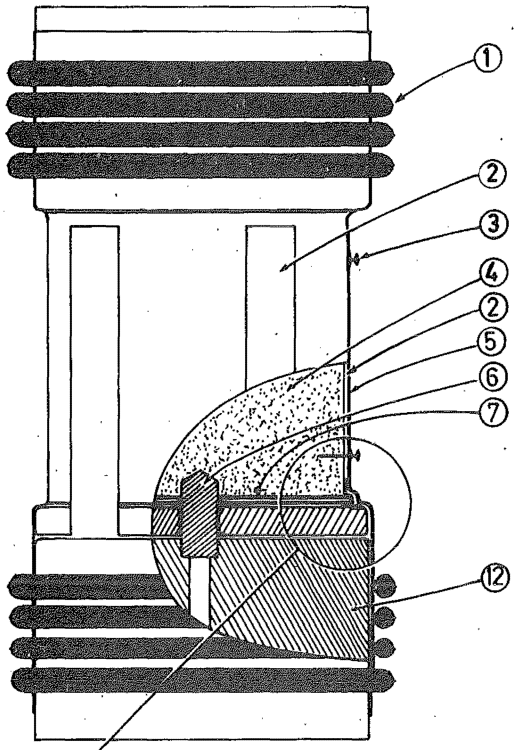

(a)

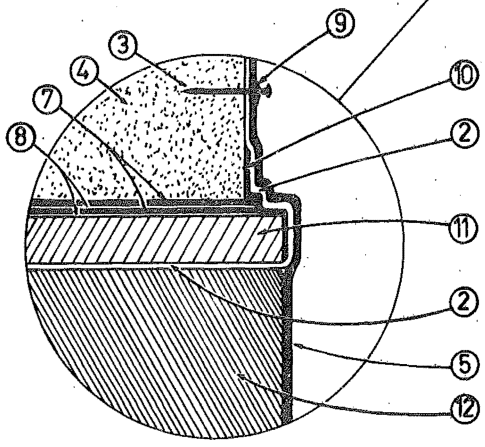

(b)

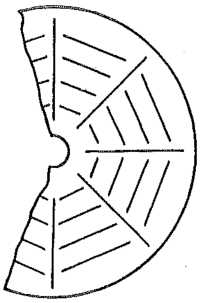

(c) Arrangement of cuts in the rubber disk of the free end

FIG. C1 ARRANGEMENT OF MOUNTED SAMPLE

APPENDIX D

PRECAUTIONS NECESSARY TO ENSURE RELIABILITY OF EXPERIMENTAL RESULTS

D.1. INTRODUCTION

The use of the apparatus described in Appendix B and the procedure outlined in Appendix C does not necessarily ensure that the observed behaviour of the soil during testing is representative of the actual behaviour of the soil in situ. There are many difficulties, due both to the concept of the triaxial test and to the peculiarities of soil as a material, that must be attended to before one can draw useful conclusions from triaxial tests. Most of these problems are well explained in the soil mechanics literature, but because they have such a bearing on the interpretation of experimental results, the manner in which these difficulties were handled is described in this appendix.

The items discussed are: leakage, uniformity of deformation and of stress distribution, accuracy of deformation measurement, equalisation of pore pressure, degree of pore pressure response, degree of saturation, and the effect of temperature variations.

D.2. LEAKAGE

In all types of triaxial tests some assumption is made

about the overall volume of the sample. Leakage of cell fluid into the sample through the membrane or past some mechanical connection, or conversely leakage of pore fluid from the sample violates the original assumption and leads to errors of unknown magnitude. The problem of leakage has been discussed very fully by Poulos[61] and the procedures recommended by him have largely been followed here.

The majority of the tests reported in this thesis are of the undrained type. Because of the comparatively long duration of the tests, at least two days and in some cases several weeks, and the small value for the slope of the rebound line, any leakage is very critical. In the following paragraphs a simplified analysis is presented of the effect of leakage in an undrained test. Poulos pointed out that leakage of a given amount is more significant in an undrained test than in a drained test.

Consider a sample normally consolidated to point A in Fig. D.1.

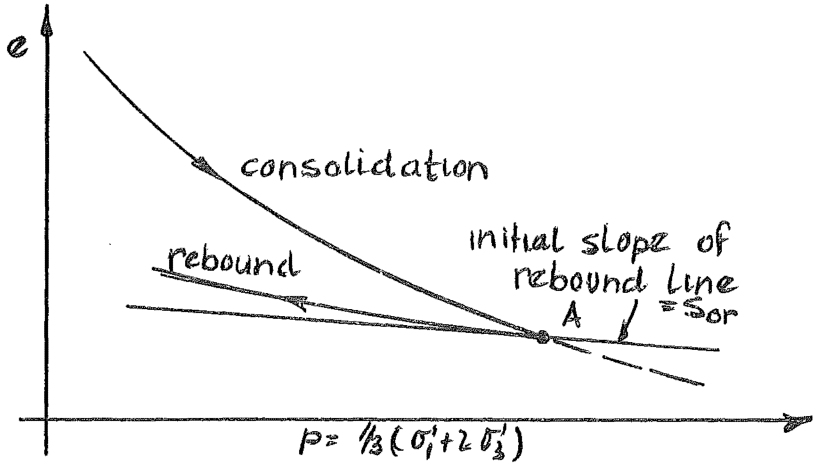

FIG. D.1. INITIAL SLOPE OF REBOUND LINE FOR LEAKAGE ESTIMATE

If some leakage of cell fluid occurs into the sample at A the effective stress is reduced and the void ratio is increased. The argument here is concerned with the magnitude of this decrease in effective stress in comparison with the volume of leakage.

At A:-

$$\frac{\Delta e \text{ (rebound)}}{\Delta p} = S_{or} \qquad \ldots\ldots\ldots\ldots\ldots\ldots\ldots\ldots \text{(i)}$$

Where S_{or} is the slope of the rebound line at the point where it moves away from the normal consolidation line. From the definition of void ratio, and some simple manipulation:-

$$\Delta e = \frac{\Delta V(1 + e)}{V} \qquad \ldots\ldots\ldots\ldots\ldots\ldots\ldots\ldots \text{(ii)}$$

where e is the void ratio of the sample, V the volume of leakage and V is the total volume of the sample.

Examination of the rebound curves in a consolidation test shows that the initial slope of the rebound line is very small. Also the presence of shearing stress during a strength test could have some effect on the appropriate value of S_{or}. However, in this discussion estimates of the influence of leakage will be based on the assumption that S_{or} is equal to the initial slope of the rebound line in a consolidation test. This should at least give a fairly good idea of the significance of leakage, even if the value of S_{or} appropriate to a particular stage of a test is not as simply related to C'_c. This assumption means that S_{or} is given by:-

$$S_{or} = \frac{C'_c}{2.30p} \qquad \text{..... (iii)}$$

Where C'_c is the slope of the initial part of the swelling line on the (e, $\log_{10}$p) diagram. Combining equation (i), (ii) and (iii) gives:-

$$\frac{\Delta V}{V} = \frac{C'_c}{2.30(1+e)} \frac{\Delta p}{p} \qquad \text{..... (iv)}$$

From the consolidation curve in Appendix A the value of C'_c for the initial stages of unloading is 0.00746. As an example, the change in volume needed to give a 1% decrease in effective stress for a sample of this compacted soil at a void ratio of 0.65 is:-

$$\frac{\Delta V}{V} = \frac{0.00746 \times 0.01}{2.30 \times 1.65} = 1.97 \times 10^{-5}$$

i.e. an increase in sample volume due to a cell fluid leakage of 0.002% leads to a 1% decrease in effective stress. The calculation underlines the critical effect that leakage has on the results of undrained triaxial tests. For a $1\frac{1}{2}$" x $1\frac{1}{2}$" Dia. sample, this corresponds to an increase in sample volume of $0.86(mm)^3$. It must be emphasised that this estimate is only approximate because of the difficulty in determining the value of S_{or} appropriate to a particular stage of a test. However it does indicate that even a small amount of leakage can be critical.

Three sources of leakage may contribute to an increase

in sample volume (generally the leakage is into the sample because the cell pressure is used for consolidation). The most significant type of leakage is the transfer of cell fluid through the rubber membrane into the sample; next most important is leakage past the bindings sealing the rubber membrane to the pedestals; and finally leakage may occur from any of the fittings and joints in the pore pressure measuring system.

In the following estimates of leakage, the values used for the permeability of rubber and for the rate of leakage past the bindings are those measured by Poulos[61], although the values in the present apparatus will not be the same it is expected that the order of magnitude of the various factors will be the same.

(a) Membrane leakage

With a pressure difference of 25 psi, a membrane thickness of 0.010" and a coefficient of permeability for the rubber of 6.8×10^{-16} cm/sec, the rate at which water enters the sample by permeation through the membrane is $0.19(\text{mm})^3$/day.

Note that this is only leakage due to permeation of water through the membrane. Tests performed by Poulos suggest that because of the differences in ionic concentration between cell water and sample water, osmosis will provide an additional leakage of water into the sample.

(b) Leakage past bindings

Poulos found that the rate of leakage into the sample

between the rubber membrane and the top and bottom pedestals can be considerable. However this can be greatly reduced by using highly polished stainless steel platens smeared with silicone grease, and several O-rings. The only precautions necessary is to ensure that the feathered edge of the O-ring is not twisted. In this way the total leakage of water into a sample past the bindings could be of the order of $0.20(mm)^3$/day for a pressure difference of 25 psi.

(c) Leakage from valves and fittings

Poulos tested an extensive range of valves and fittings commonly used in soil mechanics equipment. The results suggested that the rate of leakage through most commercially available valves and fittings can be alarming. Because of this all joints in the system for measuring pore pressures were sealed with araldite, and only one mechanical connection was allowed. This was the valve connecting the back pressure and drainage line to the sample, and for this a special "leak proof" valve was made. Essentially a needle valve in which a stainless steel stem could be screwed down tightly onto a brass seating, this had a measured rate of water leakage of $0.005(mm)^3$/day under a pressure difference of 80 psi. A cross-section of the valve is shown in Fig.B.10.

Thus the leakage rate, with water as a cell fluid and a consolidation pressure of 25 psi is about $0.4(mm)^3$/day. Considering that this does not include any contribution from

osmosis, and takes no account of the uncertain value of S_{or} and the fact that in many of the tests the consolidation pressure was greater than 25 psi, this rate of leakage is quite unacceptable because it suggests that p will decrease by at least 1% every few days. Castor oil was used as a cell fluid to reduce this leakage to an acceptable level. The oil is about 1000 times more viscous than water and since it is immiscible with water no osmosis can occur. With castor oil as a cell fluid tests of considerable duration were performed without the influence of leakage becoming significant.

D.3. UNIFORMITY OF DEFORMATION

It is well known that the frictional restraint imposed at the ends of a soil sample by the platens can influence its measured strength. However it has been shown that when the ratio of sample height to sample diameter is in excess of two the frictional restraint has a negligible effect. Even though strength may be unaffected, the frictional restraint has a considerable influence on the deformed shape of the sample. In any investigation concerned with stress-deformation properties rather than strength this non-uniformity is most undesirable as it makes the measurement of strains truly corresponding to the applied stress most difficult if not impossible.

Fortunately a means of producing a uniform deformed

shape has been developed by Rowe and Barden[69]. This consists of using a cylindrical sample with a height to diameter ratio of one, and using specially prepared "frictionless ends" for the sample. It has been shown that this gives strength parameters essentially the same as those from 2:1 samples. The advantage of free ends is that the deformed shape of the sample remains uniform, so that the assumption that the deformed sample is a cylinder is very nearly true. Visual examination shows that up to strains of 9 or 10% the shape of the sample is uniform. The uniformity of internal deformation has been investigated by Kirkpatrick and Belshaw[35] using X-rays to determine the displacement of lead shot buried within the sample. This work indicates that the use of free ends with a 1:1 sample does indeed achieve a uniform state of deformation throughout the sample.

D.4. MEASUREMENT OF AXIAL DEFORMATION

The conventional means of measuring the deformation of a soil sample is to use a dial gauge mounted so that the relative movement between the loading ram and the cell base is determined. This is quite adequate for much routine work particularly when large samples are tested. However many factors may contribute errors to these measurements which are neither systematic nor self compensating. Examples are the bedding errors between various surfaces such as the loading

ram and top platen, platen and sample (both ends), deflection of the cell base under load, and distortion of the cell when the cell pressure is changed. In addition to these errors the use of frictionless ends introduces a further uncertainty because of the stretching of the rubber and extrusion of silicone grease. Barden and Khayatt[4] suggest that these bedding errors can be calibrated by replacing the sample with a steel block. This was tried but with little success perhaps because with a sample $1\frac{1}{2}$" high small errors have a greater significance.

All these errors could be entirely eliminated if the actual deformation between points on the sample itself were measured. This was accomplished by using a cathetometer to measure the distance between the heads of two $\frac{1}{2}$" stationery pins pushed into the sample about $\frac{1}{4}$" from each end. In this way it was possible to determine the distance between the pins to within 0.0005" to 0.001". For all tests the strains determined from the cathetometer and pins were smaller than those determined with the dial gauge at the same level of stress. Furthermore the difference between the two strains at a given stress was not consistent from test to test. This is, no doubt, related to the difficulty encountered in attempting to calibrate for the bedding errors.

When the sample is unloaded, the effect of these bedding errors is even more significant. The values of the unloading modulus used in Chapter 4 differ by a factor of two when

calculated from strains determined by the two methods.

D.5. DEGREE OF PORE PRESSURE RESPONSE

The classical method of measuring pore water pressure using a null balance system has two main disadvantages. These are the constant attention required and the possibility of leakage occurring past any one of the valves and fittings required in the system. For the testing reported in this thesis a strain gauged diaphragm was used as explained in Appendix B. The basic idea underlying this is that the volumetric requirement of the diaphragm is so small that the assumption of null balance is justified. Considering the relative volumetric stiffnesses of the diaphragm and the sample, Whitman, Healy and Richardson[85] have derived the following formula for calculating the degree of pore pressure response:-

$$RP = \frac{1}{1 + B_v}$$

Where RP is the ratio of the measured pressure to the pressure that would be recorded with a true null balance system.

B_v is the ratio of the volumetric flexibility of the measuring system to that of the sample:

$$B_v = C_1/m_v V$$

Where C_1 = flexibility of the measuring system ($in^5/_{16}$)

m_v = coefficient of compressibility of the soil ($in^2/_{16}$)

V = the volume of the soil sample (in^3)

Insertion of the appropriate values shows that for the combination of soil and transducer used here the measured pressure will be better than 99.9% of the pressure that would be recorded with a perfect null balance system, the properties of the particular transducer used can be found in Appendix E.

D.5. TIME REQUIRED FOR PORE PRESSURE EQUALISATION

Related to the above discussion about the degree of pore pressure response is the time required for the pore pressures to distribute themselves throughout the sample and give a correct reading at the sensory element. This can be quite a serious problem when samples are tested with conventional end platens and a height to diameter ratio of 2. The dead zones at the ends of the sample are not subjected to the same stresses as the centre part and for a soil of low permeability the time required for equalisation of the pore pressure throughout the sample imposes severe restrictions on the rate at which a test may proceed.

In describing the use of free ends in section D.3 it was emphasised that these gave a sample with a uniform deformed shape. Just as important however is the fact that uniform deformed shape gives a more uniform distribution of pore water pressure throughout the sample. This means that the time required for pore pressure equalisation is drastically reduced,

so the rate of loading may be increased.

An additional measure used to promote rapid equalisation was the side drainage system shown in Fig. C.1: the drains made contact with the porous stone by passing beneath the perspex disc forming the lower free end. The time for pore pressure equalisation was measured in the stress controlled tests as explained in Appendix C.

D.6. DEGREE OF SATURATION

When compacted, the soil samples are not fully saturated. Unfortunately this represents a very considerable complication as the effective stresses acting in a partially saturated soil are most difficult to evaluate. To remove this problem altogether it was decided to saturate the samples before testing. In many applications of compacted soils the material eventually becomes saturated by percolation and perhaps by additional consolidation after placement. Thus saturating the compacted samples can be justified on practical grounds as well as experimental ones.

Back pressuring was used to saturate the samples because other means have been shown to be inadequate, Lowe and Johnstone[46]. Since the range of consolidation pressures used was not particularly large, it was always possible to use back pressures in excess of 100 psi. The following formula has been suggested by Lowe and Johnstone[46] for calculating the back

pressure required for saturation:-

$$U_{as} = U_{ao} \frac{(1-H)}{H} (1-S_o)$$

Where U_{as} is the required back pressure

U_{ao} is the initial pressure of the air in the pores

S_o the initial degree of saturation

H Henry's coefficient of solubitily for air in water (approx. 0.02 at 20°C)

The back pressure used was always greater than that required by the formula so that any additional air trapped between the sample and the membrane can also be dissolved.

As explained in Appendix C several samples were tested for saturation by increasing the cell pressure by a 10 or 20 psi increment and noting the pore pressure response. All these tests indicated that the samples were saturated.

D.7. INFLUENCE OF TEMPERATURE VARIATIONS

Examination of any of the various theoretical treatments of the electrical double layer that surrounds a clay particle immersed in an aqueous environment suggests that fluctuations in temperature will have an effect on the behaviour of soils containing some proportion of clay particles. This has been demonstrated by Mitchell and Campanella[50] and also by Henkel and Sowa[28] who showed that several cycles around a fixed temperature variation path leads to a gradual increase in pore

water pressure. This suggests that long term tests on clay soils must be conducted at constant temperature. For this reason all the experimental work was carried out in a constant temperature room. The average temperature of the room was 20°C subject to fluctuations of $\frac{1}{2}$°C about the mean, with a period of 20-30 minutes.

The most significant temperature effect encountered in the investigation was traced to the affect of temperature fluctuations on the pore pressure transducer. Since this was a closed system with the sample any temperature change registered as a change in pore pressure. The temperature variation mentioned in the above paragraph caused fluctuations in pore pressure of about 1 psi, but this was overcome by lagging the pressure transducer as explained in Section B.4.

APPENDIX E

DESIGN AND CONSTRUCTION OF THE PORE PRESSURE TRANSDUCER

E.1. INTRODUCTION

The pore water pressure transducer has already been described briefly in Appendix B. Fig. B.1 shows how the transducer is incorporated into the hydraulic circuit and Fig. B.10 gives a cross-section of the transducer. In Appendix B, Section B.4. some of the general features of the operation and construction of the transducer are explained. However, a successful transducer must fulfil other criteria not treated in Appendix B, and these are discussed here. Also the procedure for cementing the strain gauges to the diaphragm is set out.

E.2. DESCRIPTION OF THE TRANSDUCER

After some preliminary calculations a stainless steel diaphragm 0.033" thick and 1"D was decided upon. Four Budd C9-121A foil strain gauges were cemented to the diaphragm as shown in Fig.E.1 and wired as a four arm strain bridge. The two gauges near the centre of the diaphragm register tensile strain and those at the edges compressive strain.

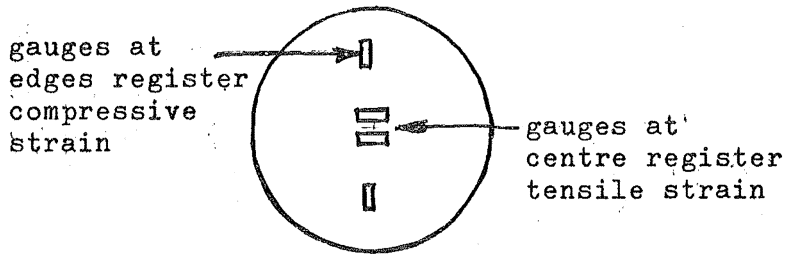

FIG.E.1. ARRANGEMENT OF STRAIN GAUGES

Under the following headings the various criteria that the transducer must meet are described briefly, and the performance of the transducer under each of the categories is enumerated.

(i) Stability

Obviously it is important that the transducer gives a steady reading when subjected to a constant pressure for some time. As explained in Appendix B this criterion of performance was not particularly easy to fulfil. The problem was that the cement fixing the strain gauge to the diaphragm tended to creep, indicating an apparent change of pressure. This was eventually overcome by using the process explained in Section 3 of this appendix.

In all cases the drift of the transducer as finally developed was less than 0.1 psi over a period of three weeks when under a pressure difference of 20 psi.

(ii) Compliance

There are two reasons why the volumetric requirement of the transducer should be small. Firstly, if the diaphragm is relatively flexible the measured pressure will be somewhat lower than the theoretical pressure, and secondly the time required for sufficient water to deflect the diaphragm to drain from the sample will make the duration of the test exceedingly long.

The volumetric compliance of the diaphragm alone is 2.6×10^{-6} in^3/psi. When the 0.33 in^3 of water behind the diaphragm and in the connecting pipe is included the total compliance of the transducer becomes 3.7×10^{-6} in^3/psi. For the soil tested this means that in all tests the measured pore water pressures were better than 99.9% of the theoretical response and for the load increments used the time for pore pressure equalisation throughout the sample was less than 10 minutes.

(iii) Leakage

As explained in Appendix D the consequences of even a small amount of leakage are critical. For this reason all joints between the components of the transducers were sealed with Araldite. The only mechanical connection was the valve in the drainage system, with which special care was taken to ensure leak proof qualities.

(iv) Sensitivity

The sensitivity of the completed transducers ranged between 10 and 15 microstrain/psi. The actual strain readings were taken with a Budd Model P 350 strain indicator, which was found to be capable of resolving strain differences down to 1 microstrain quite accurately, so it was possible to measure pressure changes as small as 0.1 psi.

(v) Linearity

The calibration curves for all four transducers were linear to within 1% of the calibrated range. That is, effects due to non-linearity and hysteresis were always less than 1% of the working range of the transducer.

(vi) Safety against overpressure

The differential pressure across the diaphragm was always less than 100 psi in the tests. However if at any stage there had been an accidental loss of cell or back pressure the diaphragm might have been subjected to pressures considerably in excess of 100 psi. This eventuality would not have damaged the transducer as the gauges and the diaphragm were capable of withstanding pressures in excess of 200 psi without damage.

The four transducers were in constant use for a period of eighteen months during which they performed in a most satisfactory manner.

E.3. PROCEDURE FOR CEMENTING THE STRAIN GAUGES TO THE DIAPHRAGM

The method is outlined step by step in the following paragraphs.

(i) Cleaning

The diaphragm was roughened with fine emery paper and given a thorough degreasing with cleaning fluid (1 part of xylol to 2 parts of methyl ethyl ketone).

(ii) Roughening the backing of the gauge

The epoxy backing of the gauges as supplied was very smooth. Before use this was roughened to improve the bond between the Araldite and the gauge.

The gauge was mounted grid downwards on a piece of Sellotape and the back was rubbed gently with very fine emery powder. When this was completed the gauge backing had lost its shiny appearance.

(iii) Cleaning the gauge.

After stage (iii) the Sellotape was trimmed so that the grid side of the gauge was still covered, but no tape projected over the edges.

The gauge was then swirled about in a beaker of cleaning fluid and left to dry in air.

(iv) Mounting the gauges on the diaphragm

The gauges were mounted on the required part of the diaphragm with a further piece of Sellotape trimmed so that three edges of the gauge were free. This allowed any excess

Araldite to flow from under the gauge.

(v) Mixing of Araldite

Araldite AY103 and hardener HY951 were used in the ratio 100:8½ by weight. A quantity 20-40 gr. was prepared, and after vigorous stirring the mixture was put in an oven for a few minutes to remove the air bubbles.

(vi) Application of Araldite

A generous amount of warm, air free Araldite was applied under each gauge. The gauges were then covered with a thick piece of polythene and this was topped with a piece of Perspex. Over this a flat piece of steel was placed which was loaded with weights in excess of 20 lb. The purpose of the weight was to squeeze out the excess Araldite from under the gauge.

(vii) Curing

The whole assembly was placed in an oven at 212°F and about eight hours later the weights were removed. The temperature of the oven was then raised gradually to 300°F and held there for four hours. After this the oven was cooled to 180°F and held there for five days. During this final stage of the curing operation the Sellotape could be removed and any excess Araldite cut away from around the gauge.

(viii) Cycling

Before the transducer was calibrated it was cycled 10-20 times through a pressure range well beyond the expected

working range. This worked out any change in the zero of the transducer caused by cold working of the strain gauges.

APPENDIX F

LISTING OF REDUCED EXPERIMENTAL RESULTS FOR UNDRAINED TESTS

This appendix contains a listing of all the reduced experimental results for all of the undrained tests. Also included is a listing of the computer programme used in analysing these results.

Initially a fairly complete description of each test and the sample is given. For the CSR tests (Constant Strain Rate) the various strain rates used are given in brackets with the title. Also after the title, on the same line, the type of loading (parallel or perpendicular to the direction in which the compactive effort was applied to the material) is given.

The particulars of the test are followed by the listing of reduced results in seven columns. The headings of the columns are:-

"Time Elapsed", gives the total time in minutes since the first axial load was applied to the sample.

"Axial Def", gives the axial strain calculated according to Eq.(3.22).

'Q', gives the stress component q calculated from Eq.(3.20).

'P', gives the stress component p calculated from Eq.(3.19).

'N', gives the stress ratio $\eta' = q/(p+3.0)$.

'SIGMA1', gives the values of the major principal stress σ'_1.

'SIGMA3', gives the minor principal stress σ'_3.

```
C*************************************************************************
C
C    TO CALCULATE EFFECTIVE STRESSES AND STRAIN FROM THE RESULTS OF AN UNDRAINED
C    TRIAXIAL TEST
C
C*************************************************************************
0001        DIMENSION TITLE(20),NOTES(20),SM(3),TS(3),SP(3),TC(3)
0002        INTEGER TITLE,SM,SP,TS,TC
0003        INTEGER TITLE,TD,TH,TM,TP
0004        REAL MC1,MC2,MC(6),MD,MCA
C
C    FROM DATA READ INFORMATION ABOUT THE TEST IS CALCULATED AND PRINTED
C
0005      175 READ(1,100) OL,OD,OP,W0,N
0006        AO = 3.1412*OD*OD/4.0
0007        IF(OD.EQ.0.) GO TO 56
0008        READ(1,101) (TITLE(I),I=1,20)
0009        WRITE(6,104) (TITLE(I),I=1,20)
0010        READ(1,107)(SM(I),I=1,3),(SP(I),I=1,3),(TS(I),I=1,3),(TC(I),I=1,3)
0011        WRITE(6,108)(SM(I),I=1,3),(SP(I),I=1,3)
0012        WRITE(6,601) (TS(I),I=1,3),(TC(I),I=1,3)
0013        WRITE(6,105) OL,AO
0014        WRITE(6,602) OP
0015        IF(N.EQ.0) GO TO 131
0016        DO 6 J=1,N
0017        READ(1,99) (NOTES(I),I=1,20)
0018        WRITE(6,98) J,(NOTES(I),I=1,20)
0019        IF(J.NE.1) GO TO 6
0020        WRITE(6,97)
0021      6 CONTINUE
0022      131 READ(1,109) W1,W2,W3,W4,W5,W6
0023        MC1 = (W2-W3)/(W3-W1)
0024        MC2 = (W5-W6)/(W6-W4)
0025        WRITE(6,110) MC1,MC2
0026        MD = 3.802*W0/5.317
0027        OD=MD/(1.+.5*(MC1+MC2))
0028        WRITE(6,111) OD
0029        VR = 158.50/OD-1.
0030        SR=100.0*(MD*(1.+VR)/(62.4*VR))-254.0/VR
0031        WRITE(6,112) SR
0032        WRITE(6,113) VR
0033        READ(1,109) W7,W8,W9,W10,W11,W12,W13,W14,W15
0034        MC(3)=(W8-W9)/(W9-W7)
0035        MC(4)=(W11-W12)/(W12-W10)
0036        MC(5)=(W14-W15)/(W15-W13)
0037        WRITE(6,114) MC(3),MC(4),MC(5)
C
C    TO CALCULATE THE FINAL VOID RATIO THE AVERAGE OF THE TWO SMALLEST FINAL
C    MOISTURE CONTENTS IS USED
C
0038        B1=0.5*(MC(3)+MC(4))
0039        B2=0.5*(MC(4)+MC(5))
0040        B3=0.5*(MC(5)+MC(3))
0041        MCA=B1
0042        IF(MCA.GT.B2) MCA=B2
0043        IF(MCA.GT.B3) MCA=B3
0044        VRF=2.54*MCA
0045        WRITE(6,115) VRF
C
C    A CORRECTION IS MADE TO THE INITIAL AREA OF THE SAMPLE TO ALLOW FOR THE
C    CHANGE DURING CONSOLIDATION
C
0046        AC=AO*(1.-.333*ALOG((1.+VR)/(1.+VRF)))**2
0047        READ(1,100)F,G
0048        J=1
0049        L=1
0050        IF(N.LT.3) K=24
0051        IF(N.GT.2) K=28
0052        IF(N.GT.6) K=32
0053      27 WRITE(6,200)
0054        WRITE(6,201)
C
C    THE MEASURED VALUES FOR EACH EXPERIMENTAL POINT ARE READ AND THE
C    REQUIRED PARAMETERS CALCULATED AND PRINTED
```

F4

```
0055          26 READ(1,102) TD,TH,TM,TP,Y,P,B,FT,EB
0056             T = TP/60.+TM+60.*TH+1440.*TD
0057             IF(T.NE.0.0) GO TO 615
0058             DO 19 IK=K,55
0059             WRITE(6,117)
0060          19 CONTINUE
0061             GO TO 175
0062         615 IF(J.NE.1) GO TO 3
0063             TO=T
0064             PO=P
0065             BO=B
0066             DT=0.
0067             EL=0.
0068             Q=0.
0069             U=0.
0070             SL1=ET-EB
0071             GO TO 93
0072           3 DT=T-TO
0073             SL2=ET-EB
0074             DLM=1.-SL2/SL1
0075             EL=EL+DLM
0076             SL1=SL2
0077             Q=F*(P-PO)/AC*(1.-EL)
0078             U=G*(BO-B)
0079          93 S3D=OP-U
0080             S1D=S3D+Q
0081             PRES=(S1D+2.*S3D)/3.
0082             R2=Q/PRES
0083             WRITE(6,106)DT,EL,Q,PRES,R2,S1D,S3D
0084             K=K+1
0085             J=J+1
0086             L=L+1
0087             IF(L.NE.5)GO TO 26
0088             WRITE(6,605)
0089             L=1
0090             K4=K/4
0091             IF(K4.NE.9) GO TO 26
0092             K=1
0093             WRITE(6,619)
0094             WRITE(6,201)
0095             GO TO 26
0096          97 FORMAT(1H+,10X,'NOTES')
0097          98 FORMAT(1HO,15X,I2,2X,20A4)
0098          99 FORMAT(20A4)
0099         100 FORMAT(4G10.4,I2,8X,G10.4)
0100         101 FORMAT(20A4)
0101         102 FORMAT(I2,I2,I2,I2,2X,5G10.4)
0102         104 FORMAT(1H1,10X,20A4,//)
0103         105 FORMAT(1HO,10X,'ORIGINAL LENGTH ',F5.3,'IN',7X,'ORIGINAL AREA',
                11X,F5.3,'SQ.IN.')
0104         106 FORMAT(1H , 9X,F8.1,3X,F6.4,3X,F6.2,3X,F6.2,3X,F5.3,3X,F6.2,3X
                1F6.2)
0105         107 FORMAT(4(I2,1X,I2,1X,I2,2X))
0106         108 FORMAT(1HO,10X,'SOIL MIXED',3(I3),5X,'SAMPLE PREPARED',3(I3))
0107         109 FORMAT(9G8.3)
0108         110 FORMAT(1HO,10X,'MOISTURE CONTENT OF COMPACTED SAMPLE',F7.4,4X,
                1F7.4)
0109         111 FORMAT(1HO,10X,'DRY DENSITY OF COMPACTED SAMPLE ',F6.2, 'LB/FT3')
0110         112 FORMAT(1HO,10X,'DEGREE OF SATURATION OF COMPACTED SAMPLE',F6.2,
                1'PER CENT')
0111         113 FORMAT(1HO,10X,'INITIAL VOID RATIO ',1X,F6.4)
0112         114 FORMAT(1HO,10X,'FINAL MOISTURE CONTENT ',F7.4,5X,F7.4,5X,F7.4)
0113         115 FORMAT(1HO,10X,'FINAL VOID RATIO ',F6.4,//)
0114         117 FORMAT('     ')
0115         200 FORMAT(1H ,11X,'TIME'6X,'AXIAL')
0116         201 FORMAT(1H ,10X,'ELAPSED',5X,'DEF',7X,'Q',8X,'P',7X,'N',5X,'SIGMA1'
                1,3X,'SIGMA3',/)
0117         601 FORMAT(1HO,10X,'TEST STARTED',3(I3),3X,'TEST COMPLETED',3(I3))
0118         602 FORMAT(1HO,10X,'CONSOLIDATION PRESSURE',F7.2,'PSI')
0119         605 FORMAT(1H ,'     ')
0120         619 FORMAT(1H1,10X,1X,'TIME',6X,'AXIAL')
0121          56 STOP
0122             END
```

CSR TEST 001 (0.0024IN/MIN) PARALLEL

SOIL MIXED 20 8 68 SAMPLE PREPARED 21 8 68

TEST STARTED 26 8 68 TEST COMPLETED 26 8 68

ORIGINAL LENGTH 1.552IN ORIGINAL AREA 1.752SQ.IN.

CONSOLIDATION PRESSURE 10.00PSI

NOTES 1 1X1 SAMPLE FRICTIONLESS ENDS, SIDE DRAINS

2 SIDE DRAINS CONTINUOUS AT ENDS. CONSIDERABLE RESTRAINT

3 LOAD MEASURED WITH PROVING RING %1LB#0.0006IN<

4 DEFORMATION MEASURED WITH DIAL GAUGE

MOISTURE CONTENT OF COMPACTED SAMPLE 0.2556 0.2556

DRY DENSITY OF COMPACTED SAMPLE 93.81LB/FT3

DEGREE OF SATURATION OF COMPACTED SAMPLE 94.15PER CENT

INITIAL VOID RATIO 0.6896

FINAL MOISTURE CONTENT 0.2724 0.2724 0.2724

FINAL VOID RATIO 0.6919

TIME ELAPSED	AXIAL DEF	Q	P	N	SIGMA1	SIGMA3
0.0	0.0	0.0	10.00	0.0	10.00	10.00
1.9	0.0019	1.42	9.39	0.151	10.34	8.92
2.8	0.0032	1.70	9.13	0.186	10.26	8.56
5.1	0.0065	2.17	8.38	0.259	9.83	7.66
7.4	0.0097	2.63	8.00	0.329	9.75	7.12
9.9	0.0129	3.28	7.58	0.432	9.77	6.49
16.0	0.0195	7.90	8.04	0.982	13.31	5.41
21.4	0.0260	10.44	7.63	1.368	14.59	4.15
27.9	0.0327	13.30	8.85	1.502	17.72	4.42
35.6	0.0426	18.43	11.37	1.620	23.66	5.23
44.0	0.0527	24.25	14.39	1.685	30.56	6.31
54.1	0.0629	31.10	18.21	1.708	38.94	7.84
64.4	0.0732	38.85	22.95	1.693	48.85	10.00
74.6	0.0837	47.01	27.83	1.689	59.17	12.16
85.3	0.0942	55.49	32.82	1.691	69.81	14.32
96.0	0.1049	63.84	37.94	1.683	80.50	16.66
106.2	0.1157	71.28	41.59	1.714	89.11	17.83
116.1	0.1266	77.44	45.80	1.691	97.43	19.99
130.8	0.1435	85.85	51.58	1.665	108.81	22.96
138.9	0.1533	89.85	54.26	1.656	114.16	24.31
147.0	0.1640	93.32	56.05	1.665	118.26	24.94
160.5	0.1871	100.45	61.48	1.634	128.45	28.00
169.1	0.1990	102.86	63.01	1.632	131.58	28.72
183.8	0.2207	105.91	66.99	1.581	137.60	31.69
184.0	0.2231	106.23	67.19	1.581	138.01	31.78
192.9	0.2356	107.50	67.61	1.590	139.28	31.78
203.5	0.2524	109.11	68.87	1.584	141.61	32.50
219.9	0.2783	110.47	71.12	1.553	144.77	34.30
228.0	0.2935	110.76	71.58	1.547	145.42	34.66
233.9	0.3053	110.81	72.14	1.536	146.01	35.20
242.5	0.3192	110.66	73.89	1.498	147.66	37.00
244.0	0.3003	0.33	22.17	0.015	22.39	22.06

CSR TEST 003 (0.0024IN/MIN) PARALLEL

SOIL MIXED 30 8 68 SAMPLE PREPARED 4 9 68

TEST STARTED 9 9 68 TEST COMPLETED 12 9 68

ORIGINAL LENGTH 2.971IN ORIGINAL AREA 1.757SQ.IN.

CONSOLIDATION PRESSURE 10.00PSI

NOTES 1 2X1 SAMPLE FRICTIONLESS ENDS,SIDE DRAINS

2 LOAD MEASURED WITH PROVING RING (1LB = 0.0006 INCHES)

3 DEFORMATION MEASURED WITH DIAL GAUGE

MOISTURE CONTENT OF COMPACTED SAMPLE 0.2639 0.2639

DRY DENSITY OF COMPACTED SAMPLE 94.24LB/FT3

DEGREE OF SATURATION OF COMPACTED SAMPLE 98.32PER CENT

INITIAL VOID RATIO 0.6319

FINAL MOISTURE CONTENT 0.2587 0.2595 0.2557

FINAL VOID RATIO 0.6532

TIME ELAPSED	AXIAL DEF	Q	P	N	SIGMA1	SIGMA3
0.0	0.0	0.0	10.00	0.0	10.00	10.00
0.4	0.0003	0.19	9.97	0.019	10.10	9.91
1.0	0.0007	0.57	9.92	0.058	10.30	9.73
1.5	0.0010	0.86	9.93	0.087	10.50	9.64
2.0	0.0014	0.96	9.78	0.098	10.42	9.46
2.6	0.0017	1.34	9.64	0.139	10.53	9.19
4.0	0.0022	3.44	9.80	0.351	12.09	8.65
5.5	0.0027	5.25	9.77	0.537	13.27	8.02
6.9	0.0034	6.58	9.58	0.687	13.97	7.39
9.9	0.0051	8.67	9.47	0.915	15.25	6.58
12.6	0.0068	10.37	9.59	1.081	16.50	6.13
15.3	0.0085	10.92	9.50	1.149	16.78	5.86
17.8	0.0102	13.17	10.07	1.308	18.85	5.68
20.4	0.0119	14.57	10.54	1.383	20.25	5.68
23.1	0.0136	15.96	11.00	1.451	21.64	5.68
25.8	0.0153	17.35	11.46	1.513	23.03	5.68
28.5	0.0171	18.73	12.10	1.547	24.59	5.86
31.3	0.0188	20.10	12.65	1.589	26.05	5.95
34.0	0.0205	21.38	13.35	1.602	27.60	6.22
36.6	0.0222	22.75	13.98	1.627	29.15	6.40
39.3	0.0240	24.11	14.53	1.660	30.60	6.49
42.2	0.0257	25.47	15.25	1.670	32.23	6.76
46.0	0.0281	27.45	16.27	1.687	34.57	7.12
47.8	0.0292	28.26	16.72	1.690	35.56	7.30
50.5	0.0309	29.69	17.47	1.700	37.26	7.57
53.3	0.0327	31.12	18.21	1.709	38.96	7.84
56.2	0.0344	32.54	19.23	1.692	40.92	8.38
63.9	0.0379	35.56	20.77	1.712	44.48	8.92
68.3	0.0414	39.19	22.61	1.733	48.74	9.55
73.2	0.0450	41.51	24.02	1.728	51.69	10.18
78.7	0.0485	44.37	25.87	1.715	55.45	11.08
84.3	0.0521	47.47	27.53	1.724	59.18	11.71
92.7	0.0574	51.98	30.30	1.716	64.95	12.97
100.9	0.0628	56.26	32.98	1.706	70.49	14.23
108.3	0.0682	60.66	35.71	1.699	76.15	15.49
117.4	0.0737	64.92	38.30	1.695	81.58	16.66
125.5	0.0792	69.12	41.14	1.680	87.22	18.10
133.6	0.0847	73.00	43.60	1.674	92.27	19.27
143.3	0.0902	76.91	46.26	1.663	97.53	20.62
153.3	0.0977	81.73	49.57	1.649	104.06	22.33
160.5	0.1033	85.08	51.86	1.641	108.58	23.50
167.0	0.1071	87.12	53.44	1.630	111.52	24.40
175.2	0.1128	90.21	55.82	1.616	115.96	25.78
182.8	0.1185	92.84	57.87	1.604	119.76	26.92

TIME ELAPSED	AXIAL DEF	Q	P	N	SIGMA1	SIGMA3
190.4	0.1242	95.25	59.75	1.594	123.25	28.00
197.9	0.1300	97.45	61.47	1.585	126.44	28.99
205.4	0.1359	99.53	63.16	1.576	129.51	29.98
212.6	0.1418	101.24	64.63	1.567	132.12	30.88
219.8	0.1477	102.82	66.05	1.557	134.60	31.78
226.9	0.1536	103.72	67.16	1.544	136.31	32.59
234.0	0.1596	105.40	68.53	1.538	138.80	33.40
241.3	0.1657	106.48	69.70	1.528	140.69	34.21
248.6	0.1718	107.53	70.59	1.523	142.28	34.75
256.8	0.1787	108.75	71.45	1.522	143.95	35.20
265.5	0.1861	109.95	72.75	1.511	146.05	36.10
275.6	0.1944	111.29	73.74	1.509	147.93	36.64
285.4	0.2029	112.50	74.95	1.501	149.95	37.45
294.8	0.2113	113.57	75.94	1.496	151.65	38.08
304.1	0.2199	114.50	76.97	1.488	153.30	38.80
313.4	0.2286	115.36	77.79	1.483	154.70	39.34
322.5	0.2374	116.17	78.60	1.478	156.05	39.88
331.7	0.2463	116.84	79.55	1.469	157.44	40.60
341.2	0.2552	117.51	80.49	1.460	158.83	41.32
350.9	0.2643	118.12	81.05	1.457	159.80	41.68
360.6	0.2735	118.66	81.95	1.448	161.06	42.40
371.4	0.2829	119.13	82.65	1.441	162.07	42.94
379.9	0.2923	119.39	83.28	1.434	162.87	43.48
389.5	0.3019	119.71	83.92	1.426	163.73	44.02
398.7	0.3116	119.76	84.39	1.419	164.23	44.47
401.3	0.3133	119.33	84.25	1.416	163.80	44.47
403.4	0.3138	116.09	82.81	1.402	160.20	44.11
407.5	0.3135	108.05	79.68	1.356	151.71	43.66
415.0	0.3130	96.75	75.73	1.278	140.23	43.48
424.0	0.3126	83.59	70.80	1.181	126.53	42.94
572.0	0.3124	83.15	69.22	1.201	124.65	41.50
802.0	0.3124	83.15	69.22	1.201	124.65	41.50
1356.0	0.3124	83.22	69.42	1.199	124.90	41.68
1682.0	0.3124	83.15	69.58	1.195	125.01	41.86
2012.0	0.3124	83.15	69.94	1.189	125.37	42.22
2021.3	0.3123	69.27	65.85	1.052	112.03	42.76

TIME ELAPSED	AXIAL DEF	Q	P	N	SIGMA1	SIGMA3
2028.5	0.3121	65.08	63.73	1.021	107.12	42.04
2037.4	0.3116	46.14	55.80	0.827	86.56	40.42
2042.3	0.3111	39.25	52.24	0.751	78.41	39.16
2045.6	0.3106	34.85	50.06	0.696	73.29	38.44
2049.4	0.3101	29.72	47.27	0.629	67.08	37.36
2052.0	0.3096	26.44	45.36	0.583	62.99	36.55
2054.3	0.3091	23.48	43.48	0.540	59.13	35.65
2056.4	0.3086	20.72	42.02	0.493	55.83	35.11
2058.4	0.3081	18.42	40.71	0.452	52.99	34.57
2060.0	0.3076	16.57	39.37	0.421	50.42	33.85
2061.5	0.3072	14.79	38.24	0.387	48.10	33.31
2063.1	0.3067	13.01	37.11	0.351	45.78	32.77
2064.2	0.3062	12.42	36.46	0.341	44.74	32.32
2066.5	0.3052	9.18	34.39	0.267	40.51	31.33
2068.8	0.3042	7.06	32.96	0.214	37.67	30.61
2070.8	0.3033	5.14	31.42	0.163	34.85	29.71
2072.7	0.3023	3.41	30.13	0.113	32.40	28.99
2074.3	0.3013	2.01	29.03	0.069	30.37	28.36
2083.0	0.3008	2.61	27.97	0.093	29.71	27.10
2131.0	0.3005	2.95	27.90	0.106	29.87	26.92
2162.0	0.3004	3.08	27.95	0.110	30.00	26.92
2166.5	0.3003	8.17	28.38	0.288	33.83	25.66
2169.8	0.3013	12.98	28.64	0.453	37.29	24.31
2173.1	0.3018	17.65	29.29	0.602	41.06	23.41
2178.0	0.3028	24.17	30.75	0.786	46.86	22.69
2185.8	0.3042	32.98	33.41	0.987	55.40	22.42
2190.3	0.3054	39.90	36.17	1.103	62.77	22.87
2196.8	0.3067	48.19	39.83	1.210	71.96	23.77
2204.4	0.3081	58.16	44.33	1.312	83.10	24.94
2213.3	0.3096	69.67	49.96	1.394	96.41	26.74
2221.7	0.3111	80.34	55.32	1.452	108.88	28.54
2229.0	0.3125	89.52	60.18	1.488	119.86	30.34
2234.5	0.3140	96.02	63.97	1.501	127.98	31.96
2238.4	0.3155	100.01	66.74	1.499	133.41	33.40
2241.3	0.3165	102.28	68.75	1.488	136.94	34.66
2243.5	0.3167	103.83	69.99	1.483	139.21	35.38

TIME ELAPSED	AXIAL DEF	Q	P	N	SIGMA1	SIGMA3
2245.6	0.3168	105.24	71.09	1.480	141.25	36.01
2247.6	0.3214	105.83	71.92	1.472	142.47	36.64
2250.8	0.3239	107.19	73.09	1.467	144.55	37.36
2253.7	0.3264	108.21	74.06	1.461	146.20	37.99
2816.0	0.3307	103.63	72.53	1.429	141.62	37.99
3195.0	0.3310	103.20	71.76	1.438	140.56	37.36
3449.0	0.3310	103.07	72.08	1.430	140.79	37.72
3453.5	0.3315	109.52	73.96	1.481	146.97	37.45
3466.0	0.3421	112.19	72.15	1.555	146.94	34.75
3472.5	0.3469	115.05	80.21	1.434	156.91	41.86
3478.5	0.3550	115.11	80.95	1.422	157.69	42.58
3482.9	0.3597	115.31	81.29	1.419	158.16	42.85
3485.0	0.3611	113.23	80.50	1.407	155.99	42.76
3495.3	0.3611	97.88	74.85	1.308	140.10	42.22
3511.0	0.3597	76.32	67.03	1.139	117.91	41.59
3520.0	0.3587	63.98	61.84	1.035	104.49	40.51
3527.6	0.3576	53.69	57.33	0.937	93.12	39.43
3534.3	0.3566	38.69	51.16	0.756	76.95	38.26
3537.3	0.3560	34.10	49.00	0.696	71.73	37.63
3546.8	0.3545	28.99	45.31	0.640	64.64	35.65
3554.5	0.3529	19.83	40.01	0.496	53.23	33.40
3560.3	0.3513	13.48	36.27	0.372	45.26	31.78
3565.1	0.3498	8.53	33.09	0.258	38.78	30.25
3569.0	0.3482	4.87	30.52	0.159	33.77	28.90
3572.3	0.3466	2.19	28.37	0.077	29.83	27.64
3602.0	0.3466	2.75	27.48	0.100	29.31	26.56
4292.0	0.3465	3.44	28.61	0.120	30.90	27.46

CSR TEST 004 (0.0024IN/MIN) PARALLEL

SOIL MIXED 30 8 68 SAMPLE PREPARED 19 9 68

TEST STARTED 23 9 68 TEST COMPLETED 25 9 68

ORIGINAL LENGTH 2.971IN ORIGINAL AREA 1.757SQ.IN.

CONSOLIDATION PRESSURE 10.00PSI

NOTES 1 2X1 SAMPLE FRICTIONLESS ENDS,SIDE DRAINS

2 LOAD MEASURED WITH LOAD BEAM (1LB.=0.00001IN.)

3 DEFORMATION MEASURED WITH DIAL GAUGE

4 TOP PLATEN INCORRECTLY MOUNTED, SLIGHT TILT THROUGHOUT TEST.

MOISTURE CONTENT OF COMPACTED SAMPLE 0.2558 0.2608

DRY DENSITY OF COMPACTED SAMPLE 94.64LB/FT3

DEGREE OF SATURATION OF COMPACTED SAMPLE 97.25PER CENT

INITIAL VOID RATIO 0.6748

FINAL MOISTURE CONTENT 0.1722 0.2349 0.2332

FINAL VOID RATIO 0.5149

TIME ELAPSED	AXIAL DEF	Q	P	N	SIGMA1	SIGMA3
0.0	0.0	0.0	10.00	0.0	10.00	10.00
0.8	0.0003	2.45	9.92	0.247	11.55	9.10
1.2	0.0007	2.31	10.23	0.226	11.77	9.46
2.4	0.0017	2.71	10.54	0.257	12.35	9.64
4.4	0.0035	3.79	11.26	0.337	13.79	10.00
6.4	0.0052	5.14	12.16	0.423	15.59	10.45
9.5	0.0070	5.00	12.39	0.403	15.72	10.72
10.8	0.0087	6.47	12.52	0.517	16.83	10.36
12.8	0.0105	10.63	12.37	0.859	19.46	8.83
14.8	0.0123	15.71	12.54	1.253	23.01	7.30
17.0	0.0140	20.11	14.00	1.436	27.41	7.30
19.0	0.0158	24.49	16.09	1.522	32.42	7.93
21.3	0.0179	14.82	13.68	1.083	23.56	8.74
23.5	0.0175	18.97	17.40	1.090	30.05	11.08
24.5	0.0168	11.50	15.63	0.735	23.30	11.80
25.5	0.0161	6.02	14.62	0.412	18.63	12.61
26.3	0.0154	3.61	13.81	0.262	16.22	12.61
27.8	0.0147	1.21	13.28	0.091	14.09	12.88
55.0	0.0147	2.28	12.56	0.181	14.08	11.80
57.0	0.0154	11.78	13.21	0.892	21.06	9.28
57.9	0.0161	16.86	14.36	1.174	25.60	8.74
59.0	0.0168	21.39	15.51	1.379	29.77	8.38
59.9	0.0175	25.38	16.84	1.507	33.76	8.38
60.8	0.0183	28.17	17.95	1.569	36.73	8.56
61.7	0.0190	30.68	19.24	1.595	39.69	9.01
62.5	0.0197	31.99	20.12	1.590	41.45	9.46
63.4	0.0204	33.83	21.19	1.597	43.74	9.91
64.3	0.0211	35.14	21.89	1.605	45.32	10.18
66.4	0.0229	38.93	24.24	1.606	50.19	11.26
68.6	0.0247	42.30	26.17	1.616	54.37	12.07
73.8	0.0282	48.36	30.08	1.608	62.32	13.96
77.1	0.0318	53.71	33.30	1.613	69.11	15.40
81.3	0.0354	59.28	36.78	1.612	76.30	17.02
85.7	0.0390	64.94	40.11	1.619	83.40	18.46
89.8	0.0426	70.42	43.37	1.624	90.32	19.90
94.2	0.0463	75.73	46.58	1.626	97.07	21.34
98.5	0.0499	81.00	49.69	1.630	103.69	22.69
102.8	0.0536	86.35	52.91	1.632	110.48	24.13
105.8	0.0525	49.99	41.96	1.191	75.29	25.30
107.5	0.0514	34.18	35.61	0.960	58.40	24.22
108.9	0.0503	25.31	31.76	0.797	48.63	23.32
110.4	0.0492	17.19	27.97	0.615	39.43	22.24
111.8	0.0481	12.68	25.57	0.496	34.02	21.34
112.8	0.0474	9.59	24.00	0.399	30.39	20.80
114.0	0.0463	6.09	22.20	0.275	26.76	20.17
115.3	0.0452	3.38	20.40	0.166	22.65	19.27
116.8	0.0441	0.91	19.12	0.048	19.73	18.82
122.0	0.0437	2.73	18.20	0.150	20.02	17.29
125.3	0.0452	19.86	20.40	0.974	33.64	13.78
126.5	0.0463	27.23	22.50	1.210	40.65	13.42
128.1	0.0474	34.71	25.17	1.379	48.31	13.60
129.5	0.0484	41.40	28.12	1.472	55.72	14.32
130.8	0.0495	49.11	31.32	1.568	64.06	14.95
132.4	0.0506	57.05	35.05	1.628	73.08	16.03
133.8	0.0517	63.44	38.17	1.662	80.46	17.02
135.2	0.0528	70.44	41.58	1.694	88.54	18.10
136.4	0.0540	74.86	44.13	1.696	94.04	19.18
137.8	0.0551	79.02	46.69	1.692	99.37	20.35
139.1	0.0562	82.39	48.89	1.685	103.82	21.43
140.4	0.0573	84.98	50.39	1.687	107.04	22.06
142.5	0.0591	88.78	53.09	1.672	112.28	23.50
144.7	0.0610	92.57	55.44	1.670	117.15	24.58
149.0	0.0647	99.20	59.72	1.661	125.85	26.65
153.2	0.0684	104.50	63.28	1.651	132.95	28.45
158.4	0.0721	110.14	66.78	1.649	140.21	30.07
161.5	0.0759	115.72	70.35	1.645	147.50	31.78
164.8	0.0797	120.88	73.69	1.640	154.28	33.40
170.3	0.0834	126.74	77.36	1.638	161.85	35.11
174.4	0.0872	131.68	80.89	1.628	168.68	37.00
178.8	0.0911	136.81	84.04	1.628	175.25	38.44
182.9	0.0949	141.53	87.15	1.624	181.50	39.97
187.3	0.0987	146.44	90.31	1.621	187.94	41.50
191.7	0.1026	151.43	93.78	1.615	194.73	43.30
195.9	0.1065	156.36	97.04	1.611	201.28	44.92
200.1	0.1104	160.52	100.05	1.604	207.06	46.54
204.6	0.1092	87.93	74.86	1.175	133.48	45.55
207.5	0.1080	64.76	65.07	0.995	108.24	43.48
209.0	0.1069	51.61	58.70	0.879	93.11	41.50
210.6	0.1057	38.67	52.41	0.738	78.19	39.52
211.1	0.1045	28.98	47.20	0.614	66.52	37.54
212.4	0.1034	22.31	43.18	0.517	58.05	35.74
214.8	0.1022	16.60	39.83	0.417	50.90	34.30
215.0	0.1010	12.59	37.24	0.338	45.63	33.04
217.0	0.1006	12.35	35.72	0.346	43.95	31.60
253.0	0.1002	12.36	35.09	0.352	43.33	30.97
339.0	0.1002	15.54	35.25	0.441	45.61	30.07
415.0	0.1002	16.52	35.85	0.461	46.86	30.34
418.2	0.0999	6.73	34.29	0.196	38.78	32.05
419.4	0.0987	3.31	31.89	0.104	34.10	30.79
420.9	0.0975	0.86	29.91	0.029	30.48	29.62
440.0	0.0972	4.17	28.67	0.146	31.45	27.28
443.3	0.0975	14.23	30.04	0.474	39.53	25.30
447.3	0.0987	30.15	32.29	0.934	52.39	22.24
449.6	0.0999	41.00	35.46	1.156	62.79	21.79
450.0	0.1010	50.36	39.03	1.290	72.60	22.24
452.4	0.1022	61.65	43.78	1.408	84.88	23.23
453.2	0.1033	62.06	45.27	1.371	86.64	24.58
454.2	0.1045	83.04	53.43	1.554	108.79	25.75
456.0	0.1057	93.51	58.36	1.602	120.70	27.19
457.0	0.1068	104.80	64.10	1.635	133.97	29.17
458.8	0.1080	114.61	69.17	1.657	145.58	30.97
460.4	0.1092	124.51	74.36	1.674	157.37	32.86
461.8	0.1104	131.85	78.70	1.675	166.60	34.75
463.2	0.1115	138.44	82.52	1.678	174.81	36.37
464.5	0.1127	143.69	85.98	1.671	181.77	38.08
467.3	0.1143	148.73	89.55	1.661	188.70	39.97
468.5	0.1162	154.05	93.30	1.651	196.00	41.95
470.6	0.1182	158.26	96.41	1.641	201.92	43.66
475.0	0.1222	165.67	101.94	1.625	212.39	46.72
480.5	0.1261	171.81	106.15	1.619	220.69	48.88
483.9	0.1301	176.71	110.12	1.605	227.93	51.22
488.3	0.1341	181.19	113.51	1.596	234.30	53.11
492.5	0.1381	184.57	116.52	1.584	239.57	55.00
496.9	0.1422	188.25	119.46	1.576	244.96	56.71
501.2	0.1462	191.54	122.18	1.568	249.87	58.33
506.5	0.1503	194.67	124.75	1.560	254.53	59.86

TIME ELAPSED	AXIAL DEF	Q	P	N	SIGMA1	SIGMA3
509.9	0.1544	197.52	127.23	1.552	258.91	61.39
513.8	0.1585	199.77	129.24	1.546	262.42	62.65
518.0	0.1627	202.20	131.31	1.540	266.11	63.91
522.3	0.1668	204.93	133.66	1.533	270.28	65.35
526.5	0.1710	207.29	135.71	1.527	273.90	66.61
531.8	0.1697	110.63	101.42	1.091	175.17	64.54
533.6	0.1685	83.44	89.38	0.933	145.01	61.57
535.3	0.1672	63.86	79.80	0.800	122.37	58.51
537.1	0.1660	161.03	109.31	1.473	216.66	55.63
538.5	0.1647	37.71	66.13	0.570	91.27	53.56
540.0	0.1635	28.78	60.63	0.475	79.82	51.04
541.4	0.1622	20.96	55.87	0.375	69.84	48.88
542.8	0.1610	15.86	52.37	0.303	62.94	47.08
544.1	0.1597	10.63	48.82	0.218	55.91	45.28
545.3	0.1585	7.21	46.33	0.156	51.14	43.93
546.8	0.1572	3.78	43.84	0.086	46.36	42.58
547.9	0.1560	1.15	41.70	0.028	42.47	41.32
551.5	0.1572	29.79	43.15	0.690	63.01	33.22
553.2	0.1585	45.20	46.67	0.969	76.80	31.60
554.7	0.1597	57.47	50.76	1.132	89.07	31.60
557.8	0.1622	82.02	60.74	1.350	115.42	33.40
559.3	0.1635	94.86	66.46	1.427	129.70	34.84
560.7	0.1647	107.10	72.34	1.481	143.74	36.64
562.4	0.1660	121.34	79.52	1.526	160.41	39.07
563.9	0.1672	134.07	85.83	1.562	175.21	41.14
565.4	0.1685	145.62	91.93	1.584	189.01	43.39
567.0	0.1697	157.94	98.65	1.601	203.94	46.00
568.4	0.1710	166.26	103.49	1.607	214.33	48.07
569.9	0.1722	173.89	108.10	1.609	224.03	50.14
572.3	0.1735	179.24	112.05	1.600	231.54	52.30
573.0	0.1752	183.14	115.33	1.588	237.42	54.28
577.3	0.1794	189.79	121.14	1.567	247.67	57.88
581.6	0.1837	193.69	125.05	1.549	254.18	60.49
585.8	0.1879	196.21	127.69	1.537	258.50	62.29
589.9	0.1922	197.81	129.49	1.528	261.36	63.55
594.0	0.1965	198.72	131.05	1.516	263.53	64.81

TIME ELAPSED	AXIAL DEF	Q	P	N	SIGMA1	SIGMA3
598.2	0.2009	201.35	133.01	1.514	267.24	65.89
602.4	0.2052	203.06	134.57	1.509	269.94	66.88
606.6	0.2096	203.87	135.83	1.501	271.74	67.87
607.5	0.2096	199.79	134.74	1.483	267.93	68.14
609.0	0.2096	197.64	133.48	1.481	265.24	67.60
614.0	0.2096	195.49	132.13	1.479	262.46	66.97
618.3	0.2096	194.41	131.41	1.479	261.02	66.61
1320.0	0.2100	184.64	126.27	1.462	249.36	64.72
1324.5	0.2096	118.22	105.93	1.116	184.74	66.52
1325.7	0.2083	82.89	91.18	0.909	146.44	63.55
1328.4	0.2070	61.57	81.10	0.759	122.15	60.58
1330.2	0.2056	44.18	72.34	0.611	101.79	57.61
1331.8	0.2043	31.70	65.39	0.485	86.52	54.82
1333.2	0.2030	23.84	60.70	0.393	76.59	52.75
1334.7	0.2017	16.06	55.76	0.288	66.47	50.41
1336.1	0.2004	10.33	52.14	0.198	59.03	48.70
1337.3	0.1991	6.21	49.06	0.127	53.20	46.99
1339.7	0.1978	1.96	46.11	0.043	47.42	45.46
1342.6	0.1991	38.88	48.88	0.795	74.80	35.92
1344.3	0.2004	54.69	53.07	1.030	89.53	34.84
1345.4	0.2017	68.93	58.27	1.183	104.22	35.29
1347.5	0.2030	85.72	64.94	1.320	122.09	36.37
1349.2	0.2043	100.40	71.82	1.398	138.75	38.35
1350.5	0.2056	114.82	78.42	1.464	154.97	40.15
1352.4	0.2069	132.42	87.17	1.519	175.45	43.03
1354.3	0.2083	148.67	95.11	1.563	194.22	45.55
1355.8	0.2096	161.53	102.27	1.579	209.96	48.43
1358.5	0.2122	168.28	108.57	1.550	220.76	52.48
1359.5	0.2135	170.99	110.20	1.552	224.19	53.20
1362.3	0.2162	174.25	112.99	1.542	229.16	54.91
1364.3	0.2184	176.73	115.08	1.536	232.90	56.17
1368.8	0.2229	181.74	118.82	1.530	239.98	58.24
1373.2	0.2274	185.74	122.22	1.520	246.05	60.31
1377.3	0.2319	188.73	124.75	1.513	250.57	61.84
1381.5	0.2364	189.69	126.51	1.499	252.97	63.28
1385.8	0.2410	191.45	128.63	1.488	256.26	64.81

TIME ELAPSED	AXIAL DEF	Q	P	N	SIGMA1	SIGMA3
1390.0	0.2455	193.47	130.47	1.483	259.45	65.98
1394.3	0.2502	194.84	132.01	1.476	261.90	67.06
1398.4	0.2548	195.55	133.41	1.466	263.78	68.23
1402.8	0.2595	196.34	134.40	1.461	265.29	68.95
1407.8	0.2581	102.90	101.00	1.019	169.60	66.70
1410.1	0.2567	72.37	88.21	0.820	136.46	64.09
1411.9	0.2553	53.16	78.48	0.677	113.92	60.76
1413.6	0.2538	38.55	71.18	0.542	96.88	58.33
1415.1	0.2524	28.05	65.16	0.431	83.86	55.81
1416.5	0.2511	20.06	60.34	0.332	73.71	53.65
1418.0	0.2497	13.47	56.25	0.239	65.23	51.76
1419.4	0.2483	7.67	52.52	0.146	57.63	49.96
1420.8	0.2469	3.58	49.71	0.072	52.10	48.52
1422.2	0.2455	0.72	47.50	0.015	47.98	47.26
1423.4	0.2441	0.31	46.28	0.007	46.49	46.18
1424.5	0.2427	0.51	45.27	0.011	45.61	45.10
1425.9	0.2413	0.31	44.93	0.007	45.14	44.83
1427.0	0.2400	0.31	44.75	0.007	44.96	44.65
1457.0	0.2400	0.21	44.00	0.005	44.14	43.93
1569.0	0.2400	0.10	43.69	0.002	43.76	43.66
1735.0	0.2400	0.10	43.78	0.002	43.85	43.75

CSR TEST 005 (0.0024IN/MIN)PARALLEL

SOIL MIXED 24 9 68 SAMPLE PREPARED 26 9 68

TEST STARTED 30 9 68 TEST COMPLETED 31 9 68

ORIGINAL LENGTH 1.502IN ORIGINAL AREA 1.7585Q.IN.

CONSOLIDATION PRESSURE 10.00PSI

NOTES 1 1X1 SAMPLE. NO SIDE DRAINS

2 LOAD MEASURED WITH LOAD BEAM %1LB # 0.00001IN<

3 DEFORMATION MEASURED WITH DIAL GAUGE

MOISTURE CONTENT OF COMPACTED SAMPLE 0.2558 0.2608

DRY DENSITY OF COMPACTED SAMPLE 94.79LB/FT3

DEGREE OF SATURATION OF COMPACTED SAMPLE 97.64PER CENT

INITIAL VOID RATIO 0.6720

FINAL MOISTURE CONTENT 0.2652 0.2608 0.2544

FINAL VOID RATIO 0.6544

TIME ELAPSED	AXIAL DEF	Q	P	N	SIGMA1	SIGMA3
0.0	0.0	0.0	10.00	0.0	10.00	10.00
0.5	0.0007	2.17	10.09	0.215	11.54	9.37
1.3	0.0020	2.04	8.88	0.230	10.24	8.20
2.6	0.0040	6.24	8.30	0.752	12.46	6.22
4.3	0.0067	7.24	7.73	0.936	12.56	5.32
6.3	0.0101	8.73	7.69	1.136	13.51	4.78
8.4	0.0134	9.71	7.66	1.268	14.13	4.42
10.9	0.0168	10.94	7.98	1.371	15.27	4.33

TIME ELAPSED	AXIAL DEF	Q	P	N	SIGMA1	SIGMA3
12.5	0.0202	12.28	8.42	1.458	16.61	4.33
14.8	0.0192	3.89	6.44	0.604	9.03	5.14
15.5	0.0182	1.63	5.68	0.287	6.77	5.14
16.1	0.0172	0.63	5.35	0.117	5.77	5.14
17.0	0.0168	1.01	4.94	0.204	5.61	4.60
22.0	0.0168	1.13	4.98	0.227	5.73	4.60
25.0	0.0168	1.13	4.98	0.227	5.73	4.60
26.7	0.0175	4.77	5.29	0.902	8.47	3.70
27.8	0.0189	8.41	6.50	1.293	12.11	3.70
28.5	0.0202	10.77	7.56	1.425	14.74	3.97
29.4	0.0216	11.63	7.94	1.466	15.69	4.06
30.7	0.0236	13.11	8.61	1.523	17.35	4.24
32.8	0.0270	14.31	9.10	1.572	18.64	4.33
34.8	0.0305	15.50	9.77	1.587	20.10	4.60
36.8	0.0339	16.92	10.42	1.624	21.70	4.78
38.9	0.0374	18.09	11.08	1.633	23.14	5.05
41.1	0.0409	19.87	12.03	1.651	25.28	5.41
43.2	0.0443	21.63	12.89	1.678	27.31	5.68
45.3	0.0478	23.38	13.92	1.679	29.51	6.13
47.5	0.0513	25.11	14.77	1.700	31.51	6.40
49.8	0.0503	10.56	10.82	0.976	17.86	7.30
50.7	0.0492	7.17	9.24	0.776	14.02	6.85
52.0	0.0471	3.53	7.40	0.478	9.75	6.22
52.9	0.0457	1.95	6.51	0.300	7.81	5.86
53.8	0.0443	1.10	5.87	0.187	6.60	5.50
54.6	0.0429	0.12	5.36	0.023	5.44	5.32
59.0	0.0419	0.12	4.73	0.026	4.81	4.69
98.5	0.0419	1.35	4.87	0.277	5.77	4.42
99.9	0.0429	4.77	4.93	0.968	8.11	3.34
101.3	0.0450	9.16	6.30	1.453	12.41	3.25
102.6	0.0471	12.06	7.54	1.600	15.58	3.52
104.0	0.0492	16.66	9.88	1.685	20.99	4.33
105.3	0.0513	19.41	11.34	1.712	24.28	4.87
106.7	0.0534	23.00	13.08	1.759	28.41	5.41
108.0	0.0556	24.88	14.42	1.725	31.01	6.13
109.8	0.0584	26.97	15.48	1.742	33.46	6.49

TIME ELAPSED	AXIAL DEF	Q	P	N	SIGMA1	SIGMA3
190.9	0.1321	65.81	41.39	1.590	85.26	19.45
193.0	0.1359	67.62	42.80	1.580	87.88	20.26
195.2	0.1398	69.40	44.11	1.573	90.38	20.98
197.3	0.1437	71.06	45.39	1.566	92.76	21.70
199.4	0.1476	72.59	46.62	1.557	95.01	22.42
201.4	0.1515	74.10	47.84	1.549	97.24	23.14
203.5	0.1554	75.49	48.93	1.543	99.26	23.77
205.6	0.1594	77.07	50.09	1.539	101.47	24.40
207.7	0.1633	78.52	51.11	1.536	103.46	24.94
211.8	0.1610	26.07	31.38	0.831	48.76	22.69
213.5	0.1586	13.88	24.80	0.560	34.05	20.17
215.0	0.1562	7.66	20.38	0.376	25.49	17.83
216.3	0.1538	4.22	18.07	0.234	20.88	16.66
217.5	0.1514	1.41	15.33	0.092	16.27	14.86
220.0	0.1510	2.61	14.74	0.177	16.48	13.87
223.0	0.1510	2.71	14.50	0.187	16.31	13.60
228.0	0.1510	3.15	14.65	0.215	16.75	13.60
263.0	0.1510	3.47	14.76	0.235	17.07	13.60
265.8	0.1514	11.72	15.71	0.746	23.52	11.80
267.5	0.1538	22.40	18.19	1.232	33.12	10.72
268.9	0.1562	31.51	21.94	1.436	42.95	11.44
270.5	0.1585	42.28	27.15	1.557	55.34	13.06
272.1	0.1609	53.97	33.57	1.608	69.55	15.58
273.5	0.1633	61.84	38.35	1.612	79.58	17.74
275.8	0.1673	69.74	43.69	1.596	90.18	20.44
278.0	0.1713	73.64	46.79	1.574	95.88	22.24
280.1	0.1753	76.24	49.09	1.553	99.92	23.68
284.5	0.1835	80.29	52.60	1.526	106.13	25.84
288.8	0.1916	83.00	54.95	1.511	110.28	27.28
293.0	0.1999	85.22	56.95	1.496	113.76	28.54
297.2	0.2082	87.06	58.64	1.485	116.68	29.62
301.2	0.2167	89.04	60.38	1.475	119.74	30.70
305.4	0.2252	90.45	61.93	1.460	122.23	31.78
309.6	0.2338	91.60	63.21	1.449	124.28	32.68
313.6	0.2426	92.78	64.51	1.438	126.36	33.58
317.8	0.2514	94.19	65.79	1.432	128.58	34.39

TIME ELAPSED	AXIAL DEF	Q	P	N	SIGMA1	SIGMA3
111.8	0.0619	29.27	17.06	1.716	36.57	7.30
114.0	0.0655	31.43	18.32	1.716	39.27	7.84
116.1	0.0691	33.80	19.65	1.721	42.18	8.38
118.3	0.0727	36.16	21.24	1.702	45.35	9.19
120.4	0.0763	38.03	22.59	1.684	47.94	9.91
122.5	0.0799	40.12	23.91	1.678	50.66	10.54
124.6	0.0835	42.07	25.19	1.670	53.24	11.17
126.8	0.0872	44.00	26.38	1.668	55.71	11.71
128.8	0.0908	45.80	27.70	1.654	58.23	12.43
131.0	0.0945	48.28	29.24	1.651	61.43	13.15
133.1	0.0982	50.16	30.59	1.640	64.03	13.87
135.3	0.1019	52.48	32.17	1.631	67.16	14.68
137.4	0.1056	54.44	33.55	1.623	69.84	15.40
140.0	0.1056	31.79	26.63	1.194	47.82	16.03
141.6	0.1034	16.62	20.22	0.822	31.30	14.68
143.1	0.1011	8.96	15.69	0.571	21.66	12.70
144.0	0.0996	6.10	13.83	0.441	17.90	11.80
145.0	0.0982	3.92	12.57	0.312	15.18	11.26
145.8	0.0967	2.43	11.89	0.204	13.51	11.08
147.0	0.0952	1.04	9.99	0.104	10.68	9.64
155.0	0.0949	2.55	9.23	0.276	10.93	8.38
159.0	0.0949	2.78	9.31	0.298	11.16	8.38
163.0	0.0949	2.78	9.31	0.298	11.16	8.38
168.0	0.0949	2.78	9.31	0.298	11.16	8.38
169.5	0.0959	10.06	10.11	0.995	16.82	6.76
171.0	0.0981	16.95	12.23	1.386	23.53	6.58
172.4	0.1004	24.39	15.43	1.581	31.69	7.30
173.9	0.1026	32.13	19.72	1.629	41.14	9.01
174.3	0.1048	39.72	23.60	1.683	50.08	10.36
177.7	0.1086	48.10	28.55	1.685	60.62	12.52
179.0	0.1108	51.50	31.13	1.655	65.46	13.96
180.3	0.1131	53.53	32.79	1.632	68.48	14.95
182.5	0.1168	58.83	35.55	1.655	74.77	15.94
184.7	0.1206	59.59	36.79	1.620	76.52	16.93
186.7	0.1244	61.58	38.36	1.605	79.41	17.83
188.4	0.1282	63.65	39.68	1.604	82.11	18.46

TIME ELAPSED	AXIAL DEF	Q	P	N	SIGMA1	SIGMA3
322.1	0.2603	95.53	66.86	1.429	130.55	35.02
326.4	0.2693	96.51	68.09	1.417	132.43	35.92
330.4	0.2785	97.24	68.87	1.412	133.70	36.46
335.8	0.2877	98.08	69.87	1.404	135.26	37.18
339.0	0.2971	98.95	70.97	1.394	136.94	37.99
343.2	0.3066	100.00	71.86	1.392	138.53	38.53
347.4	0.3163	100.45	72.64	1.383	139.61	39.16
421.0	0.3182	90.57	66.47	1.363	126.85	36.28
611.0	0.3182	89.09	65.44	1.361	124.83	35.74
619.9	0.3163	25.18	43.41	0.580	60.20	35.02
621.3	0.3143	18.59	38.52	0.483	50.91	32.32
622.3	0.3124	11.78	26.26	0.449	34.11	22.33
623.3	0.3104	6.35	31.02	0.205	35.25	28.90
624.3	0.3085	3.09	28.49	0.109	30.55	27.46
625.2	0.3065	0.71	26.62	0.027	27.09	26.38
633.0	0.3056	2.22	24.51	0.091	25.99	23.77
1293.0	0.3056	5.06	25.46	0.199	28.83	23.77

CSR TEST 006 (0.00024IN/MIN) PARALLEL

SOIL MIXED 25 9 68 SAMPLE PREPARED 2 10 68

TEST STARTED 5 10 68 TEST COMPLETED 8 10 68

ORIGINAL LENGTH 1.551IN ORIGINAL AREA 1.760SQ.IN.

CONSOLIDATION PRESSURE 10.00PSI

NOTES 1 1X1 SAMPLE FRICTIONLESS ENDS, SIDE DRAINS

2 DEFORMATION MEASURED WITH DIAL GAUGE

3 FINAL SHAPE OF SAMPLE TAPERED, MORE EXPANSION AT TOP

MOISTURE CONTENT OF COMPACTED SAMPLE 0.2571 0.2546

DRY DENSITY OF COMPACTED SAMPLE 94.99LB/FT3

DEGREE OF SATURATION OF COMPACTED SAMPLE 97.20PER CENT

INITIAL VOID RATIO 0.6687

FINAL MOISTURE CONTENT 0.2701 0.2646 0.2972

FINAL VOID RATIO 0.6791

TIME ELAPSED	AXIAL DEF	Q	P	N	SIGMA1	SIGMA3
0.0	0.0	0.0	10.00	0.0	10.00	10.00
0.7	0.0006	1.14	9.57	0.119	10.33	9.19
1.1	0.0013	1.01	9.35	0.108	10.02	9.01
1.5	0.0019	1.26	9.16	0.138	10.00	8.74
2.3	0.0032	2.27	8.82	0.257	10.33	8.07
3.3	0.0048	2.14	8.37	0.255	9.80	7.66
4.4	0.0065	2.76	8.09	0.341	9.93	7.17
6.3	0.0097	2.63	7.95	0.330	9.70	7.08
8.4	0.0129	2.99	7.58	0.395	9.57	6.58
10.6	0.0162	6.65	7.00	0.950	11.43	4.78
12.8	0.0195	8.42	7.09	1.187	12.71	4.29
14.9	0.0227	9.87	7.26	1.360	13.84	3.97
17.0	0.0260	11.07	7.48	1.480	14.86	3.79
19.1	0.0293	12.50	7.87	1.589	16.20	3.70
21.2	0.0327	13.81	8.30	1.663	17.51	3.70
23.3	0.0360	14.98	8.78	1.705	18.77	3.79
25.4	0.0393	16.26	9.30	1.748	20.14	3.88
27.5	0.0427	17.65	10.03	1.759	21.80	4.15
29.6	0.0460	19.28	10.85	1.777	23.70	4.42
33.9	0.0528	22.97	12.80	1.795	28.11	5.14
38.1	0.0596	26.25	14.61	1.797	32.11	5.86
42.3	0.0664	30.07	16.78	1.792	36.83	6.76
47.5	0.0733	33.47	19.00	1.762	41.31	7.84
50.6	0.0802	37.06	21.27	1.742	45.98	8.92
50.8	0.0802	29.97	20.17	1.486	40.15	10.18
53.2	0.0788	16.29	15.52	1.049	26.38	10.09
54.2	0.0774	10.60	12.99	0.816	20.06	9.46
55.6	0.0754	5.37	10.35	0.519	13.93	8.56
56.4	0.0740	3.86	9.22	0.419	11.79	7.93
57.4	0.0726	2.11	8.36	0.252	9.77	7.66
59.2	0.0726	3.05	7.51	0.406	9.54	6.49
62.7	0.0726	3.16	7.54	0.419	9.65	6.49
83.7	0.0726	3.28	7.49	0.438	9.68	6.40
153.7	0.0726	3.87	7.69	0.503	10.27	6.40
2785.7	0.0726	2.69	8.47	0.318	10.26	7.57
3053.7	0.0726	2.93	8.55	0.343	10.50	7.57
3056.2	0.0733	11.59	9.27	1.250	17.00	5.41
3057.2	0.0747	17.06	11.01	1.550	22.38	5.32
3058.1	0.0760	20.54	12.35	1.664	26.04	5.50
3059.1	0.0774	25.40	14.51	1.751	31.44	6.04
3059.9	0.0788	29.32	16.53	1.773	36.08	6.76
3060.9	0.0802	32.29	17.88	1.806	39.41	7.12
3061.8	0.0816	35.26	19.59	1.800	43.10	7.84
3063.1	0.0837	37.26	20.98	1.776	45.82	8.56
3065.2	0.0872	39.89	22.76	1.753	49.35	9.46
3067.2	0.0908	42.26	24.45	1.729	52.62	10.36
3069.4	0.0943	44.50	25.91	1.717	55.58	11.08
3073.8	0.1014	48.57	28.71	1.692	61.09	12.52
3078.1	0.1086	52.58	31.31	1.679	66.36	13.76
3082.3	0.1158	56.06	34.00	1.649	71.37	15.31
3086.7	0.1231	59.70	36.38	1.641	76.18	16.48
3090.8	0.1304	63.26	38.92	1.626	81.09	17.83
3095.1	0.1378	66.64	41.30	1.613	85.73	19.09
3099.4	0.1453	69.95	43.67	1.602	90.30	20.35
3104.0	0.1535	73.44	46.09	1.593	95.05	21.61
3107.8	0.1604	75.82	48.05	1.578	98.60	22.78
3111.9	0.1680	78.49	50.20	1.563	102.53	24.04
3115.9	0.1758	81.30	52.40	1.552	106.60	25.30
3120.5	0.1836	83.72	54.38	1.540	110.19	26.47
3124.8	0.1915	85.67	56.02	1.529	113.13	27.46
3128.8	0.1994	87.56	57.73	1.517	116.10	28.54
3133.0	0.2075	88.98	59.28	1.501	118.60	29.62
3137.3	0.2156	90.75	60.95	1.489	121.45	30.70
3141.6	0.2238	91.86	62.31	1.474	123.55	31.69
3145.7	0.2321	92.91	63.56	1.462	125.50	32.59
3149.8	0.2404	94.01	64.83	1.450	127.50	33.49
3163.7	0.2413	86.43	60.77	1.422	118.39	31.96
3166.1	0.2447	95.20	65.22	1.460	128.69	33.49
3168.3	0.2489	95.52	65.96	1.448	129.64	34.12
3172.4	0.2575	96.30	66.85	1.441	131.05	34.75
3176.4	0.2662	96.85	67.84	1.428	132.41	35.56
3180.6	0.2749	97.80	68.79	1.422	133.99	36.19
3184.9	0.2838	98.77	69.92	1.413	135.77	37.00
3189.1	0.2928	99.59	70.56	1.411	136.95	37.36
3193.2	0.3019	100.07	71.44	1.401	138.15	38.08
3251.7	0.3033	89.49	65.39	1.369	125.05	35.56
4213.7	0.3037	84.77	62.65	1.353	119.16	34.39
4217.6	0.3065	103.17	70.13	1.471	138.91	35.74
4218.6	0.3112	103.44	70.76	1.462	139.72	36.28
4222.7	0.3205	103.49	71.86	1.440	140.85	37.36
4227.0	0.3300	103.83	72.69	1.428	141.91	38.08
4230.2	0.3396	103.93	73.44	1.415	142.73	38.80
4233.4	0.3444	103.99	73.64	1.412	142.97	38.98
4240.2	0.3454	95.40	69.70	1.369	133.30	37.90
4257.7	0.3454	93.50	68.35	1.368	130.68	37.18
4271.7	0.3454	92.92	67.97	1.367	129.92	37.00
4278.7	0.3454	92.59	67.86	1.364	129.59	37.00
4280.9	0.3444	55.31	56.34	0.982	93.21	37.90
4282.0	0.3435	39.47	49.17	0.803	75.48	36.01
4283.2	0.3415	25.95	42.59	0.609	59.89	33.94
4283.9	0.3405	19.49	39.18	0.497	52.17	32.68
4284.5	0.3395	15.18	36.84	0.412	46.96	31.78
4285.4	0.3376	10.96	33.99	0.322	41.30	30.34
4286.5	0.3357	5.87	30.68	0.191	34.59	28.72
4287.4	0.3337	3.11	28.68	0.109	30.75	27.64
4288.4	0.3318	0.42	26.88	0.016	27.16	26.74
4320.7	0.3315	3.88	25.51	0.152	28.10	24.22
4334.7	0.3315	4.14	25.60	0.162	28.36	24.22

CSR TEST 007 (0.00024IN/MIN) PARALLEL

SOIL MIXED 25 9 68 SAMPLE PREPARED 9 10 68

TEST STARTED 14 10 68 TEST COMPLETED 16 10 68

ORIGINAL LENGTH 1.570IN ORIGINAL AREA 1.766SQ.IN.

CONSOLIDATION PRESSURE 10.00PSI

NOTES 1 TOP END, ONE PIECE OF RUBBER. BOTTOM END, TWO PIECES.

2 SLIP PLANES FIRST NOTICED AT AXIAL DEF. OF 0.140

3 UNIFORM DEFORMED SHAPE TO DEF. OF 0.105,THEN BASE EXPANDED

4 DEFORMATION MEASURED WITH DIAL GAUGE

MOISTURE CONTENT OF COMPACTED SAMPLE 0.2617 0.2566

DRY DENSITY OF COMPACTED SAMPLE 94.78LB/FT3

DEGREE OF SATURATION OF COMPACTED SAMPLE 97.93PER CENT

INITIAL VOID RATIO 0.6723

FINAL MOISTURE CONTENT 0.2504 0.2621 0.2675

FINAL VOID RATIO 0.6509

TIME ELAPSED	AXIAL DEF	Q	P	N	SIGMA1	SIGMA3
0.0	0.0	0.0	10.00	0.0	10.00	10.00
3.4	0.0006	0.38	10.04	0.038	10.29	9.91
7.8	0.0013	1.15	9.66	0.119	10.43	9.28
21.3	0.0032	3.05	8.95	0.341	10.98	7.93
42.7	0.0064	7.35	7.59	0.968	12.49	5.14
65.9	0.0100	9.09	7.27	1.250	13.33	4.24
83.7	0.0129	10.32	7.32	1.410	14.20	3.88
103.9	0.0161	11.79	7.63	1.545	15.49	3.70
125.3	0.0193	13.38	8.16	1.640	17.08	3.70
146.6	0.0226	14.83	8.64	1.716	18.53	3.70
169.7	0.0261	16.89	9.51	1.776	20.76	3.88
189.3	0.0292	18.19	10.21	1.781	22.34	4.15
210.5	0.0326	19.86	11.04	1.799	24.28	4.42
231.1	0.0358	21.63	12.08	1.791	26.50	4.87
252.3	0.0391	23.52	12.98	1.812	28.66	5.14
273.3	0.0424	25.39	14.05	1.807	30.98	5.59
294.9	0.0459	27.25	15.12	1.802	33.29	6.04
315.9	0.0492	28.97	16.06	1.804	35.37	6.40
343.2	0.0535	31.37	17.67	1.776	38.58	7.21
351.8	0.0558	32.98	18.47	1.785	40.46	7.48
377.9	0.0592	34.30	19.45	1.763	42.32	8.02
400.2	0.0626	36.57	20.75	1.762	45.13	8.56
420.2	0.0660	37.74	21.68	1.741	46.84	9.10
441.3	0.0695	39.62	22.85	1.734	49.26	9.64
462.0	0.0729	41.36	23.97	1.726	51.54	10.18
489.7	0.0775	43.75	25.48	1.717	54.65	10.90
506.3	0.0802	44.91	26.23	1.712	56.17	11.26
525.3	0.0833	46.39	27.26	1.702	58.19	11.80
548.8	0.0871	48.41	28.48	1.700	60.75	12.34
569.9	0.0906	49.97	29.63	1.687	62.94	12.97
588.9	0.0938	51.52	30.59	1.684	64.94	13.42
610.2	0.0973	53.16	31.77	1.673	67.21	14.05
634.5	0.1012	55.11	32.96	1.672	69.70	14.59
673.8	0.1079	58.00	35.18	1.648	73.85	15.85
700.1	0.1124	59.97	36.47	1.644	76.45	16.48
1328.7	0.1129	54.28	33.49	1.621	69.68	15.40
1338.7	0.1129	42.30	29.95	1.412	58.15	15.85
1341.7	0.1126	37.45	28.24	1.326	53.21	15.76
1344.4	0.1123	33.27	26.49	1.256	48.67	15.40
1350.7	0.1116	25.60	23.21	1.103	40.28	14.68
1356.0	0.1108	20.86	21.09	0.989	35.00	14.14
1362.1	0.1101	17.47	19.24	0.908	30.89	13.42
1366.8	0.1094	13.51	17.38	0.777	26.39	12.88
1372.4	0.1087	11.14	16.05	0.694	23.48	12.34
1376.2	0.1080	9.21	14.96	0.616	21.10	11.89
1381.0	0.1073	7.51	13.76	0.546	18.77	11.26
1385.7	0.1065	6.15	12.95	0.475	17.05	10.90
1390.1	0.1058	4.90	12.17	0.403	15.44	10.54
1394.9	0.1051	3.88	11.47	0.338	14.06	10.18
1399.4	0.1044	2.97	10.99	0.270	12.97	10.00
1403.0	0.1037	2.51	10.57	0.238	12.24	9.73
1407.5	0.1030	2.06	9.97	0.207	11.34	9.28
1411.9	0.1023	1.37	9.56	0.144	10.47	9.10
1416.2	0.1015	0.69	8.97	0.077	9.43	8.74
1421.1	0.1008	0.23	8.64	0.027	8.79	8.56
1510.2	0.1008	1.83	8.63	0.212	9.85	8.02
1523.8	0.1008	5.73	8.85	0.648	12.67	6.94
1528.6	0.1015	8.70	9.21	0.945	15.01	6.31
1533.6	0.1023	11.22	9.87	1.136	17.35	6.13
1538.3	0.1030	13.38	10.68	1.253	19.60	6.22
1543.1	0.1037	15.31	11.32	1.352	21.53	6.22
1549.1	0.1044	18.38	12.62	1.457	24.87	6.49
1553.9	0.1051	20.53	13.60	1.509	27.29	6.76
1558.6	0.1058	22.80	14.54	1.568	29.74	6.94
1563.3	0.1065	25.29	15.73	1.608	32.59	7.30
1568.1	0.1073	27.77	16.92	1.642	35.43	7.66
1572.9	0.1080	30.25	18.10	1.671	38.27	8.02
1577.8	0.1087	33.06	19.40	1.704	41.44	8.38
1582.5	0.1094	35.88	20.88	1.718	44.80	8.92
1587.3	0.1101	38.46	22.19	1.733	47.83	9.37
1592.0	0.1108	41.03	23.59	1.740	50.94	9.91
1596.9	0.1116	43.60	24.89	1.752	53.96	10.36
1601.7	0.1123	45.95	26.22	1.753	56.85	10.90
1607.2	0.1130	48.40	27.48	1.761	59.75	11.35
1611.0	0.1137	49.37	28.35	1.742	61.26	11.89
1615.7	0.1144	50.57	29.11	1.737	62.82	12.25
1620.1	0.1152	51.77	29.96	1.728	64.47	12.70
1633.7	0.1173	54.57	31.97	1.707	68.35	13.78
1641.9	0.1188	55.83	32.75	1.705	69.97	14.14
1650.8	0.1202	57.09	33.62	1.698	71.68	14.59
1659.9	0.1217	58.33	34.48	1.692	73.37	15.04
1664.4	0.1224	58.96	35.05	1.682	74.36	15.40
1674.4	0.1242	59.84	35.62	1.680	75.51	15.67
1685.9	0.1261	61.27	36.63	1.673	77.48	16.21
1695.7	0.1279	62.04	37.34	1.661	78.70	16.66
1706.9	0.1297	63.24	38.01	1.664	80.17	16.93
1728.1	0.1334	64.96	39.39	1.649	82.70	17.74
1749.8	0.1371	66.44	40.61	1.636	84.90	18.46
1779.8	0.1423	68.78	42.11	1.633	87.96	19.18
1826.2	0.1488	71.07	44.04	1.614	91.42	20.35
1846.3	0.1540	73.12	45.35	1.612	94.10	20.98
1856.1	0.1558	73.83	45.59	1.619	94.81	20.98
1876.9	0.1596	75.00	46.79	1.603	96.79	21.79
1912.3	0.1660	76.86	48.31	1.591	99.55	22.69
1921.2	0.1676	77.47	48.60	1.594	100.25	22.78
1944.5	0.1718	78.55	49.50	1.587	101.87	23.32
1963.5	0.1752	79.70	50.25	1.586	103.38	23.68
1988.2	0.1798	80.71	51.21	1.576	105.02	24.31
2005.9	0.1830	81.66	51.98	1.571	106.42	24.76
2024.8	0.1866	82.54	52.63	1.568	107.66	25.12
2048.2	0.1910	83.43	53.47	1.560	109.09	25.66
2067.6	0.1946	84.40	54.15	1.558	110.42	26.02
2086.0	0.1981	85.05	54.73	1.554	111.43	26.38
2114.5	0.2034	86.01	55.50	1.550	112.84	26.83
2128.5	0.2064	86.40	55.99	1.543	113.59	27.19
2154.7	0.2114	87.26	56.73	1.538	114.90	27.64
2175.3	0.2153	88.03	57.34	1.535	116.03	28.00
2191.8	0.2186	88.56	57.79	1.532	116.83	28.27
2224.8	0.2251	89.30	58.67	1.522	118.20	28.90
2790.7	0.2261	84.25	54.82	1.537	110.99	26.74
2796.8	0.2268	90.88	58.11	1.564	118.70	27.82
2818.1	0.2309	91.28	59.42	1.536	120.27	28.99
2839.6	0.2351	91.66	59.99	1.528	121.10	29.44
2860.5	0.2392	92.03	60.48	1.522	121.83	29.80
2881.8	0.2434	92.30	61.02	1.513	122.55	30.25
2919.6	0.2489	93.06	61.54	1.512	123.58	30.52

TIME ELAPSED	AXIAL DEF	Q	P	N	SIGMA1	SIGMA3
2937.9	0.2547	93.39	62.01	1.506	124.27	30.88
2975.5	0.2626	94.19	62.91	1.497	125.70	31.51
3006.4	0.2691	94.57	63.48	1.490	126.53	31.96
3039.5	0.2761	95.14	64.03	1.486	127.46	32.32
3069.7	0.2823	95.70	64.58	1.482	128.38	32.68
3101.2	0.2895	96.01	65.22	1.472	129.23	33.22
3138.9	0.2976	96.71	65.91	1.467	130.38	33.67
3175.6	0.3051	97.53	66.63	1.464	131.65	34.12
3234.6	0.3182	98.30	67.43	1.458	132.96	34.66
3274.9	0.3271	98.65	68.08	1.449	133.85	35.20

TIME ELAPSED	AXIAL DEF	Q	P	N	SIGMA1	SIGMA3
53.8	0.0080	6.23	7.85	0.794	12.00	5.77
64.6	0.0096	7.49	7.64	0.981	12.63	5.14
84.9	0.0129	8.86	7.28	1.216	13.19	4.33
105.6	0.0161	9.84	7.43	1.324	13.99	4.15
126.5	0.0193	11.31	7.74	1.461	15.28	3.97
147.6	0.0226	12.53	8.15	1.538	16.50	3.97
166.0	0.0254	13.87	8.59	1.614	17.84	3.97
188.2	0.0290	15.18	9.30	1.632	19.42	4.24
210.8	0.0325	16.99	10.08	1.685	21.41	4.42
230.0	0.0356	18.17	10.84	1.677	22.95	4.78
253.0	0.0391	20.20	11.78	1.714	25.25	5.05
272.4	0.0423	21.61	12.61	1.713	27.02	5.41
293.7	0.0456	23.49	13.60	1.727	29.26	5.77
314.8	0.0490	25.11	14.50	1.732	31.24	6.13
338.1	0.0527	27.20	15.92	1.709	34.05	6.85
359.1	0.0559	29.53	17.05	1.732	36.74	7.21
387.4	0.0605	32.03	18.61	1.722	39.96	7.93
399.5	0.0625	33.41	19.25	1.736	41.52	8.11
425.1	0.0666	35.89	20.79	1.726	44.72	8.83
441.8	0.0693	37.82	21.98	1.721	47.19	9.37
465.0	0.0730	40.40	23.38	1.728	50.31	9.91
484.3	0.0762	42.39	24.76	1.712	53.02	10.63
533.3	0.0842	48.13	28.29	1.701	60.38	12.25
547.5	0.0866	49.64	29.25	1.697	62.34	12.70
568.4	0.0901	51.67	30.46	1.696	64.91	13.24
589.7	0.0936	54.14	32.10	1.687	68.19	14.05
608.7	0.0968	56.27	33.53	1.678	71.04	14.77
634.8	0.1011	58.76	35.26	1.667	74.43	15.67
653.3	0.1042	60.74	36.64	1.658	77.13	16.39
674.6	0.1078	63.01	37.93	1.661	79.94	16.93
696.4	0.1115	65.14	39.36	1.655	82.79	17.65
717.2	0.1150	66.93	40.59	1.649	85.21	18.28
738.3	0.1186	68.92	41.88	1.646	87.83	18.91
760.7	0.1222	70.66	43.09	1.640	90.20	19.54
781.8	0.1259	72.27	44.26	1.633	92.44	20.17
804.8	0.1251	40.82	33.06	1.235	60.27	19.45

CSR TEST 008 (0.00024IN/MIN) PARALLEL

SOIL MIXED 25 9 68 SAMPLE PREPARED 18 10 68

TEST STARTED 24 10 68 TEST COMPLETED 24 10 68

ORIGINAL LENGTH 1.574IN ORIGINAL AREA 1.764SQ.IN.

CONSOLIDATION PRESSURE 10.00PSI

NOTES 1 VERY UNIFORM DEFORMED SHAPE

2 NO SLIP PLANES VISIBLE AT END OF TEST

3 DEFORMATION MEASURED WITH DIAL GAUGE

MOISTURE CONTENT OF COMPACTED SAMPLE 0.2522 0.2602

DRY DENSITY OF COMPACTED SAMPLE 95.23LB/FT3

DEGREE OF SATURATION OF COMPACTED SAMPLE 97.97PER CENT

INITIAL VOID RATIO 0.6644

FINAL MOISTURE CONTENT 0.2411 0.2569 0.2569

FINAL VOID RATIO 0.6324

TIME ELAPSED	AXIAL DEF	Q	P	N	SIGMA1	SIGMA3
0.0	0.0	0.0	10.00	0.0	10.00	10.00
4.1	0.0006	0.51	9.90	0.052	10.24	9.73
8.6	0.0013	1.02	9.62	0.106	10.30	9.28
-17.0	0.0019	1.41	9.48	0.148	10.42	9.01
17.4	0.0026	1.79	9.43	0.190	10.62	8.83
20.8	0.0032	1.79	9.25	0.193	10.44	8.65
32.0	0.0048	2.68	8.82	0.304	10.61	7.93
43.5	0.0064	3.95	8.53	0.463	11.16	7.21

TIME ELAPSED	AXIAL DEF	Q	P	N	SIGMA1	SIGMA3
810.4	0.1244	33.67	29.95	1.124	52.40	18.73
816.6	0.1237	26.73	26.92	0.993	44.74	18.01
821.6	0.1229	22.48	24.78	0.907	39.77	17.29

CSR TEST 009 (0.0006IN/MIN) PARALLEL

SOIL MIXED 14 11 68 SAMPLE PREPARED 2 1 69

TEST STARTED 6 1 69 TEST COMPLETED 6 1 69

ORIGINAL LENGTH 1.551IN ORIGINAL AREA 1.750SQ.IN.

CONSOLIDATION PRESSURE 5.94PSI

NOTES 1 SLIP PLANE IN UPPER HALF OF SAMPLE AT DEFORMATION OF 0.105

MOISTURE CONTENT OF COMPACTED SAMPLE 0.2599 0.2513

DRY DENSITY OF COMPACTED SAMPLE 93.74LB/FT3

DEGREE OF SATURATION OF COMPACTED SAMPLE 93.98PER CENT

INITIAL VOID RATIO 0.6908

FINAL MOISTURE CONTENT 0.2715 0.2765 0.2798

FINAL VOID RATIO 0.6959

TIME ELAPSED	AXIAL DEF	Q	P	N	SIGMA1	SIGMA3
0.0	0.0	0.0	5.94	0.0	5.94	5.94
1.8	0.0014	0.51	5.48	0.093	5.82	5.31
6.0	0.0018	1.65	5.50	0.300	6.60	4.95
8.9	0.0028	2.28	5.26	0.434	6.78	4.50
12.8	0.0042	3.29	5.15	0.640	7.34	4.05
17.1	0.0049	4.05	5.04	0.804	7.74	3.69
25.1	0.0085	4.42	5.07	0.871	8.02	3.60
34.5	0.0110	5.79	5.35	1.082	9.21	3.42
42.0	0.0153	6.64	5.63	1.179	10.06	3.42
51.0	0.0178	7.62	5.78	1.319	10.86	3.24
59.0	0.0214	8.47	6.15	1.376	11.80	3.33
66.9	0.0239	9.44	6.57	1.438	12.86	3.42
76.8	0.0279	10.52	7.11	1.480	14.12	3.60
84.7	0.0319	11.58	7.64	1.516	15.36	3.78
93.5	0.0348	13.02	8.30	1.569	16.98	3.96
101.2	0.0392	14.43	8.95	1.612	18.57	4.14
109.3	0.0425	15.72	9.74	1.614	20.22	4.50
118.0	0.0458	17.24	10.43	1.654	21.92	4.68
127.2	0.0487	18.64	11.16	1.670	23.59	4.95
134.8	0.0536	20.47	12.13	1.687	25.78	5.31
144.7	0.0573	22.67	13.14	1.726	28.25	5.58
151.7	0.0603	23.92	14.00	1.708	29.95	6.03
160.7	0.0640	25.61	15.02	1.705	32.09	6.48
169.6	0.0685	27.03	15.76	1.715	33.78	6.75
177.2	0.0727	28.79	16.80	1.714	35.99	7.20
185.0	0.0761	30.57	17.84	1.714	38.22	7.65
195.5	0.0811	32.04	18.78	1.706	40.14	8.10
207.0	0.0860	34.43	20.21	1.704	43.16	8.73
220.7	0.0926	36.49	21.43	1.702	45.76	9.27
232.3	0.0988	38.76	22.82	1.699	48.66	9.90
245.5	0.1058	41.31	24.30	1.700	51.84	10.53
258.7	0.1121	43.39	25.71	1.687	54.64	11.25
271.0	0.1184	45.77	27.23	1.681	57.74	11.97
283.0	0.1248	48.00	28.60	1.678	60.60	12.60
310.0	0.1392	52.03	31.47	1.653	66.16	14.13
326.0	0.1030	57.53	34.12	1.686	72.47	14.94

CSR TEST 010 (0.0006IN/MIN) PARALLEL

SOIL MIXED 14 11 68 SAMPLE PREPARED 7 1 69

TEST STARTED 10 1 69 TEST COMPLETED 11 1 69

ORIGINAL LENGTH 1.599IN ORIGINAL AREA 1.755SQ.IN.

CONSOLIDATION PRESSURE 15.92PSI

NOTES 1 SLIP PLANE VISIBLE AT DEFORMATION OF 0.121

MOISTURE CONTENT OF COMPACTED SAMPLE 0.2603 0.2500

DRY DENSITY OF COMPACTED SAMPLE 94.17LB/FT3

DEGREE OF SATURATION OF COMPACTED SAMPLE 94.89PER CENT

INITIAL VOID RATIO 0.6831

FINAL MOISTURE CONTENT 0.2591 0.2629 0.2608

FINAL VOID RATIO 0.6603

TIME ELAPSED	AXIAL DEF	Q	P	N	SIGMA1	SIGMA3
0.0	0.0	0.0	15.92	0.0	15.92	15.92
5.0	0.0015	2.05	15.79	0.130	17.16	15.11
7.1	0.0018	2.43	15.20	0.160	16.82	14.39
12.0	0.0028	2.82	14.61	0.193	16.49	13.67
16.8	0.0034	3.45	14.19	0.243	16.49	13.04
21.6	0.0043	4.34	13.86	0.313	16.75	12.41
28.8	0.0068	8.28	13.19	0.628	18.71	10.43
37.5	0.0105	11.43	12.53	0.912	20.15	8.72
46.2	0.0143	13.41	12.56	1.068	21.50	8.09
54.2	0.0168	15.52	12.99	1.194	23.34	7.82
62.8	0.0196	17.61	13.60	1.295	25.34	7.73
70.8	0.0233	19.05	14.08	1.353	26.78	7.73
74.6	0.0265	21.49	14.98	1.434	29.31	7.82
87.8	0.0293	22.92	15.55	1.474	30.83	7.91
96.4	0.0319	25.72	16.84	1.527	33.99	8.27
105.3	0.0354	28.10	17.91	1.569	36.64	8.54
113.3	0.0402	29.69	18.80	1.579	38.59	8.90
122.1	0.0427	32.92	20.23	1.627	42.18	9.26
130.7	0.0466	34.99	21.46	1.630	44.79	9.80
140.0	0.0492	37.46	22.65	1.654	47.62	10.16
147.8	0.0534	40.45	24.27	1.666	51.24	10.79
156.4	0.0563	43.23	25.83	1.674	54.65	11.42
164.6	0.0596	45.62	27.35	1.668	57.76	12.14
173.8	0.0632	48.57	28.69	1.693	61.07	12.50
182.0	0.0664	50.92	30.19	1.686	64.14	13.22
190.8	0.0711	53.17	31.48	1.689	66.93	13.76
199.5	0.0750	55.91	33.03	1.693	70.30	14.39
216.2	0.0810	61.09	36.19	1.688	76.92	15.83
233.0	0.0877	65.92	39.06	1.687	83.01	17.09
251.0	0.0971	70.56	41.96	1.682	89.00	18.44
267.8	0.1042	74.38	44.49	1.672	94.08	19.70
1048.1	0.1121	80.67	47.58	1.695	101.36	20.69
1065.3	0.1200	84.47	50.02	1.689	106.33	21.86
1082.6	0.1270	88.51	52.71	1.679	111.72	23.21
1099.3	0.1347	91.61	55.19	1.660	116.26	24.65
1116.0	0.1417	94.72	57.48	1.648	120.63	25.91
1132.8	0.1510	97.41	59.55	1.636	124.49	27.08

CSR TEST 011 (0.0006IN/MIN) PARALLEL

SOIL MIXED 14 11 68 SAMPLE PREPARED 14 1 69

TEST STARTED 21 1 69 TEST COMPLETED 21 1 69

ORIGINAL LENGTH 1.576IN ORIGINAL AREA 1.760SQ.IN.

CONSOLIDATION PRESSURE 21.33PSI

NOTES 1 TWO PIECES OF RUBBER WITH GREASE USED EACH END

2 UNIFORMITY OF DEFORMED SHAPE MUCH IMPROVED

MOISTURE CONTENT OF COMPACTED SAMPLE 0.2587 0.2492

DRY DENSITY OF COMPACTED SAMPLE 94.40LB/FT3

DEGREE OF SATURATION OF COMPACTED SAMPLE 95.02PER CENT

INITIAL VOID RATIO 0.6790

FINAL MOISTURE CONTENT 0.2571 0.2549 0.2532

FINAL VOID RATIO 0.6452

TIME ELAPSED	AXIAL DEF	Q	P	N	SIGMA1	SIGMA3
0.0	0.0	0.0	21.33	0.0	21.33	21.33
2.0	-.0009	0.51	21.23	0.024	21.57	21.06
3.8	-.0006	1.42	20.99	0.067	21.94	20.52
5.5	-.0000	2.31	21.11	0.110	22.65	20.34
6.8	-.0003	1.54	20.76	0.074	21.79	20.25
10.5	0.0003	2.18	20.71	0.106	22.16	19.98
13.3	0.0018	2.57	20.39	0.126	22.10	19.53
17.0	0.0025	3.08	20.20	0.152	22.25	19.17
20.8	0.0034	4.74	19.67	0.241	22.83	18.09
25.0	0.0037	6.92	18.96	0.365	23.57	16.65
29.5	0.0055	8.31	18.52	0.449	24.06	15.75
34.0	0.0077	10.33	18.02	0.573	24.91	14.58
42.8	0.0105	13.23	17.10	0.774	25.92	12.69
51.0	0.0127	15.87	16.81	0.944	27.39	11.52
59.8	0.0161	18.21	16.60	1.097	28.74	10.53
68.0	0.0189	19.93	16.81	1.185	30.10	10.17
76.5	0.0214	22.52	17.32	1.300	32.33	9.81
85.5	0.0243	25.09	18.17	1.381	34.90	9.81
93.4	0.0271	27.77	19.25	1.443	37.76	9.99
102.3	0.0303	30.42	19.95	1.525	40.23	9.81
110.3	0.0334	31.94	21.09	1.515	42.38	10.44
119.0	0.0366	35.05	22.39	1.565	45.76	10.71
127.8	0.0398	38.27	23.74	1.612	49.25	10.98
136.5	0.0433	41.20	25.16	1.637	52.63	11.43
145.5	0.0456	44.79	25.82	1.735	55.68	10.89
153.7	0.0501	48.12	26.57	1.811	58.65	10.53
161.8	0.0517	51.08	27.47	1.860	61.52	10.44
170.7	0.0566	54.70	29.12	1.878	65.59	10.89
179.0	0.0598	57.53	30.25	1.902	68.60	11.07
191.8	0.0638	63.19	33.84	1.867	75.97	12.78
205.2	0.0684	67.91	36.59	1.856	81.86	13.95
218.3	0.0743	73.31	39.65	1.849	88.52	15.21
231.3	0.0789	77.92	42.44	1.836	94.39	16.47
244.1	0.0846	83.20	45.28	1.837	100.75	17.55
257.6	0.0906	88.15	48.01	1.836	106.78	18.63
270.0	0.0950	92.50	50.45	1.833	112.12	19.62
283.3	0.1011	97.07	53.33	1.820	118.04	20.97
296.0	0.1076	100.51	55.37	1.815	122.38	21.87
309.3	0.1131	104.68	57.93	1.807	127.72	23.04
321.6	0.1196	107.41	59.83	1.795	131.44	24.03
333.4	0.1238	110.62	62.07	1.782	135.82	25.20

CSR TEST 012 (0.0006IN/MIN) PARALLEL

SOIL MIXED 20 1 69 SAMPLE PREPARED 22 1 69

TEST STARTED 27 1 69 TEST COMPLETED 27 1 69

ORIGINAL LENGTH 1.567IN ORIGINAL AREA 1.753SQ.IN.

CONSOLIDATION PRESSURE 7.92PSI

NOTES 1 DURING TEST TOP PLATEN TILTED, MEASURED STRAIN GOOD AVERAGE

2 PORE PRESSURE RESPONSE SEEMED SLUGGISH

3 VALUES OF P TOWARDS END OF TEST TOO LOW

MOISTURE CONTENT OF COMPACTED SAMPLE 0.2640 0.2559

DRY DENSITY OF COMPACTED SAMPLE 93.28LB/FT3

DEGREE OF SATURATION OF COMPACTED SAMPLE 94.43PER CENT

INITIAL VOID RATIO 0.6993

FINAL MOISTURE CONTENT 0.2750 0.2731 0.2709

FINAL VOID RATIO 0.6908

TIME ELAPSED	AXIAL DEF	Q	P	N	SIGMA1	SIGMA3
0.0	0.0	0.0	7.92	0.0	7.92	7.92
2.0	0.0	0.77	8.00	0.096	8.51	7.74
2.9	-.0009	0.13	7.69	0.017	7.78	7.65
7.2	-.0006	1.28	7.63	0.168	8.48	7.20
11.7	0.0006	1.79	7.26	0.246	8.45	6.66
15.3	-.0003	1.28	6.91	0.185	7.76	6.48
19.2	-.0003	1.15	6.68	0.172	7.45	6.30
23.7	0.0006	1.79	6.72	0.266	7.91	6.12
28.2	0.0024	3.19	6.46	0.493	8.59	5.40
32.7	0.0027	4.71	6.52	0.723	9.66	4.95
36.2	0.0036	5.35	6.19	0.863	9.76	4.41
40.3	0.0053	6.35	6.26	1.015	10.49	4.14
44.8	0.0059	6.99	6.11	1.144	10.77	3.78
50.0	0.0071	7.61	6.14	1.240	11.21	3.60
53.4	0.0086	8.23	6.34	1.298	11.83	3.60
57.0	0.0107	8.59	5.38	1.596	11.11	2.52
61.5	0.0119	9.47	5.59	1.695	11.90	2.43
70.2	0.0149	10.95	6.26	1.749	13.56	2.61
78.2	0.0182	12.29	5.81	2.117	14.00	1.71
87.0	0.0212	14.01	6.83	2.051	16.17	2.16
103.8	0.0273	17.65	6.87	2.568	18.64	0.99
112.4	0.0300	19.58	7.16	2.736	20.21	0.63
125.2	0.0331	22.24	8.94	2.487	23.77	1.53
129.2	0.0211	25.26	9.50	2.659	26.34	1.08
137.2	0.0402	27.96	10.04	2.785	28.68	0.72
146.0	0.0430	31.67	11.19	2.831	32.30	0.63
154.9	0.0458	33.65	11.67	2.884	34.10	0.45
162.9	0.0489	36.33	12.47	2.913	36.69	0.36
171.7	0.0517	39.98	13.51	2.960	40.16	0.18
180.5	0.0563	42.68	14.77	2.890	43.22	0.54
193.2	0.0610	47.75	16.10	2.966	47.93	0.18
206.7	0.0651	52.79	18.14	2.911	53.33	0.54
219.2	0.0696	57.42	19.86	2.891	58.14	0.72
232.7	0.0750	62.52	21.74	2.876	63.42	0.90
245.2	0.0810	66.45	23.77	2.796	68.07	1.62
258.7	0.0852	71.18	25.35	2.808	72.80	1.62
271.0	0.0904	75.07	27.72	2.708	77.77	2.70
284.4	0.0952	78.72	28.76	2.737	81.24	2.52
296.9	0.1011	81.77	31.04	2.635	85.55	3.78
310.2	0.1060	84.18	31.57	2.666	87.69	3.51

CSR TEST 013 (0.0006IN/MIN) PARALLEL

SOIL MIXED 1 3 69 SAMPLE PREPARED 7 3 69

TEST STARTED 10 3 69 TEST COMPLETED 10 3 69

ORIGINAL LENGTH 1.602IN ORIGINAL AREA 1.755SQ.IN.

CONSOLIDATION PRESSURE 64.60PSI

NOTES 1 EXCEPTIONALLY UNIFORM DEFORMED SHAPE

2 SLIP PLANE JUST VISIBLE ON SURFACE OF STRIPPED SAMPLE

3 HEIGHT OF STRIPPED SAMPLE, 1.400, 1.401, 1.404, 1.405 IN.

4 DIAM. OF STRIPPED SAMPLE, 1.555, 1.565, 1.570, 1.551 IN.

5 DISTANCE BETWEEN PINS BEFORE SATURATION, 3.176 CM.

6 DISTANCE BETWEEN PINS AFTER SATURATION, 3.188 CM.

MOISTURE CONTENT OF COMPACTED SAMPLE 0.2654 0.2540

DRY DENSITY OF COMPACTED SAMPLE 93.88LB/FT3

DEGREE OF SATURATION OF COMPACTED SAMPLE 95.86PER CENT

INITIAL VOID RATIO 0.6883

FINAL MOISTURE CONTENT 0.2363 0.2373 0.2375

FINAL VOID RATIO 0.6015

TIME ELAPSED	AXIAL DEF	Q	P	N	SIGMA1	SIGMA3
0.0	0.0	0.0	64.60	0.0	64.60	64.60
2.0	0.0010	0.79	64.68	0.012	65.21	64.42
4.0	-.0000	4.22	64.21	0.066	67.02	62.80
5.5	-.0006	4.75	63.30	0.075	66.47	61.72
7.0	-.0013	6.60	62.75	0.105	67.15	60.55
8.8	-.0003	6.72	62.16	0.108	66.64	59.92
11.8	-.0032	8.20	60.94	0.134	66.41	58.21
16.7	-.0035	10.31	59.22	0.174	66.09	55.78
25.0	-.0042	13.63	57.08	0.239	66.17	52.54
34.5	-.0042	15.22	55.00	0.277	65.15	49.93
44.0	-.0029	28.01	52.43	0.534	71.10	43.09
53.4	-.0032	39.13	50.01	0.782	76.10	36.97
62.5	-.0016	46.19	48.86	0.945	79.65	33.46
70.3	0.0016	50.25	48.41	1.038	81.91	31.66
79.7	0.0039	55.26	48.82	1.132	85.66	30.40
88.5	0.0084	58.93	49.50	1.190	88.79	29.86
96.5	0.0110	63.46	50.74	1.251	93.05	29.59
114.7	0.0178	71.95	53.66	1.341	101.63	29.68
122.5	0.0204	75.63	55.34	1.367	105.76	30.13
131.7	0.0234	80.42	57.39	1.401	111.00	30.58
140.7	0.0264	84.80	59.66	1.421	116.19	31.39
149.5	0.0303	89.31	61.97	1.441	121.51	32.20
158.2	0.0310	93.59	64.03	1.462	126.42	32.83
167.0	0.0347	98.19	66.55	1.475	132.01	33.82
175.3	0.0363	102.85	69.18	1.487	137.75	34.90
184.0	0.0427	106.97	71.46	1.497	142.77	35.80
192.5	0.0430	111.22	73.77	1.508	147.92	36.70
201.5	0.0447	116.43	76.86	1.515	154.48	38.05
210.3	0.0504	119.74	78.95	1.517	158.78	39.04
219.0	0.0518	124.94	81.77	1.528	165.06	40.12
227.5	0.0528	129.30	84.39	1.532	170.59	41.29
236.2	0.0582	133.27	86.88	1.534	175.73	42.46
244.0	0.0596	137.29	89.21	1.539	180.74	43.45
262.5	0.0668	146.08	94.75	1.542	192.14	46.06
279.7	0.0726	153.96	99.72	1.544	202.36	48.40
298.0	0.0782	162.40	105.14	1.545	213.41	51.01
314.5	0.0844	168.89	109.47	1.543	222.06	53.17
332.0	0.0932	175.40	114.07	1.538	231.00	55.60
350.0	0.0988	182.26	118.60	1.537	240.11	57.85
355.0	0.0825	-0.12	36.30	-.003	36.22	36.34
360.0	0.0825	0.0	35.71	0.0	35.71	35.71

CSR TEST 014 (0.0006IN/MIN) PARALLEL

SOIL MIXED 1 3 69 SAMPLE PREPARED 10 3 69

TEST STARTED 12 3 69 TEST COMPLETED 12 3 69

ORIGINAL LENGTH 1.619IN ORIGINAL AREA 1.755SQ.IN.

CONSOLIDATION PRESSURE 49.40PSI

NOTES 1 VERY UNIFORM DEFORMED SHAPE

2 SLIP PLANE JUST VISIBLE AT END OF TEST

3 DISTANCE BETWEEN PINS AFTER SATURATION 3.072 CM.

4 DISTANCE BETWEEN PINS AFTER CONSOLIDATION 3.013 CM.

5 FINAL HEIGHT OF SAMPLE, 1.415, 1.421, 1.426, 1.430 IN.

MOISTURE CONTENT OF COMPACTED SAMPLE 0.2672 0.2605

DRY DENSITY OF COMPACTED SAMPLE 93.40LB/FT3

DEGREE OF SATURATION OF COMPACTED SAMPLE 96.16PER CENT

INITIAL VOID RATIO 0.6970

FINAL MOISTURE CONTENT 0.2418 0.2417 0.2379

FINAL VOID RATIO 0.6091

TIME ELAPSED	AXIAL DEF	Q	P	N	SIGMA1	SIGMA3
0.0	0.0	0.0	49.40	0.0	49.40	49.40
2.4	-.0007	8.84	48.93	0.181	54.82	45.98
4.8	0.0003	13.44	47.85	0.281	56.81	43.37
6.8	0.0010	16.72	46.60	0.359	57.75	41.03
8.3	0.0020	18.41	45.73	0.403	58.00	39.59
9.8	0.0020	21.18	44.31	0.478	58.43	37.25
13.9	0.0033	25.22	42.69	0.591	59.50	34.28
19.3	0.0056	28.96	40.69	0.712	60.00	31.04
28.3	0.0080	34.52	38.95	0.886	61.96	27.44
37.3	0.0110	38.45	38.10	1.009	63.73	25.28
45.3	0.0140	41.71	38.19	1.092	66.00	24.29
54.3	0.0173	45.33	38.68	1.172	68.90	23.57
62.8	0.0200	48.30	39.40	1.226	71.60	23.30
70.3	0.0231	52.02	40.73	1.277	75.41	23.39
79.8	0.0261	55.32	42.10	1.314	78.98	23.66
87.8	0.0295	55.89	42.65	1.310	79.91	24.02
96.8	0.0333	61.03	44.72	1.365	85.41	24.38
105.6	0.0367	65.00	46.59	1.395	89.92	24.92
124.6	0.0429	73.42	50.92	1.442	99.87	26.45
131.4	0.0460	76.45	52.47	1.457	103.44	26.99
139.6	0.0484	80.14	54.51	1.470	107.94	27.80
153.3	0.0533	86.34	58.11	1.486	115.67	29.33
165.8	0.0578	92.51	61.43	1.506	123.10	30.59
174.6	0.0613	96.13	63.71	1.509	127.80	31.67
207.1	0.0743	110.90	72.60	1.528	146.53	35.63
218.3	0.0786	115.48	75.38	1.532	152.37	36.89
226.3	0.0818	118.83	77.58	1.532	156.80	37.97
239.8	0.0872	124.39	81.23	1.531	164.16	39.77
252.3	0.0934	129.29	84.58	1.529	170.77	41.48
270.6	0.0999	136.90	89.63	1.527	180.90	44.00
287.5	0.1057	142.96	93.54	1.528	188.85	45.89
305.5	0.1138	149.02	97.72	1.525	197.07	48.05
323.3	0.1216	154.31	101.65	1.518	204.52	50.21
329.3	0.1044	-0.35	29.21	-.012	28.98	29.33
339.3	0.1044	-0.35	28.85	-.012	28.62	28.97

CSR TEST 015 (0.00012/0.0006IN/MIN) PARALLEL

SOIL MIXED 1 3 69 SAMPLE PREPARED 14 3 69

TEST STARTED 15 3 69 TEST COMPLETED 15 3 69

ORIGINAL LENGTH 1.582IN ORIGINAL AREA 1.746SQ.IN.

CONSOLIDATION PRESSURE 33.43PSI

NOTES 1 STRAIN RATE CHANGED AT DEFORMATION OF 0.035

2 EXCEPTIONALLY UNIFORM DEFORMED SHAPE, NO SLIP PLANES

3 HEIGHT OF STRIPPED SAMPLE, 1.417, 1.417, 1.420, 1.422 IN.

4 CRACK AT TOP OF STRIPPED SAMPLE, PHOTOGRAPHED

MOISTURE CONTENT OF COMPACTED SAMPLE 0.2699 0.2585

DRY DENSITY OF COMPACTED SAMPLE 93.49LB/FT3

DEGREE OF SATURATION OF COMPACTED SAMPLE 96.50PER CENT

INITIAL VOID RATIO 0.6954

FINAL MOISTURE CONTENT 0.2445 0.2460 0.2443

FINAL VOID RATIO 0.6208

TIME ELAPSED	AXIAL DEF	Q	P	N	SIGMA1	SIGMA3
0.0	0.0	0.0	33.43	0.0	33.43	33.43
9.0	-.0013	1.32	32.97	0.040	33.85	32.53
18.0	-.0010	1.98	32.65	0.061	33.97	31.99
26.0	0.0007	2.37	32.42	0.073	34.00	31.63
34.0	0.0007	3.16	31.87	0.099	33.98	30.82
43.5	0.0007	4.74	31.23	0.152	34.39	29.65
60.0	0.0003	4.61	30.65	0.150	33.72	29.11
84.5	0.0033	4.07	29.93	0.136	32.64	28.57
116.5	0.0049	6.95	28.37	0.245	33.00	26.05
171.0	0.0085	15.94	26.23	0.608	36.86	20.92
215.0	0.0115	20.84	24.99	0.834	38.88	18.04
258.0	0.0151	24.14	24.56	0.983	40.65	16.51
300.0	0.0178	27.18	24.76	1.098	42.88	15.70
344.3	0.0214	30.17	25.40	1.188	45.51	15.34
385.0	0.0241	32.92	26.22	1.255	48.17	15.25
430.0	0.0271	34.49	26.93	1.281	49.92	15.43
472.0	0.0311	38.05	28.20	1.349	53.57	15.52
514.0	0.0352	41.45	29.61	1.400	57.24	15.79
524.0	0.0399	45.29	31.52	1.437	61.71	16.42
533.0	0.0423	48.71	33.47	1.456	65.94	17.23
542.3	0.0450	52.10	34.96	1.490	69.69	17.59
550.0	0.0484	55.30	36.65	1.509	73.52	18.22
559.5	0.0515	59.12	38.65	1.530	78.06	18.94
568.0	0.0560	62.94	40.73	1.545	82.69	19.75
575.3	0.0577	66.06	42.67	1.548	86.71	20.65
584.3	0.0622	69.94	44.77	1.562	91.40	21.46
593.0	0.0657	73.75	46.85	1.574	96.02	22.27
601.5	0.0685	77.21	48.73	1.585	100.20	22.99
611.0	0.0716	80.98	51.15	1.583	105.14	24.16
619.3	0.0748	85.10	53.52	1.590	110.25	25.15
632.0	0.0804	90.03	56.24	1.601	116.26	26.23
645.0	0.0857	95.66	59.92	1.597	123.69	28.03
658.7	0.0903	100.45	62.77	1.600	129.74	29.29
672.0	0.0957	105.93	66.58	1.591	137.20	31.27
685.5	0.1029	111.00	69.62	1.594	143.62	32.62
697.0	0.1061	114.96	72.47	1.586	149.11	34.15
711.5	0.1119	119.48	75.60	1.580	155.25	35.77
718.0	0.0951	0.48	21.53	0.022	21.85	21.37
727.0	0.0948	0.60	21.48	0.028	21.88	21.28

CSR TEST 016 (0.00012/0.0006IN/MIN) PARALLEL

SOIL MIXED 1 3 69 SAMPLE PREPARED 16 3 69

TEST STARTED 17 3 69 TEST COMPLETED 17 3 69

ORIGINAL LENGTH 1.625IN ORIGINAL AREA 1.755SQ.IN.

CONSOLIDATION PRESSURE 22.85PSI

NOTES 1 EXCEPTIONALLY UNIFORM DEFORMED SHAPE, NO SLIP PLANES

2 CHANGE IN STRAIN RATE AT DEF. OF 0.036

3 HEIGHT OF STRIPPED SAMPLE 1.497", 1.493", 1.490", 1.490"

MOISTURE CONTENT OF COMPACTED SAMPLE 0.2574 0.2647

DRY DENSITY OF COMPACTED SAMPLE 93.90LB/FT3

DEGREE OF SATURATION OF COMPACTED SAMPLE 96.40PER CENT

INITIAL VOID RATIO 0.6879

FINAL MOISTURE CONTENT 0.2527 0.2529 0.2492

FINAL VOID RATIO 0.6375

TIME ELAPSED	AXIAL DEF	Q	P	N	SIGMA1	SIGMA3
0.0	0.0	0.0	22.85	0.0	22.85	22.85
43.0	0.0003	0.65	22.71	0.029	23.14	22.49
51.0	0.0000	1.17	22.70	0.051	23.48	22.31
69.0	-.0003	1.95	22.15	0.088	23.45	21.50
84.0	0.0000	2.21	21.79	0.101	23.26	21.05
120.0	0.0000	4.28	20.68	0.207	23.53	19.25
162.0	-.0003	5.71	19.89	0.287	23.70	17.99
203.0	-.0018	4.94	19.37	0.255	22.66	17.72
246.5	0.0003	11.81	18.33	0.644	26.20	14.39
288.0	0.0027	15.14	17.82	0.850	27.91	12.77
330.0	0.0054	17.68	17.94	0.985	29.73	12.05
378.0	0.0090	20.06	18.20	1.103	31.57	11.51
415.0	0.0123	21.79	18.68	1.166	33.21	11.42
465.0	0.0156	24.40	19.46	1.254	35.73	11.33
500.0	0.0180	26.12	20.22	1.292	37.63	11.51
533.0	0.0208	28.47	21.18	1.344	40.16	11.69
585.0	0.0238	30.78	22.31	1.380	42.83	12.05
627.0	0.0266	33.22	23.39	1.420	45.54	12.32
669.0	0.0296	35.89	24.73	1.451	48.66	12.77
681.0	0.0336	38.88	26.45	1.470	52.37	13.49
687.5	0.0361	41.91	27.82	1.506	55.76	13.85
696.0	0.0392	44.89	29.53	1.520	59.46	14.57
705.0	0.0448	45.50	30.19	1.507	60.52	15.02
714.0	0.0466	49.37	32.11	1.538	65.02	15.65
721.5	0.0501	52.27	33.70	1.551	68.55	16.28
728.5	0.0548	55.32	35.53	1.557	72.41	17.09
737.3	0.0567	58.39	37.27	1.567	76.20	17.81
744.0	0.0595	61.39	38.36	1.600	79.29	17.90
748.0	0.0637	64.40	40.81	1.578	83.74	19.34
764.5	0.0665	67.60	42.77	1.580	87.84	20.24
772.5	0.0684	70.36	44.59	1.578	91.50	21.14
781.3	0.0716	73.86	46.48	1.589	95.72	21.86
789.0	0.0774	76.75	48.25	1.591	99.42	22.67
798.3	0.0787	79.63	50.11	1.589	103.20	23.57
807.5	0.0822	82.78	52.15	1.587	107.34	24.56
816.3	0.0855	85.93	54.19	1.586	111.48	25.55
824.3	0.0887	88.81	56.05	1.584	115.26	26.45
833.0	0.0917	92.07	57.95	1.589	119.33	27.26
842.0	0.0959	94.80	60.03	1.579	123.23	28.43
850.0	0.0985	97.80	61.84	1.532	127.04	29.24
855.0	0.0834	-0.59	17.07	-.035	16.68	17.27
1383.0	0.0821	-0.60	16.17	-.037	15.77	16.37

CSR TEST 017 (0.00012/0.0006IN/MIN) PARALLEL

SOIL MIXED 1 3 69 SAMPLE PREPARED 18 3 69

TEST STARTED 20 3 69 TEST COMPLETED 20 3 69

ORIGINAL LENGTH 1.546IN ORIGINAL AREA 1.760SQ.IN.

CONSOLIDATION PRESSURE 63.60PSI

NOTES 1 CHANGE IN STRAIN RATE AT DEF. OF 0.020

2 GOOD DEFORMED SHAPE, NO SLIP PLANES ON STRIPPED SAMPLE

3 PHOTOGRAPHS TAKEN OF DEFORMED SAMPLE

MOISTURE CONTENT OF COMPACTED SAMPLE 0.2667 0.2558

DRY DENSITY OF COMPACTED SAMPLE 93.83LB/FT3

DEGREE OF SATURATION OF COMPACTED SAMPLE 96.31PER CENT

INITIAL VOID RATIO 0.6892

FINAL MOISTURE CONTENT 0.2334 0.2358 0.2367

FINAL VOID RATIO 0.5959

TIME ELAPSED	AXIAL DEF	Q	P	N	SIGMA1	SIGMA3
0.0	0.0	0.0	63.60	0.0	63.60	63.60
8.0	-.0004	0.0	63.60	0.0	63.60	63.60
16.8	-.0004	0.26	63.60	0.004	63.77	63.51
25.0	-.0004	1.32	63.41	0.021	64.29	62.97
34.0	-.0004	2.11	63.22	0.033	64.63	62.52
42.0	-.0004	2.64	62.77	0.042	64.53	61.89
60.5	-.0004	4.75	61.67	0.077	64.84	60.09
85.0	-.0007	5.67	60.00	0.094	63.78	58.11
129.5	-.0007	10.94	64.28	0.170	71.57	60.63
172.0	-.0014	14.25	54.58	0.261	64.08	49.83
218.0	-.0007	15.16	53.26	0.285	63.37	48.21
260.0	0.0000	24.90	50.93	0.489	67.53	42.63
306.0	0.0014	36.71	48.39	0.759	72.86	36.15
353.0	0.0046	44.33	47.15	0.940	76.70	32.37
411.0	0.0097	51.54	47.12	1.094	81.48	29.94
443.0	0.0107	55.27	47.55	1.162	84.40	29.13
489.0	0.0147	59.85	48.63	1.231	88.53	28.68
529.0	0.0176	64.08	49.95	1.283	92.67	28.59
574.0	0.0205	68.79	51.61	1.333	97.47	28.68
604.0	0.0238	74.99	54.04	1.388	104.03	29.04
612.0	0.0267	79.26	56.27	1.409	109.11	29.85
621.0	0.0300	84.10	58.60	1.435	114.67	30.57
630.0	0.0326	89.10	61.08	1.459	120.48	31.38
639.0	0.0370	93.65	63.59	1.473	126.02	32.37
649.0	0.0396	99.47	66.61	1.493	132.92	33.45
660.0	0.0437	105.09	69.83	1.505	139.89	34.80
667.0	0.0459	109.50	72.29	1.515	145.29	35.79
681.0	0.0511	116.90	76.38	1.531	154.31	37.41
693.3	0.0560	123.52	80.47	1.535	162.82	39.30
700.5	0.0594	127.66	83.02	1.538	168.13	40.47
712.0	0.0632	132.94	86.22	1.542	174.85	41.91
721.0	0.0678	137.46	89.17	1.542	180.81	43.35
735.0	0.0731	144.00	93.42	1.541	189.42	45.42
748.0	0.0769	150.58	97.59	1.543	197.98	47.40
761.0	0.0827	156.65	101.51	1.543	205.94	49.29
773.3	0.0866	162.12	105.13	1.542	213.21	51.09
787.5	0.0928	167.71	108.88	1.540	220.69	52.98
800.0	0.0979	172.59	112.40	1.536	227.46	54.87
813.0	0.1030	177.76	116.01	1.532	234.52	56.76
825.0	0.1089	180.58	118.57	1.523	238.96	58.38
835.0	0.0918	-0.24	35.89	-.007	35.73	35.97
1460.0	0.0914	-0.24	35.89	-.007	35.73	35.97

CSR TEST 018 (0.00012/0.0006IN/MIN) PERPENDICULAR

SOIL MIXED 18 3 69 SAMPLE PREPARED 24 3 69

TEST STARTED 26 3 69 TEST COMPLETED 31 3 69

ORIGINAL LENGTH 1.577IN ORIGINAL AREA 1.765SQ.IN.

CONSOLIDATION PRESSURE 62.85PSI

NOTES 1 GOOD DEFORMED SHAPE, NO SLIP PLANES OBSERVED

2 CHANGE IN STRAIN RATE AT DEF. OF 0.023

MOISTURE CONTENT OF COMPACTED SAMPLE 0.2578 0.2626

DRY DENSITY OF COMPACTED SAMPLE 94.31LB/FT3

DEGREE OF SATURATION OF COMPACTED SAMPLE 97.12PER CENT

INITIAL VOID RATIO 0.6806

FINAL MOISTURE CONTENT 0.2428 0.2442 0.2351

FINAL VOID RATIO 0.6069

TIME ELAPSED	AXIAL DEF	Q	P	N	SIGMA1	SIGMA3
0.0	0.0	0.0	62.85	0.0	62.85	62.85
10.0	0.0004	2.61	62.55	0.042	64.29	61.68
19.0	0.0004	3.65	62.09	0.059	64.52	60.87
28.5	0.0007	5.73	61.52	0.093	65.34	59.61
45.0	0.0007	5.73	60.44	0.095	64.26	58.53
62.0	-.0004	7.04	59.53	0.118	64.22	57.18
88.0	-.0008	10.44	58.23	0.179	65.19	54.75
118.0	-.0004	21.65	56.12	0.386	70.55	48.90
157.0	0.0000	33.11	53.28	0.621	75.35	42.24
202.0	0.0041	41.80	50.95	0.820	78.82	37.02
247.0	0.0068	47.52	50.25	0.946	81.93	34.41
294.0	0.0090	52.71	50.27	1.048	85.41	32.70
332.0	0.0120	56.67	50.96	1.112	88.74	32.07
375.0	0.0143	60.78	51.88	1.172	92.40	31.62
405.0	0.0154	63.53	52.71	1.205	95.06	31.53
465.0	0.0196	69.27	54.89	1.262	101.07	31.80
503.0	0.0223	72.52	56.15	1.291	104.50	31.98
514.0	0.0257	78.74	59.31	1.328	111.80	33.06
523.0	0.0292	81.50	60.77	1.341	115.10	33.60
532.0	0.0323	84.77	62.58	1.355	119.09	34.32
540.0	0.0350	88.69	64.51	1.375	123.64	34.95
548.0	0.0377	91.45	66.15	1.382	127.12	35.67
556.0	0.0412	95.11	68.18	1.395	131.59	36.48
569.0	0.0467	100.16	71.13	1.408	137.90	37.74
583.0	0.0506	105.20	74.16	1.419	144.29	39.09
596.0	0.0557	110.29	77.29	1.427	150.82	40.53
608.0	0.0593	114.66	80.19	1.430	156.63	41.97
621.0	0.0644	119.03	83.09	1.433	162.44	43.41
634.0	0.0692	123.40	85.89	1.437	168.16	44.76
647.0	0.0744	127.89	89.10	1.435	174.36	46.47
660.0	0.0780	131.96	91.72	1.439	179.69	47.73
673.0	0.0805	135.93	94.48	1.439	185.10	49.17
686.0	0.0853	139.74	97.19	1.438	190.35	50.61
698.5	0.0898	143.56	99.90	1.437	195.61	52.05
711.0	0.0939	146.46	102.13	1.434	199.77	53.31
724.0	0.0984	149.37	104.36	1.431	203.94	54.57
737.0	0.1030	152.01	106.50	1.427	207.84	55.83
749.0	0.1076	154.38	108.19	1.427	211.11	56.73
756.0	0.0930	-0.12	34.55	-.003	34.47	34.59
1995.0	0.0926	-0.24	34.51	-.007	34.35	34.59

CSR TEST 019 (0.0006/0.00012IN/MIN) PARALLEL

SOIL MIXED 18 3 69 SAMPLE PREPARED 28 4 69

TEST STARTED 1 5 69 TEST COMPLETED 2 5 69

ORIGINAL LENGTH 1.532IN ORIGINAL AREA 1.762SQ.IN.

CONSOLIDATION PRESSURE 32.59PSI

NOTES 1 SAMPLE CONSOLIDATED TO 63.45PSI AND UNLOADED TO 32.59PSI

2 STRAIN RATE CHANGED ON FIRST LOADING AT DEF. OF 0.04

3 AT DEF. OF 0.10 SAMPLE UNLOADED THEN RELOADED AT 0.00012IN/MIN

4 VERY UNIFORM DEFORMED SHAPE

5 SLIP PLANE JUST VISIBLE AT END OF SECOND LOADING

6 HEIGHT OF STRIPPED SAMPLE, 1.339, 1.341, 1.338, 1.332 IN.

7 DIAM. OF STRIPPED SAMPLE, 1.561, 1.576, 1.560, 1.575 IN.

MOISTURE CONTENT OF COMPACTED SAMPLE 0.2644 0.2542

DRY DENSITY OF COMPACTED SAMPLE 94.14LB/FT3

DEGREE OF SATURATION OF COMPACTED SAMPLE 96.35PER CENT

INITIAL VOID RATIO 0.6837

FINAL MOISTURE CONTENT 0.2455 0.2463 0.2453

FINAL VOID RATIO 0.6233

TIME ELAPSED	AXIAL DEF	Q	P	N	SIGMA1	SIGMA3
0.0	0.0	0.0	32.59	0.0	32.59	32.59
11.5	0.0008	0.65	32.81	0.020	33.24	32.59
20.0	0.0008	1.95	32.97	0.059	34.27	32.32
29.0	0.0008	3.24	33.13	0.098	35.29	32.05
38.0	0.0008	4.28	33.39	0.128	36.24	31.96
45.0	0.0004	5.32	33.73	0.158	37.28	31.96
69.0	0.0011	5.83	34.26	0.170	38.15	32.32
89.5	0.0015	8.68	34.67	0.250	40.46	31.78
137.0	0.0042	19.78	35.31	0.560	48.50	28.72
182.5	0.0069	29.78	35.59	0.837	55.44	25.66
227.0	0.0103	34.81	35.55	0.979	58.76	23.95
271.0	0.0130	38.95	36.12	1.078	62.09	23.14
313.5	0.0161	43.04	37.13	1.159	65.82	22.78
357.0	0.0200	46.56	38.30	1.216	69.34	22.78
434.0	0.0250	53.28	40.90	1.303	76.42	23.14
487.0	0.0293	57.96	43.00	1.348	81.64	23.68
531.5	0.0328	62.01	44.89	1.381	86.23	24.22
574.0	0.0364	65.79	46.87	1.404	90.73	24.94
615.0	0.0395	67.94	48.40	1.404	93.69	25.75
626.5	0.0451	74.99	51.92	1.444	101.91	26.92
636.0	0.0479	79.84	54.52	1.464	107.75	27.91
643.5	0.0511	83.39	56.52	1.475	112.11	28.72
653.0	0.0547	87.61	59.00	1.485	117.41	29.80
662.0	0.0575	92.24	61.63	1.497	123.12	30.88
670.5	0.0619	96.31	63.97	1.505	128.18	31.87
681.0	0.0664	101.19	67.04	1.509	134.50	33.31
701.0	0.0745	110.04	72.78	1.512	146.14	36.10
714.0	0.0807	115.75	76.39	1.515	153.56	37.81
731.0	0.0885	123.28	81.42	1.514	163.61	40.33
744.5	0.0943	129.07	85.33	1.513	171.38	42.31
757.0	0.0993	134.79	89.31	1.509	179.17	44.38
775.0	0.0817	-0.12	26.16	-.005	26.08	26.20
1410.0	0.0809	0.0	27.46	0.0	27.46	27.46
1449.0	0.0821	1.55	27.44	0.056	28.47	26.92
1458.0	0.0825	3.10	27.32	0.113	29.39	26.29
1470.0	0.0829	6.33	27.54	0.303	33.09	24.76
1488.0	0.0838	19.15	28.35	0.675	41.12	21.97
1515.0	0.0862	29.89	30.85	0.969	50.78	20.89
1568.0	0.0896	49.87	38.95	1.280	72.20	22.33
1619.0	0.0921	70.47	49.06	1.436	96.04	25.57
1669.0	0.0962	91.03	59.87	1.520	120.56	29.53
1721.5	0.0996	109.63	70.39	1.557	143.48	33.85
1769.0	0.1038	121.21	77.67	1.561	158.48	37.27
1825.0	0.1076	130.43	84.08	1.551	171.03	40.60
1862.0	0.1114	135.40	87.89	1.541	178.16	42.76
1912.0	0.1152	140.68	91.81	1.532	185.60	44.92
1980.0	0.1204	146.48	95.91	1.527	193.56	47.08
2055.0	0.1272	153.72	101.38	1.516	203.86	50.14
2137.0	0.1363	159.52	106.10	1.503	212.45	52.93
2195.0	0.1407	163.29	108.98	1.498	217.84	54.55
2265.0	0.1477	167.71	112.61	1.489	224.42	56.71
2270.0	0.1287	199.83	260.03	0.768	393.25	193.42
2295.0	0.1283	201.29	260.52	0.773	394.71	193.42

CSR TEST 020 (0.0006/0.00012/0.000024IN/MIN) PARALLEL

SOIL MIXED 18 3 69 SAMPLE PREPARED 6 5 69

TEST STARTED 10 5 69 TEST COMPLETED 12 5 69

ORIGINAL LENGTH 1.589IN ORIGINAL AREA 1.760SQ.IN.

CONSOLIDATION PRESSURE 12.69PSI

NOTES 1 INITIAL CONSOLIDATION TO 47.60PSI, UNLOADED TO 12.69PSI

2 SLIP PLANES JUST VISIBLE AT DEFORMATION OF 0.1013

3 TEST STOPPED AT DEFORMATION OF 0.2230;SOME BARRELLING

4 HEIGHT OF STRIPPED SAMPLE, 1.257, 1.253, 1.255, 1.259 IN.

5 DIAM. TOP STRIPPED SAMPLE,1.683, 1.722, 1.732, 1.700 IN.

6 DIAM. BOTT. STRIPPED SAMPLE, 1.613, 1.617, 1.621, 1.611 IN.

7 STR. RA. CHANGES .12-6AT2.2,6-.024AT5.6,.024-6AT7.3

8 STR. RA. CHANGES, 6-.024AT9.5,.024-6AT11.2

MOISTURE CONTENT OF COMPACTED SAMPLE 0.2628 0.2578

DRY DENSITY OF COMPACTED SAMPLE 94.01LB/FT3

DEGREE OF SATURATION OF COMPACTED SAMPLE 96.39PER CENT

INITIAL VOID RATIO 0.6860

FINAL MOISTURE CONTENT 0.2486 0.2476 0.2427

FINAL VOID RATIO 0.6227

TIME ELAPSED	AXIAL DEF	Q	P	N	SIGMA1	SIGMA3
0.0	0.0	0.0	12.69	0.0	12.69	12.69
8.0	-.0004	0.52	12.86	0.040	13.21	12.69
17.0	-.0008	1.30	12.94	0.101	13.81	12.51
24.0	-.0015	1.82	13.12	0.139	14.33	12.51
42.0	-.0015	3.26	13.42	0.243	15.59	12.33
65.0	-.0027	4.18	13.90	0.300	16.69	12.51
95.0	-.0034	6.79	14.68	0.462	19.21	12.42
129.0	-.0049	7.72	15.71	0.491	20.86	13.14
171.0	-.0057	10.34	16.59	0.623	23.48	13.14
212.0	-.0049	15.95	17.11	0.933	27.74	11.79
258.0	-.0030	21.67	18.56	1.167	33.01	11.34
307.0	-.0011	26.19	20.52	1.276	37.98	11.79
342.0	0.0019	29.09	21.58	1.348	40.97	11.88
397.0	0.0053	33.27	23.60	1.410	45.78	12.51
431.5	0.0080	35.63	24.84	1.435	48.59	12.96
478.0	0.0110	39.38	26.54	1.484	52.79	13.41
522.0	0.0141	42.72	28.28	1.511	56.76	14.04
562.0	0.0164	45.69	29.90	1.528	60.36	14.67
606.0	0.0203	49.21	31.70	1.552	64.51	15.30
625.0	0.0226	53.93	34.09	1.582	70.04	16.11
631.5	0.0253	57.07	36.03	1.584	74.08	17.01
641.0	0.0292	60.51	38.08	1.589	78.42	17.91
650.0	0.0316	63.89	39.84	1.604	82.43	18.54
658.0	0.0347	67.45	42.10	1.602	87.07	19.62
667.0	0.0382	70.71	43.91	1.610	91.05	20.34
676.0	0.0402	74.44	46.14	1.613	95.77	21.33
684.0	0.0438	77.52	48.25	1.607	99.93	22.41
692.0	0.0461	81.42	50.36	1.617	104.64	23.22
701.5	0.0481	85.22	52.62	1.620	109.43	24.21
710.0	0.0509	88.92	54.93	1.619	114.21	25.29
718.0	0.0553	92.20	57.10	1.615	118.57	26.37
1378.0	0.0649	102.33	62.28	1.643	130.50	28.17
1630.0	0.0690	106.61	64.88	1.643	135.95	29.34
1644.0	0.0735	116.35	70.73	1.645	148.30	31.95
1660.5	0.0804	121.34	74.56	1.627	155.45	34.11
1678.0	0.0870	126.89	78.48	1.617	163.07	36.18
1696.0	0.0944	132.10	82.37	1.604	170.44	38.34
1860.0	0.0978	129.38	80.39	1.609	166.64	37.26
2143.0	0.1015	134.10	83.04	1.615	172.44	38.34
2736.0	0.1120	141.89	87.89	1.614	182.48	40.59
2750.0	0.1197	150.29	93.75	1.603	193.94	43.65
2762.0	0.1248	152.61	95.87	1.592	197.61	45.00
2780.0	0.1351	154.86	98.33	1.575	201.57	46.71
2796.0	0.1425	157.89	101.05	1.562	206.31	48.42
2813.0	0.1522	160.53	103.46	1.552	210.48	49.95
2832.0	0.1637	162.59	105.86	1.536	214.25	51.66
2847.0	0.1704	164.64	107.62	1.530	217.38	52.74
2864.0	0.1798	166.28	109.52	1.518	220.37	54.09
2880.0	0.1885	167.70	111.43	1.505	223.23	55.53
2897.0	0.1995	168.24	112.69	1.493	224.85	56.61
2914.0	0.2083	168.76	114.03	1.480	226.54	57.78
2941.0	0.2232	169.81	116.63	1.456	229.84	60.03
2967.0	0.2361	170.39	117.73	1.447	231.32	60.93
2985.0	0.2202	87.67	143.97	0.609	202.42	114.75

CSR TEST 021 (0.000024/0.00012/0.0006IN/MIN) PARALLEL

SOIL MIXED 18 3 69 SAMPLE PREPARED 12 5 69

TEST STARTED 14 5 69 TEST COMPLETED 16 5 69

ORIGINAL LENGTH 1.671IN ORIGINAL AREA 1.760SQ.IN.

CONSOLIDATION PRESSURE 46.45PSI

NOTES 1 GOOD DEFORMED SHAPE UP TO DEFORMATION OF 0.1050

2 HEIGHT OF STRIPPED SAMPLE 1.318, 1.332, 1.340, 1.330 IN.

3 STRAIN RATE CHANGES, .12-6AT1.4,6-.12AT3.2,.12-.024AT4.7

4 STR. RA. CHANGES, .024-.12AT5.7,.12-.024AT11.8,.024-.12AT15.9

MOISTURE CONTENT OF COMPACTED SAMPLE 0.2633 0.2548

DRY DENSITY OF COMPACTED SAMPLE 94.16LB/FT3

DEGREE OF SATURATION OF COMPACTED SAMPLE 96.30PER CENT

INITIAL VOID RATIO 0.6833

FINAL MOISTURE CONTENT 0.2470 0.2422 0.2576

FINAL VOID RATIO 0.6212

TIME ELAPSED	AXIAL DEF	Q	P	N	SIGMA1	SIGMA3
0.0	0.0	0.0	46.45	0.0	46.45	46.45
9.0	0.0004	3.25	45.91	0.071	48.08	44.83
18.0	-.0004	4.03	45.27	0.089	47.96	43.93
25.5	-.0000	4.81	44.90	0.107	48.11	43.30
44.0	0.0	6.50	43.67	0.149	48.00	41.50
65.0	-.0000	6.50	42.86	0.152	47.19	40.69
86.0	-.0000	7.54	42.03	0.179	47.06	39.52
128.0	0.0000	9.36	40.75	0.230	46.99	37.63
197.0	0.0004	12.87	39.31	0.327	47.89	35.02
224.0	0.0004	14.95	38.47	0.389	48.44	33.49
297.0	0.0000	18.73	37.57	0.498	50.06	31.33
324.0	0.0026	24.26	36.18	0.671	52.35	28.09
367.0	0.0071	29.57	35.16	0.841	54.87	25.30
390.0	0.0112	32.15	35.03	0.918	56.46	24.31
456.0	0.0154	37.78	34.92	1.082	60.11	22.33
491.0	0.0177	40.63	35.42	1.147	62.51	21.88
517.0	0.0196	42.34	35.81	1.182	64.04	21.70
558.0	0.0230	45.11	36.56	1.234	66.63	21.52
604.0	0.0249	48.70	37.75	1.290	70.22	21.52
643.0	0.0280	51.46	39.03	1.318	73.34	21.88
670.0	0.0299	53.63	39.94	1.343	75.69	22.06
692.0	0.0310	52.18	39.27	1.329	74.06	21.88
732.0	0.0314	52.79	39.48	1.337	74.67	21.88
1269.0	0.0383	62.41	43.85	1.423	85.46	23.05
1380.0	0.0399	64.06	44.76	1.431	87.47	23.41
1464.0	0.0414	65.45	45.41	1.441	89.04	23.59
1560.0	0.0426	67.74	46.35	1.461	91.51	23.77
1671.0	0.0442	69.25	47.30	1.464	93.47	24.22
1798.0	0.0461	71.34	47.55	1.500	95.11	23.77
1926.0	0.0477	74.07	49.90	1.484	99.28	25.21
1932.0	0.0477	76.05	50.56	1.504	101.26	25.21
1940.0	0.0481	77.26	51.32	1.505	102.83	25.57
1953.0	0.0485	77.97	52.10	1.497	104.08	26.11
2002.0	0.0516	81.66	54.32	1.503	108.76	27.10
2057.0	0.0551	86.15	56.90	1.514	114.33	28.18
2085.0	0.0563	88.99	58.47	1.522	117.80	28.81
2132.0	0.0595	93.09	60.92	1.528	122.98	29.89
2166.0	0.0611	96.11	62.65	1.534	126.72	30.61
2170.0	0.0615	94.24	62.02	1.519	124.85	30.61
2188.0	0.0619	93.22	61.41	1.518	123.56	30.34
2771.0	0.0694	104.70	67.49	1.551	137.29	32.59
2858.0	0.0714	106.28	68.29	1.556	139.14	32.86
2864.0	0.0714	110.27	70.16	1.572	143.67	33.40
2882.0	0.0730	111.41	71.26	1.563	145.53	34.12
2917.0	0.0754	114.24	73.28	1.559	149.44	35.20
2989.0	0.0810	119.40	76.71	1.557	156.31	36.91
3046.0	0.0839	123.80	79.62	1.555	162.15	38.35
3164.0	0.0936	132.51	85.40	1.552	173.74	41.23
3192.0	0.0948	134.68	86.84	1.551	176.63	41.95
4414.0	0.1129	149.99	96.27	1.558	196.26	46.27
4450.0	0.1133	155.57	99.66	1.561	203.37	47.80
4489.0	0.1175	157.13	101.17	1.553	205.92	48.79
4545.0	0.1221	159.51	103.13	1.547	209.47	49.96
4572.0	0.1242	160.84	104.20	1.544	211.43	50.59
4619.0	0.1276	163.28	106.10	1.539	214.95	51.67
4966.0	0.1331	163.49	106.08	1.541	215.07	51.58
5750.0	0.1459	171.07	111.30	1.537	225.35	54.28
6449.0	0.1576	175.53	114.41	1.534	231.43	55.90
7064.0	0.1681	178.32	116.78	1.527	235.66	57.34
7214.0	0.1689	179.32	117.47	1.526	237.02	57.70
7309.0	0.1751	184.96	122.14	1.514	245.45	60.49
7407.0	0.1823	186.87	124.22	1.504	248.80	61.93
7499.0	0.1867	189.23	126.09	1.501	252.24	63.01
7561.0	0.1912	190.40	127.29	1.496	254.22	63.82
7704.0	0.2016	192.41	129.49	1.486	257.76	65.35
7719.0	0.1843	-0.21	41.16	-.005	41.02	41.23

CSR TEST 022 (0.00012/0.000024IN/MIN) PERPENDICULAR

SOIL MIXED 18 3 69 SAMPLE PREPARED 21 5 69

TEST STARTED 23 5 69 TEST COMPLETED 25 5 69

ORIGINAL LENGTH 1.595IN ORIGINAL AREA 1.758SQ.IN.

CONSOLIDATION PRESSURE 46.68PSI

NOTES 1 HEIGHT OF STRIPPED SAMPLE 1.415, 1.416, 1.432, 1.441

2 SAMPLE BULGED TO ONE SIDE TOWARDS THE END OF THE TEST

3 LOAD CELL OFF FOR 2ND AND 3RD READINGS VALUES INTERPOLATED

4 STRAIN RATE CHANGE AT DEF. OF 0.0185, 0.0650

MOISTURE CONTENT OF COMPACTED SAMPLE 0.2614 0.2577

DRY DENSITY OF COMPACTED SAMPLE 94.30LB/FT3

DEGREE OF SATURATION OF COMPACTED SAMPLE 96.84PER CENT

INITIAL VOID RATIO 0.6808

FINAL MOISTURE CONTENT 0.2435 0.2452 0.2408

FINAL VOID RATIO 0.6151

TIME ELAPSED	AXIAL DEF	Q	P	N	SIGMA1	SIGMA3
0.0	0.0	0.0	46.68	0.0	46.68	46.68
8.0	0.0004	1.04	47.03	0.022	47.72	46.68
17.0	-.0007	2.09	47.38	0.044	48.77	46.68
39.0	-.0000	3.26	45.25	0.072	47.42	44.16
63.0	-.0011	5.22	44.28	0.118	47.76	42.54
86.0	-.0007	6.14	43.24	0.142	47.33	41.19
129.0	-.0022	9.80	41.58	0.236	48.11	38.31
164.0	-.0022	11.37	40.57	0.280	48.15	36.78
212.0	-.0041	13.23	39.48	0.335	48.30	35.07
259.0	-.0041	25.02	38.28	0.654	54.96	29.94
307.0	-.0022	33.86	37.99	0.891	60.56	26.70
377.0	0.0026	42.54	38.63	1.101	66.99	24.45
464.0	0.0078	51.12	40.86	1.251	74.94	23.82
489.0	0.0089	53.78	41.84	1.285	77.69	23.91
524.0	0.0119	56.84	43.13	1.318	81.02	24.18
567.0	0.0137	60.85	44.73	1.360	85.30	24.45
612.0	0.0186	64.52	46.41	1.390	89.42	24.90
1532.0	0.0284	80.47	54.51	1.476	108.16	27.69
1887.0	0.0353	86.45	57.77	1.497	115.40	28.95
3009.0	0.0495	104.03	68.40	1.521	137.75	33.72
3370.0	0.0533	109.28	71.77	1.523	144.62	35.34
4217.0	0.0654	120.93	79.25	1.526	159.87	38.94
4245.0	0.0674	125.05	81.25	1.539	164.62	39.57
4307.0	0.0722	127.80	83.88	1.524	169.08	41.28
4367.0	0.0777	130.89	86.26	1.517	173.52	42.63
4472.0	0.0861	136.01	90.13	1.509	180.80	44.79
4560.0	0.0942	139.77	93.00	1.503	186.18	46.41
4639.0	0.1028	142.55	95.37	1.495	190.40	47.85
4750.0	0.1142	146.27	98.50	1.485	196.01	49.74
4845.0	0.1238	149.27	101.03	1.478	200.54	51.27
4852.0	0.1058	0.0	30.30	0.0	30.30	30.30
4897.0	0.1058	0.0	29.76	0.0	29.76	29.76
5025.0	0.1049	-0.12	29.90	-.004	29.82	29.94

CSR TEST 023 (0.00012/0.000024IN/MIN) PERPENDICULAR

SOIL MIXED 18 3 69 SAMPLE PREPARED 2 6 69

TEST STARTED 4 6 69 TEST COMPLETED 5 6 69

ORIGINAL LENGTH 1.585IN ORIGINAL AREA 1.762SQ.IN.

CONSOLIDATION PRESSURE 43.45PSI

NOTES 1 VERY UNIFORM DEFORMED SHAPE

2 HEIGHT OF STRIPPED SAMPLE 1.481, 1.473, 1.456, 1.452

3 DIAM OF STRIPPED SAMPLE (TOP) 1.536,1.542,1.515,1.543

4 DIAM OF STRIPPED SAMPLE (BOTT) 1.502,1.523,1.503,1.535

5 STRAIN RATE CHANGE AT DEF. OF 0.0125, 0.0445, 0.0492

MOISTURE CONTENT OF COMPACTED SAMPLE 0.2585 0.2570

DRY DENSITY OF COMPACTED SAMPLE 94.46LB/FT3

DEGREE OF SATURATION OF COMPACTED SAMPLE 96.57PER CENT

INITIAL VOID RATIO 0.6779

FINAL MOISTURE CONTENT 0.2460 0.2478 0.2417

FINAL VOID RATIO 0.6194

TIME ELAPSED	AXIAL DEF	Q	P	N	SIGMA1	SIGMA3
0.0	0.0	0.0	43.45	0.0	43.45	43.45
9.0	-.0004	1.30	43.16	0.030	44.03	42.73
21.0	-.0011	2.99	43.01	0.069	45.00	42.01
35.0	-.0007	3.89	41.87	0.093	44.46	40.57
63.0	-.0007	3.76	40.47	0.093	42.98	39.22
88.0	-.0004	6.23	38.96	0.160	43.11	36.88
135.0	0.0007	19.44	36.88	0.527	49.84	30.40
180.0	0.0029	27.94	35.12	0.795	53.75	25.81
225.0	0.0065	33.50	34.82	0.962	57.15	23.65
270.0	0.0098	38.27	35.15	1.089	60.66	22.39
312.0	0.0123	42.28	35.94	1.176	64.13	21.85
322.0	0.0156	47.88	37.90	1.263	69.82	21.94
331.0	0.0186	50.79	39.14	1.298	73.00	22.21
341.0	0.0230	53.99	40.39	1.337	76.38	22.39
348.0	0.0248	56.92	41.63	1.367	79.58	22.66
356.5	0.0289	59.83	43.05	1.390	82.94	23.11
367.0	0.0330	64.22	45.24	1.420	88.05	23.83
374.0	0.0349	67.10	46.65	1.438	91.38	24.28
381.0	0.0382	69.73	48.33	1.443	94.82	25.09
391.0	0.0416	73.22	50.13	1.461	98.94	25.72
399.0	0.0454	76.65	52.08	1.472	103.18	26.53
480.0	0.0507	81.02	54.62	1.483	108.63	27.61
489.0	0.0541	86.38	57.66	1.498	115.25	28.87
498.5	0.0568	89.07	59.55	1.496	118.93	29.86
508.0	0.0598	92.56	61.88	1.496	123.59	31.03
515.0	0.0637	94.61	63.20	1.497	126.27	31.66
524.0	0.0679	97.08	64.92	1.495	129.64	32.56
532.0	0.0706	99.94	66.77	1.497	133.40	33.46
545.0	0.0764	103.26	69.32	1.490	138.16	34.90
557.0	0.0819	107.18	71.71	1.495	143.16	35.98
571.0	0.0870	110.26	74.17	1.486	147.68	37.42
584.7	0.0925	113.71	76.58	1.485	152.39	38.68
597.0	0.0988	116.54	78.88	1.477	156.57	40.03
609.0	0.1044	119.65	80.99	1.477	160.76	41.11
620.0	0.0872	0.0	23.74	0.0	23.74	23.74

STC TEST 001 PARALLEL

SOIL MIXED 14 11 68 SAMPLE PREPARED 3 12 68

TEST STARTED 10 12 68 TEST COMPLETED 19 12 68

ORIGINAL LENGTH 1.660IN ORIGINAL AREA 1.753SQ.IN.

CONSOLIDATION PRESSURE 10.00PSI

NOTES 1 SLIP PLANES NOTICED AFTER FIRST LOADING TO 160LB

MOISTURE CONTENT OF COMPACTED SAMPLE 0.2643 0.2549

DRY DENSITY OF COMPACTED SAMPLE 93.56LB/FT3

DEGREE OF SATURATION OF COMPACTED SAMPLE 95.00PER CENT

INITIAL VOID RATIO 0.6942

FINAL MOISTURE CONTENT 0.2733 0.2718 0.2662

FINAL VOID RATIO 0.6833

TIME ELAPSED	AXIAL DEF	Q	P	N	SIGMA1	SIGMA3
0.0	0.0	0.0	10.00	0.0	10.00	10.00
30.0	0.0032	5.71	7.45	0.766	11.26	5.55
60.0	0.0137	11.30	6.99	1.616	14.53	3.23
90.0	0.0249	16.76	9.01	1.861	20.18	3.42
120.0	0.0344	22.13	11.51	1.923	26.26	4.13
135.0	0.0334	16.62	9.86	1.685	20.94	4.32
150.0	0.0321	11.09	8.02	1.383	15.42	4.32
165.0	0.0311	5.55	5.92	0.938	9.62	4.07
210.0	0.0255	0.0	3.29	0.0	3.29	3.29
225.0	0.0275	5.57	4.25	1.312	7.96	2.39
240.0	0.0301	11.11	6.16	1.805	13.57	2.45
255.0	0.0327	16.63	8.51	1.953	19.60	2.97
270.0	0.0356	22.10	11.05	2.001	25.78	3.68
285.0	0.0360	16.57	9.46	1.752	20.51	3.94
300.0	0.0353	11.05	7.62	1.450	14.99	3.94
315.0	0.0333	5.54	5.53	1.002	9.22	3.68
345.0	0.0291	0.0	3.10	0.0	3.10	3.10
360.0	0.0301	5.56	3.98	1.395	7.69	2.13
375.0	0.0333	11.08	6.08	1.821	13.47	2.39
390.0	0.0356	16.58	8.30	1.997	19.35	2.78
405.0	0.0376	22.06	10.77	2.047	25.48	3.42
420.0	0.0376	16.54	9.19	1.799	20.22	3.68
435.0	0.0366	11.04	7.42	1.487	14.78	3.74
450.0	0.0350	5.53	5.33	1.038	9.01	3.49
585.0	0.0310	0.0	3.03	0.0	3.03	3.03
600.0	0.0320	5.55	3.92	1.417	7.61	2.07
615.0	0.0343	11.07	5.95	1.860	13.33	2.26
630.0	0.0369	16.55	8.23	2.012	19.27	2.71
645.0	0.0396	22.01	10.63	2.071	25.30	3.29
660.0	0.0386	16.53	9.06	1.824	20.08	3.55
675.0	0.0379	11.02	7.29	1.512	14.64	3.61
690.0	0.0363	5.52	5.26	1.049	8.94	3.42
1410.0	0.0317	0.0	3.61	0.0	3.61	3.61
1425.0	0.0343	5.53	4.30	1.287	7.99	2.45
1440.0	0.0349	11.06	6.27	1.764	13.64	2.58
1455.0	0.0376	16.54	8.42	1.965	19.45	2.91
1470.0	0.0392	22.02	10.76	2.046	25.44	3.42
1485.0	0.0392	16.51	9.18	1.798	20.19	3.68
1500.0	0.0385	11.02	7.42	1.486	14.76	3.74
1515.0	0.0376	5.51	5.39	1.023	9.06	3.55
1530.0	0.0339	0.0	3.16	0.0	3.16	3.16
1545.0	0.0346	5.53	4.10	1.348	7.79	2.26
1560.0	0.0366	11.04	6.07	1.819	13.43	2.39
1575.0	0.0385	16.53	8.22	2.010	19.24	2.71
1590.0	0.0405	21.99	10.62	2.070	25.28	3.29
1605.0	0.0405	16.49	9.05	1.823	20.04	3.55
1620.0	0.0399	11.00	7.35	1.498	14.68	3.68
1635.0	0.0375	5.51	5.26	1.049	8.94	3.42

TIME ELAPSED	AXIAL DEF	Q	P	N	SIGMA1	SIGMA3
1680.0	0.0339	0.0	2.97	0.0	2.97	2.97
1695.0	0.0349	5.53	3.91	1.414	7.60	2.07
1710.0	0.0382	11.02	5.93	1.857	13.28	2.26
1725.0	0.0395	16.51	8.15	2.026	19.16	2.65
1740.0	0.0415	21.97	10.49	2.095	25.13	3.16
1755.0	0.0412	16.48	8.91	1.849	19.90	3.42
1770.0	0.0402	11.00	7.15	1.538	14.48	3.49
1785.0	0.0385	5.51	5.13	1.074	8.80	3.29
1800.0	0.0349	0.0	2.84	0.0	2.84	2.84
1815.0	0.0365	5.52	3.84	1.437	7.52	2.00
1830.0	0.0382	11.02	5.80	1.899	13.15	2.13
1845.0	0.0398	16.50	8.02	2.058	19.02	2.52
1860.0	0.0418	21.96	10.35	2.121	24.99	3.03
1875.0	0.0418	16.47	8.78	1.875	19.76	3.29
1890.0	0.0408	10.99	7.02	1.566	14.35	3.36
1905.0	0.0388	5.51	5.06	1.088	8.73	3.23
2010.0	0.0352	0.0	2.91	0.0	2.91	2.91
2865.0	0.0385	11.02	6.32	1.743	13.67	2.65
2880.0	0.0425	21.95	10.80	2.032	25.43	3.49
2895.0	0.0514	32.61	16.61	1.963	38.35	5.74
2910.0	0.0627	42.96	22.51	1.908	51.15	8.19
2925.0	0.0624	32.23	18.81	1.714	40.30	8.07
2940.0	0.0617	21.50	15.04	1.430	29.38	7.87
2955.0	0.0590	10.78	10.56	1.021	17.75	6.97
2970.0	0.0523	0.0	4.78	0.0	4.78	4.78
2985.0	0.0546	10.83	7.10	1.527	14.32	3.49
3000.0	0.0587	21.57	11.52	1.873	25.90	4.32
3015.0	0.0620	32.25	16.43	1.963	37.92	5.68
3030.0	0.0668	42.78	21.94	1.950	50.45	7.68
3045.0	0.0664	32.09	18.44	1.740	39.84	7.74
3060.0	0.0657	21.41	14.69	1.458	28.96	7.55
3075.0	0.0634	10.73	10.22	1.050	17.38	6.65
3105.0	0.0563	0.0	4.71	0.0	4.71	4.71
3120.0	0.0593	10.78	7.01	1.537	14.20	3.42
3135.0	0.0630	21.47	11.48	1.870	25.80	4.32
3150.0	0.0657	32.12	16.26	1.976	37.67	5.55
3165.0	0.0698	42.64	21.70	1.965	50.12	7.48
3180.0	0.0691	32.00	18.22	1.757	39.55	7.55
3195.0	0.0674	21.37	14.48	1.476	28.73	7.36
3210.0	0.0664	10.70	10.08	1.061	17.22	6.52
3420.0	0.0589	0.0	4.78	0.0	4.78	4.78
3435.0	0.0616	10.75	7.01	1.535	14.17	3.42
3450.0	0.0656	21.41	11.46	1.868	25.74	4.32
3465.0	0.0680	32.04	16.29	1.966	37.65	5.61
3480.0	0.0721	42.53	21.53	1.975	49.89	7.36
3495.0	0.0711	31.93	18.06	1.768	39.35	7.42
3510.0	0.0704	21.31	14.39	1.480	28.60	7.29
3525.0	0.0684	10.68	10.01	1.066	17.13	6.45
3540.0	0.0619	0.0	4.65	0.0	4.65	4.65
4230.0	0.0619	0.0	5.36	0.0	5.36	5.36
4245.0	0.0643	10.72	7.45	1.440	14.60	3.87
4260.0	0.0680	21.36	11.90	1.796	26.14	4.78
4275.0	0.0707	31.95	16.65	1.919	37.95	6.00
4290.0	0.0734	42.47	21.71	1.957	50.02	7.55
4305.0	0.0734	31.85	18.30	1.741	39.53	7.68
4320.0	0.0724	21.26	14.57	1.459	28.74	7.48
4335.0	0.0697	10.66	10.20	1.045	17.31	6.65
4350.0	0.0629	0.0	4.97	0.0	4.97	4.97
4380.0	0.0669	10.69	7.18	1.489	14.31	3.61
4395.0	0.0693	21.33	11.63	1.834	25.85	4.52
4410.0	0.0724	31.89	16.31	1.955	37.57	5.68
4425.0	0.0751	42.39	21.42	1.979	49.69	7.29
4440.0	0.0747	31.81	18.09	1.759	39.29	7.48
4455.0	0.0741	21.22	14.43	1.471	28.58	7.36
4470.0	0.0713	10.64	10.06	1.057	17.16	6.52
4485.0	0.0652	0.0	4.84	0.0	4.84	4.84
4575.0	0.0645	0.0	4.71	0.0	4.71	4.71
4590.0	0.0682	10.68	7.04	1.516	14.16	3.49
4605.0	0.0716	21.28	11.42	1.864	25.60	4.32
4620.0	0.0747	31.81	16.15	1.969	37.36	5.55
4635.0	0.0771	42.30	21.20	1.996	49.40	7.10
4650.0	0.0768	31.74	17.87	1.776	39.03	7.29

TIME ELAPSED	AXIAL DEF	Q	P	N	SIGMA1	SIGMA3
4665.0	0.0754	21.19	14.16	1.496	28.29	7.10
4680.0	0.0733	10.62	9.86	1.077	16.94	6.32
4695.0	0.0668	0.0	4.71	0.0	4.71	4.71
4920.0	0.0668	0.0	4.97	0.0	4.97	4.97
4935.0	0.0696	10.66	7.17	1.487	14.28	3.61
4950.0	0.0726	21.25	11.54	1.842	25.71	4.45
4965.0	0.0754	31.79	16.15	1.969	37.34	5.55
4980.0	0.0774	42.29	21.19	1.995	49.39	7.10
4995.0	0.0774	31.72	17.86	1.776	39.01	7.29
5010.0	0.0767	21.16	14.15	1.495	28.26	7.10
5025.0	0.0743	10.61	9.86	1.076	16.93	6.32
5040.0	0.0682	0.0	4.78	0.0	4.78	4.78
8595.0	0.0678	0.0	6.13	0.0	6.13	6.13
8610.0	0.0702	10.65	7.68	1.387	14.79	4.13
8625.0	0.0740	21.22	12.11	1.753	26.26	5.03
8640.0	0.0767	31.74	16.65	1.907	37.81	6.07
8655.0	0.0794	42.20	21.49	1.964	49.62	7.42
8670.0	0.0791	31.66	18.10	1.749	39.21	7.55
8685.0	0.0777	21.14	14.47	1.461	28.56	7.42
8700.0	0.0750	10.60	10.24	1.035	17.31	6.71
8715.0	0.0695	0.0	5.23	0.0	5.23	5.23
8730.0	0.0719	10.64	7.35	1.446	14.44	3.81
8745.0	0.0756	21.18	11.71	1.809	25.83	4.65
8760.0	0.0777	31.71	16.25	1.951	37.39	5.68
8775.0	0.0801	42.17	21.02	2.006	49.13	6.97
8790.0	0.0801	31.62	17.70	1.786	38.79	7.16
8805.0	0.0787	21.11	14.14	1.494	28.21	7.10
8820.0	0.0767	10.58	9.98	1.060	17.03	6.45
8835.0	0.0701	0.0	5.03	0.0	5.03	5.03
10140.0	0.0701	0.0	5.74	0.0	5.74	5.74
10155.0	0.0759	21.18	11.90	1.780	26.02	4.84
10170.0	0.0807	42.14	21.34	1.975	49.43	7.29
10185.0	0.0948	62.23	33.32	1.868	74.81	12.58
10200.0	0.1325	79.52	46.05	1.727	99.07	19.55
10215.0	0.1322	59.67	38.79	1.538	78.57	18.90
10230.0	0.1304	39.86	31.16	1.279	57.73	17.87

TIME ELAPSED	AXIAL DEF	Q	P	N	SIGMA1	SIGMA3
10245.0	0.1282	19.98	22.27	0.897	35.59	15.61
10260.0	0.1181	0.0	10.39	0.0	10.39	10.39
10320.0	0.1224	20.11	14.38	1.398	27.79	7.68
10335.0	0.1270	40.01	23.08	1.734	49.76	9.74
10350.0	0.1346	59.50	32.74	1.818	72.40	12.90
10365.0	0.1553	77.43	44.78	1.729	96.40	18.97
10380.0	0.1550	58.10	37.88	1.534	76.62	18.51
10395.0	0.1546	38.75	30.53	1.269	56.36	17.61
10410.0	0.1524	19.43	22.02	0.882	34.97	15.55
10440.0	0.1431	0.0	10.84	0.0	10.84	10.84
12870.0	0.1431	0.0	11.93	0.0	11.93	11.93
12885.0	0.1460	19.57	15.17	1.290	28.22	8.65
12900.0	0.1501	38.96	23.50	1.658	49.47	10.52
12915.0	0.1553	58.08	32.59	1.782	71.31	13.22
12930.0	0.1731	75.81	44.11	1.719	94.64	18.84
12945.0	0.1719	56.93	37.36	1.524	75.32	18.38
12960.0	0.1719	37.96	30.39	1.249	55.70	17.74
12975.0	0.1701	19.02	22.15	0.859	34.83	15.80
12990.0	0.1603	0.0	11.55	0.0	11.55	11.55
13050.0	0.1647	19.14	14.57	1.313	27.34	8.19
13065.0	0.1689	38.10	22.70	1.678	48.10	10.00
13080.0	0.1730	56.86	31.60	1.799	69.50	12.64
13095.0	0.1896	74.29	43.15	1.722	92.67	18.38
13110.0	0.1885	55.80	36.60	1.525	73.79	18.00
13125.0	0.1873	37.25	29.64	1.257	54.47	17.22
13140.0	0.1854	18.67	21.71	0.860	34.15	15.48
13230.0	0.1758	0.0	11.55	0.0	11.55	11.55

STC TEST 002 PARALLEL

SOIL MIXED 14 11 68 SAMPLE PREPARED 30 11 68

TEST STARTED 4 12 68 TEST COMPLETED 8 12 68

ORIGINAL LENGTH 1.634IN ORIGINAL AREA 1.750SQ.IN.

CONSOLIDATION PRESSURE 10.00PSI

NOTES 1 PRESSURE LOST DURING SATURATION, SAMPLE LOADED BY HANGER

2 TEST CONTINUED AS THIS LOADING IMPOSED STRESS LESS THAN 5PSI

MOISTURE CONTENT OF COMPACTED SAMPLE 0.2556 0.2625

DRY DENSITY OF COMPACTED SAMPLE 93.38LB/FT3

DEGREE OF SATURATION OF COMPACTED SAMPLE 94.37PER CENT

INITIAL VOID RATIO 0.6974

FINAL MOISTURE CONTENT 0.2693 0.2663 0.2623

FINAL VOID RATIO 0.6714

TIME ELAPSED	AXIAL DEF	Q	P	N	SIGMA1	SIGMA3
0.0	0.0	0.0	10.00	0.0	10.00	10.00
30.0	0.0000	1.44	10.05	0.144	11.01	9.57
60.0	0.0012	2.88	9.30	0.310	11.22	8.34
90.0	0.0021	4.32	8.48	0.509	11.36	7.04
120.0	0.0038	5.75	7.88	0.730	11.71	5.96
150.0	0.0092	8.58	7.38	1.162	13.10	4.52
180.0	0.0157	11.36	8.02	1.417	15.59	4.23
210.0	0.0208	14.13	9.09	1.555	18.51	4.38
240.0	0.0251	16.88	10.22	1.652	21.47	4.59
270.0	0.0290	19.62	11.56	1.696	24.64	5.03
300.0	0.0360	22.26	12.66	1.758	27.50	5.24
330.0	0.0427	27.63	15.46	1.787	33.88	6.25

TIME ELAPSED	AXIAL DEF	Q	P	N	SIGMA1	SIGMA3
465.0	0.0504	32.88	18.29	1.798	40.22	7.33
495.0	0.0564	38.13	21.27	1.793	46.68	8.56
525.0	0.0639	43.23	24.26	1.781	53.08	9.86
555.0	0.0695	48.34	27.27	1.773	59.49	11.15
1266.0	0.0790	53.16	30.46	1.745	65.90	12.74
1305.0	0.0825	58.25	33.09	1.760	71.93	13.68
1365.0	0.0899	63.03	36.27	1.738	78.30	15.26
1395.0	0.0977	67.71	39.27	1.724	84.41	16.71
1425.0	0.1068	72.18	42.35	1.704	90.47	18.29
1455.0	0.1154	76.59	45.34	1.689	96.40	19.81
1485.0	0.1253	80.78	48.39	1.669	102.24	21.46
1515.0	0.1374	84.64	51.34	1.649	107.77	23.12
1545.0	0.1499	88.32	54.15	1.631	113.03	24.71
1575.0	0.1637	91.72	57.01	1.609	118.16	26.44
4520.0	0.1870	93.85	59.74	1.571	122.31	28.46
4535.0	0.1870	84.47	57.26	1.475	113.58	29.11
4550.0	0.1873	75.05	54.05	1.389	104.08	29.03
4565.0	0.1863	65.76	50.66	1.298	94.50	28.75
4580.0	0.1863	46.97	43.32	1.084	74.63	27.66
4595.0	0.1852	37.62	39.20	0.960	64.28	26.66
4610.0	0.1831	18.86	30.20	0.624	42.78	23.92
5785.0	0.1745	0.0	19.66	0.0	19.66	19.66

STC TEST 003 PARALLEL

SOIL MIXED 14 11 68 SAMPLE PREPARED 30 11 68

TEST STARTED 4 12 68 TEST COMPLETED 5 12 68

ORIGINAL LENGTH 1.628IN ORIGINAL AREA 1.753SQ.IN.

CONSOLIDATION PRESSURE 10.00PSI

NOTES 1 PRESSURE LOST DURING SATURATION, SAMPLE LOADED BY HANGER

2 TEST CONTINUED AS THIS LOADING IMPOSED STRESS LESS THAN 5PSI

MOISTURE CONTENT OF COMPACTED SAMPLE 0.2560 0.2628

DRY DENSITY OF COMPACTED SAMPLE 93.34LB/FT3

DEGREE OF SATURATION OF COMPACTED SAMPLE 94.39PER CENT

INITIAL VOID RATIO 0.6981

FINAL MOISTURE CONTENT 0.2587 0.2605 0.2599

FINAL VOID RATIO 0.6585

TIME ELAPSED	AXIAL DEF	Q	P	N	SIGMA1	SIGMA3
0.0	0.0	0.0	10.00	0.0	10.00	10.00
30.0	0.0003	1.16	9.91	0.117	10.68	9.52
60.0	0.0010	2.89	9.76	0.297	11.69	8.80
90.0	0.0020	4.34	9.44	0.459	12.34	8.00
120.0	0.0030	5.78	9.04	0.639	12.89	7.12
150.0	0.0078	8.63	9.11	0.947	14.86	6.24
180.0	0.0139	11.43	9.73	1.175	17.35	5.91
210.0	0.0180	14.23	10.66	1.335	20.14	5.91
240.0	0.0227	16.99	11.66	1.457	22.99	6.00
270.0	0.0269	19.74	12.90	1.531	26.06	6.32
300.0	0.0324	22.43	13.95	1.608	28.91	6.48
332.0	0.0387	27.86	16.56	1.682	35.14	7.28

TIME ELAPSED	AXIAL DEF	Q	P	N	SIGMA1	SIGMA3
465.0	0.0457	33.19	19.30	1.720	41.42	8.24
495.0	0.0516	38.48	22.18	1.734	47.83	9.36
525.0	0.0648	43.36	24.94	1.739	53.84	10.48

STC TEST 004 PARALLEL

SOIL MIXED 14 11 68 SAMPLE PREPARED 9 12 68

TEST STARTED 20 12 68 TEST COMPLETED 6 1 69

ORIGINAL LENGTH 1.668IN ORIGINAL AREA 1.750SQ.IN.

CONSOLIDATION PRESSURE 9.76PSI

NOTES 1 SLIP PLANE JUST VISIBLE WHEN LOAD INCREASED TO 150LB

2 CREEP DEFORMATION OF 0.065 UNDER LOAD OF 150LB FOR TWO DAYS

MOISTURE CONTENT OF COMPACTED SAMPLE 0.2652 0.2517

DRY DENSITY OF COMPACTED SAMPLE 93.81LB/FT3

DEGREE OF SATURATION OF COMPACTED SAMPLE 95.21PER CENT

INITIAL VOID RATIO 0.6895

FINAL MOISTURE CONTENT 0.2573 0.2580 0.2518

FINAL VOID RATIO 0.6466

TIME ELAPSED	AXIAL DEF	Q	P	N	SIGMA1	SIGMA3
0.0	0.0	0.0	9.76	0.0	9.76	9.76
15.0	0.0009	1.45	9.60	0.151	10.57	9.12
30.0	0.0006	0.0	9.52	0.0	9.52	9.52
45.0	0.0006	1.45	9.60	0.151	10.57	9.12
60.0	0.0006	2.90	9.29	0.313	11.22	8.32
75.0	0.0015	4.35	8.65	0.503	11.55	7.20
90.0	0.0032	5.79	7.93	0.731	11.79	6.00
105.0	0.0029	4.35	7.68	0.566	10.58	6.24
120.0	0.0021	2.90	7.44	0.390	9.38	6.48
135.0	0.0021	1.45	7.36	0.197	8.33	6.88
150.0	0.0021	0.0	7.20	0.0	7.20	7.20
4215.0	0.0024	0.0	9.76	0.0	9.76	9.76

TIME ELAPSED	AXIAL DEF	Q	P	N	SIGMA1	SIGMA3
4230.0	0.0027	1.45	9.84	0.147	10.81	9.36
4245.0	0.0027	2.90	9.52	0.304	11.46	8.56
4260.0	0.0029	4.35	9.29	0.468	12.18	7.84
4290.0	0.0035	5.79	8.97	0.646	12.83	7.04
4335.0	0.0050	7.23	8.16	0.885	12.98	5.76
4350.0	0.0068	8.66	7.92	1.093	13.69	5.03
4365.0	0.0095	10.07	7.67	1.313	14.39	4.31
4380.0	0.0127	11.48	7.74	1.483	15.39	3.91
4385.0	0.0127	10.04	7.42	1.353	14.11	4.07
4400.0	0.0127	8.61	7.02	1.226	12.76	4.15
4410.0	0.0127	7.17	6.70	1.070	11.49	4.31
4420.0	0.0115	5.74	6.39	0.899	10.22	4.47
4430.0	0.0115	4.31	5.91	0.729	8.78	4.47
4440.0	0.0112	2.87	5.75	0.500	7.67	4.79
4450.0	0.0109	1.44	5.27	0.273	6.23	4.79
5555.0	0.0101	0.0	5.59	0.0	5.59	5.59
5565.0	0.0101	2.88	5.75	0.500	7.67	4.79
5580.0	0.0103	5.75	6.07	0.948	9.90	4.15
5595.0	0.0115	8.62	6.79	1.270	12.53	3.91
5610.0	0.0121	10.05	7.18	1.399	13.88	3.83
5625.0	0.0133	11.47	7.58	1.514	15.22	3.75
5640.0	0.0148	12.88	8.13	1.585	16.72	3.83
5655.0	0.0169	14.28	8.59	1.662	18.12	3.83
5670.0	0.0190	15.68	9.06	1.731	19.51	3.83
5685.0	0.0214	17.06	9.68	1.763	21.05	3.99
5700.0	0.0232	18.45	10.22	1.805	22.52	4.07
5715.0	0.0253	19.83	10.84	1.829	24.06	4.23
5730.0	0.0265	21.22	11.47	1.850	25.61	4.39
5765.0	0.0293	22.57	12.08	1.869	27.12	4.55
5775.0	0.0290	19.75	11.22	1.761	24.39	4.63
5785.0	0.0293	19.75	11.22	1.761	24.38	4.63
5795.0	0.0289	16.93	10.28	1.647	21.56	4.63
5805.0	0.0296	14.10	9.49	1.485	18.89	4.79
5815.0	0.0286	11.29	8.72	1.295	16.24	4.95
5825.0	0.0277	8.48	7.70	1.101	13.35	4.87
5835.0	0.0280	5.65	6.52	0.867	10.28	4.63

TIME ELAPSED	AXIAL DEF	Q	P	N	SIGMA1	SIGMA3
5845.0	0.0268	2.83	5.42	0.522	7.30	4.47
14370.0	0.0235	0.0	5.43	0.0	5.43	5.43
14385.0	0.0241	5.67	5.88	0.964	9.66	3.99
14400.0	0.0262	11.32	7.53	1.504	15.07	3.75
14415.0	0.0280	16.95	9.64	1.758	20.94	3.99
14430.0	0.0295	19.74	10.73	1.839	23.89	4.15
14445.0	0.0311	22.53	11.90	1.893	26.92	4.39
14460.0	0.0317	23.92	12.61	1.897	28.55	4.63
14475.0	0.0335	25.28	13.22	1.912	30.07	4.79
14490.0	0.0344	26.66	13.92	1.915	31.69	5.03
14505.0	0.0356	28.02	14.54	1.928	33.22	5.19
14520.0	0.0368	29.39	15.15	1.940	34.74	5.35
14535.0	0.0381	30.75	15.92	1.931	36.42	5.67
14550.0	0.0390	32.12	16.54	1.942	37.95	5.84
14565.0	0.0414	33.43	17.30	1.932	39.58	6.16
14575.0	0.0414	27.86	15.52	1.795	34.09	6.24
14585.0	0.0405	22.31	13.83	1.613	28.70	6.40
14595.0	0.0399	16.74	11.90	1.407	23.06	6.32
14605.0	0.0387	11.17	9.72	1.150	17.17	6.00
14615.0	0.0378	5.59	7.46	0.750	11.19	5.59
14625.0	0.0338	0.0	4.63	0.0	4.63	4.63
14750.0	0.0338	0.0	5.03	0.0	5.03	5.03
15660.0	0.0359	11.21	7.17	1.563	14.64	3.43
15675.0	0.0396	22.33	11.84	1.886	26.72	4.39
15690.0	0.0417	27.85	14.40	1.934	32.96	5.11
15705.0	0.0451	33.30	17.17	1.939	39.37	6.08
15720.0	0.0463	36.03	18.56	1.941	42.58	6.56
15735.0	0.0485	38.71	19.94	1.941	45.75	7.04
15750.0	0.0510	41.37	21.47	1.927	49.04	7.68
15765.0	0.0538	44.00	22.90	1.921	52.23	8.24
15925.0	0.0556	43.91	22.71	1.933	51.99	8.08
15935.0	0.0556	41.16	21.88	1.881	49.32	8.16
15945.0	0.0556	38.42	20.96	1.833	46.58	8.16
15955.0	0.0550	32.95	19.14	1.721	41.11	8.16
15965.0	0.0547	27.47	17.31	1.587	35.63	8.16
15975.0	0.0544	21.98	15.41	1.427	30.06	8.08

TIME ELAPSED	AXIAL DEF	Q	P	N	SIGMA1	SIGMA3
15985.0	0.0534	16.50	13.18	1.252	24.18	7.68
15995.0	0.0519	11.02	10.87	1.014	18.22	7.20
16005.0	0.0507	8.28	9.72	0.852	15.23	6.96
16015.0	0.0513	5.51	8.31	0.663	11.99	6.48
16025.0	0.0488	2.76	6.84	0.404	8.68	5.92
16190.0	0.0463	0.0	5.59	0.0	5.59	5.59
19845.0	0.0460	0.0	6.24	0.0	6.24	6.24
19860.0	0.0491	16.58	10.08	1.645	21.13	4.55
19875.0	0.0522	27.54	14.78	1.864	33.14	5.59
19890.0	0.0559	38.41	19.92	1.928	45.52	7.12
19905.0	0.0568	41.11	21.22	1.937	48.63	7.52
19920.0	0.0587	43.76	22.59	1.938	51.76	8.00
19935.0	0.0593	46.47	23.97	1.939	54.95	8.48
19950.0	0.0618	49.07	25.48	1.926	58.19	9.12
19965.0	0.0640	51.68	26.83	1.926	61.28	9.60
19995.0	0.0669	54.23	28.32	1.915	64.47	10.24
20005.0	0.0672	51.50	27.25	1.890	61.58	10.08
20015.0	0.0675	48.78	26.42	1.846	58.94	10.16
20025.0	0.0669	43.39	24.70	1.756	53.63	10.24
20035.0	0.0665	37.98	22.74	1.670	48.06	10.08
20045.0	0.0659	27.14	18.81	1.443	36.90	9.76
20055.0	0.0647	16.31	14.48	1.127	25.35	9.04
20065.0	0.0634	10.89	11.95	0.911	19.20	8.32
20075.0	0.0615	5.45	9.42	0.579	13.05	7.60
20130.0	0.0559	0.0	6.16	0.0	6.16	6.16
20145.0	0.0602	16.39	10.26	1.598	21.18	4.79
20160.0	0.0652	32.60	17.18	1.897	38.91	6.32
20175.0	0.0674	43.36	22.21	1.952	51.12	7.76
20190.0	0.0693	48.70	24.87	1.958	57.33	8.64
20205.0	0.0703	51.33	26.31	1.951	60.53	9.20
20220.0	0.0712	53.98	27.75	1.945	63.74	9.76
20235.0	0.0731	56.56	29.25	1.933	66.96	10.40
20250.0	0.0750	59.13	30.83	1.918	70.25	11.12
20265.0	0.0782	61.61	32.30	1.907	73.37	11.76
20295.0	0.0817	64.04	33.83	1.893	76.53	12.48
20305.0	0.0817	61.37	32.86	1.868	73.78	12.40

TIME ELAPSED	AXIAL DEF	Q	P	N	SIGMA1	SIGMA3
20315.0	0.0817	58.71	31.89	1.841	71.03	12.32
20325.0	0.0814	53.39	30.12	1.773	65.71	12.32
20335.0	0.0807	42.74	26.49	1.613	54.98	12.24
20345.0	0.0792	26.76	20.52	1.304	38.36	11.60
20355.0	0.0782	16.07	15.92	1.010	26.63	10.56
20365.0	0.0769	10.73	13.42	0.800	20.57	9.84
20375.0	0.0747	5.38	10.59	0.508	14.18	8.80
20385.0	0.0734	2.69	9.22	0.292	11.01	8.32
21405.0	0.0699	0.0	7.60	0.0	7.60	7.60
21420.0	0.0728	16.17	10.98	1.472	21.76	5.59
21435.0	0.0785	37.49	20.33	1.844	45.33	7.84
21450.0	0.0833	53.28	28.16	1.892	63.68	10.40
21465.0	0.0849	58.50	30.86	1.896	69.87	11.36
21480.0	0.0881	63.60	33.84	1.879	76.24	12.64
21495.0	0.0919	68.61	36.95	1.857	82.69	14.09
21510.0	0.0977	73.41	39.92	1.839	88.86	15.45
21525.0	0.1042	78.09	42.92	1.819	94.98	16.89
21685.0	0.1085	77.72	43.04	1.806	94.85	17.13
22380.0	0.1108	77.52	43.05	1.801	94.73	17.21
23100.0	0.1108	77.52	42.49	1.824	94.17	16.65
24315.0	0.1114	77.46	41.91	1.848	93.55	16.09
24610.0	0.1114	77.46	41.19	1.881	92.83	15.37
24630.0	0.1111	72.32	39.64	1.825	87.85	15.53
24640.0	0.1114	67.13	38.23	1.756	82.98	15.85
25695.0	0.1101	41.37	30.92	1.338	58.50	17.13
25705.0	0.1101	41.37	30.44	1.359	58.02	16.65
25715.0	0.1082	25.92	24.01	1.080	41.28	15.37
25760.0	0.1059	15.59	18.32	0.851	28.71	13.12
25770.0	0.1049	10.40	16.27	0.639	23.21	12.80
25780.0	0.1032	5.21	13.50	0.386	16.97	11.76
25810.0	0.0990	0.0	9.76	0.0	9.76	9.76

STC TEST 005 PARALLEL

SOIL MIXED 14 11 68 SAMPLE PREPARED 8 1 69

TEST STARTED 22 1 69 TEST COMPLETED 25 1 69

ORIGINAL LENGTH 1.548IN ORIGINAL AREA 1.755SQ.IN.

CONSOLIDATION PRESSURE 9.45PSI

NOTES 1 SAMPLE STOOD FOR SOME HOURS UNDER LOAD BEFORE UNLOADING

MOISTURE CONTENT OF COMPACTED SAMPLE 0.2583 0.2523

DRY DENSITY OF COMPACTED SAMPLE 94.05LB/FT3

DEGREE OF SATURATION OF COMPACTED SAMPLE 94.63PER CENT

INITIAL VOID RATIO 0.6853

FINAL MOISTURE CONTENT 0.2625 0.2636 0.2594

FINAL VOID RATIO 0.6628

TIME ELAPSED	AXIAL DEF	Q	P	N	SIGMA1	SIGMA3
0.0	0.0	0.0	9.45	0.0	9.45	9.45
10.0	0.0000	1.44	9.53	0.151	10.49	9.05
20.0	0.0006	2.87	9.21	0.312	11.12	8.25
50.0	0.0016	4.30	8.00	0.538	10.87	6.57
60.0	0.0031	5.73	7.92	0.724	11.74	6.01
70.0	0.0056	7.15	7.43	0.962	12.19	5.04
90.0	0.0088	8.55	7.01	1.219	12.71	4.16
105.0	0.0110	9.95	7.24	1.374	13.87	3.92
120.0	0.0141	11.33	7.54	1.503	15.10	3.76
135.0	0.0164	12.72	7.92	1.606	16.41	3.68
150.0	0.0186	14.10	8.30	1.698	17.71	3.60
165.0	0.0218	15.47	8.76	1.766	19.07	3.60

TIME ELAPSED	AXIAL DEF	Q	P	N	SIGMA1	SIGMA3
210.0	0.0253	16.81	9.13	1.842	20.33	3.52
225.0	0.0288	19.54	10.12	1.932	23.14	3.60
250.0	0.0346	22.20	11.56	1.920	26.36	4.16
450.0	0.0356	22.18	13.00	1.706	27.78	5.61
1290.0	0.0362	22.16	12.67	1.749	27.45	5.28
1295.0	0.0362	22.16	12.27	1.806	27.05	4.88
1305.0	0.0362	19.39	11.27	1.721	24.20	4.80
1315.0	0.0356	16.63	10.03	1.659	21.12	4.48
1325.0	0.0359	13.86	8.94	1.550	18.18	4.32
1335.0	0.0349	11.10	7.94	1.397	15.34	4.24
1345.0	0.0349	8.32	6.86	1.214	12.41	4.08
1355.0	0.0336	6.94	6.40	1.085	11.03	4.08
1365.0	0.0336	5.56	5.86	0.949	9.56	4.00
1375.0	0.0330	4.17	5.55	0.751	8.33	4.16
1385.0	0.0327	2.78	5.09	0.546	6.94	4.16
1395.0	0.0320	1.39	4.47	0.311	5.39	4.00
1425.0	0.0304	0.0	3.68	0.0	3.68	3.68
1435.0	0.0304	1.39	3.91	0.357	4.84	3.44
1445.0	0.0310	2.79	4.05	0.688	5.91	3.12
1455.0	0.0310	4.18	4.27	0.977	7.06	2.88
1465.0	0.0314	5.57	4.66	1.196	8.37	2.80
1475.0	0.0320	8.35	5.50	1.517	11.07	2.72
1485.0	0.0327	11.12	6.27	1.774	13.68	2.56
1500.0	0.0339	13.88	7.19	1.931	16.45	2.56
1515.0	0.0352	16.64	8.35	1.993	19.44	2.80
1530.0	0.0362	19.39	9.51	2.040	22.43	3.04
1545.0	0.0375	22.13	10.58	2.092	25.33	3.20
1560.0	0.0395	24.85	12.05	2.063	28.61	3.76
1575.0	0.0420	27.54	13.18	2.089	31.54	4.00
1590.0	0.0460	30.17	14.70	2.052	34.81	4.64
1605.0	0.0496	32.78	15.97	2.053	37.83	5.04
1620.0	0.0532	35.38	17.40	2.034	40.99	5.61
1635.0	0.0575	37.93	18.81	2.017	44.10	6.17
1650.0	0.0614	40.47	20.22	2.002	47.19	6.73
1665.0	0.0647	43.01	21.22	2.027	49.90	6.89
1680.0	0.0684	45.52	22.54	2.019	52.89	7.37

TIME ELAPSED	AXIAL DEF	Q	P	N	SIGMA1	SIGMA3
1695.0	0.0724	47.99	23.52	2.040	55.52	7.53
1710.0	0.0765	50.44	24.02	2.100	57.65	7.21
1740.0	0.0819	52.78	24.80	2.128	59.99	7.21
1755.0	0.0825	52.74	24.95	2.114	60.11	7.37
1785.0	0.0832	52.70	25.42	2.074	60.55	7.85
1821.0	0.0835	52.68	25.57	2.060	60.69	8.01
1930.0	0.0846	52.63	29.23	1.800	64.32	11.69
2745.0	0.0856	52.57	29.46	1.785	64.50	11.93
2755.0	0.0856	49.94	28.18	1.772	61.47	11.53
2765.0	0.0859	47.29	26.90	1.758	58.43	11.13
2775.0	0.0856	44.68	25.87	1.727	55.65	10.97
2785.0	0.0849	42.09	24.92	1.689	52.98	10.89
2795.0	0.0852	39.44	23.72	1.663	50.01	10.57
2835.0	0.0846	36.84	22.45	1.641	47.01	10.17
2855.0	0.0846	34.21	21.17	1.616	43.98	9.77
2865.0	0.0842	31.59	20.46	1.544	41.52	9.93
2875.0	0.0842	28.96	19.66	1.473	38.97	10.01
4255.0	0.0842	26.32	19.03	1.384	36.57	10.25
4265.0	0.0836	21.07	17.36	1.214	31.40	10.33
4275.0	0.0829	15.82	15.36	1.030	25.91	10.09
4285.0	0.0822	10.55	13.13	0.804	20.16	9.61
4295.0	0.0808	7.93	12.17	0.651	17.46	9.53
4305.0	0.0808	6.61	11.65	0.567	16.06	9.45
4315.0	0.0805	5.29	10.73	0.493	14.26	8.97
4325.0	0.0795	3.97	10.29	0.386	12.94	8.97
4335.0	0.0785	2.65	9.69	0.273	11.46	8.81
4345.0	0.0775	1.33	8.85	0.150	9.73	8.41
4355.0	0.0764	0.0	8.33	0.0	8.33	8.33

STC TEST 006 PERPENDICULAR

SOIL MIXED 20 1 69 SAMPLE PREPARED 11 2 69

TEST STARTED 19 2 69 TEST COMPLETED 21 2 69

ORIGINAL LENGTH 1.643IN ORIGINAL AREA 1.769SQ.IN.

CONSOLIDATION PRESSURE 10.24PSI

NOTES 1 AFTER CONSOLIDATION SAMPLE STOOD UNDER NO LOAD FOR FIVE DAYS

2 PORE WATER PRESSURE DECREASED BY 1.29PSI

MOISTURE CONTENT OF COMPACTED SAMPLE 0.2619 0.2605

DRY DENSITY OF COMPACTED SAMPLE 94.06LB/FT3

DEGREE OF SATURATION OF COMPACTED SAMPLE 96.85PER CENT

INITIAL VOID RATIO 0.6850

FINAL MOISTURE CONTENT 0.2704 0.2675 0.2611

FINAL VOID RATIO 0.6712

TIME ELAPSED	AXIAL DEF	Q	P	N	SIGMA1	SIGMA3
0.0	0.0	0.0	10.24	0.0	10.24	10.24
10.0	0.0012	1.42	10.20	0.139	11.14	9.72
20.0	0.0012	2.84	10.09	0.281	11.98	9.14
30.0	0.0009	4.26	10.05	0.424	12.89	8.63
40.0	0.0021	5.67	9.61	0.590	13.40	7.72
50.0	-.0239	7.27	9.38	0.776	14.22	6.95
60.0	0.0026	8.50	9.20	0.924	14.87	6.37
120.0	0.0029	8.50	8.75	0.971	14.42	5.92
130.0	0.0031	9.91	9.03	1.098	15.64	5.73
145.0	0.0049	11.31	9.17	1.233	16.71	5.40
160.0	0.0061	12.71	9.25	1.374	17.72	5.02
175.0	0.0073	14.10	9.65	1.461	19.06	4.95
190.0	0.0114	16.85	10.57	1.595	21.81	4.95
255.0	0.0126	16.83	10.56	1.594	21.78	4.95
270.0	0.0144	19.60	11.68	1.679	24.75	5.14
285.0	0.0171	22.34	12.85	1.739	27.75	5.40
300.0	0.0207	25.04	14.07	1.780	30.77	5.73
315.0	0.0246	27.72	15.35	1.806	33.83	6.11
360.0	0.0249	27.71	15.15	1.828	33.63	5.92
375.0	0.0273	30.40	16.44	1.849	36.71	6.31
405.0	0.0279	30.38	16.43	1.849	36.69	6.31
425.0	0.0298	33.08	17.85	1.854	39.91	6.82
440.0	0.0331	35.72	19.31	1.850	43.12	7.40
455.0	0.0352	38.38	20.58	1.865	46.17	7.79
470.0	0.0395	40.94	22.08	1.854	49.37	8.43
485.0	0.0419	43.56	23.66	1.841	52.70	9.14
500.0	0.0444	46.16	25.11	1.838	55.89	9.72
605.0	0.0462	46.07	25.79	1.786	56.51	10.43
750.0	0.0469	46.04	25.91	1.777	56.61	10.56
1475.0	0.0472	46.03	25.45	1.808	56.14	10.11
1495.0	0.0475	43.31	24.74	1.750	53.61	10.30
1505.0	0.0481	37.87	22.80	1.661	48.04	10.18
1515.0	0.0472	32.49	20.94	1.552	42.60	10.11
1535.0	0.0469	32.50	20.94	1.552	42.61	10.11
1545.0	0.0472	27.08	19.01	1.424	37.06	9.98
1555.0	0.0466	21.67	16.95	1.279	31.40	9.72
1565.0	0.0472	32.49	19.97	1.627	41.63	9.14
1695.0	0.0475	43.31	24.16	1.793	53.03	9.72
1710.0	0.0478	54.12	28.15	1.922	64.23	10.11
1725.0	0.0524	53.85	29.48	1.827	65.38	11.53
1740.0	0.0580	58.89	32.19	1.829	71.45	12.56
1755.0	0.0639	63.84	35.45	1.801	78.01	14.17
1785.0	0.0649	63.77	35.88	1.777	78.40	14.63
1800.0	0.0693	68.76	38.19	1.800	84.03	15.27
1815.0	0.0699	68.72	38.18	1.800	83.99	15.27
1830.0	0.0702	68.69	38.62	1.779	84.41	15.72
1845.0	0.0747	73.62	41.49	1.775	90.57	16.95
1860.0	0.0820	78.26	44.32	1.766	96.50	18.24
1875.0	0.0829	78.18	45.07	1.735	97.19	19.01
2020.0	0.0852	77.99	45.91	1.699	97.90	19.91
2125.0	0.0858	77.93	46.22	1.686	98.17	20.24
2140.0	0.0880	82.92	48.46	1.711	103.74	20.82
2240.0	0.0916	82.60	49.19	1.679	104.26	21.66
2845.0	0.0935	82.43	48.87	1.687	103.83	21.40
3000.0	0.0938	82.40	48.80	1.688	103.73	21.33
3010.0	0.0938	77.25	46.95	1.645	98.45	21.20
3020.0	0.0938	72.10	45.37	1.589	93.43	21.33
3030.0	0.0938	66.95	43.65	1.534	88.28	21.33
3040.0	0.0935	61.82	41.62	1.485	82.83	21.01
3050.0	0.0935	56.67	39.84	1.423	77.62	20.95
3060.0	0.0929	51.55	37.87	1.361	72.24	20.69
3150.0	0.0926	41.26	33.15	1.245	60.66	19.40
3160.0	0.0913	30.99	29.08	1.065	49.74	18.75
3170.0	0.0903	20.68	23.84	0.867	37.63	16.95
3180.0	0.0890	15.53	21.16	0.734	31.51	15.98
3190.0	0.0880	10.37	18.15	0.571	25.06	14.69
3200.0	0.0848	5.20	14.94	0.348	18.41	13.21
3210.0	0.0832	2.61	13.24	0.197	14.97	12.37
3220.0	0.0819	0.0	11.27	0.0	11.27	11.27
3250.0	0.0813	0.0	11.08	0.0	11.08	11.08

STC TEST 007 PERPENDICULAR

SOIL MIXED 20 1 69 SAMPLE PREPARED 22 2 69

TEST STARTED 24 2 69 TEST COMPLETED 25 2 69

ORIGINAL LENGTH 1.642IN ORIGINAL AREA 1.769SQ.IN.

CONSOLIDATION PRESSURE 7.05PSI

NOTES 1 PORE PRESSURE RESPONSE SEEMED SLUGGISH

2 VALUES OF P TOWARDS END OF TEST TOO LOW

MOISTURE CONTENT OF COMPACTED SAMPLE 0.2559 0.2564

DRY DENSITY OF COMPACTED SAMPLE 93.93LB/FT3

DEGREE OF SATURATION OF COMPACTED SAMPLE 94.64PER CENT

INITIAL VOID RATIO 0.6874

FINAL MOISTURE CONTENT 0.2772 0.2793 0.2683

FINAL VOID RATIO 0.6928

TIME ELAPSED	AXIAL DEF	Q	P	N	SIGMA1	SIGMA3
0.0	0.0	0.0	7.05	0.0	7.05	7.05
10.0	0.0	1.41	7.09	0.199	8.03	6.62
30.0	-.0003	2.82	7.13	0.396	9.01	6.18
60.0	0.0009	4.23	6.87	0.615	9.69	5.46
75.0	0.0026	5.63	7.05	0.798	10.80	5.18
90.0	0.0049	7.02	6.94	1.011	11.61	4.60
105.0	0.0078	8.39	7.25	1.157	12.85	4.45
120.0	0.0139	11.12	7.87	1.413	15.29	4.17
135.0	0.0195	13.83	8.92	1.550	18.14	4.31
150.0	0.0242	16.51	10.03	1.646	21.04	4.53
195.0	0.0299	19.15	4.85	3.946	17.62	-1.53
210.0	0.0325	21.83	5.82	3.752	20.37	-1.46
225.0	0.0367	24.45	6.69	3.654	22.99	-1.46
240.0	0.0412	27.04	7.63	3.545	25.65	-1.39
255.0	0.0515	32.10	10.32	3.109	31.72	-0.38
270.0	0.0603	37.10	11.85	3.132	36.58	-0.52
285.0	0.0710	41.92	14.10	2.973	42.05	0.13
300.0	0.0810	46.65	15.82	2.948	46.92	0.27
315.0	0.0929	51.16	18.48	2.768	52.59	1.43
390.0	0.0941	51.09	19.83	2.577	53.89	2.80
405.0	0.1037	55.61	21.26	2.616	58.33	2.72
435.0	0.1194	59.60	23.31	2.557	63.05	3.45
450.0	0.1494	67.17	28.50	2.357	73.28	6.11
15.0	0.1537	66.82	30.48	2.193	75.03	8.20
30.0	0.1824	73.78	32.08	2.300	81.26	7.48
60.0	0.1855	73.50	32.63	2.252	81.63	8.13
720.0	0.1869	73.37	33.82	2.170	82.73	9.36
1410.0	0.1901	73.09	36.68	1.993	85.40	12.31
1420.0	0.1901	63.95	33.70	1.898	76.34	12.39
1430.0	0.1894	54.87	30.67	1.789	67.25	12.39
1440.0	0.1883	45.78	27.29	1.678	57.81	12.02
1450.0	0.1862	27.54	21.35	1.290	39.71	12.17
1460.0	0.1831	9.22	14.45	0.638	20.59	11.38
1470.0	0.1800	4.63	12.56	0.368	15.64	11.02
1555.0	0.1782	2.32	11.07	0.209	12.61	10.29
1565.0	0.1765	0.0	10.08	0.0	10.08	10.08

STC TEST 008 PERPENDICULAR

SOIL MIXED 20 1 69 SAMPLE PREPARED 22 2 69

TEST STARTED 24 2 69 TEST COMPLETED 25 2 69

ORIGINAL LENGTH 1.637IN ORIGINAL AREA 1.772SQ.IN.

CONSOLIDATION PRESSURE 5.42PSI

NOTES 1 DEFORMED SHAPE CONCAVE BETWEEN PINS

MOISTURE CONTENT OF COMPACTED SAMPLE 0.2547 0.2587

DRY DENSITY OF COMPACTED SAMPLE 94.34LB/FT3

DEGREE OF SATURATION OF COMPACTED SAMPLE 95.89PER CENT

INITIAL VOID RATIO 0.6801

FINAL MOISTURE CONTENT 0.2739 0.2833 0.2763

FINAL VOID RATIO 0.6987

TIME ELAPSED	AXIAL DEF	Q	P	N	SIGMA1	SIGMA3
0.0	0.0	0.0	5.42	0.0	5.42	5.42
10.0	0.0000	1.40	5.37	0.261	6.30	4.90
25.0	0.0010	2.80	5.19	0.539	7.06	4.26
40.0	0.0029	4.19	5.14	0.815	7.93	3.74
70.0	0.0058	5.57	5.28	1.056	8.99	3.42
85.0	0.0084	6.95	5.74	1.211	10.37	3.42
100.0	0.0119	8.30	6.19	1.342	11.73	3.42
115.0	0.0174	11.01	7.35	1.498	14.69	3.68
130.0	0.0230	13.69	8.63	1.586	17.75	4.07
145.0	0.0282	16.34	9.96	1.640	20.85	4.52
160.0	0.0332	18.96	11.42	1.661	24.06	5.10
205.0	0.0395	21.53	12.73	1.692	27.08	5.55
220.0	0.0421	24.15	14.24	1.696	30.35	6.19
235.0	0.0468	26.70	15.74	1.697	33.54	6.84
250.0	0.0566	31.72	18.83	1.684	39.98	8.26
265.0	0.0654	36.66	21.96	1.669	46.40	9.74
280.0	0.0496	42.60	25.55	1.667	53.96	11.35
295.0	0.0817	46.31	28.47	1.627	59.34	13.03
310.0	0.0925	50.85	31.79	1.600	65.69	14.84
325.0	0.1034	55.27	35.00	1.579	71.84	16.58
400.0	0.1069	55.05	34.80	1.582	71.50	16.45
415.0	0.1141	59.57	38.24	1.558	77.95	18.38
445.0	0.1299	63.38	41.38	1.532	83.64	20.25
460.0	0.1431	67.22	44.53	1.510	89.35	22.13
625.0	0.1508	66.61	43.88	1.518	88.29	21.67
640.0	0.1590	70.68	47.17	1.498	94.29	23.61
670.0	0.1647	70.21	47.01	1.493	93.82	23.61
730.0	0.1662	70.08	46.78	1.498	93.50	23.42
1420.0	0.1715	69.63	46.11	1.510	92.53	22.90
1430.0	0.1715	64.99	44.63	1.456	87.96	22.96
1440.0	0.1715	60.35	43.08	1.401	83.31	22.96
1450.0	0.1700	55.81	41.31	1.351	78.52	22.71
1460.0	0.1704	51.14	39.56	1.293	73.65	22.51
1470.0	0.1704	46.49	37.56	1.238	68.55	22.06
1480.0	0.1696	37.22	33.50	1.111	58.32	21.09
1565.0	0.1681	27.97	28.93	0.967	47.58	19.61
1575.0	0.1670	18.67	24.41	0.765	36.86	18.19
1585.0	0.1639	9.37	18.80	0.498	25.05	15.68
1595.0	0.1632	7.03	17.31	0.406	22.00	14.97
1650.0	0.1616	4.70	15.50	0.303	18.63	13.93
1660.0	0.1598	2.35	13.88	0.170	15.45	13.10
1685.0	0.1560	0.0	11.81	0.0	11.81	11.81

STC TEST 009 PERPENDICULAR

SOIL MIXED 1 3 69 SAMPLE PREPARED 2 3 69

TEST STARTED 14 3 69 TEST COMPLETED 15 3 69

ORIGINAL LENGTH 1.579IN ORIGINAL AREA 1.762SQ.IN.

CONSOLIDATION PRESSURE 19.21PSI

NOTES 1 VERY UNIFORM DEFORMED SHAPE, NO SLIP PLANES VISIBLE

MOISTURE CONTENT OF COMPACTED SAMPLE 0.2610 0.2631

DRY DENSITY OF COMPACTED SAMPLE 93.43LB/FT3

DEGREE OF SATURATION OF COMPACTED SAMPLE 95.58PER CENT

INITIAL VOID RATIO 0.6964

FINAL MOISTURE CONTENT 0.2537 0.2504 0.2430

FINAL VOID RATIO 0.6266

TIME ELAPSED	AXIAL DEF	Q	P	N	SIGMA1	SIGMA3
0.0	0.0	0.0	19.21	0.0	19.21	19.21
10.0	-.0000	1.46	19.22	0.076	20.19	18.73
20.0	0.0010	2.92	19.30	0.151	21.24	18.33
30.0	0.0003	4.38	19.15	0.229	22.06	17.69
40.0	0.0006	5.83	19.07	0.306	22.96	17.13
50.0	0.0010	7.29	19.00	0.384	23.86	16.57
60.0	0.0016	8.74	18.52	0.472	24.35	15.61
70.0	0.0016	10.20	18.52	0.551	25.32	15.12
80.0	0.0016	11.65	18.61	0.626	26.38	14.72
90.0	0.0026	14.55	18.69	0.779	28.40	13.84
105.0	0.0039	17.44	18.94	0.921	30.57	13.12
120.0	0.0058	20.31	19.49	1.042	33.03	12.72
135.0	0.0087	23.14	20.28	1.141	35.71	12.56
150.0	0.0107	25.99	21.22	1.224	38.55	12.56
165.0	0.0113	25.97	21.14	1.229	38.45	12.48
183.0	0.0139	28.78	22.31	1.290	41.50	12.72
195.0	0.0152	31.61	23.50	1.345	44.58	12.96
210.0	0.0178	34.40	24.91	1.381	47.84	13.44
225.0	0.0188	34.36	24.82	1.385	47.72	13.36
240.0	0.0205	37.16	26.15	1.421	50.93	13.76
255.0	0.0231	39.91	27.63	1.445	54.24	14.32
270.0	0.0254	42.66	29.11	1.466	57.55	14.88
285.0	0.0287	45.35	30.48	1.488	60.72	15.37
300.0	0.0310	48.07	31.95	1.505	64.00	15.93
315.0	0.0334	50.78	33.49	1.516	67.35	16.57
332.0	0.0364	53.43	34.94	1.529	70.56	17.13
345.0	0.0367	53.42	34.93	1.529	70.54	17.13
360.0	0.0387	56.11	36.47	1.538	73.88	17.77
375.0	0.0407	58.79	38.17	1.540	77.36	18.57
390.0	0.0434	61.42	39.76	1.545	80.71	19.29
420.0	0.0467	63.99	41.10	1.557	83.76	19.77
435.0	0.0481	66.67	42.72	1.561	87.16	20.49
450.0	0.0555	71.67	45.98	1.559	93.76	22.09
465.0	0.0613	76.71	49.10	1.562	100.24	23.54
480.0	0.0664	81.73	52.46	1.558	106.95	25.22
495.0	0.0750	86.38	55.69	1.551	113.28	26.90
510.0	0.0823	91.06	58.85	1.547	119.56	28.50
525.0	0.0897	95.64	62.14	1.539	125.90	30.26
560.0	0.0918	95.42	61.83	1.543	125.44	30.02
585.0	0.0989	99.94	65.26	1.531	131.88	31.95
605.0	0.1070	104.24	68.38	1.525	137.87	33.63
780.0	0.1106	103.82	67.43	1.540	136.65	32.83
790.0	0.1106	98.63	65.70	1.501	131.46	32.83
800.0	0.1106	93.44	64.37	1.452	126.67	33.23
810.0	0.1106	83.06	60.59	1.371	115.97	32.91
820.0	0.1113	72.62	56.63	1.282	105.04	32.43
830.0	0.1095	51.97	47.99	1.083	82.64	30.66
840.0	0.1092	31.20	38.66	0.807	59.46	28.26
1585.0	0.1092	31.20	36.66	0.851	57.46	26.26
1595.0	0.1074	20.84	32.97	0.632	46.86	26.02
1605.0	0.1052	10.45	26.86	0.389	33.82	23.38
1615.0	0.1034	5.23	23.76	0.220	27.25	22.01
1625.0	0.1009	0.0	19.93	0.0	19.93	19.93
1635.0	0.1006	0.0	19.69	0.0	19.69	19.69

STC TEST 010 PERPENDICULAR

SOIL MIXED 1 3 69 SAMPLE PREPARED 15 3 69

TEST STARTED 18 3 69 TEST COMPLETED 19 3 69

ORIGINAL LENGTH 1.645IN ORIGINAL AREA 1.762SQ.IN.

CONSOLIDATION PRESSURE 14.81PSI

NOTES 1 SOME SLIGHT BARRELLING IN DEFORMED SHAPE

2 SLIP PLANE AT DEFORMATION OF 0.1004

MOISTURE CONTENT OF COMPACTED SAMPLE 0.2547 0.2529

DRY DENSITY OF COMPACTED SAMPLE 94.04LB/FT3

DEGREE OF SATURATION OF COMPACTED SAMPLE 94.08PER CENT

INITIAL VOID RATIO 0.6854

FINAL MOISTURE CONTENT 0.2598 0.2698 0.2563

FINAL VOID RATIO 0.6555

TIME ELAPSED	AXIAL DEF	Q	P	N	SIGMA1	SIGMA3
0.0	0.0	0.0	14.81	0.0	14.81	14.81
19.0	0.0003	1.44	14.49	0.099	15.44	14.01
34.0	0.0003	2.87	14.73	0.195	16.64	13.77
85.0	0.0003	4.31	14.16	0.304	17.03	12.73
101.0	0.0009	5.74	14.00	0.410	17.82	12.09
113.0	0.0016	7.17	14.00	0.512	18.77	11.61
130.0	0.0028	8.59	13.27	0.647	18.99	10.40
143.0	0.0038	10.01	13.58	0.737	20.26	10.24
160.0	0.0041	11.44	13.42	0.853	21.04	9.60
182.0	0.0075	14.25	13.95	1.021	23.45	9.20
193.0	0.0110	17.04	14.72	1.157	26.08	9.04
206.0	0.0151	19.80	15.32	1.292	28.52	8.72
270.0	0.0199	22.52	16.39	1.374	31.40	8.88
289.0	0.0230	25.25	17.78	1.420	34.61	9.36
299.0	0.0266	27.95	18.76	1.490	37.40	9.44
319.0	0.0307	30.62	20.29	1.509	40.70	10.08
336.0	0.0349	33.25	21.49	1.547	43.66	10.40
416.0	0.0398	35.84	23.31	1.537	47.21	11.37
435.0	0.0414	38.54	24.13	1.597	49.82	11.29
446.0	0.0453	41.12	25.79	1.594	53.21	12.09
480.0	0.0518	43.56	27.65	1.576	56.69	13.13
498.0	0.0555	46.11	28.90	1.596	59.64	13.53
521.0	0.0614	48.51	30.10	1.612	62.44	13.93
537.0	0.0657	50.97	31.80	1.603	65.78	14.81
555.0	0.0724	53.27	33.53	1.589	69.04	15.77
570.0	0.0781	55.59	34.62	1.606	71.68	16.09
612.0	0.0845	57.83	36.33	1.592	74.88	17.05
630.0	0.0907	60.06	37.47	1.603	77.51	17.45
648.0	0.0979	62.17	38.98	1.595	80.43	18.25
685.0	0.1182	65.83	42.28	1.557	86.17	20.34
706.0	0.1323	69.77	44.23	1.577	90.74	20.98
1389.0	0.1405	69.11	45.78	1.510	91.85	22.74
1399.0	0.1405	59.23	42.24	1.402	81.73	22.50
1414.0	0.1398	49.40	38.97	1.268	71.90	22.50
1429.0	0.1387	29.68	31.51	0.942	51.30	21.62
1439.0	0.1358	14.89	24.26	0.614	34.18	19.30
1451.0	0.1315	4.99	18.15	0.275	21.48	16.49
1466.0	0.1269	0.0	14.09	0.0	14.09	14.09

STC TEST 011 PERPENDICULAR

SOIL MIXED 1 3 69 SAMPLE PREPARED 15 3 69

TEST STARTED 18 3 69 TEST COMPLETED 19 3 69

ORIGINAL LENGTH 1.596IN ORIGINAL AREA 1.767SQ.IN.

CONSOLIDATION PRESSURE 11.02PSI

NOTES 1 SOME SLIGHT BARRELLING IN DEFORMED SHAPE

2 SLIP PLANE AT DEFORMATION OF 0.0953

MOISTURE CONTENT OF COMPACTED SAMPLE 0.2528 0.2553

DRY DENSITY OF COMPACTED SAMPLE 94.20LB/FT3

DEGREE OF SATURATION OF COMPACTED SAMPLE 94.54PER CENT

INITIAL VOID RATIO 0.6827

FINAL MOISTURE CONTENT 0.2653 0.2699 0.2638

FINAL VOID RATIO 0.6719

TIME ELAPSED	AXIAL DEF	Q	P	N	SIGMA1	SIGMA3
0.0	0.0	0.0	11.02	0.0	11.02	11.02
9.0	-.0003	1.42	10.91	0.130	11.86	10.44
24.0	-.0000	2.84	10.74	0.265	12.64	9.79
66.0	-.0000	4.26	10.38	0.411	13.22	8.96
82.0	0.0006	5.68	10.20	0.557	13.99	8.31
98.0	0.0009	7.10	10.03	0.708	14.76	7.67
111.0	0.0024	8.51	9.99	0.852	15.66	7.15
128.0	0.0050	9.90	10.06	0.984	16.66	6.76
140.0	0.0062	11.30	10.34	1.093	17.87	6.57
159.0	0.0089	14.08	11.20	1.257	20.59	6.51
174.0	0.0134	16.82	12.31	1.367	23.52	6.70
192.0	0.0197	19.50	13.65	1.429	26.65	7.15
256.0	0.0233	22.21	14.94	1.486	29.74	7.54
269.0	0.0267	24.90	16.48	1.511	33.08	8.18
285.0	0.0327	27.49	17.99	1.528	36.32	8.83
299.0	0.0358	30.14	19.52	1.544	39.61	9.47
327.0	0.0407	32.71	21.15	1.547	42.96	10.25
397.0	0.0463	35.24	22.64	1.557	46.13	10.89
415.0	0.0497	37.81	24.27	1.558	49.48	11.66
432.0	0.0565	40.22	25.97	1.548	52.79	12.57
459.0	0.0641	42.56	27.66	1.539	56.03	13.47
485.0	0.0697	44.94	29.36	1.531	59.32	14.37
502.0	0.0748	47.33	30.92	1.530	62.47	15.15
524.0	0.0825	49.54	32.63	1.518	65.66	16.12
534.0	0.0886	51.80	34.22	1.514	68.76	16.95
554.0	0.1006	53.68	35.75	1.501	71.53	17.86
584.0	0.1068	55.84	37.25	1.499	74.48	18.63
615.0	0.1180	60.16	39.59	1.520	79.69	19.53
624.0	0.1180	55.14	37.72	1.462	74.48	19.34
642.0	0.1177	45.13	33.87	1.333	63.96	18.82
666.0	0.1160	30.15	27.39	1.101	47.49	17.34
695.0	0.1124	12.61	18.90	0.667	27.31	14.70
706.0	0.1104	7.58	16.19	0.468	21.25	13.66
717.0	0.1074	2.54	12.70	0.200	14.40	11.86
732.0	0.1044	0.0	10.89	0.0	10.89	10.89

STC TEST 012 PARALLEL

SOIL MIXED 18 3 69 SAMPLE PREPARED 19 3 69

TEST STARTED 31 3 69 TEST COMPLETED 31 3 69

ORIGINAL LENGTH 1.617IN ORIGINAL AREA 1.753SQ.IN.

CONSOLIDATION PRESSURE 0.90PSI

NOTES 1 NO SLIP PLANES ON STRIPPED SAMPLE

2 SAMPLE ALLOWED TO CREEP FOR SIX DAYS UNDER MAXIMUM LOAD

MOISTURE CONTENT OF COMPACTED SAMPLE 0.2646 0.2546

DRY DENSITY OF COMPACTED SAMPLE 93.96LB/FT3

DEGREE OF SATURATION OF COMPACTED SAMPLE 96.00PER CENT

INITIAL VOID RATIO 0.6869

FINAL MOISTURE CONTENT 0.2730 0.2711 0.2778

FINAL VOID RATIO 0.6910

TIME ELAPSED	AXIAL DEF	Q	P	N	SIGMA1	SIGMA3
0.0	0.0	0.0	0.90	0.0	0.90	0.90
5.0	0.0003	0.0	0.90	0.0	0.90	0.90
25.0	0.0012	1.42	1.05	1.353	2.00	0.58
35.0	0.0048	2.83	1.14	2.497	3.02	0.19
65.0	0.0114	4.22	1.60	2.642	4.41	0.19
75.0	0.0186	5.59	2.25	2.487	5.97	0.38
118.0	0.0265	6.93	2.89	2.400	7.51	0.58
135.0	0.0317	8.27	3.53	2.344	9.04	0.77
197.0	0.0385	9.58	4.22	2.269	10.61	1.03
213.0	0.0426	10.91	4.92	2.216	12.19	1.29
224.0	0.0491	12.19	5.74	2.125	13.86	1.67
235.0	0.0519	13.50	6.37	2.120	15.37	1.87
252.0	0.0582	14.75	7.11	2.076	16.94	2.19
263.0	0.0620	16.03	7.79	2.057	18.48	2.45
291.0	0.0728	18.48	9.25	1.997	21.58	3.09
305.0	0.0754	19.75	10.00	1.975	23.17	3.42
320.0	0.0809	20.94	10.78	1.942	24.74	3.80
330.0	0.0841	22.17	11.45	1.936	26.23	4.06
340.0	0.0893	23.34	12.23	1.909	27.79	4.45
355.0	0.0932	24.53	13.01	1.885	29.37	4.83
375.0	0.0939	24.52	12.94	1.894	29.29	4.77
393.0	0.0958	25.75	13.68	1.883	30.84	5.09
405.0	0.0998	26.92	14.39	1.871	32.34	5.41
417.0	0.1047	28.05	15.15	1.851	33.85	5.80
430.0	0.1080	29.21	15.93	1.834	35.40	6.19
525.0	0.1110	29.12	15.89	1.832	35.30	6.19
780.0	0.1120	29.08	15.75	1.846	35.14	6.06
1450.0	0.1130	29.05	15.61	1.860	34.98	5.93
2265.0	0.1137	29.03	15.54	1.868	34.89	5.87
3513.0	0.1140	29.02	15.60	1.860	34.95	5.93
4945.0	0.1140	29.02	15.67	1.852	35.01	6.00
6360.0	0.1144	29.01	15.73	1.844	35.07	6.06
7805.0	0.1144	29.01	15.86	1.829	35.20	6.19
8750.0	0.1147	29.00	15.92	1.821	35.25	6.25
8760.0	0.1150	23.94	14.43	1.659	30.39	6.45
8770.0	0.1140	18.92	12.56	1.507	25.18	6.25
8814.0	0.1140	13.88	10.43	1.331	19.68	5.80
8880.0	0.1127	8.84	8.11	1.091	14.00	5.16
8905.0	0.1100	5.07	6.14	0.826	9.52	4.45
8945.0	0.1077	2.54	4.59	0.554	6.28	3.74
8962.0	0.1020	0.0	2.83	0.0	2.83	2.83

STC TEST 014 PERPENDICULAR

SOIL MIXED 18 3 69 SAMPLE PREPARED 8 5 69

TEST STARTED 13 5 69 TEST COMPLETED 19 5 69

ORIGINAL LENGTH 1.559IN ORIGINAL AREA 1.774SQ.IN.

CONSOLIDATION PRESSURE 10.83PSI

NOTES 1 REASONABLE DEFORMED SHAPE

2 HEIGHT OF STRIPPED SAMPLE 1.439, 1.434, 1.424, 1.432 IN.

MOISTURE CONTENT OF COMPACTED SAMPLE 0.2582 0.2615

DRY DENSITY OF COMPACTED SAMPLE 94.00LB/FT3

DEGREE OF SATURATION OF COMPACTED SAMPLE 96.19PER CENT

INITIAL VOID RATIO 0.6862

FINAL MOISTURE CONTENT 0.2623 0.2650 0.2662

FINAL VOID RATIO 0.6697

TIME ELAPSED	AXIAL DEF	Q	P	N	SIGMA1	SIGMA3
0.0	0.0	0.0	10.83	0.0	10.83	10.83
10.0	0.0010	1.42	10.72	0.132	11.67	10.25
20.0	0.0014	2.83	10.55	0.269	12.44	9.60
30.0	0.0010	4.25	10.18	0.417	13.02	8.77
90.0	0.0028	5.66	9.56	0.592	13.33	7.67
105.0	0.0028	7.07	9.51	0.744	14.23	7.15
120.0	0.0045	8.47	9.33	0.908	14.98	6.51
135.0	0.0066	9.86	9.28	1.063	15.86	5.99
150.0	0.0090	11.25	9.48	1.186	16.98	5.73
190.0	0.0142	13.98	10.20	1.371	19.52	5.54
205.0	0.0188	16.70	11.30	1.478	22.44	5.73
220.0	0.0241	19.38	12.65	1.533	25.57	6.19

TIME ELAPSED	AXIAL DEF	Q	P	N	SIGMA1	SIGMA3
235.0	0.0287	22.05	14.05	1.569	28.75	6.70
260.0	0.0337	24.67	15.44	1.598	31.89	7.22
275.0	0.0387	27.27	16.95	1.609	35.14	7.86
260.0	0.0441	29.83	18.45	1.617	38.34	8.51
305.0	0.0495	32.36	20.07	1.612	41.64	9.28
320.0	0.0553	34.84	21.61	1.613	44.84	9.99
335.0	0.0619	37.26	23.12	1.612	47.96	10.70
365.0	0.0685	39.64	24.69	1.606	51.12	11.47
380.0	0.0729	42.08	26.28	1.602	54.33	12.25
395.0	0.0792	44.41	27.89	1.592	57.50	13.09
410.0	0.0863	46.66	29.48	1.583	60.58	13.93
425.0	0.0935	48.86	31.12	1.570	63.69	14.83
440.0	0.0988	51.14	32.65	1.566	66.74	15.60
545.0	0.1034	50.88	32.56	1.562	66.48	15.60
560.0	0.1057	53.28	33.82	1.576	69.34	16.05
575.0	0.1134	55.34	35.73	1.549	72.62	17.28
590.0	0.1238	57.17	37.31	1.533	75.42	18.25
750.0	0.1305	56.74	37.16	1.527	74.99	18.25
1400.0	0.1332	56.56	36.84	1.535	74.55	17.99
2045.0	0.1328	56.59	36.98	1.530	74.70	18.12
3720.0	0.1336	56.53	37.54	1.506	75.23	18.70
4293.0	0.1340	56.51	37.86	1.493	75.53	19.02
4527.0	0.1336	56.53	37.87	1.493	75.55	19.02
4535.0	0.1340	54.05	37.17	1.454	73.20	19.15
4545.0	0.1336	49.16	35.73	1.376	68.50	19.34
4555.0	0.1324	39.38	31.96	1.232	58.21	18.83
4565.0	0.1328	29.52	27.83	1.061	47.51	17.99
4575.0	0.1313	19.72	23.14	0.852	36.29	16.57
4585.0	0.1285	9.89	17.67	0.560	24.27	14.38
4595.0	0.1265	4.96	14.68	0.338	17.98	13.02
4605.0	0.1254	2.48	12.95	0.192	14.60	12.12
4615.0	0.1222	0.0	11.09	0.0	11.09	11.09

STC TEST 015 PERPENDICULAR

SOIL MIXED 18 3 69 SAMPLE PREPARED 8 5 69

TEST STARTED 13 5 69 TEST COMPLETED 19 5 69

ORIGINAL LENGTH 1.601IN ORIGINAL AREA 1.781SQ.IN.

CONSOLIDATION PRESSURE 14.89PSI

NOTES 1 LOST CELL PRESSURE DURING SATURATION, SAMPLE CRACKED

2 HEIGHT OF STRIPPED SAMPLE 1.408, 1.414, 1.411, 1.403 IN.

MOISTURE CONTENT OF COMPACTED SAMPLE 0.2582 0.2569

DRY DENSITY OF COMPACTED SAMPLE 94.57LB/FT3

DEGREE OF SATURATION OF COMPACTED SAMPLE 96.77PER CENT

INITIAL VOID RATIO 0.6760

FINAL MOISTURE CONTENT 0.2557 0.2712 0.2580

FINAL VOID RATIO 0.6523

TIME ELAPSED	AXIAL DEF	Q	P	N	SIGMA1	SIGMA3
0.0	0.0	0.0	14.89	0.0	14.89	14.89
10.0	-.0003	1.42	14.64	0.097	15.59	14.17
20.0	0.0003	2.83	14.63	0.194	16.52	13.69
30.0	0.0003	4.25	14.22	0.299	17.06	12.81
85.0	0.0007	5.66	13.65	0.415	17.43	11.77
100.0	0.0017	7.07	13.32	0.531	18.04	10.97
115.0	0.0021	8.48	12.99	0.653	18.65	10.16
130.0	0.0034	9.89	12.66	0.781	19.25	9.36
145.0	0.0048	11.28	12.40	0.910	19.92	8.64
185.0	0.0083	14.05	12.29	1.144	21.65	7.60
200.0	0.0107	16.82	13.05	1.289	24.26	7.44
215.0	0.0159	19.52	13.95	1.400	26.96	7.44

TIME ELAPSED	AXIAL DEF	Q	P	N	SIGMA1	SIGMA3
230.0	0.0187	22.25	14.86	1.498	29.69	7.44
255.0	0.0236	24.91	15.90	1.566	32.51	7.60
270.0	0.0240	24.90	16.14	1.543	32.74	7.84
255.0	0.0275	27.56	17.11	1.611	35.48	7.92
300.0	0.0310	30.21	18.39	1.643	38.53	8.32
315.0	0.0363	32.77	20.13	1.628	41.98	9.20
330.0	0.0406	35.35	21.39	1.653	44.95	9.60
360.0	0.0452	37.88	23.19	1.633	48.45	10.56
375.0	0.0478	40.48	24.46	1.655	51.45	10.97
390.0	0.0535	42.92	26.23	1.636	54.85	11.93
405.0	0.0579	45.39	27.62	1.644	57.88	12.49
420.0	0.0626	47.82	29.31	1.632	61.19	13.37
435.0	0.0674	50.22	29.63	1.695	63.11	12.89
540.0	0.0699	50.08	30.22	1.657	63.61	13.53
555.0	0.0721	52.59	31.06	1.693	66.12	13.53
570.0	0.0784	54.85	31.49	1.742	68.06	13.21
585.0	0.0840	57.11	31.77	1.798	69.84	12.73
750.0	0.0892	56.79	33.02	1.720	70.88	14.09
1395.0	0.0907	56.69	33.55	1.690	71.34	14.65
2040.0	0.0911	56.67	33.78	1.678	71.56	14.89
3715.0	0.0919	56.62	35.21	1.608	72.96	16.33
4287.0	0.0922	56.60	35.84	1.579	73.57	16.97
5960.0	0.0926	56.58	37.27	1.518	74.99	18.41
5975.0	0.0930	61.69	38.74	1.593	79.87	18.17
5990.0	0.1043	66.00	40.66	1.623	84.66	18.65
6005.0	0.1268	69.29	41.59	1.666	87.79	18.49
6020.0	0.1459	72.62	42.94	1.691	91.35	18.73
6035.0	0.1495	72.31	42.76	1.691	90.97	18.65
6062.0	0.1523	72.08	42.68	1.689	90.73	18.65
6369.0	0.1559	71.77	43.86	1.636	91.70	19.94
7307.0	0.1595	71.46	45.28	1.578	92.92	21.46
7318.0	0.1595	66.70	43.53	1.532	88.00	21.30
7330.0	0.1599	61.90	41.61	1.488	82.88	20.98
7340.0	0.1595	57.17	39.95	1.431	78.07	20.90
7350.0	0.1575	33.43	31.56	1.059	53.85	20.42
7394.0	0.1551	19.16	25.04	0.765	37.81	18.65
7405.0	0.1535	9.60	20.09	0.478	26.49	16.89
7415.0	0.1503	4.82	17.14	0.281	20.35	15.53
7425.0	0.1503	2.41	15.45	0.156	17.06	14.65
7490.0	0.1475	0.0	13.13	0.0	13.13	13.13

STC TEST 016 PARALLEL

SOIL MIXED 18 3 69 SAMPLE PREPARED 21 5 69

TEST STARTED 22 5 69 TEST COMPLETED 23 5 69

ORIGINAL LENGTH 1.568IN ORIGINAL AREA 1.758SQ.IN.

CONSOLIDATION PRESSURE 5.36PSI

NOTES 1 SLIP PLANE AT DEFORMATION OF 0.0890

2 SATURATION CHECK AT END OF TEST,100PER CENT

MOISTURE CONTENT OF COMPACTED SAMPLE 0.2641 0.2554

DRY DENSITY OF COMPACTED SAMPLE 93.98LB/FT3

DEGREE OF SATURATION OF COMPACTED SAMPLE 96.10PER CENT

INITIAL VOID RATIO 0.6866

FINAL MOISTURE CONTENT 0.2656 0.2617 0.2594

FINAL VOID RATIO 0.6618

TIME ELAPSED	AXIAL DEF	Q	P	N	SIGMA1	SIGMA3
0.0	0.0	0.0	5.36	0.0	5.36	5.36
10.0	0.0000	1.44	5.19	0.277	6.15	4.71
20.0	0.0018	2.87	4.96	0.578	6.87	4.01
30.0	0.0046	4.29	4.73	0.908	7.59	3.30
40.0	0.0095	5.69	4.87	1.169	8.67	2.97
50.0	0.0145	7.08	5.27	1.344	9.99	2.91
60.0	0.0202	8.45	5.79	1.459	11.42	2.97
70.0	0.0241	9.81	6.44	1.524	12.98	3.17
80.0	0.0281	11.17	7.02	1.591	14.47	3.30
90.0	0.0314	12.52	7.79	1.607	16.14	3.62
100.0	0.0353	13.86	8.43	1.644	17.67	3.81
120.0	0.0394	15.18	9.07	1.675	19.19	4.01

TIME ELAPSED	AXIAL DEF	Q	P	N	SIGMA1	SIGMA3
130.0	0.0412	16.53	9.77	1.691	20.79	4.26
140.0	0.0445	17.85	10.60	1.684	22.50	4.65
150.0	0.0467	19.17	11.30	1.697	24.08	4.91
160.0	0.0489	20.50	11.93	1.717	25.60	5.10
170.0	0.0518	21.79	12.75	1.709	27.28	5.49
180.0	0.0544	23.09	13.44	1.718	28.84	5.75
190.0	0.0574	24.37	14.13	1.725	30.38	6.00
200.0	0.0630	26.92	15.75	1.709	33.70	6.78
210.0	0.0667	29.50	17.19	1.716	36.86	7.36
287.0	0.0690	29.43	17.17	1.714	36.78	7.36
300.0	0.0709	32.04	18.55	1.727	39.91	7.88
310.0	0.0750	34.55	20.23	1.708	43.26	8.71
320.0	0.0803	36.99	21.75	1.700	46.42	9.42
1165.0	0.0834	36.87	21.78	1.693	46.36	9.49
1175.0	0.0841	39.47	22.84	1.728	49.15	9.68
1185.0	0.0860	42.02	24.46	1.718	52.47	10.46
1195.0	0.0926	44.32	26.13	1.696	55.68	11.36
1205.0	0.0987	46.61	27.67	1.685	58.74	12.13
1215.0	0.1061	48.80	29.30	1.665	61.83	13.04
1225.0	0.1120	51.03	30.82	1.656	64.84	13.81
1783.0	0.1163	50.78	30.67	1.656	64.53	13.74
1795.0	0.1163	45.70	29.04	1.574	59.51	13.81
1805.0	0.1163	40.63	27.35	1.485	54.43	13.81
1820.0	0.1139	28.00	22.37	1.252	41.04	13.04
1832.0	0.1124	15.30	16.27	0.941	26.47	11.16
1843.0	0.1112	10.22	13.93	0.734	20.74	10.52
1853.0	0.1088	5.12	11.00	0.465	14.42	9.29
1865.0	0.1069	2.57	9.31	0.276	11.02	8.46
1873.0	0.1026	0.0	7.49	0.0	7.49	7.49

APPENDIX G

LISTING OF REDUCED EXPERIMENTAL RESULTS FOR THE DRAINED TESTS

As in Appendix F the actual listing of the stress-strain data is preceded by a description of the sample.

The headings of the first five columns in the listing of results are the same as those in Appendix F, the remaining four are:-

'VOID R', gives the void ratio of the sample.

'QR', gives the value of q_r calculated from Eq.(5.13).

'NQR', gives the ratio $q_r/(p+3.0)$.

'DS', gives the evaluation of Drucker's Stability condition using Eq.(5.11).

```
C*************************************************************************
C
C   TO CALCULATE EFFECTIVE STRESSES AND STRAIN FROM THE RESULTS OF A DRAINED
C   TRIAXIAL TEST
C
C*************************************************************************
0001        DIMENSION TITLE(20),NOTES(20),SM(3),SP(3),TS(3),TC(3)
0002        DIMENSION Q(100),PRES(100),EL(100)
0003        DIMENSION T(100),Y(100),P(100),B(100),ET(100),EB(100),VRA(100)
0004        INTEGER TITLE,SM,SP,TS,TC
0005        INTEGER TITLE,TD,TH,TM,TP
0006        REAL MC1,MC2,MC(6),MD,MCA
C
C   FROM DATA READ INFORMATION ABOUT THE TEST IS CALCULATED AND PRINTED
C
0007      175 READ(1,100) OL,OD,OP,WO,N
0008          IF(OL.EQ.0.) GO TO 56
0009          AO = 3.1412*OD*OD/4.0
0010          IF(OD.EQ.0.) GO TO 56
0011          READ(1,101) (TITLE(I),I=1,20)
0012          WRITE(6,104) (TITLE(I),I=1,20)
0013          READ(1,107)(SM(I),I=1,3),(SP(I),I=1,3),(TS(I),I=1,3),(TC(I),I=1,3)
0014          WRITE(6,108)(SM(I),I=1,3),(SP(I),I=1,3)
0015          WRITE(6,601) (TS(I),I=1,3),(TC(I),I=1,3)
0016          WRITE(6,105) OL,AO
0017          WRITE(6,602) OP
0018          IF(N.EQ.0) GO TO 131
0019          DO 6 J=1,N
0020          READ(1,99) (NOTES(I),I=1,20)
0021          WRITE(6,98) J,(NOTES(I),I=1,20)
0022          IF(J.NE.1) GO TO 6
0023          WRITE(6,97)
0024        6 CONTINUE
0025      131 READ(1,109) W1,W2,W3,W4,W5,W6
0026          MC1 = (W2-W3)/(W3-W1)
0027          MC2 = (W5-W6)/(W6-W4)
0028          WRITE(6,110) MC1,MC2
0029          MD = 3.802*WO/5.317
0030          DD=MD/(1.+.5*(MC1+MC2))
0031          WRITE(6,111) DD
0032          VR = 158.50/DD-1.
0033          SR=100.0*(MD*(1.+VR)/(62.4*VR))-254.0/VR
0034          WRITE(6,112) SR
0035          WRITE(6,113) VR
0036          READ(1,109) W7,W8,W9,W10,W11,W12,W13,W14,W15
0037          MC(3)=(W8-W9)/(W9-W7)
0038          MC(4)=(W11-W12)/(W12-W10)
0039          MC(5)=(W14-W15)/(W15-W13)
0040          WRITE(6,114) MC(3),MC(4),MC(5)
C
C   TO CALCULATE THE FINAL VOID RATIO THE AVERAGE OF THE TWO SMALLEST FINAL
C   MOISTURE CONTENTS IS USED
C
0041          B1=0.5*(MC(3)+MC(4))
0042          B2=0.5*(MC(4)+MC(5))
0043          B3=0.5*(MC(5)+MC(3))
0044          MCA=B1
0045          IF(MCA.GT.B2) MCA=B2
```

```
0046              IF(MCA.GT.B3) MCA=B3
0047              VRF=2.54*MCA
0048              WRITE(6,115) VRF
                  C
                  C    A CORRECTION IS MADE TO THE INITIAL AREA OF THE SAMPLE TO ALLOW FOR THE
                  C    CHANGE DURING CONSOLIDATION
                  C
0049              AC=A0*(1.-.333*ALOG((1.+VR)/(1.+VRF)))**2
0050              READ(1,900) VRI
0051            900 FORMAT(F10.4)
0052              VS=W0/((1.+(MC1+MC2)/200.)*2.54)
0053              READ(1,100)F,G
                  C
                  C    THE MEASURED VALUES FOR EACH EXPERIMENTAL POINT ARE READ AND THE
                  C    REQUIRED PARAMETERS CALCULATED AND PRINTED
                  C
0054              DO 901 JK=1,100
0055              READ(1,102)TD,TH,TM,TP,Y(JK),P(JK),B(JK),ET(JK),EB(JK)
0056              TL=TP/60.+TM+TH*60.+TD*1440.
0057              IF(JK.EQ.1) TLI=TL
0058              T(JK)=TL-TLI
0059              IF(JK.EQ.1) GO TO 901
0060              IF(TL.EQ.0.) GO TO 906
0061            901 CONTINUE
0062            906 VRA(1)=VRI
0063              DO 902 KI=2,JK
0064              DB=(B(KI-1)-B(KI))
0065              IF(DB.LT.-10.) DB=0.
0066              DV=DB*0.01971
0067              DVR=DV/VS
0068              VRA(KI)=VRA(KI-1)+DVR
0069            902 CONTINUE
0070              VRC=VRA(JK)-VRF
0071              DO 903 KI=1,JK
0072            903 VRA(KI)=VRA(KI)-VRC
0073              EL(1)=0.
0074              PRES(1)=OP
0075              Q(1)=0.
0076              AA=AC
0077              DO 904 KI=2,JK
0078              DLM=1.-(ET(KI)-EB(KI))/(ET(KI-1)-EB(KI-1))
0079              EL(KI)=EL(KI-1)+DLM
0080              DVV=(VRA(KI)-VRA(KI-1))/(1.+VRA(KI))
0081              DRR=0.5*(DVV-DLM)
0082              AA=AA*(1.-DRR)**2
0083              Q(KI)=F*(P(KI)-P(1))/AA
0084              PRES(KI)=OP+0.333*Q(KI)
0085            904 CONTINUE
0086              J=1
0087              L=1
0088              IF(N.LT.3) K=24
0089              IF(N.GT.2) K=28
0090              IF(N.GT.6) K=32
0091             27 WRITE(6,200)
0092              WRITE(6,201)
0093              EM=2850.+126.000*EXP((0.754-VRA(KI))/0.0357)
0094              DO 905 KI=1,JK
0095              SIG=OP+Q(KI)
```

```
0096          907 R2=Q(KI)/PRES(KI)
0097              WRITE(6,106) T(KI),EL(KI),Q(KI),PRES(KI),R2,VRA(KI)
              C*****************************************************************************
              C
              C   CALCULATION OF ELASTIC AND PLASTIC COMPONENTS OF STRAIN
              C
              C*****************************************************************************
0098              IF(EL(KI).LE.0.0) GO TO 910
0099              DP=PRES(KI)-PRES(KI-1)
0100              DQ=Q(KI)-Q(KI-1)
0101              DVV=-(VRA(KI)-VRA(KI-1))/(1.+VRA(KI))
0102              DVE= 0.0112*DP/(PRES(KI)*(1.+VRA(KI)))
0103              DVP=DVV-DVE
0104              DE=EL(KI)-EL(KI-1)
0105              DEF=DQ/EM
0106              DEP=DE-DEE-0.333*DVP
0107              IF(DEP.LE.0.0) GO TO 910
0108              DS =DVP*DP+DEP*DQ
0109              QL=Q(KI)+PRES(1)*DVV/DE
0110              NQR=QL/(PRES(KI)+3.0)
0111              WRITE(6,96) QL,NQR,DS
0112          910 K=K+1
0113              J=J+1
0114              L=L+1
0115              IF(L.NE.5) GO TO 905
0116              WRITE(6,605)'
0117              L=1
0118              K4=K/4
0119              IF(K4.NE.9) GO TO 905
0120              K=1
0121              WRITE(6,619)
0122              WRITE(6,201)
0123          905 CONTINUE
0124              GO TO 175
0125           96 FORMAT(1H+,58X,F6.2,3X,F5.3,3X,F6.4)
0126           97 FORMAT(1H+,10X,'NOTES')
0127           98 FORMAT(1HO,15X,I2,2X,20A4)
0128           99 FORMAT(20A4)
0129          100 FORMAT(4G10.4,I2,8X,G10.4)
0130          101 FORMAT(20A4)
0131          102 FORMAT(I2,I2,I2,I2,2X,5G10.4)
0132          104 FORMAT(1H1,10X,20A4,//)
0133          105 FORMAT(1HO,10X,'ORIGINAL LENGTH ',F5.3,'IN.',7X,'ORIGINAL AREA',
                 11X,F5.3,'SQ.IN.')
0134          106 FORMAT(1H , 1X,F8.1,3X,F6.4,3X,F6.2,3X,F6.2,3X,F5.3,3X,F5.3)
0135          107 FORMAT(4(I2,1X,I2,1X,I2,2X))
0136          108 FORMAT(1HO,10X,'SOIL MIXED',3(I3),5X,'SAMPLE PREPARED',3(I3))
0137          109 FORMAT(9G8.3)
0138          110 FORMAT(1HO,10X,'MOISTURE CONTENT OF COMPACTED SAMPLE ',F7.4,4X,
                 1F7.4)
0139          111 FORMAT(1HO,10X,'DRY DENSITY OF COMPACTED SAMPLE ',F6.2, 'LB/FT3')
0140          112 FORMAT(1HO,10X,'DEGREE OF SATURATION OF COMPACTED SAMPLE',F6.2,
                 1'PER CENT')
0141          113 FORMAT(1HO,10X,'INITIAL VOID RATIO ',1X,F6.4)
0142          114 FORMAT(1HO,10X,'FINAL MOISTURE CONTENT ',F7.4,5X,F7.4,5X,F7.4)
0143          115 FORMAT(1HO,10X,'FINAL VOID RATIO ',F6.4,//)
0144          117 FORMAT('     ')
0145          200 FORMAT(1H , 3X,'TIME',5X,'AXIAL')
0146          201 FORMAT(1H , 3X,'ELAPSED',3X,'DEF',8X,'Q',8X,'P',7X,'N',6X,'VOID R'
                 1,5X,'QR',6X,'NQR',5X,'DS',//)
0147          601 FORMAT(1HO,10X,'TEST STARTED',3(I3),3X,'TEST COMPLETED',3(I3))
0148          602 FORMAT(1HO,10X,'CONSOLIDATION PRESSURE',F7.2,'PSI')
0149          605 FORMAT(1H ,'    ')
0150          619 FORMAT(1H1, 3X,   'TIME',5X,'AXIAL')
0151          998 FORMAT(1HO,F10.4)
0152           56 STOP
0153              END
```

DSC 001 PARALLEL

SOIL MIXED 14 7 69 SAMPLE PREPARED 2 8 69

TEST STARTED 3 8 69 TEST COMPLETED 8 8 69

ORIGINAL LENGTH 1.596IN. ORIGINAL AREA 1.760SQ.IN.

CONSOLIDATION PRESSURE 20.55PSI

NOTES 1 DEFORMED SHAPE OF SAMPLE SKEWED

2 NO DATA ON FINAL M/C USED VALUES FOR STC 016

MOISTURE CONTENT OF COMPACTED SAMPLE 0.2624 0.2569

DRY DENSITY OF COMPACTED SAMPLE 96.44LB/FT3

DEGREE OF SATURATION OF COMPACTED SAMPLE102.50PER CENT

INITIAL VOID RATIO 0.6435

FINAL MOISTURE CONTENT 0.2571 0.2549 0.2532

FINAL VOID RATIO 0.6452

TIME ELAPSED	AXIAL DEF	Q	P	N	VOID R	QR	NQR	DS
0.0	0.0	0.0	20.55	0.0	0.626			
38.0	-.0004	5.20	22.28	0.233	0.625			
91.0	0.0007	11.52	24.39	0.472	0.625			
140.0	0.0021	16.17	25.94	0.624	0.624	23.41	0.0	0.0026
213.0	0.0052	23.03	28.22	0.816	0.623	27.20	0.0	0.0130
296.0	0.0077	30.62	30.75	0.996	0.622	36.02	0.000	0.0082
415.0	0.0126	41.06	34.22	1.200	0.621	43.76	0.000	0.0315
499.0	0.0151	48.66	36.75	1.324	0.620	51.53	0.000	0.0083
557.0	0.0169	53.78	38.46	1.398	0.620	55.47	0.000	0.0043
621.0	0.0211	59.11	40.23	1.469	0.620	59.51	0.000	0.0175
690.0	0.0218	64.50	42.03	1.535	0.620			
750.0	0.0240	69.30	43.63	1.588	0.620	69.21	0.000	0.0061
795.0	0.0257	72.38	44.65	1.621	0.620	72.06	0.000	0.0038
1349.0	0.0243	76.55	46.04	1.663	0.620			
1406.0	0.0297	79.96	47.18	1.695	0.620	79.40	0.000	0.0161
1501.0	0.0336	85.65	49.07	1.745	0.621	84.14	0.000	0.0166
1600.0	0.0376	90.95	50.84	1.789	0.621	88.78	0.000	0.0159
1680.0	0.0394	93.86	51.81	1.812	0.622	89.72	0.000	0.0037
1747.0	0.0430	96.10	52.55	1.829	0.623	94.04	0.000	0.0072
1847.0	0.0463	98.01	53.19	1.843	0.623	94.53	0.000	0.0056
1943.0	0.0510	98.56	53.37	1.847	0.624	96.24	0.000	0.0026
2045.0	0.0562	100.15	53.90	1.858	0.625	97.97	0.000	0.0077
2100.0	0.0577	100.03	53.86	1.857	0.626	95.73	0.000	-.0002
2817.0	0.0610	100.10	53.88	1.858	0.626	97.63	0.000	0.0002
2885.0	0.0654	100.75	54.10	1.862	0.627	99.49	0.000	0.0028
2949.0	0.0692	101.11	54.22	1.865	0.627	99.81	0.000	0.0013
3041.0	0.0751	100.66	54.07	1.862	0.628	99.54	0.000	-.0027
3115.0	0.0793	100.62	54.06	1.861	0.628	99.45	0.000	-.0002
3118.0	0.0789	100.66	54.07	1.862	0.628			
3213.0	0.0846	101.98	54.51	1.871	0.628	101.38	0.000	0.0071
3268.0	0.0872	103.22	54.92	1.879	0.628	102.80	0.000	0.0030
3411.0	0.0963	102.10	54.55	1.872	0.629	101.20	0.000	-.0105
3549.0	0.1029	99.42	53.66	1.853	0.630	97.82	0.000	-.0188
4485.0	0.1079	58.26	39.95	1.458	0.638	36.98	0.0	-.5147
4581.0	0.1118	63.40	41.66	1.522	0.638	63.79	0.000	0.0152
4699.0	0.1180	69.25	43.61	1.588	0.638	69.60	0.000	0.0302
4345.0	0.1263	70.83	44.14	1.605	0.638	70.34	0.000	0.0126
4918.0	0.1298	71.83	44.47	1.615	0.639	70.89	0.000	0.0034
5018.0	0.1076	38.69	33.43	1.157	0.639			
5235.0	0.1192	4.31	21.99	0.196	0.639	4.20	0.0	-.6154

DSC 002 PARALLEL

SOIL MIXED 14 7 69 SAMPLE PREPARED 15 7 69

TEST STARTED 17 7 69 TEST COMPLETED 24 7 69

ORIGINAL LENGTH 1.601IN. ORIGINAL AREA 1.769SQ.IN.

CONSOLIDATION PRESSURE 35.79PSI

NOTES 1 AT END OF TEST HEIGHT OF SAMPLE 1.447, 1.453, 1.457, 1.454IN

MOISTURE CONTENT OF COMPACTED SAMPLE 0.2582 0.2544

DRY DENSITY OF COMPACTED SAMPLE 92.42LB/FT3

DEGREE OF SATURATION OF COMPACTED SAMPLE 91.06PER CENT

INITIAL VOID RATIO 0.7150

FINAL MOISTURE CONTENT 0.2455 0.2463 0.2453

FINAL VOID RATIO 0.6233

TIME ELAPSED	AXIAL DEF	Q	P	N	VOID R	QR	NQR	DS
0.0	0.0	0.0	35.79	0.0	0.612			
17.0	0.0003	0.65	36.01	0.018	0.612	1.70	0.0	0.0002
34.0	0.0007	0.92	36.09	0.025	0.612	0.92	0.0	0.0001
65.0	-.0003	1.44	36.27	0.040	0.612			
104.0	0.0007	1.57	36.31	0.043	0.612	1.22	0.0	0.0001
133.0	-.0000	2.09	36.49	0.057	0.612			
190.0	0.0003	3.53	36.97	0.096	0.612	3.53	0.0	0.0002
238.0	0.0007	3.53	36.97	0.096	0.612	5.62	0.0	-.0000
310.0	-.0003	4.19	37.19	0.113	0.612			
346.0	-.0000	4.06	37.14	0.109	0.612			
409.0	0.0007	4.06	37.14	0.109	0.612	5.11	0.0	-.0000
468.0	-.0000	4.06	37.14	0.109	0.612			
557.0	0.0003	4.06	37.14	0.109	0.612	1.97	0.0	-.0000
649.0	0.0010	3.79	37.05	0.102	0.612	3.27	0.0	-.0002
722.0	-.0000	3.40	36.92	0.092	0.612			
797.0	-.0003	3.93	37.10	0.106	0.612			
1474.0	0.0003	3.93	37.10	0.106	0.612	-7.64	0.0	-.0000
1952.0	-.0003	3.01	36.79	0.082	0.613			
2239.0	0.0000	2.75	36.71	0.075	0.613	-3.51	0.0	-.0001
3442.0	0.0016	21.44	42.93	0.499	0.612			
3500.0	0.0039	31.93	46.42	0.688	0.612	39.88	0.0	0.0098
5757.0	0.0052	39.97	49.10	0.814	0.612	38.66	0.0	0.0022
5817.0	0.0069	49.11	52.14	0.942	0.611	57.92	0.000	0.0042
5877.0	0.0088	57.42	54.91	1.046	0.611	62.65	0.000	0.0075
6012.0	0.0138	75.67	60.99	1.241	0.609	80.26	0.000	0.0472
6093.0	0.0158	85.14	64.14	1.327	0.609	90.50	0.000	0.0073
6172.0	0.0191	93.94	67.07	1.401	0.609	95.81	0.000	0.0192
6247.0	0.0221	101.83	69.70	1.461	0.609	102.64	0.000	0.0156
6324.0	0.0254	108.75	72.00	1.510	0.609	109.36	0.000	0.0169
6402.0	0.0288	114.73	73.99	1.551	0.609	114.73	0.000	0.0154
6512.0	0.0321	122.58	76.61	1.600	0.609	121.76	0.000	0.0184
6585.0	0.0355	126.97	78.07	1.626	0.609	125.65	0.000	0.0123
7261.0	0.0392	133.70	80.31	1.665	0.609	130.74	0.000	0.0192
7333.0	0.0426	136.91	81.38	1.682	0.610	134.78	0.000	0.0096
7404.0	0.0460	139.34	82.19	1.695	0.610	137.53	0.000	0.0075
7478.0	0.0484	141.53	82.92	1.707	0.610	138.37	0.000	0.0046
7580.0	0.0542	144.10	83.78	1.720	0.611	142.03	0.000	0.0141
7657.0	0.0577	145.62	84.28	1.728	0.611	142.73	0.000	0.0049
7745.0	0.0611	147.01	84.75	1.735	0.612	143.74	0.000	0.0046
7836.0	0.0660	147.58	84.93	1.738	0.612	145.10	0.000	0.0027
8629.0	0.0705	148.31	85.18	1.741	0.613	145.28	0.000	0.0033
8639.0	0.0702	149.34	85.52	1.746	0.613			
8641.0	0.0702	149.10	85.44	1.745	0.613			
8751.0	0.0765	145.31	84.18	1.726	0.614	143.71	0.000	-.0104
8848.0	0.0825	144.47	83.90	1.722	0.614	143.55	0.000	-.0052
8985.0	0.0903	144.46	83.89	1.722	0.614	143.40	0.000	-.0001
9072.0	0.1131	141.93	83.05	1.709	0.615	141.72	0.000	-.0586

APPENDIX H

LISTING OF CALCULATED PLASTIC STRAIN INCREMENTS FOR THE UNDRAINED TESTS

The results given in Appendix F are the reduced experimental results. These are the raw data recorded reduced to the required stresses and the axial strain. In this Appendix the components of elastic and plastic strain and increments of these are calculated from the definitions given in Chapter 5. The listing of the computer programme used is also included.

The data in the various columns of the listings are:-

'EL', gives the axial strain of the sample.

'EE', gives the elastic component of this strain. This is calculated by summation of the elastic strain increments calculated from Eq.(5.9).

'EP', gives the total shear distortion calculated by summing increments of this calculated from Eq.(5.10).

'VP', gives the total plastic volumetric strain. This is calculated by summing the increments calculated with Eq.(5.7).

'DEP', the fifth column, gives the increment of plastic distortion calculated from Eq.(5.10). This expressed as a percentage.

'DVP', in the sixth column, is the increment of plastic volumetric strain calculated from Eq.(5.7). This is also given in percent.

'QC' in column seven is the stress component q defined in Eq.(3.20).

'PC' in column eight is the stress component p defined in Eq.(3.19).

'THETA' in column nine is the angle giving the direction of the plastic strain increment vector, it is defined in Eq.(5.12).

'NI', is the stress ratio η', defined in Eq.(4.1).

'DS', is the value of the left hand side of the inequality (5.11) which Drucker's stability postulate requires to be positive for stable plastic deformation.

'BM', is the friction parameter calculated from Eq.(5.17).

```
C ***************************************************************************
C
C   CALCULATES ELASTIC AND PLASTIC COMPONENTS OF STRAIN
C
C ***************************************************************************
0001        DIMENSION TITLE(20)
0002        DIMENSION EL(100), QC(100), PC(100),PN(100)
0003      1 READ(1,100) VR
0004        IF(VR.EQ.0.0) GO TO 56
0005        READ(1,101) (TITLE(I),I=1,20)
0006        WRITE(3,102) (TITLE(I),I=1,20)
0007        WRITE(3,131)
0008        DO 2 N=1,100
0009        READ(1,103) EL(N),QC(N),PC(N)
0010        IF(PC(N).EQ.0.0) GO TO 3
0011      2 CONTINUE
0012      3 N=N-2
0013        K=1
0014        EM=1./(2850.+126.*PC(1))
0015        EE=0.
0016        EP=0.
0017        VP=0.
0018        DO 9 JL=1,N
0019        IF(EL(JL).GT.0.0) GO TO 8
0020        PN(JL)=QC(JL)/(PC(JL)+3.)
0021        WRITE(3,136)EL(JL),QC(JL),PC(JL),PN(JL)
0022      9 CONTINUE
0023      8 K=JL*2
0024        ETA1=(PC(JL-1)+3.)/(PC(1)+3.)
0025        ZETAS1=0.066*(3.35-(ETA1-2.55)**2)
0026        ZEASS1=SQRT(ZETAS1)
0027        ZETA1=0.240-ZEASS1
0028        DO 4 J=JL,N
0029        PN(J)=QC(J)/(PC(J)+3.)
0030        DQ=QC(J)-QC(J-1)
0031        DP=PC(J)-PC(J-1)
0032        DE=EL(J)-EL(J-1)
0033        DEE=DQ*EM
0034        ETA=(PC(J)+3.)/(PC(1)+3.)
0035        ZETAS=0.066*(3.35-(ETA-2.55)**2)
0036        IF(ZETAS.LT.0.0) ZETAS=0.0
0037        ZETASS=SQRT(ZETAS)
0038        IF(DP.LT.0.0) ZETA=0.240-ZETASS
0039        IF(DP.GT.0.0) ZETA=0.240+ZETASS
0040        IF(ETA.GT.2.55) ZETA=0.71
0041        DZETA=ZETA-ZETA1
0042        DVP=-0.0108*(((1.-ZETA)*DP-(PC(J)+3.)*DZETA)/((PC(J)+3.)*(1.-ZETA
           1)))/(1.+VR)
0043        ZETA1=ZETA
0044        DEP=DE-DEE+0.333*DVP
0045        DS=DQ*DEP+DP*DVP
0046        DEEE=DE-DEP
0047        EE=EE+DEEE
0048        EP=EP+DEP
0049        DEP=DEP*100.
0050        VP=VP+DVP
0051        AM=DVP/(DEP*(1.+3./PC(J)))+PN(J)*DQ*EM/(2.*DEP)+PN(J)
0052        DVP=DVP*100.
0053         DEE=DEE*100.
0054        DE=DE*100.
0055        DEEE=DEEE*100.
0056        IF(DEP.EQ.0.) GO TO 6
0057        XXX=DVP/DEP
0058        RBETA=ATAN (XXX)
0059        BETA=RBETA*57.296
0060        WRITE(3,135) EL(J),EE,EP,VP,DEP,DVP,QC(J),PC(J),BETA,PN(J),DS,AM
0061        GO TO 7
0062      6 WRITE(3,129) EL(J),EE,EP,VP,DEP,DVP,QC(J),PC(J),PN(J),DS,AM
0063      7 K=K+2
0064        IF(K.GT.50) WRITE(6,133)
0065        IF(K.GT.50) K=1
0066      4 CONTINUE
```

```
0067              DO 5 J=K,50
0068            5 WRITE(3,134)
0069              GO TO 1
0070          100 FORMAT(G10.4)
0071          101 FORMAT(20A4)
0072          102 FORMAT(1H1,26X,20A4//)
0073          103 FORMAT(F10.4,2F10.2)
0074          129 FORMAT(1HO,6F8.4,2F8.2,10X,3F3.4)
0075          131 FORMAT(1HO,4X,'EL',6X,'EE',6X,'EP',6X,'VP',6X,'DEP',5X,'DVP',6X,
                 1'QC',6X,'PC',5X,'THETA',4X,'N1',6X,'DS',6X,'BM',//)
0076          133 FORMAT(1H1,' ',//////////)
0077          134 FORMAT(1HO,' ')
0078          135 FORMAT(1HO,6F8.4,3F8.2, 1X,3F8.4)
0079          136 FORMAT(1HO,F8.4,38X,F10.2,3X,F5.2,7X,F10.4)
0080           56 STOP
0081              END
```

STC TEST 002 PARALLEL

EL	EE	EP	VP	DEP	DVP	QC	PC	THETA	N1	DS	BM
0.0						0.0	10.00		0.0		
0.0						1.44	10.05		0.1103		
0.0012	0.0002	0.0010	0.0005	0.1037	0.0519	2.82	9.35	26.57	0.2283	0.0011	0.2325
0.0021	0.0003	0.0018	0.0011	0.0782	0.0595	4.12	8.62	37.29	0.3546	0.0006	0.3609
0.0038	0.0005	0.0033	0.0019	0.1520	0.0753	5.89	7.81	26.35	0.5449	0.0021	0.5492
0.0092	0.0010	0.0082	0.0023	0.4875	0.0417	8.62	7.41	4.89	0.8280	0.0131	0.8292
0.0157	0.0007	0.0150	0.0054	0.6761	0.3086	11.77	8.09	24.53	1.0613	0.0234	1.0652
0.0208	0.0014	0.0194	0.0053	0.4459	-0.0026	14.37	9.23	-0.33	1.1750	0.0116	1.1758
0.0251	0.0020	0.0231	0.0053	0.3703	-0.0062	16.74	10.21	-0.95	1.2672	0.0087	1.2681
0.0290	0.0026	0.0264	0.0052	0.3243	-0.0081	19.33	11.39	-1.44	1.3433	0.0083	1.3444
0.0360	0.0036	0.0324	0.0051	0.6017	-0.0111	23.22	13.25	-1.05	1.4289	0.0232	1.4299
0.0427	0.0047	0.0380	0.0050	0.5618	-0.0128	27.49	15.43	-1.31	1.4916	0.0237	1.4928
0.0504	0.0062	0.0442	0.0048	0.6200	-0.0178	33.41	18.65	-1.64	1.5432	0.0361	1.5447
0.0564	0.0074	0.0490	0.0046	0.4830	-0.0203	37.94	21.22	-2.41	1.5665	0.0214	1.5679
0.0639	0.0088	0.0551	0.0043	0.6040	-0.0323	43.50	24.48	-3.06	1.5830	0.0325	1.5843
0.0695	0.0100	0.0595	0.0039	0.4420	-0.0344	47.88	27.06	-4.45	1.5928	0.0185	1.5940
0.0790	0.0119	0.0671	0.0034	0.7579	-0.0492	55.10	30.03	-3.72	1.6682	0.0533	1.6695
0.0825	0.0127	0.0698	0.0029	0.2725	-0.0538	57.55	33.00	-11.16	1.5986	0.0051	1.5985
0.0899	0.0143	0.0756	0.0023	0.5809	-0.0555	63.33	36.38	-5.45	1.6082	0.0317	1.6092
0.0977	0.0153	0.0824	0.0019	0.6805	-0.0386	66.89	38.88	-3.24	1.5972	0.0233	1.5977
0.1068	0.0166	0.0902	0.0015	0.7740	-0.0481	71.82	42.25	-3.56	1.5872	0.0365	1.5878

STC TEST 016 PARALLEL

EL	EE	EP	VP	DEP	DVP	QC	PC	THETA	M1	DS	BM
0.0						0.0	5.36		0.0		
0.0						1.44	5.19		0.1758		
0.0018	0.0003	0.0015	0.0003	0.1482	0.0256	2.86	4.97	9.80	0.3588	0.0020	0.3604
0.0046	0.0006	0.0040	0.0005	0.2515	0.0268	4.18	4.75	6.07	0.5394	0.0033	0.5404
0.0095	-0.0007	0.0102	0.0058	0.6192	0.5260	5.80	4.87	40.35	0.7370	0.0107	0.7425
0.0145	-0.0003	0.0148	0.0057	0.4612	-0.0048	7.11	5.30	-0.59	0.8566	0.0060	0.8569
0.0202	0.0002	0.0200	0.0057	0.5217	-0.0071	8.73	5.93	-0.77	0.9776	0.0084	0.9779
0.0241	0.0005	0.0236	0.0056	0.3551	-0.0068	9.88	6.47	-1.09	1.0433	0.0040	1.0436
0.0281	0.0010	0.0271	0.0055	0.3573	-0.0082	11.29	7.15	-1.31	1.1123	0.0050	1.1128
0.0314	0.0013	0.0301	0.0054	0.2947	-0.0072	12.45	7.72	-1.39	1.1614	0.0034	1.1619
0.0353	0.0019	0.0334	0.0053	0.3339	-0.0099	14.31	8.60	-1.70	1.2336	0.0061	1.2344
0.0394	0.0022	0.0372	0.0053	0.3799	-0.0069	15.29	9.15	-1.05	1.2584	0.0037	1.2588
0.0412	0.0025	0.0387	0.0052	0.1500	-0.0066	16.27	9.66	-2.51	1.2851	0.0014	1.2860
0.0445	0.0030	0.0415	0.0051	0.2752	-0.0120	18.06	10.67	-2.49	1.3211	0.0048	1.3220
0.0467	0.0034	0.0433	0.0050	0.1849	-0.0084	19.20	11.29	-2.61	1.3436	0.0021	1.3444
0.0489	0.0037	0.0452	0.0049	0.1838	-0.0091	20.37	11.93	-2.84	1.3644	0.0021	1.3652
0.0518	0.0042	0.0476	0.0048	0.2439	-0.0122	21.85	12.75	-2.87	1.3873	0.0035	1.3881
0.0544	0.0046	0.0498	0.0047	0.2220	-0.0110	23.06	13.42	-2.84	1.4044	0.0026	1.4051
0.0574	0.0050	0.0524	0.0045	0.2567	-0.0142	24.42	14.22	-3.16	1.4181	0.0034	1.4187
0.0630	0.0059	0.0571	0.0042	0.4720	-0.0316	27.15	15.83	-3.83	1.4418	0.0124	1.4425
0.0667	0.0065	0.0602	0.0040	0.3060	-0.0270	29.09	16.96	-5.04	1.4574	0.0056	1.4580
0.0690	0.0070	0.0620	0.0037	0.1831	-0.0216	30.49	17.76	-6.72	1.4687	0.0024	1.4693
0.0709	0.0074	0.0635	0.0035	0.1490	-0.0210	31.69	18.46	-8.01	1.4767	0.0016	1.4772
0.0750	0.0082	0.0668	0.0031	0.3319	-0.0403	33.97	19.88	-6.93	1.4847	0.0070	1.4851
0.0803	0.0091	0.0712	0.0027	0.4346	-0.0447	36.81	21.57	-5.87	1.4982	0.0116	1.4987
0.0834	0.0098	0.0736	0.0024	0.2451	-0.0278	38.77	22.67	-6.48	1.5103	0.0045	1.5110
0.0841	0.0100	0.0741	0.0023	0.0527	-0.0075	39.29	22.97	-8.10	1.5129	0.0003	1.5138
0.0860	0.0104	0.0756	0.0021	0.1473	-0.0182	40.58	23.72	-7.06	1.5187	0.0018	1.5195
0.0926	0.0116	0.0810	0.0016	0.5411	-0.0513	44.17	26.01	-5.42	1.5226	0.0183	1.5232
0.0987	0.0124	0.0863	0.0013	0.5324	-0.0346	46.50	27.64	-3.72	1.5176	0.0118	1.5190
0.1061	0.0131	0.0930	0.0009	0.6636	-0.0334	48.80	29.30	-2.88	1.5108	0.0147	1.5111

CSR TEST 009 (0.0006IN/MIN) PARALLEL

EL	EE	EP	VP	DEP	DVP	QC	PC	THETA	NI	DS	BM
0.0						0.0	5.94		0.0		
0.0014	-0.0002	0.0016	0.0005	0.1564	0.0509	0.02	5.46	18.04	0.0024	-0.0002	0.0045
0.0018	0.0002	0.0016	0.0005	0.0073	0.0011	1.21	5.45	8.46	0.1432	0.0001	0.1474
0.0028	0.0006	0.0022	0.0007	0.0612	0.0144	2.78	5.32	13.23	0.3341	0.0009	0.3368
0.0042	0.0005	0.0037	0.0009	0.1418	0.0230	2.99	5.12	9.20	0.3682	0.0003	0.3693
0.0049	-0.0007	0.0056	0.0057	0.1949	0.4770	4.21	5.13	67.77	0.5178	0.0024	0.5337
0.0085	0.0003	0.0082	0.0030	0.2569	-0.2644	4.75	5.05	-45.82	0.5901	0.0016	0.5838
0.0110	-0.0011	0.0121	0.0077	0.3923	0.4707	5.27	5.23	50.19	0.6403	0.0029	0.6481
0.0153	-0.0006	0.0159	0.0077	0.3817	-0.0042	6.96	5.67	-0.62	0.8028	0.0064	0.8032
0.0178	-0.0005	0.0183	0.0077	0.2345	-0.0024	7.49	5.86	-0.58	0.8454	0.0012	0.8456
0.0214	-0.0001	0.0215	0.0076	0.3277	-0.0043	8.60	6.22	-0.75	0.9328	0.0036	0.9331
0.0239	0.0001	0.0238	0.0076	0.2286	-0.0041	9.32	6.55	-1.03	0.9759	0.0016	0.9762
0.0279	0.0004	0.0275	0.0075	0.3630	-0.0067	10.57	7.14	-1.06	1.0424	0.0045	1.0428
0.0319	0.0008	0.0311	0.0074	0.3612	-0.0071	11.88	7.76	-1.12	1.1041	0.0047	1.1045
0.0348	0.0011	0.0337	0.0074	0.2596	-0.0062	12.90	8.29	-1.38	1.1426	0.0026	1.1431
0.0392	0.0018	0.0374	0.0073	0.3726	-0.0123	15.18	9.69	-1.88	1.1962	0.0083	1.1970
0.0425	0.0030	0.0395	0.0033	0.2062	-0.3919	14.94	9.29	-62.25	1.2156	0.0011	1.2011
0.0458	-0.0004	0.0462	0.0154	0.6697	1.2095	17.21	10.47	61.03	1.2777	0.0295	1.2923
0.0487	0.0000	0.0487	0.0154	0.2534	-0.0072	18.44	11.08	-1.62	1.3097	0.0031	1.3103
0.0536	0.0007	0.0529	0.0152	0.4236	-0.0126	20.68	12.21	-1.70	1.3596	0.0093	1.3604
0.0573	0.0012	0.0561	0.0151	0.3187	-0.0114	22.39	13.11	-2.04	1.3898	0.0053	1.3906
0.0603	0.0016	0.0587	0.0150	0.2549	-0.0119	23.87	13.97	-2.67	1.4066	0.0037	1.4074
0.0640	0.0021	0.0619	0.0149	0.3244	-0.0133	25.35	14.85	-2.35	1.4202	0.0047	1.4207
0.0685	0.0026	0.0659	0.0147	0.3948	-0.0171	27.13	15.88	-2.49	1.4370	0.0069	1.4375
0.0761	0.0036	0.0725	0.0143	0.2958	-0.0175	30.18	17.67	-3.39	1.4601	0.0039	1.4605
0.0811	0.0043	0.0768	0.0141	0.4345	-0.0282	32.20	18.89	-3.71	1.4710	0.0084	1.4714
0.0860	0.0049	0.0811	0.0138	0.4286	-0.0300	34.05	20.02	-4.00	1.4791	0.0076	1.4794
0.0926	0.0057	0.0869	0.0134	0.5803	-0.0375	36.47	21.47	-3.70	1.4904	0.0135	1.4907
0.0988	0.0064	0.0924	0.0131	0.5493	-0.0319	38.63	22.77	-3.33	1.4990	0.0115	1.4993
0.1058	0.0072	0.0986	0.0127	0.6189	-0.0357	41.12	24.31	-3.30	1.5057	0.0149	1.5060
0.1121	0.0079	0.1042	0.0124	0.5580	-0.0309	43.34	25.71	-3.17	1.5096	0.0120	1.5099
0.1184	0.0087	0.1097	0.0121	0.5550	-0.0308	45.67	27.18	-3.18	1.5133	0.0125	1.5136
0.1248	0.0093	0.1154	0.0118	0.5714	-0.0273	47.81	28.54	-2.73	1.5159	0.0119	1.5162

CSR TEST 010 (0.0006IN/MIN) PARALLEL

EL	EE	EP	VP	DEP	DVP	QC	PC	THETA	N1	DS	BM
0.0						0.0	15.92		0.0		
0.0015	-0.0018	0.0033	0.0064	0.3270	0.6448	1.83	16.25	63.11	0.0951	0.0081	0.1118
0.0018	-0.0007	0.0025	0.0035	-0.0781	-0.2932	2.34	15.41	75.08	0.1271	0.0021	0.1584
0.0028	-0.0007	0.0035	0.0040	0.1018	0.0481	3.03	14.51	25.30	0.1730	0.0003	0.1771
0.0034	-0.0006	0.0040	0.0041	0.0541	0.0133	3.53	14.27	13.83	0.2044	0.0002	0.2066
0.0043	-0.0006	0.0049	0.0044	0.0869	0.0266	4.11	13.81	17.03	0.2445	0.0004	0.2472
0.0068	0.0000	0.0068	0.0047	0.1871	0.0325	7.69	13.28	9.86	0.4724	0.0065	0.4747
0.0105	0.0008	0.0097	0.0050	0.2942	0.0328	11.90	12.78	6.35	0.7541	0.0122	0.7561
0.0143	0.0012	0.0131	0.0051	0.3368	0.0027	14.04	12.74	0.46	0.8920	0.0072	0.8926
0.0168	0.0003	0.0165	0.0087	0.3441	0.3581	15.26	13.00	46.14	0.9537	0.0051	0.9626
0.0196	0.0007	0.0189	0.0086	0.2368	-0.0011	17.34	13.56	-0.28	1.0471	0.0049	1.0480
0.0233	0.0012	0.0221	0.0086	0.3239	-0.0025	19.54	14.29	-0.45	1.1301	0.0071	1.1309
0.0265	0.0016	0.0249	0.0086	0.2749	-0.0039	21.67	15.14	-0.80	1.1946	0.0058	1.1954
0.0293	0.0020	0.0273	0.0085	0.2373	-0.0045	23.67	15.99	-1.09	1.2464	0.0047	1.2474
0.0319	0.0023	0.0296	0.0085	0.2317	-0.0035	24.99	16.56	-0.86	1.2776	0.0030	1.2782
0.0354	0.0028	0.0326	0.0084	0.3013	-0.0060	27.26	17.63	-1.14	1.3214	0.0068	1.3222
0.0402	0.0035	0.0367	0.0084	0.4137	-0.0080	30.35	19.14	-1.10	1.3708	0.0127	1.3717
0.0427	0.0040	0.0387	0.0083	0.2001	-0.0081	32.64	20.66	-2.32	1.3795	0.0045	1.3808
0.0466	0.0046	0.0420	0.0082	0.3294	-0.0057	35.49	21.63	-0.98	1.4409	0.0093	1.4421
0.0492	0.0049	0.0443	0.0082	0.2223	-0.0055	37.23	22.58	-1.42	1.4554	0.0038	1.4564
0.0534	0.0057	0.0477	0.0081	0.3443	-0.0097	40.75	24.47	-1.61	1.4834	0.0119	1.4847
0.0563	0.0062	0.0501	0.0080	0.2398	-0.0074	43.07	25.79	-1.77	1.4960	0.0055	1.4972
0.0596	0.0068	0.0528	0.0079	0.2725	-0.0083	45.73	27.26	-1.74	1.5112	0.0071	1.5125
0.0632	0.0074	0.0558	0.0078	0.3008	-0.0089	48.46	28.78	-1.69	1.5249	0.0081	1.5260
0.0711	0.0085	0.0626	0.0076	0.4073	-0.0107	53.51	31.67	-1.51	1.5434	0.0115	1.5443
0.0750	0.0091	0.0659	0.0075	0.3312	-0.0109	56.19	33.24	-1.88	1.5505	0.0087	1.5515
0.0810	0.0103	0.0707	0.0073	0.4722	-0.0250	61.99	36.64	-3.03	1.5638	0.0265	1.5653
0.0877	0.0120	0.0757	0.0069	0.5032	-0.0384	69.47	40.87	-4.36	1.5835	0.0360	1.5853
0.0971	0.0118	0.0853	0.0068	0.9607	-0.0091	68.32	41.69	-0.54	1.5288	-0.0111	1.5285
0.1042	0.0128	0.0914	0.0065	0.6053	-0.0268	72.97	43.98	-2.54	1.5532	0.0275	1.5540
0.1121	0.0144	0.0977	0.0061	0.6311	-0.0443	79.97	47.43	-4.01	1.5858	0.0426	1.5869

CSR TEST 013 (0.0006IN/MIN) PARALLEL

EL	EE	EP	VP	DEP	DVP	QC	PC	THETA	N1	DS	BM
0.0						0.0	64.60		0.0		
0.0						0.79	64.68		0.0117		
0.0						4.21	64.20		0.0626		
0.0						4.74	63.30		0.0715		
0.0						6.59	62.75		0.1002		
0.0						6.72	62.16		0.1031		
0.0						8.19	60.94		0.1281		
0.0						10.31	59.22		0.1657		
0.0						13.62	57.08		0.2267		
0.0						15.21	55.00		0.2622		
0.0						28.00	52.42		0.5052		
0.0						39.10	50.00		0.7377		
0.0						46.16	48.85		0.8903		
0.0035	0.0003	0.0032	0.0001	0.3198	0.0125	49.94	48.38	2.23	0.9720	0.0120	0.9729
0.0057	0.0000	0.0057	0.0022	0.2493	0.2027	54.14	48.65	39.11	1.0482	0.0110	1.0567
0.0102	0.0006	0.0096	0.0022	0.3914	0.0043	60.74	49.84	0.62	1.1495	0.0259	1.1505
0.0128	0.0007	0.0121	0.0022	0.2453	0.0016	62.41	50.63	0.37	1.1637	0.0041	1.1641
0.0197	0.0017	0.0180	0.0022	0.5970	0.0034	72.75	54.11	0.32	1.2739	0.0618	1.2749
0.0223	0.0020	0.0203	0.0022	0.2299	-0.0009	76.03	55.58	-0.22	1.2979	0.0075	1.2987
0.0253	0.0024	0.0229	0.0022	0.2616	-0.0018	80.18	57.47	-0.39	1.3259	0.0108	1.3268
0.0282	0.0028	0.0254	0.0022	0.2410	-0.0032	85.45	60.19	-0.77	1.3523	0.0126	1.3535
0.0322	0.0035	0.0287	0.0021	0.3380	-0.0045	92.10	63.30	-0.75	1.3891	0.0223	1.3903
0.0329	0.0036	0.0293	0.0021	0.0577	-0.0013	93.40	64.00	-1.29	1.3940	0.0007	1.3952
0.0365	0.0041	0.0324	0.0021	0.3064	-0.0051	99.10	67.15	-0.96	1.4127	0.0173	1.4137
0.0445	0.0053	0.0392	0.0020	0.5334	-0.0086	112.00	74.40	-0.92	1.4470	0.0544	1.4481
0.0465	0.0056	0.0409	0.0019	0.1713	-0.0014	115.10	75.14	-0.48	1.4730	0.0053	1.4741
0.0523	0.0064	0.0459	0.0019	0.4987	-0.0091	123.70	81.20	-1.04	1.4691	0.0423	1.4701
0.0536	0.0066	0.0470	0.0018	0.1106	-0.0009	125.80	81.68	-0.48	1.4856	0.0023	1.4868
0.0546	0.0068	0.0478	0.0018	0.0864	-0.0052	127.10	84.69	-3.43	1.4494	0.0010	1.4498
0.0601	0.0075	0.0526	0.0017	0.4796	-0.0051	134.65	87.70	-0.62	1.4846	0.0361	1.4855
0.0614	0.0075	0.0539	0.0017	0.1231	-0.0007	135.38	88.08	-0.33	1.4864	0.0009	1.4867
0.0686	0.0086	0.0600	0.0016	0.6182	-0.0101	146.20	94.88	-0.93	1.4937	0.0662	1.4947
0.0745	0.0093	0.0652	0.0016	0.5124	-0.0087	154.41	100.39	-0.98	1.4935	0.0416	1.4944

CSR TEST 014 (0.0006IN/MIN) PARALLEL

EL	EE	EP	VP	DEP	DVP	QC	PC	THETA	N1	DS	BM
0.0						0.0	49.40		0.0		
0.0						8.84	48.93		0.1702		
0.0						13.44	47.85		0.2643		
0.0						16.72	46.60		0.3371		
0.0018	0.0001	0.0017	0.0003	0.1658	0.0312	18.95	45.07	10.64	0.3942	0.0032	0.3963
0.0018	-0.0013	0.0031	0.0055	0.1422	0.5216	21.81	45.13	74.75	0.4531	0.0044	0.4881
0.0031	0.0000	0.0031	0.0031	0.0019	-0.2454	26.02	42.56	-89.56	0.5711	0.0064	-0.5811
0.0055	0.0003	0.0052	0.0035	0.2139	0.0438	29.71	40.75	11.57	0.6791	0.0071	0.6816
0.0078	0.0005	0.0073	0.0038	0.2048	0.0338	33.02	39.46	9.37	0.7777	0.0063	0.7799
0.0108	0.0010	0.0098	0.0042	0.2465	0.0369	38.99	38.17	8.52	0.9470	0.0142	0.9497
0.0138	0.0005	0.0133	0.0069	0.3563	0.2654	41.90	38.26	36.68	1.0155	0.0106	1.0229
0.0172	0.0009	0.0163	0.0069	0.3005	0.0013	45.52	38.91	0.25	1.0861	0.0109	1.0869
0.0199	0.0012	0.0187	0.0069	0.2372	0.0008	48.52	39.68	0.20	1.1368	0.0071	1.1377
0.0229	0.0015	0.0214	0.0069	0.2670	0.0003	51.52	40.69	0.06	1.1792	0.0080	1.1800
0.0259	0.0019	0.0240	0.0069	0.2666	-0.0005	54.53	41.89	-0.12	1.2147	0.0080	1.2155
0.0293	0.0022	0.0271	0.0069	0.3043	-0.0015	57.73	43.30	-0.27	1.2469	0.0097	1.2475
0.0331	0.0026	0.0305	0.0069	0.3382	-0.0026	61.45	45.07	-0.43	1.2783	0.0125	1.2790
0.0365	0.0031	0.0334	0.0068	0.2960	-0.0034	65.34	46.94	-0.65	1.3084	0.0115	1.3092
0.0427	0.0040	0.0387	0.0068	0.5293	-0.0057	73.40	50.10	-0.62	1.3823	0.0425	1.3834
0.0458	0.0044	0.0414	0.0067	0.2646	-0.0064	77.33	53.27	-1.39	1.3743	0.0102	1.3752
0.0482	0.0047	0.0435	0.0067	0.2113	-0.0027	79.85	54.39	-0.74	1.3914	0.0053	1.3921
0.0531	0.0055	0.0476	0.0066	0.4135	-0.0077	86.56	58.16	-1.06	1.4153	0.0275	1.4164
0.0576	0.0061	0.0515	0.0065	0.3873	-0.0068	92.04	61.38	-1.01	1.4296	0.0210	1.4306
0.0611	0.0066	0.0545	0.0065	0.3025	-0.0054	96.19	63.85	-1.03	1.4389	0.0124	1.4398
0.0784	0.0088	0.0696	0.0063	0.3708	-0.0069	115.11	75.84	-1.06	1.4600	0.0156	1.4608
0.0817	0.0092	0.0725	0.0062	0.2870	-0.0041	118.89	77.64	-0.81	1.4743	0.0108	1.4753
0.0870	0.0098	0.0772	0.0062	0.4704	-0.0074	124.07	81.07	-0.90	1.4758	0.0241	1.4765
0.0932	0.0105	0.0827	0.0061	0.5504	-0.0088	130.12	85.10	-0.92	1.4770	0.0329	1.4777
0.0997	0.0112	0.0885	0.0060	0.5735	-0.0101	136.76	89.51	-1.01	1.4783	0.0376	1.4791
0.1056	0.0119	0.0937	0.0059	0.5241	-0.0093	142.46	93.28	-1.01	1.4796	0.0295	1.4804
0.1137	0.0126	0.1011	0.0058	0.7384	-0.0109	148.63	97.46	-0.84	1.4795	0.0451	1.4800
0.1215	0.0133	0.1082	0.0056	0.7135	-0.0117	154.31	101.65	-0.94	1.4745	0.0400	1.4750

CSR TEST 015 (0.00012/0.0006IN/MIN) PARALLEL

EL	EE	EP	VP	DEP	DVP	QC	PC	THETA	N1	DS	BM
0.0						0.0	33.43		0.0		
0.0						1.32	32.97		0.0367		
0.0						1.98	32.65		0.0555		
0.0						2.37	32.42		0.0669		
0.0						3.16	31.87		0.0906		
0.0						4.74	31.23		0.1385		
0.0						4.61	30.65		0.1370		
0.0033	-0.0001	0.0034	0.0002	0.3423	0.0188	4.18	30.02	3.14	0.1266	-0.0016	0.1271
0.0049	0.0002	0.0047	0.0007	0.1294	0.0483	7.48	28.51	20.49	0.2374	0.0035	0.2412
0.0085	0.0009	0.0076	0.0015	0.2914	0.0818	14.25	26.29	15.69	0.4865	0.0179	0.4898
0.0115	0.0017	0.0098	0.0019	0.2207	0.0382	20.75	25.38	9.83	0.7311	0.0140	0.7342
0.0151	0.0021	0.0130	0.0022	0.3155	0.0315	24.63	24.71	5.70	0.8888	0.0120	0.8905
0.0178	0.0018	0.0160	0.0042	0.3052	0.2030	26.92	24.93	33.64	0.9638	0.0074	0.9703
0.0214	0.0022	0.0192	0.0043	0.3138	0.0038	30.27	25.57	0.70	1.0595	0.0105	1.0604
0.0241	0.0025	0.0216	0.0043	0.2391	0.0021	32.50	26.23	0.50	1.1119	0.0053	1.1127
0.0271	0.0029	0.0242	0.0043	0.2658	0.0011	34.94	27.08	0.23	1.1616	0.0065	1.1624
0.0311	0.0033	0.0278	0.0043	0.3549	-0.0003	38.12	28.34	-0.05	1.2163	0.0113	1.2171
0.0352	0.0038	0.0314	0.0043	0.3577	-0.0024	41.76	30.01	-0.38	1.2651	0.0130	1.2659
0.0399	0.0043	0.0356	0.0042	0.4255	-0.0035	44.82	31.49	-0.47	1.2995	0.0130	1.3001
0.0423	0.0047	0.0376	0.0042	0.1952	-0.0041	47.89	32.97	-1.21	1.3314	0.0059	1.3327
0.0450	0.0053	0.0397	0.0041	0.2126	-0.0056	51.81	34.90	-1.50	1.3670	0.0082	1.3686
0.0484	0.0059	0.0425	0.0041	0.2837	-0.0058	55.65	36.82	-1.18	1.3975	0.0108	1.3987
0.0515	0.0063	0.0452	0.0040	0.2636	-0.0054	58.80	38.53	-1.18	1.4158	0.0082	1.4168
0.0560	0.0070	0.0490	0.0039	0.3789	-0.0078	63.64	41.21	-1.18	1.4395	0.0181	1.4406
0.0622	0.0080	0.0542	0.0038	0.3791	-0.0078	70.22	44.92	-1.18	1.4654	0.0181	1.4665
0.0657	0.0086	0.0571	0.0038	0.2949	-0.0063	73.96	47.01	-1.23	1.4789	0.0109	1.4800
0.0685	0.0091	0.0594	0.0037	0.2313	-0.0058	77.26	48.91	-1.44	1.4883	0.0075	1.4896
0.0716	0.0096	0.0620	0.0036	0.2547	-0.0066	81.01	51.10	-1.49	1.4974	0.0094	1.4987
0.0748	0.0101	0.0647	0.0036	0.2686	-0.0062	84.49	53.13	-1.33	1.5053	0.0092	1.5064
0.0804	0.0110	0.0694	0.0035	0.4739	-0.0103	90.33	56.62	-1.24	1.5151	0.0273	1.5162
0.0857	0.0118	0.0739	0.0034	0.4516	-0.0101	95.63	59.85	-1.29	1.5216	0.0236	1.5226
0.0903	0.0125	0.0778	0.0033	0.3887	-0.0104	100.42	62.94	-1.53	1.5229	0.0183	1.5240
0.0957	0.0132	0.0825	0.0032	0.4670	-0.0114	105.31	66.09	-1.39	1.5242	0.0225	1.5251
0.1029	0.0142	0.0887	0.0030	0.6242	-0.0163	111.69	70.30	-1.50	1.5237	0.0391	1.5246
0.1061	0.0143	0.0918	0.0029	0.3019	-0.0051	112.85	71.46	-0.97	1.5156	0.0034	1.5158
0.1119	0.0153	0.0966	0.0028	0.4815	-0.0185	119.37	75.56	-2.20	1.5195	0.0306	1.5206

CSR TEST 016 (0.00012/0.0006IN/MIN) PARALLEL

EL	EE	EP	VP	DEP	DVP	QC	PC	THETA	N1	DS	BM
0.0						0.0	22.85		0.0		
0.0						0.65	22.71		0.0253		
0.0						1.17	22.70		0.0455		
0.0						1.94	22.15		0.0771		
0.0						2.20	21.78		0.0888		
0.0						4.27	20.67		0.1804		
0.0						5.70	19.89		0.2490		
0.0						4.93	19.36		0.2205		
0.0						11.78	18.32		0.5525		
0.0029	0.0005	0.0024	0.0003	0.2413	0.0277	15.10	17.80	6.55	0.7260	0.0079	0.7278
0.0056	-0.0001	0.0057	0.0033	0.3276	0.3029	17.58	17.90	42.76	0.8411	0.0084	0.8496
0.0092	0.0004	0.0088	0.0033	0.3137	0.0005	20.24	18.31	0.09	0.9498	0.0083	0.9505
0.0125	0.0007	0.0118	0.0033	0.2957	-0.0001	22.20	18.81	-0.03	1.0179	0.0058	1.0185
0.0158	0.0011	0.0147	0.0033	0.2923	-0.0011	24.34	19.57	-0.21	1.0784	0.0062	1.0791
0.0182	0.0014	0.0168	0.0033	0.2057	-0.0019	26.27	20.30	-0.54	1.1275	0.0040	1.1283
0.0210	0.0018	0.0192	0.0032	0.2409	-0.0031	28.45	21.24	-0.73	1.1737	0.0052	1.1745
0.0240	0.0023	0.0217	0.0032	0.2546	-0.0043	30.97	22.40	-0.97	1.2193	0.0064	1.2202
0.0268	0.0027	0.0241	0.0032	0.2392	-0.0046	33.22	23.51	-1.11	1.2531	0.0053	1.2540
0.0298	0.0032	0.0266	0.0031	0.2496	-0.0058	36.00	24.89	-1.33	1.2908	0.0069	1.2918
0.0338	0.0036	0.0302	0.0030	0.3579	-0.0054	38.31	26.13	-0.87	1.3151	0.0082	1.3157
0.0363	0.0040	0.0323	0.0030	0.2079	-0.0055	40.62	27.37	-1.51	1.3375	0.0047	1.3386
0.0394	0.0047	0.0347	0.0029	0.2483	-0.0071	44.02	29.09	-1.64	1.3718	0.0083	1.3731
0.0450	0.0051	0.0399	0.0029	0.5141	-0.0068	46.52	30.71	-0.75	1.3800	0.0127	1.3805
0.0468	0.0056	0.0412	0.0028	0.1316	-0.0060	49.18	32.13	-2.62	1.3999	0.0034	1.4020
0.0550	0.0069	0.0481	0.0026	0.3922	-0.0093	56.13	35.93	-1.36	1.4418	0.0166	1.4430
0.0569	0.0072	0.0497	0.0026	0.1559	-0.0043	58.00	36.89	-1.57	1.4540	0.0029	1.4553
0.0597	0.0077	0.0520	0.0025	0.2284	-0.0071	60.82	38.54	-1.78	1.4641	0.0063	1.4654
0.0639	0.0085	0.0554	0.0024	0.3445	-0.0107	64.94	41.06	-1.78	1.4739	0.0139	1.4751
0.0667	0.0090	0.0577	0.0023	0.2261	-0.0088	67.86	42.96	-2.24	1.4765	0.0064	1.4778
0.0686	0.0094	0.0592	0.0023	0.1514	-0.0065	69.95	44.25	-2.44	1.4804	0.0031	1.4818
0.0718	0.0099	0.0619	0.0022	0.2655	-0.0092	72.90	46.03	-1.98	1.4868	0.0077	1.4880
0.0776	0.0109	0.0667	0.0020	0.4860	-0.0166	77.97	49.11	-1.96	1.4963	0.0241	1.4973
0.0789	0.0111	0.0678	0.0020	0.1080	-0.0046	79.14	49.86	-2.45	1.4972	0.0012	1.4982
0.0824	0.0117	0.0707	0.0018	0.2866	-0.0137	82.51	52.03	-2.73	1.4994	0.0094	1.5005